PHOTOGRAPH THIS SHEET

DTIC FILE COPY

AD-A223 020

DTIC ACCESSION NUMBER

LEVEL

INVENTORY 1

MATERIALS 88

DOCUMENT IDENTIFICATION

13 MAY 88

DISTRIBUTION STATEMENT A

Approved for public release;
Distribution Unlimited

DISTRIBUTION STATEMENT

| ACCESSION FOR | |
|---|---|
| NTIS GRA&I | X |
| DTIC TAB | |
| UNANNOUNCED | |
| JUSTIFICATION | per form 50 |
| BY | |
| DISTRIBUTION / | |
| AVAILABILITY CODES | |
| DIST | AVAIL AND/OR SPECIAL |
| A-1 | |

DISTRIBUTION STAMP

DTIC
ELECTE
JUN 18 1990
S D

DATE ACCESSIONED

DATE RETURNED

90 06 14 098

DATE RECEIVED IN DTIC

REGISTERED OR CERTIFIED NO.

PHOTOGRAPH THIS SHEET AND RETURN TO DTIC-FDAC

DTIC FORM 70A
MAR 86

DOCUMENT PROCESSING SHEET

PREVIOUS EDITION MAY BE USED UNTIL STOCK IS EXHAUSTED.

The Institute of Metals

# Materials

Materials and Engineering Design

London
9-13 May
1988

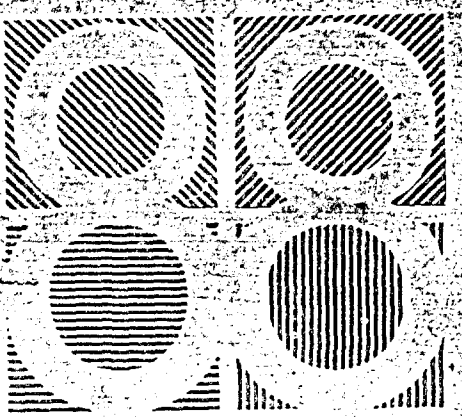





PREPRINT

RD 5994-MS-02
DAJA 45-88-M-0127

# MATERIALS AND ENGINEERING DESIGN

9–13 May 1988 Royal Lancaster Hotel, London

This report is

The second in the series of international materials engineering conferences established by The Institute of Metals in May 1987, organised in conjunction with the National Physical Laboratory and the University of Sheffield. The event is co-sponsored by The Design Council, The Institute of Ceramics and The Plastics and Rubber Institute.

CONTENTS OF PREPRINT



Keywords: Symposia, Knowledge-Based Systems, Fiber Reinforced Plastics, Transputer-based Finite Element techniques, Coatings, Welded Components, CREEP, Damage Mechanics, Metal Matrix Composites, Fracture (Mechanics), FATIQUE (Mechanics), Corrosion, Explosive Cladding, ALLOYS

XG

---



Compiled from original typescripts and illustrations provided by the authors

Printed and made in England by
Inprint of Luton, Bedfordshire.

# THE INTERACTION OF DESIGN, MANUFACTURING METHOD AND MATERIAL SELECTION

J. A. Charles

Dr Charles is in the Department of Materials Science at the University of Cambridge

SYNOPSIS

The characterisation of a design in terms of function, appearance, manufacturing method and cost is considered. The interacting influences of design, fabrication and materials selection are not always appreciated, with resultant inefficiency or failure. This is considered in an historical setting, highlighting the changes in circumstance which now require better communication of information for such interaction to occur. The role of the computer in the provision of databases from standardised information and the development of 'intelligent' selector systems with input to models from consideration of microstructural engineering is outlined. The greatly increased range of materials to be considered and the need for integration of design, processing and materials expertise, poses problems for the teaching of materials engineering where, again, the computer has an important role to play in developing understanding.

In this very important area of industrial and educational endeavour interaction should progress towards integration.

It has been suggested[1] that any design can be characterised in terms of:

(1) Function
(2) Appearance
(3) Manufacturing Method
(4) Cost

## (1) Function and Design Synthesis

In considering the design of a component it is first necessary to define function precisely, i.e. what the component has to do.

We have to search out and bring together sufficient basic ideas for the achievement of function to an acceptable degree - let us call this design synthesis (Fig. 1[2]). This stage may be built on previous experience and expertise or it may be truly innovative. It may also be constrained by market research which indicates the customer pull in a certain direction which will affect the design, and it will generally be restricted in its technical development by cost requirements, particularly in a cost-oriented rather than a performance-oriented product. Perfection may be too expensive and the designer has to know when to stop in what is essentially an open-ended exercise with diminishing returns down any particular synthesis track.

At several stages decisions have to be made. Initially these will be in the context of dimensions, tolerances, materials and manufacturing method, and at these stages external advice will need to be available to the designers, particularly as the range of materials and manufacturing methods, and the impact that this can have in design, is continuing to expand at a rapid rate. How that advice can be provided is a matter to be considered later. For decision making to be effective it requires a high degree of technical expertise and must be as numerate as possible. Computer-aided design and the development of data banks of stress analysis formulae and comparative materials properties are making the process of design increasingly sophisticated. A significant aspect of this can be that increasingly quantitative design practice is likely to move designs closer to the margin of failure, i.e. designs become more critical. This must be the result of cost control where there is confidence in the design process. On the other hand a quantitative understanding of, say, fracture mechanics in relation to a design will reduce the likelihood of the introduction of gross error.

Having achieved what appears to be the basis of a satisfactory design, analysis must follow to determine whether function has been achieved to the required level. This is, of course, where testing comes in and, later on, the reactions of the market.

It will be noted from Fig. 1 that the introduction of a new product which achieves good sales may well be next associated with a cost reduction exercise involving a degree of redesign. It is frequently the case that new products are associated with overdesign, since underdesign would not create a market. Gross overdesign is, however, uneconomic and the more numerate the original design has been the nearer to optimisation one can be initially, provided the full requirements of the function have been properly analysed. In any case, once a market is established overdesign can be trimmed back as a result of service experience. Thus design synthesis is essentially an iterative process, but one where it pays to get as nearly to the optimum

solution the first time round. In this the value of proper interaction of materials selection and consideration of the manufacturing method in relation to the design, on as numerate a basis as possible, cannot be over-emphasised.

(2) Appearance

It is worth distinguishing between design and appearance, since to the general public at least the two may appear synonymous. There is no reason why functional equipment should not be designed for an appearance which satisfies a taste or fashion subjectively if this does not reduce effectiveness of the design in relation to its function or its economic viability. One recalls the fashion for inessential decorative trim on motor cars which promoted corrosion beneath at fixing points and which was not related to function. In so many examples also such inessential complexities of form make cleaning and maintenance more difficult, increasing the cost or energy of ownership and can even make designs inadmissible on safety grounds. In the design of cars what is pleasing to the eye may not necessarily give the lowest drag coefficient or a design which excels in this latter respect may not be easy for other than the young to enter or leave! There has to be a reconciliation between priorities in terms of fuel economy, comfort in use and "looks" as subjectively judged by the customer.

(3) Manufacturing Method

The manufacturing method is of the greatest significance in determining the successful application of a given material to a design.

Firstly, the required properties may be largely developed in a component as a result of the manufacturing method applied - as, for example, in the cold presswork and drawing of low carbon steel and brass. Here the levels of strength required in a component are developed during the forming process such that it is capable of accepting work hardening to the final level required for strength. There are, of course, numerous other examples of this general principle.

In the context of more advanced materials it can now even be said that the manufacturing method for the component itself creates the material chemically or mechanically and the three aspects of design, manufacturing method and material must perforce be considered together.

Secondly, it has to be recognized that individual components may be designed to satisfactory function in themselves, but incorporation by manufacture into a larger overall design introduces complications of behaviour which have to be properly assessed.

Considering one or two examples of this. If welding is to be used to join steel components into a structure the influence that the welding operation has on the local properties and geometry is extremely important, particularly in relation to fatigue resistance under fluctuating load, where performance of the component will generally not match the fatigue life of the separate components in the non-welded state. To maximise fatigue strength in the overall design the perfection and geometry of the welds themselves, the position of stress concentrations in the structure relative to the welds and the influence of the heating/cooling cycle in relation to the hardenability of the steel and thus its effect on microstructure, yield strength and toughness have to be understood as an important aspect of the overall interactive process relating design, material and manufacturing method. The word understood is emphasised since there may well be circumstances where existing specifications and associated codes of practice and data bases do not cover even reasonable rather than remote possibilities as they arise in modern practice. If, for example, welding is to be used to join lengths of line-pipe in a carbon-manganese steel of considerable hardenability, specifications will advise the design-engineer that certain welding procedures with pre- and postheating should be followed. This will ensure that brittle, hydrogen-sensitive martensite-containing microstructures in the parent pipe do not result. Present specifications would not say, however, that similar care should be exercised in any other procedure involving heating/rapid cooling which might be applied to the pipe, as, for example, when induction-bending. With proper understanding or advice of the reasons why the care in welding is necessary the engineer will be concerned to ensure that similar caution is applied to the products of bending, which may well require post-bend heat treatment.

Another example where manufacturing method may alter the response of individual components when assembled into an overall design is surface durability, often the primary consideration in the selection of a material. Welding, or other local heating in the course of fabrication can produce changes in microstructure leading to differences in potential between adjoining surfaces in the one material with enhanced local corrosion. Mechanical joints are also notorious for introducing crevice corrosion as the result of differential aeration, and worse, the smaller the crevice in the first instance the more intense the crevice attack as the result of differential aeration up to the point where electrolyte penetration ceases. Thus, even where a material with acceptable intrinsic corrosion resistance has been selected, joining processes may introduce corrosive failure.

Casting

If a casting is considered to be the most appropriate manufactured form for a component the design developed for function may not be ideal for the production of a fully-sound product in the material chosen on the basis of bulk properties. In this matter careful integration of design for casting and required function has to be exercised.

In the field of casting there is considerable activity to develop fully satisfactory 3-D solid model data bases and software which can represent the solidification process in all its aspects, fluid flow in the mould, heat transfer, solidification mechanism and resultant microstructure, shrinkage, solute segregation, internal stress development etc. Progress is being made, particularly in the USA, and a number of relatively simple software packages are available for certain aspects of casting technology which can reduce the heavy dependence on experience, but it is heartening to know that there is collaborative effort between academics such as Prof. Cross at Thames Polytechnic and Prof. Lewis at Univ. of Swansea, the National Engineering Laboratory at East Kilbride and SCRATA in Sheffield, which will hopefully lead to a major jump in UK expertise in modelling and get 3-D solid modelling and the

expression of design data in digital form accepted and implemented in the industry.

When one gets down to the real problems that such a commitment entails it is evident that there is still a lack of realistic values for parameters such as shrinkage characteristics (particularly for non-isotropic materials) and for the heat transfer characteristics across various interfaces. Further, whilst proper control over mould conditions, metal quality, pouring rates etc. is always essential for good, reproducible practice, it would be the more so if the full benefit of any predicted optimum casting regime were to be achieved.

(4) Cost

Whilst in any given set of circumstances the competition between materials or components may be finally decided on costs where otherwise similar performance in relation to function is obtainable, the precise level of performance and cost must depend on the type of application involved.

In the interaction between performance and cost it is possible to see a continuous spectrum stretching from, at one end, applications which demand the maximum achievement of performance (i.e. performance-oriented products) to, at the other end, applications in which considerations of cost must be predominant (i.e. cost-oriented products).

In the context of cost the properties of a given design and material may be regarded according to the extent to which they are cost-effective; that is to say, the extent to which they may be dispensed with in the interests of reducing costs. The designer will be prepared to incur costs for the provision of a certain property in proportion to the penalties that will result when it is absent. One of the contributions that the materials engineer can make as a member of a design project team is this ability to distinguish between material-sensitive and design-sensitive properties. A tough material is one that is resistant to the initiation and propagation of cracks, whereas a tough design is one that is free from notches and stress raisers. It may be quite expensive to obtain an especially tough material for a critical application but relatively cheap to free a design from stress-raising geometry. It is technical incompetence to solve a problem more expensively than is necessary. The cost of any improvement in technology either as regards material or design must be more than recouped from corresponding savings resulting from improved performance, in other than highly performance-oriented applications. The inevitable result is, of course, that cost-effective decisions generally act to inhibit purely technological advance.

## Present Practice

There is no doubt that in terms of numeracy in design, quality control in materials and the understanding and control of manufacturing methods, there has been continuous progress in the engineering world. Sometimes still, however, elementary mistakes are made using conventional materials and new materials and techniques are not considered.

As an example the majority of engineering component failures occur by fatigue mechanisms and yet frequently one encounters a lack of even elementary understanding of the effect that design can have on fatigue performance. We are all familiar with the story of the effect of the window design in the original Comet in generating fatigue cracks and the effect that these had on the overall fracture toughness of the design. Yet not infrequently one encounters stress-concentrating designs which could so easily be modified - for example, in coal grinding equipment which it is known would be subject to heavy vibrational stresses where square apertures were oxygen-cut in the casing. Not only was the overall design of the apertures wrong, the oxygen-cutting left kerf lines on the cut surface, which could act as crack-initiation sites.

Thus, whilst we acknowledge that interaction between design, fabrication and materials selection is essential, and there are numerous books and papers to guide us, a proper understanding of the principles involved is not always evident. Why is this?

## Historical Background

Certainly the interactive process that we have been discussing is in no way new and it is interesting to look back in relation to what we now see as a vitally important aspect of competitive engineering practice - the selection of a design and a material for a function incorporating an understanding of how the material may be produced to that shape to acceptable properties. The technology of prehistory provides fascinating examples of just the sort of deductive processes that must be involved. It may be interesting to look at a few examples.

The earliest is a Minoan dagger from Gournia in S.E. Crete, circa 1500 BC, Fig. 2, where a tin-bronze blade cast to a blank, forged and work-hardened in the cutting edge and fluted surface, has pure copper rivets, capable of appreciable cold-heading with work-hardening, attaching the handle to the blade. Minoan daggers of this time have no extended tang so that the rivets have to be stout and strong, as indeed they are here. These rivets have been decoratively silver-capped at each end and show a silver-copper eutectic at the interface with indication that it was produced by diffusion - i.e. the Sheffield plate system 'invented' by Bolsover in 1743 (Fig. 3). The bond was achieved by locally applied heat and pressure probably from a blowpipe flame, and as a result, the derived eutectic would be squeezed out of the joint, requiring 'filing' to fit through the tang at the rivet diameter. Here we see a clear example of control of design in relation to manufacture. The final geometry indicates that the copper rivet was chamfered slightly under the silver cap so that the gap thus created accommodated the eutectic solder and did not increase the diameter of the rivet (Fig. 4). Thus in this example we see the choice of material in relation to function and manufacture, viz bronze for the blade and copper for the rivets, and a further control of design to facilitate manufacture.

The Egyptian Late Kingdom bronze cats (c. 500 BC) Fig. 5, were made in large numbers - an early example of bulk production. For economy they were produced as hollow castings by the lost wax technique on a clay core, with a wall thickness of ~ 2 mm for the usual sizes. For those with experience in bronze founding it would clearly be seen to be very difficult to run such a thin-walled casting in a straight tin-bronze at an acceptable superheat. The effect of lead on the

fluidity of tin-bronze is very marked - almost certainly because the film of molten lead surrounding the first-forming wall dendrites produced in solidification greatly reduces the thermal diffusivity and thus the heat flow to the wall from the metal moving through the central aperture. The effect can be clearly demonstrated by fluidity spirals [3].

In the case of the Egyptian cats the lead content of the bronze is often very high and usually of the order of 12%, which enables the thin-walled castings to be run. Whilst such high lead contents would not be acceptable in a bronze to be used for a purpose where strength and toughness were a requirement such as a sword blade, the material is perfectly satisfactory for a statuette. Clearly this is a case of the use of a chosen material to enable the ready bulk-production of the required castings at lowest cost, incorporating the hollow design. Early Caananite earrings were put together by soldering (Fig.6a) but probably successful sales resulted in reconsideration of the manufacturing method to reduce effort and increase production and we find that one-piece investment castings follow (Fig. 6b).

Thus the type of empirical reiterative process for the interaction of design, material selection and manufacturing method without numeracy is not new. In the early days of technology the designer and the manufacturing craftsman with an intimate knowledge of the materials then available, were usually one and the same person, and there were no barriers of knowledge and understanding between the two functions, a situation which continued for a very long time. With the growth of population and increased complexity of social organisation the craft units enlarged but were still usually in the control of a master craftsman/owner who would increasingly become separated from the practical execution of the work, but who had training and experience in every quarter. As well as representing the craft group or company commercially he would still be directly involved with design and developments of practice. At a much later stage we see this very clearly at Ironbridge in the activities of the Darby and Reynolds families, who became increasingly metallurgical engineers and designers, both of plant processes and products, but who understood their materials within the limits of the day.

By the end of the eighteenth century the iron and steel industry, for example, was already highly capitalistic in its organisation and there was increasing separation between design, manufacture and the supply of materials, with growth accelerated by the demands of new machines and by the needs of war. In steel, production was being concentrated in Sheffield, particularly once the Hunstman crucible process was established in the latter half of the eighteenth century.

It is interesting to reflect on the position of Bessemer in all this. In his autobiography he describes a situation in 1854 where he had designed a field gun which provided a method of rotating projectiles for more accurate flight which, when tested in France made him conscious of the need to produce "a superior description of cast iron" - presumably since a higher pressure developing behind the shell had caused barrels to burst. He says then [4] "my knowledge of iron metallurgy was very limited and consisted only of such facts as an engineer must necessarily observe in a foundry or smith's shop, but this was in one sense an advantage to one, for I had nothing to unlearn" . . . "the object I set before myself was to produce a metal having characteristics comparable with wrought iron or steel and yet capable of being run into a mould or ingot in a fluid condition."

Clearly, Bessemer was just sufficiently near to working practice to be able to personally use his undoubted intellect to observe and deduct from experiments and to eventually generate the material that he needed - acid Bessemer steel.

## Standard Specifications

As production increased, at numerous centres each with their own practice and their own design of product based upon craft experience and rule of thumb and with relatively poor and slow inter-producer communication, problems arose with such engineering components as rails and sections, where there was a bewildering range of slightly different dimensions and shapes. Combined with a large range of compositions or 'brands" associated with the different producing works this made the substitution of alternative sources for a particular construction very difficult. The confusion led to the birth in 1901 of the Engineering Standards Committee through pressure from Sir John Wolfe Barry. Sir John, in addressing the British Association in 1906 said "if high class standard specifications were generally acknowledged it would inevitably tend to improve manufacture and assist British manufacturers to meet competition."

Here we see the beginning of the use of a language relating to design, manufacture and materials, which was becoming essential for communication in a situation where by now the designer, materials producer and manufacturer had become separated in their roles. The data contained in a specification could be referred to for design purposes and eventually codes of practice would provide the information as to how specified materials could be suitably manufactured, for example, how a particular steel should be welded. As specifications developed the values for properties contained therein could be assumed by the engineer for empirical and continuum design purposes without detailed understanding of the way in which the properties were related to the microstructure of the material. Thus the language was most effective as between the individual materials and standard component producers and the engineer.

The role of the industrial metallurgist became clearly divided into two areas, firstly in the extraction and fabrication of metals serving the individual materials producers, and then increasingly, the assessment of materials performance in user industries, including failure analysis, advising on improvement in the choice of material and methods of manufacture. To a large extent the second role was to investigate situations where the information from standards or the use of the standard had been inadequate for the production of a satisfactory design. My consulting experience has led me to the firm opinion that many manufacturing companies in the engineering field still have inadequate expert materials input in their activities, whether from design engineers with knowledge themselves or from associated materials engineers. It is a situation which, in general, does not seem to have improved. There are several reasons that could be postulated for this: engineering courses in University have

become increasingly crowded with less time to devote to a more detailed treatment of the materials component. Another probability is that the proportion of qualified engineers employed in industry has not risen adequately. Materials scientists/engineers are also still sometimes seen as advisors only to be called in when something goes wrong, and not involved in the initial design process. All this in the situation where the number of engineering materials available is growing significantly with the introduction of a large range of non-metallic materials, to include particularly engineering polymers and composites, let alone the continued development of metallic materials.

## The role of the computer

One may even question now whether any individual materials scientist or materials engineer is likely to be able to provide the whole range of expertise necessary at adequate depth; this in the context of a world situation where one technical article is being published per minute, much of it devoted to new materials. Will he or she be able to give the best advice to design engineers, as perhaps metallurgists were once able to do in a more restricted field.

Perhaps the language of communication through printed specifications for standard materials and components, whilst necessary in relation to the production of those materials and components, has to be amplified and made more flexible for design. Increasingly, whilst good handbooks for engineering designers exist, which give good guidance in the use of standards, information retrieved from computer data bases is providing a more flexible and rapid approach with up-to-date information suited to the general increase in computer literacy and computer use in industrial practice. For example, requirements for sub-contractors will increasingly be issued in digital format via electronic communication with their databases, a vital aspect of multiple sourcing to ensure the consistency of dimensions essential for transfer line CNC machining operations. It is significant that so much of this present conference will be taken up with papers on computer-aided design, data bases and expert systems for materials selection, and it is not proposed to go into detail in these respects. What is clear, however, is that there is a vast amount of activity in these areas - one might even term it an explosive activity. Valiant attempts have been made to influence and control development through such agencies as the National Bureau of Standards[5], the Commission of the European Communities, who held a workshop at Petten in 1984[6] and the Committee on Data for Science and Technology (CODATA) and its workshop in 1985[7]. The proceedings of these workshops indicate clearly the major requirements for development in materials databases and the selection programmes that may be based upon them.

Clearly the databases need to be sufficiently large so that there may be balanced response to an inquiry. There also needs to be proper indication of the quality of the information in some relatable way. The database needs to be user-friendly - I was interested to read a reported comment by Dr Norman Waterman (Quotec)[8] where he concentrated on the problem of introducing new materials to Senior Engineers, many of whom obtained their understanding of materials through their apprenticeship or early training and needed access to information on newer materials in a more accessible form than words and numbers and paper. In terms of user-friendliness the development of a materials-selector system based on graphical relationships or charts is very promising, particularly in the context of teaching.

A very important requirement is that there should be standardisation of information in databases in terms of test methods, units, assessment criteria etc., so that there is compatability enabling useful access between bases. Without standardisation of databases integrated information management and computer-controlled technology will be greatly hampered. This is particularly true since it is unlikely that one massive database could be developed to suit all needs and it is most likely that growth will be in the generation of individual bases to suit specific industrial needs.

In these databases and associated selector programmes there is clearly more difficulty in dealing with existing non-quantitative property assessments for such features as appearance, processability, corrosion resistance and wear resistance. In general the best that can be done at present is the incorporation of low level information into the databases in the form of agreed codes interpreted from published empirical observations. These are hopes, however, that expert systems can be developed which will enable precise corrosion-response prediction from models incorporating the many variables in a corrosion process - composition and condition of environment, temperature, flow rate etc., based on the available fundamental electrochemical understanding together with accumulated experience to fill the gaps[9].

A present weakness may also be that quantitative cost effectiveness of potential material choices, where the cost data needs continuous updating, is at present not always available from databases, and at the end of the day this is likely to be the deciding factor between alternatives with reasonable fulfilment of function, particularly in a cost-oriented product.

## Standardisation in the field of engineering plastics

An area in which there is a great need for improvement, standardisation and comparability of data is in the field of engineering plastics, so much based on the very same "local" formula and 'own brand' approach which typified the early days of metal production growth. There are approximately 25,000 commercially-named plastics on the market, a number which is continuously expanding a modification of molecular architecture, blending, the addition of fillers and fibres etc. continues. For the design engineers working with plastics this vast range of possibilities and a relative scarcity of standardised quantitative design data has made selection procedures difficult, not only in comparing against metal alternatives, but even within the field of plastics themselves. ICI with their Dutch subsidiary LNP Plastics have issued a computer software package for the selection of "engineering plastics on screen" (EPOS)[10]. Other manufacturers have similar packages, but like ICI, are bound to cover their own range of materials, which may leave some gaps, and will not evaluate relative costs for similar, if not identical, materials from other manufacturers. One of the few systems which is commercially available and which contains independent

information on the properties and sources of plastics is Plascam (RAPRA). The British Plastics Federation in consultation with the National Physical Laboratory and the UK Plastics industry are now recommending a simple comprehensive system to cover the basic properties of plastics and are working to that end. Major databases exist for metals (e.g. Metadex) with selection programmes such as the ASM metal selector.

Returning to the historical scenario it is clear that it is becoming increasingly important in relation to design to get back full circle to the original situation where the design synthesis and manufacture have a high level of current materials expertise in the same camp, but now utilising the power of the computer to provide immediate information and advice from standardised data banks with linked access, quite beyond the capability of individual expertise or written communication.

## Microstructural engineering

How can the materials selector programmes that are developed for this purpose be made most efficient? Increasingly the fabrication history of a component decides the final properties and whether the properties are isotropic or not. It has always been true to an extent in terms of directionality of properties in metals such as steel, the effect of section thickness on local properties, the introduction of single crystal turbine blades etc. but it has become increasingly marked in the field of composites where specific properties may be introduced at a particular section of the component by suitable manipulation of the reinforcement content or directionality. The microstructure of components in both metals and non-metals, which controls properties, is generated by an engineering requirement in the fabrication process for the particular shape, i.e. external design, but increasingly materials themselves may now be designed for required performance within a specific region of a component. This not only concerns mechanical and physical but also chemical properties where the primary requirement of surface stability under the pertaining environmental conditions can be satisfied by localised surface treatment or coatings.

I recall being intrigued by the occasion many years ago when I first encountered the term 'microstructural engineering' from Dr David Hills of Sheffield Polytechnic, a term he used to describe a course primarily concerned with the processing of materials to a required microstructure and properties. It appealed to me because it implied a need to integrate engineering use with an understanding of the generation of microstructure and the way in which it controls properties in varying section or shape.

## Continuum and atomistic modelling - Selector systems

As Prof. Ashby has pointed out in an earlier conference[11] the continuum design approach with proper information provides a description of material response to certain stimuli such as tensile stress at room temperature, but gives no help in predicting response to a new stimulus because it contains no information about mechanisms, nor can it predict the magnitude of a property in a material in a particular design. Whilst the extension of empiricism with the continuum modelling approach has been made much more powerful in recent years by the introduction of computer facility in finite element analysis, CAD/CAM, large data bases etc. there is increasingly a need for input which understands the microstructural engineering context of the empirical continuum information. For this to be fully effective it has to be numerate information. The development of intelligence systems is needed which can analyse the design and the mechanical property and surface stability requirements and indicate not only the best material but also the effects of microstructural control in that material and the preferred condition of use. Taking the concept of microstructural engineering to its ultimate Ashby uses the term 'atomistic modelling'. Here the numerate information from models for such processes as fatigue and creep could be used to assist to an engineering solution. That the involvement of such atomistic modelling could give an engineering solution directly seems still a long way off - the number of microscopic parameters involved is large and for independent use would require a great deal more comparable data and understanding than we presently have. However, as Ashby indicates there may be considerable scope for the current design philosophy to be improved by model-informed empiricism with input from atomistic information to give, for example, an engineering solution for design against creep which is 'intelligent' and which uses an 'intelligent' data base.

In terms of quality of information it is clear that the development of useful 'intelligent' systems incorporating the microstructural and atomistic information which can integrate design, material choice and fabrication route through refined models needs the incorporation of expertise from really experienced and well qualified individuals who are not likely to be very young and may not be sufficiently comfortable with the computer to pass their experience directly into it[9]. In fact, there are not a large number of metallurgists/materials engineers working at the interface between their subject and engineering and also with an interest in computing, and both attributes are essential for the task. Essentially we seek to create computerised intelligence systems which will bring to the designer the direct involvement with the material in both structure, properties and its manufacture that originally existed with the smith when the demands were relatively simple, empirical and humanly encompassable. How far this is truly achievable is a matter of debate. Experts tend to react with examples rather than with rules, even though the rules may remain in their subconcious. Where they are forced back to the rules background the result of their input to intelligence systems may be more likely to give a system reacting at the level of an expert novice than reproducing their own thinking expertise. Symbol manipulation does not create a mind.

## Educational Aspects

My own materials expertise is of the traditional metallurgical variety based on youthful industrial experience, widespread consultative activity and teaching Materials Selection to final year students in a short course for over twenty years. The course that I have given has been structured so that after discussing the methodology of materials selection and ramifications in terms of costs, failure analysis, specifications etc. the

greater part is taken up with case studies of selection in practice. A similar approach is taken in the advanced student text published with the late F.A.A. Crane of Imperial College[2] with the inclusion of aspects of continuum design in relation to stiffness, fatigue strength etc. which are an essential part of the background required. The increased amount of information to be encompassed in such courses is making treatment in this now traditional manner difficult. With the much greater range of materials now to be covered there will need to be suitable computer software to enable students to become familiar with the characteristics of materials and the levels of property involved. The Peritus-Ed software package designed for teaching (Metal Systems Ltd) covers both metals and plastics and uses a graphics environment called GEM In this respect I believe the graphical relationship approach from the data base which Cebon and Ashby are developing further in the Engineering Dept. at Cambridge is also ideally student-friendly.

As far as engineers are concerned experience has convinced me that the increased criticality of design and required material condition means that in general engineers must have a better knowledge of microstructure than at present, so as to develop an appreciation of the non-continuum factors which can so markedly affect material performance. I am conscious also that the materials scientist or metallurgist needs to be able to appreciate the continuum approach to behaviour and be numerate in both this aspect and the atomistic processes involved in relation to microstructural phase control. Plumbridge[12] sees the solution in producing graduates as "materials engineers" who will possess the dual attitudes of scientist and engineer. Hopefully, however it is achieved, generations of design engineers and materials men will in the future be able to carry on in conjunction the work of providing the interlocking computerised intelligence systems for the full integration of design, manufacture and material selection which we need in a world of ever-increasing complexity and speed.

Throughout this paper the theme has been one of interaction of design, manufacturing method and material selection. From what has been said, however, it must be clear that what is needed is not only interaction but progress towards integration.

**References**


(1) H.J. Sharp, Engineering Materials - Selection and Value Analysis, Iliffe 1966.

(2) F.A.A. Crane and J.A. Charles, Selection and Use of Engineering Materials.

(3) J.A. Charles, Trans. I.I.M. C, June 1982, 51.

(4) H. Bessemer, Autobiography, Engineering, 1905.

(5) National Bureau of Standards, Computerised Materials Data Systems, Fairfield Glade Workshop, TN, Nov. 7-11, 1982.

(6) CEC, Factual Material Data Banks Workshop, JRC Petten 14-16 Nov. 1984, ECSC-EEC-EAEC Brussels, Luxembourg 1985.

(7) CODATA, Materials Data for Engineering, Schluchsee Workshop, FRG, Sept. 22-27, 1985, Fach-Informations Zentrum 1986.

(8) E. Briscoe, SAMPE Journal Jan/Feb 1987.

(9) C. Edeleanu, 29th SAMPE Symposium, April 3-5 1984, 532-536.

(10) Design Engineering, May 1987, 91.

(11) M.F. Ashby, Technology in the 1990's, Royal Society 1987, 87.

(12) W.J. Plumbridge, Metals and Materials, Jan. 1988, 4, 1, 31.

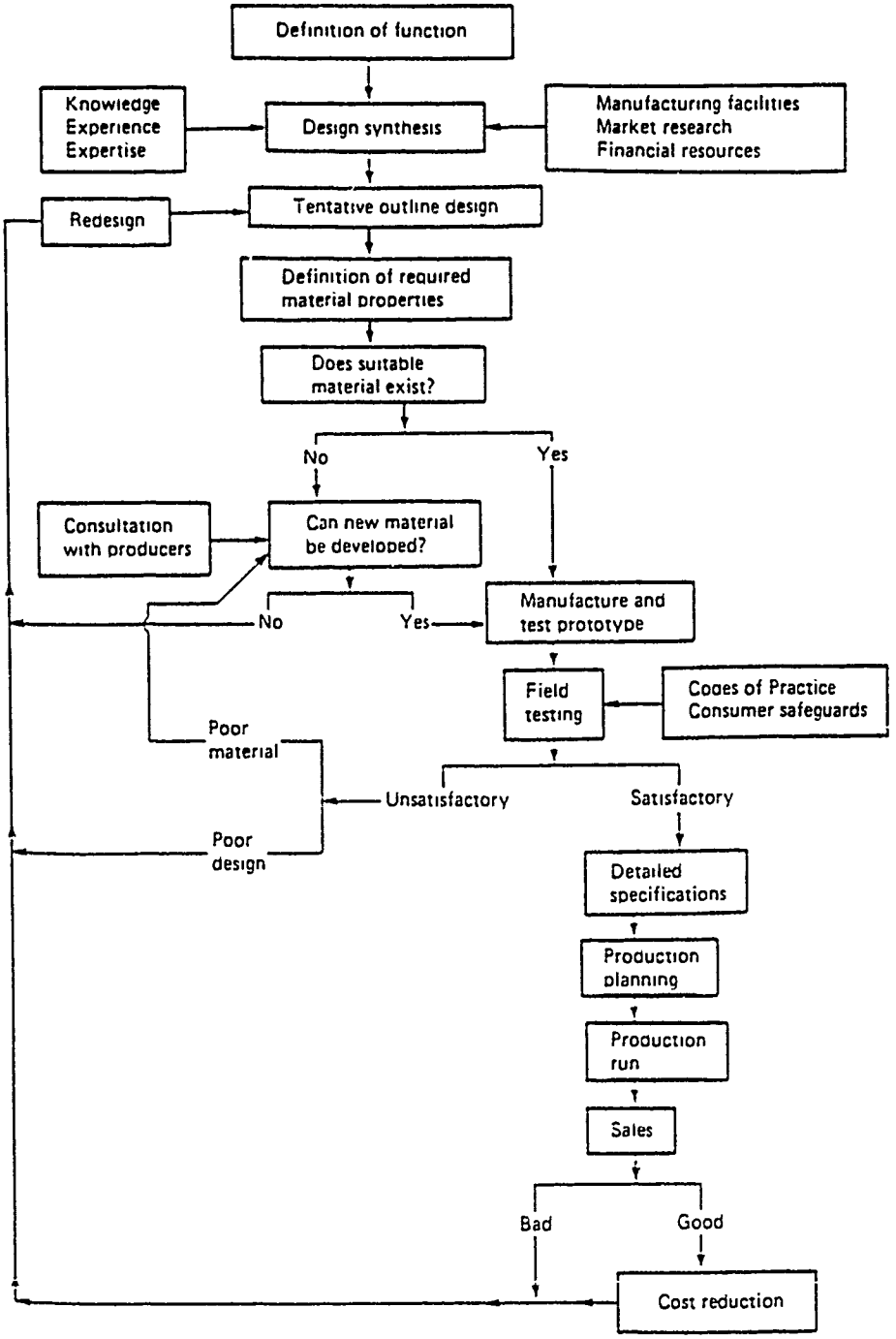


Fig. 1 Iterative processes in design

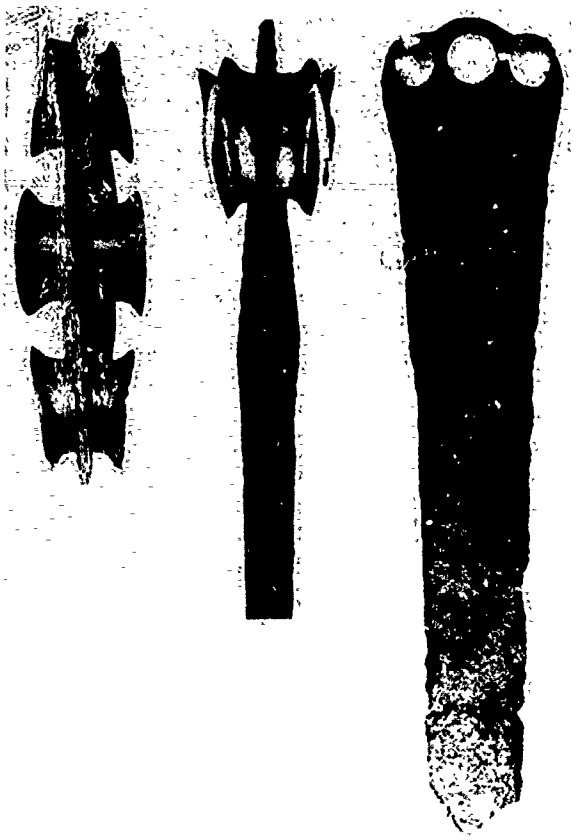

Fig. 2 Minoan dagger, 21 cm long

Fig. 3 Microstructure of interface between copper rivet and silver cap. X 225

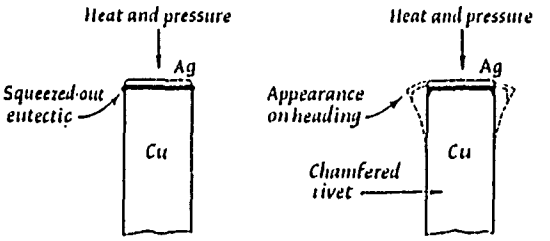


Fig. 4 Use of chamfered rivet to accommodate exuding eutectic from joint

Fig. 5 Egyptian bronze cats, ~1/2 size

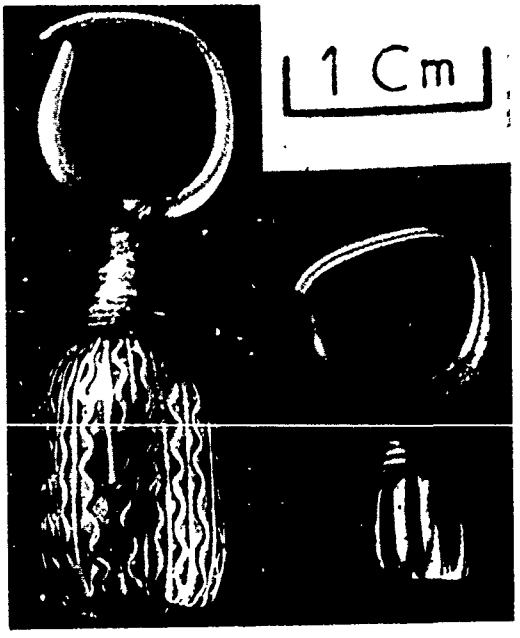


Fig. 6 Caananite earrings, Late Bronze Age

# MATERIALS SELECTION IN CONCEPTUAL DESIGN

Michael F. Ashby

Dr Ashby is in the Engineering Department at the University of Cambridge, Cambridge CB2 2PZ, U.K.

## SYNOPSIS

Information on material properties is essential to engineering design. The breadth and precision of the data that the designer requires depend on the stage the design has reached: at the start (the "conceptual" stage), low-level data for all materials; at the end (the "detailed design" stage), data at a high level of precision for one or a few materials. This paper describes a procedure for materials selection in mechanical design which allows the identification, from among the full range of materials available to the engineer, the subset most likely to perform best in a given application.

## 1. INTRODUCTION

There are, it is said, more than 50,000 materials available to the engineer*. It is convenient to catalogue them in the six broad classes shown in Figure 1 - metals, polymers, elastomers, ceramics, glasses and composites. Within a class, there is some commonality in properties, processing and use-pattern. Ceramics, for instance, have high moduli, polymers have low; metals can be shaped by casting and forging, composites require lay-up or special moulding techniques. But this compartmentalisation has its dangers: it can lead to specialisation (the metallurgist who knows nothing of polymers) and to conservative thinking ("we use steel because we have always used steel").

*Materials enter all engineering design, from the most integrated of microelectronics to the most massive of civil engineering structures. The cost of materials in microelectronics is a small fraction (5% or less) of the cost of the product. By contrast, in mechanical and civil engineering, material costs often exceed 50% of the product cost, and the volume of material used is very large. So we will restrict ourselves to the materials of mechanical and civil engineering. It is here that the competition between materials is greatest, and opportunities for innovation are most marked.

There was a time when metals so dominated mechanical design that ignorance of the potential of other materials was hardly a handicap. But that has dramatically changed. The range of materials available to the engineer is larger, and is growing faster, than ever before (see also the paper by Dr J. A. Charles in this volume). New materials create opportunities for innovation: for new products, and for the evolutionary advance of existing products to give greater performance at lower cost. Markets are captured by the innovative use of new materials, and lost by the failure to perceive the opportunities they present. But how is one to find one's way through the enormous catalogue, narrowing it down to a single, sensible, choice? Can one devise a rational procedure for material selection? To answer that, we must first look briefly at the design process.

## 2. MATERIALS DATA IN THE DESIGN PROCESS

The central column of the flow chart of Figure 2 shows, much simplified, the stages of the design process (Pahl and Beitz, 1984; French, 1985). A market need is identified. A concept for a product which meets that need is devised. If approximate calculations (left hand columns) show that, in principle, the concept will work, the design proceeds to the embodiment stage: a more detailed analysis, leading to a set of working drawings giving the size and layout of each component of the product, estimates of its performance, cost, and so forth. If the outcome is successful, the designer proceeds to the detailed design stage: full analysis (using computer methods if necessary) of critical components, preparation of detailed production drawings, specification of tolerance, precision, joining methods, finishing and so forth.

Materials selection (Dieter, 1983; Crane and Charles, 1984) enters at every stage of the design process. But the nature of the data for material properties needed at each stage differs greatly in its level of precision and breadth (Figure 2, right hand columns). At the conceptual design stage, the designer requires approximate data for the widest possible range of materials. All options are open: a polymer may be the best choice for one concept, a metal for another, even though the function is the same. That sort of data is found in low-precision tables such as those of the Fulmer Materials

Optimiser (1974), the Materials Selector (1987) or in Materials Selection Charts of the sort shown later in this article. The low level of precision is not a problem; it is perfectly adequate for this task. The problem is access: how can the data be presented to give the designer the greatest freedom in considering alternatives? The Charts help here. Examples will be given in a moment.

Embodiment design needs data at the second level of precision and detail. The more detailed calculations involved in deciding on the scale and lay-out of the design require the use of more detailed compilations: multi-volume handbooks like The ASM Metals Handbook (1973), Smithells (1984), The Handbook of Plastics and Elastomers (1975), the Handbook of Properties of Technical and Engineering Ceramics (Morrel 1985, 1987), or computer data-bases which contain the same information. They list, plot and compare properties of a single class of materials, and allow choice at a level of detail not possible from the broader compilations which include all materials.

The final stage of detailed design requires a still higher level of precision and detail. This is best found in the data-sheets issued by the material producers themselves. A given material (low-density polyethylene, for instance) has a range of properties, which derive from differences in the way differeent producers make it. At the detailed-design stage, a supplier should be identified, and the properties of his product used in the design calculation. But sometimes even this is not good enough. If the component is a critical one (meaning that its failure could, in some sense or another, be disastrous) then it may be prudent to conduct in-house tests, measuring the critical property on a sample of the batch of material that will be used to make the product itself.

This paper concerns the first level of data - the broad, low precision compilation - and ways of presenting it which simplify the task of selection.

## 3. MATERIALS SELECTION IN CONCEPTUAL DESIGN

It is important, as we have said, to start the design process with the full menu of materials in mind; failure to do so may mean a missed opportunity. The immensely wide choice is narrowed, first, by primary constraints dictated by the design, and then by seeking the subset of materials which maximise the performance of the components. One way of doing this quickly and effectively is with Materials Selection Charts.

The idea behind the charts is illustrated by Figure 3. One material property (the modulus in this case) is plotted against another (the density) on logarithmic scales. When this is done, it is found that data for a given class of materials (engineering polymers, for example) cluster together; they can be enclosed in a single balloon. The balloon is constructed to enclose all members of the class - even those not explicitly listed on the Chart. The result displays, in a conveniently accessible way, data for E and $\rho$ for all materials.

Primary constraints in materials selection are imposed by characteristics of the design of a component which are non-negotiable: the temperature and environment to which it is exposed, its weight, its cost and so forth. If these are specified, all but a subset of materials which satisfy these constraints can be eliminated. A primary constraint corresponds to a horizontal or vertical line on the diagram: all materials to one side of the line can be rejected.

Further narrowing is achieved by seeking the combination of properties which maximise the performance of the component. For most common load-bearing components, performance is limited, not by a single property, but by a combination of them. The lightest tie rod which will carry a given axial load is that with the greatest value of $\sigma_y/\rho$, (where $\sigma_y$ is the yield strength and $\rho$ is the density of the material). The lightest column which will support a given compressive load without buckling is that with the greatest value of $E^{1/2}/\rho$ (where E is Young's modulus). The best material for a spring, regardless of its shape or the way it is loaded, is that with the greatest value of $\sigma_y^2/E$. Ceramics with the best thermal shock resistance are those with the largest value of $\sigma_f/\alpha E$ (where $\sigma_f$ is the fracture stress and $\alpha$ is the thermal coefficient of expansion); and so forth. There are numerous such combinations, depending on the application. Those for some simple loading geometries are listed in Figure 4; there are many more.

The charts can be used to select materials which maximise any one of these combinations. Look again at Figure 3: it shows modulus, E, plotted against density, $\rho$, on log scales. The condition

$$E/\rho = C$$

or, taking logs,

$$\log E = \log \rho + \log C$$

is a family of straight parallel lines of slope 1, one line for each value of the constant C. The condition

$$E^{1/2}/\rho = C$$

gives another set, this time with a slope of 2; and

$$E^{1/3}/\rho = C$$

gives yet another set with slope 3.

It is now easy to read off the materials which are optimal for each loading geometry - assuming, of course, that nothing else (corrosion resistance, for instance) matters. If a straight-edge is laid parallel to the $E^{1/2}/\rho = C$ line, all the materials which lie on the line will perform equally well as a light column loaded in compression; those above the line are better, those below, worse. If the straight-edge is translated towards the top left corner of the diagram, the choice narrows. At any given position of the edge, two materials which lie on its edge are equally good, and only the subsets which remain above are better. The same procedure, applied to the tie ($E/\rho$) or plate

in bending ($E^{1/3}/\rho$), lead different equivalences and optimal subsets of materials.

In mechanical design, the properties which, singly or in combination, usually limit performance are twelve in number. They are listed in Table 1; they include density, cost, stiffness, strength, thermal properties, wear properties and creep resistance. Charts exist (Ashby, 1988) for all of them, combined in the ways which occur most frequently.

We now introduce four of the Charts through brief examples of the way each allows materials to be selected for particular applications.

TABLE 1: BASIC SUBSET OF MATERIAL PROPERTIES

| | |
|---|---|
| Relative cost, $C_R$ | (-) |
| Density, $\rho$ | ($Mg/m^3$) |
| Young's modulus, E | (GPa) |
| Strength, $\sigma_y$ | (MPa) |
| Damping coefficient, tan($\delta$) | (-) |
| Thermal conductivity, $\lambda$ | (W/mK) |
| Thermal diffusivity, $a$ | ($m^2/s$) |
| Thermal expansion, $\alpha$ | (1/K) |
| Strength at temperature, $\sigma_T$ | (MPa) |
| Wear rate, W/A | (-) |
| Corrosion resistance | (-) |

## 4. THE MATERIALS SELECTION CHARTS AND THEIR USES

### 4.1 Materials for Table Legs

Luigi Tavolino, furniture designer, conceives of a light-weight table of daring simplicity: a flat sheet of toughened glass supported on slender, unbraced, cylindrical legs (Figure 5). The legs must be solid (to make them thin) and as light as possible (to make the table easier to move). They must support the load imposed on them by the table top and whatever is placed upon it, without buckling. What materials could one recommend?

Slenderness imposes a primary constraint: slender columns must be stiff, that is, they must be made of a material with a high modulus, E. Lightness, while still supporting the design load, puts a further restriction on the material choice: Figure 4 (and the discussion of the last section) suggest that the choice should focus on materials with high values of $E^{1/2}/\rho$. The appropriate chart is shown in Figure 6 (a). On it, Young's modulus, E, is plotted against density, $\rho$; it is the chart of which Figure 3 is a schematic. Materials of a given class cluster together: metals in the top right, composites near the middle, polymers near the bottom, and so forth. Figure 6 (b) shows the selection procedure. A line of slope 1/2 is drawn on the diagram; it links materials with equal values of $E^{1/2}/\rho$. Materials above the line are better choices for this application than materials on the line; materials below are worse. The line is displaced upwards until a reasonably small selection of materials is left above it. They are identified on Figure 6 (b): woods, composites (particularly CFRP) and certain special engineering ceramics. Metals are out: they are far too heavy; polymers too: they are not nearly stiff enough. The choice is further narrowed by the primary constraint that, for slenderness, E must be large. A horizontal line on the diagram links materials with equal values of E; those above are stiffer. Figure 6 (b) shows that this now eliminates woods. CFRP is the best choice: it gives legs which weigh the same as the wooden ones but are much thinner. At this stage, other aspects of the design must be examined: strength, cost and so forth. Other charts help with this, but that requires more space than is available here.

### 4.2 Materials for the Forks of a Racing Bicycle

The first consideration in bicycle design (Figure 7) is strength. Stiffness matters, of course; but the initial design criterion is that the frame and forks should not yield or fracture in normal use. The loading on the frame is not obvious; in practice it is a combination of axial loading and bending. That on the forks is simpler: it is predominantly bending. If the bicycle is for racing then the weight is a primary consideration: the forks should be as light as possible. Then (see Figure 4) one should choose a material with the greatest value of $\sigma_y^{2/3}/\rho$.

The appropriate chart is shown in Figure 8 (a): strength (yield strength for ductile materials, crushing strength for brittle) plotted against density. As before, members of one class of material cluster together in one area of the chart: metals near the top right, polymers in the middle, structural foams in the bottom left. Figure 8 (b) shows the selection procedure. A line of slope 2/3 is drawn on to the chart; it links materials with the same value of $\sigma_y^{2/3}/\rho$, that is materials which (as far as strength is concerned) are equally good for making the forks of a racing bicycle. All materials above the line are better; those below are worse.

Four materials are singled out. High strength aluminium (7075, T6) and titanium alloys are equally good; Reynolds 531 (a high strength steel popular for bicycle frames) is a little less good; CFRP is definitely better. At this stage it is necessary to examine other aspects of the material choice: stiffness, resistance to fracture and so forth (charts exist which help with this), and to examine the cost of fabrication (though, to the committed racing cyclist, cost is irrelevant). CFRP emerges from such an analysis as an attractive, though expensive, choice; and, of course, it is used in exactly this applications.

### 4.3 Materials for Springs

Springs come in many shapes (Figure 9), and have many purposes. Regardless of their shape or use, the best material for a spring of minimum volume (for a watch, for instance) is that with the greatest value of $\sigma_y^2/E$. We will not go into that now, but simply use the result as a way of introducing the chart shown in Figure 10 (a): modulus, E, plotted against strength, $\sigma_y$. As always, materials group together by class, though with some overlap. This diagram has many uses; one is the identification of good materials for springs.

The procedure is shown in Figure 10 (b). A line of slope 1/2 links materials with the same value of $\sigma_y^2/E$. As the line is moved to the right (to increasing values of $\sigma_y^2/E$ ) a smaller selection of materials is left exposed. The result is shown in the figure, where candidate materials are identified. The best choices are a high-strength steel (spring steel, in fact) and, at the other end of the line, rubber. But certain other materials are suggested too: CFRP (now used for truck springs), titanium alloys (good but expensive), glass (used in galvanometers) and nylon (children's toys often have nylon springs). Note how the procedure has identified the best candidates from almost every class: metals, glasses, polymers and composites.

## 4.4 Safe Pressure Vessels

Pressure vessels, from the simplest aerosol can to the biggest boiler, are designed, for safet , to yield before they break. The details of this design method vary. Small pressure vessels are usually designed to allow general yield at a pressure still too low to propagate any crack the vessel may contain ("yield before break"); then materials with the largest possible value of $K_{1c}/\sigma_y$ are the best choice - they will tolerate the biggest flaw. With large pressure vessels this may not be possible; instead, safe design is achieved by ensuring that the smallest crack that will propagate unstably has a length greater than the thickness of the vessel wall ("leak before break"), and the best choice of material is one with a large value of $K_{1c}^2/\sigma_y$. That covers safety; the actual pressure that the vessel can hold is proportional to $\sigma_y$ itself, so the designer seeks to maximise this too.

These selection criteria are most easily applied by using the Chart shown in Figure 12 (a). On it, the fracture toughness, $K_{1c}$ , is plotted against strength, $\sigma_y$ . Strong, tough, materials lie towards the top right; hard, brittle materials in the bottom right, and so on. The three criteria appear as lines of slope 1, 1/2 and as lines that are vertical. Take "yield before break" as an example (Figure 12 (b)). A diagonal line corresponding to $K_{1c}/\sigma_y = C$ links materials with equal performance; those above the line are better. The line shown on Figure 12 (b) excludes everything but the toughest steels, copper and aluminium alloys, though some polymers nearly make it (pressurised lemonade and beer containers are made of these polymers).

The pressure which the vessel can hold depends also on the magnitude of $\sigma_y$ itself. The vertical line excludes all materials with a yield strength below 100 MPa, leaving only tough steels and copper alloys. Large pressure vessels are always made of steel. Those for models - a model steam traction engine, for instance - are copper; it is favoured, in the small scale application, because of its greater resistance to corrosion.

## 5. CONCLUSIONS

Materials are evolving faster than ever before. New and improved materials create opportunities for innovation. The opportunities can be missed unless a rational procedure for material selection is followed.

At the conceptual stage, while the design is still fluid, the designer must consider the full menu of materials: metals, polymers, elastomers, ceramics, glasses and numerous composites. Material data for a single class or sub-group of materials (suitable for the embodiment stage) are available in handbooks and computerised data bases; and the precise, full, data for a single material (needed at the detailed-design stage) are available fror the supplier of the material, or can be generated by in-house tests.

The difficult step is the first: choosing from the vast range of engineering materials an initial subset on which design calculations can be based. One approach to this problem is described here. Data for the mechanical and thermal properties of all materials are presented as a set of Materials Selection Charts. The axes are chosen to display the common performance-limiting properties: modulus, strength, toughness, density, thermal conductivity, wear-rate and so forth. The logarithmic scales allow performance-limiting combinations of properties (like $E^{1/2}/\rho$ or $\sigma_y^2/E$ ) to be examined and compared.

The examples given in the text show how the charts give a broad overview of material performance in a given application, and allow a subset of materials (often drawn from several classes) to be identified quickly and easily. The uses are much wider than those shwon here; charts exist which help with problems of dynamics, heat transfer, thermal stress, wear and cost. They help, too, in finding a niche for new materials: plotted on to the charts, the applications in which the new material offers superior performance become apparent.

At present, the charts exist as hand-drawn diagrams like those shown here. But is is an attractive (and attainable) goal to store the data from which they are constructed in a data base coupled to an appropriate graphics display to allow charts with any combination of axes to be presented; and to construct on them lines which isolate materials with attractive values of performance-limiting properties (just as in the examples) leading to a print-out of candidate materials with their properties. A micro-computer based system of this sort is at present under development in the Engineering Department at Cambridge.

## REFERENCES


Ashby, M.F. (1987) "Materials Selection in Design", Internal Report, CUED, Cambridge (to be published).

ASM Metals Handbook (1973) 8th Edition, American Society for Metals, Columbus, Ohio, U.S.A.

Crane F.A.A. and Charles J.A. (1984) "Selection and Use of Engineering Materials", Butterworths, London.

Dieter G.E. (1983) "Engineering Design, A Materials and Processing Approach", McGraw Hill, London.

French M.J. (1985) "Conceptual Design for Engineers", The Design Council, London, and Springer, Berlin.

Fulmer Materials Optimiser, (1974) Fulmer Research Institute, Stoke Poges, Bucks, U.K.

Handbook of Plastics and Elastomers, (1975) Editor C.A. Harper, McGraw Hill, New York, U.S.A.

Materials Selector (1976) Materials Engineering, Special Issue, Reinhold, Stamford, Conn, U.S.A.

Morrell R. (1985, 1987) "Handbook of Properties of Technical and Engineering Ceramics" Parts I and II, National Physical Laboratory, HMSO, London.

Pahl G. and Beitz W. (1984) "Engineering Design", The Design Council, London, and Springer, Berlin.

Smithells, C.J. (1984) "Metals Reference Book", 6th Edition, Butterworths, London, U.K.

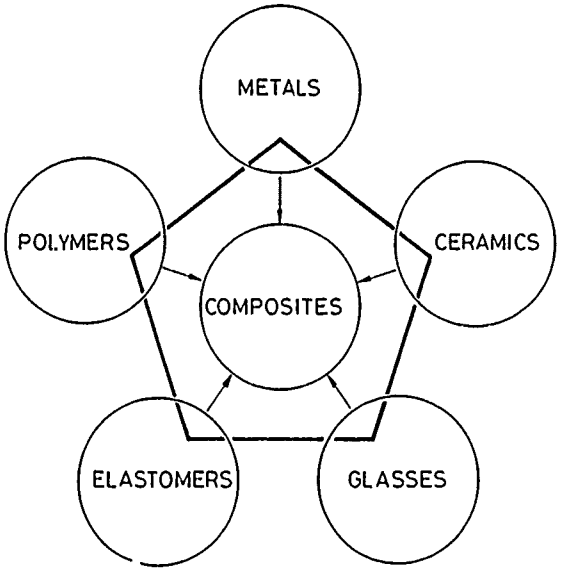


Figure 1. The menu of engineering materials. Each class has properties which occupy a particular part (or "field") of each of the Materials Selection Charts, shown later.

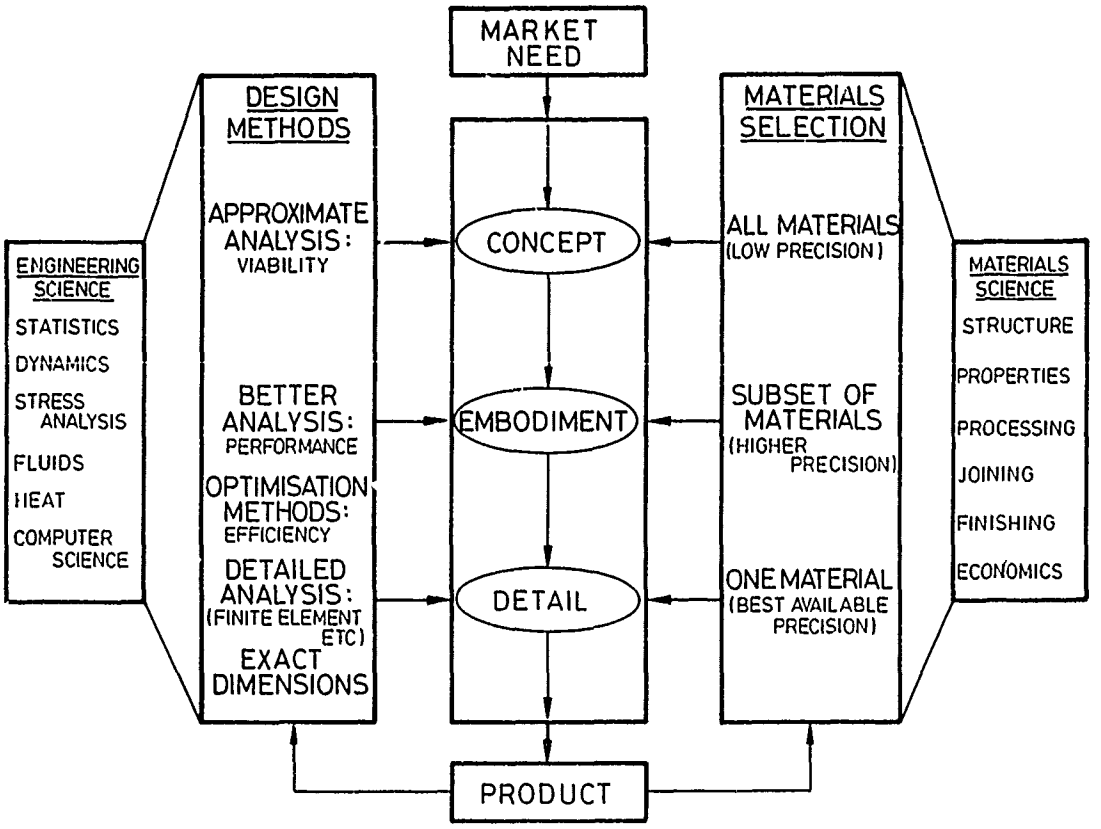


Figure 2. The Design Process, much simplified (central column), showing how Engineering Science and Materials Science interface with each stage. The breadth and precision of the materials data required at each stage differ greatly.

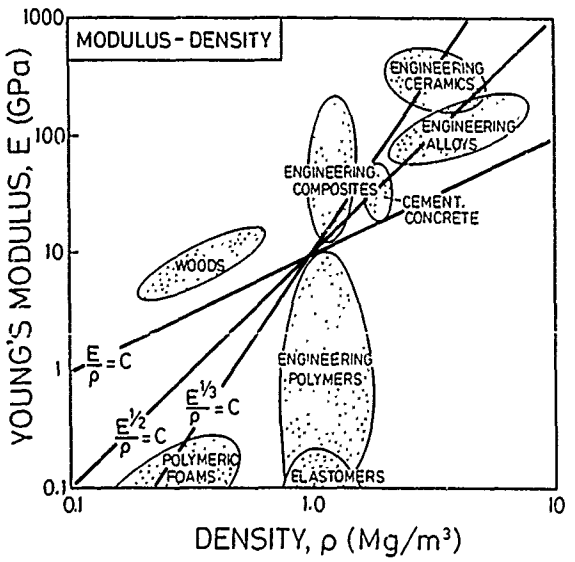


Figure 3. A schematic of a Materials Selection Chart - Young's modulus, E, is plotted against the density, $\rho$, on log scales. Each class of material (Fig 1) occupies a characteristic part of the chart. The log scales allow performance criteria (such as $E/\rho$ or $E^{1/2}/\rho$) to be examined in an easy way.

| MODE OF LOADING | | MINIMISE WEIGHT FOR GIVEN STIFFNESS | DUCTILE STRENGTH | BRITTLE STRENGTH |
|---|---|---|---|---|
| TIE<br>F, $\ell$ SPECIFIED<br>r FREE | 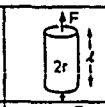 | $\frac{E}{\rho}$ | $\frac{\sigma_y}{\rho}$ | $\frac{K_{Ic}}{\rho}$ |
| TORSION BAR<br>T, $\ell$ SPECIFIED<br>r FREE | 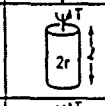 | $\frac{G}{\rho}$ | $\frac{\sigma_y}{\rho}$ | $\frac{K_c}{\rho}$ |
| TORSION TUBE<br>T, $\ell$, r SPECIFIED<br>t FREE | 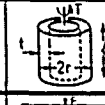 | $\frac{G}{\rho}$ | $\frac{\sigma_y}{\rho}$ | $\frac{K_c}{\rho}$ |
| BENDING OF RODS AND TUBES<br>F, $\ell$ SPECIFIED<br>r OR t FREE |  | $\frac{E^{1/3}}{\rho}$ | $\frac{\sigma_y^{1/2}}{\rho}$ | $\frac{K_c^{1/2}}{\rho}$ |
| BUCKLING OF SLENDER COLUMN OR TUBE<br>F, $\ell$ SPECIFIED<br>r OR t FREE | 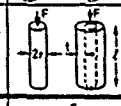 | $\frac{E^{1/2}}{\rho}$ | - | - |
| BENDING OF PLATE<br>F, $\ell$, w SPECIFIED<br>t FREE | 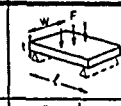 | $\frac{E^{1/2}}{\rho}$ | $\frac{\sigma_y^{1/2}}{\rho}$ | $\frac{K_{Ic}^{1/2}}{\rho}$ |
| BUCKLING OF PLATE<br>F, $\ell$, w SPECIFIED<br>t FREE | 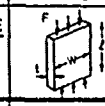 | $\frac{E^{1/2}}{\rho}$ | – | – |
| CYLINDER WITH INTERNAL PRESSURE<br>p, r SPECIFIED<br>t FREE | 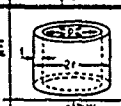 | $\frac{E}{\rho}$ | $\frac{\sigma_y}{\rho}$ | $\frac{K_{Ic}}{\rho}$ |
| ROTATING CYLINDER<br>w, r SPECIFIED<br>t FREE | 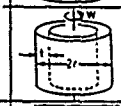 | $\frac{E}{\rho}$ | $\frac{\sigma_y}{\rho}$ | $\frac{K_{Ic}}{\rho}$ |
| SPHERE WITH INTERNAL PRESSURE<br>p, r SPECIFIED<br>t FREE | 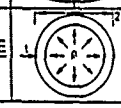 | $\frac{E}{(1-\nu)\rho}$ | $\frac{\sigma_y}{\rho}$ | $\frac{K_{Ic}}{\rho}$ |

Figure 4. The property-combinations which determine performance in minimum-weight design. For minimum cost design, $\rho$ is replaced by $C_\rho \rho$ where $C_\rho$ is the cost per unit weight of the material.

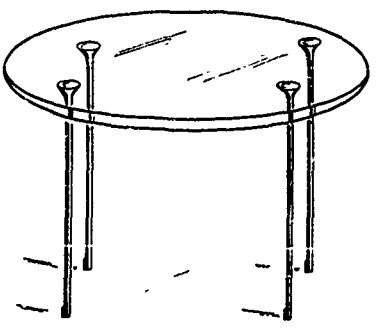

Figure 5. A light-weight table with slender cylindrical legs. The legs must be slender and must not buckle elastically when the table is loaded. That requires a material with high values of both $E$ and $E^{1/2}/\rho$.

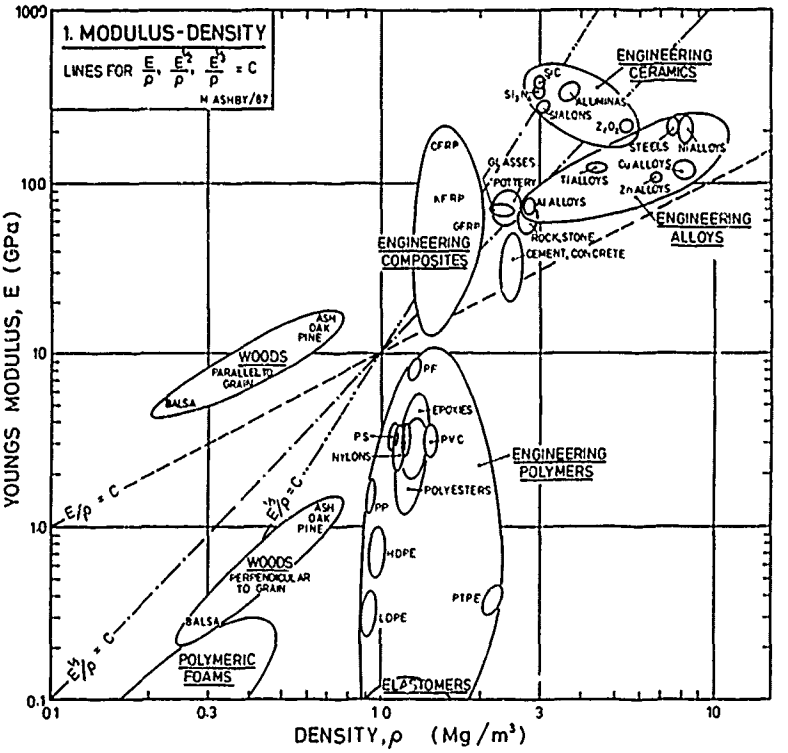


Figure 6,a (above). Materials Selection Chart 1: Young's modulus against density. The balloons enclose data for a given class of material.
Figure 6,b (below) Materials for light, slender columns. Wood is a good choice; so is a composite such as CFRP, which (having a higher modulus) gives a column which is both light and slender.

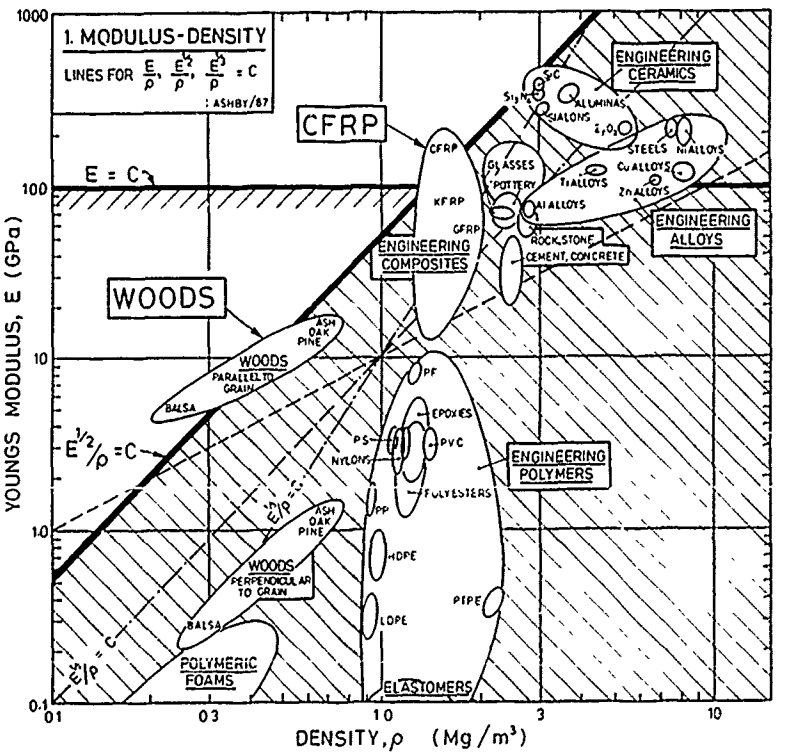

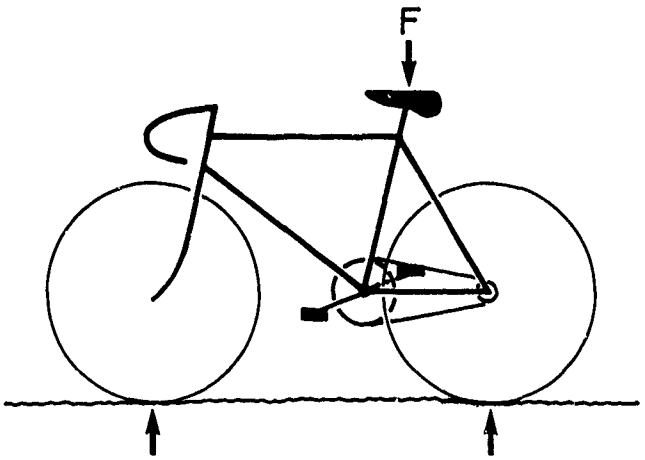


Figure 7. The bicycle. The forks are loaded in bending. The lightest forks which will not collapse plastically are those made with the material with the greatest value of $\sigma_y^{2/3}/\rho$.

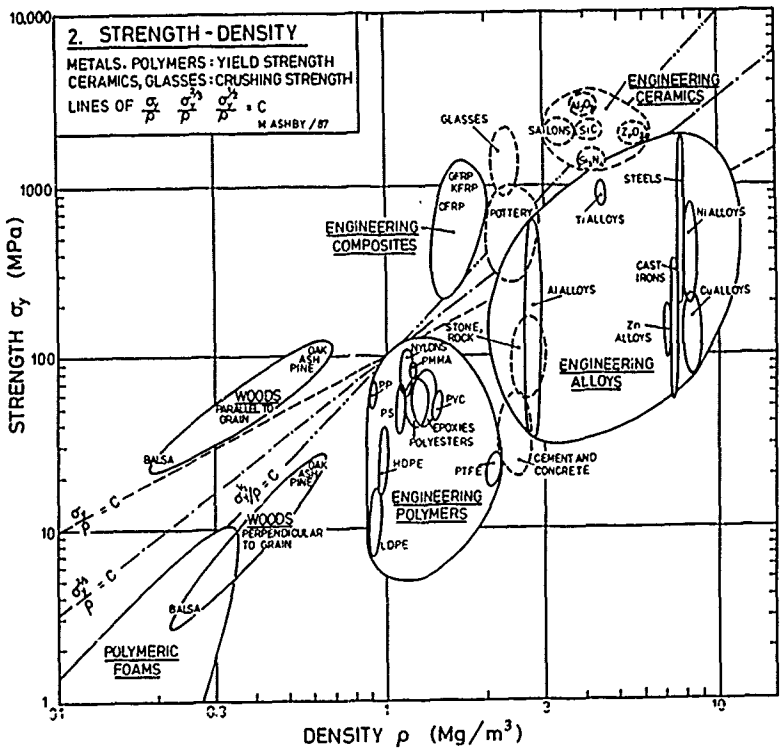


Figure 8,a Materials Selection Chart 2: Strength (the yield strength $\sigma_y$ for ductile materials, the compressive crushing strength for brittle solids) plotted againt density, $\rho$.

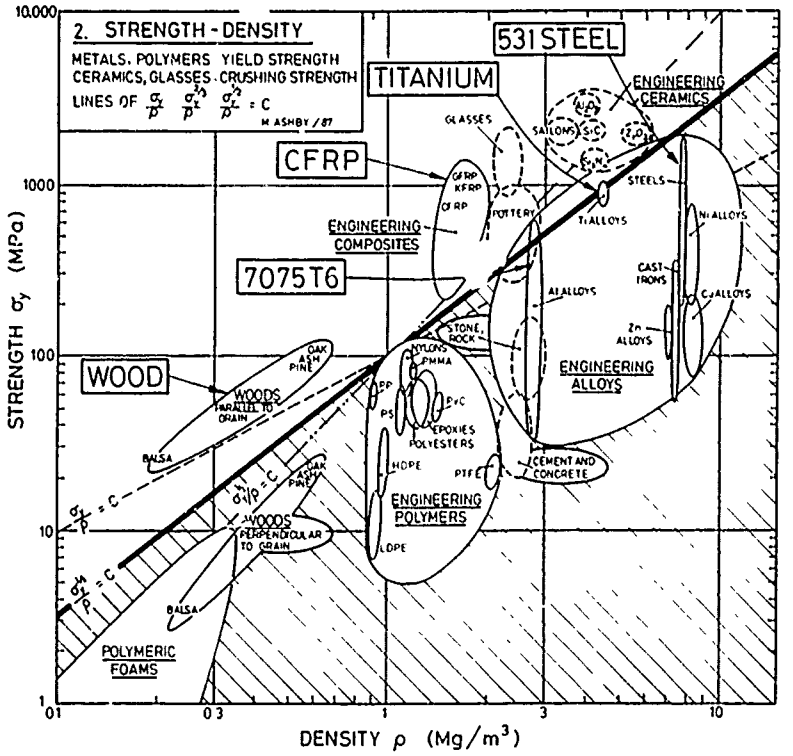


Figure 8,b Materials for the forks of a racing bicycle. Forks made of a titanium alloy or of 7075 aluminium alloy perform better than steel; CFRP is better still. But other aspects of the design (stiffness, resistance to fracture, fabrication costs, etc) must be examined before a final choice is made.

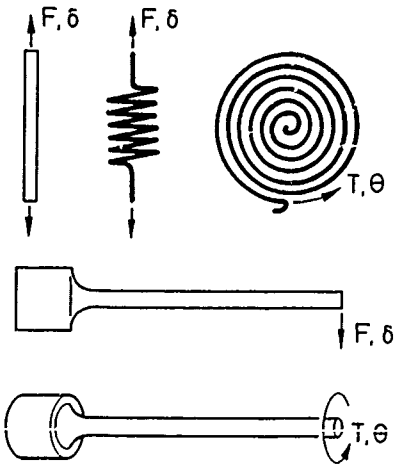


Figure 9. Springs. The best material for any spring, regardless of its shape or the way in which it is loaded, is that with the highest value of $\sigma_y^2/E$ .

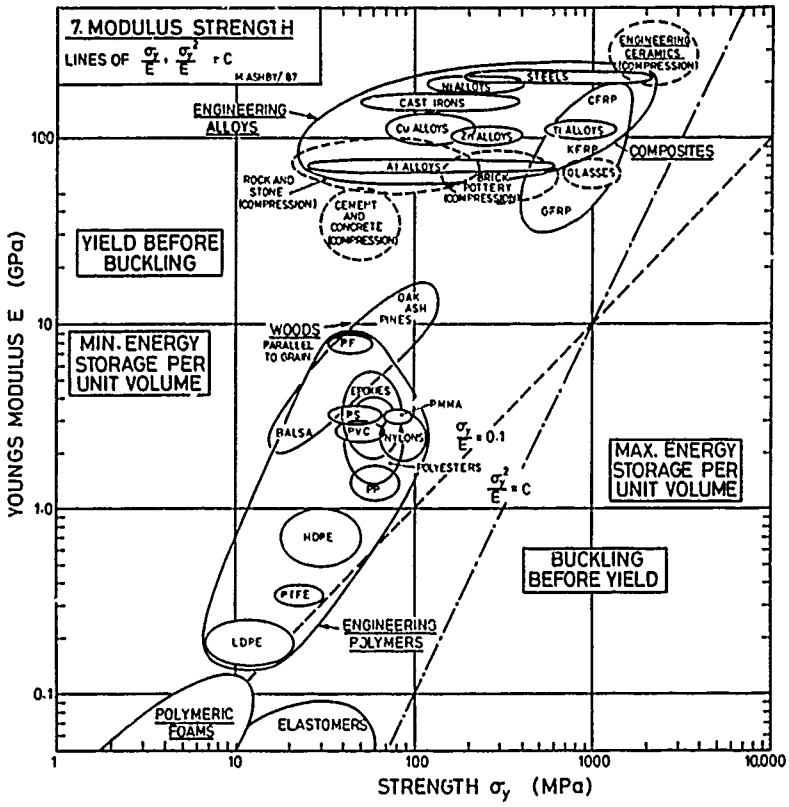


Figure 10,a (above). Materials Selection Chart 7: Young's modulus, E, plotted against strength $\sigma_y$ (the yield strength for ductile materials, the compressive crushing strength for brittle solids). Figure 10,b (below). Materials for springs. Rubber, of course, is good. High strength ("spring") steel is good. But glass and CFRP both, under the right circumstances, make excellent springs.

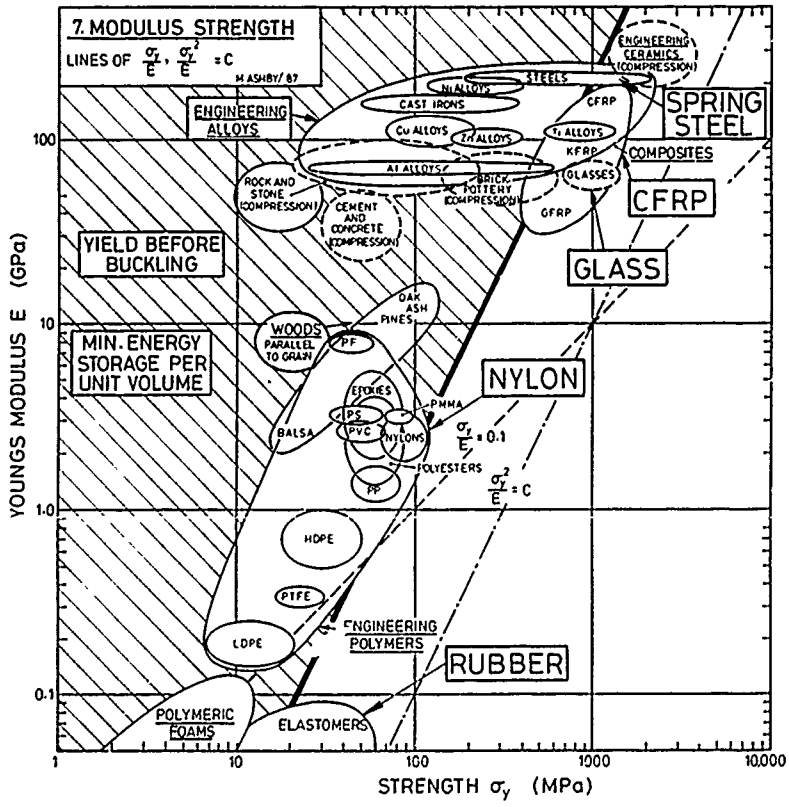

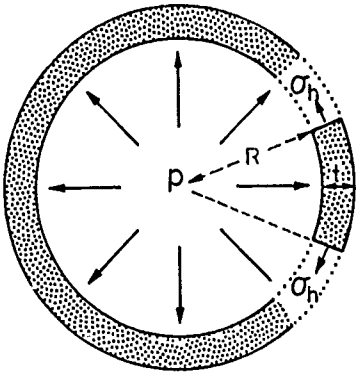


Figure 11. A pressure vessel containing a flaw. Safe design requires that pressure vessels should leak before they break. The best material is then that with the greatest value of $K_{Ic} / \sigma_y$.

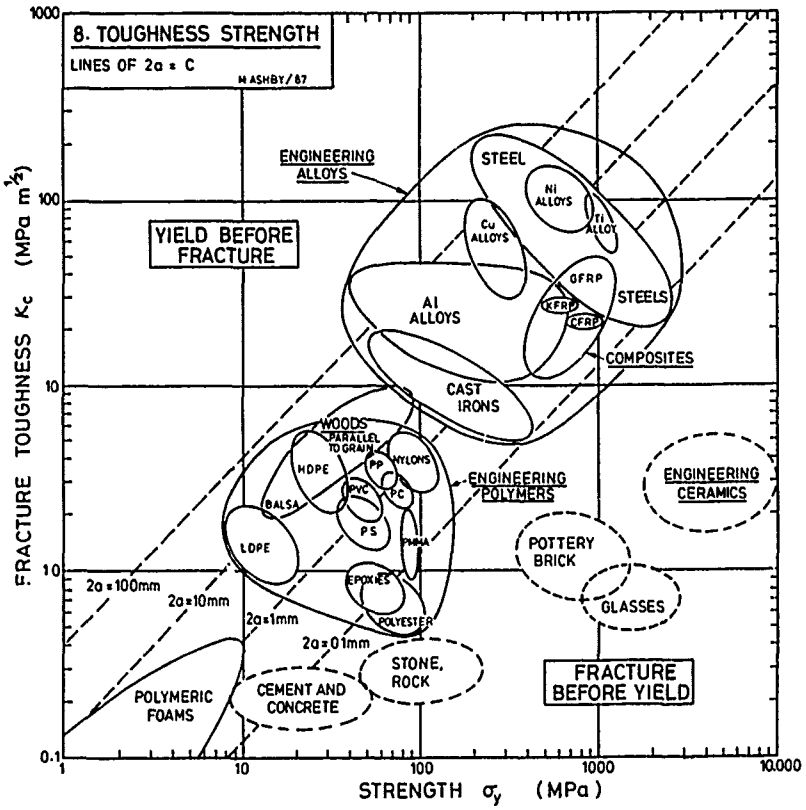


Figure 12,a (above). Materials Selection Chart 8: fracture toughness, $K_{1c}$, plotted against strength $\sigma_y$. Figure 12,b (below). Materials for pressure vessels. Steel, copper alloys and aluminium alloys best satisfy the "yield before break" criterion. In addition, a high yield strength allows a high working pressure. The materials in the remaining triangle are the best choice.

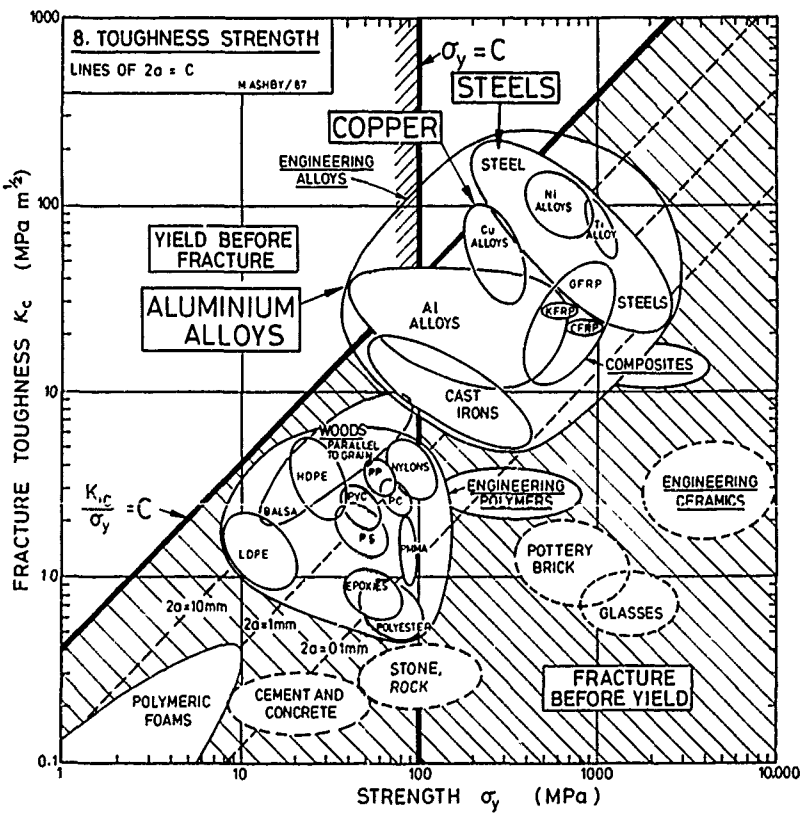

# DESIGNING WITH CERAMICS

by

D.G.Brandon

Department of Materials Engineering
Technion - Israel Institute of Technology
Haifa 32000, Israel

## 1. INTRODUCTION

In a very successful trilogy of books on design, written in the early seventies [1-3], Gordon Glegg wrote as the opening sentence to the first chapter of the first book: "Sometimes the problem is to discover what the problem is." This article attempts to go no further than this. The author is a generalist rather than a specialist. His background is in education and research, rather than industry and development. His conclusions are qualitative rather than quantitative. Nevertheless, and in spite of the caveats, we will attempt to discover "what the problem is", to outline the prerequisite information for successful design, and to give a clear explanation of why designing with ceramics seems to be so different from designing with metals. We will also attempt to define some design strategies suitable for structural ceramics.

## 2. PREREQUISITES FOR DESIGN

Before considering specific designs for a structural component, the designer must first satisfy himself that he has certain basic information available. This information can be summarised by the following check-list for those actions which are required of the designer before he settles down to the real work:

1. Define engineering requirements.
2. Identify critical parameters.
3. Select candidate materials.
4. Determine material properties.
5. Weight relative importance of all factors.
6. Establish alternative processing routes.

This check-list translates into quite specific information requirements which are the prerequisites for successful design. This information, which has to be made available to the designer, should be as accurate and as complete as possible. Every scientist, engineer and technologist associated with the supply of materials, the manufacture of components or the operation of engineering systems should be aware of the designer's needs, for it is in his own interest to contribute his expertise to the design process. In effect, design is too important to be left to the designer.

## 3. ADVANTAGES OF STRUCTURAL CERAMICS

The range of structural ceramics now commercially available is attractive to

the materials engineer because these materials would seem to have singular advantages when compared to the alternatives:

1. Low density, which could reduce the weight of a system and minimise inertial forces.
2. Low thermal conductivity, reducing heat losses and providing thermal insulation for heat-sensitive components.
3. High temperature capability, allowing for higher operating temperatures and a possible improvement in thermodynamic efficiency.
4. High hardness, and hence improved wear resistance and longer life for sliding parts.
5. Low thermal expansion and high stiffness, leading to improved dimensional stability and tighter tolerances under conditions of variable load and temperature.

Given these advantages, it can come as something of a shock to the materials engineer to discover that these "improved" properties are seldom of direct or immediate interest to the designer. For example, the systems designer would probably define the requirements for future heat engine development as follows:

1. Minimise the size and weight of the power unit without increasing its cost.
2. Reduce environmental pollution in order to comply with legal restrictions.
3. Improve fuel efficiency and versatility in order to reduce running costs.
4. Minimise maintenance requirements, for example by eliminating the cooling system.
5. Ensure a guaranteed life for the component, which implies a combination of high component reliability with no unnecessary overdesign.
6. Respond to unpredictable market forces.

When the materials engineer does finally have a mandate from the designer to go ahead and recommend a specific ceramic for a structural component, he will be faced with several basic problems characteristic of the currently available high performance ceramics:

1. Poor reliability in service, usually associated with an inherent brittleness.
2. High costs of raw materials, especially specialty products such as ultra-fine powders, ceramic whiskers or organometallic precursors.
3. High production costs, either because of the long processing times or because of the high capital expenditure on equipment.
4. High rejection rates associated with processing defects and the failure of components to pass proof testing.

## 4. CRITERIA FOR CERAMIC DESIGN

It is important to state clearly just why the design approach to ceramics has to be different from that used for metals and alloys, since this basic difference is the only justification for considering structural ceramics as a separate class of materials. The first point to be made is that metals can relieve local stress concentrations by plastic yielding. This spreads the load over the cross-section and leads to a condition sometimes referred to as "plastic shakedown". Ceramics, on the otherhand, are liable to fail catastrophically from points of local stress concentration and have no inherent capacity for plastic yielding, except under conditions of extreme constraint. The second point is that metals are as strong in tension as they are in compression, while although ceramics can be very strong in compression, they are normally very weak in tension. This is best illustrated by the familiar biaxial-stress failure diagram (fig.1), which shows the limiting stress conditions for plastic yielding in metals according to the von Mises

criterion (fig.1 a), compared with the conditions for fast tensile fracture in ceramics according to a Weibull criterion (fig.1 b).

Katz [4], in a review of American heat-engine programmes, has given a list of seven "rules of thumb" for designing with ceramics:

1. Avoid point loads.
2. Maintain structural compliance.
3. Avoid stress concentrators.
4. Minimize the impact of thermal stresses.
5. Keep components as small as possible.
6. Minimize the severity of impact.
7. Machine components very carefully.

These rules relate to processing (rule 7) and assembly (rule 2), as well as to functional design. They also include (rule 5) a reference to the problems associated with manufacturing ceramic components in large cross-sections and complex shapes. Finally, rule 4 draws attention to the importance of thermal stresses in ceramic components, which may result from operating transients in start-up or shut-down, as well as from thermal gradients or thermal expansion incompatibilities during operation. Thermal stresses in ceramics often play a decisive role in determining performance because of the combination of inherent brittle behaviour with poor thermal conductivity and poor elastic compliance.

Kochendorfer [5], in an excellent summary of work on structural ceramic design for heat engines performed at DFVLR, in Germany, has emphasised the advantages of designing ceramic components to operate in compression, in order to use their high compressive strength and as far as possible avoid operating in tension. These compressive stresses may be introduced during assembly, for example by introducing a shrink-fit assembly, or they may be actual operating stresses. In a gas turbine rotor, compressive operating stresses in the blades may be achieved by attaching them to a rotating rim, rather than at the hub, and such designs have been investigated both at DFVLR and at ONERA, in France. Of course, this imposes high tensile stresses on the supporting rim. An alternative, discussed by Kochendorfer, is to construct a shell blade mounted on a metal root, which is attached to the hub in the usual way, fig.2.

A further example, given in the same article [5], is the redesign of a diesel engine piston and cylinder assembly, fig.3. The aluminium alloy cylinder and piston are replaced by a reaction-bonded silicon nitride piston and reaction-sintered silicon carbide cylinder. The load is transferred to the camshaft by a ball joint in a conical metal insert. The insert is operating in tension, but the ceramic piston is in compression. Because of the low thermal expansion coefficient of the ceramic, the high wear resistance and the high elastic modulus, no piston rings are neccessary.

The silicon carbide cylinder is held in compression by casting an aluminium alloy sleeve around the outside. Normally, the compressive residual casting stresses in the cylinder would be relieved by thermal expansion of the aluminium during operation, and repeated thermal cycling might be expected to remove the beneficial compressive stresses completely. In the DFVLR design this is avoided by wrapping a prefabricated silicon carbide-fibre reinforced aluminium alloy bandage around the cast sleeve after machining.

## 5. RELIABILITY AND FAILURE

The materials engineer can reduce the in service uncertainties in the performance of ceramics, both by

establishing reliable material properties, and by developing reliable theories of failure. Reliable material properties require that the measurable properties should be reproducible; that is, that the properties of commercial grades should not vary from batch to batch. However, they also require agreement within the engineering community on the methods, standards and definitions to be used in determining material properties. The present situation is far from satisfactory, with very few generally agreed standards. The problem is well recognised and international cooperation is underway to establish recognised standards, noteably through VAMOS.

Adequate theories of failure for ceramics can only be developed if the failure modes have first been clearly identified. So far, only four failure modes can be said to be generally recognised:

1. Fast fracture, associated with catastrophic crack propagation.
2. Slow crack growth, either due to environmental attack ("static fatigue") or to diffusion-assisted crack growth at high temperatures.
3. Creep fracture occuring by the nucleation, growth and coalescence of cavities.
4. Surface oxidation or environmental attack leading to a loss of strength of the material.

Of these four failure modes, the theoretical treatment of the first two is sufficiently complete to be useful in formulating design criteria. The theoretical treatment of creep failure in ceramics is currently the subject of considerable research, but has yet to yield a coherent design methodology.

Fast fracture is most commonly treated using a Weibull analysis in which the probability of failure is defined by:

$$P_f = 1-\exp[-(\sigma_{max}/\sigma_u)^m.V_e$$

The effective volume $V_e$ is defined by integrating the known stress distribution over the volume of the component:

$$V_e = \int(\sigma/\sigma_{max})^m dV$$

The expected average strength is then given by:

$$\sigma = \sigma_u.V_e^{-1/m}.\Gamma(1+1/m)$$

The Weibull parameters are $\sigma_u$ and m, and $\sigma_{max}$ is the maximum stress acting on the component.

Some indication of the success of this analysis is given in fig.4, which shows the dependence of mean strength on effective volume for a pressureless-sintered silicon nitride, and compares the calculated result with three types of mechanical test - flexure, torsion and tension [6].

Successful treatment of slow crack growth is based on the determination of the stress intensity dependence of the crack growth rate [7]:

$$dc/dt = AK_I^n$$

Here A and n are material constants. The minimum life of the component $L_{min}$ is related to a proof-stress $\sigma_p$ and to the fracture toughness $K_{Ic}$:

$$L_{min} = 2(\sigma_p/\sigma_a)^{n-2}/[(n-2)A\sigma_a^2Y^2K_{Ic}^{n-2}]$$

Y is a geometrical constant and $\sigma_a$ is the applied stress on the component. Fig.5 gives an example of calculated life levels for three different levels of proof-stress as a function of applied stress, also for pressureless sintered silicon nitride [6].

In both the above cases certain material parameters are assumed to be "known" - $\sigma_o$ and m in the case of fast fracture, and $K_{Ic}$, A and n in the case of slow crack growth. Clearly, the accuracy with which these parameters are in fact known will have a direct bearing on the reliability of the design analysis.

In practice design is an iterative process in which a protoype is first designed against the expected primary failure mode, and then proof-tested to identify the actual failure mode and limits to performance. The cycle of redesign and retesting is then repeated, until either the performance objectives of the project are realised or the project is abandoned. This process is well illustrated by the progress of the DARPA-Ford 820 stator development project (fig.6) [4], in which repeated redesign has led to a continuous increase in observed life, accompanied by a marked change in the primary failure mode of the stator blades.

## 6. MATERIALS SELECTION

The selection of candidate materials is a process of compromise which must include availability, ease of processing and reliability, as well as the relative properties of the materials considered. Materials selection typically involves a trade-off between the various material properties. Table 1 compares the typical thermal properties and strength levels which are currently achievable with three broad classes of monolithic ceramics: silicon carbides and nitrides, aluminas and zirconias, and complex oxides (mullite and cordierite).

From this table it is clear that no single class of high performance ceramics is capable of simultaneously fulfilling requirements for low thermal expansion, low thermal conductivity and high strength. Design solutions must be sought to make up for the deficient properties of each class. An example is provided by the silicon nitride pre-combustion chamber illustrated in fig.7 [6]. While silicon nitride has a low heat capacity, a low thermal expansion coefficient and excellent high temperature resistance, the thermal conductivity of silicon nitride is as high as that of a nickel-base super alloy. The design for the mounting of this component thus includes three features:

1. A compliant gasket, to reduce operating stresses.
2. A metal sleeve, to introduce compressive prestresses.
3. An air gap, to improve thermal isolation of the prechamber.

This last feature makes up for the poor thermal insulation provided by the silicon nitride.

## 7. COMPUTER-AIDED DESIGN

Computer-aided design (CAD) and finite element methods (FEM) are essential features of successful component design. However, these methods are only as reliable as the data introduced into the calculations. Three problem areas can be identified. The first is in establishing the finite element mesh. Regions of maximum stress and temperature can only be identified if the mesh is sufficiently fine to avoid smearing out the stress and temperature gradients. It may be necessary to perform the calculation in two stages, identifying critical areas in the first stage and then using a finer mesh, with boundary conditions defined by the first mesh, to explore the critical regions further.

The second problem area concerns the boundary conditions for the calculations. If the normal operating conditions of an engine are known, then these can be fed in as the boundary conditions for a new,

ceramic component; but then the new component will itself change the operating conditions (for example, the mean gas temperature). Ideally, the whole heat engine system should be included in the model, but this is distinctly impracticable. In practice, the boundary conditions must be redefined by a process of iteration, in which the changes in the operating conditions of neighbouring components are also considered.

The third problem area is the verification of material properties. As indicated in previous sections, this is non-trivial. In the case of monolithic ceramics, the manufacturer's data for the elastic modulus, the thermal expansion coefficient and the thermal conductivity ought to be sufficiently accurate and reliable, but until acceptable international standards are available (and are adhered to) the same is certainly not true of the strength and toughness. Thus, in performing calculations for engine components, the selection of the Weibull parameters is generally inexact, both because of the absence of reliable data and because of the cost of acquiring new data.

An example of a FEM calculation for the assembly, thermal and operating stresses in a silicon nitride piston cap mounted in a precast aluminium alloy stub with a compliant insulating gasket is shown in fig.8. The maximimum tensile stresses in this design are the hoop stresses at the periphery of the cap. At maximum operating temperatures these could reach 80 MPa, which is about 10% of the average strength calculated for the effective volume under stress. In other words, this design incorporates a safety factor of 10 against fast fracture!

## 8. DISCUSSION AND CONCLUSIONS

The various factors which have been discussed in this contribution can be compressed into five independent design strategies for high performance ceramics:

1. Separation of Engineering Functions.

This involves trying to separate the different engineering requirements. For example, a wear-resistant coating may be a more sensible design solution than the replacement of a metal component by a ceramic. This strategy is well-illustrated by the Ford diesel engine programme [8] which envisages three stages in the introduction of ceramics into the engine, fig.9:

1. Ceramic thermal barrier coatings.
2. Ceramic inserts held in compression.
3. Ceramic structural components.

2. Compliant Assembly.

A push-fit assembly and the use of flexible mountings and gaskets helps to avoid stress concentrations and point loads on the ceramic components, and allows for some relative movement of these components during operation of the system.

3. Compressive Prestresses.

Cast or brazed ceramic inserts can be designed to operate under residual compressive stresses that are introduced during the casting. With care, accurate shrink-fit assemblies can achieve the same objective. Compressive prestresses reduce the operating tensile stresses and make maximum use of the high compressive strength of ceramics.

4 Compressive Operating Stresses.

If possible, the ceramic component should be designed to operate in compression rather than in tension, as illustrated in figs.2 and 3. This strategy is more likely to be successful if the component is symmetrical and is adequately supported by a metal, which supplies the tensile strength for the

structure. As a strategy for the design of structural components it should be given priority.

5. High Safety Factors.

Given the current uncertainties in the determination of material properties, in material reliability and in the modelling of ceramic failure processes, the introduction of a high safety factor is a most sensible feature in any design for ceramic components.

No mention has yet been made of current attempts to improve the strength, toughness and damage tolerance of structural ceramics. This has been achieved by three routes:

1. Zirconia toughening, involving a stress-induced phase transformation.
2. Whisker strengthening or particle hardening, in which a second phase is incorporated in the matrix.
3. Fibre toughening, in which ceramic fibres are used to improve damage tolerance by preventing catastrophic failure.

Two questions have to be asked in the development of these new materials.
Firstly, is the improvement in tensile strength achieved at the expense of a reduced fracture toughness? This is most commonly the price which is paid for the ultra high strength grades of transformation toughened zirconia.
Secondly, is the improvement in damage tolerance accompanied by a loss of compressive strength? This is certainly the case for cont. ous fibre-toughened ceramic matrix comp ·ites. These may fail prematurely in compression, either by the buckling of the fibres or by shear at the fibre-matrix interface.

Finally, the message of this paper could be put into a single sentence and expressed as a unique guiding principle:

**"High performance structural ceramics should be treated like bricks and concrete and not like iron and steel."**

ACKNOWLEDGMENTS

I should like to express my appreciation to my colleagues Yehudah Tzabari and Rachman Chaim for reading and criticising this manuscript.

REFERENCES

1. G.L.Glegg, "The Design of Design", C.U.P. (1971)

2. G.L.Glegg, "The Selection of Design", C.U.P. (1972)

3. G.L.Glegg, "The Science of Design", C.U.P. (1973)

4. R.N.Katz, "Applications of High Performance Ceramics in Heat Engine Design", Matls.Sci.Eng., 71, 227 (1985)

5. R.Kochendorfer, "Design Aspects for Reliable Ceramic Structures", Ceramic Materials and Components for Engines, Ed. W.Bunk and H.Hausner, D.K.G. (1986) p.1081

6. H.Kawamoto, T.Shimizu, M.Suzuki and H.Miyazaki, "Strength Analysis of Silicon Nitride Swirl Chamber for High-Power Turbocharged Diesel Engines", Ceramic Materials and Components for Engines, Ed. W.Bunk and H.Hausner, D.K.G. (1986) p.1035

7. S.M.Wiederhorn and E.R.Fuller Jr., "Structural Reliability of Ceramic Materials", Matls.Sci.Eng., 71, 169 (1985)

8. A.F.McLean, "Materials Approach to Engine/Component Design", Ceramic Materials and Components for Engines, Ed. W.Bunk and H.Hausner, D.K.G. (1986) p.1023

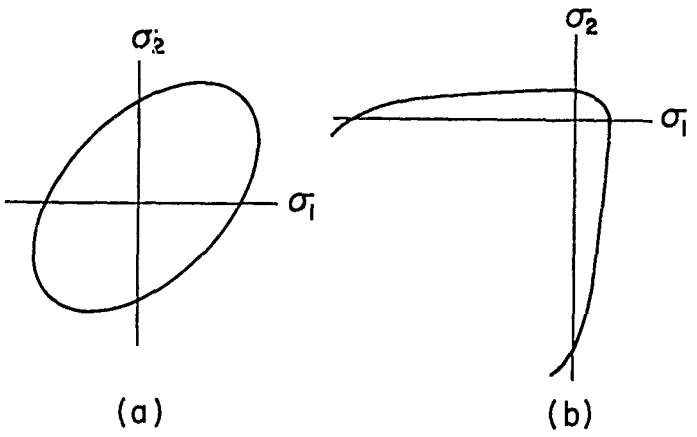


Fig.1 Biaxial stress failure criteria for (a) metals - von Mises criterion for plastic yielding, and (b) ceramics - Weibull criterion for fast fracture.

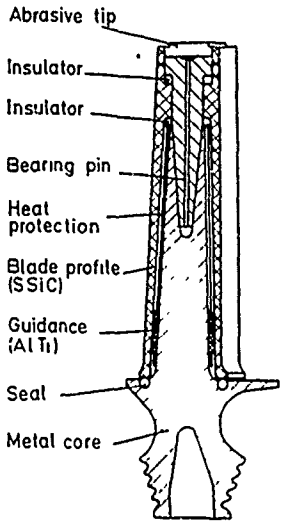


Fig.2 Tie-rod turbine blade design with a hollow ceramic airfoil [5].

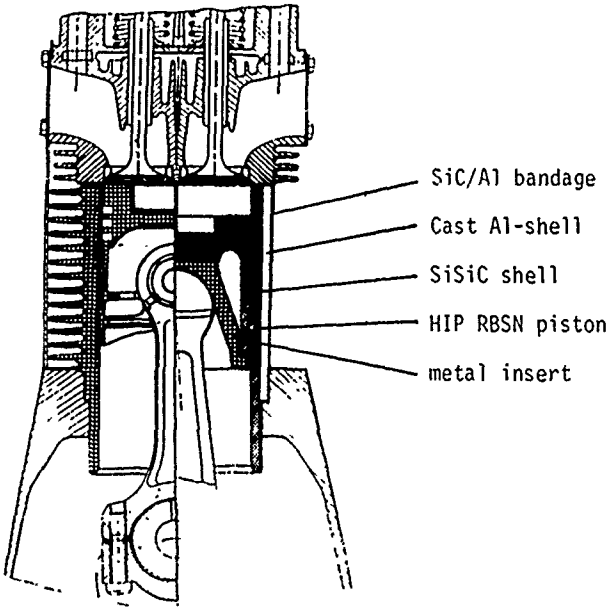


Fig.3 Ceramic and conventional designs for a diesel piston/cylinder combination [5].

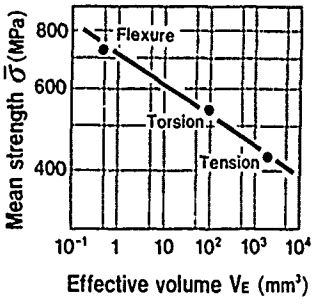


Fig.4 Calculated and observed mean fast fracture stress as a function of effective volume for a pressureless-sintered silicon nitride [6].

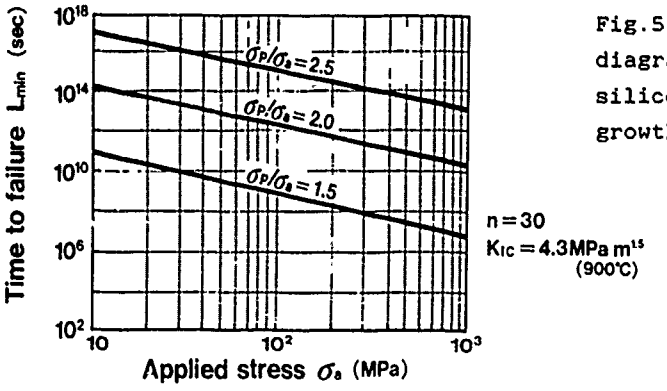


Fig.5 Calculated proof-test failure diagram for a pressureless- sintered silicon nitride failing by slow crack growth [6].

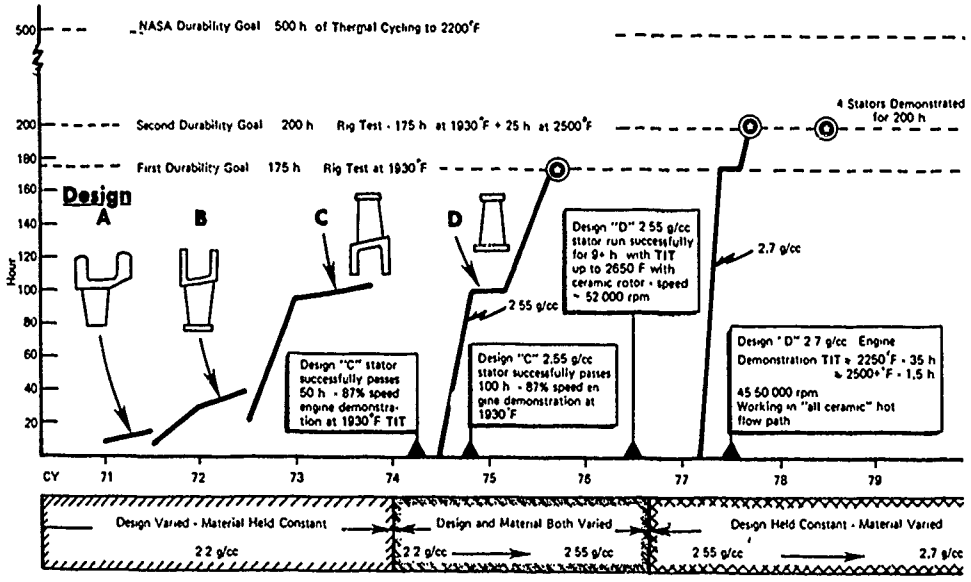


Fig.6 A brittle materials design case history: the DARPA-Ford 820 stator blade development project (TIT - turbine inlet temperature) [4].

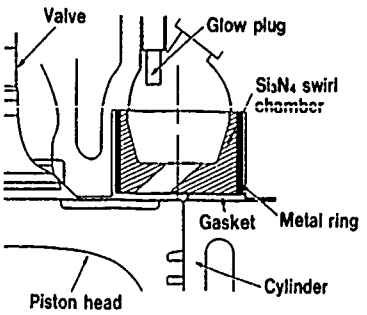


Fig.7 Mounting and assembly of a silicon nitride precombustion (swirl) chamber [6].

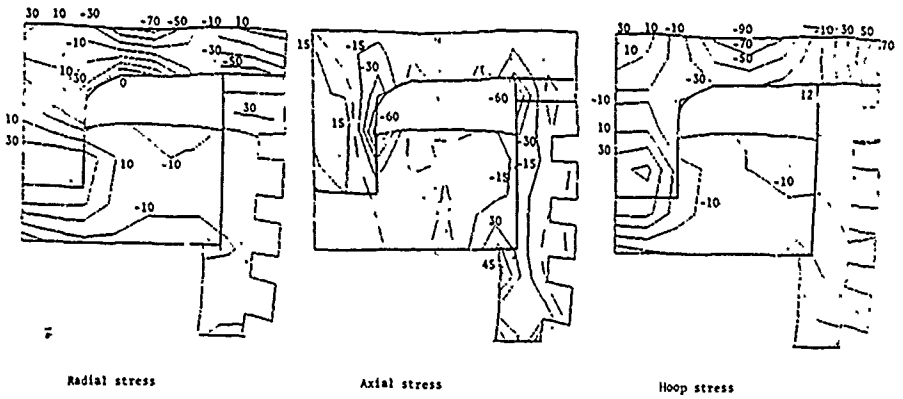


Fig.8 CAD/FEM calculation of the temperature and stress distributions in a silicon nitride piston cap.

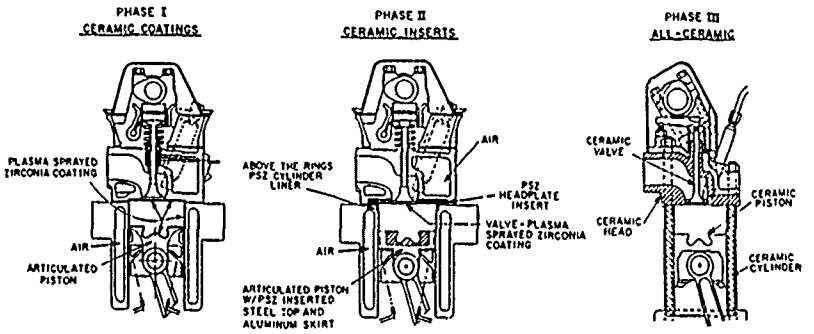


Fig.9 Successive stages in the development of an uncooled, low heat rejection, high speed, direct injection diesel [8].

# COMPOSITE MANUFACTURE AND DESIGN INTENT - A QUESTION OF COMPROMISE

J W Johnson

Dr Johnson is Manager of Composites Manufacturing R & D in the Manufacturing Technology Group at Rolls-Royce plc, and also Visiting Professor in The Dept of Materials Science and Engineering, University of Surrey.

## SYNOPSIS

For the designer, new to continuous fibre reinforced composites, the novelty and great variety of the raw materials, the unusual character of the manufacturing processes, in which the material and shape are created at the same time, frequently combine to cause a real dilemma. In practice compromises are required at each stage of the design-make cycle, but without the means to effectively quantify the end-effects of such concessions. The relationships between raw-material, manufacturing process and engineering needs are reviewed in this paper, and the way forward to a more quantifiable system, through the development of process modelling, is suggested.

## COMPETING FACTORS

For composites, probably more than for any other comparable group of materials at present, the relationship between raw materials, manufacturing processes, design and functional performance is complicated, hedged about by trade-offs and other imponderable compromises. Consequently component manufacture can only be treated as an independent activity at the risk of ultimate failure. The most usual practical approach adopted is a compromise between the conflicting requirements of design, engineering needs, manufacturing difficulties and cost. Typical factors driving the rationalisation process are:-

(a) Component loading needs Fig 1
(b) Material performance Issues Fig 2
(c) Component Manufacturing Factors Fig 3

In the case of hardware for military purposes, additional complications arise out of the requirement for the structures to have survivability in the face of various damage threats ranging from missiles to radiation, and the need to demonstrate repairability when damaged. Civil applications likewise place great emphasis on damage tolerance, damage resistance and repair - but in this case arising out of accidental handling or foreign object damage rather than, hopefully, from any premeditated intent.

Finally and more generally it is essential that the customer be assured that the quality of the product as intended for use, can be maintained throughout a production run and the life of the component in the application. This need brings in its train the absolute imperative to maintain rigid controls over materials supplied and manufacturing processes - usually addressed by the adoption of some system of material and process specifications subject to vigorous regular audit. Thus for a given material selected for any application it is necessary to have or develop

(d) Comprehensive Materials Database Fig 4

(e) Component Quality Standards Fig 5

Some of the factors so far discussed are forward driving, that is tending to impose (engineering) constraints on manufacture, and some clearly are reverse acting, limiting the objective of the engineering need by what can be guaranteed to be reliably achieved in practice.

Besides the clear and essential differences there is a good deal of commonality between manufacturing processes; the need to manipulate fibre at some stage and the properties of the resin matrix, for example. The interactive relationship can be usefully demonstrated by the construction of a fabrication chart.

This can take many forms but is helpful in identifying those elements of a process which are generic and those which are process specific. Thus the elements requiring compromise are usually adjusted within the framework of the total process and may well dictate the ultimate fabrication method used.

The basis for the formation of a typical sequence Fig 6 is:

(i) The reinforcement and its textile form

(ii) The matrix material and associated secondary processes.

(iii) Preliminary/intermediate forming operation

(iv) Final consolidation procedure

Acquisition of packages of technology covering the various operational stages shown in this chart, and their representations by mathematical or computer models, is the ultimate aim of process modelling, a subject of great current interest in the materials field and arising again later.

Despite their obvious inter-relationships however the consolidation processes in common-use all possess individual characteristics and consequently parts made by any particular process are likely to exhibit a range of faults and properties specific to that technique.

One process characteristic of importance is the accuracy with which any method produces parts conforming in shape and dimensions to the intended design. A simple classification allows of division into a system of three categories:-

(1) One surface defined, thickness not controlled directly
(eg autoclaving)

(2) Two surfaces defined, thickness approx. controlled.
(eg matched-die moulding)

(3) All surfaces defined, thickness accurately controlled.
(eg. resin injection)

A brief discussion of the development of a small compressor blade for the RB162 engine in glass fibre reinforced, polyimide resins by matched die moulding, illustrates the need for a concessionary approach, taking account of manufacturing limitations.

PROBLEM FOCUS - RB162 COMPRESSOR BLADE

An exploded view of the laminate lofting diagram of this blade, which is scarcely 6 cm long overall, is shown in Fig 7. Some of the large number of laminates shown are preplied multiple stacks, and the total needed is over 80 laminate shapes, cut from unidirectional prepreg with a thickness of about 0.15mm. An early problem for manufacturing with this product concerns the need for accurate placement of the laminates, one on top of the other, in space and the cumulative effects of "bulk factor" problems in the laminate preform.

BULK FACTOR AND LOFTING

The issues are demonstrated by the idealised representation of the construction of an ovoid shape from flat thin laminates as shown in Fig 8. The points to be made are first, that some arbitrary decision has to be made to terminate the laminate boundaries within the envelope of the die (usual solution) or to extend slightly outside of it. Either choice leads to an unsatisfactory situation, with an excess of fibre in one case or resin rich areas in the other. Alternatively (and again usually) the laminates may be laid to follow the external or die profile, in which case the faults referred to develop internally, and additionally, the material will not conform to the external shape if it has more than slight double curvature. Second, where the component is suffering rapid changes in thickness, the accuracy needed on laminate placement and positioning may be very high and infact difficult to meet.
Third, excess laminate thickness, or "bulk factor", created by the presence of excess resin to be removed in the moulding process, leads to the requirement for gross laminate movement during consolidation and the real risk of lateral displacement.

MATCHED DIE MOULDING

As shown by the above classification matched die moulding is often selected for its good surface finish, accurate reproduction of opposing surface profiles, and in principle, its provision for active control of component thickness by the use of moulding stops. Unfortunately there is an underlying dilemma which is difficult to resolve. This is that voidage can only be eliminated by maintenance of hydraulic pressure in the matrix. However pressure falls dramatically when the fixed stops are reached if the matrix is still fluid at this point. In practice therefore a void free component is only achieved if resin gellation and the attainment of the stop dimensions occur simultaneously. In the case of the RB162 blade the need to attain the higher void-free quality of moulded product forced an important change in philosophy. The approach adopted was to plan to mould without the use of fixed stops, a plan however which relinquished active thickness control

and placed reliance on indirect methods by careful control of process parameters, particularly resin viscosity and residual solvent in the prepreg and precured materials.

## PROCESS AND MATERIALS TRADE-OFF

The need to maintain critical parameter values in processing has a direct significance for the details of the specification and supply of raw material and an effect on the ultimate properties of the system.

For the polyimide resin system in use for the RB162 blade - Kerimid 601 (Rhone Poulenc), a solid at room temperature - the critical element was solvent type and its residual level. In practice, the only viable solvent found, N - methyl 2-pyrrolidone (NMP) was found to intereact in a complex manner with the resin, affecting storage life, handling characteristics, flow during moulding and thermal ageing of the cure composite. Some of these effects were mutually incompatible. Although tack and drape could be induced into the prepreg at room temp by the use of high solvent levels, equally importantly, storage life was reduced, and residual solvent reduced glass transition temperature affecting high temperature properties. By contrast completely solvent free prepregs gave good high temperature properties initially, but poor ultimate thermo-oxidative stability and were dry and very fragile to handle at RT.

## MATERIAL SPECIFICATION

The material selected on the basis of a balance of all these conflicting factors called up a tightly controlled NMP content and closely defined limits on dry resin and glass cloth distribution in order to meet the engineering tolerances. See Fig 9. Even so. the specification needed to contain sufficient lattitude to allow the manufacturer controlled leeway on the acceptable limits of batch to batch variability. It will be obvious from a consideration of Fig 9 that to reach the target thickness/ply moulding line from the two extremes of the specification box requires very different precuring treatments to control resin loss. These precure treatments, as with the moulding process itself, were controlled by mandatory laboratory sampling and monitoring.

## FUTURE DIRECTIONS

The penalties accepted for adopting the approach described are, complex and tight laboratory supervision of shop-floor production as routine practice.

The lessons learned could be multiplied by many other examples of component histories. The manufacturing cycle for composites is very sensitive to changes in resin formulation and this has led the industry increasingly to the development of formulated resin systems having a limited minimum-viscosity behaviour through a moulding cycle. In most commercial systems the viscosity is modified by the use of thermoplastic or other additives to limit its fluidity and create a more passive, handleable system.

In recent years however, there has been an increasing effort to bring the design and manufacturing issues into a common forum and quantify the issues, so that the problems and compromises necessary in the development phase can be addressed outside of the need for an iterative experimental approach involving hardware manufacture, since this is so expensive.

If the initiative succeeds it will be through the medium of computer modelling of the manufacturing process. Starting from the creation of a comprehensive data base for particular resin systems, a great deal of work is currently being expended on the development of mathematical models to describe process elements which can be synthesised to predict the course and result of selected manufacturing operations.

In practice the data bases are used to compile a number of sub-models (for example resin cure, or flow) and the sub-models are integrated to simulate the process cycle of interest, most often autoclaving at present. The simulated model can then be used to review manufacturing options and ultimately actively control the actual moulding cycle. Fig 10 illustrates the schematic relationships envisaged.

Progress in this area has been surprisingly rapid bearing in mind the practical complications. Apart from the value of a coherent data base, sub-model development can provide a rapid, easy means of screening for materials equivalence and substitution, optimisation of limited elements of the cycle and so-on. Thus even an incomplete model can provide valuable opportunities for reducing the essential experimental content of any development.

Fig 11 shows the computer output of a dynamic simulation of resin cure for BSL 914 (Ciba-Geigy) using a model developed at Rolls-Royce by W R Jones. It shows how, having established a database and model, the methodology permits a very thorough exploration of the manufacturing envelope, allowing the influence of temperature profiles (ramp rates and isothermal treatments), gellation times, estimates of degree of cure etc, to be investigated at great length.

Modelling of thermoset composite manufacture is a very ambitious and

complex task for the industry to undertake, involving, as it does, chemical reactions, evolution of volatiles from some systems, and other difficulties. The basis for all useful models will be an extensive and accurate data base embracing raw materials, tooling, consumables etc, which is time consuming and expensive to obtain initially. These facts will inevitably hinder the speed and scope of modelling development. However great strides appear to have been made recently and there seems to be every hope that the compromises which are an essential feature of the debate between engineering needs and manufacturing expediency can be placed on a firmer quantitative footing and explored before commitment to manufacture. Only in this way will the industry reduce its development costs, produce reliable and reproducible components which are fit for the intended application.

---

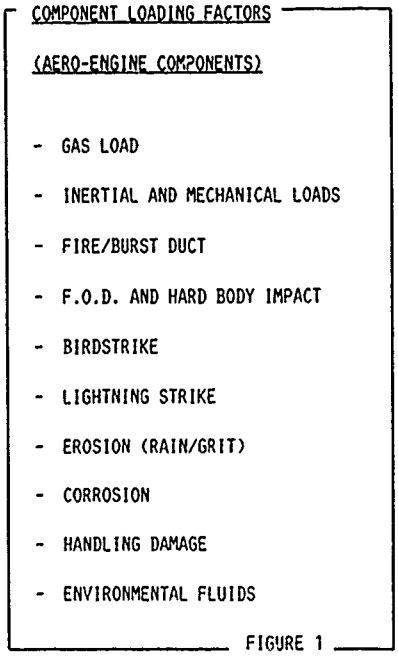

FIGURE 1

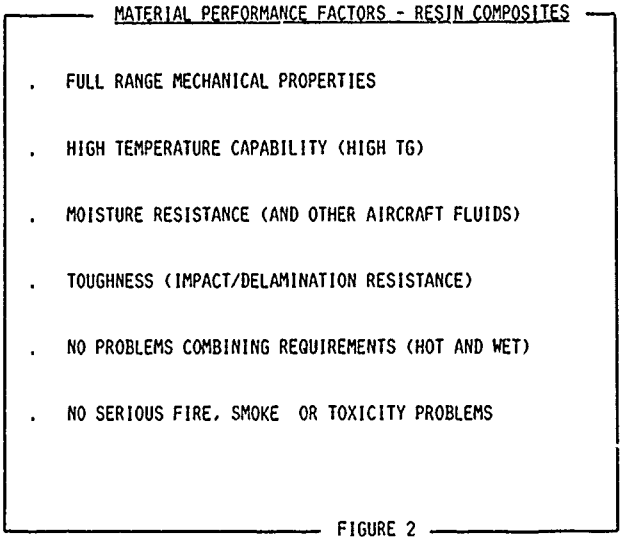

FIGURE 2

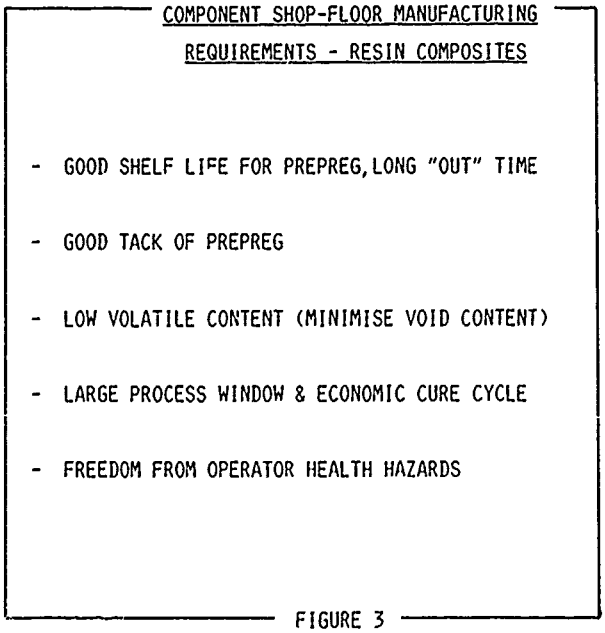

FIGURE 3

COMPREHENSIVE DATA BASE

- MATERIALS CONTROLLED BY SPECIFICATIONS

FIBRE : TYPE, MECHANICAL PROPS, FIL COUNT, TWIST, SIZE, WEAVE ETC

RESIN : TYPE, COMPOSITION, TEMP RANGE VISCOSITY, IMPREGNATION METHOD

PREPREG : FIBRE, RESIN, VOLATILE CONTENTS, TACK, GEL-TIME, STORAGE LIFE

CURED LAMINATE : VOID CONTENT, FIBRE FRACTION, TENSILE STRENGTH (0°,±45°, 90°) TENSILE MODULUS (0°, 90°), ILSS, STRENGTH RETENTION ON AGEING AT 95% RH AND 50°C ENGINE FLUIDS

. AUDITS OF SUPPLIER PLANT/FACILITY, BATCH TO BATCH REPRODUCIBILITY

FIGURE 4

PROCESS CONTROL - COMPONENT QUALITY STANDARDS

. DEFINED QUALITY STANDARDS FOR
  - VISUAL INSPECTION
  - DIMENSIONAL CHECKS
  - OTHER DESTRUCTIVE AND NDE TESTS

. IDENTIFICATION OF POTENTIAL DEFECTS
  - FIBRE MISALIGNMENT, KINKING, ETC
  - FOREIGN BODY INCLUSIONS
  - VOIDAGE
  - RESIN RICH/FIBRE RICH AREAS
  - SURFACE DEFECTS, BLISTERING, CRACKS
  - GENERAL DIMENSIONAL FAULTS

. QUALITY ACCEPTANCE STANDARDS TO DEFINE TYPE, NUMBER AND LOCATION OF ALLOWABLE DEFECTS

FIGURE 5

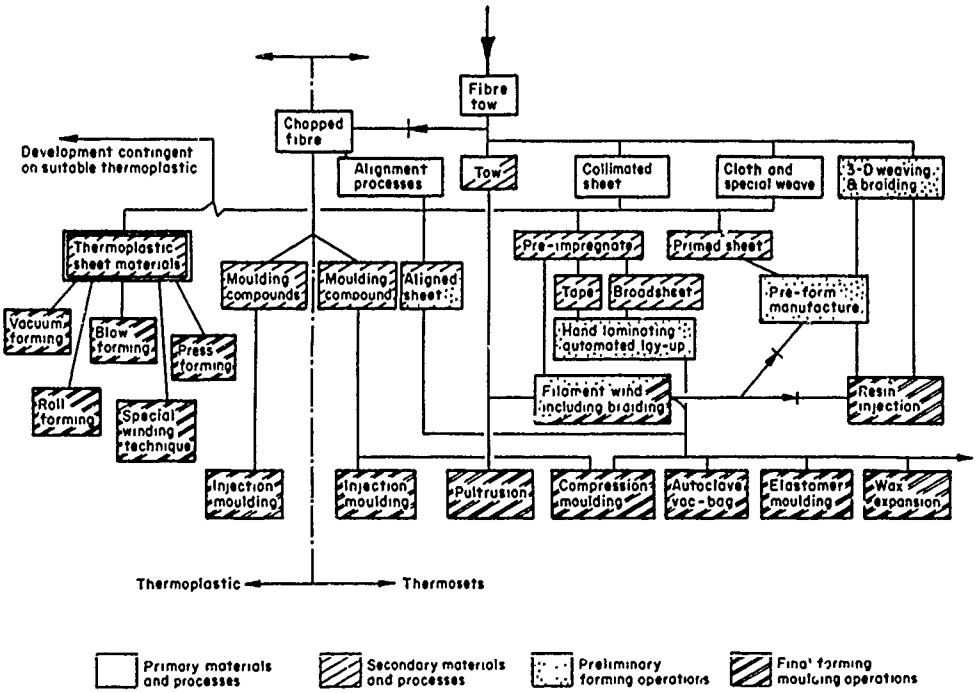


Fig 6 Fabrications chart for fibre reinforced resin composites.

**RB 162-86 exploded rotor blade -diagrammatic form**

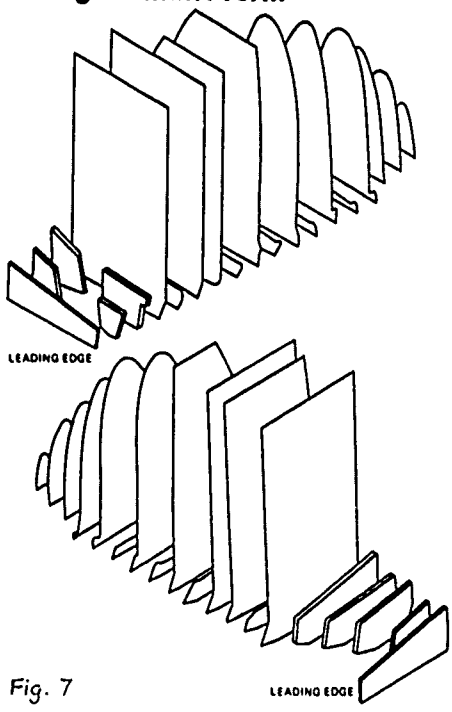


Fig. 7

LOFTING AND BULK-FACTOR PROBLEMS

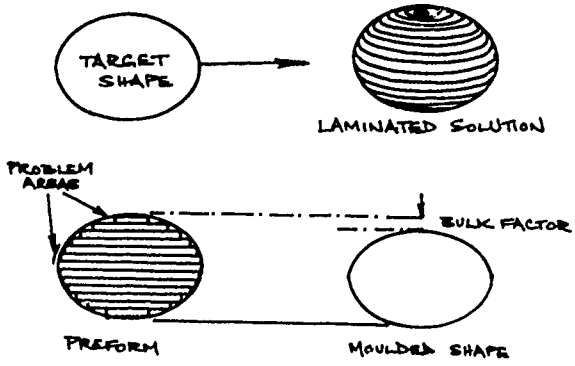


Fig. 8

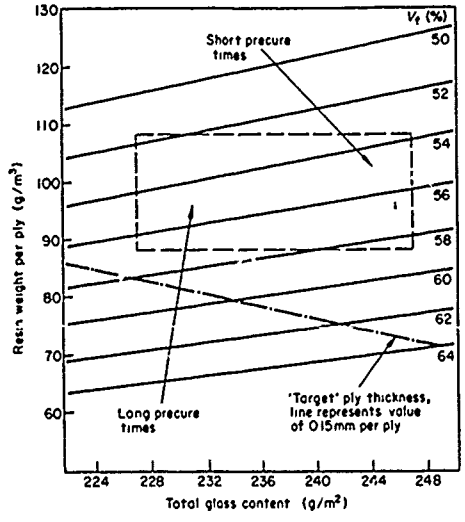


Fig 9 Basic specification for Kerimid 601 glass fibre prepreg.

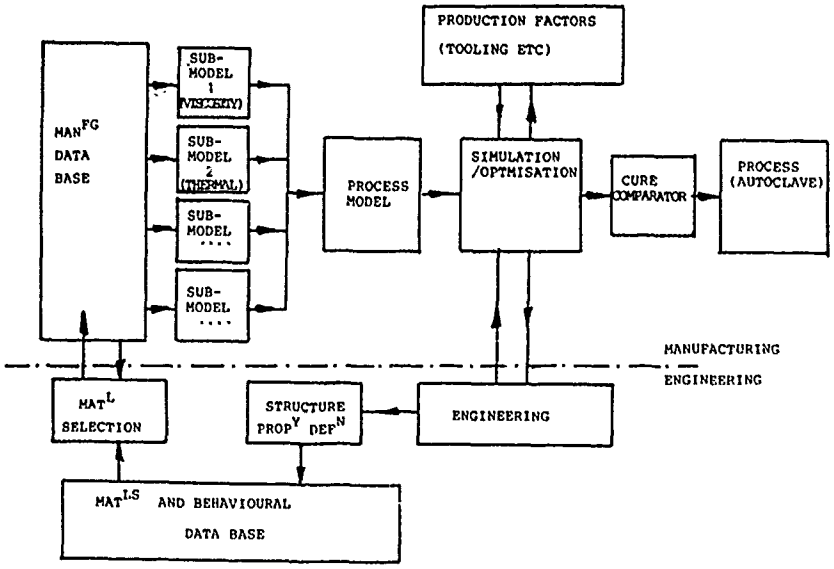


Fig 10 Schematic diagram of the factors involved in process modelling and their inter-relationships.

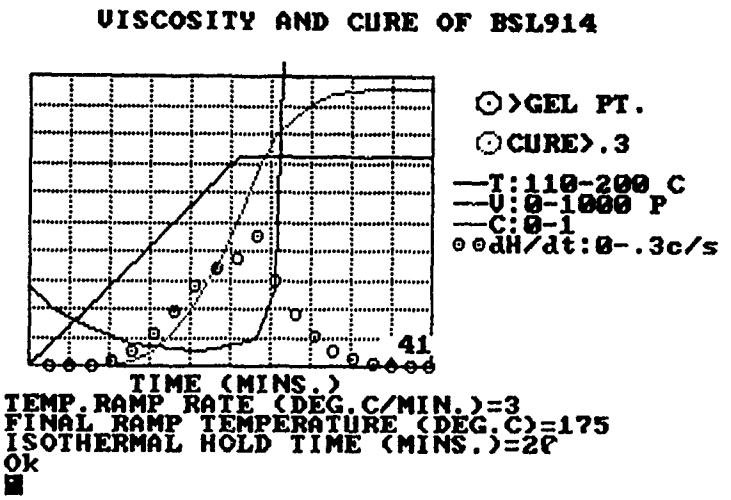


Fig 11 Computer simulation of cure cycle for BSL 914 systems.

# STRUCTURAL ASSESSMENT OF METAL COMPONENTS

I. W. Goodall and R. A. Ainsworth

Central Electricity Generating Board, Berkeley Nuclear Laboratories, Berkeley, Gloucestershire, GL13 9PB

SYNOPSIS

This paper describes high temperature design and assessment procedures for metal components. The procedures have similarities with approaches at low temperature and reference stress techniques enable the latter approaches to be extended to the creep range. Simplified methods of analysis are described both for defect-free and defective components.

## 1 INTRODUCTION

This paper is concerned with design and assessment procedures for metal components which operate at high temperatures. For such applications it is necessary to ensure that component lifetime is not limited by:-

(i) excessive inelastic deformation,
(ii) ratchetting or incremental growth,
(iii) excessive crack propagation,
(iv) creep rupture damage,
(v) combined creep and fatigue damage.

The first three of these mechanisms are also addressed at low temperature. There, elastic analysis, limit analysis and shakedown analysis can be used to ensure that applied stress levels do not exceed some material strength level. Defect assessments, by the CEGB's R6 procedure [1] for example, can also be carried out provided a material toughness level is specified in addition to the strength level.

Extension of assessment methods to high temperature applications is complicated by time-dependent creep deformation, and by the need to consider the possibility of failure by the time-dependent damage mechanisms listed above. In principle, inelastic analysis by finite-element methods offers a means of performing high temperature assessments. However, in recent years significant progress has been made in the development of simplified analysis methods both for defect-free [2] and defective components [3]. Within the CEGB, these methods are being incorporated into a comprehensive procedure, termed R5, for assessing the structural integrity of high temperature plant. The procedure addresses:

- simplified methods of analysis,
- creep-fatigue crack initiation,
- creep crack growth,
- creep-fatigue crack growth,
- similar metal and transition joint welds.

In the following sections, the R5 procedures are illustrated by discussion of simplified stress analysis methods, and by discussion of creep crack growth assessment.

## 2 SIMPLIFIED METHODS OF ANALYSIS

The simplified methods of analysis being incorporated in R5 are based upon proposals made some time ago utilizing the shakedown concept [2, 4]. The proposals ensure that the lifetime is not limited by the mechanisms listed in Section 1, apart from assessment of crack growth which requires separate calculation by the methods of Section 3 below. Thermal striping, dynamic loading and buckling also require separate assessments.

The simplified methods are applicable provided it is possible to demonstrate that global shakedown criteria are satisfied. However, limited areas of cyclic plasticity due to local or F-stresses may be taken into account, as may the action of creep during periods of steady operation. At highly stressed points within a component, this leads to creep relaxation and a typical stress-strain response for a cyclic loading history is shown in Figure 1. In general, the hysteresis loop is not closed and the creep deformation is enhanced by the cyclic loading. The procedure outlined below provides a simplified method of describing this response and estimating the associated deformation and creep rupture damage.

### 2.1 Procedure

The methodology described in [2, 4] has now been developed into a step-by-step procedure [5]. The steps are listed below and further details are given in the following sub-sections, as indicated. The presentation is necessarily brief and further details are contained in the R5 document [6].

(i) Determine the loading and temperature history during the lifetime of the component, and perform an elastic calculation of stresses and strains. This step may be performed using standard analysis methods and is not discussed further here.

(ii) Demonstrate that excessive plastic deformation will not occur before the steady cyclic state and shakedown is reached. This step may be achieved by limiting the elastically calculated stresses and stress ranges to multiples of the yield stress, as in low temperature applications. Alternatively, the shakedown analysis of step (iv) may be used directly. A factor of 0.9 is applied to the yield stress for creep applications to ensure that plastic strains are negligible [6].

(iii) Calculate a reference stress and hence the creep rupture endurance (see Section 2.2).

(iv) Generate candidate residual stress fields in order to produce a steady cyclic stress history and assess shakedown (Section 2.3). Where the elastic stresses are split into categories at step (i), local or F-stresses may be excluded from the shakedown assessment. Where this split is not performed, only an approximate satisfaction of shakedown is required: this should demonstrate that at least 80% of any structural section forms a continuous ligament over which strict shakedown is satisfied.

(v) Assess creep-fatigue damage, with inclusion of local or F-stresses in the steady cycle where these have been excluded at step (iv). (Section 2.4).

(vi) Ensure that the amount of creep strain is not excessive, and that any component distortion limits are not exceeded. (Section 2.5).

## 2.2 Calculation of Reference Stress

Creep rupture due to primary stresses is based on a reference stress calculation. The reference stress is defined as

$$\sigma_{ref} = P\sigma_y/P_L\ (\sigma_y) \qquad (1)$$

where P is the applied load and $P_L$ is the value of P corresponding to plastic collapse assuming a perfectly plastic material of yield stress $\sigma_y$. In its simplest form, the limit load is based on the elastically calculated membrane and bending stress resultants at each section. Alternatively, the methods of limit analysis may be used. The reference stress of eqn (1) is also used in the assessment of defective components in Section 3: in such cases limit load solutions are available for a wide range of structures with cracks [7].

Creep rupture is avoided provided

$$K_2\ \sigma_{ref} \leq S_R \qquad (2)$$

where $S_R$ is the material operating stress for the operating life. The factor $K_2$ is different for creep ductile and creep brittle materials and also depends on the stress concentration in the feature as described in [2, 4, 6].

## 2.3 Shakedown Analysis

Before shakedown calculations can be used to estimate stress histories in the creep range, it is necessary to ensure that global shakedown would be achieved in the absence of creep (step ii of Section 2.1). This requires that during the early cycles, a constant residual stress field develops as a result of plastic yielding such that in subsequent cycles, the component response to load changes is linear. In essence this constant residual stress field when added to the elastic stress history produces a 'safe' stress history, that is a stress history in which the stresses are less than or equal to the yield stress at every point in the component for all load combinations during the cycle. In practice it is not necessary to perform cyclic elastic-plastic calculations to determine this residual stress field as there are well-established shakedown theorems. One of these states that shakedown will occur if any time-independent residual stress field can be found such that the sum of the residual stresses and the elastically calculated stresses produces a 'safe' stress history. This may be expressed mathematically as

$$f\left[\tilde{\sigma}(t) + \rho\right] \leq K_1\ \sigma_y;\ \text{all time t, all positions} \qquad (3)$$

Here f is the yield function, $\tilde{\sigma}(t)$ is the elastically calculated stress history, $\rho$ is any time-independent residual stress field and $\sigma_y$ is the yield stress at the appropriate temperature. The factor $K_1$ is determined experimentally and relates $\sigma_y$ to the ability of the material to resist ratchetting.

When load cycles occur in the creep range, a residual stress field develops as a result of both plastic and creep strains. However, provided the shakedown criteria (3) are satisfied, a simplified estimate of the stress history in the steady cyclic state can be taken as $\tilde{\sigma}(t) + \rho$ where $\rho$ is, again, a constant residual stress field. The concept is very similar to that at low temperature: a constant residual stress field $\rho$ must be found such that $\tilde{\sigma}(t) + \rho$ is a 'safe' stress history. But now 'safe' requires not only that the yield stress is not exceeded but also that any creep damage will be satisfactorily limited. A further theorem shows that it is permissible to choose $\rho$ in order to minimise the creep damage during dwell at high temperature [2]. In practice, $\rho$ is chosen to minimise the stress at the start of the creep dwell. Inequalities (3) must be satisfied for conditions below the creep range, and stresses applying at temperatures within the creep range are required to satisfy

$$f\left[\tilde{\sigma}(t) + \rho\right] \leq \sigma_T;\ \text{all dwell periods, all positions} \qquad (4)$$

where the user must determine $\sigma_T$ subject to $\sigma_T \leq K_1\sigma_y$. The stress history $\tilde{\sigma}(t) + \rho$ is used in the calculations of creep damage in Section 2.4. Guidance on determining $\sigma_T$ is given in [6]. As a guide, $\sigma_T$ may be derived from the

rupture stress for the operational lifetime, by analogy with inequality (2), although for load cycles of varying severity, it may be helpful to consider larger values of $\sigma_T$ for some cycles. Note that if $\sigma_T$ is set too low, then it may not be possible to satisfy inequality (4), whereas if $\sigma_T$ is set equal to $K_1\sigma_y$ the estimates of creep damage may be too pessimistic.

### 2.4 Assessment of Creep-Fatigue Damage

In order to assess creep-fatigue damage, it is necessary to derive a total (elastic plus plastic) strain range. This may exceed the elastically calculated strain range and three sources of enhancement need to be considered:

(i) the change in Poisson's ratio from elasticity to plasticity,
(ii) the effects of creep relaxation during a hold period on subsequent plastic straining,
(iii) increased strain due to stress reduction according to Neuber's rule.

The adjustment for Poisson's ratio follows accepted practice [8]. Adjustments for the other two effects are illustrated in Figure 2, which shows equivalent stress range against equivalent strain range. The reduction in stress level $\Delta\bar{\sigma}_r$ during the dwell period is added to the elastically calculated stress range, and this point is joined to the material curve for cyclic stress range against cyclic strain range by the Neuber construction. This gives the enhancement $\Delta\bar{\varepsilon}_{pl}$ due to effects (ii) and (iii) above.

Two options are available for estimating creep-fatigue damage. The simpler is to assume that the stress does not relax during the dwell periods, so that the stress level calculated in Section 2.3 can be used to derive a creep damage fraction by comparison with minimum stress rupture data at the same temperature. Creep-fatigue damage is then assessed by combining the creep damage fraction with a fatigue damage fraction derived from the total strain range calculated above, and identifying the worst combination relative to an interaction diagram such as that in ASME Code-Case N-47 [8].

The second option uses the ductility exhaustion method [9] to assess creep damage, with allowance made for stress relaxation during the dwell. The stress relaxation will be associated with some degree of elastic follow-up or forward creep, which is estimated in Section 2.5 below. The damage summation is then expressed as an exhaustion of available ductility over a history of varying strain rates rather than as a stress-based life-fraction rule. Details are contained in [6].

### 2.5 Calculation of Creep Strain and Distortion

The shakedown analysis of Section 2.3 leads to a steady stress cycle. This can be used to estimate average strain levels within a component using average isochronous curves for the corresponding temperature. The accumulated strain should be less than 2% at the end of the operational lifetime, and this should be sufficient to avoid excessive distortion.

When using the ductility exhaustion method, it is additionally necessary to estimate the forward creep strain during dwell periods. This will depend on geometry, constraint of the structure, temperature distribution and the level of primary load. The amount of creep strain is related to the stress relaxation, in terms of uniaxial equivalents, by

$$\dot{\bar{\varepsilon}}_c = Z\dot{\bar{\sigma}}/E \qquad (5)$$

where E is the elastic modulus, and the factor Z=1 for relaxation at constant strain, and $Z \to \infty$ for constant load. The procedure [6] provides guidance on estimating Z and, for example, a value Z=3 is recommended for isothermal structures free of geometric features likely to result in excessive elastic follow-up.

## 3 CRACK GROWTH ASSESSMENT

Although the basic design of metal components assumes the absence of defects, it is important to have the facility to evaluate defect tolerance. This may be used in design to optimise material selection, inspectability and geometric details, or during service to re-assess plant found to contain defects, for example.

This section contains a description of the R5 procedures for assessing creep crack growth under steady loading [10, 11]. The approach is similar to that in R6 [1] for low temperature applications, being based on simplified methods. The crack tip characterising parameter J [12] is replaced by the parameter $C^*$ at high temperature. Section 3.1 contains an introduction to $C^*$ and the approximate techniques used for its evaluation. Section 3.2 outlines the assessment procedure within R5 [11] and this is illustrated in Section 3.3 by means of a worked example.

### 3.1 The $C^*$ Parameter

For a material with a creep law described by the constants $\alpha$, $\sigma_o$, $\dot{\varepsilon}_o$, n as

$$\dot{\varepsilon} = \alpha\,\dot{\varepsilon}_o\,(\sigma/\sigma_o)^n, \qquad (6)$$

the steady state stress field in terms of polar co-ordinates $(r,\theta)$ centred at the crack tip, is

$$\sigma_{ij}/\sigma_o = (C^*/\alpha I_n \sigma_o \dot{\varepsilon}_o r)^{1/(n+1)}\,\tilde{\sigma}_{ij}(\theta,n) \qquad (7)$$

for $r \to 0$. $I_n$ is a known function of n and $\tilde{\sigma}_{ij}$ is a known dimensionless function of $\theta$ and n; these functions are independent of geometry. Thus, the near-tip stress field is characterised completely by the parameter $C^*$ which is analogous to J [12] and can be similarly written as a path-independent line integral. As $C^*$ characterises the near-tip stress field, and indeed the strain rate and displacement rate fields, it is a suitable

parameter for characterising creep crack growth.

To use the $C^*$ parameter it is necessary to be able to estimate it, in order to collect materials data and to assess cracks in components. For the material law of eqn (6), dimensional arguments require $C^*$ to have the form

$$C^* = \alpha \sigma_o \dot{\varepsilon}_o b h_1(n) (P/P_o)^{n+1} \qquad (8)$$

where P is the applied load, $P_o$ is a normalising load proportional to $\sigma_o$ and some section area, b is a characteristic length and $h_1$ is a non-dimensional function of geometry and n. Values of $h_1$ have been tabulated for a range of crack sizes, geometries and creep indices in [13].

Equation (8) may be written in a more convenient form for interpreting materials data, by noting that for a material law of eqn (6), the load-point displacement rate $\dot{\Delta}$ obeys

$$\dot{\Delta} = \alpha \dot{\varepsilon}_o b h_3(n) (P/P_o)^n \qquad (9)$$

where $h_3$ is a dimensional function of geometry and n. Combining eqns (8) and (9)

$$C^* = [P \dot{\Delta}/B(w-a)] F(n, a/w) \qquad (10)$$

where B is specimen thickness, w-a is remaining ligament ahead of a crack of length a, and F is a function which includes $h_1/h_3$ and the area term in $P_o/\sigma_o$ relative to B(w-a). It transpires that F is insensitive to n for many test specimen geometries and therefore formulae for $C^*$ can be written in terms of load-point displacement rate without detailed knowledge of the material creep law [14]. Thus, measurements of displacement and crack length during a test enable data to be collected as $\dot{a}$ ($C^*$).

Unfortunately, displacement rates can rarely be measured in service and estimates of $C^*$ cannot be readily derived from eqn (10). Equation (8) is also inconvenient as detailed finite-element solutions are required to generate $h_1$. However, eqn (8) may be written in terms of the reference stress of eqn (1) and the corresponding creep strain rate $\dot{\varepsilon}_{ref}$ derived from eqn (7), as [15]

$$C^* = \sigma_{ref} \dot{\varepsilon}_{ref} R \qquad (11)$$

since $P_L$ ($\sigma_o$) is proportional to $P_o$. Although R depends on n in general, it transpires that the approximation of R in terms of the stress intensity factor K:

$$R = K^2/\sigma_{ref}^2 \qquad (12)$$

which ensures that eqn (11) is accurate for n=1, is accurate for a wide range of geometries and stress indices [16]. An example of a comparison of eqn (11) (with R given by eqn 12) with eqn (8) is shown in Figure 3 taken from [16]. The load factor is the ratio of the loads at which eqn (11) and eqn (8) give the same value of $C^*$. It can be seen that the load factor is close to unity for a wide range of stress indices and crack sizes. Similar results are obtained for a wide range of geometries [16] so that the approximation of eqn (11) is reasonable for practical applications.

As stress intensity factor solutions and limit loads for flawed structures are widely available, eqn (11) enables $C^*$ to be evaluated for complex structures. In addition, the independence of eqn (11) of detailed material laws, enables creep laws other than Norton's law to be used and enables realistic strain hardening rules to be employed in estimating $C^*$ as the reference stress increases as a crack grows in a structure. An example is given in Section 3.3,

### 3.2 Assessment Procedure

As with the basic stress analysis procedure of Section 2.1, a step-by-step procedure has been developed for crack growth assessment. These steps are set out below in terms of an assessment of whether a defect of current size $a_o$ will lead to failure during the desired additional service life $t_s$.

(i) Define the steady service load and temperature at the time of the assessment, $t_o$.

(ii) Calculate the time for failure by continuum damage/creep rupture mechanisms, $t_{CD}$. In this time widespread and significant creep damage occurs throughout the ligament ahead of the crack irrespective of whether any crack growth occurs. Thus, $t_{CD}$ sets an upper bound on the overall service life and the desired lifetime is not obtainable if $t_{CD}$ is shorter. $t_{CD}$ is calculated from the rupture time from uniaxial data at a stress equal to the reference stress of eqn (1) with the limit load defined for the crack size, $a_o$. The normal design margins in eqn (2) should ensure that creep rupture does not occur in the service life except for deep cracks.

(iii) Calculate the incubation time, $t_I$, during which a defect blunts as a consequence of creep straining, but does not show any significant extension. Clearly, if the calculated incubation time is shorter than the life seen to date, it must be assumed that the crack is already growing. In other cases crack incubation may occupy part or all of the desired additional service life. The procedure [10, 11] uses reference stress methods to estimate $t_I$ according to

$$\varepsilon_c \{\sigma_{ref}(a_o), t_I\} = 0.5 [\delta_I/R(a_o)]^{n/n+1} \qquad (13)$$

where $\delta_I$ is the COD for incubation from specimen tests, $\varepsilon_c$ is the accumulated creep strain at the reference stress during the period $t_I$, and R is defined by eqn (12). Eqn (13) is based on widespread creep conditions and is not applicable if such conditions are not established. The requirement may be conveniently expressed by

$$\varepsilon_c \{\sigma_{ref}(a_o), t_I\} > \sigma_{ref}(a_o) / E \qquad (14)$$

When inequality (14) is violated, the

incubation stage should be neglected in the assessment.

(iv) Calculate the crack size at the end of life from

$$a_g = a_o + \int \dot{a} \{C^*(a)\}\, dt \qquad (15)$$

where it has been assumed that crack growth rates are a function of $C^*$, as defined by data from test specimens, using eqn (10). The value of $C^*$ for the component is obtained from eqn (11) in conjunction with material creep strain data. The procedure [10, 11] defines conditions under which $C^*$ correlations can validly be applied. The integration of eqn (15) is only performed for times exceeding $t_i$, and indeed is not required if incubation occupies all of the desired service life.

(v) As the crack grows, the remaining ligament ahead of the crack reduces leading to higher rates of creep damage accumulation. As a consequence, there is a reduction in the time for continuum damage/creep rupture failure, $t_{CD}(a)$, to the extent that this may become shorter than the remaining desired life $t_s + t_o - t$, at some time t when the crack size is a(t). In this case the desired service life is not attainable. Step (v) requires this check to be made by recalculation of $t_{CD}$ as the crack grows. The calculation is similar to that in step (i) but using the limit load for the current crack size to define the reference stress.

(vi) Calculate the margin of safety for the end-of-life defect size, $a_g$, for all possible load conditions, including overloads as well as the steady operating loads which lead to creep crack growth. The end-of-life safety margin may be obtained by using defect assessment procedures such as R6 [1]. The mechanical properties used in these assessments may be adversely affected by the creep damage accumulated in a component and, therefore, larger factors of safety may be necessary than in the absence of creep.

(vii) As the procedure and calculations in steps (i) and (vi) do not specifically contain margins or factors, apart from the end-of-life safety margin in step (vi), confidence in an assessment should be obtained by assessing the sensitivity of the results to variations in the input parameters according to the principles of Section 12 of R6 [1]. Conservatism is assured by the use of lower and upper bound materials data as appropriate but, in addition, confidence is gained when it is possible to demonstrate that small changes in the input parameters do not lead to dramatic reductions in the end-of-life load margins.

### 3.3 Worked Example

To illustrate the procedure of Section 3.2, a cylindrical pressure vessel containing circumferential defects is considered. The geometry and dimensions are shown in Figure 4. The pipe was made of $^1/_2Cr^1/_2Mo^1/_4V$ steel in the normalised and tempered condition. The example is taken from an experimental pressure vessel programme [17] and detailed calculations have been reported elsewhere [18]. For the vessel examined, only data from material similar but not identical to the pressure vessel steel are available. Therefore, a conservative application of the procedure of Section 3.2 using lower bound creep rupture and crack initiation data and upper bound creep strain and creep crack growth data is not attempted. Instead, the steps of Section 3.2 are followed below in conjunction with mean data from specimen tests.

(i) The vessel was tested at 565°C and a constant internal pressure of 62.5 MPa.

(ii) A limit load solution for the defective pipe is contained in [7] and for the initial crack size of 30 mm, the reference stress is obtained from eqn (1) as

$$\sigma_{ref}(a_o) = 150 \text{ MPa}$$

Mean creep rupture data are available and are shown in Figure 5. Entering this curve at the reference stress leads to the rupture time of 2957h as indicated. As noted in Section 3.2, this time sets an upper bound on the overall life attainable.

(iii) In order to calculate the incubation time from eqn (13) it is necessary to have uniaxial creep strain data and an incubation COD. Strain data are given in [18] and shown in Figure 6 for a stress of 150 MPa; the stress index is n=10.6. The incubation COD, $\delta_i$=0.11mm [19]. Stress intensity factor solutions for this geometry are readily calculated [18] enabling R to be obtained from eqn (12) as $R(a_o)$=19mm. Then the right-hand-side of eqn (13) defines $\varepsilon_c$=0.0045 which is in excess of the elastic strain in inequality (14) so that eqn (13) can validly be used to define $t_i$. This is $t_i$=612h as indicated in Figure 6. It is apparent that incubation is predicted to occur in the vessel before failure by continuum damage (2957h from step ii) so that crack growth may occupy a significant fraction of life.

(iv) The crack size at any time is obtained by integration of eqn (15) for times greater than 612h. $C^*$ is readily calculated from eqn (11) with both $\sigma_{ref}$ and R updated as the crack grows. The creep strain rate is also updated using a strain hardening rule. Creep crack growth data are given in [19] and fit

$$\dot{a} = 0.3\ (C^*)^{0.85}/(100\varepsilon_f)$$

where $\varepsilon_f$ is the uniaxial ductility which is stress dependent. The resulting prediction of crack size against time is shown in Figure 7.

The crack growth calculations were terminated at a crack size of 48 mm when it can be seen that the crack growth rate is very high. This crack size is reached after 1930h

(v) For a crack size of 48 mm, the reference stress of eqn (1) is 330 MPa which corresponds to a rupture time $t_{CD}(a)$ of 10h from Figure 5. The total failure time of the vessel cannot be more than 1930+10=1940h. Thus, there is little benefit in extending the calculations of step (iv) to greater crack sizes.

(vi) This step is not considered here as R6 analyses have been reported extensively and reference may be made to the R6 documentation [1].

(vii) Sensitivity analyses for the vessel are reported in [20] and are not considered here as they are simply a repetition of the calculations in the above steps covering realistic variations in the material properties.

The above example has demonstrated that a crack growth assessment according to the procedure of Section 3.2 is straightforward to perform. The actual test vessel data, with crack size monitored by potential drop techniques, are compared to the assessment in Figure 7. As the assessment is based on mean data from material similar, but not identical, to the pipe steel, the overall agreement is good. In particular, the assessment identifies the observed behaviour of failure occurring as a result of creep crack incubation and growth.

Acknowledgement: This work was carried out at the Berkeley Nuclear Laboratories of the Technology, Planning and Research Division and the paper is published by permission of the Central Electricity Generating Board. The authors acknowledge the contributions of their colleagues within the CEGB who have assisted in the preparation of R5.

REFERENCES

[1] I Milne, R A Ainsworth, A R Dowling and A T Stewart, Assessment of the integrity of structures containing defects, CEGB Report R/H/R6 - Revision 3 (1986).

[2] I W Goodall, F A Leckie, A R S Ponter and C H A Townley, The development of high temperature design methods based on reference stresses and bounding theorems, ASME J. Engineering Materials and Technology 101, 349-355 (1979).

[3] R A Ainsworth and I W Goodall, Defect assessments at elevated temperature, ASME J Pressure Vessel Technology 105, 263-268 (1983)

[4] R A Ainsworth and I W Goodall, Proposals for primary design above the creep threshold temperature - defect free structures, CEGB Report RD/B/N4394 (1978).

[5] A M Goodman, D E Buckthorpe, R T Rose, C H A Townley and P S White, Shakedown design rules for fast reactor application, issue 1, Structural Integrity Working Group (1987).

[6] A M Goodman, M D Heaton, D C Martin, D C Morse, J Phillips and J Fielding, R5: An assessment procedure for the high temperature response of structures, volume 2 : proposed analysis and assessment methods for defect-free structures, CEGB Report (1988).

[7] A G Miller, Review of limit loads of structures containing defects - 3rd edition, CEGB Report TPRD/B/0093/N82 - Revision 2 (1987).

[8] ASME, Boiler and pressure vessel code, Code-Case N47-17 (1979).

[9] R Hales, Fatigue Fract Engng. Mater Struct 6, 121-135 (1983).

[10] R A Ainsworth, G G Chell, M C Coleman, I W Goodall, D J Gooch, J R Haigh, S T Kimmins and G J Neate, CEGB Assessment procedure for defects in plant operating in the creep range, Fatigue Fract Engng Mater Struct. 10, 115-127 (1987).

[11] R A Ainsworth, M C Coleman, I W Goodall, J R High, S T Kimmins, G J Neate and R J Slominski, R5 : An assessment procedure for the high temperature response of structures, Volume 4 : Proposed assessment procedure for defects under steady loading, CEGB Report TPRD/B/1006/R87 (1987).

[12] J R Rice, A path independent integral and the approximate analysis of strain concentrations by notches and cracks, J Appl Mech 35, 379-386 (1968).

[13] V Kumar, M D German and C F Shih, An engineering approach for elastic-plastic fracture, EPRI Report NP1931 (1981)

[14] M P Harper and E G Ellison, The use of the $C^*$ parameter in predicting creep crack propagation rates, J Strain Analysis 12, 167-179 (1977).

[15] R A Ainsworth, Some observations on creep crack growth, Int J Fracture 20, 147-159 (1982).

[16] A G Miller and R A Ainsworth, Consistency of numerical results for power-law hardening materials, and the accuracy of the reference stress approximation for J, CEGB Report TPRD/B/1005/R87 (1987).

[17] M C Coleman, A T Price and J A Williams, Crack growth in pressure vessels under creep conditions, Fracture 1977, Volume 2, 649-662, Waterloo, Canada (1977).

[18] R A Ainsworth and M C Coleman, Example of an application of an assessment procedure for defects in plant operating in the creep range, Fatigue Fract. Engng Mater Struct 10, 129-140 (1987).

[19] G J Neate, Creep crack growth in $1/2$CrMoV steel at 838K, I : behaviour at a constant load, Mater Sci Engng 82, 59-76 (1986).

[20] R A Ainsworth, Structural assessment of creep crack growth, Post-SMiRT Seminar on Inelastic Analysis and Life Prediction in High Temperature Environment, Paris (1987).

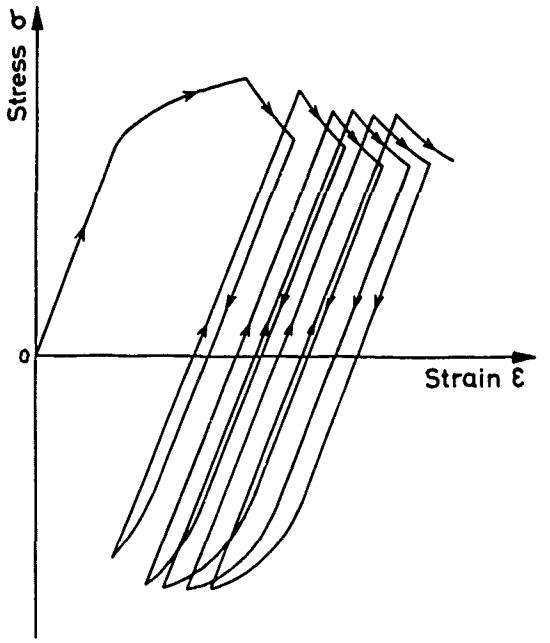


Figure 1 Schematic stress-strain history showing creep deformation enhanced by the high stress levels regenerated by cyclic loading.

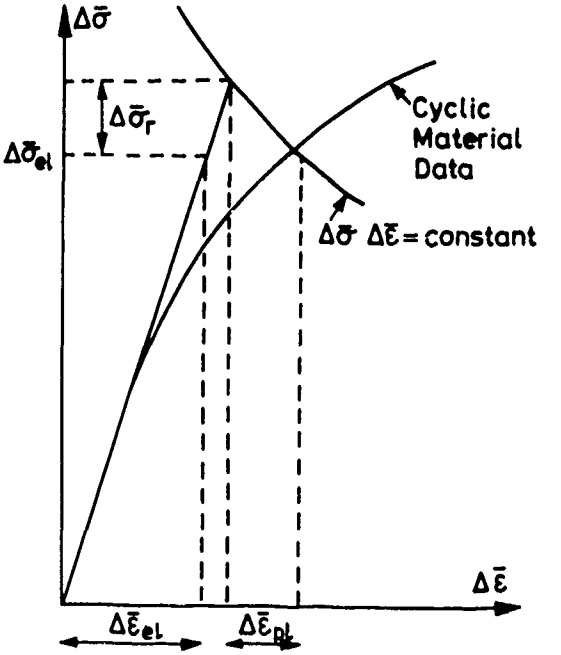


Figure 2 Illustration of plastic strain range enhancement when creep relaxation is significant.

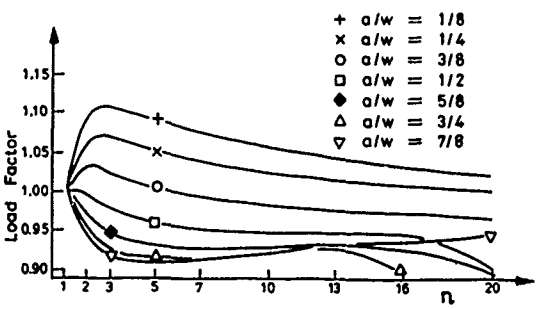


Figure 3 Comparison of eqns (8) and (11) for a plane stress double-edge notched plate in tension.

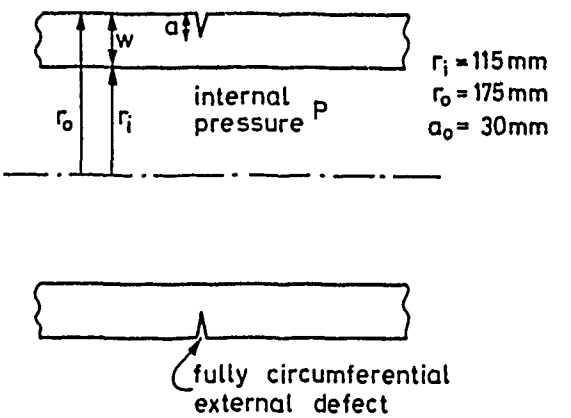


Figure 4 Geometry of externally circumferentially cracked pipe.

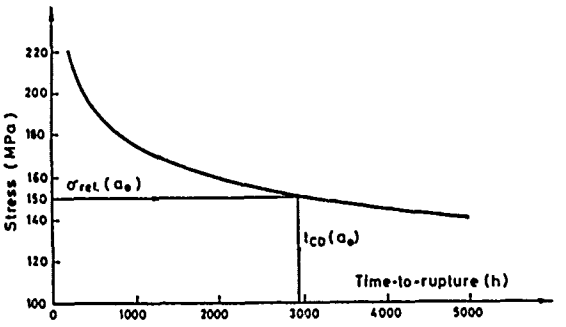


Figure 5 Uniaxial stress/time-to-rupture data illustrating calculation of $t_{CD}$.

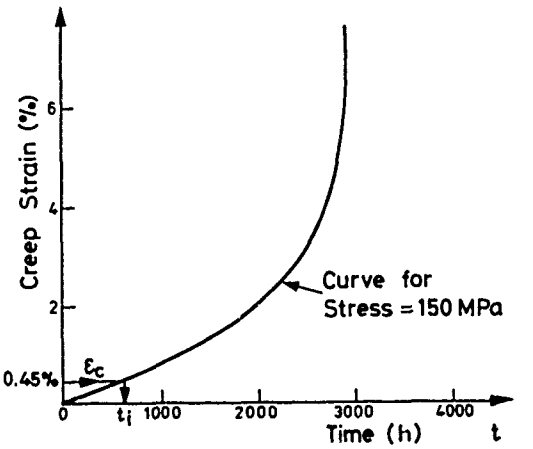


Figure 6 Creep strain data illustrating calculation of $t_i$.

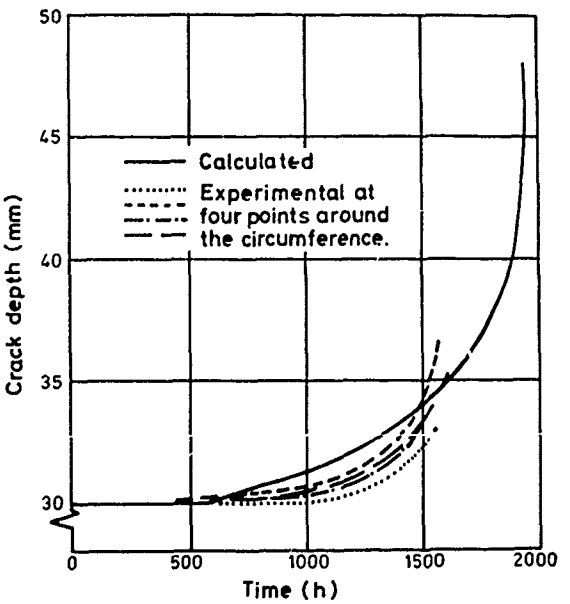


Figure 7 Calculated and measured crack size as a function of time.

# SOLID - SURFACE MODELLING AND MANUFACTURE

E B Lambourne, Deltacam Systems Ltd,
Birmingham

Ed Lambourne, director of Deltacam Systems Ltd, has fourteen years experience in CADCAM including two years of CAD software research at Cambridge University as part of the development work on DUCT which is now the key Deltacam software. His experience centres on general engineering, draughting, surface modelling, computer aided part programming, machine tool control systems, computer systems and software development.

SYNOPSIS

The development of CADCAM from its originally separate design and manufacturing components to the current complex modelling techniques is outlined. The specific characteristics of surface modelling and its applications are considered in more detail with emphasis on data exchange between systems and the use of flow analysis.

## Introduction

CADCAM - computer aided design and computer aided manufacture has its origins in the numerically controlled machine and computer graphics work applied by the then comparatively affluent aircraft and automotive industries as long ago as the mid-fifties. But because of its high cost it was well beyond the means of the rest of the engineering industry and accordingly was a virtually unknown field of activity. Later, with the advent of more compact, more powerful computers at more affordable prices, CADCAM became an attractive proposition for the smaller companies and the subject of a Government awareness scheme during the three years 1982 to 1984. The scheme involved the setting up of six practical experience centres across the UK, a series of countrywide seminars, and a mobile demonstration unit, all organised and funded by the DTI working closely with the Institution of Mechanical Engineers.

The object of the exercise was to bring to the attention of management, primarily in the mechanical engineering and allied industries, what CADCAM could do for them, how it could be applied to their particular operations and how they could benefit from its use. The underlying message was that CADCAM could improve the effectiveness of designing and manufacturing engineering components by the application of computer aids.

First reaction from some engineers was one of suspicion because of the computer connection and a feeling that there might be a hidden threat to the well-entrenched and, seemingly, perfectly satisfactory existing procedures.

Since then, a considerable proportion of those same engineers have come to appreciate that the new technology is not merely a substitute for certain manual techniques but a powerful means of helping them to improve the quality and effectiveness of their own engineering operations.

They realised that the computer provided a means of helping them to carry out tasks of designing products and of making them, leaving more time for them to apply their basic engineering skills to those problems that computers are not yet able to resolve.

## Development of CADCAM

CAD and CAM began their lives independently of each other. CAM came first, in the form of numerical control (NC) which required machining to be manually programmed as a sequence of machine tool axis motions to carry out a series of, initially, simple repetitive cutting operations without need for constant supervision. Subsequently, programming became more sophisticated with the machine tool being controlled by toolpath programs with the aid of computer based NC processors, cutting more complicated shapes with minimal operator supervision. Typically, tool path programs were entered into the machine tool system on paper tape but now, direct numerical control (DNC)

enables the most complex machining program to be downloaded directly to the machine tool controller from the computer system used to generate the tool path.

Meanwhile CAD developed in the drawing office as a quicker and more accurate method of draughting than the traditional drawing board. A keyboard, data tablet and mouse replaced the conventional instruments and the completed screen image was subsequently plotted as a high quality engineering drawing.

Initially CADCAM was a misnomer in that the CAD and CAM systems were independent of one another. A drawing from a CAD system was the starting point for preparing an NC program. Moreover the term CADCAM was set to embrace the use of computer aids for a number of other hitherto quite separate functions broadly categorised under the cover of CAPM, computer aided production management. Included were shop floor activities such as data collection, planning, estimating and production control.

A basic CAD system comprises a processor (or computer) with a terminal screen; called an engineering workstation if the screen and computer are combined, and the necessary software for creating and manipulating the drawings. Printers and plotters are customary ancillaries, the first for running off a copy of the screen image at any specified time, the latter for plotting a full scale engineering drawing from the computer model geometry. Small CAD packages confined to draughting operations can be run on PCs or microcomputers but the more comprehensive modelling software requires the greater power of 32-bit minicomputers.

CAD systems can be 2D, 2 1/2D or 3D with 3D being the obvious choice for anything beyond a fairly simple shape. The design can be developed on screen as a computer model, its geometry being automatically held in computer memory. The benefits of manipulating the computer model rather than drawing and re-drawing a manual design are apparent in the way the model can be handled. For example, among others, the model can be enlarged, reduced, rotated, repositioned, and viewed from different angles.

The more advanced modellers fall into three main categories, wire frame, solid and surface modellers and there is often some confusion as to the difference between them.

A wire frame modeller defines the shape by linking together points with lines. These lines can define the edges of a shape but do not define the areas bounded by them. Accordingly, if there are two intersecting surfaces, the wire frame modeller cannot define the position of any point on either of the two surfaces, but only the edges as represented by the interconnecting lines making up the lines in the wire frame.

A surface modeller can define the surface area between the points for which considerably more processing power as well as additional programming is necessary. Hidden surface removal is relatively simple since the system assumes that all surfaces conceal what lies behind them unless they are specifically designated transparent. An advanced surface modeller can convert the design geometry into cutter data for postprocessing to machining data enabling the designed shape to be cut on a CNC machine tool.

While a surface modeller can define highly complex surfaces, it does not ensure that the surfaces in a model actually define a solid, that is, fully enclose a volume. This more rigorous property is the feature of a solid modeller which can, by definition, tell whether any point is inside or outside the solid. This feature is particularly useful for creating assemblies of solids and clash detection. The greater integrity of the model, however, is achieved at the expense of greater computer power. In addition, solid modellers are still not able to satisfactorily represent complex surfaces to manufacturing accuracies. A particularly useful application of the solid modeller is for generating 'cutaway' or 'exploded' drawings.

Defining A 3D Shape

Deltacam Systems Ltd originated as a technical unit set up in the seventies by the Delta Group of engineering companies to advise member organisations on the introduction of numerical control machine tools as a means of improving the effectiveness of their operations. The association between this advisory service and the broader vista of CADCAM led to a widening of the brief and participation with the University of Cambridge's engineering department in the development of computer software that would overcome the difficulties of interpreting complicated 3D shapes from conventional 2D drawings.

Originally, the 2D drawing was the only means of defining an engineering component and, in most cases, is perfectly able to define a 3D shape unambiguously. The problems arise when the shape includes multi-curved sculptured surfaces as, for instance, on turbine or impeller blades, in cosmetic bottles, even in domestic pan handles. In such cases the modelmaker, whose function was to cut a hardwood model for copymilling the shape or its reverse as a cavity, had to interpret the 'grey' areas as best he could using his skill and experience. Even so he could at best only achieve a close approximation to the required shape so that, often,

substantial effort and time was spent in modifying the model, perhaps a number of times, before the designer was satisfied that it represented his intended product shape.

The product that emerged from the development work at Cambridge was DUCT, a surface modeller which was, effectively, an integrated 3D design and manufacture software package, specifically intended for complex shapes as found in plastics, glass and rubber mouldings, and in metal castings, forgings and pressings.

In 1977 the original technical advisory group was formed into Delta Computer Aided Engineering Ltd which embraced the management of the joint development work with the University of Cambridge and the expansion of its own workshop in Birmingham. Subsequently in 1982 Deltacam Systems was formed with Delta CAE being retained as the company's machining division, now equipped with a number of CNC machine tools as well as a range of conventional equipment.

Deltacam Systems acquired from the University the sole rights to market DUCT and took the University's development team on to its payroll. Currently Deltacam is responsible for the continuing development of the software and has already established distributorships in over 20 countries worldwide.

Principles of DUCT

DUCT enables a design concept to be developed to a fully surfaced shape in three dimensions, the equivalent of the pattern. Initially, the geometry is defined, usually in terms of key cross sections through the object. These sections are positioned in space by a spline curve and DUCT will automatically clothe the sections or ribs with a smooth surface. More complex parts can be designed by joining surfaces with automatic blends and constant radius fillets. The design can be automatically rendered to provide a colour shaded screen image so that the designer can visualise what his intended product will look like.

From the design geometry, DUCT's integral machining module will automatically generate tool paths which can be postprocessed and downloaded into a CNC machine tool controller. The designed shape will be precisely reproduced in every detail on the machine. Simultaneous control of up to five axes is possible to give a model, pattern, prototype, electrode, finished product or a cavity mould or die. Shrinkage, parting lines, draft angles, wall thicknesses, EDM spark gaps, can all be readily accommodated by DUCT prior to toolpath generation.

The product geometry (or 3D computer model) of the component can be created with DUCT from one of several sources. Probably the most obvious one is an input based on the designer's first sketches. From these a few lines on the screen can be progressed into the finished product although this might well not be the best way to start. The source can be a conventional 2D detail drawing from which key dimensions can be input, or a model or existing product from which a number of key contours can be input as x y z co-ordinates from which a computer model can be constructed. The designer would then develop his intended product shape on the screen as before.

DUCT is also able to receive data in digitised form from other CAD systems via both standard and certain proprietary data exchange formats - an essential in a world of proliferating CAD systems and to be considered in more detail later.

Incorporated within DUCT is a finite element mesh generator for stress or flow analysis. By interfacing with the Moldflow analysis software the effectiveness of the design for manufacture can be examined and, if necessary, modified and re-examined. Cross-sectional and surface areas and component volumes can be calculated providing accurate information about the material content of a casting or moulding. DUCT can also be used to conform to a volume constraint as, for instance, in dimensioning a bottle to provide for a specified liquid content; or to have a uniform decrease in cross sectional area along the length of a passageway as, for instance, in a turbine scroll.

One of the key features of DUCT is its visualisation facilities, which include first and third angle, isometric conic projections and stereo views. Colour shading provides the ultimate pre-production visualisation with highlights and surface emulation giving a startlingly realistic screen image.

Data Exchange

Design for manufacture requires an accurate surface modeller if the design is to be converted into cutter data for making a mould or die on a CNC machine tool. However, if the design has been carried out on a CAD system, the model geometry needs to be transferred to a surface modeller so that the manufacturing parameters can be built in. Subsequent modifications dictated by manufacturing constraints may need to be transmitted back to the designer before final approval for manufacture is given. Accordingly, there is a need for a method of exchanging data between systems.

If the two systems are identical, data exchange poses no problems. If they are different a 'software translator' can be written to convert data from the one system to the other. Such a customised translator can work well and reliably to

pre-defined rules but, where one or both of the communicating parties lacks the necessary resources to write a translator, one of the system suppliers, or a third party, can be nominated but with the risk that he may find it difficult to acquire the necessary information about the two systems. The problems multiply where data exchange is required with several CAD systems since each one will require a separate translator.

The alternative is a standard data exchange format which reduces the effort to writing an input and output translator to the standard format. This does not call for access to the confidential data structures of rival systems.

There are several data exchange interfaces of which the best known are IGES (Initial Graphics Exchange Specification) with VDA-FS, widely used in the German motor industry and SET in the French motor industry.

IGES, the best known data exchange standard in the UK, is based on the creation of a file of data common to both the systems between which data is to be exchanged and requires each system to have software interfaces to read (pre-processor PUT) and to write (post processor GET).

All the leading CADCAM software vendors, including ourselves, provide IGES pre- and post processors, our DUCT surface modeller supporting the format. IGES processors for some CAD systems can be purchased from third party software houses.

The IGES program converts between IGES format and the native data format of the particular CADCAM system, supporting a substantial range of data including point, line, arc and spline entities together with certain types of surfaces.

Additionally, notes and dimensions, non-graphical data such as specifications and geometric associativities for forming assemblies, symbols and the like, are also supported.

Although the mechanics of transferring IGES format data are relatively straightforward, the details are a little more complicated. Each CADCAM system has its own data storage method and many systems do not handle the full range of data entities covered by the IGES standard; indeed, some CADCAM systems - particularly 3D modellers are concerned with entities that IGES cannot represent. It is important, therefore, to understand why the transfer is being made, whether it is to transfer a 2D drawing with full text and dimensions or to transmit essential geometry in 3D. While, ideally, it should be perfectly feasible to transfer a complete datafile back and forth without sacrificing any information the ideal is seldom achieved in practice, the differences in the two systems permitting only common entities to survive the transfers.

IGES users should accordingly use only the highest set of common factors between the sending and receiving systems which may mean some compromising. For instance, if a 3D system is to communicate with a 2D system, the data must be compressed into 2D. Or, if the recipient does not recognise cubic splines, the sender may have to fit these with some other acceptable curve.

As IGES is more fully developed there should be fewer difficulties but even in its present state of advancement, the difficulties are by no means insurmountable. Our experience suggests that conventional 2D draughting data can be transferred with no more than minor imperfections while there are few problems with 3D line geometry.

We have accumulated a considerable amount of experience in data exchange having interchanged data between our Deltacam software and most well-known CAD systems including CV, Catia, GE Calma, Geomod, PDGS and several proprietary ones. In most cases we received data for progressing into manufacturing data.

Perhaps a classic example of our involvement in data interchange was our participation in the Ford Motor Company's pilot projects involving data from Ford's PDGS and Computervision systems being transmitted to and from DUCT using the IGES format.

A particular project was the production of a complicated exhaust manifold casting in which we collaborated with patternmakers G Perry & Sons of Leicester and J J Harvey (Manchester) and with Qualcast (Derby) Foundry. The work involved extensive IGES transfers of original design data on the manifold tracts and adjacent engine parts, such as a mounting bracket, being transferred from CV to DUCT.

The design data was used by both the foundry and the patternshops to create the computer model for the final detailed casting in DUCT, making extensive use of DUCT's 3D modelling and visualisation capabilities to accommodate engine amendments. A number of design modifications required extensive use of IGES to inter-transfer data. The foundry tooling, including pattern and core boxes were fully defined in DUCT and NC machined by Perry.

At no time during the project were paper drawings exchanged, the only communication being via IGES data files containing three dimensional geometry consisting of line and curve data.

We have also gained considerable experience with the German VDA-FS standard interface, successfully

receiving data from such companies as Volkswagen from which models have been machined.

Flow Analysis

In the case of plastics mouldings, a software program called 'Moldflow' can be interfaced with DUCT to enable optimal moulding conditions to be established. 'Moldflow' contains a comprehensive materials data base embracing the characteristics and properties of virtually all commercial plastics materials. The program will accurately predict how the designated material will behave as it fills the mould cavity. Complete mould and feed systems analysis can be carried out on the FE mesh, with comprehensive results being output from each analysis. The optimal moulding conditions can be rapidly identified from these analyses.

The DUCT/Moldflow interface allows the two systems to communicate effectively. Put simply, the interface links the DUCT modelling, Moldflow analysis and DUCT visualisation facilities in five basic steps. These are: creation of the computer model and FE mesh using DUCT; conversion of the DUCT mesh into Moldflow; performing the Moldflow analysis; conversion of the Moldflow results into DUCT images; and displaying and assessing the results in DUCT.

This procedure quickly evolves into a design cycle until both the design and its moulding quality are approved. Screen images in DUCT consist of annotated colour bands of iso-lines ie lines of equal pressure, temperature and short shot (time), drawn over the model. Current developments will lead to solid-fill colour shaded images similar to those produced by heat sensitive cameras.

Currently solidification simulation of metals in the foundry is less advanced than that of plastics but work is being carried out at several locations including, in the UK, the University of Wales in Swansea and Foseco's Tamworth plant.

In Conclusion

The main purpose of this paper was to generate greater awareness of what CADCAM, and in particular surface modelling, can contribute to the effectiveness of complex shaped product manufacture. But, beyond this, it is important to appreciate the increasing trend towards replacing conventional engineering drawings by digitised data as the prime means of communicating product geometry among customers, suppliers and sub-contractors. Without the means to deal with this form of data, manufacturers in the business of making complex shapes will find it increasingly difficult to compete in the market place.

It is certain that, over the next few years, there will be continuing change in the organisation and working practices of industry in line with advances in information technology. Awareness of new developments and of their relevance is fundamental to ensuring a profitable future for manufacturing industry.

# MODERN FINITE ELEMENT PRACTICE

T. K. Hellen

Berkeley Nuclear Labortories, Berkeley,
Glos, GL13 9PB

## SYNOPSIS

The finite element method is now a widely accepted technique for solving a wide variety of physical states in arbitrary structures. The method has been developed during the digital computer age and thus is available on a wide range of hardware, from small 16 bit word personal computers to extremely large and high powered vector processing machines. The visual display unit gives a fast direct access to the hardware and has been exploited with respect to input and output data for the benefit of the user.

Finite element data is necessarily complex. Computer models of element meshes, representing the often complicated shape of structure, can be very time consuming to generate accurately, so that much software effort has been expended in designing user-friendly data generation and results viewing packages. The VDU complements the older media of printers and digital plotters in this respect.

A description of finite element usage with particular reference to the BERSAFE system is given. This deals with the static and dynamic behaviour of loaded structures. The statics facility includes stress analysis with linear or non-linear materials response, as plasticity (time independent) and creep (time dependent), for a variety of loading forms including cyclic behaviour and thermal transients. Non-linear data is given in the form of standard laws, or, in the case of creep, a tabular form as acquired directly from experiment. Calculation facilities for cracked bodies are also available.

Examples of use are given to illustrate the various facilities.

# COMPUTER-AIDED PLASTIC PARTS DESIGN FOR INJECTION MOULDING

G. Menges, W. Michaeli, E. Baur, V. Lessenich, C. Schwenzer

Institut für Kunststoffverarbeitung (IKV) (Institute for Plastics Processing), Aachen, West Germany

## 1. INTRODUCTION

The use of technical plastics for applications in the automotive, consumer goods and electrical and household appliance industry is increasing at an annual rate of approx. 7-8%. For this reason, the plastics industry is demonstrating a considerable innovative potential in the development of special materials, plastics-oriented and multi-functional components and moulds necessary to produce these components.

In view of the increasingly more complex demands made on component characteristics, computer-aided processes for part and mould design have become generally established in the Design and Production Planning departments; CAD systems for design and modules for NC data generation are now just as widespread as programs for the simulation of flow and thermodynamic processes in injection and compression moulds.

The use of computer programs enables this innovative potential to be more extensively exploited even for complex technical mouldings by:

- Shortening development cycles,
- Minimizing the risks in component design,
- Reducing cost-intensive prototype trials by simulation,
- Greater exploitation of the power reserves in the moulding and mould,
- Allowing the viability and cost-effectiveness of a design to be assessed at the design stage

The injection moulding process permits efficient processing of various polymers with a high degree of design freedom right up to complex geometric figures with ribbed outer surfaces. Since the properties of the moulding depend to a considerable extent on the processing conditions, one of the main emphases in the use of computers to date was the application of finite element methods (FEM) to simulate flow or heat transfer processes. In general, however, these were merely "island" solutions.

## 2. CADFORM - AN OPEN SOFTWARE FOR AN INTEGRATED SOLUTION

In the long term, however, only an integrated solution which incorporates the complete part and mould design process into a common CAE concept can have any real prospects of success, due to the extensive interdependence between the individual design stages. With this aim, the IKV, in conjunction with industry, has now developed an integrated software package (CADFORM, Figure 1) which can be extended step-by-step into a comprehensive design aid system. At the same time, however, this package consists of specific injection moulding modules which can be easily coupled to existing commercial software structures via defined interfaces.

The CADFORM software package offers a concept for plastics-oriented moulding design. This package incorporates:

- Modules for initial material selection and analysis,
- Dialogue-controlled design programs for conventional dimensioning of wall thicknesses and functional elements,
- Methods and material laws for the structural analysis of mouldings using FEM,
- A "design controller" for automatic analysis of moulding geometries for plastics-oriented design and
- A program for simulation of the mould filling process.

We would now like to go on to describe the central components of the CADFORM software package for computer-aided plastics part design, whereby we will present only the programs developed at the IKV in conjunction with the plastics industry, and not the product-neutral commercial products such as the CAD software, FEM programs, preprocessor and postprocessor, NC software or the standards modules.

### 2.1 A PLANT-SPECIFIC MATERIAL DATA BANK FOR PLASTICS

Several software houses and a large number of raw material manufacturers are now offering fundamentally different data banks for polymer materials.

These data banks often contain only the materials of one manufacturer, however, and provide only material properties of general interest. These data banks also often fail to contain programs which can process and present the stored material data in a form convenient to the operator.

The starting point for the IKV material data bank was the consideration that the majority of the plastics processing companies are specialized in specific product classes. The plastics used are generally well-known from the many years of use, and the companies have gathered their own experience in the fields of design, processing and quality assurance. Since this wealth of in-house experience is always included in any decision on material selection and design, it should also be possible to store this knowledge and to call it up as required at a later date.

Figure 2 shows the concept of a material data bank as the central component of a CAE system as developed at the IKV, and which is now in widespread use:

- User-defined, plant-specific as well as standard characteristics can be defined,
- Material properties gained from in-house tests can be read in,
- If required, the material data from commercial suppliers and raw materials manufacturers can be read into the data bank,
- All programs for part and mould design require material data. For this reason, an interface for computer programs was developed which allows all the stored data to be transferred automatically to the application program without error by simply entering the appropriate trade name. This applies both to property values such as the modulus of elasticity, price or heat resistance, as well as to functional dependencies like creep curves, viscosity functions or p-v-T diagrams.

The user interface allows a wide range of interactive enquiries to be made, as shown in Figure 3:

- For the initial material selection (I), the list of requirements for the material can be directly input. The system then selects the most suitable materials according to their quality from a predetermined group of the materials stored.
- Less experienced designers are aided in entering the material requirements by a check list which systematically asks for all the significant parameters to be entered.
- Material data can not only be called up numerically and graphically; the system also allows the properties of various materials or material classes to be compared.

The high degree of flexibility in data management, the extensive access methods and the comfortable user interface make this system considerably more versatile than pure file managers. It can therefore be used as the central part of a CAE system.

## 2.2 PROGRAMS FOR THE DESIGN OF FUNCTIONAL ELEMENTS

The layout of frequently used functional elements can make it expedient to automate the geometric definition of these elements with regard to their particular requirements.

By a macro, we mean a body generated from several primitives (e.g. cylinders, prisms, solids of rotation, etc.) within a solid-based 3D CAD system (Solid Modeler) for which, however, only the principle of generation is stored, and not the dimensions of the body.

The dimensions are taken directly from preceding design and dimensioning programs. The basis for these programs is the know-how drawn from experience and part designs performed by raw materials manufacturers and in institutes over the course of the years. The functional relationships derived from this information is used as the basis for the calculation of the geometry and service life or of permissible loads.

However, the results of the calculations are then available not only in numerical form; they also provide the geometry and plastics-oriented design of the functional element calculated in the CAD system at the push of a button. A system-independent FORTRAN interface between the design program and the CAD system allow various Solid Modelers to be adapted.

These macros also call up the necessary material information directly via an interface into the material data bank. The press-fit joints shown in Figure 4, for example, require the relaxation module as a function of strain and loading time in order to be able to design the joint for transmission of a defined longitudinal force or for the necessary torque and the desired service life.

In addition to a wide range of connecting elements such as the typical plastic snap-fit joints, ultrasonic welded joints or integral hinges, this macro also permits bolted joints and the press-fit joints already mentioned to be designed.

An important macro is also that employed for the generation of gating and runner systems, since this again provides a link between the design of the moulding and of the mould.

When the designer has generated his part with regard to the function, material and production method in the CAD system, he can then design the gating and runner system in dialogue with the program for sprue gates and tunnel gates. Relevant parameters such as gate angle or gate diameter can be read in from external mould files, and therefore derived directly from the cross-sections of existing milling cutters. In addition to the moulding geometry, the FE mesh for the mould filling analysis program is automatically output, which can therefore include the gating system in the rheological calculations. The inclusion of the gating and runner system in the flow pattern calculation can be of interest particularly for the calculation of the holding pressure phase.

Injection mouldings are generally thin-walled parts, i.e. shell-like components. Ribs or cambers are therefore produced on the component in order to achieve satisfactory stiffening. Figure 5 shows the cross ribs for part of the housing of a paper cutting machine generated using the appropriate macro.

When the user has selected a suitable ribbing from the program, input of the geometric border conditions (e.g. mating dimensions, rib cross-section) is requested. After a plausibility check of the

input data, all the relevant design guidelines are examined; the material-specific draft angles can be called up from the material data bank, and the rib height and rib width checked in relation to the wall thickness of the part.

As shown in Figure 5, undesireable material accumulations can be automatically eliminated. With flat ribs, the stiffening effect resulting from the increase in section modulus can be checked. An extension to the program also enables an optimization calculation which allows the amount of material used to be minimized.

## 2.3 PROGRAMS FOR CONVENTIONAL DIMENSIONING OF WALL THICKNESS

Using CADFORM, predimensioning of wall thickness can be performed quickly using the formulae from classical mechanics for simple bending beams, torque rods and plates, and via volume-specific work of deformation for plates subject to impact loading. However, in contrast to classical design materials, the non-linear stress/strain behaviour of polymers must also be taken into consideration here.

The primary advantage of this type of program is, as with the macros, the reduction in design time. All the possible loading rates and load cases are already formulated for various parameters and can be called up via the program. The user can then calculate the deformation or stresses for selected profile cross-sections. This program in conjunction with the data bank link relieves the designer of the time-consuming searches for formulae or material data. Furthermore, errors in the application of equations are eliminated. Explanations of the calculation principles used together with graphic clarifications can be called up at any time.

## 2.4 MATERIAL LAWS AND FINITE ELEMENTS METHODS

The use of finite elements methods has become established in cases where the critical moulding areas cannot be estimated closely enough using empirical methods, or where complex or critical loads are involved.

During mechanical analysis and structure optimization using FE computer programs, the generally inhomogeneous, anisotropic and non-linear material behaviour of plastics can be numerically approximated. Measurement of the necessary material properties for non-linear analyses is extremely cost-intensive and time-consuming. Compared with the construction of prototypes, however, savings in time and costs can be achieved in particular where changes in design and/or parameter studies are required.

In addition to a non-linear FE program as well as the preprocessors and post-processors required for geometric generation and the display of results, such calculations are based on material laws which define the material behaviour of the plastics with regard to the major parameters loading rate and temperature.

Figure 6 divides the type of load application into the three areas impact, short-term and long-term loading. A guided selection process for the necessary material description is performed in the FEM interface of the IKV material data bank, which also outputs the appropriate parameters in the required format.

A large part of the load illustrated in Figure 6 is covered by the deformation model developed at the IKV, which has been verified in a large number of tests.

## 2.5 DESIGN CONTROLLER

Guidelines for part design are predetermined by the polymer behaviour and the processing method. Parts should, for example, contain no mass accumulations in order to avoid sink marks and voids. A further typical design guideline is that cavity areas should be conical in order to allow the part shrunk onto the mould core to be removed.

When designing functional elements with the help of the macro programs already mentioned, all the design rules for plastic part design will be automatically observed.

However, an examination of the finished component according to design guidelines has not yet been possible. One exception here is merely the flow pattern method which should be used during the part design in order to generate a favourable flow geometry. In many cases, however, the flow pattern is drawn up only at the part layout stage, as generation of the FE mesh is often too time-consuming.

In a prototype version of an automatic design controller, it is now possible for the first time to control a large number of the design guidelines for simple geometries, automatically and without special preparation, on the basis of the geometric information stored in the CAD system data bank. The system can examine the stored geometries for large flat areas, sharp corners and edges, flaws in wall strength, material accumulations, draft angles and undercuts.

At first sight, these rules may appear to be banal and immediately recognizable for the experienced designer. Injection moulded parts often have a complex geometry, however, and this can result in even simple errors in practice being overlooked on the technical drawing or on the monitor of the CAD workstation. The automatic control of the geometry therefore provides an additional check and helps to reduce costs.

Figure 7 shows schematically the methods which can be used for detecting material accumulations on a simple profile:

The solution shown on the left-hand side of the illustration is used, for example, in the foundry technique. In the cross-sectional drawing of the casting, the designer draws circles which just touch the contour. The ratio of the diameters of two neighbouring circles is then a measure of whether the examined area is at risk with regard to the formation of material accumulations.

However, this well-known manual method cannot be used in this way on a Solid Modeler, since a large number of complex calculations also have to be performed which makes this method inefficient.

A large number of spheres have to be generated in the volume and have to be moved along inside the part. In order to determine the correct sphere diameter at the relevant point, the diameter has to be varied using interval nesting until the sphere just has room in the component. The last operation in particular requires the Boolean mean to be calculated for each interval, making it one of the most complex and most critical operations for 3D Solid Modelers. Furthermore, this process results only in a vague area for the material accumulation, but not the accumulation itself.

It was therefore necessary to develop a new method which conformed to the method of operation of the CAD system used. In this case, recourse was made to perspective similarity transformation in plane cuts. Both these are standard functions of Solid Modelers.

In practice, however, this type of program generally still requires enormous calculating times and is therefore still the subject of current development work.

## 2.6 ASSISTANCE IN MOULD CONSTRUCTION

The fundamental idea of examining stored moulding geometries for specific characteristics can also be used, however, in order to allow the moulding designer to consider the problems of mould construction during the part design phase.

A major role is played here by the question of demouldability. After input of a main demoulding direction, a further CADFORM program is able to divide the adjoining surface of the object into mould, cavity and slide contours (Figure 8). Furthermore, the normal vectors of the individual surface areas of the part are considered in relation to the demoulding vector. At present, this method is still considerably time-consuming; it has the advantage, however, that the designer is forced from a very early stage to give thoughts to the mould concept. The mould parting lines can be superimposed on the screen at any time in order to check whether the newly created geometric element still fits into the mould concept or causes undercuts. Inevitable undercuts are marked accordingly and can be used as the basis for building up the slide plate contours.

The mould and slide plate contours thus derived are finally output as related contours of surface areas and no longer as a solid. This would appear expedient insofar as surface models are easier to handle than solids. Consequently, the heavily surface-orientated problems of plastic parts such as subsequent rounding, subsequent creation of draft angles or the definition of the mould parting lines can be more easily performed on the surface representation of the mould cavity than on its solid model. Calculation of the difference in the shrinkage between the moulding contour and mould contour would also appear to be easier to perform on a surface model.

This development has already been taken up by software houses, whereby the pure solid modelling systems are now being superseded by "hybrid modelling systems". This integrates 3D surface modelling into the solid-based design systems with the facility for switching between solid and surface representation as the application requires.

## 3. SIMULATION OF THE MOULD FILLING PROCESS

Since CAD systems are being used to an increasing extent for part design, the result is a complete geometric description of the part in the computer. It is therefore only logical that it should also be possible to simulate the mould filling process in the computer. This type of simulation at this early stage, i.e. before the mould design stage, allows problems which might occur during injection moulding of a part to be detected in advance and, by modification to the part geometry, to enables the problem to be completely eliminated, thereby avoiding any unnecessary costs. This results in a linking of part design and mould design.

The mould filling process is simulated using the CADMOULD-MEFISTO program, which allows the melt flow to be simulated and presented in 3D on the monitor. It incorporates programs

- For calculating the temporal melt front advance and the pressure distribution during the mould filling phase,
- For calculating the shear rates, shear stresses and melt temperatures along freely selected flow paths,
- For determining the most favourable machine operating point and its dependence on operating parameters, and
- For analysis of the holding pressure phase and estimation of the shrinkage.

Using CADMOULD-MEFISTO, the mould filling process can be simulated for even the most complex parts. Since the program operates on the basis of a 3D finite element shell model, it is not necessary to develop a 2D model. The material data required for the flow calculation are also taken directly from the IKV material data bank. When the finite elements model has been generated, the effects of changes in the number and position of the gate(s) and in wall thickness can be very easily examined. The results of these simulations allow the welding lines, air bubbles and, using the temporal curve of the velocity vectors, the molecular and fibre orientations to be derived.

Figure 9 shows an example of a mould filling simulation, in this case the assymmetric housing for a lawnmower. Starting from the gate in the centre of the mould, the melt first spreads in a circle. The lines indicate the position of the melt front at different times during the filling process.

The figure shows that the large visible surfaces of the lawnmower housing fill uniformly, so that no problems are to be expected from welding lines or air bubbles.

## 4. PERSPECTIVES AND FUTURE PROSPECTS

All CADFORM and CADMOULD programs are written in standard FORTRAN 77 in order to be independent of the computer system. During development of these programs, however, the limits of conventional programming techniques were often reached, as can be seen from the following example:

One of the macros for joint elements is used to design screw joints with metal screws in plastic tubes. After a suitable screw for the particular application has been selected from a screw manufacturers file, the surrounding plastic tube is

dimensioned and the correct torque for the automatic screw fitting calculated. The tube geometry generated in the CAD system is shown in the centre of the following illustration (Figure 10).

However, the generation of this tube geometry also involves a number of non-geometric relationships which exist only in the head of the designer, but which are not stored in the system data bank:

- o For the program shown in the previous illustration for the generation of mould contours and checking of the demouldability it would be expedient, for example, for the system to be able to recognize the demoulding direction embossed on the plastic tube as quickly as the human eye.

- o Upper and lower edges and the related surfaces lie in two mould halves. Automatic recognition of this information would be expedient for the tolerance program which already exists as a macro and which, depending on the material, the restrictions and a desired degree of precision, enters acceptable moulding tolerances onto the moulding drawing.

- o The information that, depending on the selected material, the corresponding demoulding angle is embossed on the tube during production is not contained in the geometric data base of the CAD system. It would be desireable, however, that these parameters be automatically modified when a new material is selected, since interactive modification of complex solid geometries is possible only with a great degree of difficulty with current CAD systems.

A demand to be made on the CAD software houses is therefore that not only the management of the geometric data, but also part-specific non-geometric data and functional relationships for a complete product should be taken into consideration and linked to the geometric data.

New concepts in CAD systems are based on "product models" which store the generated geometries along with their behaviour within their environment. Using object-oriented systems, it should then be possible to achieve the following results:

- Function of the individual geometries in the overall structure (e.g. snap-fit joints as elastic connecting elements),
- Material-specific parameters (e.g. material-specific draft angles or roundings),
- Analogies to similar components already manufactured and whose behaviour in practice is known (management of knowledge gained from experience),
- Procedures in production and mould construction (particularly important for fibre composites),
- Measures for structure optimization,
- (Company-specific) standards to be applied, lists of dimensions or tolerance charts,
- Links with suppliers' catalogues, warehouse files, etc.,
- Independent proposal of favourable demoulding directions and automatic generation/modification of the drafting angles.

In addition to the possibilities shown in Figure 9, it would also be expedient for the system to make proposals, based on the association between the solid (body of revolution) and its function (positioning and fixing the screw), for the exact positioning of the element (e.g. to warn against positioning the element in the area of the weld lines), to point out the necessity for prototype tests and to define the test conditions.

These potentials cannot be satisfactorily met with the current generation of CAD systems, and we will have to wait and see to what extent it will be possible to incorporate these into the new generation of CAD systems, e.g. by using object-oriented programming or with artificial intelligence.

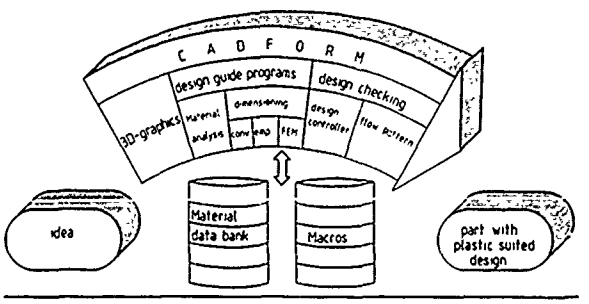


Figure 1: CADFORM: Computer-aided part design

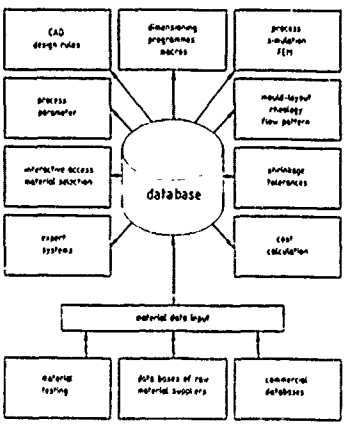


Figure 2: The data bank in a CAD environment

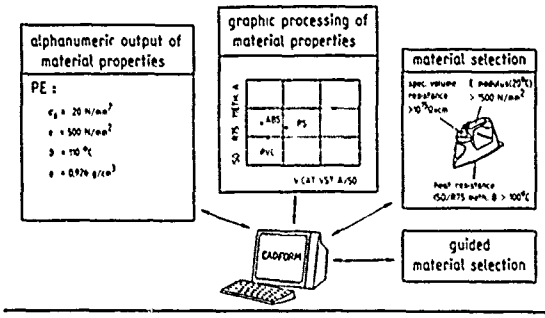


Figure 3: Applications of the data bank

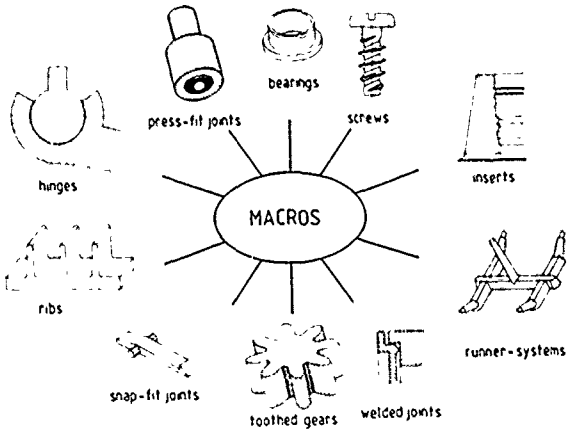


Figure 4: Macros

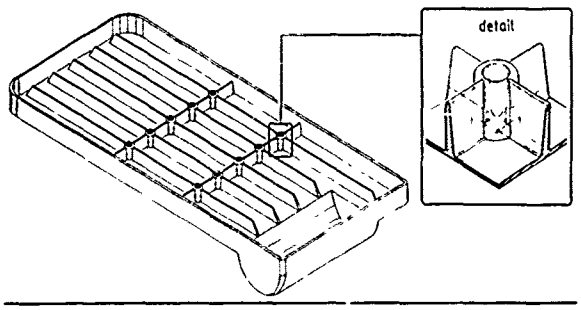


Figure 5: Optimized ribbing on a paper cutting machine (view from below)

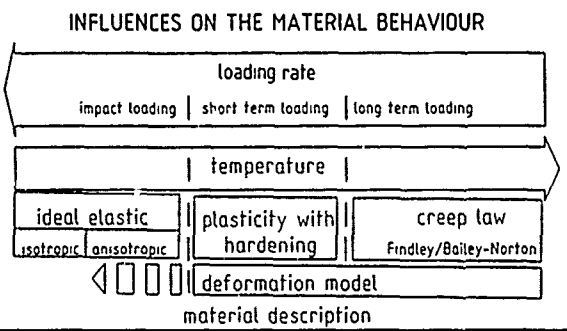


Figure 6: Operative ranges of material laws

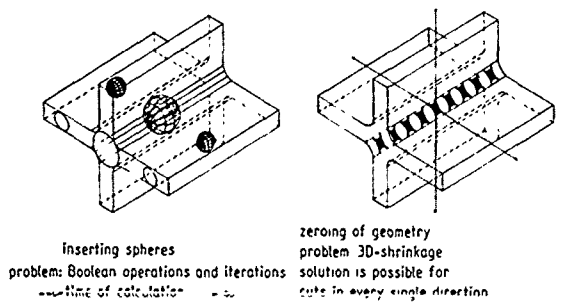


Figure 7: Determination of material accumulations

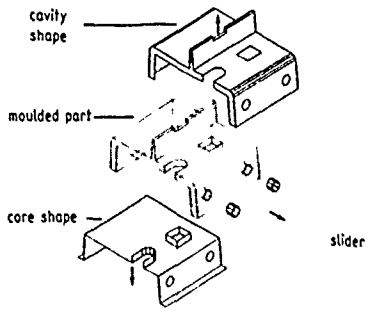


Figure 8: Generation of the mould contours from the component geometry


Figure 9: Filling pattern for a lawnmower housing

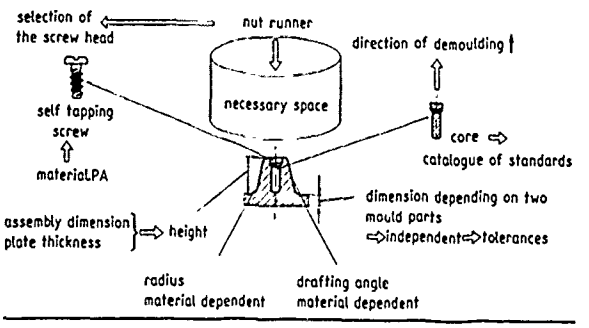


Figure 10: Options of object-oriented CAD systems

# Computer-Aided Modelling of Metal Forming Processes

I.St. Doltsinis

The author is at the Institute for Computer Applications (ICA), University of Stuttgart, West Germany.


## Synopsis

A brief review is given on the numerical finite element methodology developed at the Institute for Computer Applications (ICA) for the computer simulation of industrial metal forming processes. It deals with large elastoplastic deformations and with the viscous approach to forming processes. Both formulations may interact with the thermal phenomena appearing during the course of the deformation process. An essential constituent of the computation procedure is the treatment of the unsteady contact developing between the work-piece material and the die during forming, and of the associated friction phenomena. Also of importance for industrial applications is automatic mesh generation as well as variable discretisation adaptable to the development of the numerical solution.


## Introduction

Reliable computational methods are now available for the numerical analysis of metal forming processes. The simulation techniques developed so far on the basis of the finite element concept account for the appropriate constitutive model under the observance of the finite kinematics involved in the physical problem. When modelling the material response, the inelastic constituent of the material – of plastic, viscous or viscoplastic origin – may be combined with either an hyperelastic or an hypoelastic constituent. Under certain conditions, elastic effects can be neglected, and a viscous approach to the inelastic deformation problem proves satisfactory.

In the deforming solid, thermal effects can arise, due to external thermal action as well as friction and local dissipation. This necessitates a coupled thermomechanical analysis of the forming process. The applied methodology relies on a consecutive treatment of the interacting thermal and mechanical problems.

The treatment of the unsteady contact developing between the work-piece material and the die in the course of the forming process is an essential constituent of the computer procedure. Also important is the possibility of a redefinition of the finite element mesh which ensures a certain quality of the numerical solution [13,15, 16]. Automatic generation of meshes for finite element computations may considerably facilitate the description of complicated problems. In particular, the surface of the die often possesses a complex geometry while the solid workpiece is initially of a simple shape. For this reason, the generation of meshes for arbitrary three-dimensional surfaces has been attacked first. As a result a systematic for mesh generation has been developed in conformity with the simulation software existing at ICA, [15].

The validity of the numerical analysis of a forming process depends strictly on the relevance of the imposed boundary conditions [17, 18] and on the adequate constitutive description of the work-piece material [17, 19]. For this reason the development of the computation methodology at ICA is accompanied by numerical investigations of the specific experiments performed at the 'Institut für bildsame Formgebung' in Aachen. This resarch work aims at the correct modelling of mechanical and thermal boundary conditions, such as the coefficients for friction and for heat transfer between the work-piece material and the die, and at the characterisation of the material in the range of hot-working.

For typographical brevity, the paper deals merely with the basic ingredients of the computational methodology for the simulation of metal forming processes. It is to be supplemented in the oral presentation by subjects of specific interest, such as details on mesh generation and mesh adaptation to the solution, the physical-numerical modelling of the boundary conditions and of the material behaviour, and by the demonstration of industrial applications.

# Methodology of Computation

## Large Deformation Processes

For a numerical analysis of the forming process the workpiece material is represented by a finite element mesh. The actual geometry is then specified by the coordinates of the mesh nodal points collected in the vector array $\boldsymbol{X}$. Accordingly, the applied forces form the vector $\boldsymbol{R}$. The forces resulting at the nodal points from stresses $\boldsymbol{\sigma}$, via the accumulation of elemental contributions, are collected

in the vector $\boldsymbol{S}$. With the above definitions quasistatic deformation in the finite element representation of the work-piece material is governed by the matrix equation

$$\boldsymbol{R}(t, \boldsymbol{X}) = \boldsymbol{S}(\boldsymbol{\sigma}, \boldsymbol{X}) \tag{1}$$

which expresses the equilibrium condition at time instant $t$. The applied forces may depend on the time and on the actual geometry of the deforming solid. The dependence of the stress resultants on the stress and on the actual geometry as indicated in (1) is not given explicitly, but stands for a series of computer operations.

The significance of the history of deformation in the simulation of forming processes calls for an application of incremental continuation techniques to the numerical treatment of the equilibrium equation (1). Thereby, starting with a known equilibrium state of the solid at time ${}^{a}t$, the next state at time $t = {}^{a}t + \tau = {}^{b}t$ is obtained, so that the equilibrium condition (1) is satisfied for applied forces advanced in accordance with the time increment and for the new stresses and geometry of the solid.

The stress $\boldsymbol{\sigma}$ is related via the relevant material law to the kinematics of the deformation process and depends on the temperature. Certain representative material laws are defined in the following and are discussed with respect to the associated computational implications. For the present purpose any details concerning appropriate definitions of stress and strain in the presence of large elastoplastic deformations are omitted, cf [1].

### Elastoplastic Materials

For a material possessing an hyperelastic (elastic) constituent [2, 4], stresses can be connected with the elastic part of strain and the temperature. Elastic strains may be defined for given strains $\boldsymbol{\gamma}$ and inelastic strains $\boldsymbol{\eta}$. Therefore,

$$\boldsymbol{\sigma} = \boldsymbol{f}(\boldsymbol{\gamma}, \boldsymbol{\eta}, T) = \boldsymbol{\kappa}[\boldsymbol{\gamma} - \boldsymbol{\eta} - \boldsymbol{\alpha}(T - {}^{\circ}T)] \tag{2}$$

where local stresses and strains are collected in vector arrays and $T$ denotes the absolute temperature. The customary linear thermoelastic constitutive expression appears as a particular form of the general relation in (2). Here, $\boldsymbol{\kappa}$ denotes the elastic material stiffness matrix, the vector $\boldsymbol{\alpha}$ comprises the coefficients of thermal expansion, ${}^{\circ}T$ is the reference temperature. The material characteristics may depend on the local process variables.
In the case of an hypoelastic (rate elastic) material [3, 5], a relation connecting rate variables may be written in analogy to (2) as

$$\dot{\boldsymbol{\sigma}} = \boldsymbol{g}(\dot{\boldsymbol{\gamma}}, \dot{\boldsymbol{\eta}}, \dot{T}) = \boldsymbol{\lambda}[\dot{\boldsymbol{\gamma}} - \dot{\boldsymbol{\eta}} - \boldsymbol{\beta}\dot{T}] \tag{3}$$

The variables appearing in (3) represent time rates from the point of view of the material. For economy of presentation, the same symbols have been used in (2) and (3). However, the rate variables in (3) may be defined directly and independently of the total variables in (2), cf. [5].

The strain variables $\boldsymbol{\gamma}, \dot{\boldsymbol{\gamma}}$ may be expressed directly in terms of the kinematics of the deformation process. The inelastic strains $\boldsymbol{\eta}, \dot{\boldsymbol{\eta}}$ are still to be specified and may be of plastic, viscous or of viscoplastic origin [6, 7]. In either case, the inelastic constitutive concept provides an expression for the rate quantity $\dot{\boldsymbol{\eta}}$ which completes the evaluation fo the rate constitutive relation for $\dot{\boldsymbol{\sigma}}$ in (3). If $\dot{\boldsymbol{\eta}}$ is a purely plastic strain, it may be represented by an associated modification of the instantaneous stiffness matrix $\boldsymbol{\lambda}$ of the material.

The stress $\boldsymbol{\sigma}$ required in the equilibrium condition (1) is determined by an integration of $\dot{\boldsymbol{\sigma}}$ whith respect to time. The integration procedure is an approximate, incremental one [8]. As $\dot{\boldsymbol{\sigma}}$ in the material law (3) is defined from the material point of view, while $\boldsymbol{\sigma}$ in the equilibrium condition (1) refers to a spatially fixed frame, the integration must properly account for the finite kinematics of the deformation process, cf. [9] for example.

When an elastic relation is applicable, the stress $\boldsymbol{\sigma}$ is directly provided by an evaluation of (2). However, this case requires an integration procedure for the transition from the rate quantity $\dot{\boldsymbol{\eta}}$ to the total quantity $\boldsymbol{\eta}$.

### Iterative Solution Procedure

As a result of the above discussion the stress state $\boldsymbol{\sigma}$ at a given time instant $t$ may be considered a function of the deformed geometry $\boldsymbol{X}$ of the solid, and of the temperature. The temperature distribution in the finite element mesh is specified by the vector array $\boldsymbol{T}$ which comprises the temperatures at the nodal points. Accordingly, the equilibrium condition (1) may be written as

$$\boldsymbol{R}(t, \boldsymbol{X}) - \boldsymbol{S}(\boldsymbol{X}, \boldsymbol{T}) = \boldsymbol{o} \tag{4}$$

In the case of isothermal processes ($\boldsymbol{T} = \text{const.}$), temperature is not an active variable. Then the residual form (4) may be solved for the deformed geometry $\boldsymbol{X}$ by the application of the iteration scheme

$$\boldsymbol{X}_{i+1} = \boldsymbol{X}_i + \boldsymbol{H}_i[\boldsymbol{R}_i - \boldsymbol{S}_i] \tag{5}$$

Following the recurrence formula in (5), the $i$th iteration cycle starts with an approximation to the solution of (4) and supplies a new estimate with the aid of the iteration matrix $\boldsymbol{H}_i$. The matrix $\boldsymbol{H}$ may be considered an auxiliary one, usually chosen with respect to best numerical properties and computational convenience. It can be seen from (5) that convergence of the iteration process implies that the equilibrium condition (4) is fulfilled. For an assessment of the convergence properties of the iteration procedure (5), we deduce for the difference between consecutive iterations the expression

$$\mathrm{d}_{i+1}\boldsymbol{X} = [\boldsymbol{I} + \boldsymbol{H}\boldsymbol{G}]\mathrm{d}_i\boldsymbol{X} \tag{6}$$

where $\boldsymbol{I}$ denotes the identity matrix and

$$\boldsymbol{G} = \frac{\mathrm{d}}{\mathrm{d}\boldsymbol{X}}[\boldsymbol{R} - \boldsymbol{S}] \tag{7}$$

is the gradient of the residuum with respect to the geometry. The requirement for convergence is based on

the spectral norm of the magnification matrix in (6) and reads,

$$\|\boldsymbol{I} + \boldsymbol{H}\boldsymbol{G}\| < 1 \tag{8}$$

Accordingly, convergence depends on the relation of the iteration matrix $\boldsymbol{H}$ to the gradient matrix $\boldsymbol{G}$ of the system.

### Thermomechanical Coupling

In the non-isothermal case, the temperature in the solid appears as an additional variable of the process and is governed by the energy balance. The finite element formulation of the thermal problem leads to the matrix equation

$$\dot{\boldsymbol{Q}} - \boldsymbol{C}\dot{\boldsymbol{T}} - \boldsymbol{L}\boldsymbol{T} = \boldsymbol{o} \tag{9}$$

where $\dot{\boldsymbol{Q}}$ is the heat flux vector, $\boldsymbol{C}$ denotes the heat capacity matrix and $\boldsymbol{L}$ the heat conductivity matrix of the discretised solid material. Thermal effects can arise in the deforming solid by externally applied thermal action and irreversible, as well as reversible, deformations. As a consequence, $\boldsymbol{L}$ is extended to account for reversible mechanical effects, dissipative mechanical contributions are considered in $\dot{\boldsymbol{Q}}$, cf. [4]. Furthermore, equation (9) requires knowledge of the actual geometry of the solid, while the temperature appears in the stress-strain relations for the material. Therefore, thermal and mechanical phenomena are coupled.

When the mechanical coupling terms in (9) are assumed frozen ($\boldsymbol{X}$ = const.), the unknown quantities are $\dot{\boldsymbol{T}}$ and $\boldsymbol{T}$. They are linked via an approximate integration of the temperature rate within the small time interval $\tau = {}^{b}t - {}^{a}t$. One obtains the relation

$${}^{b}\boldsymbol{T} = {}^{a}\boldsymbol{T} + (1-\zeta)\tau\,{}^{a}\dot{\boldsymbol{T}} + \tau\zeta\,{}^{b}\dot{\boldsymbol{T}} \tag{10}$$

with the parameter $0 \le \zeta \le 1$. When $\zeta = 0$, the approximate integration in (10) is explicit and requires the temperature rate at the beginning of the time interval. In this case, equation (9) is stated at $t = {}^{a}t$ for $\dot{\boldsymbol{T}} = {}^{a}\dot{\boldsymbol{T}}$ with $\boldsymbol{T} = {}^{a}\boldsymbol{T}$ known. When $\zeta > 0$, the integration is implicit and (9) is considered at $t = {}^{b}t$ with $\boldsymbol{T} = {}^{b}\boldsymbol{T} = \boldsymbol{T}\left({}^{b}\dot{\boldsymbol{T}}\right)$ in accordance with (10) and requires a solution for $\dot{\boldsymbol{T}} = {}^{b}\dot{\boldsymbol{T}}$.

The coefficient matrixes $\boldsymbol{C}$ and $\boldsymbol{L}$ in (9) as well as the vector $\dot{\boldsymbol{Q}}$ may depend also on the temperature $\boldsymbol{T}$ which leads, in the implicit case $\zeta > 0$, to an nonlinear expression for $\dot{\boldsymbol{T}}$. In this case, the iterative scheme of (5) as applied to the solution of (4) may analogously be used to solve the residual form (9) governing the transient temperature distribution in the solid. The same scheme is also applicable to the explicit case $\zeta = 0$.

A solution technique for the coupled system of the thermomechanical equations (4) and (9) is based on the consecutive treatment of the individual problems [4, 5].
Thereby, the equilibrium condition (4) is fulfilled first and yields the deformed geometry $\boldsymbol{X}$, while the estimated distribution of temperature is held fixed, $\boldsymbol{T}$ = const.. The computed mechanical variables are subsequently used in the thermal equation (9) which is solved for $\boldsymbol{T}$ while $\boldsymbol{X}$ = const., and the iteration cycle is repeated.

### The Viscous Approach

In certain situations relevant to metal forming processes the solid may be described within the conceptual basis of a viscous material. Such an approach is well-suited for superplastic deformation [10] and may adequately be used also in the rigid-plastic constitutive assumption. The material law establishes then a relation between the Cauchy stress $\boldsymbol{\sigma}$ and the corresponding rate of deformation $\boldsymbol{\delta}$ which is defined by the symmetric part of the velocity gradient in the material. The isothermal response is given by

$$\boldsymbol{\sigma} = \boldsymbol{\mu}\,\boldsymbol{\delta} \tag{11}$$

where $\boldsymbol{\mu}$ denotes the viscosity matrix of the material. Isotropic materials are characterised by the deviatoric viscosity coefficient $\mu$ and the volumetric viscosity coefficient $\kappa$. If we consider isochoric inelastic deformations, $\kappa$ has not any physical relevance. Nevertheless, it may be used as a penalty factor in connection with a penalty approach to the isochoric condition [10], and is chosen according to numerical aspects. The deviatoric viscosity coefficient $\mu$ is then the relevant material characteristic, and may be specified using uniaxial experimental data [10]. A finite element formulation of the problem of viscous isochoric deformations on the basis of the penalty approach demands some caution [11]. In the classical velocity method both the deviatoric and the hydrostatic stresses are directly linked with the assumed velocity distribution in the element via the rate of deformation in (11). The deviatoric response of the element is obtained by standard integration over the element domain. In order to prevent overconstraint, the penalty volumetric response of the element is evaluated by a reduced integration rule. Alternatively, in a mixed formulation, the hydrostatic stress may first be approximated to a lower order and then be related to the velocities via the associated finite element expression of the penalty form of the isochoric condition, cf. [11].

As a result, the stress state $\boldsymbol{\sigma}$ in the viscous solid appears as a function of the velocity field represented by the vector array $\boldsymbol{V}$, which comprises the velocities of the nodal points in the finite element mesh. This dependence transfers to the stress resultants $\boldsymbol{S}$ in the equilibrium condition (1) so that quasistatic deformation in the finite element representation of viscous solids is governed by the matrix equation

$$\boldsymbol{R}(t, \boldsymbol{X}) = \boldsymbol{S}(\boldsymbol{V}, \boldsymbol{X}) = \bar{\boldsymbol{D}}(\boldsymbol{V}, \boldsymbol{X})\boldsymbol{V} \tag{12}$$

The indicated dependence of the viscosity matrix $\bar{\boldsymbol{D}}$ of the system on the velocity reflects a non-linear constitution of the viscous material. The dependence on the geometry accounts for the actual configuration of the solid. As a matter of fact, both the velocity $\boldsymbol{V}$ and the deformed geometry $\boldsymbol{X}$ appear as unknown quantities in (12). They are to be linked via an approximate integration of the

velocity within the time interval $\tau = {}^b t - {}^a t$ by the expression

$$ {}^b\boldsymbol{X} = {}^a\boldsymbol{X} + (1-\zeta)\tau\,{}^a\boldsymbol{V} + \zeta\tau\,{}^b\boldsymbol{V} \qquad (13) $$

which is analogous to expression (10) for the temperature. In the explicit case ($\zeta = 0$) the approximate integration requires the solution of (12) at the beginning of the time interval $t = {}^a t$, for $\boldsymbol{V} = {}^a\boldsymbol{V}$ with $\boldsymbol{X} = {}^a\boldsymbol{X}$ known. In the implicit case ($\zeta > 0$), (12) must be solved at $t = {}^b t$, for $\boldsymbol{V} = {}^b\boldsymbol{V}$ with $\boldsymbol{X} = {}^b\boldsymbol{X} = \boldsymbol{X}({}^b\boldsymbol{V})$ in accordance with (13).

In either case, (12) is nonlinear in the velocities and may be solved by the application of the iteration procedure (5) in the form,

$$ \boldsymbol{V}_{i+1} = \boldsymbol{V}_i + \boldsymbol{H}_i[\boldsymbol{R}_i - \boldsymbol{S}_i] \qquad (14) $$

The remarks made in concern with the convergence properties of the iteration scheme (5) are analogously applicable also to (14). In particular, convergence depends due to (8) on the relation of the iteration matrix $\boldsymbol{H}$ to $\boldsymbol{G}$ which, in the present case, is the gradient of the residuum $[\boldsymbol{R}-\boldsymbol{S}]$ with respect to the velocity $\boldsymbol{V}$. In most cases the choice

$$ \boldsymbol{H} = \bar{\boldsymbol{D}}^{-1} \qquad (15) $$

proves satisfactory.

When the considered deformation process is non-isothermal, the viscous constitutive relation (11) must be modified according to the appearance of a temperature rate, cf. (3). In addition, the viscosity characteristics of the material are usually sensitive to the temperature, [12, 17]. Consequently, the temperature becomes significant and must be treated as an additional variable in the equilibrium condition (12).

The transient distribution of the temperature in the solid during the course of the deformation process is governed by the thermal equation (9), which is coupled to the mechanical equation (12) via the deforming geometry of the solid and the mechanical dissipative phenomena. A solution of the arising coupled thermomechanical system is achieved along the lines previously discussed in the context of thermally and mechanically coupled large elastoplastic deformations, cf. also [12].

## Boundary Conditions

### Contact with the Die

In forming processes, deformation of the work-piece material is often constrained by a die, which is assumed to be rigid in the following. The tasks associated with the consideration of the unsteady contact between work-piece material and die in the numerical analysis concern mainly the specification of the surface limiting the motion of the material, the test for contact or penetration, and the accounting for the boundary conditions upon contact [13].

For general situations a discretised description of the geometry of the die surface is convenient. This is done by the use of individual surface elements in a mesh on the potential contact surface of the die. The surface limiting the motion of the work-piece material is then completely specified by the coordinates of the mesh nodal points, the topological description of the surface elements, and by the geometrical properties of the elements. In addition, it is useful to record the surface elements connected to each nodal point. The numbering order of the element nodal points defines the sign of the surface normal, which we assume to be positive by convention when pointing into the space prohibited for the material motion. A normal uniquely defined for each element simplifies the subsequent procedure and, for this reason, plane elements are assumed in what follows.

The test for contact requires a comparison of the actual position of the work-piece material with that of the die. For this purpose let us consider a nodal point $m$ on the surface of the discretised material and obtain first the nodal point $k$ of the die surface closest to $m$ by the condition of minimum distance,

$$ \boldsymbol{x}_{km}^t \boldsymbol{x}_{km} = \min\left(\boldsymbol{x}_{jm}^t \boldsymbol{x}_{jm}\right) \;;\; j = 1, \cdots, K \qquad (16) $$

where $\boldsymbol{x}_{km}$ denotes the radius vector from $k$ to $m$. At the beginning of the computation the search comprises each of the $K$ nodal points of the discretised die surface. Later on, the procedure is first restricted to the vicinity of the previous neighbour $k$ of $m$ and is extended to other nodal points if necessary. Subsequently, the particular surface element e is specified which contains the projection

$$ \boldsymbol{y}_{km} = \left[I - \boldsymbol{n}_e \boldsymbol{n}_e^t\right] \boldsymbol{x}_{km} \qquad (17) $$

of the vector $\boldsymbol{x}_{km}$ onto the plane with normal $\boldsymbol{n}_e$. The position of the point of the work-piece material relativ to the surface of the die is ultimately indicated by the normal distance to this element,

$$ d_n = \boldsymbol{n}_e^t \boldsymbol{x}_{km} \qquad (18) $$

As long as $d_n < 0$, the nodal point has not reached the die and is left to move freely.

The numerical treatment of the phenomena occuring upon contact between the work-piece material and the die is based in the following on the viscous approach, as an example. When the material nodal point (velocity $\boldsymbol{v}$) contacts the die (velocity $\boldsymbol{w}$), the normal velocity $[\boldsymbol{v}_n - \boldsymbol{w}_n]$ directed into the die surface must be suppressed in the calculation. This implies a change in the kinematic boundary conditions for the work-piece material and affects the structure of the system matrix; it is therefore inconvenient. Alternatively, a penalty form of this contact condition reads

$$ \boldsymbol{v}_n - \boldsymbol{w}_n = -\frac{1}{k_n}\boldsymbol{F}_n \to 0 \;;\; k_n \to \infty \qquad (19) $$

and helps to express the contact pressure $\boldsymbol{F}_n$ as a viscous force which contributes to the stress resultants in (12). In this manner the contact condition modifies the viscosity matrix of the system solely through a contribution by the penalty factor $k_n$, while the structure of the matrix remains unchanged.

When penetration of the die occurs, the material point is brought back onto the die by a prescribed velocity normal

to the die surface. For this purpose the approximate time integration of (13) is applied to the desired motion of the nodal point within the time increment

$$-d_n \boldsymbol{n}_e = (1-\zeta)\tau\ {}^a[\boldsymbol{v}_n - \boldsymbol{w}_n] + \zeta\tau^b[\boldsymbol{v}_n - \boldsymbol{w}_n] \quad (20)$$

It yields the velocity ${}^a[\boldsymbol{v}_n - \boldsymbol{w}_n]$ for $\zeta = 0$, or the velocity ${}^b[\boldsymbol{v}_n - \boldsymbol{w}_n]$ for $\zeta > 0$. The calculated velocity is imposed on the respective node of the work-piece material by the penalty form (19) which is modified accordingly.

### Friction Phenomena

Sliding motion of the work-piece material with local velocity $[\boldsymbol{v}_t - \boldsymbol{w}_t]$ along the surface of the die is opposed by a friction force $\boldsymbol{F}_t$. This can be expressed by the statement

$$\boldsymbol{F}_t = -\frac{|\boldsymbol{F}_t|}{|\boldsymbol{v}_t - \boldsymbol{w}_t|}[\boldsymbol{v}_t - \boldsymbol{w}_t] \quad (21)$$

which defines the direction of the friction force beyond sticking. The material sticks as long as $|\boldsymbol{F}_t| < F_H$ , $F_H > 0$ being the sticking limit. For Coulomb-type friction,

$$|\boldsymbol{F}_t| \leq c|\boldsymbol{F}_n| \quad (22)$$

where the friction coefficient $c$ may depend on various parameters of the process [17, 18]. With (21), (22) the friction force can be determined using the quantities available in the course of the iteration process and contributes to the applied forces in (12), (14). Thereby a tendency to sticking is indicated by oscillations in the sliding velocity when approaching zero, and may lead to unreliable results. Stabilisation of the numerical results can be achieved by suppressing the sliding motion. This is an inconvenient step, because it affects the structure of the viscosity matrix of the system. An alternative is provided by the penalty formulation of the sticking condition [14], which is analogous to (19). However, the definition of an appropriate velocity criterion for the appearance of sticking is critical to both procedures, as is the definition of the penalty factor in the latter.

Expression (21) for the friction force and the penalty form of the sticking condition may be combined to a complete kinematic computational approach to friction [13]. The single form proposed reads

$$\boldsymbol{F}_t = -k_t[\boldsymbol{v}_t - \boldsymbol{w}_t] \quad (23)$$

where the factor $k_t$ is defined as the ratio

$$k_t = |\boldsymbol{F}_t|/|\boldsymbol{v}_t - \boldsymbol{w}_t| \leq k_{\max} \quad (24)$$

Limitation by $k_{\max}$ implies the penalty approach to the sticking condition. By means of equation (23), friction is accounted for throughout the numerical analysis by a viscous force in conformity with the contact pressure in (19), and contributes via $k_t$ to the viscosity matrix of the system. The present approach to the friction force seems to be insensitive to the choice of the penalty parameter $k_{\max}$, and the velocity criterion to sticking.

Finally, the alternative elastoplastic methodology should be considered for completeness. In this context kinematics are described in terms of displacements which replace the velocity variables of the viscous approach. Then, the penalty factor $k_n$ for the normal contact force in (19), as well as the factor $k_t$ for the friction force in (23), refer to relative displacements between the work-piece material and the die and contribute via the internal stress resultants in (4), (5) to the gradient matrix (7) of the elastoplastic system.

## References


[1] J. Argyris and I.St. Doltsinis, On the large strain inelastic analysis in natural formulation. Part I. Quasistatic problems, Comput. Meths. Appl. Mech. Engrg. 20 (1979) 213-251; Part II. Dynamic Problems, Comput. Meths. Appl. Mech. Engrg. 21 (1980) 91-128.

[2] E.H. Lee, Elasto-plastic deformation at finite strain, J. Applied. Mech. 36 (1961) 1-6.

[3] R. Hill, Some basic principles in the mechanics of solids without a natural time, J. Mech. Phys. Solids 7 (1959) 209-225.

[4] J. Argyris and I.St. Doltsinis, On the natural formulation and analysis of large deformation coupled thermomechanical problems, Comput. Meths. Appl. Mech. Engrg. 25 (1981) 195-253.

[5] J. Argyris, I.St. Doltsinis, P.M. Pimenta and H. Wüstenberg, Thermomechanical response of solids at high strains - natural approach, Comput. Meths. Appl. Mech. Engrg. 32 (1982) 3-57.

[6] J. Argyris, I.St. Doltsinis and M. Kleiber, Incremental formulation in nonlinear mechanics and large strain elasto-plasticity - natural approach. Part II, Comput. Meths. Appl. Mech. Engrg. 14 (1978) 259-294.

[7] J. Argyris, I.St. Doltsinis and K.J. Willam, New developments in the inelastic analysis of quasistatic and dynamic problems, Int. J. Num. Meths. Engrg. 14 (1979) 1813-1850.

[8] J. Argyris and I.St. Doltsinis, On the integration of inelastic stress-strain relations. Part 1: Foundations of method; Part 2: Developments of method, Res Mech. Lett. 1 (1981) 343-355.

[9] T.J.R. Hughes, Numerical implementation of constitutive models: Rate-independent deviatoric plasticity, In S. Nemat-Nasser et al. (eds.): Theoretical Foundation of Large-Scale Computations of Nonlinear Material Behavior, Martinus Nijhoff Publishers, (Dordrecht/Boston/Lancaster, 1984).

[10] J. Argyris and I.St. Doltsinis, A primer on superplasticity in natural formulation, Comput. Meths. Appl. Mech. Engrg. 46 (1984) 83-131.

[11] R.L. Taylor and O.C. Zienkiewicz, Mixed finite element solution of fluid flow problems, In R.H. Gallagher et al. (eds.): Finite Elements in Fluids, Vol. 4 (Wiley, New York, 1982).

[12] J. Argyris, I.St. Doltsinis, H. Fischer and H. Wüstenberg, '*Τα παντα ρει*', Comput. Meths. Appl. Mech. Engrg. 51 (1985) 289-362.

[13] I.St. Doltsinis, J. Luginsland and S. Nölting, Some developments in the numerical simulation of metal forming processes, Engineering Computations, 4 (1987) 266-280.

[14] J.T. Oden and J.A.C. Martins, Models and computational methods for dynamic friction phenomena, Comput. Meths. Appl. Mech. Engrg. 52 (1985) 527-634.

[15] I.St. Doltsinis, J.Luginsland and S. Nölting, Mesh generation and variable discretisation techniques, Conference on Automatic Mesh Generation and Adaptation, Grenoble, Oct 1-2, 1987.

[16] J. Argyris, I. St. Doltsinis and H. Friz, Three-dimensional hypersonic viscous flows with chemical reactions. First progress report on the research and development work for the European Hermes Project, RDANE 11/87, Stuttgart, Dec. 1987.

[17] M.L. Cho, G. Hirt, R. Kopp, and J. Argyris, I.St. Doltsinis, J. Luginsland, Thermomechanische Analyse des Freiformschmiedeprozesses hinsichtlich des Dichtschmiedens und der Werkstoffeigenschaften, DFG-Zwischenbericht, Januar 1986.

[18] J. Argyris, I.St. Doltsinis and J. Luginsland, Three-dimensional thermomechanical analysis of metal forming processes, Int. Workshop on Simulation of Metal Forming Processes by the Finite Element Method, 3rd June 1985, Stuttgart, Proceedings (Springer, 1986).

[19] J. Argyris and I.St. Doltsinis, Computer simulation of metal forming processes, Conf. on Numerical Methods in Industrial Forming Processes, Gothenburg, 25-29 August 1986, Proceedings.

□

# COMPUTER AIDED ENGINEERING: INTEGRATING THEMES

David R. Hayhurst

Professor of Engineering Design and Manufacture,
Department of Mechanical Engineering,
The University of Sheffield, Sheffield S1 3JD

SYNOPSIS

The paper presents an overall or systems view to design, giving consideration to marketing; the elicitation of a business specification; design and manufacture; and, to their interactions through the need for optimal materials selection. The design activity is considered at several levels of information together with the different approaches required in materials selection. The flow of information is outlined from concept to detailed design; and, the influence of Computer Aided Engineering is considered on the automation of data and information flows throughout the process. The catalysts for change are identified as being Computer Science and Computer Aided Engineering and it is argued that these will provide the integrating themes in systematised or automated design.

## 1.0 INTRODUCTION

Traditionally the interface between materials and engineering scientists has been established through materials properties such as:

1. mass, density, thermal and heat transfer;
2. electrical conductivity;
3. elastic moduli, yield strength, ductility;
4. resistance to fatigue, creep;
5. fracture and corrosion; and
6. the effects of stress-state, temperature and chemical environment.

The engineer has sought data, models, constitutive equations which quantitatively describe the above properties, and which enable reliable design decision making to take place. The main concern of the engineer has been to select, and to process materials such that, when used in service, they will satisfy all materials-related aspects of the component, system or product. Market driven need to enhance performance has stimulated materials scientists to improve the properties of existing materials, and to develop new materials with significantly better properties. The effect has been to establish research programmes directed towards a fundamental understanding of the microstructural processes which underpin the physical properties. The need to develop materials and to provide materials data which is geared to the market place, and to engineering design requirements, has not always been given prominance.

While the potential will always exist to use materials with novel properties in the marketing of products, with superior performance, to capture large market sectors; new technology is becoming available which allows better and more competitive design to take place with traditional materials. Technological change in fields such as Computer Science and Computer Aided Engineering, coupled with new marketing methods, makes possible the establishment of interfaces between Materials, Engineering and Business. These methods and tools enable the Designer to engage in multi-parameter design optimisation, involving either new, or well established materials to launch fresh products into the market place which optimally satisfy targeted consumer requirements.

This paper concerns the potential synergisms between Business, Engineering Design and Materials, which might be brough about by appropriate use of Computer Science and Computer Aided Engineering. A 'top-down' systems approach to Engineering Design is presented, starting with a market place product specification, leading through concept and embodiment design to detail design. The material selection implications are considered at all stages, and it is shown how Computer Science and Computer Aided Engineering provide the cross-disciplinary integrating links to make possible rapid design optimisations hitherto not possible.

## 2.0 TYPES OF DESIGN

The extent and style of the influence of materials selection on the design process very much depends on the type and status of the design activity. The spectrum of design types may be split up into three principal areas:

1. Original Design;
2. Adaptive Design; and
3. Variant Design.

In Original Design the process starts with the establishment of a product specification based on market research and leads to the elaboration of an original solution. Typically only 25% of all designs fall into this category. In Adaptive Design a known product or system exists for which a changed task or function is required. This necessitates the original design of parts or assemblies.

Of the order of 50% of designs fall into this area. In Variant Design a limited change is required to an existing product. Variation is required of the size or arrangement of parts of a system. Less than 25% of all design activity is in this area.

The opportunity for the selection of materials to have an impact on conceptual design is probably greatest with original designs, and it is in this area where there is most scope for imaginative, latteral thinking, to have greatest impact. In the fields of adaptive and of variant designs, preferences and predudices tend to become established and innovative use of materials tends to be driven by the more detailed, technological, design considerations.

## 3.0 SYSTEMS APPROACH TO DESIGN

In this section the 'top-down' systems approach to design will be outlined with brief reference to materials selection.

### 3.1 Business Specification

Design is the process whereby ideas, concepts, data, information, skill are put together using methods, procedures, and techniques to create or to produce artefacts, objects or systems which satisfy a predefined need, objective, or specification. The process can only satisfactorily proceed when the specification has been identified. Invariably engineering design is concerned with wealth generation in either national or world markets. Since it is the consumer in whose mind the requirements or specifications are vested, marketing techniques have to be used to elicit the dominant elements of the specification. If this is not done the designer will inevitably exercise prejudice in the decision making process.

Shown in Figure 1 are the principal components of a Business Specification; all of which, to varying degrees, may, consciously or otherwise, influence the consumer's concept of the product. Materials selection has been included at this stage, since it is important for a class of products, which include Aesthetic and Ergonomic factors; or, for products where design is constrained by manufacturing resource. The greatest potential for materials selection to influence the specification tends to occur in the case of original design.

### 3.2 Abstraction of Specification

Business specifications resulting from market research tend to be coloured either by the individual's notion of the product, be it either the researcher or the consumer. At this stage it is important that the specification be abstracted to allow consideration of the broadest possible range of solution and of associated materials. Options must not be excluded either by preference ignorance or favour.

### 3.3 Concept Design

Having established an abstracted specification the designer can now set up a broad solution field and establish independent concept variants which appeal to a broad range of available materials. Constraints must be included at this point from inventory control and from available manufacturing resource. Concept variants should be evaluated against the specified multi-disciplinary requirements and the broadest solution field and materials options passed on to Embodiment Design. As shown in Figure 2, only the coarsest sorting of materials alternatives is carried out at this stage.

### 3.4 Embodiment Design

Here the solution variants are assessed in more detail by inclusion of multi-disciplinary interactions; and, by the identification of systems and function variables. What-if type scenarios are studied by computer modelling and simulation. Constraints from manufacture and inventory control are included and studied. Checks and evaluations are carried out against the technical and economic specification. The use of value engineering methods may be included here. The first passage through this procedure leads to modification, iteration and optimisation of the process. Preliminary production-planning specifications can be prepared at this stage. As in the conceptual stage (Figure 2) a second coarse sorting of materials data and information is carried out; the complexity of the materials related computations is low and a number of alternatives may be retained at this stage.

### 3.5 Detailed Design

In this phase completion takes place of the embodiment of technical aspects, together with final instructions about layout, dimensions and surface properties of all individual components. After detailed modelling the definitive selection of materials takes place. Here value engineering plays an important rôle. A final scrutiny takes place of manufacturing methods and costs. Included in this are: the elaboration of production documents; preparation of detailed and assembly drawings; and, preparation, for production departments, of documents on assembly, transport, quality control.

As outlined in Figure 2 much higher levels of materials data, information and of constitutive equations will be used with Computer Aided Engineering techniques to achieve an optimal selection of materials.

### 3.6 Materials Selection

In progressing through the systems approach to design, outlined in Figure 2, it is evident that materials evaluation-selection takes place at all levels; the distinguishing feature is the level of information associated with the activity. At the specification stage reference to materials could be either non-existent or veiled, while at the detailed design stage materials evaluation will be a dominant activity requiring extensive provision of data, information and constitutive equations.

## 4.0 INTEGRATING POWER OF COMPUTER AIDED ENGINEERING

Shown in column 1 of Figure 3 is a block diagram which shows the information flows, particularly through the detailed design stage. The figure is most relevant to the flow of digital information during the CAE activity. At the embodiment-detailed design stage a solid-surface model of the component may be generated at a Visual Dis-

play Unit and the designer can carry out many of the functions-requirements listed in the specification of Figure 1, e.g. shape, form, colour, texture etc. This data set can be passed on as input to a pre-processor for Finite Element or simplified analysis procedures where most of the detailed materials related assessment is usually carried out, i.e. checks to verify that all possible failure modes will not be excited during the product lifetime. The block in column 1 labelled Failure Analysis represents this function; it could refer either to an experienced designer or to an Expert System which enables a non-materials specialist to carry out the same function. A post processor or results investigator is included in this process. The finite element data set, after suitable adjustment-optimisation may be passed on to a computer package for the modelling of a range of manufacturing processes which would be materials related,and require material input data. Optimisation-interaction may involve the return to earlier stages of the process and to their repetition. Directly, from this same data set it is possible to manufacture the forming die or tools which can be used in manufacture. The same, or similar,data sets can be passed on to other functions which could involve Robotic fabrication, assembly and quality assurance.

It is clear from the foregoing that it is possible to take a component through the detailed design phase with only a digital representation; and, that the materials related aspects can be studied and optimised, provided that sufficient data and information is available and accessible in an appropriate form.

## 5.0 MATERIALS DATA REQUIREMENTS

Within the Computer Aided Engineering process outlined in Figure 3 the component, product, or system is represented in digital form, and hence the designer's interactions within the materials selection process must take place through the same digital medium. This requires that laboratory data be stored in appropriate data bases from which the required design information can be generated, and accessed for input to the design process. In column 2 of Figure 3 three areas have been identified for such materials data bases.

The first is to provide data on physical properties such as those listed in the introduction to this paper. This data is for use in design calculations to ensure that the product operates satisfactorily for its lifetime without excessive deformation or failure of material elements. Depending upon the level of importance of component integrity, either simple or complex design calculations may have to be performed, each demanding a different quality of data or information. In addition, the data may be such that it has to be coupled with other data on cost, on sensitivity of manufacturing route, and on availability to the manufacturing company. Such data base technology has yet to be introduced in significant measure into the design process.

The second is to provide data concerning the behaviour of material during the manufacturing process; for example during its flow into shaping cavities; its cooling; and, the way in which these factors determine-influence its subsequent physical properties. It is clear that links between this type of data base and the first, concerning component integrity, must be available if the manufacturing route - component integrity requirements are to be correctly optimised within cost, and availability constraints.

The third is to provide data on material processes, surface durability, fabrication and quality assurance all of which enable the performance, wear, and durability to be quantified and optimised for a range of environments. In this area the data can range from simple look-up tables to more complex constitutive models of the type that may be required in the design of weldments and of adhesive bonds.

In addition to the requirements set out in column 2, further materials requirements are given in column 3 which are concerned with the design-manufacture activity within the companies involved. These factors are concerned with designing to cope with:

1) optimal use of manufacturing plant;
2) design using available materials;
3) design for correct value engineering;
4) achievement of Just in Time Manufacture and of required product quality.

The data bases associated with such activities are specific to the particular company, to the types of materials used, and to the customer profiles and job inventories. The principal materials involvement is associated with their procurement, processing, minimal storage and sales dispatch. In comparison with the materials data requirements of component integrity this field of activity is wrongly considered to "low technology"; its true merit is only apparent on consideration of economic factors.

## 6.0 THE ROLE OF COMPUTER SCIENCE

It is clear from the foregoing that the process of design-manufacture involves the creation, and the use of materials data bases of different types. The data often has to be converted into information before it can be used in the decision making processes of design. Increasingly this information is used in conjunction with computer aided engineering methods for analysis and for simulation. The potential to hold and to transfer information concerning the different phases of the design-manufacture process means that it is possible to study and to optimise the entire process. While this potential has existed for some time there are few companies who have achieved widespread use of it. Most industries have chosen to develop particular areas which are best suited to their needs.

One of the limiting factors is in providing links, or information flows, between areas of computerisation. Such links often involve human processing of information, and the associated difficulties of non-uniqueness of human judgement. Certainly in this field there is considerable potential for Expert System technology to provide an integrating role.

## 7.0 FUTURE MATERIALS REQUIREMENTS

The rates at which software is being developed for computer aided engineering, data base, and

Expert System technologies, and at which computer hardware is becoming more powerful and cheaper, must ultimately place demands on the Materials Scientists to provide enough and sufficiently detailed data to enable engineering designers to make optimal and competitive decisions. Bearing in mind the long lead times required to initiate experimental programmes, and to develop the associated modelling, it is evident that a data or an information gap could develop if the appropriate cross-disciplinary interactions are not developed sufficiently well at an early stage.

## 8.0 MANAGEMENT OF DESIGN

In the majority of companies involved in design a low priority is given to the activity; it is seen as a function carried out by draughtspersons; and, as a self-contained activity unrelated to marketing and to manufacture. In contrast, the systems approach discussed here requires that it is an "all-pervading" activity, i.e. it must be recognised at all levels of company structure. The need for communications and interactions between departments must be recognised and stimulated. Before these aims can be achieved it is necessary to establish appropriate company management structures which allow both the vertical and the horizontal information flows necessary for the systems approach in design to function.

## 9.0 CONCLUSIONS

An overall or systems approach to design has been outlined stressing the importance of the elicitation of a business specification, through marketing. The power of computer aided engineering to integrate the wide range of activities from concept, detailed design, manufacture, to processing and fabrication has been discussed. Within this range of activities, consideration has been given to the use of material data and information in the optimisation processes of design.

In this process computer aided engineering provides the tools and aids necessary to analyse, simulate, and to carry out what-if scenarios necessary in design optimisation. To underpin this activity digital materials data bases are necessary which allow the manipulation of data into the forms required by designers for decision making.

In addition, it is necessary to permit information flows within the design-manufacture activity, and to make possible optimal specialist decisions, by the use of Expert System technology.

Computer Aided Engineering and Computer Science provide the links with Materials Science necessary to make possible a computerised Systems approach to Design.

1. Product function and performance
2. Weight, Size and Maintainability
3. Market Constraints and Competition
4. Patents
5. Cost and Selling Price
6. Political, Cultural and Environmental Factors
7. Design-Manufacture Timescales
8. Aesthetics
9. Ergonomics
10. Quality
11. Product Life-cycle
12. Standards, Safety and Testing
13. Company Constraints and Manufacturing Resource
14. Sales, Packaging, Storage and Transportation
15. Materials

Figure 1. Components of Business Specification

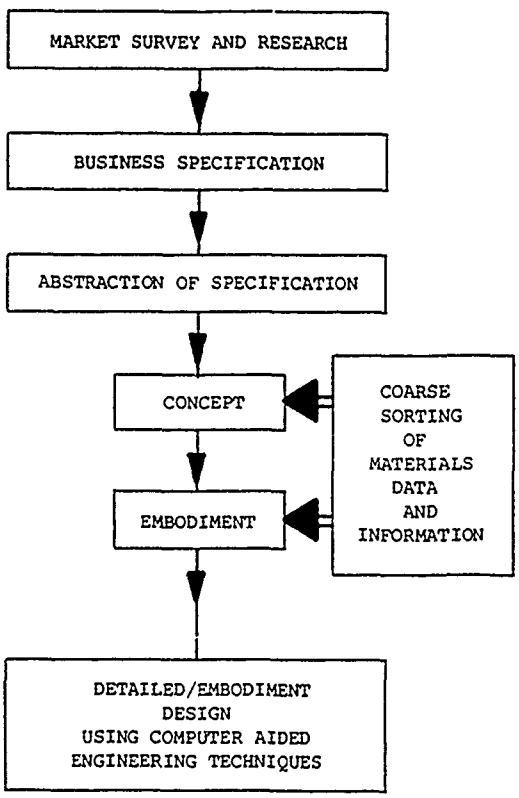


Figure 2 Materials Data Input to Concept and Embodiment Phases of Design

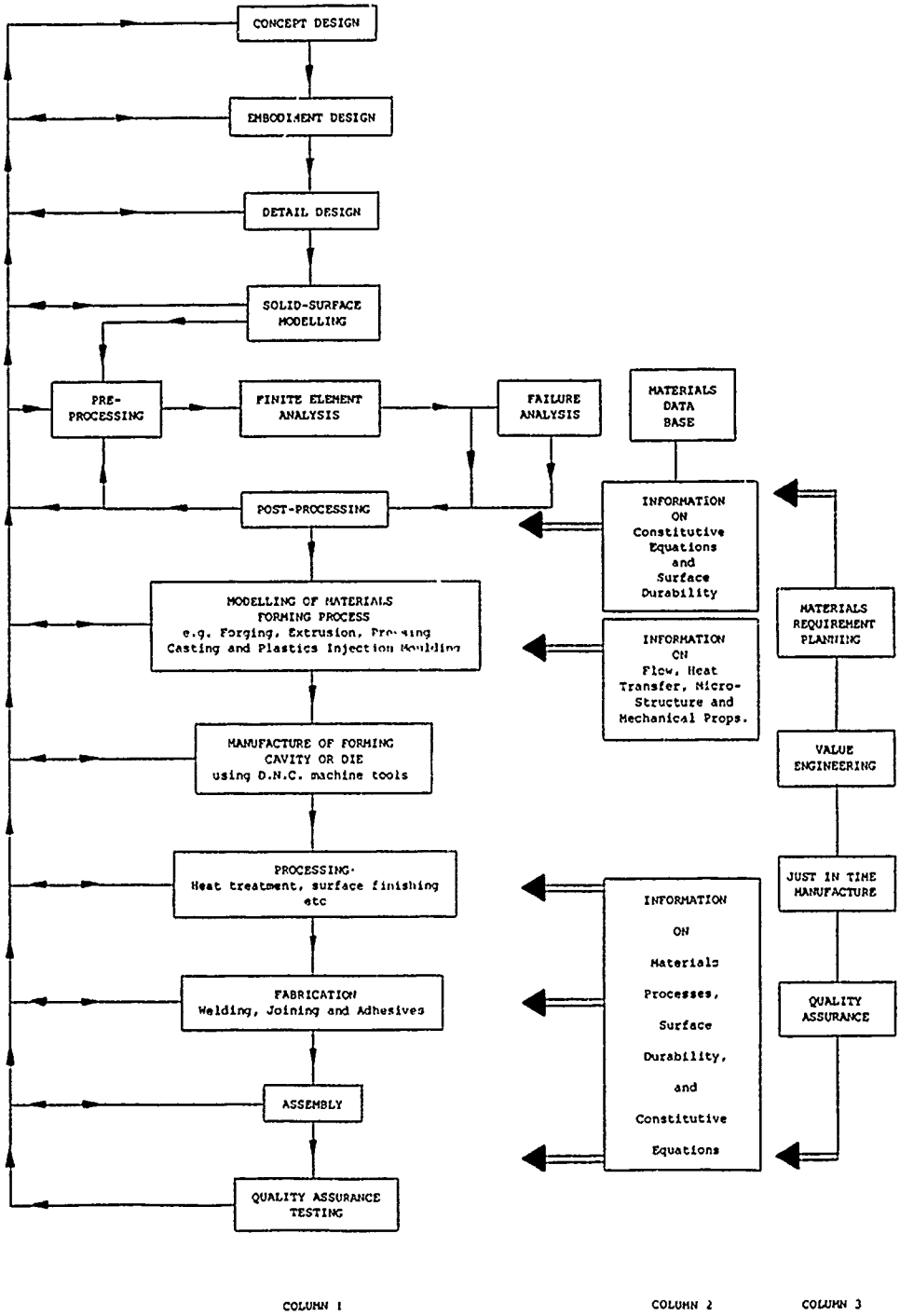


Figure 3. Detail Design - Information Flow and Material Requirements

# COMPUTERISED MATERIALS DATA AND INFORMATION - AN OVERVIEW

Keith W.Reynard

The author is Principal Consultant with Wilkinson Consultancy Services. He is the UK coordinator for the VAMAS Technical Working Area 10 - Materials Databanks, a member of the executive committee of ASTM Committee E-49 on Computerization of Material Property Data and secretary of the CODATA Commission on Industrial Data.

## SYNOPSIS

The recognised industrial need for the improved organisation and dissemination of the available information on materials and in particular the factual and numerical data required in engineering has stimulated a series of international conferences and workshops.

These have been the starting points for much work, some voluntary, some funded by the Commission of the European Communities, CEC, some by national governments. The application of computer techniques, in managing the data, in the use of expert systems, and in links with CAD and CAE to provide engineers with new and powerful tools has become the focus for the great surge of interest and work in materials data.

In Europe the five year information programme of the CEC includes the topic of materials databanks. The programmes set up by the Versailles Project on Advanced Materials and Standards, VAMAS, are well under way and practical results are beginning to appear, as they are from ASTM Committee E-49 in the USA.

The paper provides a review of what is needed, what is being done and where to find more information.

## INTRODUCTION

'Designers and manufacturers, ..... use materials for achieving function or performance. They work in a competitive climate with on-going problem-solving processes concerning their products in order to reach optimal decisions. In analogy with composition and properties, there is no clear and direct correspondence between properties and performance. This discrepancy is at the root of the present dilemma of computerised materials data systems. It is also the explanation why engineering materials data are more difficult to computerise than, for instance physical data.' (Reference 1).

'Also, most of the properties which are measured on a new material are derived from tests on laboratory specimens. These may bear little relation to those found in a component in service. Finally, figures on a data sheet are an inadequate description of a material. Selection from data sheets alone cannot cover adequately the appearence or feel of a material.' (Reference 2).

Design methods and computer programs are the lifeblood for many engineers. They criticise and refine in infinite detail the workings of a finite element stress program or the methodology of one for fatigue life prediction. Yet in using these tools they seem willing to pick up numerical materials data from any scrap of paper in a filing cabinet or any twenty year old handbook just because it is to hand. They take little thought for its origins, its processing history from measuring instrument to the paper or screen on which they find it. They ignore many possibilities of use out of context, misleading presentation, inadequate supporting information, gross error, misprint or inapplicability.

Because computers exist, because databases in other fields are common and sometimes commercially viable does it necessarily follow that materials data should also be handled this way?

Generally computerisation is desirable because much of what exists in hard copy is not presented so as to make it easy to use in more than one way, not easy to link to the design program, not easy to reorganise and manipulate into the form that the user needs. Indeed when critically evaluated much of the data available in hard copy is unusable due in the main to inadequate reporting of the original measurements, ie lack of metadata.

A few forward thinkers set up the workshop at Fairfield Glade (Reference 3). What has happened since suggests that they were right.

## WHAT KINDS OF DATA AND INFORMATION?

Before considering what is being done towards computerisation in the world of materials data, it is pertinent to consider what sort of data and who wants to use it. A clear understanding of these two aspects helps to define the problems that exist and points to some solutions.

There are many categories of information that are requested by users. Some of these are:

- Suppliers - names, stock, form of stock, price, delivery
- Manufacturers
- Identification of material from - name, number, mnemonic, composition, property(ies)
- Equivalence of materials
- Identification of a standard
- Equivalence of standards
- Physical properties
- Mechanical properties
- In-service data
- Bibliographic information
- Machinability - forming, joining, welding
- Corrosion - environmental information
- Comparative information - leading to materials selection

Thus the range of what is wanted extends from the qualitative and descriptive to precise highly refined numerical information. What is available only rarely meets the needs of the engineering user in a manner that is wholly acceptable.

## WHO WANTS MATERIALS DATA AND INFORMATION AND FOR WHAT PURPOSE?

There are many groups of scientists and engineers who need materials data and information. Their diversity coupled with the range of uses to which they will apply the information creates many of the problems facing those who seek to provide them with the appropriate service. It is easier for those with data to think of the uses to which that data might be put than to consider dispassionately the real needs of the user.

An individual user is likely to have one predominant use for data, whereas the data are frequently used in several different ways by different users. This leads to compromises in the presentation of data in hardcopy form and opportunities for the demonstration of the advantages of flexible computerised forms.

Some of the types of user and uses are listed in the table below.

| Users | Uses |
|---|---|
| Chemists | Computer aided design |
| Corrosion | Databank building |
| engineers | Design |
| scientists | analysis |
| Database managers | development |
| Data | synthesis |
| evaluators | Evaluation |
| validators | Failure investigation |
| Engineers | Marketing |
| design | Property measurement |
| development | Purchase |
| production | Research |
| research | Sales |
| Information | Selection |
| brokers | Sourcing |
| officers | Substitution |
| Librarians | Validation |
| Materials | |
| manufacturers | |
| scientists | |
| suppliers | |
| Physicists | |

Where many have gone wrong in the past when aiming to provide an information or data service, is to consider only the possible uses instead of first seeking to satisfy the real needs of real users at a price that will provide a viable system.

### Materials Selection

There are many interpretations of what is meant by selection and by whom it is carried out. This has in turn lead to misunderstandings when some have said, for various reasons, that materials selection is not needed either by engineers or as a service from a computerised data base.

Simple aspects of materials selection are frequently invoked in answer to questions such as:

What is the nearest equivalent to ....?
What is like ... but a bit better in a particular property?
What is like ... but cheaper?
What is like ... but does not need to be so good in ...?
Can we use ... for?

Usually these questions assume that the response will be a material of the same generic group, ie another steel, another brass, another grade of a particular polymer. So it is also with many other questions of selection where a new design is being advanced to a prototype. The structural and mechanical design of the component itself is done with the assumption of a material from a particular generic group, and its related and connecting components. This is because the environment of a particular organisation is geared to the accumulated experience of certain materials, to the machining and fabrication process that relate to those materials and even to customers familiar with one material and loath to 'experiment' with a product made from another (see also reference 2).

Design standards that sometimes become quasi mandatory legal documents are often written with one material specified or implied. Phrases such as 'designs carried out according to standard XY9999 are deemed to satisfy the regulations' are not unusual. They are not written by the standards authorities but usually by government departments or regulatory bodies. Such a phrase does not make the standard mandatory but it does make it extremely expensive and time consuming for a designer to argue a case for the use of an alternative material. The consequence is that the use of the traditional material described in the standard is perpetuated.

Materials selection, when it is done in a widest sense, is liable to be done at the wrong stage in the design process. This is because the optimum physical shape of a component made in brass is unlikely to be the same as that for a component with the same function made from an injection moulded plastic, nor one from steel the same as one from a glass fibre reinforced polymer. So true selection involves carrying through several parallel design routes. Inevitably this will increase the cost and the elapsed time considerably, that is unless or until, CAD is fully integrated interactively with materials information.

One can also ask, is materials selection in the widest sense not done more frequently because of the poor availability of the information needed, because the systems have so far been less than adequate, because of bad experience with 'new and advanced' materials? What is certain is that it is extremely difficult to computerise selection procedures due to the need to add know how and experience to the numerical data accessed by the selection process. There are several materials selection programs available in the UK and elsewhere, some described in papers in this conference. Others may be found in reference 10.

Just data? what about experience and knowledge?

The sort of questions that need this kind of input are:

Where can I get ...?
What is ....?
What is this standard and where can I get it?
What was .... (referring to an old specification, or name)?
Who can tell me about .....?
What are the possible problems when using .... in this situation?
What is the in service history of .... ?
Who has used .... and for what?
Why did this fail?
Why did that succeed?

Data for production engineering, ie machinability, formability, weldability, etc is more qualitative than that for mechanical properties. Yet it is no less important. The best material in terms of its properties is no use if the required component cannot be made from it economically. Several programs exist for parts of this area. CUTDATA in the US, INFOS in the FRG, USIDATA in France and a series from the Welding Institute in the UK are a few examples of the many that are available. The Open University, reference 11, has a hard copy database as part of its course PT610 Manufacture Materials and Design. Beyond this they are seeking to develop a method of answering the questions who has used this material before, what shapes were made from it, for what purpose, and most importantly what was the result.

Capturing the experience of scientists and engineers before they leave or retire from an organisation is very desirable. We are far from doing this in a way that provides useful and reusable data.

## HOW IS THE DATA TO BE PRESENTED?

Within the limits of this paper one can only touch on the possibilities. The simple answer to the question is, 'in the form best suited to the needs of the user'. There are several possibilities.

### On-line systems

In the early 1980's it was frequently thought that the best solution to the problem of providing a comprehensive service to the user was to link the many individual and specialised databases through a 'gateway'. By this means the user made a connection on-line to a single point and was automatically routed to the database that best filled his need wherever it might be in the world. Rerouting would take place as the users needs developed from data to design method to simulation to production. This 'gateway' concept has now largely been set aside as the operational difficulties became apparent but individual and linked on-line systems have their place.

### Mainframe systems

At no time in the last few years has anyone seriously proposed setting up one database that would provide everything. The practical difficulties and colossal cost of such a venture have been obvious for a long time.

In addition to their speed and capacity main frame systems provided the most promising solution to problems of security, data control within a company, linking with other data sets and design, drafting and production procedures, and provision of subsets of data for specific projects. However the rapid development of desktop hardware has nullified some of the previous advantages of the main frame.

### Floppy discs for desktop use

A large number of organisations now sell or distribute their data on floppy disc. For some this medium replaces the hard copy catalogue and adds the flexibility of use of the computer database. ICI's EPOS, Engineering Plastics On Screen is a good example where the selection of the most appropriate ICI product is far easier than from the hardcopy catalogue. (Reference 6). CUTDATA from Metcut, reference 7, assisting in the planning of machining operations is also supplied on floppy disc. A great number of others are listed and described in references 3,8,9 and 10, and in the DOMIS database. (Reference 11).

The obvious problems of unauthorised copying, modification of the data by users without suppliers or user company approval, updating of all copies, correction of errors and many others are not very different to those when hard copy is the medium. They do differ in magnitude. Copying one disc takes seconds, photocopying a manual a little longer.

Despite the problems particular to those trying to make a living from the sale of their data, it does seem that the universal availability of suitable hardware will for support the use of floppy discs.

### WORMS and CD-ROMS

The hardware to make use of these media is not yet common on the desks of engineers. Systems using this technology are predominantly offering bibliographic and encyclopaedic information rather than numerical data. With one gigabyte of memory on a disc that will slip into a pocket there must be concerns about security. On the other hand one disc can also accomodate each additional updating of a database enabling easy reference to the data used on older projects and comparison between old and new data sets. They are also at present resistant to unauthorised changes.

The high cost by comparison with floppy drives and discs and the few databases available in this form both account for the slow take up of this technology.

One of the tasks that the CODATA Task Group on Materials Database Management has set itself is to carry out a cost benefit review of access to reliable, high quality materials data. It is proposed that a workshop should be set up to bring together economists versed in the assessment of databases in other fields, the database managers and the materials community.

## WHO IS DOING WHAT?

There are three categories of activity that need to be described. Some work is being done because international groupings of countries support work, some work is the result of nationally funded activities, and some is done by individual organisations or people within countries.

### International activities

There are three international groups active in the materials information scene, CODATA, the EC and VAMAS, in the order in which they started work on this subject.

### CODATA

The Committee on Data for Science and Technology, CODATA, was established in 1966 by the International Council of Scientific Unions. Its office is in Paris and member countries provide funding which is used in part to provide for travel by the individual members of its committees and task groups. Whilst scientific in its origins there is a growing emphasis on the requirements of industry. The Commission on Industrial Data, whose Chairman is Dr J.H.Westbrook, was cosponsor of the International Workshops at Fairfield Glade 1982, and Schluchsee 1985, (references 3 and 9) taking place.

The first of these workshops took a situation in which many individuals were saying 'something ought to be done' and turned it into one where groups of people and organisations started to do something. The latter is the most recent international workshop and its recommendations cover the whole scene of computerised materials data and its applications. There are over 30 recommendations and a full listing of who is doing what, now and in the future will be found in reference 12 to be published as an updating of reference 13.

In 1987 CODATA set up a Task Group on Materials Database Management. One of the tasks it has set itself is to carry out a cost benefit review of access to reliable, high quality materials data. It is proposed that a workshop should be set up to bring together economists versed in the assessment of databases in other fields, the database managers and the materials community. The Task Group also issues a Newsletter through CODATA Paris. Two issues are now available in the CODATA Newsletters Nos 42 and 43. (Reference 14).

CODATA is revising and extending its directory in a series of chapters, those on mechanical properties of materials and on corrosion are in preparation. These chapters will provide world lists of sources of data and information.

### CEC

In between the two CODATA workshops the CEC, Commission of the European Communities, proposed a five year programme for the development of the specialised information market that included materials databanks as one priority area. To assist in establishing how far understanding of the subject had progressed and what were the priorities for action, the Petten Workshop was organised in 1984. (Reference 6). Three CEC activities have produced much of value since the workshop. The main one is the Demonstrator Programme which is supported by the other two, the online European Directory DOMIS, and MATTERM, the multilingual dictionary of terms and definitions.

### The Demonstrator Programme

This programme has several objectives that are now being met and made public. The database managers from ten systems from five countries are working together to improve the access and user friendliness, setting standards for these and for the user manual, and the system operation. These databases are in different languages and have a wide subject spread. The first objective of an agreed code of practice has been acheived (Reference 15). The next objective that each should modify their system in accordance with the proposals in the code has also been done and now the awarenes programme is under way. Dr N.Swindells of Matsel Systems has played a major role as coordinator for the working group concerned with operating standards and codes of practice for materials databases. Seminars are being held in six EC countries to make make management, scientists and engineers aware of what is available, what has been acheived by the programme and what the future actions will be in the context of a European system. In time workshops will be organised to increase still further the feedback from users. A full description of the programme with its aims in the context of the development of the information market in Europe will be found in reference 16.

### DOMIS

The Directory of Materials Data Information Sources, DOMIS, is available on-line through ECHO. (Reference 9). It has been compiled from information from all the European Community countries and has about 250 records. There is the possibility that a hard copy version will be produced in 1989.

The directory provides the name of the source, acronym, type of source and full address with telephone and telex number. The materials concerned and their properties are listed together with the form of publication (which is not necessarily computerised), the language, search mode and other information.

### MATTERM

The multilingual dictionary of technical terms and definitions, MATTERM, is being compiled from terms used in the databases in the Demonstrator System. Some 2000 terms have been collected and their definitions researched using a wide range of source material. The intention is to provide this resource in all nine languages of the EC and to mount it as a subset of

EURODICAUTOM, the online dictionary of the CEC that like DOMIS is also mounted on ECHO. To enable the widest and most flexible use a hard copy version of this dictionary will be made available.

VAMAS

Shortly after the Petten Workshop the Steering Committee of VAMAS, the Versailles Project on Advanced Materials and Standards, approved the setting up of Technical Working Area 10 - Materials Databanks. This Working Area recently published its findings and recommendations for further work. (Reference 17). Proposals based on them have been approved by the Steering Committee. These are the compilation of a worldwide inventory of materials designation systems, a workshop for national and international standards bodies and users of standards to consider the implementation of the recommendations, and a series of round-robin tests of validation and evaluation procedures for raw data. The workshop is provisionally scheduled for November 1988 at the JRC, Petten, The Netherlands.

VAMAS also publishes a Bulletin, reference 18, that provides information on the progress of all the Technical Working Areas. Some but not all of the output from the VAMAS programme is restricted to the participants.

The following table enables a comparison of which country is involved with which activity.

| Country | CODATA | EC | VAMAS |
|---|---|---|---|
| UK | + | + | + |
| Federal Republic of Germany | + | + | + |
| France | + | + | + |
| Canada | + | | + |
| Italy | + | + | |
| Japan | + | | + |
| USA | + | | + |
| Australia | + | | |
| Belgium | | + | |
| Brazil | + | | |
| China | + | | |
| Denmark | | + | |
| Eire | | + | |
| German Democratic Republic | + | | |
| Greece | | + | |
| Hungary | + | | |
| India | + | | |
| Isreal | + | | |
| Luxembourg | | + | |
| Netherlands | | + | |
| Poland | + | | |
| Portugal | | + | |
| South Africa | + | | |
| Spain | | + | |
| Sweden | + | | |
| USSR | + | | |

The VAMAS countries are those of the Economic Summit group of nations and so are a closed group as are the countries in the European Community.

CODATA on the other hand being solely a scientific and technical organisation has no geographical boundaries.

In addition the CEC is also a member of VAMAS in its own right, though this does not make all the countries of the EC members.

National activites

The very significant participation of individuals and organisations in the UK in international activities to some extent compensates for the absence until recently of any national programme. The PROMAT, Profit Through Materials Technology, activity of the Department of Trade and Industry, DTI, aims to ensure that industry at large gives the attention to materials technology which its importance deserves and that companies know where to look for the expertise and advice which they may need to investigate and exploit particular opportunities. In addition the DTI has provided funds for the setting up of the Materials Information Centre within the Design Council (reference 19).

The French National CODATA Committee, several of whom had participated in the Petten and Schluchsee workshops, held their own workshop in 1986 with about 250 participants. This was followed by a second meeting in Bordeaux in November 1987 at which the databases compiled by CETIM, Centre Technique des Industries Mecaniques, were demonstrated.

In the FR of Germany there is at present no nationally coordinated activity but FIZ in Karlsruhe and in Berlin, BFI in Dusseldorf, the DKI in Darmstadt and others have well developed databases, are doing significant work supporting the development of computerisation and participating in international activities.

Dr Kozlov, the member of the CODATA Task Group on Materials Database Management from the USSR has compiled a list of over 200 databases dealing with subjects from rubber to those related to the environment.

China has a large number of databases mostly for use on personal computers and is active in CODATA. (Reference 21).

In Japan where some government funds are available for database development the most important related to materials are those on fine ceramics, fatigue, and steels and alloys. There is also considerable support and participation in the work of VAMAS and CODATA. (Reference 22).

In the USA three activities should be mentioned, one of which, ASTM Committee E-49 on the Computerization of Material Property Data, is open to all to join and support. E-49 came into being shortly after the Schluchsee workshop. There were participants from twelve countries at the recent symposium, and many from outside the US contribute to the work of the Task Groups.

There is no other such broad activity across the range of basic topics necessary for the establishment of high quality databases taking place in any other country. Even the CEC programme of work on materials does not touch on

many of the important aspects of the data that are of concern to E-49.

As at the meeting in November 1987 there were four subcommittees each with several task groups as follows:

E-49.01 Subcommittee - Identification of Materials

Objectives: to identify and select those descriptors and coding systems necessary to adequately describe and differentiate materials for a computerised materials database.

This Subcommittee has task groups on the identification of, metals and alloys*, ceramics*, composites*, and polymers*.

E-49.02 Subcommittee - Reporting of Materials Property Data

Objectives: to develop guidelines for the presentation of material properties data to be included in computerized materials properties databases. Specifically to list the metadata that it is necessary to record for test results to be useable, and the metadata that are desirable in addition.

This has task groups on reporting properties for use in computerized materials property databases and in particular reporting fracture test methods*, mechanical test methods*, fatigue test methods*, corrosion data*, and weld property data.

E-49.03 Subcommittee - Terminology

Objectives: to develop a standard terminology for use in building and accessing computerized materials property databases including definitions, units, symbols, nomenclature, and abbreviations.

E-49.04 Subcommittee - Database Interfaces and Functionalities

Objectives: to develop standard guides and practices to facilitate the transfer, processing, and presentation of materials data among distributed databases and users, including areas such as data exchange formats, data security, search and presentation capabilities, and data quality and reliability.

Here the task groups are concerned with materials data interchange formats*, and with data quality.

Several drafts are making good progress and it expected that they will either become standards in their own right or become part of existing standards for test methods.

This brief outline shows that E-49 is tackling the basic nuts and bolts of the materials database scene. It is to be hoped that the international participation in this Committee will increase so that the standards and guides produced will be applicable across all national standards from the start and a lengthy period of harmonisation of differing national products will not be necessary.

The other two activities are the MIST Project (Materials Information for Science and Technology), reference 19, and the National Materials Property Data Network Inc. reference 20. The MIST Project is a programmme to build a demonstration computerised materials data system and the NMPDM is similar in many aspects to the European Demonstrator. As it is not government funded it has had to take a much more commercial approach than the European programme.

Behind all the work in the US is the support of the Office of Standard Reference Data of the National Bureau of Standards.

## WHERE IS IT ALL LEADING?

Computerisation of information is not just a matter of blind copying from paper to disc, that would merely aggravate the situation and disseminate errors and misleading information more widely. It is easier to take and use data out of context from a computerised source than from a textbook or manual, and that is easy enough.

Slowly new tools are being made and old tools sharpened or modified to handle materials data in ways that are appropriate to the needs of present day science and engineering. If progress seems slow to those not directly involved it is because some parts of the work are extremely difficult, because in places there is a lack of government support, because all industry has not yet learned the true value of good data nor the true cost of that which is inferior. Reference 24 contains many papers that show an understanding of what can be achieved.

Hopefully as a result of conferences like this the number of those who understand what needs to be done will grow and they too will share in the work that has to be done.

## ACKNOWLEDGEMENT

The author wishes to acknowledge the pleasure, the interest and the stimulation that has come from listening to, and working and talking with those whose names appear in this paper and the references, and many others in the materials community.

## REFERENCES

1. A paradox in the development of computerized materials data systems. G.Ostberg, in Nonbibliographic data banks in science and technology. Papers presented at a CODATA/Unesco/DFI Seminar, Stockholm, 15-22 October, 1983. Editors S.Schwarz, D.G.Watson, O.Alvfeldt. Available from CODATA, 51 boulevard de Montmorency, 75016 Paris, France

2. Materials for profit. N.Waterman, Engineering, Vol.228 No.1, January 1988, pp16-18. Available from The Design Council, 28 Haymarket, London SW1Y 4SU.

* The asterisks after the task group subjects indicate that a draft is in progress.

3. Computerized Materials Data Systems. The proceedings of a workshop devoted to discussion of problems confronting their development, Fairfield Glade, Tennessee, USA, 7-11 November 1982. Editors J.H.Westbrook and J.R.Rumble. Available from The Office of Standard Reference Data, National Bureau of Standards, Gaithersburg, MD 20899, USA.

4. Materials Information Directory 1988. Editor K.W.Reynard. To be published in May 1988 by The Design Council, 28 Haymarket, London SW1Y 4SU.

5. Manufacture Materials Design, course PT6[illegible], The Open University, Walton Hall, Milton Keynes MK7 6AA.

6. Engineering Plastics on Screen, EPOS, The comprhensive catalogue of engineering plastics. ICI Petrochemicals and Plastics Division Engineering Plastics Sales Office, P.O.Box 90, Wilton, Middlesbrough, Cleveland, TS6 8JE.

7. CUTDATA, Machining Parameters Database, Metcut Research Associates, Inc. Manufacturing Technology Division, 11240 Cornell Park Drive, Cincinnati, Ohio 45242-1812, USA

8. Factual Material Data Banks. The proceedings of a CEC workshop at JRC Petten, The Netherlands, 14-16 November 1984. Editors H.Kroeckel, K.W.Reynard and G.Steven. ISBN 92 825 5322 1. Available from the Office for Official Publications of the European Communities, Luxembourg, reference EUR 9768 EN.

9. Materials Data Systems for Engineering. The proceedings of a CODATA workshop, Schluchsee, Federal Republic of Germany, 22-27 September 1985. Editors J.H.Westbrook, H.Behrens, G.Dathe and S.Iwata. ISBN 3 88127 100 7. Available from Technische Verarbeitung und Alleinvertrieb, Fachinformationszentrum Energie Physik Mathematik GmbH, 7514 Eggenstein-Leopoldshafen 2, Karlsruhe, FRG.

10. 1st International Symposium on Computerization and Networking of Materials Property Databases. ASTM Committee E-49, Philadelphia, 2-4 November 1987, proceedings to be published by ASTM, 1916 Race Street, Philadelphia, PA 19103, USA.

11. DOMIS, Directory of Materials Data Information Sources, ECHO Customer Service, 177, route d'Esch, L-1471 Luxembourg.

12. Schluchsee, Materials Data Systems for Engineering. The thirty recommendations, what's happened? K.W.Reynard and J.H.Westbrook. To be published.

13. Materials data and information. K.W.Reynard. Metals and Materials, Volume 2, No 3, March 1986, pp 147-150. Available from the Institute of Metals, 1 Carlton House Terrace, London SW1Y 5DB.

14. CODATA Newsletter. ISSN 0538 6918. No 42 November 1987, No 43 January 1988. Editor W.G.Jackson, The Institute of Metals, 1 Carlton House Terrace, London SW1Y 5D[illegible]. Availabilty as reference 1 or through the National Committee in each member country.

15. A code of practice, for use in the Materials Data Base Demonstrator Programme. MDP(Mat-02)-OS-03 1987. Available from Commission of the European Communities, DGXIII/B, Batiment Jean Monnet, Plateau du Kirchberg, L-2920, Luxembourg.

16. European Activities Towards the Integration and Harmonisation of Materials Data Systems. H.Kroeckel and G.Steven. To be published in reference 10.

17. Factual materials databanks - the need for standards. VAMAS Technical Working Area 10 Report July 1987. Editors H.Kroeckel, K.W.Reynard and J.Rumble. Distributed in the UK by the Division of Materials Applications, NPL, Teddington TW11 OLW. Elsewhere apply to the local VAMAS representative or to the Secretary of VAMAS, Dr B.Steiner, Institute for Materials Science and Engineering, National Bureau of Standards, Gaithersburg, MD 20899, USA.

18. VAMAS Bulletins. 1 to 7 issued, No 7 January 1988. Availability as for reference 17.

19. The Materials Information Centre, The Design Council, 28 Haymarket, London SW1Y 4SU.

20. Banques de Donnees Factuelles sur les Materiaux. Actes de la journee d'etude. Paris la Defense, France, 20 November 1986. Editor B.Marx. ISBN 2 906826 00 6. Availability as reference 1.

21. Materials Data Activities in China. L.Yunwen. to be published in reference 10.

22. Japan Progress on Materials Databases. S.Nishijima, Y.Monma and M.Kanao. To be published in reference 10.

23. Materials Information for Science and Technology (MIST): Project Overview. W.Grattidge, J.H.Westbrook, J.McCarthy, C.Northrup. NBS Special Publication 726. Available from the Superintendent of Documents, U.S.Government Printing Office, Washington, DC 20402, USA.

24. Overview of the National Materials Property Data Network. Dr J.G.Kaufman. Available from The National Materials Property Data Network Inc, 2540 Olentangy River Road, P.O.Box 02224, Columbus, Ohio 43202, USA.

25. The Promise of Advanced Materials. The proceedings of a Discussion Meeting held at the Royal Society 4-5 June 1986. Available from The Royal Society, 6 Carlton House Terrace, London SW1Y 5AG.

□

D. PHELAN

INSTITUTE OF METALS AND MATERIALS AUSTRALASIA
DATA BANK

D. PHELAN is in the Department of Mechanical Engineering at Chisholm Institute of Technology Victoria, Australia.

## SYNOPSIS

The development of an industrially acceptable mater als data base requires contributions from many different types of people having a wide variety of industrial backgrounds. The Institute of Metals and Materials Australasia is endeavouring to increase Australian industry's awareness of materials data bases while at the same time encourage it to contribute to and develop the Institute's materials data base.

## INTRODUCTION

Some two years ago the then federal Australian Department of Science sponsored two conferences/workshops to discuss areas of importance with respect to advanced materials. One of the outcomes of the conference was a short list of ten areas of research worthy of some concentration of effort and resources. Included in this list was a reference to materials data bases. At the time of this recommendation, there was no substantial work being carried out any-where within Australia into computerised materials data bases and it would be a fair comment to suggest that most, if not all of Australian Industry had little or no experience with materials data bases. Consequently, the Institute of Metals and Materials Australasia (IMMA) decided to initiate a pilot study of the requirements of a computerised data base suitable for Australian conditions. IMMA was aware of the difficulties involved, and the scope of the task needed to be undertaken, if an industrially acceptable data base was to be developed. Ostberg [1] has pointed out the paradox associated with computerized materials data systems where most such systems have only been used by those involved in their respective developments, while Westbrook [2] has discussed ' degree of difficulty associated with de nition and standardization of data.

Initially, it was proposed that po tial users should be canvassed as to thei views and expectations of a computerised materials database, however, it soon became ap a nt that because of the above mentioned lack e xp re of Australian Industry to materials data bases, no firm opinions were held with respect to the structure of such, apart from the belief that a need for data bases existed. It was therefore concluded that before industry could be expected to constructively contribute to defining their requirements, they would need some form of exposure to materials data bases.

## STRUCTURE

IMMA subsequently decided to construct an initial data base of some three hundred and fifty metals and alloys which could be thought of as a sample or starter data base. In addition, it was proposed that the data base software should provide users with editing facilities to allow for personal customising of data in order to help them define their requirements. The editing emphasis dictated the need for the proposed system to run on a personal micro computer and it was decided that an IBM PC or compatible would be used. Users of the system were seen as potential sources of data, and a user group was envisaged as being set up once some degree of experience had been developed in the use of the system. It was decided that the material record structure should simulate that which is common to many material data handbooks. Namely:-

1. Prior uses and applications.
2. Chemical composition.
3. Related specifications.
4. Mechanical properties.
5. Property rankings within a material system.

A full record structure showing the above five fields for the wrought copper alloy CC601 is shown in figure 1. One reason for the slow growth in the commercialization of materials data bases as discussed by Ostberg [1,3], is the difficulty of quantifying or qualifying all aspects of material data or material performance. Many material applications have been developed empirically and although there may always be a relationship between basic material quantitative data and application the link is often very obscure. Therefore, while not under rating the importance of quantitative data, it was felt that an important aspect of the IMMA data base should be a text field containing the main material uses and

applications, and, in addition, interrogation of this field should be possible via text query searching.

## SEARCHING

The software used to write the IMMA programme is a fourth generation package which incorporates a pattern matching algorithm allowing for text searching which is considered to be one of the strengths of the system. The use field which can contain up to two thousand characters, contains references to prior uses, applications and a general description of a material's main properties and functions. The IMMA data base will supply, via text searching, materials whose use field contains key words or approximations to key words searched on. Furthermore, the list of selected materials will be ranked in order of degree of match between the text query and the use field of the selected records.

Figure 2 shows the results of a text search of cast aluminium alloys using "high strength and corrosive resistant" as the search query. The list of suitable matches, places the alloy CC601 at the top due to the reference to both strength and corrosion resistance (as opposed to corrosive resistant). A similar response would have been obtained using the query " corrosion resistant and high strength".

The material selection part of the design process is not easily defined and varies from a designer making repeated use of a familiar commercial specification, through to a full translation of component functional requirements into quantitative property values followed by a data bank search. Albeit an anathema to the material scientist, text searching of the use field allows for a replication of one common way in which engineers go about selecting materials, that is, selection based upon prior uses and applications.

Text searching also provides for the inclusion of data on difficult to quantify properties, as well as allowing for the inclusion of all possible combinations of properties. Any special property possessed by a material can be referred to in the use field, as opposed to having one vast property encompassing template which would give a very unwieldy record structure. Also provided is an immediate classification of product types such as thin walled die castings, crankcase housings, etc., which can be searched on.

The pattern searching can also be used to search through the specifications field which, as well as containing international specifications, also includes common commercial trade names. The specification search option provides for searching for an exact match, where the specification to be searched on can be accurately detailed such as LM26 or in the case of searching for an obscure, vaguely remembered trade name, approximate matchings can be listed.

Alloys contained in the starter data bank have a full chemical description with chemical searches done by specifying upper and lower limits for one or more elements. The mechanical properties associated with the starter data base vary with alloy system, but are restricted to the types more generally found in text and material data handbooks. No attempt has been made to place any statistical significance on the mechanical properties quoted, except to state that they are either minimum or typical values. It is possible for the user to change the structure of the mechanical property file of any alloy system within the data base to include additional properties, and subsequently add their own data. Searching, using minimum mechanical properties, is provided for. Within any one alloy system, non-numeric rankings (A-D) are given for groups of properties, with the properties contained within each group varying with alloy system. For instance, pressure tightness is an important property of cast aluminium alloys, but of no importance within the wrought aluminium alloy system. Searching on these ratings is there-fore restricted to one alloy system per search.

## SCREEN PRESENTATION

The screen presentation is such that most data for a particular material can be included in one screen display. Windowing and scrolling allows for the displaying of up to two thousand characters in the use field, and the mechanical properties of as many tempers as are present, for any particular alloy. Only seven of a material's mechanical properties can be displayed on the screen, even though the data base may contain many more. If more than seven are present, the user can select, via the editing facilities, which seven are to be included in a full screen display. It can be argued that most users would not be interested in more tnan seven mechanical properties at any one time. To fit most of the data associated with one material record into one screen display it is necessary to use abbreviations and special IMMA alloy designations. These abbreviations are explained by help screen pages which are obtained by pressing the relevant alloy special function key F1, F2, F3 etc., at any stage of running the programme.

## EDITING

All of the data contained in the data base, which is password protected, can be edited by the user, and the mechanical property files can be modified to allow for the inclusion of any additionally required mechanical properties. Furthermore, it is possible for the user to introduce into the data base a completely new material system including all property fields that are to be associated with this new system. Indeed, early indications suggest that many users have intentions of using the programme to develop their own-inhouse specialized data base, as opposed to requiring a large general purpose data base. After a new material system, and the associated data, has been inserted into the data base, it can then be downloaded onto a floppy disc backup, which can be used to transfer this new system into another user's data base, using the main menu import option. It is proposed that this transportation of data will occur within a user group, with IMMA acting as an intermediary vetting agent. As well as allowing for the introduction of new material systems into the data base, existing ones may be overwritten and updated.

## FUTURE DEVELOPMENTS

A polymeric data base is planned for the near future, but with a slightly different structure from that of the metals one. It is also proposed that a front end should be attached to the data base which would assist users to select which material system/s to consider.

## CONCLUSIONS

A computerised metals data base has been constructed which can be compared with the structure of many engineering materials handbooks, that is, at this stage of its development it is seen as just another material reference source, though a powerful one, which may provide a solution to a material selection, specification or chemical query, etc. problem. The driving software is expected to be periodically altered in response to users' recommendations, and the development of the data base assisted by user data input as provided by the programme's editing functions.

## REFERENCES


1. Westbrook J.H., "Some considerations in the design of properties files for a computerized materials information system," The Role of Data in Scientific Progress, P.S. Glaeser (ed.) Elsevier Science Publishers B.V. (North Holland) CODATA 1985.
2. Ostberg G., "A Paradox in the Development of computerised Materials Data Systems," Materials & Design vol. 5 February/March 1984.
3. Ostberg G., Rydnert B., Normann R., "Conditions for Development & Operation of Computerised Materials Data Bases", The Role of Data in Scientific Progress, P.S. Glaeser (ed.) Elsevier Science Publishers B.V. (North Holland) CODATA 1985.

ALLOY : CC601 Used in applications where corrosion resistance combined with high strength is required. Used in food, chemical, marine applications and in pa rticular automotive wheels. Its potential is increased by heat treatment.

| | | | | |
|---|---|---|---|---|
| Si 6.5-7.5 | Fe 0.20 | Cu 0.05 | Mn 0.05 | Mg 0.25-0.35 Cr - |
| Ni - | Zn 0.05 | Pb - | Ti 0.20 | Al Rem |

PREV. A.D.C. - BS LM25 AL ASSCTN. A356.1
EURO_ALLOY AlSi7Mg JIS C4CV OTHERS B135

| ALLOY | TEMPER | TYPE | MIN UTS MPa | TYP UTS MPa | TYP YLD MPa | MIN ELONG % | TYP ELONG % | BRIN HARD | FAT STR. MPa |
|---|---|---|---|---|---|---|---|---|---|
| CC601 | T1 | P | 140 | 195 | 95 | 3 | 6 | - | - |
| CC601 | T1 | S | 130 | 160 | 90 | 2 | 5 | 55 | - |
| CC601 | T5 | P | 170 | 180 | 140 | - | 6 | 60 | - |
| CC601 | T5 | S | 155 | 180 | 130 | - | 3 | 60 | 55 |
| CC601 | T6 | P | 220 | 275 | 185 | 5 | 10 | 100 | 90 |
| CC601 | T6 | S | 205 | 255 | 185 | 3 | 5 | 70 | 60 |

| S-CAST | P-CAST | D-CAST | CORR. RES | MACH | PRESS. TIGHT | WELD |
|---|---|---|---|---|---|---|
| A | A | - | A | B | A | A |

SPACE BAR FOR MORE TEMPER PROPERTIES Q TO QUIT

Figure 1.

CC601
Used in applications where corrosion resistance combined with high strength is required. Used in food, chemical, marine applications and in particular auto motive wheels. Its potential is increased by heat treatment.
AC601
Used in applications where corrosion resistance combined with high strength is required. Used in food, chemical, marine applications and in particular auto motive wheels. Its potential is increased by heat treatment.
AA319
Used for special automotive pistons. Low thermal expans.on rate combined wi th high hot strength and good wear resistance.
AC603
Easily cast into sand or permanent moulds. Exhibiting good electrical condu ctivity and high strength.
AA603
Easily cast into sand or permanent moulds. Exhibiting good electrical condu ctivity and high strength.
AA607
Good fluidity and corrosion resistance combined with hardness. Extensively used for low pressure permanent mould castings.

SPACE BAR TO CONTINUE OR P TO SEE PROPERTIES OR Q TO QUIT

Figure 2.

G S Dodd and A H Fairfull

# KNOWLEDGE-BASED SYSTEMS IN MATERIALS SELECTION

Mr Dodd and Dr Fairfull are with Matsel Systems Limited, Cunard Building, Liverpool L3 1EG

## SYNOPSIS

Effective materials selection in design is crucial to the creation of successful products. At the conceptual stage the approach must be problem-oriented and consider all materials objectively, avoiding restraints other than those imposed by the design brief. The components of design can be generalised as the interactive parameters of shape, material and manufacturing method. The conceptual design specifies each of these within fairly wide limits, leading to the recommendation of the most suitable materials class. The problem-oriented approach can then be re-applied, provided that detailed information is available. Since the parameters are interactive, an optimum solution requires the facility to refine the specification iteratively. Neither a database nor a question and answer type expert system can provide these features satisfactorily, and it is preferable to use a knowledge-based system. An example of such a system, called PERITUS, is described.

## INTRODUCTION

Information about engineering materials can be divided into two broad categories; data, and knowledge. Data can be defined as the results of measurements, whereas knowledge represents the connections between items of data - this knowledge coming from, and contributing to, an understanding of the results. In using materials information within engineering, some applications require the use of data, some the use of knowledge, and some a combination of both.

Collections of data and knowledge exist in 'systems' such as books, reports, libraries, computer packages etc. The usefulness of such systems is determined by their structure and means of operation, the origins of the information they contain, and the user interfaces by which the information is extracted. The success of systems developments for specific applications depends on conscious design for appropriate interaction of these components - such applications include materials selection for new designs, provision of data for design calculations, provision of information for purchasing, creation of knowledge from existing collections of data, and support for the creation of new standards.

Each application requires a different system design, and particularly in the case of computer packages it has become clear from recent experience within the EEC and elsewhere that a single, universal system is not practically achievable.

## PROBLEM ORIENTED MATERIALS SELECTION IN DESIGN

The selection of materials at the conceptual stage of design is the most potentially complex application, and also has the most far-reaching implications. The problem oriented approach involves breaking down the design brief into a number of smaller problems or requirements, which are then satisfied individually or in combination. The advantage of this technique is that the resulting solutions are more likely to be novel and closer to the optima, when compared to the alternative approach of making calculated 'guesses' and subsequently checking their viability.

The methodical breaking down of the design brief into component tasks allows it to be viewed objectively, enabling possibly innovative solutions to be produced which still incorporate the necessary performance aspects. It has been shown (1) that information is required about four factors:

- the purpose or FUNCTION of the item to be designed
- the PROPERTIES of the MATERIAL from which it will be made
- the MANUFACTURING METHOD by which it will be made
- the SHAPE and dimensions of the item.

The last three factors are interactive variables, and since the fixing of one or more of them has a determining influence on the others, a system which supports the design function should include the capability to allow for these interactions. Many design problems for example are initiated by re-assessment of an existing product for which a material has already been successfully utilised. In order to apply the problem oriented approach in this situation, it

is necessary to re-consider the functions performed by that material along with the other functional requirements of the design. Thus the 'old' material may provide stiffness along with resistance to corrosion, whereas a new design might combine the functions differently by adapting the shape of the component to provide stiffness from a cheaper, low modulus material with the same corrosion resistant capabilities.

This kind of approach requires ready access to information about a wide range of materials and processes, it being fundamental to the success of the method to consider not simply 'expected', familiar or similar materials. Also, since in general the creation of new products involves cooperation between design engineers and materials specialists, each of whom draw on both world knowledge and personal (company) experience, a further requirement is the capability to handle both world and company-specific knowledge as appropriate.

## SUITABILITY OF TYPES OF COMPUTER SYSTEM FOR MATERIALS SELECTION IN DESIGN

### Data Bases

Most computerised collections of materials properties are organised into the form of data bases, or data banks, which typically have fixed record structures and search procedures. A disadvantage of this type of system for design applications is that as a consequence of the fixed structure there are invariably gaps in the data for certain combinations of material and property. Searches for materials with particular property values thus reject materials with inadequate values AND materials for which the properties have not been measured.

Since in general there is no facility to display the data base contents in advance of the search procedure, it can be difficult to establish whether the system contains the information required for particular design problems. Data bases are more effective at a much later stage in the design process when the material name has already been identified, and the system can then be used to display the properties associated with that particular material and its condition.

### Expert Systems

Expert systems have been developed (2) for supporting the materials aspect of the design function, as indeed they have been applied to other areas of traditionally human expertise. These systems can be described as collections of experience stored as rules. For practical purposes they can only be applied in situations where the task is well defined, and where the full range of knowledge is small enough for the rules to be readily established in advance.

In practice, the design of the user-interface to expert systems can make them frustrating to use if based on a simple method of question and answer. In the absence of a facility to view the total system content, the user's specific requirements cannot be formulated in terms of the knowledge which the system contains.

### Knowledge Based Systems

Research carried out by Matsel Systems Limited has shown that neither data bases nor rule-based expert systems are ideally suited to solving the general problem of materials selection in innovative design, and that this has led to scepticism over the suitability of computer systems in general for this application. The nature of the problem is that each design situation has sufficient originality such that, by definition, the rules for dealing with it cannot be anticipated in advance. A system is therefore required which establishes the feasibility of new situations as they arise, using existing data and knowledge. Since a problem can often be approached in several different ways depending on the preference of the user, the system must also be able to accommodate different approaches with equal ease.

The range of possible problems is very large, and it is therefore necessary to avoid excessive numbers of outcomes. This is accomplished by building the system around a methodology for approaching the problem, incorporating sets of general scenarios (which can be displayed in advance) to limit the scope, and providing some form of interactive optimisation procedure to assist in finalising the solutions. The PERITUS system and its user interface were designed in terms of these requirements, and a description of the system will show how they have been addressed.

## THE PERITUS MATERIALS SELECTION AND EVALUATION SYSTEM

The concept of the PERITUS system has been described in more detail elsewhere (1) but briefly it consists of three main parts or stages. In order of use of the full system, these are as follows:

(i) The Director stage initiates the process by considering the fundamentals of conceptual design. This enables an analysis of the general requirements to be made in terms of the possible combinations and interactions of shape, material and processing method. The analysis identifies appropriate manufacturing methods and general classes, or sub-classes, of suitable materials.

(ii) The Presort stage enables a more detailed examination of the requirements to be made at the embodiment stage of design, and operates within individual materials classes. The Presort search procedure can be introduced from sub-classes recommended by the Director stage, from qualitative or quantitative more specific design requirements, or from the basis of a known material on which it is wished to improve. By any of these approaches, the objective is to arrive at a shortlist of candidate materials.

The Presort stage is itself knowledge based - for example the effects of section size, shape, and processing method on material properties are considered.

(iii) The Evaluation stage is intended to allow the unranked shortlists produced by the Presort procedure to be considered in more depth, and to suggest means of ordering the shortlists to help to achieve optimum decisions. This evaluation is carried out by a graphical comparison of material

property profiles with, importantly, no weighting factors since these would distort the overall interpretation. The graphical display represents a distortion-free profile of the combination of properties.

The role of the user interface to PERITUS is to present the system in such a way that the user can formulate his own ideas within the context of the system content. The user interface to all parts of the system is based on the GEM graphics environment (3) which provides facilities for windows and drop-down menus. In association with the facility to scroll through the content of each materials class, this ensures that all the information contained in the system can be dispalyed. Unlike the question and answer approach, the profile of requirements can be built up in any order as the user's ideas develop. Requirements set earlier can be returned to at any stage and altered, and the implications examined for any or all of the resulting combinations. Also, by creating the system in modular form, modules can be added or modified to deal with particular materials classes or knowledge - thus some modules can be based on company or private knowledge, whilst others are based on public knowledge.

PERITUS is an on-line service accessed via the public data network. The central computer controls access to private/public information, automatically logs operations carried out by users, and provides for instant updates to the distributed outlets. The user interface is a suite of programs which enables an IBM PC or its equivalent to be used as a local terminal. Thus the control of the windows and menus is done in the terminal and only the essential search information is sent over the data network to and from the central computer.

At present the Presort and Evaluation stages make up the commercial release of PERITUS. In this form, the user must make the initial decision about which class of materials to examine. The Director stage, with the unique capability to consider shape and processing methods across different materials classes, is in advanced prototype form and will soon be commercially available to enhance the existing product.

## CONCLUSIONS

1. Materials selection at the conceptual stage of design is best accomplished by a problem oriented approach whereby the design brief is broken down into a number of smaller components. This method is most likely to produce optimum or novel solutions which still satisfy the functional requirements.

2. The interactions between shape, material properties and manufacturing method must be included in any design procedure. These factors cannot be considered in isolation.

3. Neither data bases nor question and answer type expert systems are ideally suited to solving problems of material selection in conceptual design. This has lead to scepticism concerning the ability of computer systems in general to fulfill a useful role in this application.

4. Recent research has shown however, that knowledge-based systems, such as the PERITUS system, can tackle design problems using a problem oriented methodology, and that it is in this area that future rapid development is likely to occur.

## References


1. Swindells, N & Swindells, R. J., System for Engineering Materials Selection, Metals and Materials, 1 (1985) pp. 301-304.

2. Fehsenfeld, B. et al, Expertensystem zur Anwendung Neuer Werkstoffe, German Chapters of the ACM, 28 (1987) pp.198-209.

3. GEM is a trademark of Digital Research Inc. and Digital Research (UK) Ltd.

M. TISZA - L. TOTH

# A COMBINED MULTI-PURPOSE DATABANK FOR COMPUTER AIDED ENGINEERING

Dr. Tisza and Dr. Toth are at the Department of Mechanical Engineering, Technical University of Heavy Industry in Miskolc

## SYNOPSYS

A properly built CAD/CAM system should be based on a unified database containing a large amount of information on geometric parameters, material properties, technological and tool parameters. Analysing realized CAD systems, it may be stated that material databases are not generally involved. The paper analyses a complex CAD/CAM system which contains material databases as a fundamental part of the integrated system.

## INTRODUCTION

In recent years, mechanical engineering may be characterized by rapid development and wide-spreading application of Computer Aided Engineering (CAE). It involves from the beginning of product design, through the geometrical modelling, technological and tool design, process planning, NC-postprocessing, up to the control of manufacturing processes the whole process of engineering activity. In a properly built computerized system all the forementioned processes are based on a unified database as a central part of the system. This database should contain a large amount of information including geometric parameters, material properties, technological and tool parameters, etc.

Analysing the database structure of existing CAD systems, it may be stated that they are well equipped with all the necessary geometric information concerning the geometric modelling but they include significantly less data on materials. This is certainly due to the fact that CAD systems are generally developed by computer scientists and design engineers not by material scientists /1/.

In our opinion, material databases should be a fundamental part of an integrated databank. In this case, CAD systems are capable to carry out various optimization tasks taking material properties into consideration, as well.

At our department an integrated CAD/CAM system has been developed for multi-purpose application /2/. It can be applied for very different purposes involving material selection for various constructional, technological and tool design processes (eg. testing of materials, dimensioning of different structures, heat-treatment, metal forming, machining, welding, etc.), as it is shown in Fig. 1.

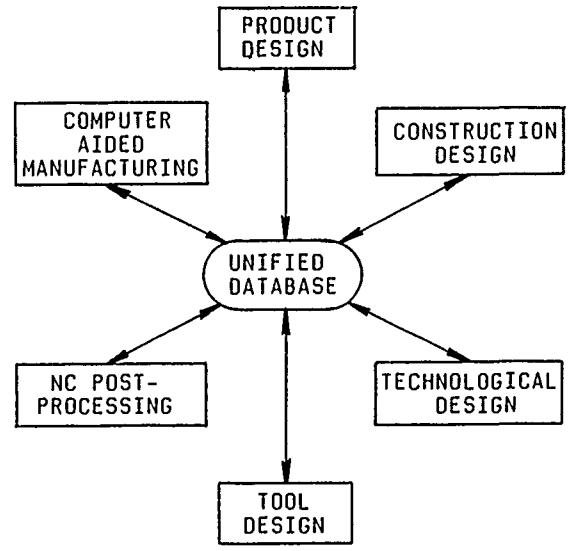


Fig. 1.
General scheme of complex CAD/CAM system

The system has been developed following a modular build-up principle. It means that each modul (e.g. product modelling module, technological design module, etc.) can be applied independently and as a part of the integrated CAD system. Each module is based on a unified database since many data stored in the databank may be important for each module.

In the following, the system will be analysed first of all from the wievpoint of multi-purpose database system. Owing to the limited extent of the paper only two short examples will be shown about the multi-user application. One of the examples may be regarded as a constructional, whereas the other as a technological application.

## THE UNIFIED DATABASE

There are generally three main classes of databases: hierarchical, network and relational /3/. In hierarchical databases, data-element have a father-son relationship. Different elements can be found by moving up and down tree structures. In a network database, the elements are linked together in closed loop whilst in relational databases elements can be accessed by key attributes. Our database takes the advantages of each of these three types, although it mainly hierarchical and ralational. In the following, only the material database will be analysed.

Since it is a database for multi-purpose application it contains a large amount of data accessable for different users. Thus, it is very important that database should remain independent of application programs, but it should provide the necessary access for them. It is assured by the special database management system.

The main modules of database management system are the database utilities module, the administrator and the working module.

The database utilities module is used to create and maintain the database, to determine keys, master schedules and the links between them. It can provide also special utilities: listing, reporting, etc.

The administrator module is used to set up sophisticated security and access rights. A security and access level is allocated for each user and it makes possible to access only those databases he needs. The access is realized through the working module.

Creating the database structure and database management system, it have to be kept in mind that various data in databases are not of equal importance for individual users.

Thus, there are some data which are necessary for each module in the whole integrated system and there are many groups of properties which are important for some special modules (e.g. forgeability for metal forming module, weldability for welding module, etc.). Thus, data on materials are structured in several groups. There are some basic data which identify the material (e.g. material designation, code of standardization, chemical composition) these are regarded as primary data. In secondary data-groups material properties of different kind can be found (e.g. mechanical properties like ultimate tensile strength, yield limit, etc., fracture mechanical properties like fracture toughness, etc., technological parameters like formability, machinability, etc.).

## EXAMPLES OF APPLICATION

Considering the limited extent of the paper, two special applications will briefly be analysed: one of them is a construction design type, whilst the other is a technological one.

### Application of combined database for design of welded structure possessing initial cracks of known size.

It is well known that operating structures often contain cracks of different sizes arising from either manufacturing or operating conditions. Thus, it is a frequent demand to give reliable answer for many questions in connection with the conditions of further applicability of these structures, e.g.:

- What type and size of cracks may be permitted for a given structure under given operating conditions?

- How long can this structure work without the risk of failure, etc.

These types of questions can be answered on the basis of theory of fracture mechanics. For this purpose a modular program-system has been developed. This program-system basically consists of three main modules:

(1) A database-handling module
The main task of it to assure the access to the main database described formerly. It is used first of all for material selection taking fracture mechanical aspects into consideration.

(2) Module of structural elements
It contains a large amount of information on various structural elements (concerning geometric parameters, mechanical models, etc.).

(3) Computational module
It carries out the necessary calculations based on the theory of fracture mechanics taking into consideration both the material properties and the specifics of structural elements. This module is capable of carrying out various calculations, e.g.:

- in what conditions can the supposed crack propagate;
- how long can the structure be used at a given level of cyclic loading without the risk of failure, or

- how large loads can be applied to achieve a given life-time;
- how can the operating conditions effect the life-time, etc.

All the forementioned questions and many other design tasks can be solved utilizing the possibilities provided by the interactive dialogue system.

## Application of combined database to manufacturing processes

Following from the main research fields of our department, most of the application programs have been developed for technological and tool design of various mechanical technologies (e.g. machining, metal forming, heat-treatment, welding, etc.). In the following, the program-package elaborated for metal forming will be analysed /5/.

This program-system is capable of designing both sheet and bulk metal forming processes, involving blanking, piercing, cutting, bending, deep-drawing as individual sheet metal forming technologies and as complex sheet metal forming in progressive dies, as well as upsetting, several types of extrusion and wire-drawing.

These pogram modules are also capable to determine blank shapes and sizes, to elaborate various layout alternatives for optimum material utilization, to calculate technological and tool parameters, to carry out process planning, etc. All these modules are based on the unified database containing a large amount of information both on raw and tool materials.

## CONCLUSIONS

In this paper a complex multi-purpose CAD/CAM system was analysed from the wievpoint of unified database. On the basis of it, the following main conclusions may be drawn:

- A unified database should be the central part of any CAD/CAM system.
- In engineering applications material databases should be an integrated part of the unified database.
- Material databases should contain a large amount of information both on raw and tool materials.
- Since material databases can be used for very different purposes, various data are not of equal importance for different users. Therefore, database should be carefully structured according to the demands of application programs.
- Since the unified database can be accesed by different users owing to its multi-user character, it is very important that it should remain independent of application programs, but it should provide the necessary acces for them.

## REFERENCES


/1/ THOMPSON, W.: CAD/CAM - A state of the Art, 2nd ICTP Conf. Stuttgart, 22-28. August. 1987. p.11-124.

/2/ TISZA, M.-ROMVARI, P.-RACZ, P.: A complete CAD/CAM Package for Sheet Metal Forming, 26th MTDR Conf. Manchester, 17-19. Sept. 1986. p.33-39.

/3/ GRUM, J.: A material database, 26th MTDR Conf. Manchester, 17-19. Sept. 1986. p. 23-29.

/4/ TOTH, L.: The reliability of cracked structure elements, 9th Int. Colloquium on Mechanical Fatique of Metals, Smolenice, 29-30. Nov. 1987.

/5/ TISZA, M.: A CAD/CAM system for deep-drawing, 2nd ICTP Conf., Stuttgart, 24-28. August. 1987. p. 145-152.

B. Fehsenfeld, S. Harris, R. Küke

# Expert System New Materials - Fibre-Reinforced Plastics

Krupp Forschungsinstitut
Münchener Straße 100
4300 Essen 1
FRG

SYNOPSIS:
Expert systems are technologically the most advanced knowledge-based systems. They make it possible to present and process knowledge which is resident in the form of facts and rules. They can be used equally for analysis, interpretation and diagnosis as well as for synthesizing, planning and configurational tasks. In the conceptual product design phase expert systems can usefully complement the existing CAD systems since the actual design drawing phase is preceded by a longer phase for specifications preselection and decision-making in which the possible solutions for the product to be manufactured have to be compared from various points of view. Beyond this expert systems can further support the designer in for example, the selection of new engineering materials such as cermets, p/m products and fibre-reinforced plastics, which are being increasingly used in more and more applications. Just such a "New Materials" expert system for fibre-reinforced plastics has been developed at Krupp Forschungsinstitut, the Group's central research establisment. In it dimensioning, production and cost-efficiency have been implemented. This expert system helps the designer who is used to working with conventional metallic engineering materials to come to terms with new materials. In its current stage of development the system is geared to clarifying the question, so significant in mechanical engineering, as to whether a metal component subject to external stress can be costefficiently replaced by a fibre composite.

## 1. INTRODUCTION:

More and more new engineering materials with enhanced properties are thrusting forward from the area of basic research into practical application. Vigorous research activities[1] in fields such as ceramics, powder metallurgy and fibre composites - to name but a few - are providing additional impetus.

Assessing new materials for use in machinery and industrial plant requires domain knowledge that is seldom available in the design and engineering departments maintained by plantmakers and machine builders. In order to remedy this deficiency an expert system was developed which can provide advice for designers and engineers faced with the problem of introducing new engineering materials. Without the knowledge processing software which has increasingly been adopted over the past few years it would have been impossible to tackle such a complex problem with even the prospect of success. Fibre-reinforced plastics were chosen as a first venture into the complexities of new materials application. For this group of materials many years industrial experience is available. Such materials are used almost routinely in aircraft construction and lightweight structures, for example. And machine builders and plantmakers, in particular, often encounter problems which could be solved by fibre-composite properties such as high strength, low thermal expansion and high corrosion resistance. This is shown by numerous solutions which have actually been realized such as the carbon-fibre-reinforced rotary spindle[2], the carbon-fibre-reinforced robot arm[3] and fibreglass reinforced leaf springs for commercial vehicles[4].

## 2. THE PROBLEM AT HAND

The task of the system outlined here is to investigate load-bearing metal components and select those which from the technical and economic points of view are potential candidates for replacement by fibre composites. This investigation takes place ahead of the actual design process and represents a feasibility analysis.

With fibre composites, by contrast to metal, the design engineer has no resource to a clearly defined range of proven materials. Rather, he has to match material properties to the given application by selecting the appropriate fibre and resin and suitably building up the laminate. Even during the design phase the question of manufacturability has to be borne in mind. The usual manufacturing techniques such as pultrusion, filament- winding, hand-laminating and lay-up impose major manufacturing constraints which have to be taken into account at an early stage. The decision as to whether a metallic component can be replaced by composite materials requires wide-ranging domain knowledge. The entire genesis of a fibre-composite component has to be considered, from material selection through proportioning to manufacture. This strongly intermeshing process which takes place during the decision-making phase is incorporated in the expert system outlined here.

## 3. MADE OF OPERATION

### 3.1 FORMS OF KNOWLEDGE REPRESENTATION

Knowledge representation in the computer must be matched to the problem at hand and indirectly support its solution. This is of fundamental importance for the performance capability and upgradability of an expert system. Widely used knowledge representation devices are semantic networks, frames, scripts, predicate logic and rules[5]. For the domain specific knowledge (fibre and resin properties, material compatibilities, manufacturing techniques, design methods) and application specific knowledge (component properties, operating conditions, optimization criteria) available in the present case, hybrid representation was the obvious choice. Frames are used to present declarative knowledge or facts while rules are a vehicle for encoding procedural knowledge.

The frame concept[6] is particulary well suited to describing objects existing in the real world, viz, by their properties and their relationships. In Fig. 1 knowledge about the material is represented in a frame structure. Each object possesses the properties that are typical of such an object. Objects of the same type are combined in classes and these, if possible, in meta-classes. Apart from the materials, production techniques,

component description and suggested possible solutions were also represented in an frame structure.

A production rule system[7] and the associated knowledge is of a quite different nature. It is the obvious way of encoding heuristics which are normally only weakly structured. Production rules are a formal way for the decentralized representation of recommendations, instructions and strategies. By way of these simple IF-THEN rules it is possible to link objects of the most widely differing types and draw conclusions depending on object properties. Dynamic knowledge in its entirety was represented in a production rules system. Apart from search-strategy representation, this includes checking on the compatibility of object statuses in materials selection proportioning methods and production processes.

3.2 SYSTEM ARCHITECTURE:
Fig. 2 shows the architecture of the expert system. The component to be investigated is specified interactively via the man-machine interface. Menu and window capabilities permit rapid and error-free input of the mainly verbal component description. The system proposes plausible basic assumptions. Questions are aked concerning the material used, geometry, dimensions, design peculiarities and type of loading. Operating conditions are described in terms of the thermal, chemical and physical stresses to which the component is subjected and which may affect the properties of the material used.

The component's functionality is defined by stating the principal mechanical stresses.

After describing actual status, relating entirely to the metallic component, the desired condition of the hypothetical fibre-composite component has to be specified. Desirable and undesirable component properties as well as possible unchangeable parameters such as restricted dimensions are fixed. Weight and cost of the fibre-composite component are evaluation criteria for possible solutions.

Entries are checked for completeness and consistency. Only then does the search begin for a solution embracing a fibre/resin/production-process triple compatible with the technical and economic specifications input by the user.

The search space is determined by the variables fibre, resin and production process. Proceeding from the completely undefined starting condition, a search tree is generated. Step by step, nondetermined variables are specified or existing partial solutions refined. Fig. 3 is a schematic of such a search tree. A solution refinement means that within the object hierarchies for fibre, resin and production process the next lowest level is selected. Compatibility rules ensure that nonsensical partial solutions are blocked and removed from the search process. This prunes the search tree and speeds up the search. Evidence rules, operating via heuristic rating functions for component weight, component cost and agreement with the requirements profile determine which partial solution is to be detailed. Only the partial solution with the best rating is processed further. This search strategy is known in the literature as "best- first"[8,9]. An overall solution has been found when a partial solution can be refined no further and possesses the best rating.

The expertise of the system is a list of the best possible substitution suggestions. For each substitution suggestion shown, a detailed description and reasons can be called up. The description of the substitution suggestions contains statements on

- fibre and resin material
- dimensions of the fibre-composite component
- buildup and structure of the laminate
- laminate production process
- cost estimate for production of a component

If the system finds no substitution possibility, it indicates this to the user, stating the rules governing its decision.

4. CONCLUSIONS:
The question as to whether a load-bearing metallic component can be replaced by a fibre-composite substituto is of fundamental importance in mechanical engineering and plantmaking. The expert system outlined above can help the designer and engineer to answer this question. Further development can proceed in two directions. The knowledge areas material data, dimensioning, manufacture and cost-efficieny can be expanded in terms of their depth of information and knowledge. Also the system can be upgraded for conslusion, ist can be said that expert systems are a useful tool for material selection in design engineering.

REFERENCES


1 Bundesministerium für Foprschung und Technologie (BMFT)
(West German Ministry of Research and Technology)
Material Research 1985

2 G. Menges, K.W. Kirberg, H. Weck, L. Ophey
Maschinenmarkt 91 (1985) No. 77

3 G. Menges, K.W. Kirberg
Bundesministerium für Forschung und Technologie (BMFT)
New Materials, 1986, p. 70

4 T. Götte, R. Jacobi, A. Puck
Kunststoffe 75 (1982) 2

5 A. Barr, E.A. Feigenbaum
The Handbook of Artificial Intelligence, Vol. 1

6 M. Minsky
A Framework for Representing Knowledge
in the Psychology of Computer Vision
P. Winston (Ed.)
McGraw-Hill, New York, 1975

7 D.A. Waterman, F. Hayes-Roth
Pattern Directed Inference Systems

8 P.E. Hart, N.J. Nilsson, B. Raphael
A Formal Basis of the Heuristic Determination of Minimum Cost Paths
IEEE Transactions of SSC, 4 (1968)

9 P.E. Hart, N.J. Nilsson, B. Raphael
Correction to "A Formal Basis of Heuristic Determination Minimum Cost Paths"
SIGART Newsletter 37 (1972)

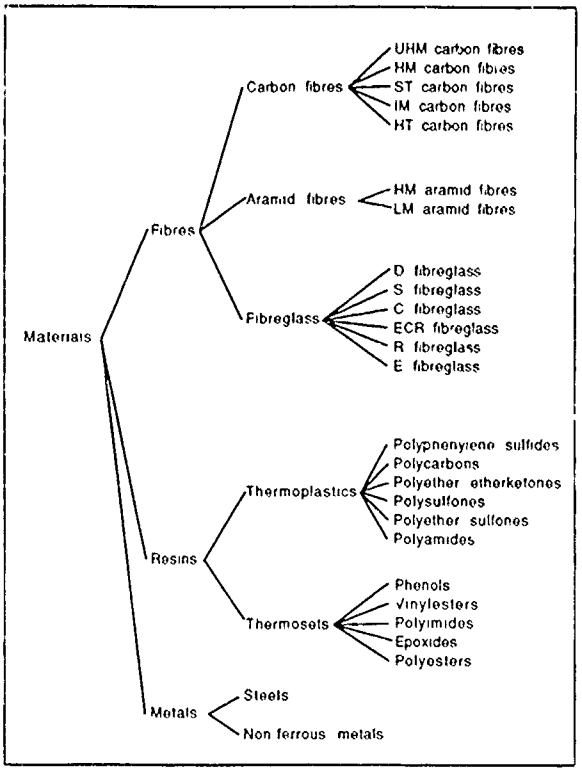


Fig. 1: Material representation in a frame structure

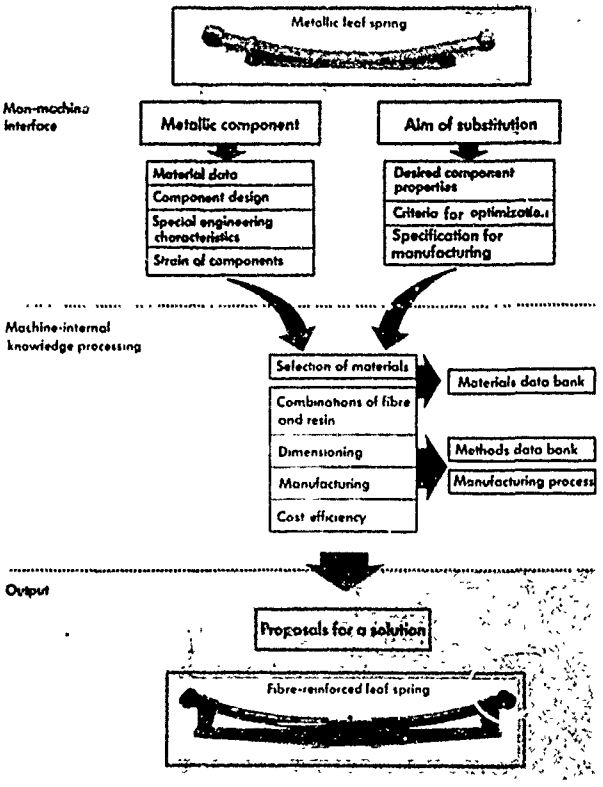


Fig. 2: The architecture of the expert system

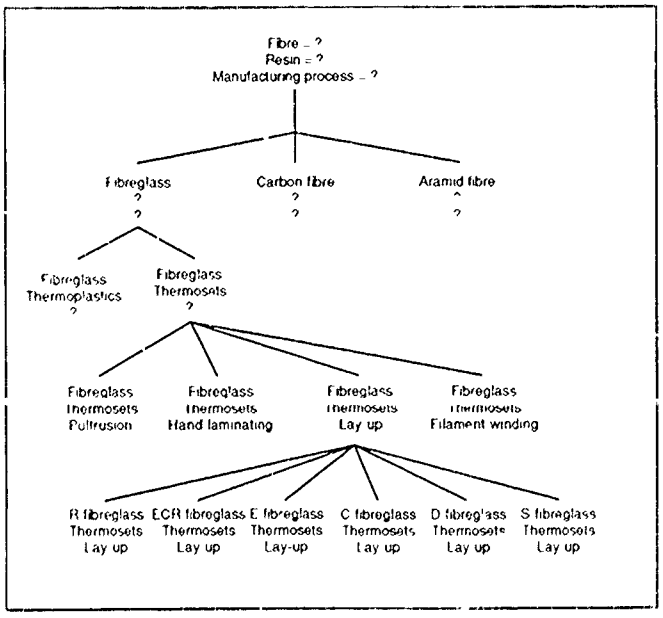


Fig. 3: Schematic of the search tree

# The Use of Models in Materials Properties Databanks

R.C. Hurst, H. Kröckel, H.H. Over, P. Vannson

C.E.C. - J.R.C. Petten, The Netherlands

## SYNOPSIS

The paper describes the material data evaluation features installed in the High Temperature Materials Databank of the CEC Joint Research Centre. The databank stores original test data and uses a number of statistical and model-based methods for the evaluation of tensile, creep, fatigue and fracture mechanics properties. Examples are presented in which data are extracted from the bank and converted into model parameters suitable for material and property evaluation, constitutive equations and engineering design analysis.

## INTRODUCTION

Computerized databases for factual data on materials, usually called Factual Materials Databanks, enable the rational storage and rapid retrieval of materials data in any form and quantity. They are entering the research and engineering activities of many institutions which generate and use materials data. Since many of these databases are designed for online operation giving them the attractive feature of remote access, they are often categorized as Information Systems like the older bibliographic databases.

Although materials databanks can of course have the task of information systems, this paper concentrates on their role as primary tools which make materials data accessible to computer treatment. This opens perspectives for a great diversity of roles, for the computer treatment of materials data is no longer a convenience but is becoming an essential pre-requisite for various applications of computer-aided engineering (CAE), as this conference may prove.

## REPRESENTATION OF KNOWLEDGE IN MATERIALS DATABANKS

An important trend marking the development of some types of materials databanks is the representation of knowledge in their computer environment which strongly diversifies and enhances the functions of databanks. A particularly powerful system evolves if a databank for materials properties is combined with the knowledge of the materials scientist who uses both knowledge and data to evaluate the behaviour of a material. The resulting computerized materials evaluation system produces data of engineering utility for computer-based calculation of strength, deformation and service life and other CAE methods.

Obviously, the computer representation of the materials scientist's knowledge which is only to a small fraction organized in the structure of mathematical logics will be difficult if not impossible to achieve. It is an open question whether artificial intelligence approaches using rule bases and inferential programmes, once better developed and applicable, can ever solve this problem in its entirety. It is however possible without difficulties to represent on a computer that part of the knowledge which operates with mathematical algorithms. The High Temperature Materials Databank of the CEC is designed on this basis as a "data and methods bank" for CAE application.

## THE USE OF MODELS

Algorithms usable in materials property databanks are in general mathematical descriptions of phenomena in continuum mechanics. They are obtained by continuum modelling which is mostly considered as empirical, as it is usually expressing results from macroscopic experimental observations, which may be exact in the mathematical sense but not necessarily representing of a physical mechanism. The application of such empirical models is in principle restricted to the range of conditions from which the experimental data is obtained. Extension of the application outside this range can only be achieved in conjunction with substantiated experience. Only then can the full application scope of the model be accepted by the scientific community and be adopted by the design engineer. The utilisation of these models in conjunction with computers is "state of the art" today and with expert assistance can be readily applied in databanks as shown in the examples at the end of this paper.

Equipping models with both a continuum mechanics and a micromechanistic foundation reduces the level of expertise required. The combination of both features in a way which Ashby (ref. 1) calls "model-informed empiricism" allows exploitation of evaluation techniques in areas where continuum mechanics models alone are not feasible. For example, in extrapolating creep data for Alloy 800 from data obtained in high stress tests, the empirical θ-projection fails to predict even the shape of the long term test curve (fig. 5). In this case, the physical "damage state variable" prediction is demonstrably more successful

(ref. 2). Although the development of physical models is not yet ripe enough for their incorporation into the evaluation library of the HTM Databank it is clear that their early acceptance depends only on the success of carefully selected verification testing rather than on lengthy experience.

## THE HIGH TEMPERATURE MATERIALS DATABANK

The HTM-DB was designed to store data obtained from tensile, creep, relaxation, fatigue, crack growth and toughness testing of metallic alloys used for high temperature applications. At present it contains mainly Alloy 800, IN738 and IN939 data, the databank structure coping adequately with other materials e.g. ODS alloys and with corrosion or irradiation test data as well.

The file and metadata structure of the databank is shown in Fig. 1. The knowledge part of the HTM-DB is implemented as an evaluation programme library comprising various data evaluation methods based mainly on accepted material models and also on statistical analysis methods. The data and knowledge parts are in general used by combining a data search with a subsequent data evaluation, but they can also be used independently.

Fig. 2 shows an example of a data search in the "command" mode leading to the finding of 41 test results for the following search criteria : test temperature in °C (tt8), carbon content in % (c), material (ma7), heat treatment (ty7), treatment temperature in °C (tt7), specimen geometry (co6), rupture time in h (rt5). The alternative "tutorial command" search mode is based upon the main menu shown in Fig. 3. The menu support makes this mode easier to use but slower. The retrieved data can then be displayed in tabular or graphical form and/or be evaluated.

The required model can be selected from the menus of the evaluation programme library. A suitable extrapolation method for the 41 creep rupture data would call on the evaluation menu sequence shown in Fig. 4.

## EXAMPLES OF MODEL BASED DATA EVALUATIONS

The acceptance of model programmes for implementation in a databank requires that only operational and well accepted models are used, independent of whether they represent physically based or empirical knowledge. In practical terms this means that the databank is better equipped with models for the more explored properties such as creep, however a number of proven methods are also available for fatigue, creep-fatigue and crack propagation. The following examples illustrate some of the models available; other examples are presented in ref. 3.

### Norton Creep Law

The Norton creep law is a semi-empirical constitutive equation which describes the stress dependence of the secondary creep rate under constant stress creep conditions as

$$\dot{\varepsilon}_{min} = A\sigma^n$$

The programme "Norton Creep Law" demands the input of the creep stress $\sigma$ and the minimum creep rate $\dot{\varepsilon}_{min}$ of different creep curves for a constant temperature. $\dot{\varepsilon}_{min}$ is established from a second order $\log\dot{\varepsilon}$ vs $\varepsilon$ plot of the creep curve. The data points are fitted with a regression analysis (Fig. 6) leading to the calculation of the Norton creep parameters A and n for a specific temperature. These parameters are inputs into finite element codes e.g. Abaqus, used for component design against creep.

### Larson-Miller Extrapolation

The Larson-Miller method is often used in design calculations for the extrapolation of long term creep rupture times from short term creep rupture data using time-temperature parameters depending on the creep stress. The Larson-Miller parameter $P_{LM}$ combines the Arrhenius function as the physical principle for temperature dependence of creep with the semi-empirical Norton creep law and the empirical Monkman Grant relationship for ductile creep rupture. The required database for the Larson-Miller extrapolation method is creep rupture time $t_r$, creep stress $\sigma$ and test temperature T for a range of stresses at different temperature levels.

Isothermal creep curves of the Larson-Miller extrapolation method for Alloy 800H are shown in Fig. 7. The L-M constant C in the equation $P_{LM} = T\ (C + \log t_r)$ is found to be 19.5 consistent with the alloy manufacturers' data.

### Paris Law

The fatigue crack growth rate da/dN dependence on the stress intensity dK can analytically be described with

$$\log \frac{da}{dN} = C_1 \sinh\ (C_2 \cdot (\log(dK) + C_3)) + C_4$$

where $C_1$, $C_2$, $C_3$ and $C_4$ are constants.

In Fig. 8, measured fatigue crack growth data are fitted using the regression analysis programme "Analytical Description" to yield the constants.

The Paris law ($da/dN = C\ dK^m$) describes the steady state region of the fatigue crack growth curve for stable crack growth and in this region sinhx is equal to the argument x. Therefore the Paris constants C and m can be determined from

$$C = 10^{(C_4 + C_1 \cdot C_2 \cdot C_3)}$$

and $$m = C_1 \cdot C_2$$

An engineer using ASME III, Appendix G needs these constants to evaluate the lifetime of a component containing cracks.

## CONCLUSIONS

The dynamic features of a materials databank which uses material models for the evaluation of the stored raw data expand its utility towards a data evaluation system converting test results into engineering parameters. Databanks of this type have an attractive potential for CAE applications. Although they can be used scientifically to support the development and verification of models, they should not implement models before these are scientifically accepted and operational. Linkage of these "data and methods banks" with CAE systems to provide materials data input will necessitate the standardization of the implemented models. Material models may in this respect turn out to become vital elements in CAE disciplines.

REFERENCES

1. M.F. Ashby : Technology of the 1990s : Advanced Materials and Predictive Design. Phil. Trans. R. Soc. Lond. A323, pp. 393-407, 1987.

2. N.G. Taylor : The Multiaxial Creep Behaviour of Alloy 800H at 800°C in Carburising Environment. Doctoral Thesis, University of Dublin. JRC Petten, December 1986.

3. H. Kröckel, H.H. Over, P. Vannson, Die Europäische Hochtemperaturwerkstoff-Datenbank Petten, In : VDI-Bericht no. 600.4, 1987.


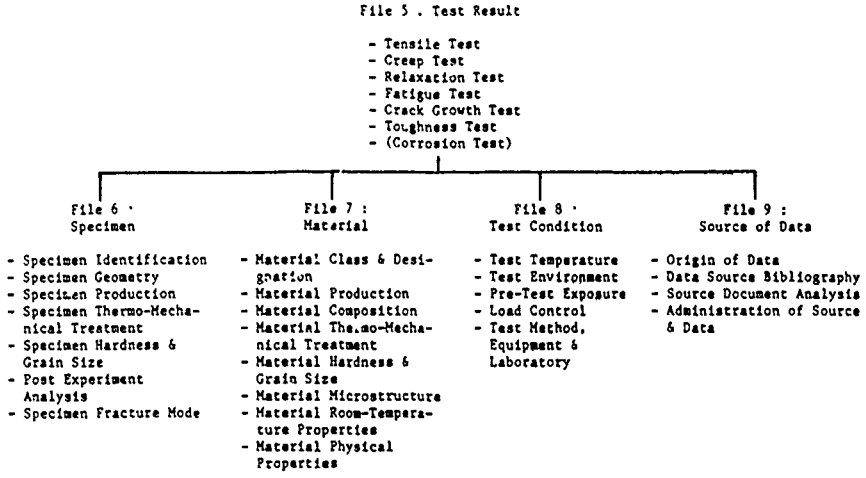


Fig. 1. File and Metadata Structure of the HTM Databank

Fig. 2. Example of a Data Search in the "Command Mode"

```
PLEASE ENTER COMMAND:
find rt5 gt 0 and tt8 = 600 thru 900
   3055 TEST RESULT(S)   FOUND HELD WITH S01
PLEASE ENTER COMMAND:
find s01 and c = .03 thru .05 and ma7 = alloy 800
    655 TEST RESULT(S)   FOUND HELD WITH S02
PLEASE ENTER COMMAND:
find s02 and ty7(1) = solution annealed
    382 TEST RESULT(S)   FOUND HELD WITH S03
PLEASE ENTER COMMAND:
find s03 and tt7(1) = 1150 and co6 = cylindrical
     41 TEST RESULT(S)   FOUND HELD WITH S04
PLEASE ENTER COMMAND:
eval s04
```

Fig. 3. The "Tutorial Command Mode"

```
*** PLEASE ENTER YOUR CHOICE ***********************************************
*                                                                           *
*                                                                           *
*                >>>  MAIN MENU: TUTORIAL COMMAND MODE  <<<                 *
*                                                                           *
*                                                                           *
*  DATA SOURCE      MATERIAL      SPECIMEN    TEST CONDITIONS   TEST RESULT  *
*                                                                           *
* A:DATA ORIGIN  B:DESIGNATION  G:...GEOMETRY  L:.TEMPERATURE  R:.....TENSILE *
*                C:COMPOSITION  H:..TREATMENT   & ENVIRONMENT  S:.....CREEP *
*                D:..TREATMENT  I:...PRE TEST  M:.....TENSILE  T:.....FATIGUE *
*                E:.HARDNESS &  MICROSTRUCTUR  N:.....CREEP   U:CRACK GROWTH *
*                   GRAIN SIZE  J:..POST TEST  O:CRACK GROWTH                *
*                F:...PHYSICAL  MICROSTRUCTUR  P:.....FATIGUE               *
*                   PROPERTIES  K:..POST TEST  Q:....PRE TEST               *
*                               EXAMINATION       EXPOSURE                  *
*                                                                           *
*************************************************************** HTM-DB ***
!                                                                           !
!      OR ENTER ONE OF THE FOLLOWING COMMANDS (TYPE FOR EXAMPLE: EVAL )     !
!*** DISPLAY EVAL ESCAPE HELP MENU MODE QUERY STOP REPORT RESET SCOPE SHOW ***!
```

MAIN MENU: EVALUATION METHODS

1. TENSILE
2. CREEP → CREEP EVALUATION MENU
3. FATIGUE
4. CREEP-FATIGUE
5. FRACTURE MECHANICS
6. STATISTICAL METHODS
7. GRAPHICAL FORMATS

CREEP EVALUATION MENU

1. CREEP CURVES
2. CREEP RELATIONS
3. CONSTITUTIVE EQUATIONS
4. EXTRAPOLATION METHODS → CREEP SUBMENU 4: EXTRAPOLATION METHODS
5. MINIMUM CREEP RATE CORRELATIONS

1. SPERA
2. ORR-SHERBY-DORN
3. LARSON-MILLER
4. SCHMIDT-GRANACHER
5. MANSON-HAFERD
6. MANSON-BROWN

Fig. 4. Example of a Menu Sequence in the Evaluation Program Library

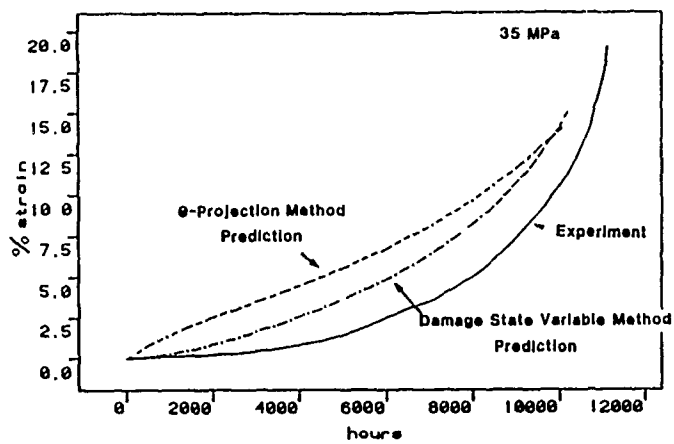


Fig. 5. Prediction of creep behaviour of Alloy 800 at 800°C using two models

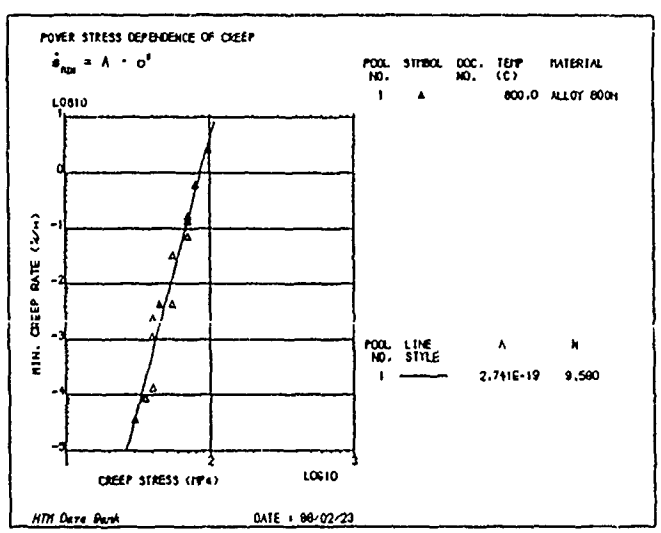


Fig. 6. Determination of the Norton Creep Law Parameters

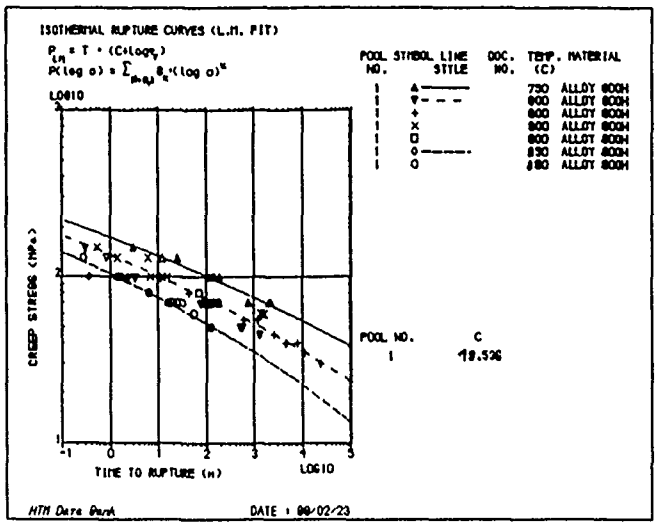


Fig. 7. Isothermal Larson-Miller Rupture Curves

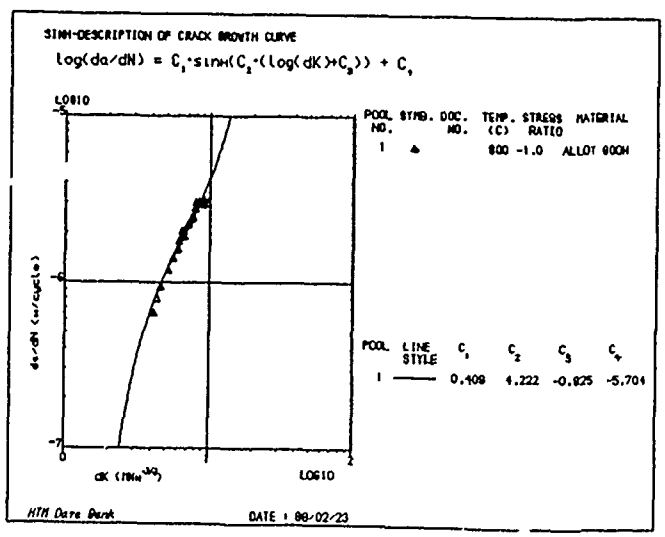


Fig. 8. Sinh-Description of a Crack Growth Curve

# STRUCTURAL SHAPE DESIGN BY TRANSPUTER BASED FINITE ELEMENT TECHNIQUES

D. R. J. Owen, Civil Engineering Department, University of Wales, Swansea, U.K.

J. S. R. Alves Filho, Instituto de Pesquisas Espaciais, Brazil, (presently at Civil Engineering Department, University of Wales, Swansea, U.K.)

SYNOPSIS

This paper describes the use of parallel processing finite element techniques for the solution of transient dynamic problems. The use of transputer equipment hosted on a desktop computer or workstation is considered for the numerical simulation of the behaviour of structures which can be modelled by either solid or thick shell elements. In this way, extremely efficient solutions for the stress and deformation histories of structures operating under fast transient loading are obtained enabling their efficient design from both a shape and material viewpoint.

## 1. INTRODUCTION

Problems involving dynamic transient behaviour which are of intense current interest arise in several branches of engineering. These include missile impact problems in space applications and nuclear containment structures, explosion simulation in pressure vessels and crash worthiness assessments in the automobile and aero industries. A computer simulation of the structural response of such structures and components, employing numerical techniques based on the finite element method, is prohibitively expensive and with present day computing resources only the most politically sensitive or high risk structures warrant such a treatment.

Nowhere is this problem more acute than in the case of laminated composite shells where even the static analysis of such structures demands extensive computer processing power. Typically for aerospace applications a composite shell will be made up of 10-20 anisotropic layers and a finite element formulation necessitates consideration of the stiffness characteristics of each layer and also, if edge effects are considered important, the independent deformation of each laminate must be accounted for.

The efficient design of such structures for operation under dynamic load conditions requires an accurate determination of the stress and deformation histories. This can only be achieved by a radical improvement in the computational solution times of the finite element method. Parallel processing offers a natural means to this end and the emergence of multi-processor machines makes such advances possible.

Despite the simplicity of the parallel processing concept, its implementation in finite element programs is not so straightforward. The exploitation of parallelism in every algorithm and the efficient use of hardware in a wide range of applications call for a great deal of expertise. This means that, while the fifth generation computers are still on the drawing board, the pursuit of parallelism and efficiency in the development of a particular application on a multi-processor machine is largely controlled by the programmer. Users of parallel computers must have a much deeper understanding of their hardware and software than before in order to derive a benefit.

The transputer is the first product available which allows the programmer to conceive a MIMD (multiple instruction, multiple data) parallel machine of his own without the need to be a computer expert. However, the great capabilities and advantages which transputers offer on a first approach do not seem to be so impressive on a closer examination of non-mandelbrot set applications. The link speed being one order of magnitude lower than the memory access time (or an integer operation on the T414; or a Flop on the T800) indicates the need for a balance between processing and communication. The less concurrency that is found and the more communication that is needed, the smaller the advantages that arise from using a transputer system for a particular application. The strong appeal of transputers is really the performance/cost ratio which is one order of magnitude higher than current supercomputers. While the latter have a ratio around 10 Flops per dollar, a T800 system could provide a ratio higher than 200.

The solution of rapid transient problems by explicit time integration allows concurrency to be widely exploited, since under these conditions the system equations become completely uncoupled. The work described in this paper is directed at developing transient dynamic solution codes for solids and laminated shells, allowing an elasto-viscoplastic material behaviour, using either a desktop computer or workstation hosted transputer system.

## 2. TRANSIENT DYNAMIC FINITE ELEMENT ANALYSIS

The discretised dynamic problem invariably gives rise

to a set of ordinary differential equations of the form, [1]

$$\underline{M}\ddot{\underline{a}}_n + \underline{C}\dot{\underline{a}}_n + \underline{P}_n(\underline{a}_n) = \underline{F}_n(t) \qquad (2.1)$$

in which dots denote differentiation in time, $\underline{a}_n$ stands for a set of parameters describing the displacements, $\underline{M}$ is the mass matrix, $\underline{C}$ is the damping matrix, $\underline{P}_n$ are the internal forces opposing the structural displacement and $\underline{F}_n$ are the activating forces. On use of virtual work principles, the appropriate terms in (2.1) are found to be

$$\underline{M} = \int_v \underline{N}^T \rho\, \underline{N}\, dv \qquad (2.2)$$

$$\underline{C} = \int_v \underline{N}^T c\, \underline{N}\, dv \qquad (2.3)$$

$$\underline{P}_n = \int_v \underline{B}_n^T \underline{\sigma}_n\, dv \qquad (2.4)$$

$$\underline{F}_n = \int_v \underline{N}^T \underline{b}\, dv + \int_s \underline{N}^T \underline{d}\, ds \qquad (2.5)$$

in which $\rho$ is the material density, c stands for velocity proportional damping forces, $\underline{b}$ are the body forces per unit volume and $\underline{d}$ are the boundary tractions. Also $\underline{N}$ represent the shape functions and subscript n denotes the value of quantities at time $t_n$. The term $\underline{\sigma}_n$ denotes the stresses which instantaneously satisfy the elasto-viscoplastic conditions and $\underline{B}_n$ is the strain/displacement matrix which varies with time for large deformation problems.

Using central difference approximations to express the terms $\ddot{\underline{a}}_n$ and $\dot{\underline{a}}_n$ in terms of the value of $\underline{a}$ at time stations $t_{n-1}$, $t_n$ and $t_{n+1}$, all at an interval $\Delta t$ apart, leads to

$$\underline{a}_{n+1} = (\underline{M} + \underline{C}\,\Delta t/2)^{-1}[\Delta t^2(\underline{P}_n + \underline{F}_n) + 2\underline{M}\underline{a}_n - (\underline{M} - \underline{C}\,\Delta t/2)\underline{a}_{n-1}] \qquad (2.6)$$

which provides a recurrence relationship for the solution of the displacements at successive time intervals. The calculation at every time step is trivial if the matrices $\underline{M}$ and $\underline{C}$ are diagonal, which can be brought about by a "lumping" procedure. In particular, the terms of the lumped mass matrix are computed from the consistent values given by (2.2) according to

$$M_i = M^e_{ii}\,\frac{M}{\Sigma M^e_{ii}} \qquad (2.7)$$

in which $M^e_{ii}$ represent the diagonal terms of the consistent mass matrix and M is the total element mass.

To diagonalise $\underline{C}$, mass proportional damping is assumed so that

$$C_i = \alpha M_i \qquad (2.8)$$

where $\alpha$ is a proportionality constant.

When (2.7) and (2.8) are used in (2.6) the problem uncouples and the equation system becomes diagonal so that

$$a_i^{n+1} = \frac{1}{M_i(1+\alpha\Delta t/2)}[\Delta t^2(P_i^n + F_i^n) + 2M_i a_i^n - M_i(1-\alpha\Delta t/2)a_i^{n-1}] \qquad (2.9)$$

The solution can then be systematically integrated in time using (2.9) to give the displacement history. The stresses can be found from

$$\underline{\sigma}_{n+1} = \underline{\sigma}_n + \underline{D}(\underline{B}\Delta\underline{a}^n - \dot{\underline{\varepsilon}}^n_{vp}\Delta t) \qquad (2.10)$$

where $\dot{\underline{\varepsilon}}^n_{vp}$ represents the viscoplastic strain rate and $\Delta\underline{a}^n$ is the displacement increment.

## 3. ELEMENT DESCRIPTION

Use of the solution procedure described above requires specification of the various terms for the particular element to be adopted for solution. For two and three dimensional solids, the description of the appropriate element matrices for use in an elastic-viscoplastic analysis is well known and full details can be found, for example, in Ref. [1].

For anisotropic laminated shells, the element description is provided in Ref. [2] and the essential characteristics are summarised below.

The shell configuration is shown in Fig.1, where it is seen that four separate coordinate systems are employed to define the element behaviour. In particular, a Cartesian system describes the element geometry, a nodal system is used to identify the nodal rotations, a local system defines the stresses and strains, as well as the material anisotropy and a natural coordinate system is employed for integration of quantities over the element. Transverse shear deformation is permitted and a layered formulation is adopted in order to model property changes through the shell thickness.

The elastic relationship between the stress and strain components can be written as

$$\underline{\sigma} = \begin{Bmatrix}\sigma_1\\ \sigma_2\\ \tau_{12}\\ \tau_{13}\\ \tau_{23}\end{Bmatrix} = \begin{bmatrix}D_1 & D_{12} & 0 & 0 & 0\\ D_{12} & D_2 & 0 & 0 & 0\\ 0 & 0 & D_3 & 0 & 0\\ 0 & 0 & 0 & D_4 & 0\\ 0 & 0 & 0 & 0 & D_5\end{bmatrix}\begin{Bmatrix}\epsilon_1\\ \epsilon_2\\ \gamma_{12}\\ \gamma_{13}\\ \gamma_{23}\end{Bmatrix} = \underline{D}\,\underline{\epsilon} \qquad (3.1)$$

where it is assumed that the through-thickness stress is negligible and

$$D_1 = E_1/(1-\nu_{12}\nu_{21}),\quad D_2 = G_{12},\ \text{etc.} \qquad (3.2)$$

where E, $\nu$ and G denote anisotropic values of the material properties.

The yield criterion is expressed in terms of the Huber-Mises condition extended to anisotropic materials [3,4] so that

$$F = \bar{\sigma} - (a_1\sigma_1^2 + 2a_{12}\sigma_1\sigma_2 + a_2\sigma_2^2 + a_3\tau_{12}^2 + a_4\tau_{13}^2 + a_5\tau_{23}^2)^{\frac{1}{2}} \qquad (3.3)$$

in which $\bar{\sigma}$ denotes the effective stress and the six anisotropic yield parameters $a_1$, $a_{12}$, etc. can be determined from independent uniaxial tests.

The viscoplastic strain rate is governed by the following flow rule

$$\dot{\varepsilon}_{vp} = \gamma < \phi(F) > \frac{\partial F}{\partial \sigma} \qquad (3.4)$$

in which $\gamma$ is the fluidity parameter and $\Phi$ denotes the flow function.

Evaluation of the $\underline{B}$ matrix is a relatively complex and computationally expensive procedure involving the derivatives of the displacements which are first evaluated in the local coordinate system and then transferred to the global system.

Since the element is based on a layered approach, the above relationships hold for each layer and a through- thickness integration procedure is adopted to provide the complete element response.

## 4. BASIC CONSIDERATIONS OF PARALLEL PROCESSING ALGORITHMS

The key idea behind parallel processing is that an algorithm consisting of M independent processes running on N processors should run N times as fast as the same process running on just one processor. Experience, however, shows that the actual speed-up is often smaller, mainly because of communication, synchronization and sharing of resources. It is therefore important to know how to take full advantage of any particular parallel machine in order to design efficient application programs.

When designing application programs for a transputer network there are basically three approaches that can be considered: a dataflow decomposition, a data structure decomposition or, the so called, processor farm scheme. While the first two approaches will always lead to specific system configurations for different types of problems, the last one is a general and simple approach which employs a fixed configuration for every application. Although the processor farm scheme will not always present the best solution and that some problems naturally call for dataflow or data structure decompositions, its generality and simplicity has great appeal and such a scheme is adopted here.

For the sake of simplicity consider a process P consisting of M concurrent (or independent) subprocesses. Each of these subprocesses takes time $t_p$ to run and only communicates at its start for input and at its end for output Also consider a transputer system with N processors. Speedup and efficiency can then be respectively defined as [5]:

$$S = \frac{T(1)}{T(N)} \qquad (4.1)$$

$$E = \frac{S}{N} \qquad (4.2)$$

where T(N) is the total runtime consumed by process P running on N processors. If it is assumed that each one of the M subprocesses runs alone in one processor, time T can be estimated as:

$$T(N) = (t_p * \iota M/N \jmath) + t_{oh} \qquad (4.3)$$

where $t_{oh}$ is the total overhead time due to communication and synchronization and the $\iota\jmath$ operator yields an integer number such that $a < \iota a \jmath < (a+1)$.

Considering expression (4.3), then (4.1) and (4.2) can be rewritten as:

$$S = \frac{t_p * M}{(t_p * \iota M/N \jmath) + t_{oh}} < N \qquad (4.4)$$

$$E = \frac{\beta}{\iota\beta\jmath + \Gamma} < 1 \qquad (4.5)$$

where: $\beta = (M/N)$ and $\Gamma = t_{oh}/t_p$.

Multi-processor machines have their performance inevitably degenerated by inter-processor communication. This overhead is not significantly dependent on the size of the message communicated therefore making the use of fewer and longer messages advantageous and highly advisable. Nevertheless, a loss in efficiency due to communication will always be present and can be represented by parameter $\Gamma$ in expression (4.5). The smaller $\beta$ is, the more important the communication overhead becomes in determining the system efficiency.

Although transputer links are synchronized, data can sometimes be not available when needed owing to the low link speed. If the process runtime $t_p$ is smaller than the time the input message takes to communicate through the link, the processor will be idle for a period of time even when all communications are done in high priority processes and data is ready on the sender. This fact helps to increase the overhead time and consequently decrease the system performance. In these cases long messages may not be the best solution and a compromise has to be reached between the number and size of messages.

## 5. COMPUTER IMPLEMENTATION

A transient dynamic finite element code has been written in OCCAM employing the theory and principles described in the previous sections. The parallel algorithm considered in this work is shown in Fig. 2 where the inclined rectangles represent the use of slave transputers through a processor farm scheme. The main loop over the number of time steps is largely a sequential process since the displacements for each step must be fed back into the next step. Concurrency can be mostly found inside the "internal stresses" and "displacement" processes where the numbers of independent subprocesses (M) are the number of elements and the number of degrees of freedom respectively. It is noted that no parallel schemes were considered in the "Input" and "Pre-processing" stages. The "output" process, though, is considered to run concurrently with the next step calculations, following a dataflow decomposition.

The element initially implemented was an isoparametric plane element. The average runtime $t_p$ measured for the various operations with this element led to the use of a linear configuration for the processor farm, since approximately 80% of the total time is spent on the internal stress calculations and the advantages of the improved efficiency of a tree configuration are outweighted by the simplicity of a linear routing scheme.

Figures 3 and 4 present the system and program structures considered. The hardware currently comprises two B004 boards (1 T414 and 2 Mbyte of RAM per board) for the ROOT and MAIN transputers and three B003 boards (4 T414 per board and 256 Kbyte of RAM per transputer) for the 12

slave processors (the workers). The first transputer, called ROOT, is linked to the host and performs all I/O operations as well as the pre-processing tasks. After all data has been input the ROOT sends the data to the MAIN transputer which then starts executing the analysis. Before receiving the data, the MAIN counts the number of slave transputers giving an identity number to each and preparing them to undertake tasks. Every slave transputer can undertake three types of task: displacement calculation, element internal stress vector or element mass matrix evaluation. In order to keep the required amount of local memory in the workers at a low level (less than 64K), all data are kept only in the ROOT and MAIN transputers and all information is sent each time it is needed.

The PRE process collects the data for the various tasks and transmits them to the workers via the SEND process which controls the number of jobs being undertaken. The POS process receives back the processed data through the GET process and assembles them suitably. The variables in MAIN (such as the displacement vector) are kept local to the PRE process. The POS process works with working-vectors which are fed back into the PRE process at the end of each task. The OUTPUT process sends to the root transputer warning or error messages and data to be output. Messages can be originated from one of the work processors or in the PRE or POS processes.

## 6. NUMERICAL RESULTS AND DISCUSSION

Results obtained with the computer implementation described in the last section (program TRANSA) are shown here in terms of the speed-up and efficiency achieved. The problem chosen for analysis was an aluminium spherical cap under a step external pressure. The efficiency obtained for various mesh sizes is shown in Figure 5. The runtime for a 12-slave farm is compared to the runtime for a 1-slave farm and the efficiency is calculated according to expressions (4.1) and (4.2). The importance of high values of $\beta$ in achieving better performances is readily seen.

The actual speed-up achieved by this implementation was assessed by comparing its results with those from the similar program DYNPAK [1], running on a micro-VAX II. The speed-up values presented in Table 1 illustrate the potential of the parallel formulation considered.

The processor farm scheme proved to be efficient for this explicit transient dynamic finite element application. Better performances can be achieved when more complex elements and material models are brought into consideration. The use of the new T800 transputers (floating point unit on-chip sustaining a rate of 1.5 MFlops) also greatly improve the performance. Floating point operations are performed in software on the present T414, which makes it slow for such scientific applications as considered here. Figure 6 illustrates a comparison between a 12-slave T414 farm and a single T800 implementation.

TABLE 1 - Comparison between DYNPAK and TRANSA times

| number of time steps | VAX time for DYNPAK [1] | time for TRANSA | speed-up |
|---|---|---|---|
| 10 | 29.9 | 7.5 | 4.0 |
| 100 | 169.9 | 19.5 | 8.7 |
| 1000 | 1484.0 | 182.3 | 8.1 |

N = 12; 64 element mesh;
time in seconds

The idea of a personal transputer-enhanced finite element system is shown by this first application to be worth considering and that the concept employed could be extended to other types of problems. This work is presently continuing with particular consideration being given to the development of concurrent equation solvers, so that parallel solution procedures can be implemented for a general range of finite element problems.

## REFERENCES


1. D. R. J. OWEN and E. HINTON
'Finite Elements in Plasticity: Theory and Pract. :' Pineridge Press, Swansea, U.K., 1980.

2. D. R. J. OWEN and G. Q. LIU
"Elasto-viscoplastic analysis of anisotropic laminated plates and shells" Engineering Computations, Vol.2, 90-95, 1985.

3. R. HILL
'The Mathematical Theory of Plasticity', Clarendon Press, Oxford, 1950.

4. D. R. J. OWEN and J. A. FIGUEIRAS
"Anisotropic elasto-plastic finite element analysis of thick and thin plates and shells" Int. J. Num. Meth. Eng. Vol.19, 541-566, 1983.

5. U. SCHENDEL
'Introduction to Numerical Methods for Parallel Computers' Ellis Horwood, U.K, 1984.

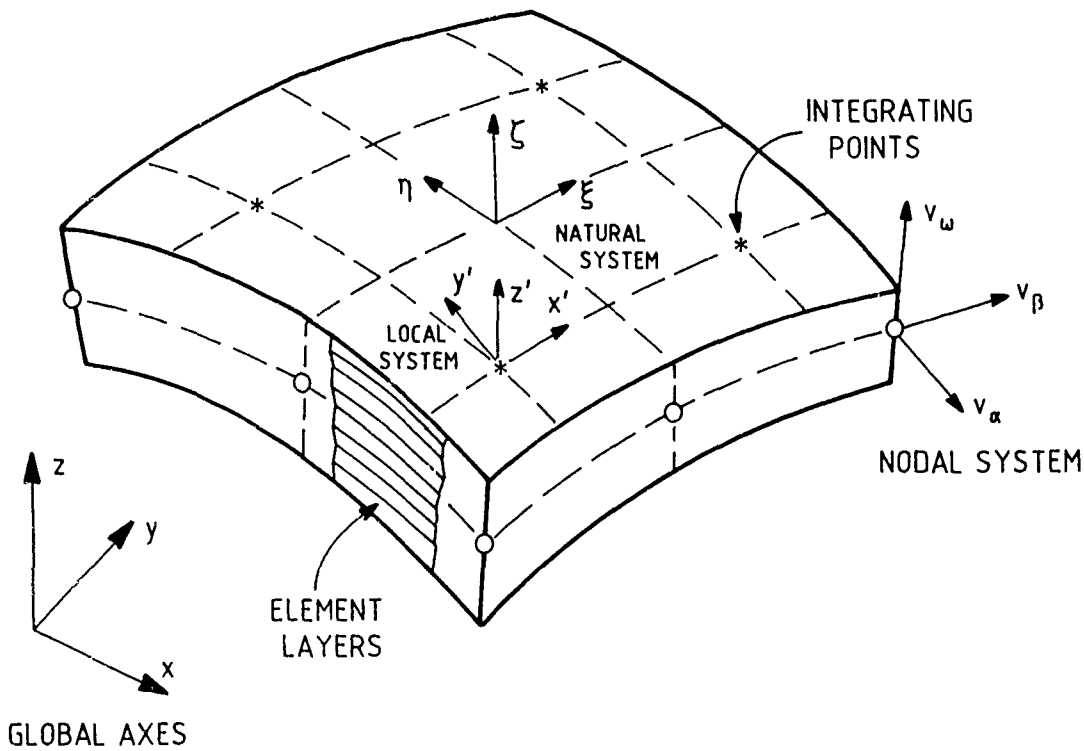


FIG. 1 Laminated anisotropic thick shell element

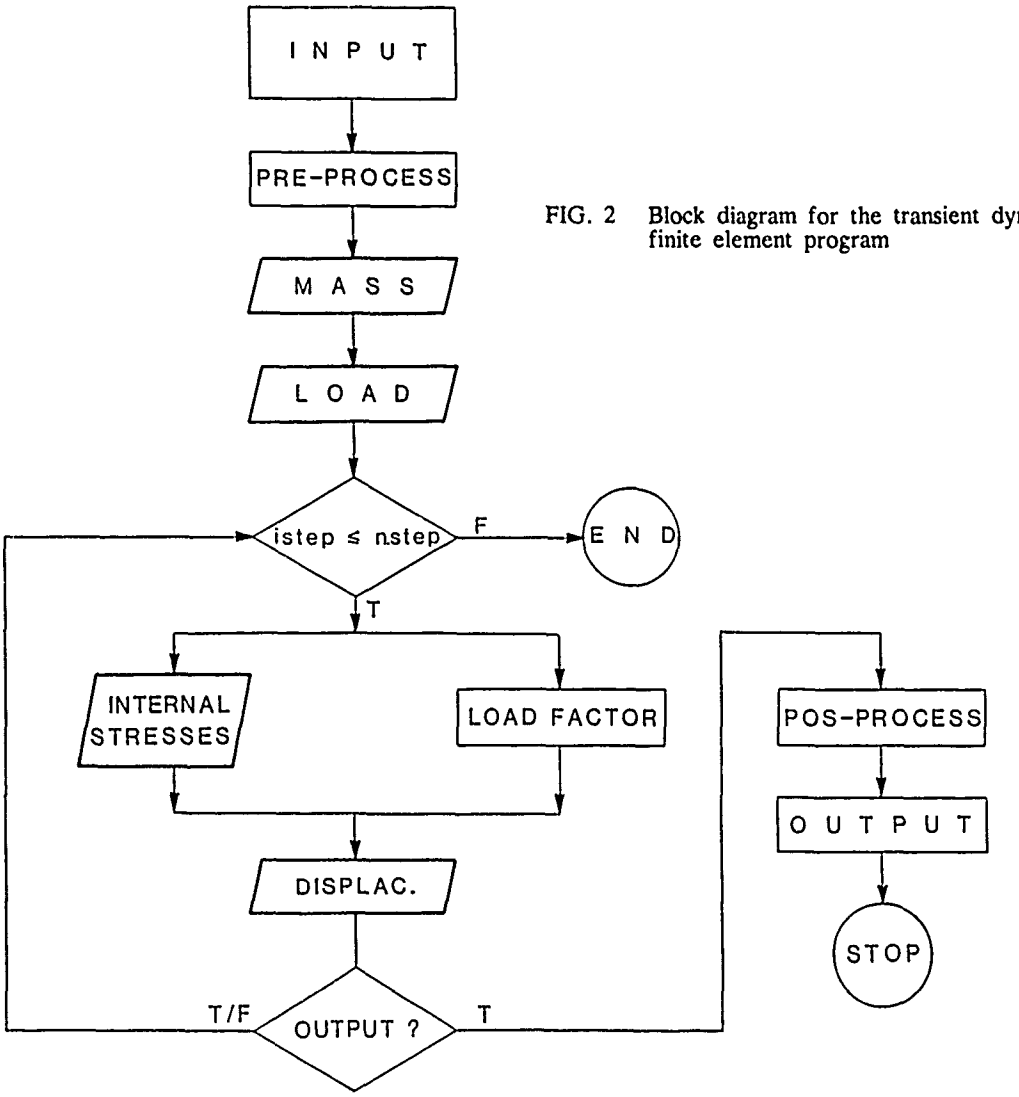


FIG. 2 Block diagram for the transient dynamic finite element program

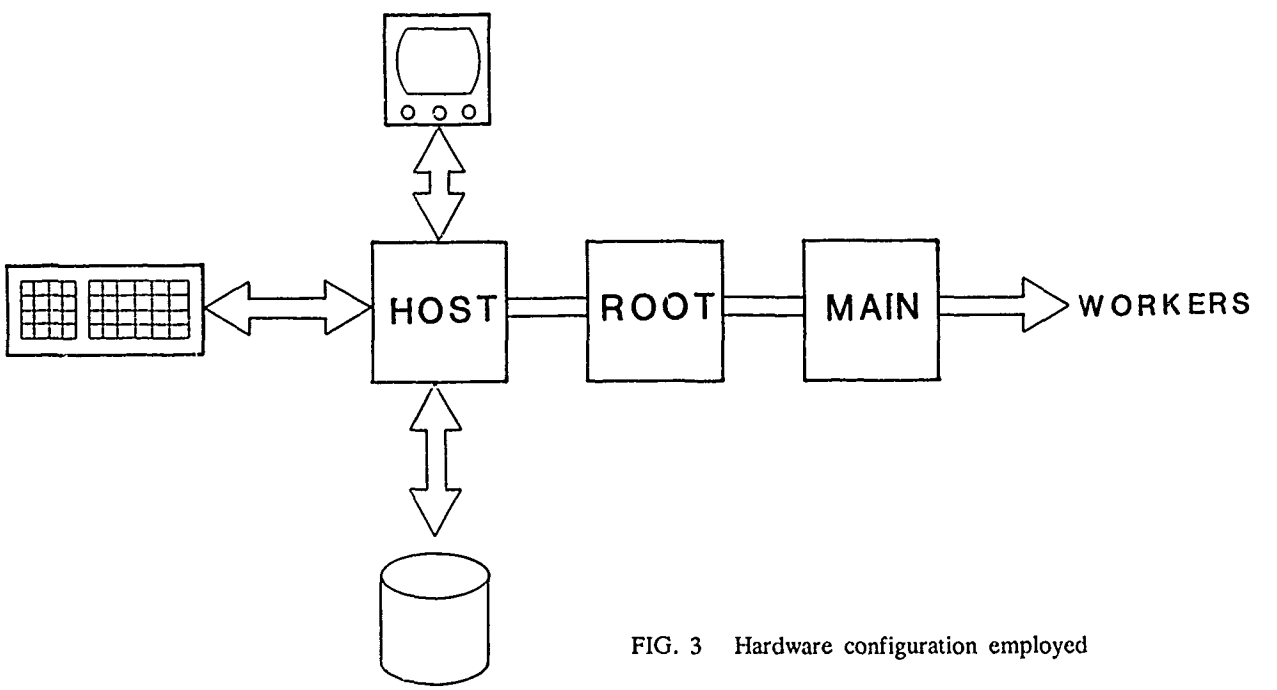


FIG. 3 Hardware configuration employed

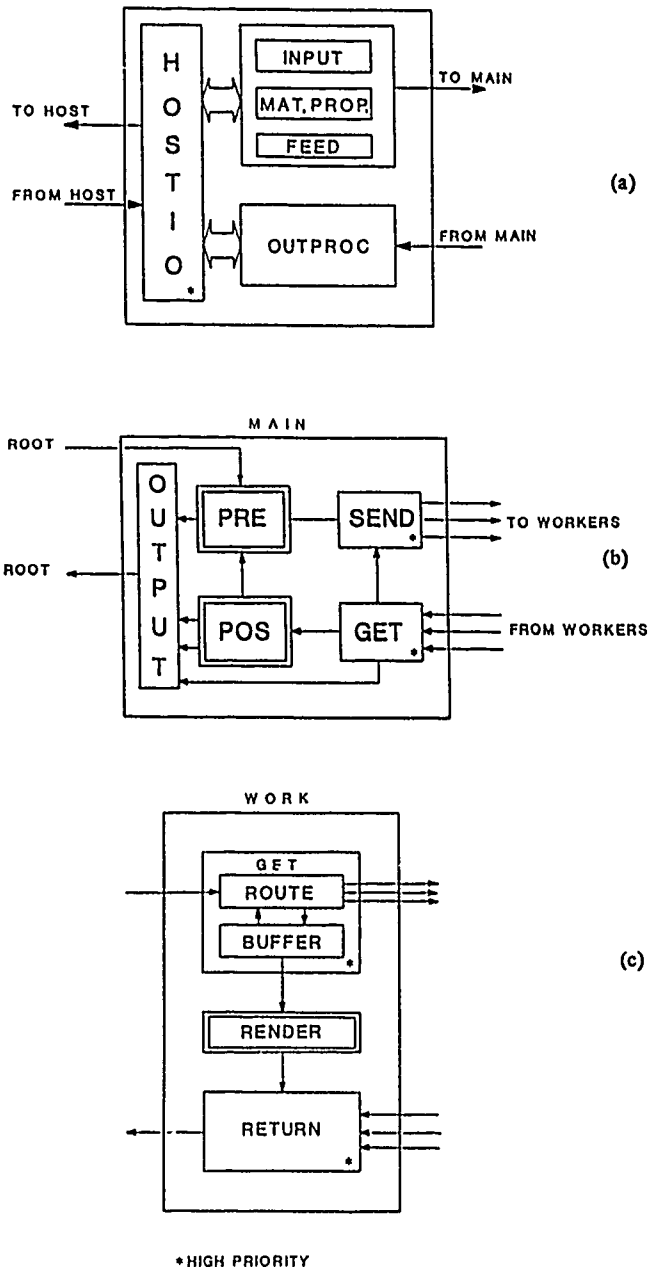


FIG. 4 Program structure for (a) the ROOT; (b) the MAIN and (c) the worker transputers

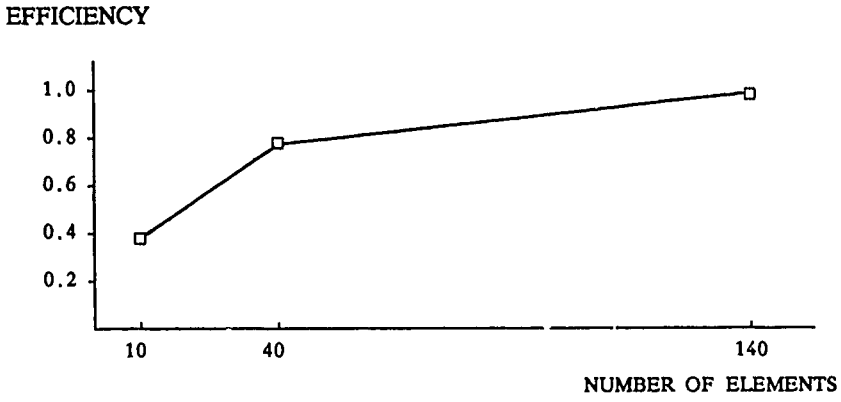


FIG. 5 Efficiency obtained for a 12-slave implementation

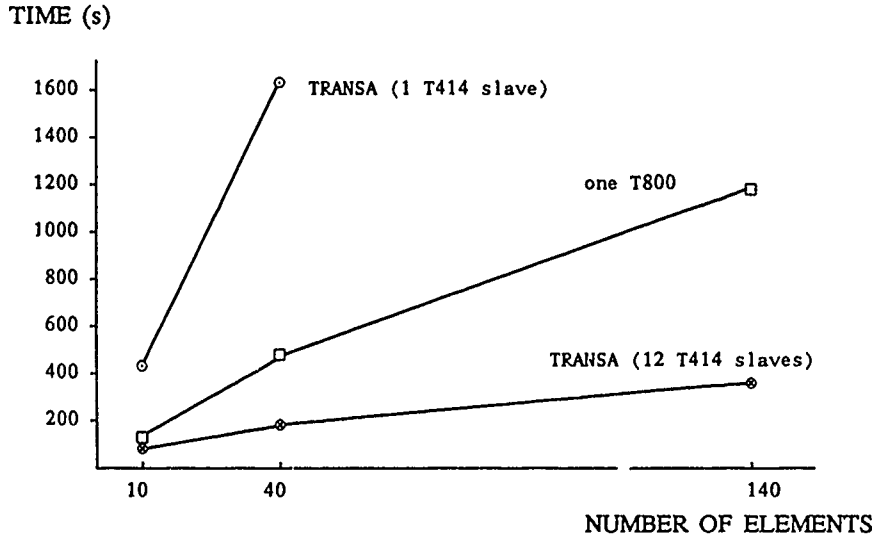


FIG. 6 Comparison between T414 and T800 transputer performance

# ROLE OF COMPUTER SCIENCE IN MATERIALS AND ENGINEERING DESIGN: PRESENT STATE AND FUTURE TRENDS

Douglas Lewin

Douglas Lewin is Professor of Computer Science and Information Engineering at the University of Sheffield

## 1. Introduction

Advances in computer technology have, and will even more in the future, radically change the methods and tools of engineering design. Computers have of course from their inception been used by engineers to perform calculations but the availability of high definition graphics workstations with appropriate software tools and support systems will revolutionise the design process.

A typical engineering workstation, available from such companies as Appollo, Sun Microsystems and DEC, would operate between 2-5 MIPS (millions of instructions per second) with a main storage of 2-32 megabytes and secondary hard disc storage of some quarter of a million gigabytes. Most systems would also comprise a graphics co-processor and high resolution (1024 x 800) display unit necessary to perform solid modelling and the representation of large hierarchical structures. Workstations would also be provided with a relevant 'tool-set', including basic compilers, linkers, operating systems, window managers etc, and application tools. For example, in the case of the mechanical engineer, for 2- and 3-dimensional design, solid and finite-element modelling and finite-element analysis.

These systems have enabled the traditional engineering design approach, based on a trial-and-error methodology in which successive generations of prototypes were designed, built, tested and analysed and then re-designed, to be superseded by computer-aided design and engineering techniques.

For instance, take the design of piston engines where the weight and balancing of moving components are directly related to the engine's structural integrity, efficiency and cost. Using CAD tools such as solid modelling software the weight of a proposed assembly, including components, could be estimated, followed by a finite-element stress analysis of a particular component say a connecting rod. Should the component not come up to specification, a new material would be chosen and its mass (weight and volume) and stress properties analysed. Repeating this procedure for several materials and designs, the engineer can evolve a satisfactory preliminary design.

Another important characteristic of the engineering workstation is that they can be linked together either locally, using for example an Ethernet, or globally via gateways to remote computing facilities. In this way users can utilise common facilities, such as specialised computing engines or centralised databases, but more important they are no longer isolated and become members of an integrated design team.

Though computer-aided engineering has radically altered and shortened the design cycle there is still a considerable need for major improvements. For example:

a) Simulation and Modelling Techniques. Many of the problems in this area are caused by lack of computing power, currently overcome by the use of supercomputers such as the CRAY X-MP which operates at 1 gigaflop (billion floating point operations per second). Supercomputers are normally employed for computational analysis based on complex mathematical models and operated in a batch mode. As well as the inherent difficulties of programming such machines there are many problems if a graphical representation of the results is required. The major problem arises due to the time required to transmit data (usually over a network) coupled with the need to perform (and output) a family of calculations to build-up a picture. This and other factors causes major difficulties when attempting to integrate supercomputers into a CAE system.

b) Storage and Acquisition of Design Data and Component Parameters. Though databases have and are being used extensively in CAD there is still a need to integrate existing data-banks and couple these effectively into all stages of the design process.

c) Disparate Tool-Sets. There are difficulties caused by the lack of standardisation and differing user interfaces, this causes major problems when transferring data and results between different application packages. A CAE system should enable a wide range of existing and new tools to be supported in an integrated environment.

d) Interfaces and Ease of Use. Current communication with the computer is limited to mouse and/or keyboard windowing systems with pull-down menus. Though these techniques are moderately effective, lack of standardisation and awkwardness in use make them unsuitable for more sophisticated future applications such as interactive three-dimensional modelling. There is also the problem of data capture and data entry, for example engineering drawings.

e) Low Level Design Tools. Current software tools are concerned primarily with design at the sub-systems and/or component levels (the functional and physical levels of design) rather than assisting at the higher behavioural level necessary to handle complex systems. Design is a top-down hierarchical process and a CAE system must reflect this, providing a compatible hierarchy of tools suitable for use at all levels. In particular tools for the specification, partitioning and evaluation of systems specifications are required. There is an inherent danger in considering the design of a component or sub-system in isolation from the total system.

f) Support Environments. Studies indicate that only some 20% of the engineer's time is concerned with design, test and evaluation, the rest of the time being spent in planning, communication and documentation tasks. Thus the engineering workstation must be able to support all these activities to provide a fully integrated CAE support system [1].

The following sections of the paper will examine in more detail some of the future trends in computer science which will provide enhanced CAE facilities.

## 2. Advances in Computer Architectures.

In the search for increased processor power many novel computer architectures and systems have been proposed.

2.1 Reduced Instruction Set Computer (RISC). Based on work by IBM in the mid 1970s which showed that only 20% of the instruction set of a computer is used in 80% of its operations researchers investigated computers with reduced and specific instruction sets. The RISC computer [2] in addition to having a basic, single cycle, load/store instruction set also utilises pipe-lined data paths and large register sets, with much of the complexity normally associated with run-time hardware being off-loaded to optimised compile-time software.

Currently there are some twentyfive different RISC chip sets available on the market, including special purpose chips for object-oriented languages, including Smalltalk 80, Lisp and multiprocessing (the Transputer). RISC systems have the potential for creating powerful workstations, based on personal computers, operating at 5-20 MIPS at very low cost. RISC microprocessors are also being used as the basis for super mini-computers, often utilising a multi-processor structure, operating at between 12-50 MIPS.

2.2 Parallel Architectures. Von Neumann processors suffer from the fundamental limitations of sequential operation. That is the program is executed serially, one step at a time, requiring repeated accesses to a common memory to retrieve (and store) instructions and data. Another basic problem is encountered in the actual process of computation, the time required, for example, to perform floating-point multiplications. This simple control-driven structure is unsuitable for many computationally demanding tasks such as the interactive simulation of complex systems and applications involving intelligent knowledge based systems (IKBS) or artificial intelligence techniques such as expert systems.

Three basic methods are currently being explored to overcome these problems:

i) Increasing the speed of a uniprocessor system by employing interleaved memory systems, multiple function units, pipelining and vector processing [4];

ii) Multi-processor systems;

iii) Highly parallel architectures including Array processors.

Super computers, such as the CRAY machines, utilise many of these techniques in particular pipelining, and vector processing using multiple function units.

A pipelined computer performs overlapped computations and data transfers to exploit temporal parallelism. An array processor uses multiple synchronised arithmetic and logic units to achieve spatial parallelism. A multiprocessor system achieves asynchronous parallelism via a set of interactive processors with shared memories, database etc.

A highly parallel architecture is comprised of a large number of computing elements, which may be expanded at approximately linear cost, and would normally solve one particular problem. An important property of such structures is the grain size or granularity, this refers to the size of a concurrent module (processes or processors, which may be executed simultaneously) and is usually directly related to the number of hardware processor modules. Fine grain systems give maximum parallelism but give rise to communication problems; if the grain is too course parallelism is limited.

Computer architectures have been classified by Flynn [5] into four basic organisations:

a) single instruction stream - single data stream (SISD) (conventional single processor machine);

b) single instruction stream - multiple data stream (SIMD) (array computers and vector processors);

c) multiple instruction stream - single data stream (MISD);

d) multiple instruction stream - multiple data stream (MIMD) (multiprocessor systems).

MIMD systems are said to be tightly coupled if the degree of interaction among the processors is high, otherwise they are considered as loosely coupled.

An example of a fine grained, massively parallel SIMD computer, is the DAP 510 machine which is structured as a two-dimensional 32 x 32 array of single-bit processing elements hosted by a SUN or VAX computer. Another example of an SIMD structure is the connection machine [6] consisting of 65,536 elementary processing unit. SIMD architectures are particularly suited to supported image processing, aerodynamic studies, weather forecasting and computer image generation including engineering graphics.

2.3 Interconnection Networks [7] [8]. The major factors which must be considered when designing a parallel processing architecture are the number of individual processors, the complexity of each processor and the degree and mode of interaction between processors. The most important characteristic of a parallel system is processor communication and the manner in which the processors are interconnected. The interconnection network determines the way processors can share information among themselves and with common memory units.

A shared memory system, see figure 1, has single or multiple global memories accessible to all processors. The mode of connection may be direct, with every processor being connected to every memory unit, via a shared communications highway or bus, or by means of a cross-bar switching circuit.

In distributed memory architectures the processor nodes have their own local memory which must be loaded with data prior to the start of a computation. Information stored in a local memory may be shared between processors using a message passing procedure. A message is sent to a specified node requesting information, if the message is accepted the data is sent back in a return message. In some structures the message would need to be passed from node to node before reaching its specified destination. The performance of these systems will critically depend on the mode of interconnection and the mapping of the data requirements of a given algorithm onto the interconnection structure. Many forms of interconnection network are possible, see figure 2, ranging from simple rings and arrays to hypercubic forms.

The hypercube structure is particularly favoured and is used for instance in Floating Point Systems T Series of machines. In this configuration each processor is connected to n others, where n is the dimension of the cube, and messages take a maximum of n steps to pass between any two processors; the cube would comprise $2^n$ processors. The advantage of this topology is that it provides the shortest routes with the minimum of connections and can be mapped onto other structures such as meshes, rings etc.

In some machines, for example the Meiko M40 computing surface machine based on transputer technology, the network topology can be configured under software control, using programmable switches, to obtain the optimum processor interconnection network for a given problem.

2.4 Other Advanced Architectures. An alternative concept to highly parallel general purpose supercomputers is the use of coprocessors, accelerators and computing engines to perform specific functions such as simulation [9] [10], optimisation, inferencing [11], graphics processing etc. The concept has also been extended to develop highly efficient language processors, where the architecture is tailored to maximise the performance of specific programming languages such as Lisp, Prolog and Smalltalk.

The approach of designing special engines to meet specific requirements has been made economically viable by the rapid development of VLSI circuit techniques and the associated CAD systems. The use of application specific integrated circuits (ASICs) means that computers can now be custom designed to meet computational and user requirements.

These ideas are of particular relevance to engineering design where the requirement is for high performance engineering workstations. Using a networked system, powerful computing engines and accelerators can be accessed as a shared resource, off-loading a simulation or optimisation problem, whilst still working on other tasks and keeping track of the remote computation by means of a window-editor.

A major innovation in this area has been the development of the Transputer [12] [13] a single chip RISC computer which can be used as a building block in parallel processing systems; communication between processors is achieved via message passing over high speed serial input-output channels. The device is programmed in Occam, a language designed to handle both sequential and parallel processors.

The Transputer has been employed as a coprocessor to host machines such as the IBM PC, and more recently Atari has developed the Abaq multiprocessor [14] with up to 12 Transputers arranged to run alone or as part of a distributed system. The Abaq runs under a Unix like operating system called Helios and compilers are being developed for Pascal, Fortran, Lisp etc.

Transputers have also been used to develop supercomputers at a fraction of the cost of current machines; work is underway in this area at the Universities of Edinburgh and Southampton. Transputer based machines of this type create the potential for desk-top supercomputer workstations which would open up a new dimension in interactive engineering design.

2.5 Programming Parallel Computers [15] [16] [17]. The programming of parallel computers presents a formidable task if the user wants to exploit the machine to the full. The structure of the problem, particularly the amount of inherent parallelism in the data, is often the determining factor in obtaining an effective solution. Users must "think parallel" a process which though inherent in many human functions is still alien to a generation of programmers versed in serial problem solving.

Though it is possible to render the parallelism of a machine transparent to the user, for example by providing automatic parallelisation of sequential code, in general the user must be more aware of the underlying hardware than is normally the case with sequential computers.

There is a fundamental problem with converting existing sequential software into parallel code in that the procedure exploits the parallelisms embedded in the algorithm (which effected a serial solution to the original problem) and does not allow the invention of new parallel forms of solution. However the use of parallelised compilers does allow existing software (for example written in FORTRAN) to be executed at higher computational speeds. For example, FORTRAN programs executed on a Transputer B004 coprocessor with IBM PC Host execute up to an order of magnitude faster.

Parallel programming calls for new models of computation. For example, message passing schemas require problems to be broken down into ideally independent parallel processes, whose communication needs can be reduced to a simple and regular exchange of messages, with the data structures being stored inside the processes. The choice of network connection is normally problem dependent and directly affects the speed of communication.

Multiprocessor systems would appear to support the object-oriented programming paradigm [18] in which entities are represented as objects which have their own private memory and an associated set of operations provided by the class to which it belongs. For example, the class "components" may consist of objects nuts, bolts, screws etc., and methods for performing operations on these objects. Computations are performed by sending messages to objects which invoke a method in the objects class.

Object-oriented programming systems (OOPS) such as Smalltalk 80 are rapidly gaining ground in model building and system simulation but do not in general map efficiently onto conventional computer architectures; there are indications that they could be better implemented using parallel structures [19].

Though there are still many major problems to be solved parallel processing holds the promise of transforming, among others, graphics and simulation techniques making it possible to interactively model and analyse natural phenomena at a level of sophistication hitherto thought impossible.

## 3. Engineering Support Environments

Computer-aided engineering has been, and will continue to be even more so in the future, heavily dependent on networked personal workstations. If full advantage is to be made of this environment then it will be essential to provide an appropriate software support environment for the management, documentation and design tools essential to the engineering design process.

The engineering support system (ESS), similar in concept to the integrated project support environment (IPSE) proposed for software engineering, is shown in figure 3. In general the ESS can be considered as consisting of various layers; there is an inner core of computing hardware, CPU, input/output, memory etc., surrounded by operating systems and language software. Next comes the general utilities software like database, graphics and network managers, with the outer layer supporting the applications and design tools.

An ESS should enable group project teams to work together sharing the same information and tools, consequently a basic requirement is for the exchange of data from any one workstation to any other on the network. Again it is essential that input/output data formats should be compatible between software tools, calling for format interchangers, and that new tools should be acceptable to the system. The last requirement depends critically on standardisation, not just language portability but also the development of interchange data formats and tool interfaces.

If design automation is really to succeed the development of a fully integrated ESS for design and manufacture, including an open-systems policy for hardware and software tools, must be given urgent priority. Currently there is too much fragmentation of effort, with engineers developing software tools to run in particular environments, defacto standards like UNIX and the IBM PC are not really adequate!

3.1 Database Technology. Engineering databases differ markedly from commercial database management (DBMS) for example, in business applications there are normally few record types, records are accessed in a regular sequential manner and the relationships between records are comparatively simple. In contrast, engineering design applications call for many record types with complex relationships between them, and random data access. Another problem with traditional DBMS is that they do not allow the modelling of engineering objects in a natural way. That is they do not support the retrieval and manipulation of such objects in a way that is familiar to engineers. Again, there is a difference between a databank (or catalogue) of engineering components and devices accessed on a linear search basis and the dynamically changing databases used in CAD applications.

Though the advantages of a shared centralised database containing all the data that design, analysis, drafting and manufacturing programs generate and utilise is obvious, the design of such a system presents a formidable task. Some of the major problems are as follows:

a) The difficulty of specifying the overall user requirements. Recent work on semantic data models [20] which allow data to be described in an abstract manner directly related to application, has been used to evolve a high-level conceptual specification for a database system.

b) The choice of a suitable data structure or model for the DBMS implementation and the associated query language, taking into account the user requirements and experience [21].

c) The database would need to be accessed in parallel by users with different needs and requirements - giving rise to problems of performance and conflicts.

d) Many different databases are already in existence and would either need to be rewritten or integrated into the DBMS.

The relational database model [22] appears to hold many advantages for CAD/CAM particularly when used in conjunction with a structured query language

(SQL) [23]. The major strength of SQL (which is keyword based) is that it deals with sets of data, the language itself being defined by relational mathematics, so there is a close match between the query language and the relational data model. Another important advantage is that SQL offers a standard method (as defined by ANSI and IBM) of querying very large databases and also facilitates the exchange of data between workstations and mainframe machines.

Again object-oriented databases [24] [25] have been proposed for supporting engineering applications. An object is perceived as an entry that can be manipulated as a whole, for example a geometric object that has to be rotated in space. Using this approach the user can manipulate permanent data objects by application specific operators. This behavioural approach to databases has it origins in programming languages, particularly the notion of abstract data types.

Research is also in progress in the following areas:

a) Distributed database systems, in which data is kept at widely dispersed locations connected by networks. The major problems are concerned with communication and conflict issues - the transfer of data between machines causing bottlenecks.

b) Database machines specialised computer architectures, often using parallel processing techniques, have been designed as intelligent back-ends to host machines and dedicated to data management or specialised database tasks.

For instance, a 16,000-processor Connection machine has been used for high speed querying of a large database [26] based on a free-text search algorithm. Later work has suggested that the form of search algorithm is critical and that current mass storage devices do not provide sufficient I/O bandwidth to justify highly parallel database machines.

Other work in progress [27] based on the transputer, utilises existing databases in conjunction with separate application oriented user databases. Queries are sent to the user database, which could initially be either empty or pre-loaded, and if the required data is not present the query is processed and sent to the main database. The required information is returned direct to the user and also stored in the user application database, analogous to a cache memory system. The application database could also contain rules and inferencing procedures to enable it to function as a knowledge base. Techniques of this type would be ideally suited to a locally distributed engineering database management system.

The use of parallel processing techniques, especially those based on multiprocessor systems, show considerable promise for database and retrieval systems particularly in the area of intelligent storage systems such as, for example, in associative processing.

3.2 Methods and Tools. Initially computers were used primarily for the calculation intensive stages of design. Advances in computer performance and interactive graphics stimulated new methods of analysis and more detailed modelling and simulation techniques allowing the investigation of a greater solution space. Unfortunately the impact of CAD systems has been largely restricted to the more detailed levels of design as opposed to the initial conceptual and requirements specification stages.

The design process may be considered as consisting of a number of interacting hierarchical levels, see figure 4. At each level of the process a set of specifications will be generated detailing the results of the relevant design stage. Note that interaction between all stages is essential to optimise a design; note also that the semantic content of a design specification must be preserved and correctly mapped onto the next level of design. Current CAD systems are primarily concerned with optimising the design at the sub-system and components level with a corresponding restricted solution space in terms of the total design. The effect of a radical or major change in design or materials at these levels on the behavioural level is seldom contemplated. Even more important there are few CAD tools available for this purpose and none of these to the author's knowledge integrated into the total design process.

Software tools available for system design are mostly concerned with the creation of dataflow and structure diagrams and general systems documentation. The Design software package, developed and marketed by Meta Software Corporation of Cambridge Massachusetts, has all these facilities and also allows the setting up of "grammar rules" for drawing the diagrams. If a rule is violated, such as the rules for the proper attachment of input-output connections to a sub-system module, appropriate error messages are generated.

Another design system as SADT [28], structured analysis and design technique, which has had considerable success in problem analysis, requirements definition and functional specification.

Research is also underway in developing tools for the conceptual creative levels of design employing developments in artificial intelligence techniques in particular IKBS. The major problems being investigated are formalisms for knowledge representation and the strategies for reasoning, including the identification and significance of interactive relationships, using these representations.

The use of expert systems technology [29] in CAE is now well established with many applications being described in the literature [30]. The term expert system describes software embodying a collection of knowledge, facts and rules together with an inferencing machine that mimics the procedures that a human might employ to solve a particular problem.

An effective expert system application should satisfy the following criteria:

a) applications must have well defined domains of interest;

b) experts (people recognised as performing the desired task in a superior manner) must be available;

c) the experts must be able to verbalise the execution of the desired task.

Thus it is very apparent that the elicitation and representation of expert knowledge is the key and the major stumbling block to the design of effective expert systems. Unfortunately it is all too easy to develop an expert system, using for example an expert system shell, in which the "experts" knowledge is gathered inexpertly resulting in an expert system with one particular approach to solving the problem frozen in the model.

Another important aspect is that the usefulness of an expert system tool depends on how well it integrates with the total CAE system, in particular the ability to access and use other programs and data. Too often expert system applications are designed out of context with the rest of the system.

Computer Scientists are all too aware that the claim made for expert systems using the long established AI rules and frames techniques have been overplayed and that much more fundamental research is required. There is also considerable work in hand on logic programming [31], though again many would question the value of monotonic logic systems in IKBS applications. Another problem arising with expert systems is the large computational load required, for example in undertaking forward and backward chaining; research in the use of parallel architectures and specially designed 'expert systems on a chip' is being actively pursued.

Notwithstanding, within a restricted and well defined domain expert systems are beginning to find industrial application, for example in the real-time adaptive tuning of control parameters, such as the gain in feedback loops.

## 4. Summing Up

Arising from this survey the following points seem worthy of further consideration:

a) that advances in computer architectures, particularly the availability of supercomputer power in a personal workstation, opens up a new dimension in interactive modelling and simulation;

b) that there is a need for more fundamental research in computer science, particularly in the areas of AI and the use and programming of parallel computers;

c) that the specific problems of CAE, such as the development of a fully integrated engineering support environment including the use of engineering databases, should be urgently investigated, preferably by interdisciplinary teams;

d) that engineers should be more aware of current work in computer science before embarking on the development of applications software;

e) that computer scientists should attempt to understand the overall engineering dimension and make themselves aware of engineering problems and requirements.

A more important and pressing issue is the question of the new product liability laws which came into effect in March 1988. Under these laws a designer could be held legally responsible, and charged under criminal procedures, for any damage to person or property resulting from malfunctioning of a product traceable to a design error. This raises many frightening prospects when employing new technology, particularly when design decisions could be based on computer modelling and expert systems techniques.

## References and Bibliography


1. Engineering Support Systems: User Requirements
   L Bezanson et al
   IEEE Micro 5 no.5 p36-50 October 1985
2. A Survey of RISC Processors and Computers of the Mid-1980s
   C Gimarc and V Milutinovic
   IEEE Computer 20 no.9 p59-69 September 1987
3. Advanced Computer Architectures
   G Fox and P Messina
   Scientific American 257 no.4 p45-52 October 1987
4. Computer Architecture and Parallel Processing
   K Horang and F Briggs
   McGrew Hill 1985
5. Very High Speed Computing Systems
   M J Flynn
   Proc IEEE 54 p1901-1909 1966
6. The Connection Machine
   W D Hillis
   MIT Press 1985
7. A Survey of Interconnection Networks
   T Feng
   IEEE Computer 14 no.12 p13-27 December 1981
8. Interconnection Networks - special issue
   IEEE Computer 20 no.6 June 1987
9. A Survey of Hardware Accelerators Used in CAD
   T Blank
   IEEE Design and Test of Computers 1 no.3 p21-39 August 1984
10. MARS: A Multiprocessor-based programmable accelerator
    D Agrawal et al
    IEEE Design and Test of Computers 4 no.5 p28-36 October 1987
11. Expert System on a Chip: An engine for real-time approximate reasoning
    M Togai and H Watanabe
    IEEE Expert 1 no.3 p55-62 Fall 1986
12. The Transputer
    P Walker
    Byte 10 no.5 p219-235 May 1985
13. The IMS T800 Transputer
    M Homewood, D May, D Shephard and R Shepherd
    IEEE Micro 7 no.5 p10-26 October 1987
14. Atari Abaq
    Personal Computer World p105-110 February 1988
15. Programming for Parallelism
    T Karp
    IEEE Computer 20 no.5 p43-57 May 1987
16. A Parallel Architecture comes of age at last
    P Wiley
    IEEE Spectrum 24 no.6 p46-50 June 1987
17. Supercomputer Languages
    R H Perrott and A Zarea-Aliabadi
    ACM Computing Surveys 18 no.1 p5-22 March 1986
18. Elements of Object-Oriented Programming
    G Pascoe
    Byte 11 no.8 p139-144 August 1986
    (This is a special issue on Object-oriented languages)

19. DOOM: A decentralised Object-oriented machine
W Bronnenberg et al
IEEE Micro 7 no.5 p52-69 October 1987
20. Database Description with SDM: A Semantic database model
M Hammer and D McLeod
ACM Trans. Database Systems 6 no.3 p351-366 Sept.1981
21. A Framework for Choosing a Database Query Language
M Jarke and Y Vassiliou
ACM Computing Surveys 17 no.3 p313-340 September 1985
22. A Relational model for large shared data banks
E Codd
Commun.ACM 13 no.6 p377-387 June 1970
23. SQL/Data Systems, concepts and facilities
IBM Report GH 24-5013, IBM Corp. January 1981
24. Database facilities for engineering design
C M Eastman
Proc. IEEE 69 no.10 p1249-1263 October 1981
25. Views, objects and Databases
G Wiederhold
IEEE Computer 19 no.12 p37-44 December 1986
26. Parallel Free-Text Search on the Connection Machine
C Stanfill and B Kahle
Comm.ACM 29 no.12 p1129-1239 December 1986
27. Private communication February 1988
Dr J Kerridge, Department of Computer Science, University of Sheffield.
28. Applications and Extensions of SADT
D Ross
IEEE Computer 18 no.4 p25-34 April 1985
29. Expert Systems, Knowledge Engineering and AI tools-An Overview
C Williams
IEEE Expert 1 no.4 p66-70 Winter 1986
30 Knowledge-Based Engineering systems: Research in Progress
IEEE Software 3 no.2 p48-60 March 1986
31. Logic Programming and Prolog: A Tutorial
R Davis
IEEE Software 2 no.5 p53-62 September 1985

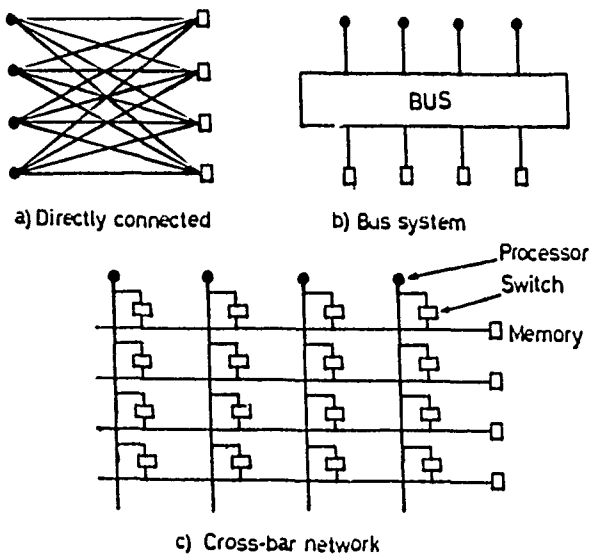


FIG 1 – SHARED MEMORY SYSTEMS

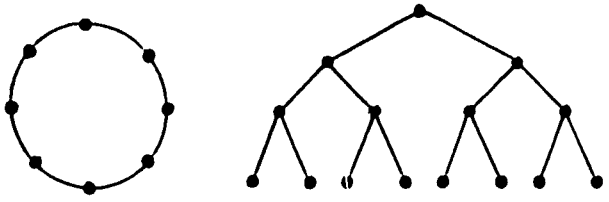

a) Ring b) Tree

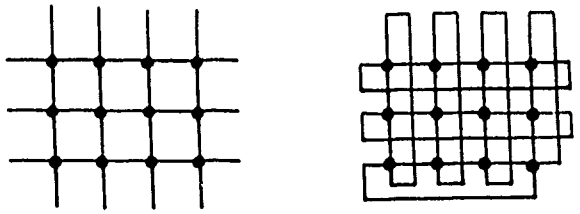

c) Planar array d) Mesh

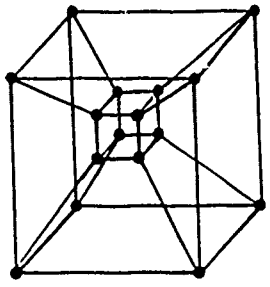

e) Hypercube

FIG 2 - DISTRIBUTED MEMORY SYSTEMS

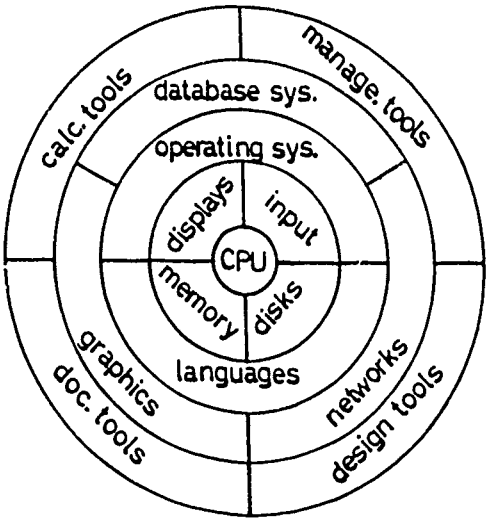


FIG 3 - ENGINEERING SUPPORT SYSTEM

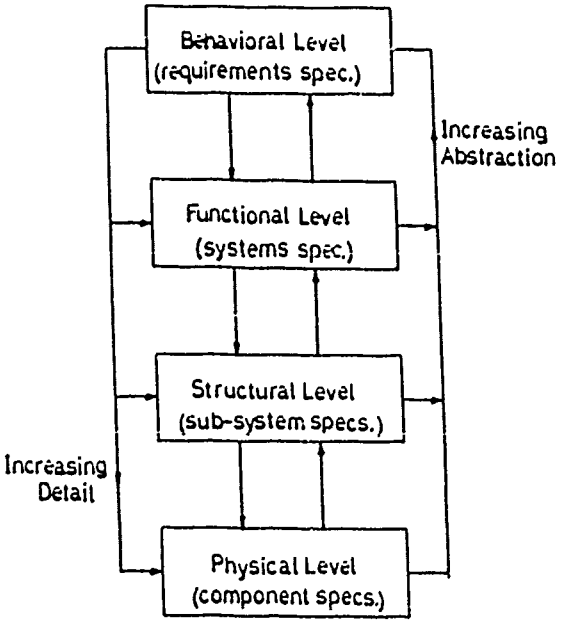


FIG 4 - DESIGN HIERARCHY

# CERAMIC WEAR TESTING FOR DESIGN

M G Gee and E A Almond

Drs M G Gee and E A Almond are in the Division of Materials Applications at the National Physical Laboratory, Teddington, Middlesex

SYNOPSIS

Before the service performance of ceramic wear components can be predicted confidently from laboratory data it is necessary to ensure that reproducible and reliable results are obtained in laboratory wear tests. Attempts at standardisation have recognised the importance of maintaining load, velocity, test geometry and the specimen's surface-finish constant, but there is still considerable scatter caused by some unidentified variables. Possible sources of variability include variations in environment and vibrational characteristics of the test machine. However, even when all the external test parameters have been accounted for, some unexpected microstructural mechanism may intervene and prevent wear behaviour from being extrapolated beyond the conditions used in a standardised laboratory test.

## INTRODUCTION

A yardstick for success in understanding an engineering property is for it to be expressible in a form that can be incorporated quantitatively into a design for a component or structure. The pressure for this kind of numerical information has grown considerably in recent years with the setting up of property data banks, expert systems and computer aided design procedures. It is unfortunate that this quest for data is being extended to wear properties even though for each wear application there is a unique set of conditions and behaviour that cannot yet be extrapolated from laboratory tests or predictive models. This applies especially to the relatively new field of sliding wear of ceramics operating under unlubricated conditions. However the sparsity of data has one advantage, since it offers a period for a critical appraisal of test techniques and requirements before ideas and perceptions become entrenched and stultified by masses of unreliable and conflicting prematurely gathered test data.

## VARIABILITY AND WEAR

There are currently national and international exercises to investigate the repeatability and reproducibility of dry sliding wear tests on ceramics [1,2]. It is important to note that these projects are not concerned with establishing the relevance of the results to an application. This is a distant target. They are solely concerned with identifying the factors that cause variability in the results of wear tests. The known sources of variability that have been kept constant are test geometry and specimen dimensions, test load, relative velocity of the wear interface, length of time of test and surface finish of the wear surfaces. Even with this degree of test control the repeatability and reproducibility of tests carried out internationally for the wear test methods group of VAMAS (Versailles Project on Advanced Materials and Standards) in 38 laboratories were only 5-14% and 13-35% (Table 1) when the results were analysed assuming a normal distribution of results [1]. For these levels of scatter a Weibull analysis is probably more appropriate and in a project performed by a UK wear test methods group (UKWTM), tests on steel specimens [2] gave indications of a bimodal distribution (Fig 1). The reason for this appeared to be that two different designs of machine were used by the participants, and this introduced an effect from an unknown source of variability, even though the test conditions were nominally identical.

An illustration of the degree of variability that can occur if specimen composition, load, test geometry, and interface velocity are not standardised is shown in Fig 2 . In these results it can be seen that the coefficient of friction varied from 0.2 to about 1, and the wear rates varied by up to four orders of magnitude for a 95% and a 99.5% alumina tested in pin-on-ring and pin on-disc geometries [3]. Applying a Weibull analysis to the data gave Weibull factors of 0.34 for the wear rate and 2.24 for the friction coefficient. When the results were examined in more detail it was found that wear properties varied not only with the change in composition of the alumina, but also with a change in geometry from a pin-on-ring to a pin-on-disc configuration. The latter test was the more discriminative between materials and gave much lower wear rates for the 99.5% alumina than for the 95% alumina.

## CERAMICS AND WEAR

Before examining the sources of the variability in wear results in more detail, it is useful to consider the properties of ceramics that are particularly important in determining wear behaviour, and to consider how these influence wear mechanisms.

Thus the ceramics of particular interest for sliding wear applications have high hardness and low ductility at room temperature. Consequently brittle fracture makes a greater contribution to wear damage than it would in metals. Nevertheless, significant plastic deformation can occur when ceramics are subjected to hydrostatic compressive stress fields such as those that are generated under an indenter in hardness tests, and are thought to exist in some wear situations. However, more generally, resistance to plastic and elastic deformation is high. As a result, when two wear surface are pressed together the asperities resist deformation, the true area of contact remains small and the contact stresses are correspondingly high.

A major attraction of ceramics is their high strength and creep resistance at elevated temperatures. However, this may not be true for ceramics which contain glasses or other compounds formed during sintering. These constituents have a much lower melting point than the matrix, and exhibit viscous flow at high temperatures with the result that resistance to deformation is considerably reduced. Another disadvantage is low thermal conductivity which causes high local temperatures to be generated at points of contact between two wear surfaces, and contributes to a poor thermal shock resistance.

Ceramics have a reputation for inertness and resistance to degradation in hostile environments. However, whereas this is usually true for oxides such as alumina and zirconia heated in air, nitrides and carbides oxidise. Under some circumstances this may cause the formation of a protective oxide film, but this will not stop degradation if the film is continually worn away at contacting wear surfaces.

The surfaces of ceramic components are normally machined to their final finish by abrasive techniques such as grinding and lapping. Grinding leaves surfaces which are too rough for precision applications, but more importantly, it introduces damage in the form of sub-surface cracking to a considerable depth into the ceramic. Ideally lapping and polishing should remove the damaged surface layers and leave a surface which is smoother and free of cracks and residual stresses.

## MECHANISMS OF WEAR

Wear studies on ceramics have tended to concentrate on mechanical processes, and of these, abrasion of one surface by asperities on the opposing surface, or by hard particles of wear debris trapped between the wear surfaces is likely to make a major contribution to sliding wear. On a fine scale, abrasion takes the form of ploughing and cutting of the surface leaving a characteristic grooved appearance (Fig 3). The relative contributions made by ploughing and cutting are dependent on the geometry of the abrading point, the mechanical properties of the materials and the load acting through the abrading point. At higher loads, with greater areas of contact and increased surface roughness, deformation mechanisms may include processes similar to those observed in indentation fracture such as Hertzian cone cracking or lateral cracking.

At low wear rates, flat polished surfaces are often produced. The surface is very smooth, but in materials like alumina where the crystal properties are anisotropic, the surfaces of some grains are depressed relative to the surfaces of their neighbours, while other grains may be pitted (Figs 4). Since preferential material removal occurs in grains that are oriented in crystallographically 'soft' directions, these observations indicate that polishing wear may involve plastic deformation, arising from abrasion on a very fine scale.

There is some controversy over the degree of plasticity that occurs in the wear of ceramics. Plastic deformation would certainly be expected to contribute to surface grooving in abrasive wear, but this is generally a small scale process. Also, plastic deformation is likely to occur if high temperatures are allowed to develop at points of contact between wear surfaces. However what is in dispute is an explanation for the appearance of ceramic surfaces that have undergone very high wear rates and often give the impression that they have been subjected to gross plastic deformation (Fig 5). To examine this possibility, a cross section was taken through a heavily worn surface of an alumina sample but no evidence of plastic deformation could be seen. In addition, the results of an X-ray examination of the surface indicated that if plastic deformation had occurred it was on a scale which was below the limits of detection of the technique [3]. This would correspond, at most, to a thin surface layer confined to the uppermost portions of the surface grains. Consequently an alternative explanation for the pseudo plasticity exhibited by heavily worn surfaces must be found. For example, it is possible that the distortions produced by plastic deformation could be simulated by the formation of suitable assemblies of fine non-propagating microcracks.

Failure mechanisms that are frequently neglected when considering wear are those involving fatigue by corrosion or by thermal or load cycling. Thus points of contact between two wear surfaces are usually subject to fluctuating loads as the path of the asperities traverses hills and valleys on the opposite wear surface. Similarly thermal stresses will fluctuate in regions which are alternately heated by the energy dissipated in friction and cooled during periods of non contact. Both sources of load cycling lead to the growth of fatigue cracks in the surface layers of the ceramic, and eventually cause breakaway of material from the wear surface. The process occurs at the higher wear rates and leads to rough broken surfaces. It is accelerated in a corrosive environment.

If material detached from the wear surfaces is not removed from the wear system it will undergo comminution to a fine dust but while this is occurring it will cause further damage by acting

as an abrasive. This appears to have happened in the tests on alumina referred to above. Thus very fine (20-30 nm) particles were observed by transmission electron microscopy and X-ray observation to make up a large part of the wear debris [3]. Larger particles, which were also observed, would have acted as an abrasive but it is also possible that some became entrapped in surface cracks and accelerated crack growth by wedging the cracks open. Another role that wear debris may play under some circumstances, is that of a reinforcing agent. For example particles of debris from a hard phase in a material may be pushed back into regions of a softer phase and provide a surface which has enhanced wear resistance [4].

In some ceramics if the wear surfaces reach a sufficiently high temperature a liquid phase forms and acts as a lubricant. For example the low melting point glassy phase that is present in some ceramics can melt, or for silicon based ceramics, reaction with oxygen in the surrounding atmosphere can form low melting point glasses.

## EFFECT OF CHANGING TEST VARIABLES

Some of the effects of test variables can be predicted. For example, wear rate would be expected to increase with applied load and this is generally observed in sliding wear tests on ceramics. However, estimating the magnitude of the effect is by no means straightforward and may depend on a large number of variables including the initial surface condition of the specimens. For example, in pin-on-disc experiments on a 95% alumina, when the specimens were lapped to give a smooth surface finish, low wear rates were observed [3]. When specimens with a rougher surface finish produced by grinding were tested under the same conditions, high wear rates were observed (Figs 6a and b). This result can be explained by the wear process changing from a polishing mechanism for the lapped specimens, to a fatigue mechanism for the ground specimens. Thus the surface damage in the ground specimens probably occurred by growth of networks of microcracks under the fluctuating stresses imposed at the points of contact, leading to continual breakaway of material.

The wear rate would also be expected to increase with interface velocity, and this was found to be true for a 99% alumina ceramic but results from tests on a 95% alumina exhibited a maximum in wear rate and in friction with increase in velocity (Fig 7). This can be explained by the presence of a glassy phase with a relatively low softening temperature in the 95% alumina. Thus as the sliding velocity was increased, initially there was the expected increase in wear [3]. With further increases in speed the glassy phase softened and caused added wear and increased friction as a result of adhesion between the wear surfaces. Eventually the glassy phase melted and formed a liquid lubricant at the wear interfaces, with resulting reductions in friction and wear. This is an example where a microstructural mechanism had an overriding effect on wear which prevented wear behaviour from being treated as a monotonically increasing function of interface velocity.

In addition to effects from velocity, load and surface finish, there are good reasons to expect that changes in test environment can influence the results of wear tests. Control of humidity is particularly important since a marked increase in wear and friction has been observed in wear tests on alumina when the humidity of the air surrounding the test was reduced below about 15% relative humidity. This effect was due to the removal of an adsorbed layer of water from the surface of the alumina at low humidity levels. The layer which was only a few molecules thick lubricated the two surfaces with a resultant reduction in friction and wear. A similar increase in wear rate has been observed for hot-pressed silicon nitride when the humidity was reduced below about 40% relative humidity (Fig 8). However, there was no increase in friction coefficient [5]. The mechanism is thought to be somewhat different to that for the alumina, with the high humidity stabilising a hydrated silica protective film formed by reaction of the silicon nitride with the air.

Variation in test temperature may also be a source of scatter in wear test results but the effects are relatively small for the typical fluctuations of a few degrees that occur in room temperature testing.

Effects on wear from using different designs of test machine have been referred to above, and could arise from several sources in for example the results obtained in the pin-on-disc and pin-on-ring tests shown in Fig 2 [3]. Thus, there were differences in the thermal properties of the specimens and specimen holders such that in the pin-on-disc test the disc had lower thermal capacity than that of the ring, and the wear interface was closer to the nearest metallic heat sink than in the pin-on-ring test. This would have caused the ring to be hotter than the disc, and subjected the disc to wider thermal fluctuations than the ring. The higher temperatures in the rings would have favoured the microplastic abrasion and polishing mechanisms that operate at low wear rates. In contrast, thermal fatigue of the disc would have promoted the crack initiation and propagation processes associated with high wear rates. This explanation agrees with the observation of higher wear rates in the pin-on-disc tests.

A variable that has received little attention is the difference in the vibration characteristics of test machines [3]. This was investigated by suitable instrumentation of a pin-on-disc machine where it was found that natural frequencies of 518 and 17 Hz existed at the wear interface (Fig 9). If these results are interpreted in terms of the high frequencies and probable stress concentrations at surface asperities, it can be shown that the conditions are compatible with a wear process dominated by fatigue growth of sub-surface microcracks which destroys the integrity of the surface layers. Consequently it is concluded that the vibrational characteristics of a wear system, whether it is a test machine or a wear component, can have a considerable effect on wear behaviour, and should be taken into account in any simulative test.

## DISCUSSION AND CONCLUSIONS

From the above it can be seen that even though some degree of reproducibility can be maintained under specified test conditions, extrapolation to other conditions is dangerous since unexpected microstructural mechanisms may intervene and alter the overriding wear process. Another difficulty is that there is often more than one wear mechanism operating at any given time so that it is difficult to quantify wear in terms of a single mechanism. Wear mechanisms may also depend on one another in a synergistic way so that the wear rate with both mechanisms operating is more than the sum of wear rates for the individual mechanisms.

For the same reasons, it is inappropriate to try to use quantitative data obtained from laboratory wear tests in design procedures. Reliable prediction of materials performance must wait until the interaction of test variables and wear mechanisms are more clearly defined. The long term aim of this work must be to understand wear mechanisms and their interactions in sufficient detail to be able to model the wear behaviour of ceramics quantitatively. Until this has been achieved the best approach must be to make sure that simulated laboratory tests show the same wear mechanisms as those seen in applications. When this is true, then the results of the simulative tests can be expected to give a reasonably reliable guide to the relative performance of different materials.

## REFERENCES


1 H Czichos, S Becker and J Lexow, Wear 114 (1987) 109-130
2 E A Almond and M G Gee, Wear 120 (1987) 101-116
3 M G Gee and E A Almond, Mater. Sci. Technol., to be published
4 E A Almond, L A Lay and M G Gee, Proc. 2nd Int. Conf. Science Hard Mater. Inst. Phys. CS75, Adam Hilger, Bristol 1986, 919-948
5 T E Fischer and H Tomizawa, Wear 105 (1985) 29-45


TABLE 1 Results of VAMAS Interlaboratory Exercise.

| Material pair* | S-S | A-S | S-A | A-A |
|---|---|---|---|---|
| Friction Coefficient | 0.6(18)** | 0.76(18) | 0.6(20) | 0.41(19) |
| Wear Rate um/km | 70(28) | small | 81(36) | small |
| Wear Scar Diameter mm | 2.11(13) | *** | 2.08(17) | 0.3(17) |
| Wear Track Diameter mm | *** | 0.64(20) | *** | **** |

* S is steel, A is alumina.

** Figures inside brackets give percentage variation in results defined as relative standard deviation (standard deviation divided by mean).

*** Material transferred from one specimen to the other

**** Not measured

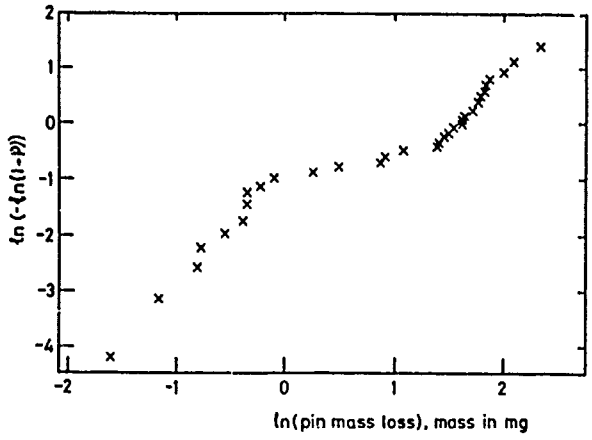


Fig 1, Weibull plot of pin mass losses.

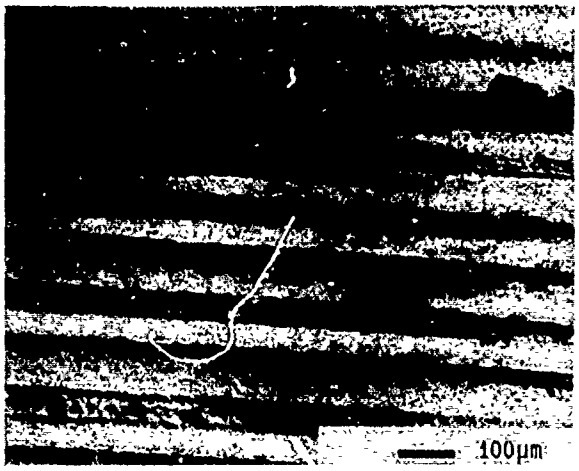


Fig 3, Optical micrograph showing abrasive grooving on surface of lightly worn 95% alumina pin.


Fig 4, Back-scattered electron micrograph of surface of lightly worn alumina pin.

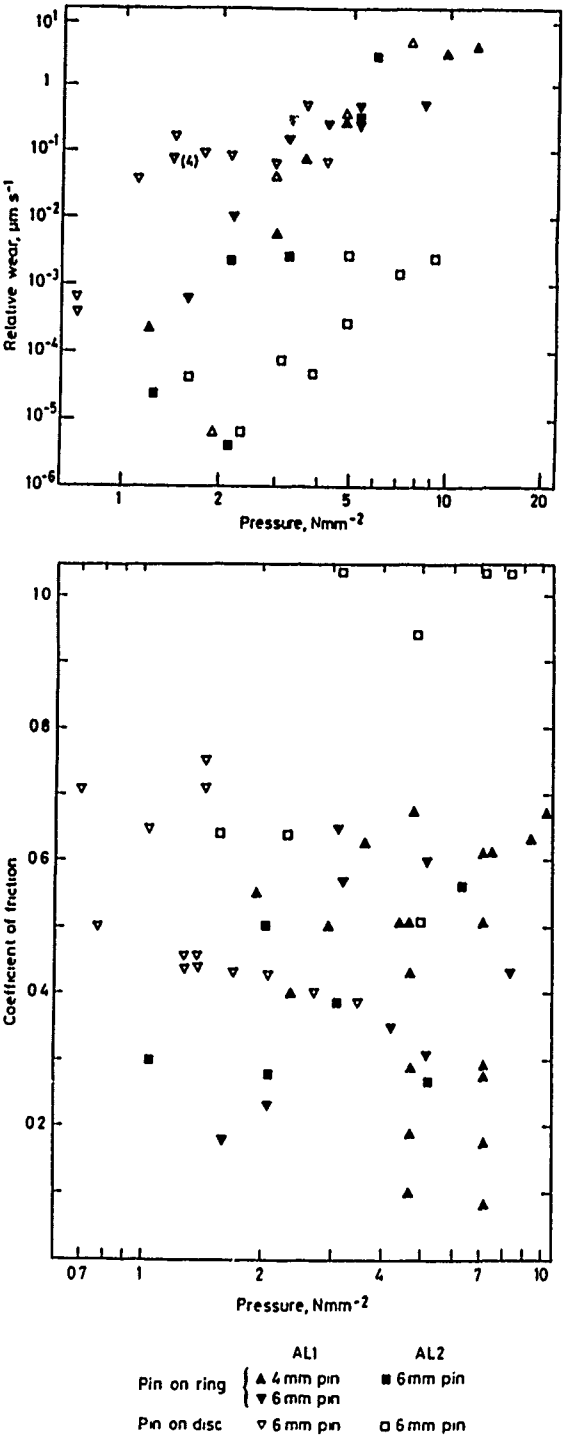


Fig 2, Results of sliding wear tests on 95% and 99.5% alumina (AL1 and AL2).

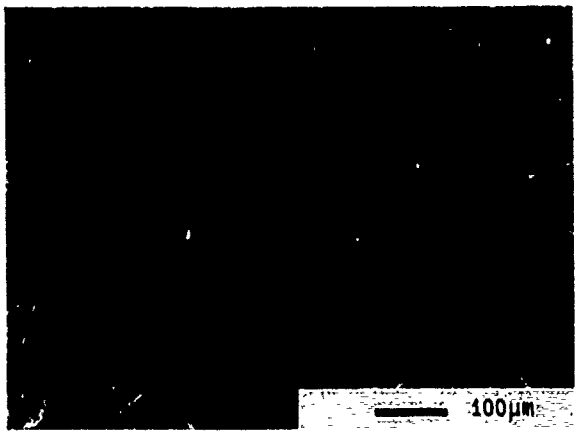


Fig 5, Scanning electron micrograph of heavily worn alumina pin.

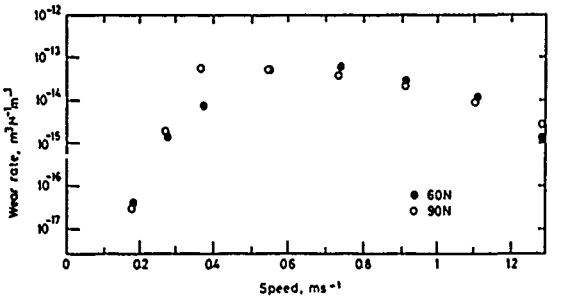


Fig 7, Variation in wear rate with interface velocity for 95% alumina.

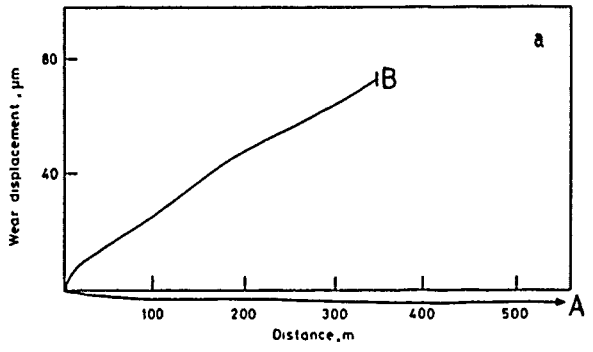


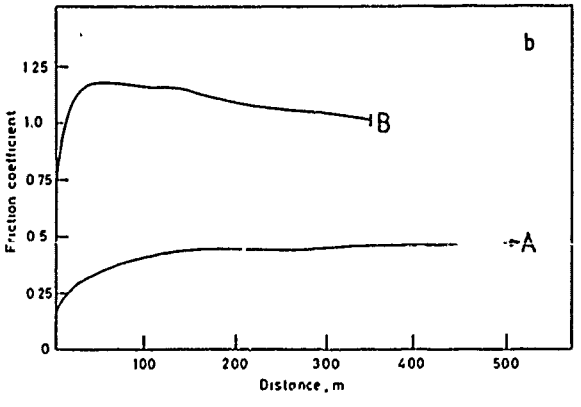


Fig 6, Results of pin-on-disc wear tests on 95% alumina given a lapped and polished surface finish (A) and a diamond ground finish (B); a) wear displacement, b) friction coefficient.

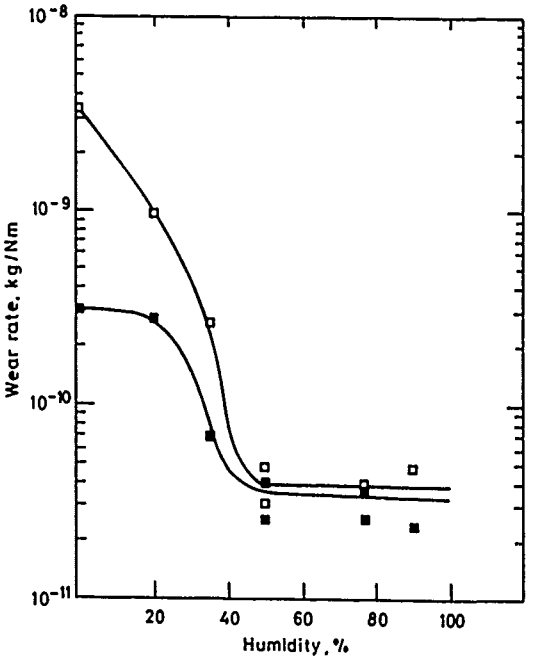


Fig 8, Variation in wear rate with relative humidity for hot-pressed silicon nitride.

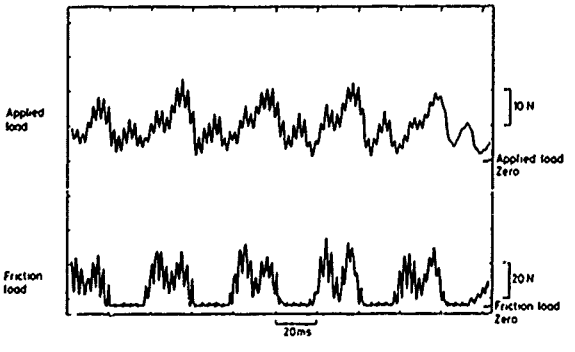


Fig 9, Fluctuations in applied load and frictional force in pin-on-disc wear tests on 95% alumina.

□

# COATING SELECTION FOR WEAR REDUCTION

Allan Matthews

Dr Matthews is 3M Reader in Surface Engineering, in the Department of Engineering Design and Manufacture at the University of Hull.

## SYNOPSIS

Effective use of coatings and treatments can extend wear lives by orders of magnitude. Designers have not used coatings as widely as they might for several reasons. One is the lack of a recognised selection procedure, another is the need to have ready access to a large amount of data on different coatings. Advances in Physical Vapour Deposition (PVD) technology, coupled with developments in computer expert systems will provide a solution to designers' problems in this area and ensure the wider use of coatings.

## INTRODUCTION

There can be no topic within the materials science field with as much potential as that of surface and coatings technology. It is now possible to 'surface engineer' components to have ideal surface and bulk properties. The realisation by many designers that these are not necessarily identical, together with process development, will bring about enormous improvements in materials and energy utilisation, and important benefits in terms of product quality, reliability and productivity.

It is well known that nearly all failures of durable components occur through surface initiated effects, such as wear, corrosion and fatigue. The surface also influences friction, and since it is the part we see, has an important aesthetic role to play. In many cases it also fulfils an optical, electrical or thermal function. The field of wear and friction control offers some of the most striking benefits for surface coatings. Indeed, modern techniques give the design engineer the capability to overcome problems which were insurmountable only a few years ago. For example, the use of thermal barrier coatings now allows gas turbines to run hotter and therefore more efficiently (Ref 1). The benefits of coatings are greater when the component is designed specifically to take advantage of the surface properties produced - a good example being the SKF and Dormer ADX Drill (Ref 2).

Clearly there is a need to encourage design engineers to employ coatings more widely. There are two main problems which prevent this. Firstly, there is no recognised procedure for selecting coatings. If such a procedure could be agreed then coatings would be specified more often and producers would have a specification by which to judge and improve their products. A second problem lies in providing data about different coatings to permit an appropriate selection. Currently, data tends to be process-specific; for example, weld-deposit and electroplating guides exist, but information is formatted differently in each case and comparison is difficult. As will be seen later in the paper, the best way around this problem is to apply computer knowledge-based 'expert' systems. These can store and manipulate large amounts of data, and follow a decision making route which in many ways mimics the human expert.

The paper will first discuss the topic of selection, tracing early approaches to the problem, and then explain how recent developments in coating and computer technology have begun to provide a solution.

## EARLY APPROACHES

All too often coatings have been seen as a 'last resort' solution to problems that had their roots in poor design or material selection. Worse still, companies usually adopt what James (Ref 3) describes as a 'positive selection approach'; that is, a solution will be tried and if it works it will be used. Rather than the progressive elimination of all feasible solutions, the first one that appears to fit the bill is used, often resulting in better solutions being rejected by default. Clearly this is an unsatisfactory state of affairs. Progressive elimination is to be preferred for many reasons, even though it is more time consuming. The discipline inherent in this approach encourages the acquisition of information (rather than the assumption of knowledge) and the investigation of alternative ways of solving minor problems obstructing highly desirable solutions. James has also stated that it is important to make expert advice available at the earliest opportunity. In his view: "Permitted freedom to contribute to the original design and to feed advice and suggestions before the design is finalised, the surface may play a significant role in producing a part with superior performance at a reasonable cost".

In many ways the approaches suggested by James (Refs 3, 4) and Smart (Ref 5), although appropriate, were constrained by the level of technology available at that time. Even so, the ideas they suggest include several valid features, which will be considered here.

Smart (Ref 5) presented a checklist to aid in selection, based on two headings: Process Selection and Materials Selection.

Process selection includes:

(i) General factors such as process availability and quantity required.
(ii) Job factors such as size, weight, and machinability.
(iii) Surface preparation factors such as undercutting and tolerances.
(iv) Finishing factors such as required finish and post-surfacing actions.

Materials selection includes:

(i) General factors such as knowledge of similar applications and cost.
(ii) Operating environment, including wear types and lubrication.
(iii) Properties required, including wear resistance, hardness, and machinability.
(iv) Substrate factors such as previous surface treatments and size.

The above provides a rather global approach which begs many questions. The properties of the same materials deposited by different techniques can, for example, be very different. The lists do not necessarily make the designer's job easier. In Ref 3, James made an effort to define the criteria and their inter-dependencies, and thereby make selection more straightforward. He did this by dividing the selection method into four distinct headings: Requirements, Limitations, Interactions, and Economics/design. He described these as follows.

Requirements:
Before any selection can begin, it is important that the function of the part and its surface should be understood. James suggests that by comparing surface and bulk requirements the designer will be able to determine whether a simple material will suffice or a composite structure is needed. Some requirements may be changed by design, including (possibly) surface requirements. By comparing requirements with resources it will be possible to make preliminary suggestions for materials and processes, but various limitations and interactions must be considered in order to select the most suitable ones.

Limitations:
Here the design requirements are applied to the preliminary choices, based on five factors: Environmental, Use, Social, Supply, and Process. 'Use' constraints refer to the operating location in which the coating will be used. A food factory or a nuclear power plant for example may impose certain specific constraints on what can be used (often based on safety legislation). Similar constraints may be associated with 'Social' aspects, Environmental, supply and process limitations are more straightforward to interpret.

Interactions:
These are split into three parts:

(i) Coating/substrates: the interaction of these two can be important, for example on adhesion, or under corrosive or stressed conditions.
(ii) Coating/process: some materials deposited by different processes give different properties. Examples are cobalt or nickel based alloys, which differ if applied by spraying or welding.
(iii) Process/substrate: the effect of the process on the substrate must be considered, eg overheating during weld cladding or hydrogen embrittlement during electroplating.

Economics and design:
James emphasizes that these factors need not necessarily be considered as constraints. For example, a design should not be considered as 'frozen' at too early stage, as a change may bring benefits in allowing a wider range of surfacing processes. He thus defines the ability to redesign as a 'resource'.

In essence James established a philosophy for selection which still applies today. This was developed by Smart, emphasising wear mechanism identification - an approach which was followed subsequently by several writers.

## THE WEAR MECHANISM APPROACH

Smart (Ref 5) used three wear type designations: Adhesion, Abrasion and Fatigue to illustrate some general rules of thumb on selection. He contended that adhesive wear in the presence of lubrication is best resisted by the use of soft, dissimilar metal coatings with little tendency to mutual solubility. Where lubrication is marginal or absent, he suggested that harder surfaces are required, the precise hardness being dictated by the contact pressure, the hardness of the contacting surface and its roughness. Abrasive wear is said to be best resisted by a coating with a high shear strength - translated into a hardness greater than 0.5 to 1.3 times that of any abrasive particles present. The thickness of the surface deposit should, according to Smart, be determined by the likely depth of abrasive penetration. In practice this will be related to the degree of load support provided by the substrate. Where low angle particle impact erosion is involved, hard materials give good resistance, even if they are brittle. With high angle impact, however, materials that are tough and ductile and can absorb substantial amounts of energy before fracture are preferred. If cavitation erosion prevails, Smart states that it is desirable to use a material with a high ultimate resilience (defined as half x ultimate tensile strength, divided by elastic modulus E). For contact fatigue resistance Smart prescribes a coating with a high yield strength ($Y$) and hardness coupled with adequate toughness. Others have specified the 'elastic strain to failure' as a determinant parameter in such situations. This has been equated (eg see Refs 6, 7) to a low ratio of $E/Y$.

From the above it can be seen that there can be no universal wear resistant coating to meet all requirements. Indeed, desirable properties

may be counteracting. As Smart points out, high hardness tends to be associated with low impact resistance, notch sensitivity and poor resistance to crack propagation. Thus selection is largely a compromise between hardness and toughness. Simplistically there should be adequate strength to resist the imposed loads, but sufficient toughness to avoid failure due to surface imperfections or incipient fatigue cracks. Smart favours an emphasis on toughness, since a higher than optimal wear rate will be preferable to catastrophic and unpredictable failure.

Wear resistance per se is not the only requirement from a coating. Farrow (Ref 8) lists these in descending importance thus:

(i) A good substrate to coating bond.
(ii) High hardness.
(iii) High structural integrity.
(iv) Chemical inertness.
(v) Low coefficient of friction.
(vi) Controllable surface topography.

If we add controllable toughness to this list, we can see that the demands placed on researchers developing suitable coatings for wear resistance are very stringent. The PVD methods are best suited to fulfilling these goals, as will be discussed in the next section.

The main drawback with an approach to coating selection which is based on identification of a dominant wear mode is that in almost all cases a number of wear modes operate. This has been succinctly summarised in a sketch produced by Farrow and Gleave (Refs 8, 9) and reproduced in Figure 1. The message from this is that wear is a process which invariably involves at least three or four interdependent mechanisms. At worst this could be said to invalidate many of the idealised approaches to wear control, such as the systems concept (Ref 10). This takes as a central goal the separation of each of the input and output variables in the tribological system - a daunting, if not impossible, task in many wear situation. Likewise, approaches based on the quantification of wear coefficients under laboratory conditions has been shown to be prone to enormous uncertainty. The ingress of small amounts of non-specified contamination can easily occur in practical situations, which can change wear coefficients by orders of magnitude.

This leaves the need to develop: i) Coatings with properties which are in general 'non-standard', that is having characteristics which would normally be expected to be mutually exclusive in traditional engineering materials. ii) Techniques of selection which can accommodate the 'human' attributes of being able to make deductions under conditions of uncertainty, and iii) Ways to transfer data on coatings to the design engineer in a readily assimilated form consistent with the selection procedure.

Technological advances in ionisation assisted PVD coatings and computer expert systems now mean that solutions to these requirements are in sight.

## THE CONTRIBUTION OF PVD COATINGS

Table 1 summarises, in a simplified form, some of the properties of the main generic groups of coatings and treatments. PVD methods stand out as offering by far the greatest scope for producing wear resistant coatings. In particular they are known for their capability to produce dense ceramic coatings at low temperature with excellent adhesion. Other benefits include their ability to replicate the original surface finish - thereby avoiding finish machining. Furthermore they are pollution-free and avoid the other possible drawbacks of electroplating: hydrogen embrittlement and build-up on corners.

Possibly more important than these attributes is the flexibility which PVD methods offer coatings technologists to 'design' coatings with specific (and often unique) properties.

Ceramic-based materials are in many ways ideal for wear resistance applications. They are hard and chemically stable - giving them excellent resistance to abrasive, adhesive and corrosive wear.

If we consider the E/Y criterion referred to earlier, ceramics rank very high in the scale of predicted wear resistance (see Table 2). They are especially effective at high temperatures, as they have excellent hot hardness and are stiff and dimensionally stable under stress. This explains their usefulness as cutting tool coatings. This field has to date been dominated by titanium nitride. Work by Kramer and Judd (Ref 11) indicates that even this material may be improved upon by other ceramics. They used Rabinowicz's abrasive wear prediction model:

$$V = \frac{L \tan \theta}{3P}$$

V = wear volume per unit sliding distance
L = normal force
$\theta$ = average tangent of roughness angle
P = surface hardness.

This gave the ranking shown in Table 3 for the relative abrasive wear rate for different ceramics.

Kramer and Judd also predicted the likely chemical dissolution rates of iron in different ceramics based on chemical data at typical cutting temperatures. This gave the relative chemical dissolution wear rates of various ceramics, shown in Table 4. Whilst recent experimental data (Ref 12) has not exactly borne out these predictions, it is still clear that PVD, by offering the potential to deposit a wide range of ceramic and cermet films, will be an increasingly important technique for producing wear resistant coatings. This becomes even more apparent when one examines recent work on the development of multi-phase coatings, such as that reported by Dr Holleck in W Germany (Ref 13).

An important point to note is that PVD techniques offer an unrivalled capability to control the coating microstructure through the fabrication parameters and constitution respectively (see Figure 2). This makes it possible to 'surface engineer' the coating/substrate system properties. The designer will in effect be seeking different attributes from the substrate, the interface, the coating bulk and the surface (Figure 3).

Holleck argues that the requirements of these different regions can be expressed according to a preferred bonding type within the coating at each point. Thus he recommends the use of a coating material with metallic bonding at the interface where good adhesion is needed, moving progressively through to (perhaps) a covalently bonded material with greater hardness at the surface. Table 5 shows the dominant

bonding mode for a number of ceramics. Table 6 indicates how the bonding type can be expected to influence coating properties.

Holleck has taken his model a stage further, by suggesting mixed phase deposits, produced (for example) by layering. It is found in practice that many mixed ceramic phases can produce improved hardness and corrosion resistance compared to the single phase ceramics on their own. Figure 4 shows how the former applies to a number of carbides. Recently, titanium aluminium nitride coatings have been shown to possess improved high temperature oxidation resistance compared to titanium nitride.

Multi-layered coatings are now widely applied by Chemical Vapour Deposition. They offer a number of advantages. Firstly, by incorporating phases with different properties (eg low heat conduction, high hot hardness, or low workpiece compatibility) the coating can be made to possess an amalgam of attributes not possible in a single coating. The layering can also impart a degree of stress equalisation through the film. (Refs 14,15). According to Almond, such films can also arrest crack propagation, a problem which otherwise increases with thickness (Ref 16). PVD techniques have a further property which can prove fortuitous or problematic depending on the application. This is the high residual compressive stress which is usually present. These can have a benefit, for example in thermal cycling applications or when a mechanical fatigue loading is to be applied; they do however impose greater demands on the substrate to coating adhesion. Specifications for these coatings in the future must therefore include a meaningful test for adhesion (Ref 17).

## THE CONTRIBUTION OF EXPERT SYSTEMS

We have seen that PVD is likely to take up an increasingly important place in the designer's armoury of coating techniques. These coatings can provide a wide range of properties, making it all the more important to have an effective selection procedure which can include a facility for data encapsulation. The increasing use of computer aided design (CAD) systems in industry, coupled with the ever reducing cost of computer memory, suggest that a solution to the problem is at hand. In particular, knowledge-based or expert systems offer the ideal structure to fulfil this type of requirement.

Expert systems are elaborate computer programmes which are specifically developed to encode expert knowledge and make it readily available to the user, often in a conversation mode interaction. Over the past 20 years specific programming languages, such as LISP and PROLOG, have been developed which are particularly suited to this purpose. Unlike conventional 'hard wired' programmes, most expert systems have a separate reasoning module or rule interpreter, which manipulates logical statements to reach a conclusion. This allows the data base (containing coating property information) to be stored separately in the programmes. Figure 5 illustrates the difference between a conventional programme and an expert system. Because the knowledge is separate from the rules the information can be updated readily without rewriting the whole system. The rules used for a consultation and the decision path can be monitored, to provide an explanation for any decisions reached. This latter point is especially important if designers are to have confidence in the system.

## THE TRIBSEL SYSTEM

A number of coating selection expert systems have been developed at the University of Hull over the past 5 years. Each one has to some extent been a development of earlier systems (eg Refs 18, 19, 20). Our initial work tended to emphasise the identification of wear mechanisms, and to apply mathematical models. In practice the number of occasions when a strictly mathematical approach to selection can be utilised were found to be very limited. Even the metal cutting situation, which is well documented and was thought to be covered by only two dominant wear mechanisms, has been found to be difficult to model (Refs 11, 12). Given these facts we have had to devise a system which short-circuits the need to identify the wear mechanisms.

The present system uses an approach based on 15 main criteria which were found to be inherent in the reasoning processes carried out by human experts. These criteria are listed in Table 7. Of course, these cannot be fully specified by just 15 questions, and 31 factors were identified which together sufficiently define all of the criteria. These are broken down into 5 factor groups: (1) Operating Constraints; (2) Processing Constraints; (3) Geometrical Constraints; (4) Topographical Constraints, and (5) Economic Constraints.

The approach used has been to consider coating and treatment technologies in generic groups. These are shown in Table 8. A consultation will start with the hypothesis that all of these will be suitable. As the user supplies information about a particular application the system uses the rules in its knowledge base to reject any that are unsuitable. Thus the process is one of 'progressive elimination' - defined by James as the optimum approach.

The sequencing of the consultation stages is devised to try to eliminate as many processes as possible early in the interaction. This ensures that the response time is kept short.

Within the heading of Operating Constraints come factors such as the maximum or minimum operating temperature, the operating environment, contact type (point, line, etc),and loading type (rolling, sliding, impact etc). In essence the system is based on an enormous amount of case history information, as recalled by several human experts after a lifetime of experience. We extracted this information by asking them when particular coating or treatment types were or were not successful. An advocate of the wear mechanism identification approach might argue that the questioning in this factor group category is merely identifying the likely wear types. At no point do we request such information from the computer, neither does it possess any knowledge of wear mechanisms.

Having eliminated certain coatings because of their non-suitability for the operating constraints, those that are left are sifted according to the constraints imposed by the processing method. These include factors such as the maximum dimension of the component which can be coated, the processing temperature and its possible influence on the component, and production capability factors such as the throughput required.

Next come geometrical constraints, such as the coating uniformity and re-entrant penetration capability of the process. These are followed by questions relating to the topographical constraints which cover aspects such as the surface finish requirements. When particular coatings or treatments cannot meet the needs indicated by the designer under each of these headings, they are rejected. The designer can ask 'why?' a particular question is being asked, and the system will respond by explaining the particular reasoning path it is using at that time. It will ultimately provide a list of coatings or treatments that will satisfy all of the indicated demands - or if none exist it will respond eaccordingly. The system has relative cost information encoded and information about economic quantities and availability which is also available to the designer. A case history file of similar applications is also being incorporated, which the computer will display if it meets an application which it has seen before.

## CONCLUSIONS

There is an urgent need in industry for a standardised selection procedure for coatings and treatments. This should ensure the appropriate and widespread use of the latest developments in this technology, such as PVD coatings. Computer expert systems offer an effective means of achieving this goal. They can incorporate up to date information and demonstrate 'human' attributes such as the ability to learn and explain their reasoning, based on their knowledge. These systems will clearly have an increasingly important role in many areas of materials engineering and design, where selection activities are carried out.

## REFERENCES


1. K S Fancey and A Matthews, J Vac Sci Technol., 1986, A4, 2656.
2. A Matthews, Engineering, December 1987, Technical File No 161.
3. D H James, Surf J., 1978, 9, 3.
4. D H James, Paper presented at the 8th Int Thermal Spraying Conf., 27 Sept - 1 Oct, 1976, 148-155, Miami, FL. American Welding Society.
5. R F Smart, Tribology Int., April 1978, 97.
6. J Halling, Tribologia - The Finnish Journal of Tribology, 1982, 1, 15.
7. A Matthews, Proceedings of the 1st Conf on Materials Engineering, Leeds, July 1984, Institution of Metallurgists, London 1984, p175.
8. M Farrow, Paper presented at the Int Conf on Metallurgical Coatings, ICMC 86, San Diego, USA, 1986.
9. M Farrow and C Gleave, Trans Inst Met Fin., 1984, 62, 2.
10. H Czichos: 'Tribology - a systems approach to the science and technology of friction, lubrication and wear'; 1978, Amsterdam, Elsevier.
11. B M Kramer and P K Judd, J Vac Sci Technol., 1985, A3, 2439.
12. W D Sproul, Surface and Coatings Technology, 1987, 33, 133.
13. H Holleck, J Vac Sci Technol., 1986, A4, 2661.
14. J Cookson, Metalworking Production, 1983, 92, 127.
15. A Matthews, Proceedings of the Vapour Deposition Seminar, Cranfield, June 1985.
16. E A Almond, Vacuum, 1984, 34, 835.
17. A Matthews and J Valli, Proceedings of the Int Seminar on Plasma Heat Treatment, Senlis, France, September 1987, PYC Edition Paris.
18. A Matthews and K G Swift, Thin Solid Films, 1983, 109, 305.
19. C S Syan, A Matthews and K G Swift, Surface and Coatings Technology, 1987, 33, 105.
20. C S Syan, A Matthews and K G Swift, Surface Engineering, 1986, 2, 249.

| TYPICAL CHARACTERISTICS | COATINGS | | | | | TREATMENTS | |
|---|---|---|---|---|---|---|---|
| | VAPOUR DEPOSITION | | HARD FACING | | ELECTRO-DEPOSITION | THERMAL | CHEMICAL |
| | PHYSICAL | CHEMICAL | THERMAL SPRAYING | WELDING | | | |
| THICKNESS (mm) | Up to 0.1 | Up to 0.1 | 0.1 - 1.0 | 2 - 20 | 0.02 - 0.5 | 1 - 6 Sub-surface | 0.2 - 2.0 Sub-surface |
| DEPOSITION RATE (Kg/hr) | Up to 0.5 per source | Up to 1 | 1 - 10 | 3 - 50 | 0.1 - 0.5 | - | - |
| SUBSTRATE MATERIAL | Wide choice | Limited by heat | May be limited by heat | Mostly copper & iron alloys | Conductors | Mostly steels | Mostly steels |
| SUBSTRATE TEMP ($^{o}C$) | 100 - 600 | 800 - 1200 | Depends on method 100 - 1000 | 1400 | 50 | 900 | Up to 900 for a thermo-chemical |
| COMPONENT SIZE | Limited by Chamber size | Limited by Chamber size | No limit | No limit | Limited by bath size | Limited by equipment | Limited by equipment |
| PRE-TREATMENT | Grit blast and /or chemical clean | Grit blast and /or chemical clean | Grit blast | Mechanical clean | Chemical clean and etch | - | - |
| TOLERANCES | Good | Fair/Good | Fair | Poor | Fair | Fair/Good | Fair/Good |
| HARDNESS ATTAINABLE ($H_v$) | 2000 + | 2000 + | 1800 (Carbides) | 900 | 1000 | 800 | 1000 |
| DEPOSITION OF SUPER-HARD CERAMICS POSSIBLE | Yes | Yes | Not without metal binder | Not without metal binder | Not without metal binder | - | - |
| FINISH MACHINING NECESSARY | No | No | Yes | Yes | Probably | Probably | Possibly |

TABLE 1 Typical characteristics of the main Surface Engineering Techniques. (These should be taken as a guide only as developments are continually expanding the boundaries of all processes).

TABLE 2 Ranking of different materials according to their $E'/Y$ ratio.

| | Elastic Modulus E ($GN/m^2$) | Yield Stress Y ($MN/m^2$) | $E'/Y$ |
|---|---|---|---|
| Copper | 124 | 60 | 1033 |
| Aluminium | 69 | 40 | 863 |
| Silver | 76 | 55 | 690 |
| Mild Steel | 196 | 220 | 445 |
| Titanium | 116 | 180 | 325 |
| EN31 Alloy Steel | 200 | 1700 | 60 |
| Alumina | 390 | 5000 | 39 |
| Titanium Carbide | 380 | 5000 | 38 |
| Titanium nitride | 300 | 5000 | 30 |
| Diamond | 1000 | 50000 | 10 |

($E'$ is the effective modulus which combines the elastic modulii of the contacting surfaces. For materials with similar E values $E' \approx 0.5E$).

TABLE 3 Predicted relative abrasive wear rates of different ceramics at 700°C (Ref 11).

| | |
|---|---|
| SiC | 0.004 |
| WC | 0.008 |
| $Si_3N_4$ | 0.030 |
| $Al_2O_3$ | 0.075 |
| HfN | 0.28 |
| HfC | 0.34 |
| ZrC | 0.79 |
| TiC | 1.0 |
| $TiO_2$ | 2.2 |
| TiN | 170 |

TABLE 4 Predicted relative chemical dissolution wear rates of different ceramics at 700°C (Ref 11).

| | |
|---|---|
| $Al_2O_3$ | 0.0000 |
| $TiO_2$ | 0.0000 |
| HfN | 0.0009 |
| TiN | 0.018 |
| HfC | 0.035 |
| ZrC | 0.36 |
| TiC | 1.0 |
| $Si_3N_4$ | 250 |
| WC | 5200 |
| SiC | 24000 |

TABLE 5 Dominant bonding types for different ceramics.

| Metallic | Covalent | Ionic |
|---|---|---|
| M | C | I |
| borides, carbides & nitrides of the transition metals. | borides carbides nitrides of Al, Si, B | oxides of Al, Zr, Ti |
| eg: TiN, TiC, VC WC, $TiB_2$ | eg: $B_4C$, SiC, BN | eg: $Al_2O_3$ $Zr_2O_3$. $TiO_2$ |

TABLE 6 Influence of bonding types on coating properties

| | Hardness | Brittleness | Melting Point | Thermal expansion Coefficient | Adhesion to Metallic Substrate |
|---|---|---|---|---|---|
| High | C | I | M | I | M |
| | M | C | C | M | I |
| Low | I | M | I | C | C |

TABLE 7 Criteria used in coating selection

| | |
|---|---|
| 1. | Operating temperature |
| 2. | Operating environment |
| 3. | Counterface material |
| 4. | Counterface hardness |
| 5. | Substrate material |
| 6. | Substrate hardness |
| 7. | Contact pressure |
| 8. | Contact geometry |
| 9. | Relative motion type |
| 10. | Relative speeds |
| 11. | Surface finish |
| 12. | Component size and shape |
| 13. | Coating thickness and uniformity |
| 14. | Quantity of parts |
| 15. | Economics, including availability |

TABLE 8 Generic groups of coatings and treatments included in TRIBSEL.

Surface treatments:

Mechanical surface working
Thermal surface hardening
Induction hardening
Carburising
Carbonitrinding
Nitrocarburising
Nitriding
Pack processes
High temperature salt bath processes

Surface coatings:

Ion-implantation (nitrogen)
Ion-implantation specials
Electrodeposited chromium
Anodising
Electroless nickel
Phosphating
Chemical vapour deposition
Physical vapour deposition (sputtered TiN)
Physical vapour deposition (ion-plated TiN)
Physical vapour deposition specials
Thermo spraying (Cr/iron alloys)
Thermo spraying (stellite)
Thermo spraying (carbides/nitrides/oxides)
Thermo spraying specials
Welding (austenitic-manganese steels)
Welding (martensitic alloys, Cr/HSS)
Welding carbides (tungsten)
Welding specials
Metallic dipped coatings
Polymetric and plastic coatings
Elastomer coatings

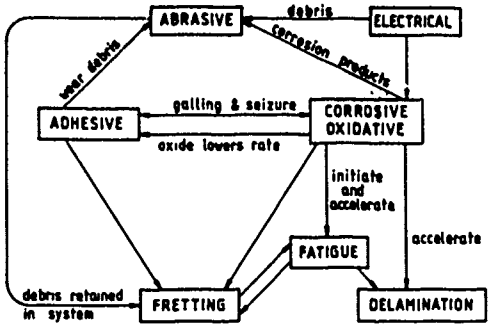


Fig 1 Interacting mechanisms in wear. (After Ref 8).

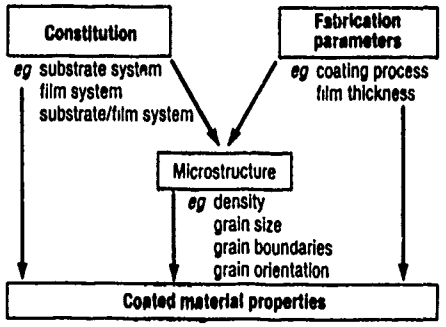


Fig 2 Factors affecting coating properties in PVD (After Ref 13).

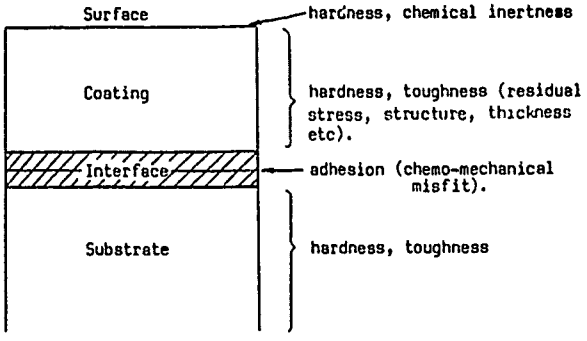


Fig 3 Requirements of the surface, coating, interface and substrate. (After Ref 13).

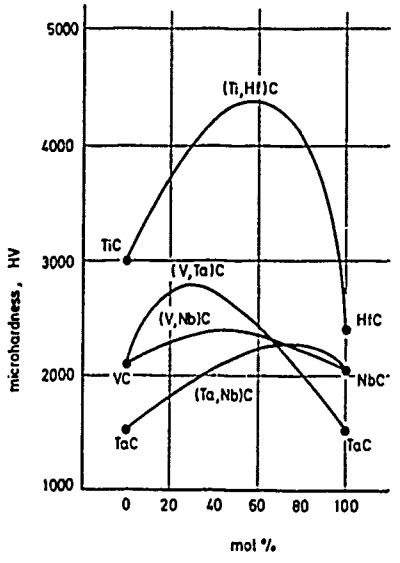


Fig 4 Microhardness of mixed carbides. (After Ref 13).

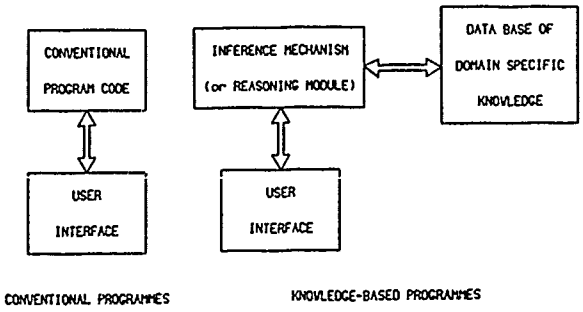


Fig 5 Comparison between a conventional programme and an expert system.

# DESIGNING FOR ADHESIVES

Dr.W.A. Lees.

Dr. Lees is the Technical Director at Permabond Adhesives Limited.

SYNOPSIS

While bonded structures, based on practical experience, have been used successfully for an extremely long time it is only recently that a better insight into the behaviour of bonded joints has allowed a more logical and scientific approach to their design. This development, based on the measurement of the true material properties of structural adhesives and mathematical models utilizing these properties, has explained the behaviour of bonded joints and has allowed their use in extremely demanding mechanical systems - as exemplified by the introduction of bonded propeller shafts based on metal/composite assemblies. The background to such applications and the behaviour of the four classical joint forms are discussed in the paper.

## 1. INTRODUCTION

There can be very few individuals who, having worked with adhesives for some time, cannot have wondered and been concerned about the occasionally anomalous performance given by the materials they have used. They will have seen that from time to time there is little or no correlation between the performance obtained on one component - perhaps a standard test piece - with that seen on another. Formulators too are puzzled when minor changes in composition have an apparently dis-proportionate effect on the "strength" of the adhesive they are working on.

For the designer and production engineer this uncertainity is most disturbing and as a consequence both become hesitant, if not reluctant, about introducing adhesives. This is most unfortunate for it is only by exploring their use that novel designs incorporating new materials can be achieved. How else may dissimilar materials be joined without introducing excess weight and high local stresses? Indeed, the only effective way of transferring substantial loads from metal to composite is by means of an adhesive. Similarly, the only effective way of joining dissimilar metals without incurring a weight penalty - from the use of fasteners - is with an adhesive.

The problem for the adhesive technologist is to give an explanation of the apparently erratic behaviour displayed by bonded joints - and it is to this end that this paper is dedicated with a view to laying a basis for rational design.

For some time now it has been the practise of the aerospace industry to regard adhesives as engineering maerials. And, while this approach has been somewhat limited by early mathemaical techniques, it has proved sufficiently successful to stimulate considerable further endeavour. As a result, it is now possible to measure the more important engineering characteristics of an adhesive and to employ them in mathematical models which can utilise the data to give a reasonably accurate picture of the stress and strain distribution within a joint.

The thick Adherend Shear Test may be used to measure the:

- Shear Modulus
- Elastic Shear Stress Limit
- Asymptotic Shear Stress

of an adhesive. These properties, coupled with the geometry of the joint and the appropriate modulus of the adherend, may be used in a Finite Element model to predict the performance of the assembly. Such calculations can be used to demonstrate why adhesives with quite dissimilar characteristics will behave in an apparently similar manner in one situation and quite differently in another where the geometry of the joint ceases to favour one of them. They may also be used to develop a joint's geometry in order to devise its optimum form.

A complete picture may only be obtained from a full three dimensional study of the forces in a joint. Such an analysis is very time consuming and for the present a simpler approach will be used.

Altogether four joint types will be discussed. They are the:-

* Co-axial (collar/pin) joint
* Contained joint - a derivative of the co-axial type
* Lap joint and the -
* Butt joint and its derivatives.

## 2. THE PRINCIPAL BONDED JOINTS

### 2.1 Co-axial assemblies.

In order to demonstrate quite clearly how stress distribution may vary it is necessary to examine the effect of changing from one extreme form of adhesive to another - from a very stiff, but tough adhesive, to a tough but very ductile adhesive.

Example 1:

Change in Stress Distribution with Loading Mode.

This simple pin and collar joint will also be used as the basis for Example 2.

It characteristics are :-

Materials

| | |
|---|---|
| Adherends | - mild steel |
| Adhesive | - tough, stiff epoxy |

Joint Geometry

| | |
|---|---|
| Description | - collar and pin |
| Collar Diameter | - infinite |
| Pin Diameter | - 10mm |
| Length of Peg Engaged | - 10mm |
| Adhesive Thickness | - 0.2mm |

Load

In Tension - 6KN )giving an 'average' stress of
In Torque - 30Nm)19MPa on the bond line.

The axial stress distribution of Example 1, when a stiff-epoxy bonded joint experiences either tensile or torsional loads, is given in Figure 1. Perhaps one of the more surprising features is that both stress distribution curves are asymetrical - the classis cusp curve, often used to illustrate stress in lap joints, is not seen. An effect generated by the mass of the collar which is so very stiff compared to the adhesive. The effect becoms more pronounced if the pin is replaced by a hollow tube. Indeed, if a tube of 1mm wall replaces the pin then the stress distribution seen in tension is almost identical to that generated by rotating the solid pin and inducing a torque load. A situation illustrated by the dashed line in Figure 1 where the two curves given there show quite clearly that any attempt to relate the true stress distribution to an average figure is most unlikely to prove useful.

Furthermore, such averages can give no insight into the creep and fatigue resistance of a joint - a subject examined in some detail in section 2.3.

Example 2:

Change in Stress Distribution with Adhesive.

When the adhesive of Example 1 is exchanged for a tough ductile acrylic the stress pattern is quite different. It is noticeable in Figure 2 that the torsional and tensile patterns have now moved closely together and that the "average" load is now a closer approximation to the model computation.

Unless it is appreciated why this should be so, and it is due to the extreme ductility of the adhesive, then the performance of the adhesives considered in the two Examples is likely to be misjudged.

Example 3:

Change in Stress Distribution with Geometry.

Here the components of Example 1 are modified further and both are now reduced to tubes of 1mm wall thickness. Figure 3 displays three versions of the classic cusp curve generated by the tensile loading of these bonded tubes when the bond line varies between 0.2mm (as in Example 1) and 0.0125mm. The adhesive in the thinnest bond line is suffering plastic deformation at the ends which are highly stressed because there is, in effect, insufficient adhesive within the joint to distribute the load along the axis and thus over a greater area - See 2.3.

It is against this background that some current attempts to extrapolate practical observations need to be judged. The enormous variation in stress pattern generated by very simple modification of a joint's geometry make a nonsence of such attemps to predict performance on anything but the narrowest spectrum of variation.

### 2.2. Contained joints.

One of the primary features of the collar and pin joint is the virtual elimination of damaging peel and cleavage forces from the joint line. This is because the maximum strain which is likely to occur in the metal - in normal use - is generally incapable of imposing a subsequent strain in the adhesive which is in excess of its elastic limit. It is for this reason that anaerobic adhesives - which are generally brittle and strain sensitive - works so well in co-axial configurations and are consequently used extensively for the mounting of bearings and the like.

It is obvious that co-axial assemblies are unsuitable for the fabrication of large

sheet structures but the principle embodied in them can be utilized in the form of the contained joint. Figures 4a - d show the conceptual development of a collar and pin assembly into the edges of a box formed from two sheets and an extrusion. Designs based on 4d are extremely strong and stable. An excellent example being the bonded assembly of needles into a ring frame - part of a knitting machine. After many millions of operations the kneedles fractured outside the joint leaving the ends firmly embedded in place. That this should occur is certainly due in a large part to the suppression of tensile forces normal to the plane of the joint lines within the ring frame - a design feature which is developed further in 2.3.

2.3. The lap joint.

Perhaps the most important point that can be made is that the lap joint can never be loaded in pure shear - even the strapped double lap (Fig.5), which would appear to allow symmetrical loading, distorts due to the way in which strain is induced.

This means that unless a positive design feature is introduced to prevent cleavage and peel forces developing a lap type joint is always at risk when high loads are likely - by either intent or accident. However, having said this, it is appropriate to point out that the loads seen in most situations are readily borne by the present generation of "Toughened" adhesives and it is only when demands are extreme that there is a need for concern.

The stress distribution of the shear vector of a loaded lap joint is important for determining the overlap necessary and the most appropriate type of adhesive. While these factors are intimately inter-related it is simpler and convenient to consider them separately.

2.3.1. Overlap length.

Practical experience has established that there is an upper limit to the load which can be carried by a lap joint no matter to what degree the overlap is extended. Example 4 is used to demonstrate that it is now possible to simulate this behaviour on a computer using models capable of handling elastic and plastic strain in the adhesive.

Example 4:

Changes in the load bearing capacity of a lap joint.

The characteristics of this simple lap joint are:-

Materials
Adherends - mild steel
Adhesive - tough, stiff epoxy.
Shear modulus 1.5 GPa, elastic limit 25 MPa, ultimate strength 43 MPa.

Joint Geometry.
Description - simple lap
Overlap length - variable 5 - 50mm
Width - 25mm
Metal thickness - 2mm
Adhesive thickness - 0.8mm

Load
Tension - variable 0 - 40 Kn.

Curve M of Figure 6 demonstrates the maximum computed load which can be carried by the lap joint described for any given overlap length. It can be seen immediately that this calculated curve follows typical practical observations very closely. An initially straight line curve falls away indicating that a further increase in overlap length does not increase the load bearing capacity of the joint at all. This follows from the progressive inability of the adhesive/adherend combination to transmit stress to the central areas of the joint as the overlap increases. A feature of the thinnest joint line curve already illustrated in Figure 3 of Example 3. This is exemplified further in Figure 7 where:-

Line 5 represents the shear stress distribution of a 5mm overlap joint sustaining the maximum load (5.5 kN) possible and correspondingly

Line 20 - a 20mm overlap, maximum load 21.6 kN.
Line 35 - a 35mm overlap, maximum load 34.1 kN.
Line 50 - a 50mm overlap, maximum load 35.1 kN.

However, returning to Figure 6 and curve M it needs to be pointed out that a suitably factored maximum load bearing capacity is often used by designers. For example, 30-40% of the observed strength of a joint, factored by 2 for a safety margin, could well be the figure used for allowable design loads. This would let our Example carry a working load of some 7kN with a 40mm overlap. It can be seen from Curve E - which represents the maximum load which can be borne without exceeding the adhesives elastic limit - that such a figure is close to inducing fatigue in the joint! Furthermore, a 7kN load is in excess of the limits indicated by curve C which represents the maximum load that can be imposed on any particular joint length without inducing long term creep problems. It needs to be said immediately that creep criteria are not properly understood let alone quantified - but it seems certain that for long term stability some point in a joint needs to experience little or no load. In this example the limit was set for computational convenience at 2MPa. That this condition is not easily achieved is amply demonstrated in Figure 7 by to the graphs 5 - 50. In a similar vein the various curves illustrated in Figure 8 indicate that a working load based on 30% of the practical maximum achievable is

probably a better criteria. This is because the 10% M curve lies below both lines C & E and is well below the latter at the most critical point in the joint - the edge.

Bearing this in mind it is worthwhile re-examining both Figures 1 and 2 though more particularly the former. In Figure 1 the maximum stress induced by the tensile load lies just over the elastic limit. But, its torsional 'average' load equivalent lies well above it and thus can be seen to be more susceptible to fatigue failure - though it would appear to be less sensitive to creep effects!

2.3.2. Suppressing peel and cleavage forces.

Whenever lap type joints need to withstand substantial loads - coming eiher by design or foreseeable accident - every effort should be made to ensure that peel and cleavage forces are minimised or suppressed. Figure 9 highlights correct and incorrect methods of designing or assembling a variety of bonded structures. The key lesson in every case is to load the joint with a combination of compression and shear forces and to avoid destructive peel and cleavage loads.

Combination joints using either screws or rivets may also be used and sheet metals can be successfully welded through a layer of suitable adhesive.

Screws, rivets or welding are useful in holding components together while the adhesive cures and, where peel or cleavage forces cannot be avoided, they can be used to counteract such loads. Although the use of bonded and rivetted (welded) joints may appear at first sight to be regressive and even counter-productive this is not so. Many modern bus and coach designs use the technique because it allows:-

* quick, simple constructive and needs -
* very few fasteners (often as little as 10% of the norm)
* thinner gauges to be used while still giving -
* stiffer structures often fabricated from -
* different materials.

2.4. The Butt joint.

The butt joint is usually regarded as an extremely poor form of lap joint. Its success depends upon both the geometry and the physical characteristics of the adherends. In its most demanding form - rod end-bonded to rod - the joint will fail readily, due to cleavage, unless at least one of the adherends is highly complient. The stable forms - seen in the shape of a bonded 'Big-Head' fastener, (which has a slender shank) and the 'L' or 'T' section stiffeners - are very robust. This follows because the geometry makes it very difficult for imposed loads to induce peel and cleavage in the plane of the joint. A point readily appreciated and already seen in the penultimate sketch of Figure 9. The various forms of the butt joint and their capabilities are not generally appreciated - a pity, since they could be utilized more widely than they are.

3. A Case history.

In 1985 and '86 Peugeot won the World Rally (Paris - Dakar) with a turbo-charged quatro version of their popular 205 saloon which was driven through a carbon fibre/epoxy propeller shaft. Both ends of the shaft were bonded into steel coupling. Similarly, in 1988 Renault announced their latest version of the Espace which is also driven through a composite shaft - in both cases considerable technical advantages were gained. The end fittings of the Renault shaft are to be seen in Plate 1.

Although details of the two shafts have not been released some concept of how their performance might have been achieved is given by the following paramentric study - based upon a mathematical model devised by AERE Harwell. In Figures 10a and b the stress pattern induced by a torque load is modified and improved as the sophistication of the component's form is developed. The basic component is an aluminium yoke bonded into a composite torque tube. In the first design (Figure 10a) the bonded portion of the yoke takes the form of a simple solid bar. In the second 10b, the end of the bar has been hollowed out and its end considerably developed - the avoidance of abrupt dimensional changes coupled with the tapering of the tubular section having very beneficial results. This may be readily appreciated by comparing the appropriate stress patterns. It can be seen that critical edge stress has been sharply reduced by transfer of load to central areas. Creep will still be avoided because two unloaded zones have been created. However, fatigue could still be a problem and its avoidance will require the bonding of both the inner and outer faces of the tube with a modified coupling (the Peugeot solution) or operating at a reduce torque or with a greater diameter.

4. SUMMARY

The mathematical models which have been developed to evaluate stress distribution in bonded joints have worked well - particularly in the case of the simpler joints - and have clearly demonstrated that the behaviour of an adhesive is not erratic but is susceptible to rational analysis. Nonetheless, there is a long way to go before adhesive technology can be considered to have become a material science. Current work is most encouraging and instructive and is establishing sensible design concepts.

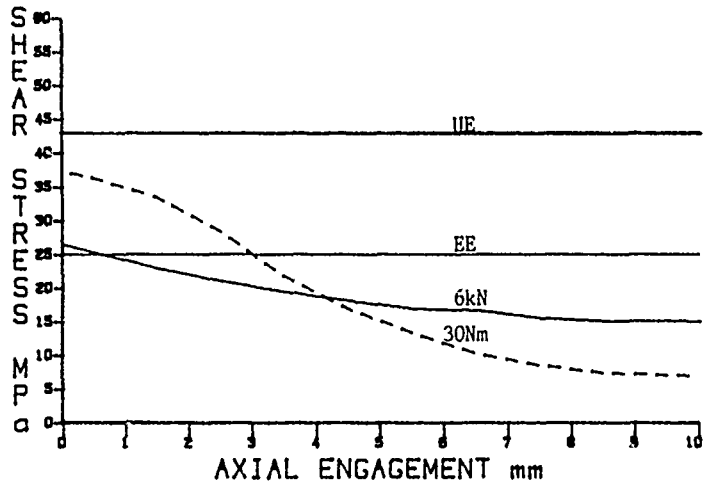


FIG. 1 STRESS DISTRIBUTION: Comparison of torque and tensile loading of a collar and pin joint - tough, stiff epoxy adhesive.

Solid line - tensile load 6kN ) 'average' 19MPa
Dashed line - torque load 30Nm )
Solid line UE - ultimate shear strength of epoxy adhesive
Solid line EE - elastic limit of epoxy adhesive

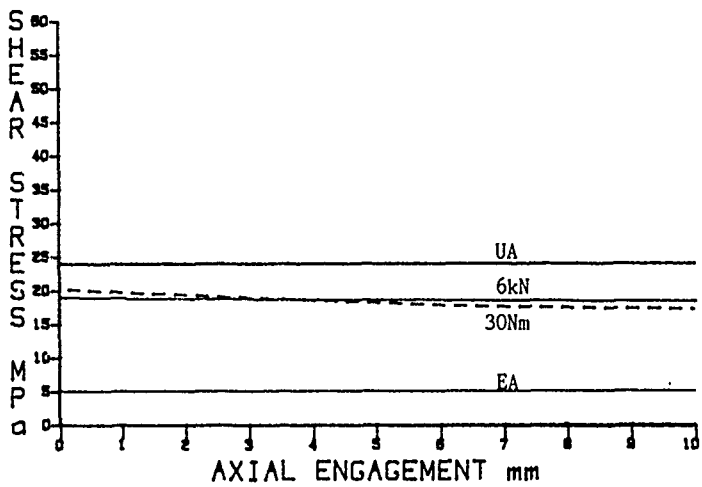


FIG. 2 STRESS DISTRIBUTION: Comparison of torque and tensile loading of a collar and pin joint - tough, ductile acrylic adhesive.

Solid line - tensile load 6kN ) 'average' 19MPa
Dashed line - torque load 30Nm )
Solid line UA - ultimate shear strength of acrylic adhesive
Solid line EA - elastic limit of acrylic adhesive

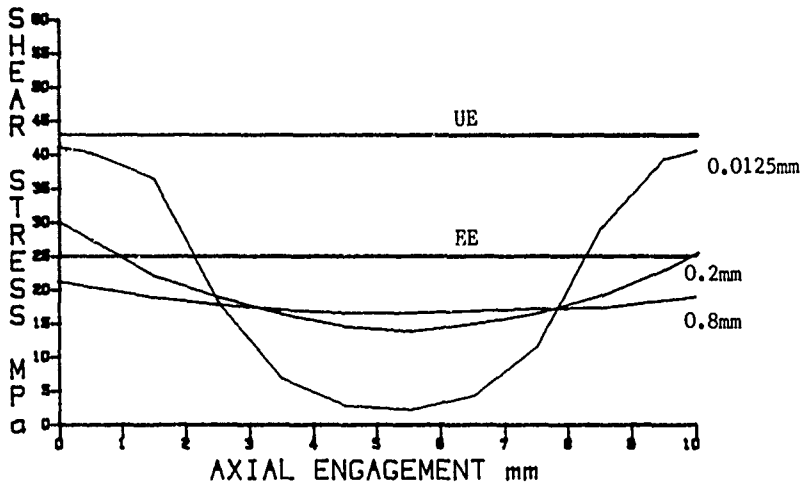


FIG. 3 STRESS DISTRIBUTION: Changes brought about by variation of bond line thickness.

Line UE - ultimate shear strength of epoxy adhesive
Line EE - elastic limit of epoxy adhesive

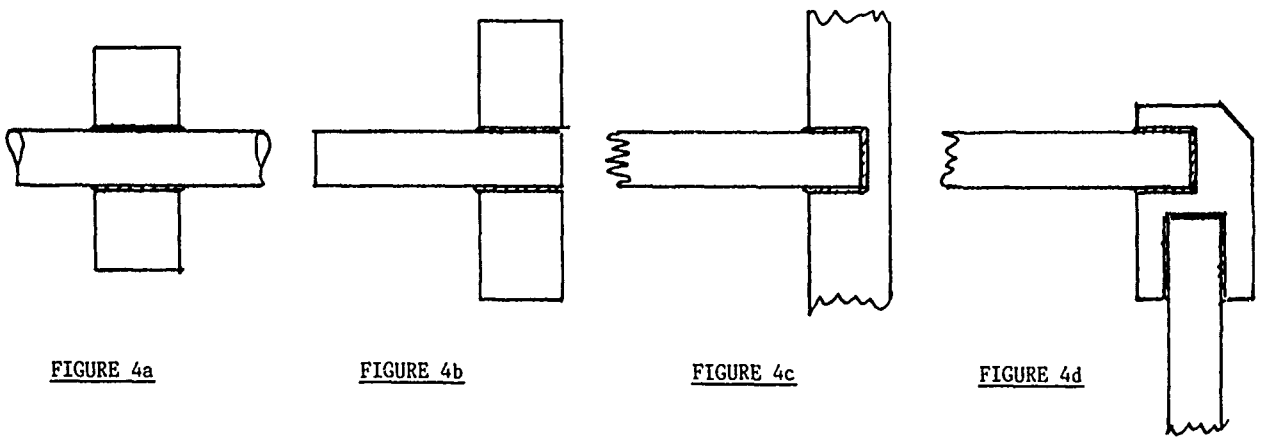

FIGURE 4a FIGURE 4b FIGURE 4c FIGURE 4d

FIG. 4 Development of a collar and pin joint into a contained joint formed from flat sheet and an extrusion.

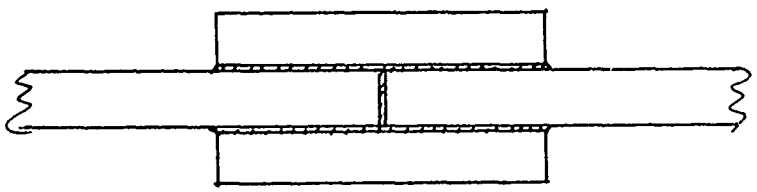

FIG. 5 A strapped double lap joint.

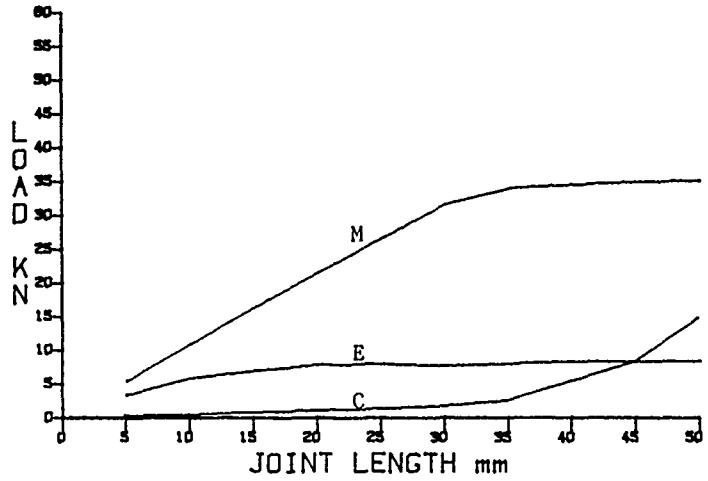


FIG. 6 Various concepts of the load bearing capacity of a model lap joint.

Line M: The maximum calculated load that can be borne
Line E: The maximum load that can be borne without exceeding the elastic limit of the adhesive
Line C: The maximum load that can be borne while leaving some portion of the joint essentially unloaded.

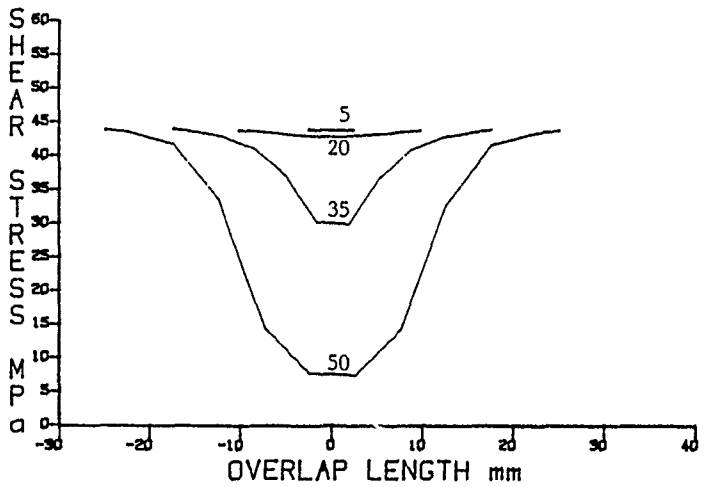


FIG. 7 STRESS DISTRIBUTION: Variation about centre line with joints of differing overlap each carrying its calculated maximum load (equivalent of Line M Fig. 6).

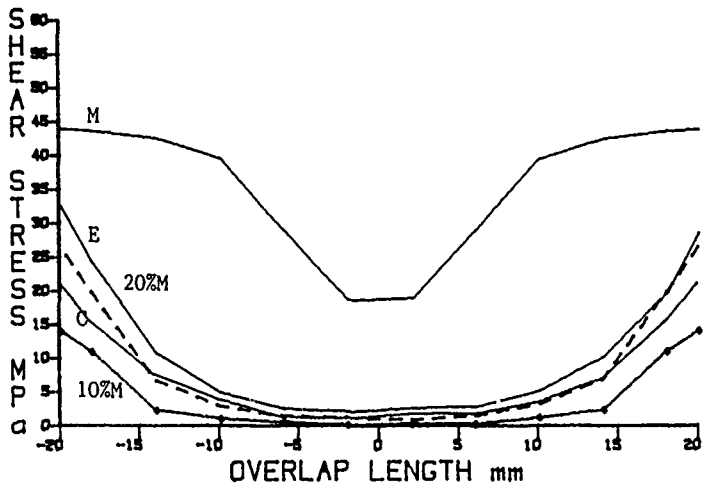


FIG. 8 STRESS DISTRIBUTION: Variation about centre line for a 40mm joint carrying a variety of loads.

Line M: The maximum calculated load that can be borne
Line E: The maximum load that can be borne without exceeding the elastic limit of the adhesive
Line C: The maximum load that can be borne while leaving some portion of the joint essentially unloaded.

Dashed line - 20% of M
Dotted solid line - 10% of M

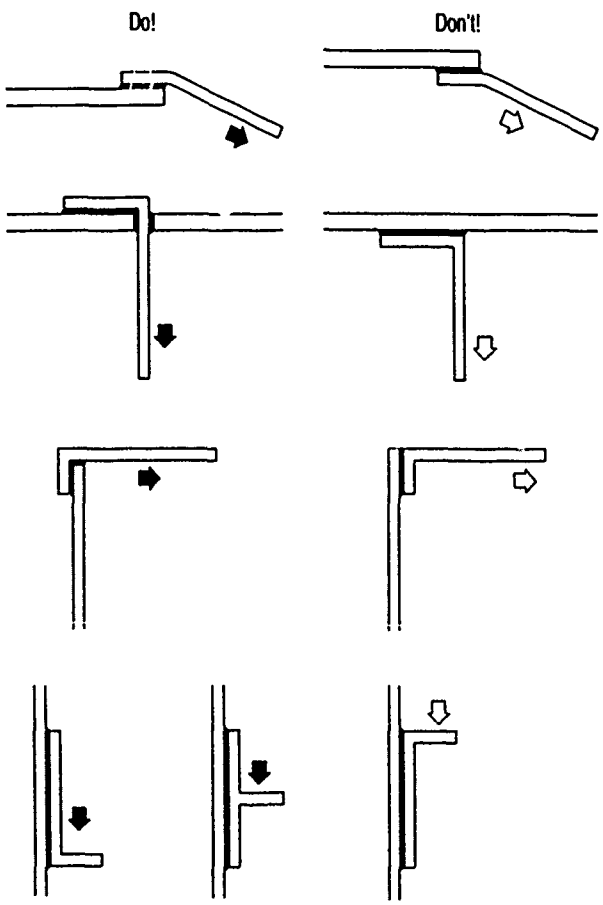


FIG. 9

Acceptable and unacceptable practice in joint design.

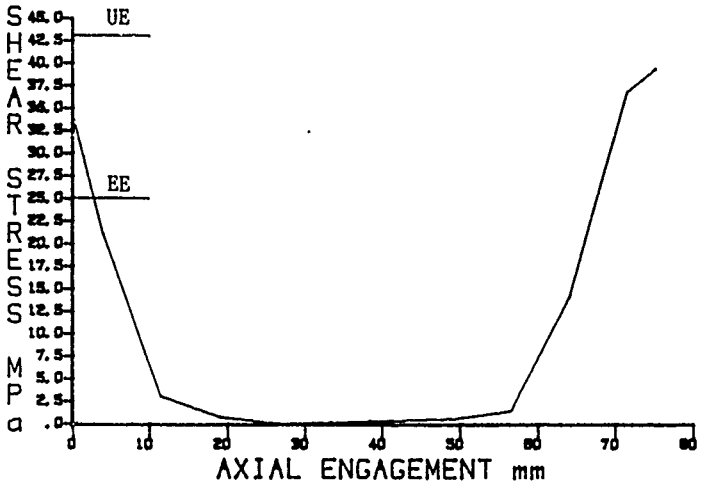


FIG. 10a STRESS DISTRIBUTION: Pattern generated by a load of 4.5KNm in the joint formed between a solid yoke and a composite torque tube.

Solid line UE - ultimate shear strength of epoxy adhesive
Solid line EE - elastic limit of epoxy adhesive.

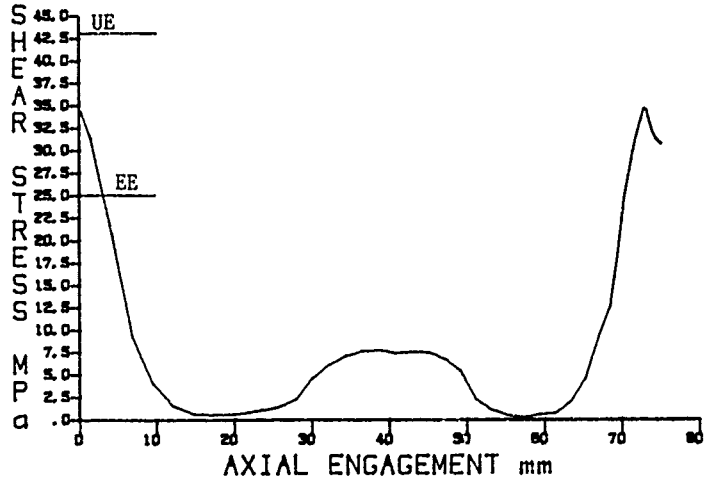


FIG. 10b STRESS DISTRIBUTION: Improved pattern given by modification of the yoke's design - incorporation of cusp and taper.

PLATE 1 The bonded couplings of the Renault Espace propeller shaft (Photograph courtesy of Uni-Cardan AG).

# DESIGN OF WELDED COMPONENTS FOR CREEP

R.W. Evans

Dr. R.W. Evans is Reader in the Department of Materials Engineering, University College of Swansea.

## SYNOPSIS

The paper describes the methods which are currently used for the design of high temperature pressure containing plant with integral welds. The procedures are shown to be successful only when large safety factors are used. It is proposed that full numerical procedures based on finite element methods are preferable, and the requirements in terms of materials creep constitutive relationships are outlined. As an example, the behaviour of a transition joint under creep conditions is simulated and a design analysis carried out. The procedure is shown to be capable of predicting the general accumulation of strain in the inhomogeneous structure as well as the rupture life and the position at which creep failure occurs.

## 1. INTRODUCTION

The construction of plant for large scale pressure containment in the chemical, oil, gas and generating industries necessarily involves welding as an integral part of the process. Such plant frequently operates at high temperatures as well as under pressure, and creep deformation can become critically important in determining plant life. Since welding often produces chemical. microstructural and mechanical discontinuities, it is not surprising that many plant failures originate at welds[1,2]. This is particularly true when transition welds between pipework of different chemical compositions (e.g. ferritic and austenitic) are necessary. It is thus surprising that at the design stage the presence of welds is often ignored in the design codes in operation.

In most cases, pipe-work design codes take into account internal pipe pressure and assume isothermal operating conditions. The design stress is taken to be that stress in the hoop direction calculated as $\sigma = PD/2W$ where P is the operating pressure, W the wall thickness and D a suitable pipe diameter (often the mean diameter). This implies that under creep conditions, the creep life will be determined by the maximum principal stress, and stress redistribution through the wall is ignored.

The values of $\sigma$ are then used, together with tensile uniaxial creep data, to determine design life. This can be done either by ensuring life is greater than $10^5$ hours, or limiting the average creep strain to less than 1% or by limiting the maximum creep rate to less than $10^{-7}$ per hour. Often the limited long term data available ensures that only the first of these criteria can be used. No direct assessment of weldments is made although a safety factor (~1.5) is always employed to determine the actual stress at which the component will operate. Only in the ASME XI Boiler and Pressure Vessel Code (section N47) are welds specifically mentioned and this places ductility limits on the average and local strains at weld sites. In view of the crude nature of this approach, it is surprising that it has been reasonably successful and this can only be attributed to the blanket cover provided to inaccuracies by the generous safety factors.

A more sophisticated method of design is to model the service conditions of the welded component by suitable computer analysis. Many good creep finite element codes are now available which make this possible and there are considerable advantages to be gained. The models have no difficulty in dealing with complex geometry and they can be readily modified to investigate other than steady operating conditions. Thus the effects of frequent temperature and pressure excursions such as occur on start up and stop or through plant running out of control can be easily estimated. However, there are several prerequisites for this approach to be successful. An accurate and efficient finite element procedure must be available together with the hardware which will allow runs to be performed in reasonable times. This latter restriction is rapidly becoming less onerous as fast cheap machines (with the possibility of parallel processing) become commercially common. Secondly, the creep properties of the material must be well understood, particularly for long service times. There are particular problems here for welds since the metallurgical structure is often complex and each structure must have its own creep constitutive equation. Lastly, the nature of creep fracture processes must be quantified again for each microstructure in the weld.

The present paper is intended to show that a careful combination of analytic and experimental work is capable of meeting these requirements. It then describes an application of the technique to the difficult problem of ferritic-austenitic transition welds and shows how the major feature of the failure of such welds can be predicted.

## 2. THE FINITE ELEMENT MODEL

The model used in this work is an elastic-viscoplastic creep analysis. The welded component is assumed to be subject to tractions given by the vector [q] over parts of its surface, although other loadings such as residual stresses and thermal stresses can be included. In response, each point in the body undergoes a displacement [u] with a corresponding strain vector [ε] given by

$$[\varepsilon] = [L][u] \tag{1}$$

where [L] is a matrix of suitable differential operators. The total strain vector is split into two parts corresponding to elastic and creep strain so that

$$[\varepsilon] = [\varepsilon_E] + [\varepsilon_c]. \tag{2}$$

Assuming isotropic material, $[\varepsilon_E]$ is related to the six component stress vector, $[\sigma]$, by means of the linear elasticity matrix [D] where

$$[\sigma] = [D]^{\prime}[\varepsilon_E] \tag{3}$$

The creep strain rate constitutive relationship is taken to be of the general form

$$[\dot{\varepsilon}_c] = \Phi(\bar{\sigma}, \bar{\varepsilon}, t, s)\frac{d\bar{\sigma}}{d[\sigma]} \tag{4}$$

where t is time, $\bar{\varepsilon}$ and $\bar{\sigma}$ are the effective strain and stress respectively, and s represents one or more structural parameters (see section 3 below). The solution to the deformation problem is formulated through a virtual work equation so that if [b] represents the vector of the body forces

$$\int_V [\varepsilon]^T [\sigma] dV - \int_s [u]^T [q] ds - \int_V [u]^T [b] dV = 0 \tag{5}$$

where the integrations are taken over volumes and surfaces as appropriate. The deforming body is now discretized into finite elements connected only at their nodal points. For any one element the nodal displacements are given by the vector $[a^e]$and the element displacements by

$$[u^e] = [N][a^e] \tag{6}$$

where [N] is a matrix of shape functions. Substitution into equation 5 yields

$$\int_V [B^e]^T [\sigma^e] dV - [F] = 0 \tag{7}$$

where

$$[B^e] = [L^e][N^e]$$

and $[F] = \int_V [N^e]^T [b] dV + \int_s [N^e]^T [q] ds$.

Similar equations are developed for all the elements and then assembled to give the general equation

$$\int [B]^T [\sigma] dV - [F] = 0 \tag{8}$$

Use of the elastic stress-strain equation gives

$$[\sigma] = [D][\varepsilon_E] = [D][\varepsilon] - [D][\varepsilon_c] \tag{9}$$

and equation 7 yields

$$\int_V [B]^T [D][B] dV [a] - [F] - [F_c] = 0,$$

i.e.

$$[K][a] = [F] + [F_c] \tag{10}$$

where [K] is the assembled stiffness matrix ar.d

$[F_c] = \int_V [B]^T [D][\varepsilon_c] dV$.

Thus,

$$[a] = [K]^{-1}([F] + [F_c])$$

and $[\sigma] = [D][B][a] - [D][\varepsilon_c]$. (11)

The creep strain vector is calculated from the creep constitutive equation by an explicit Euler time stepping regime,

$$[\varepsilon_c]_{t+\Delta t} = [\dot{\varepsilon}_c]_t \Delta t. \tag{12}$$

In order to maintain stability in the time integration, it is necessary to limit the maximum time step to[3]

$$\Delta t \le \min\left[\frac{4(1+\upsilon)}{3E} \Big/ \frac{\partial \Phi}{\partial \bar{\sigma}}\right] \tag{13}$$

where $\upsilon$ is Poisson's ratio.

## 3. THE CREEP CONSTITUTIVE EQUATION

At any given strain $\bar{\varepsilon}$ and time t the creep rate of each part of the welded structure is dependent on the function, $\Phi$, in equation 4. In general, the structure terms in this function can be complex, describing things like mobile dislocation density, subgrain size, precipitate structure, etc. Each of these will be functions of the current creep conditions so that a full constitutive equation for a single material creeping under Levy-Mises condition will be

$$[\dot{\varepsilon}_c] = \frac{3\Phi(\bar{\sigma}, \bar{\varepsilon}, t, s_1, s_2, \ldots s_k \ldots s_m)}{2\bar{\sigma}}[\sigma'] \tag{14a}$$

$$s_k = f_k(\bar{\sigma}, \bar{\varepsilon}, t) \tag{14b}$$

where $[\sigma']$ is the deviatoric stress vector.

For engineering materials, the full set of equations 14 are never known, so that various approximations must be made. One procedure which is proving to be increasingly successful is based on the θ Projection method[4]. This seeks to describe the general shape of the creep curve by the creep rate equation

$$\Phi = \theta_1\theta_2 \exp(-\theta_2 t) + \theta_3\theta_4 \exp(\theta_4 t) \tag{15}$$

and then to provide functions which express the $\theta_i$ as functions of stress and temperature over the range of operating conditions of interest. Taken in conjunction with a strain hardening rule, this approach has been very successfully applied to a number of superalloys[5] and ferritic steels[6] and its present applicability is limited only by the lack of complete data sets for the engineering materials.

In the absence of such complete data, it is possible to use Norton's Law relating the current creep rate to the stress through a simple power law,

$$\Phi = A(\bar{\sigma})^n \tag{16}$$

so that equation 14 becomes simply

$$[\dot{\varepsilon}_c] = \frac{3}{2}A(\bar{\sigma})^{n-1}[\sigma'] \tag{17}$$

It must be emphasized that A and n are not true constants and are usually functions of stress and temperature.

The analysis of a welded component is complicated by the fact that the weld and regions near it will have variable metallurgical structure. The weld metal itself is seldom of the same composition as the parent and its solidification rate will certainly be different. Most thick pipes and plates are welded by multi-pass fusion welding[7] and the thermal effects of this are to significantly alter the metallurgical structure of the parent metal to produce heat affected zones (HAZ) extending to several millimetres from the fusion line. As an example, Figure 1 shows the macrostructure of a weld in a 2¼Cr1Mo plate showing the extensive HAZ region. The detailed metallurgical explanation of such zones is well understood[8], and a typical HAZ structure in ferritic steel will exhibit (from the fusion line into the parent) coarse grained bainite, fine grained bainite and intercritical structure. Each of these will have a different creep constitutive relationship with the possibility of different stress and temperature dependence. It is necessary to determine these relationships by careful testing of specimens cut directly from the heat

affected structures or, less satisfactorily, by testing materials given heat treatments intended to simulate the structures.

## 4. CREEP FRACTURE RELATIONSHIPS

The uniaxial creep ductility of the structures in the weld can be determined readily from the creep tests conducted to obtain the constitutive relationships, but the transference of these to multiaxial stress conditions is not so straightforward as for creep deformation. Although creep fracture is intimately connected to creep deformation the exact relationship is often unclear.

In a phenomenological sense, the growth of creep damage leading to eventual rupture can be related to various components and invariants of the multiaxial stress field. The initial work of Johnson and co-workers[9] suggested that the rate of accumulation of creep damage could be related either to the magnitude of the maximum principal stress ($\sigma_1$) or the value of the effective (Von Mises) stress ($\bar{\sigma}$), depending on the material in question. Thus copper was found to obey a maximum principal stress law whereas aluminium and some of its alloys have fracture characteristics which depend on the effective stress. More recent work[10] has indicated that few materials are so clearly classified and that many engineering alloys behave in a way which is somewhere between the extremes of $\sigma_1$ and $\bar{\sigma}$ behaviour. It is usually sufficient to write[11] the rate of change of creep damage, $\omega$, as

$$\frac{d\omega}{dt} = f[(\alpha_1\sigma_1 + \alpha_2\bar{\sigma})]^{\chi} \qquad (18)$$

where f is some suitable function and $\chi$ an experimentally determined constant greater than one. $\alpha_1$ and $\alpha_2$ are then parameters such that $\alpha_1+\alpha_2=1$ and $\alpha_1 = 1$ specifies a maximum principal stress fracture material and $\alpha_2 = 1$ an effective stress material. It is normally assumed that $\omega = 0$ at zero time (initial loading) and $\omega = 1$ at fracture so that suitable integration of equation 18 through the creep loading will allow a determination of rupture time. Thus for certain simplifying assumptions[11], the rupture life, t, may be approximated by

$$t = M(\alpha_1\sigma_1 + \alpha_2\bar{\sigma})^{-\chi}. \qquad (19)$$

Thus, provided $\bar{\sigma}$ and $\sigma_1$ can be determined from the finite element model of the welded structure, estimates of real overall failure times can be made as well as determinations of the likely site of fracture in the component.

## 5. REAL WELD BEHAVIOUR

In view of the nature of the service conditions under which high temperature high pressure plant operates, it is difficult to monitor the behaviour of real welds over considerable lengths of time. In order to show the effectiveness of the modelling design technique described above, it has been applied to the creep of a commercial transition weld crept under constant stress laboratory conditions[8]. The weld was a transition weld between 2¼Cr1Mo ferritic steel and AISI type 316 austenitic steel which had been produced using an austenitic 17Cr8Ni2Mo weld metal. Specimens were machined from the weldment as shown in Figure 2. The specimens showed a complete HAZ structure as illustrated in Figure 1.

### 5a. Constitutive Equations

In order to determine the constitutive relationships required for creep properties in the numerical analysis, various creep tests were carried out on unwelded specimens[8]. Tests were carried out at 838K not only for the parent 2¼Cr1Mo steel and the weld metal, but also for samples prepared from the 2¼Cr1Mo steel after heat treatments designed to simulate the coarse grained bainite, the fine grained bainite and the 'intercritical' structures of the HAZ. After an instantaneous specimen strain on loading, the creep rate decreased gradually throughout the primary stage until a minimum rate was attained, after which the creep rate accelerated continuously to fracture. The variation of the minimum creep rate, $\dot{\epsilon}_m$, with stress, $\sigma$, is shown in Figure 3, which is plotted according to equation 16. The stress exponent, n, does not remain constant over a range of stresses. In fact, with the normalised and tempered 2¼Cr1Mo steel, the stress exponent decreased from 12 to 3 over the stress range from 250 to 150 MPa at 838K. A similar decrease in stress exponent with decreasing stress has been reported for ½Cr½Mo¼V steel[12] and for other commercial steels[13]. In contrast, no change in stress exponent was found for the simulated HAZ structures over the range considered and n was 3. As a result, the minimum creep rate stress lines for the parent material and the HAZ structures intersect at a stress of 200 MPa at 838K. The various n and A values appropriate for the different materials are shown in Table 1.

The times to rupture showed a similar variation with stress (Figure 4) with, for low stresses, the normalized 2¼Cr1Mo steel, fine grained bainite, coarse grained bainite and intercritical structure having progressively shorter rupture lives. In all cases, the rupture strains at fracture were not significantly stress dependent and the average values for the materials listed above were 13%, 14%, 4% and 16% respectively. It is not certain whether 2¼Cr1Mo steel is a maximum principal stress or an effective stress material, but some work on a chromium low alloy steel[9] suggests that it is probably the former so that $\alpha_1$ will be close to 1. In any case, for a weld specimen loaded uniformly at an average stress $\sigma_a$ the build-up in stress intensification to a value $\gamma\sigma_a$ ($\gamma > 1$) may be expected to yield locally a large reduction in rupture life. Thus the curves of Figure 4 suggest a value for $\chi$ of about 4.

### 5b. Creep of Welds

Standard constant stress creep tests were conducted on the weld samples illustrated in Figure 2 so that the variation of overall creep strain with time and the rupture time and strain were determined. In order to monitor the variation of creep strain with time for the separate parts of the structure, a micro-grid of spacing 8μm by 5μm was placed on the gauge length. At the end of the test (at fracture) the displacements of individual parts of the grid were measured and the local strains evaluated.

Figure 5 shows a measured total creep strain curve for a weld specimen tested at 100 MPa and 838K. Although the cross-weld sample failed in little more than $5\times10^3$ ks, the tests on the parent 2¼Cr1Mo steel and the weld metal were discontinued when it was established that the creep rates for these materials were still decaying even after periods twice as long as the life of the cross-weld testpiece. Microstructural examination of the failed cross-weld sample showed that fracture had occurred in an intergranular manner, as a result of crack formation in the coarse grained HAZ region of the 2¼Cr1Mo steel, at a distance of some 75-150μm from the fusion boundary. Crack development in the HAZ could be reproduced at all temperatures within the range 838 to 893K, provided only that creep tests of comparatively long duration were performed. However, at any specified temperature, the creep and fracture behaviour of the cross-weld testpieces changed markedly with increasing applied stress. In particular, at high stresses, relatively ductile failures were found to occur in regions of the parent 2¼Cr1Mo steel well away from the fusion interface.

A further feature of the difference in behaviour at high and low stresses became apparent when measurements were made of the displacements caused by the creep deformation on the regular surface grid, Figure 6. In tests of long duration, the strains were essentially zero at the fusion boundary but increased rapidly to values of 25% some 75-150μm from the boundary, and then decreased gradually with increasing distance from the weld metal, reaching a

limiting value close to the creep strain found in the 2¼Cr1Mo parent material. The position of maximum strain coincided approximately with the location of cracking in the coarse grained region of the HAZ.

In tests of comparatively short duration, the peak strain again coincided with the fracture position but, in this case, the strain increased gradually from zero at the weld interface to a maximum value several millimetres from the fusion boundary.

### 5c. Numerical Modelling

The creep deformation of the weld specimens was simulated for steady loading levels giving average cross-section stresses of 250 MPa and 100 MPa. In each case, the total of 64 time step increments were performed and the changes in general stress and strain patterns with time were calculated. For the constitutive relationship given by equation 17 the limiting time step was given by

$$\Delta t \leq \min \frac{4(1+\upsilon)(\bar{\sigma})^{1-n}}{3EAn}. \qquad (20)$$

Discretization was carried out using eight noded isoparametric quadrilaterals and the mesh geometry is shown in Figure 7.

Figure 8 shows the general pattern of stress in the specimen for a loading of 250 MPa after 64 iterations (16 ks). Contour plots are shown for both maximum principal stress and effective stress and in each case, the values shown are the ratios of the local stress at any point to the value of the uniform stress field observed immediately after (elastic) loading. The principal stress shows the greatest intensification at a point near the zone 1/zone 2 boundary (point A, Figure 7) as does the effective stress although the largest ratios are small (~1.3). Figure 9 shows similar plots for a loading of 100 MPa and in this case, both for maximum principal stress and effective stress the point at which maximum stress intensification occurs is close to the zone 4/zone 5 boundary in the heat affected zone (point B, Figure 7). The stress intensification factors after 64 iterations are approaching steady values as can be seen from Figures 10 and 11 which show the values for points A and B (Figure 7) as a function of time at both applied stress levels.

The overall stress intensification at point B for 100 MPa loading is large, reaching values of 2.8 for maximum principal stress and 2.65 for effective stress. Reference to equation 19 and the approximate n value of 4 indicates that, regardless of whether the material has a maximum principal stress or an effective stress fracture mode, the creep life at about 50μm from the weld interface (point B) will be decreased by a factor of about 60 compared to a uniformly stressed state. This accounts for the observed fracture path in the low stress weld specimens. On the other hand, the greatest stress intensification at 250 MPa at point A is only at a level of about 1.3 for maximum principal stress and 1.2 for effective stress. This is likely to lead to a life reduction of only a factor of 2.5 times and the fracture will occur at about 2.9mm from the weld interface, as is observed in practice with high stress weld specimens.

The numerical analysis also allows the calculation of creep strains in the weld specimens. Figure 12 shows the ratio of the effective strain in the x direction divided by the average effective strain. It is clear that at both low and high stress they correspond well with those observed experimentally in Figure 4.

## CONCLUSIONS

It is clear from the results of the finite element creep analysis that provided good materials property data is available for all the various metallurgical structures occurring at or near the weld zone, good quantitative understanding can be achieved of both the strain distributions and the fracture characteristics of cross-weld specimens. However the form of analysis is not restricted to this special geometry. The finite element procedure is capable of dealing with any general component form and also of incorporating other loading methods. Thus thermal stresses can be readily introduced and, provided sufficient is known about the non-steady stress and temperature response of the materials, the general loadings and temperatures can also be continually variable. The overall creep testing and numerical procedures can be used with confidence at the design stage for complex welded components.

## REFERENCES


1. L.H. Toft and D.E. Yeldham, 'International Conference on Welding Research Related to Power Plant', C.E.G.B., London, 1972, 5.
2. D. Cheetham, R. Fidler, M. Jagger and J.A. Williams, 'Residual Stresses in Weld Constructions and their Effects', The Welding Institute, London, 1977.
3. I. Cormeau, Int. J. of Numerical Meth. in Eng., 9, 1975, 109.
4. R.W. Evans and B. Wilshire, 'Creep of Metals and Alloys', Institute of Metals, London, 1985.
5. R.W. Evans and B. Wilshire, Mat. Sci. and Tech., 3, 1987, 701-706.
6. R.W. Evans and B. Wilshire, Proc. of the 3rd Int. Conf. on Numerical Methods in Fracture Mechanics, Pineridge Press, 1984, 547-560.
7. A.T. Price and J.A. Williams, 'Recent Advances in Creep and Fracture of Engineering Materials and Structures', Eds. B. Wilshire and D.R.J. Owen, Pineridge Press, Swansea, 1982, 265.
8. I.J. Chilton, A.T. Price and B. Wilshire, Metals Technology, 11, 1984, 383.
9. A.E. Johnson and J. Henderson, 'Complex Stress Creep, Relaxation and Fracture of Metallic Alloys', HMSO, Edinburgh, 1962.
10. D.R. Hayhurst, J. Mech. and Phs. Solids, 20, 1972, 381.
11. D.R. Hayhurst, 'Engineering Approaches to High Temperature Design', Eds. B. Wilshire and D.R.J. Owen, Pineridge Press, Swansea, 1983, 85.
12. B.J. Cane, 'Collaborative Programme on the Correlation of Test Data for the High Temperature Design of Welded Steel Pipe', Report RD/L/2101/M81, CEGB, 1981.
13. J.D. Parker and B. Wilshire, Mater. Sci. Eng., 29, 1977, 219.

**Table 1** Mechanical properties of materials (units are MN, m, s)

| Material | Zone (Fig. 7) | E | υ | A | n |
|---|---|---|---|---|---|
| 2¼Cr1Mo, $\bar{\sigma} < 200$ MPa | 1 | $0.1705 \times 10^{6}$ | 0.35 | $0.512 \times 10^{-14}$ | 3.0 |
| 2¼Cr1Mo, $\bar{\sigma} > 200$ MPa | 1 | $0.1705 \times 10^{6}$ | 0.35 | $0.426 \times 10^{-34}$ | 12.0 |
| HAZ, Intercritical region | 2 | $0.1705 \times 10^{6}$ | 0.35 | $0.277 \times 10^{-13}$ | 3.0 |
| HAZ, Intercritical region | 3 | $0.1705 \times 10^{6}$ | 0.35 | $0.148 \times 10^{-13}$ | 3.0 |
| HAZ, Coarse grained region | 4 | $0.1705 \times 10^{6}$ | 0.35 | $0.115 \times 10^{-13}$ | 3.0 |
| Austenitic weld metal | 5 | $0.1705 \times 10^{6}$ | 0.35 | $0.500 \times 10^{-16}$ | 3.0 |

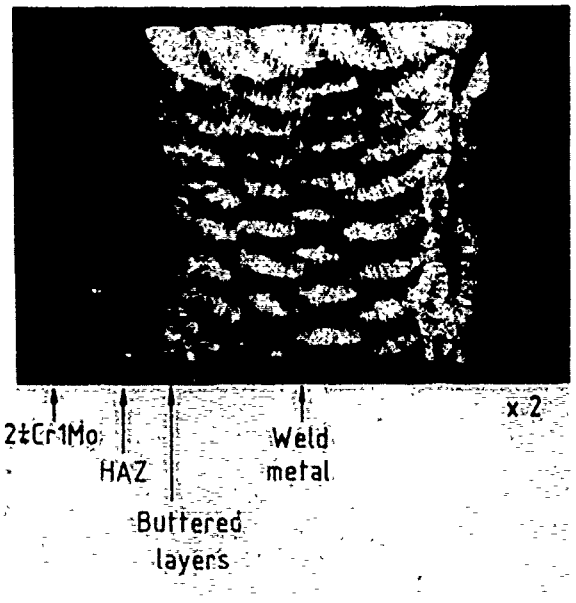


Fig. 1 Section through a multipass weld showing weld metal and HAZ regions of 2¼Cr1Mo parent steel plate.

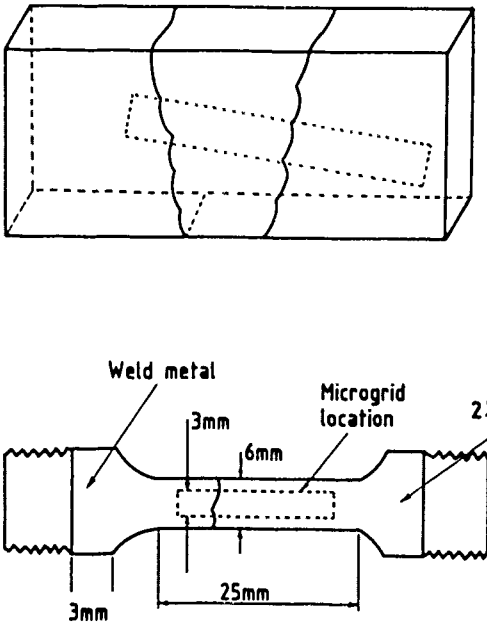


Fig. 2 Schematic representation of testpiece geometry and position of the weld interface along the gauge length.

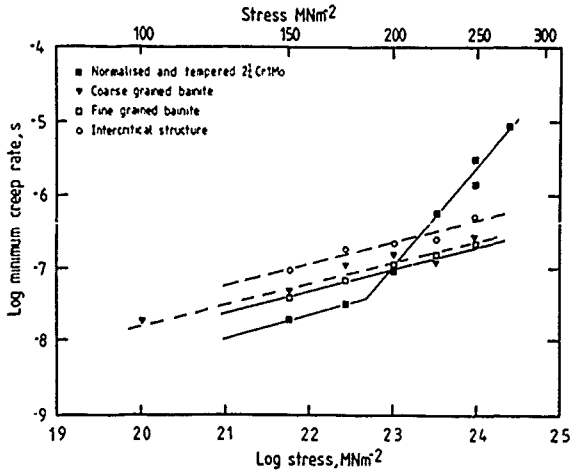


Fig. 3 Stress dependence of the minimum creep rate at 838K for 2¼Cr1Mo steel normalized and tempered, and for simulated HAZ structures.

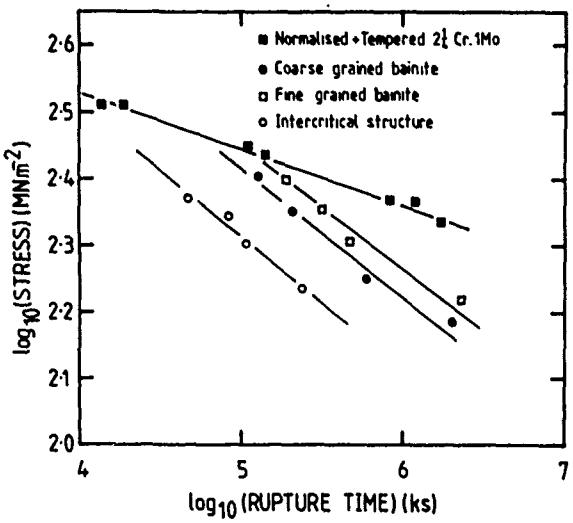


Fig. 4 Stress dependence of the rupture time at 838K for 2¼Cr1Mo steel normalized and tempered, and for simulated HAZ structures.

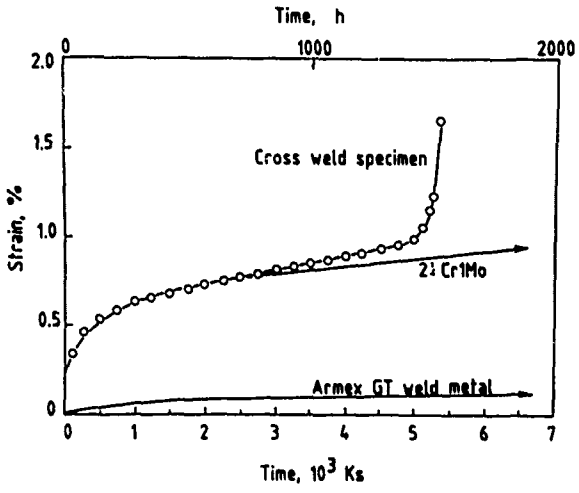


Fig. 5 Creep curve for weld testpiece at 100 MPa at 838K in relation to the strain-time behaviour observed under these conditions for 2¼Cr1Mo parent steel and Armex GT weld metal.

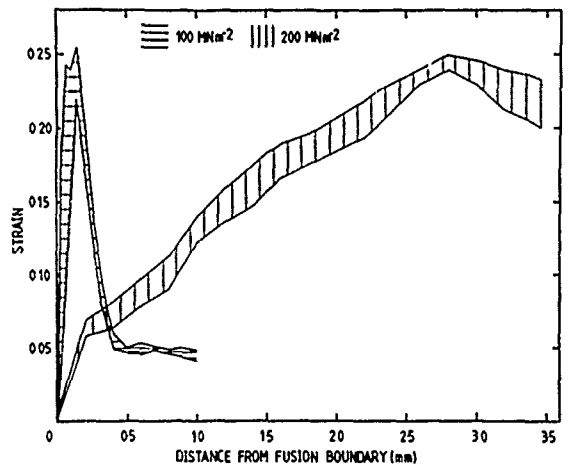


Fig. 6 Variation of local strain in weld testpieces for tests undertaken at 100 MPa and 200 MPa at 838K. In each case, fracture occurred near the point of maximum strain.

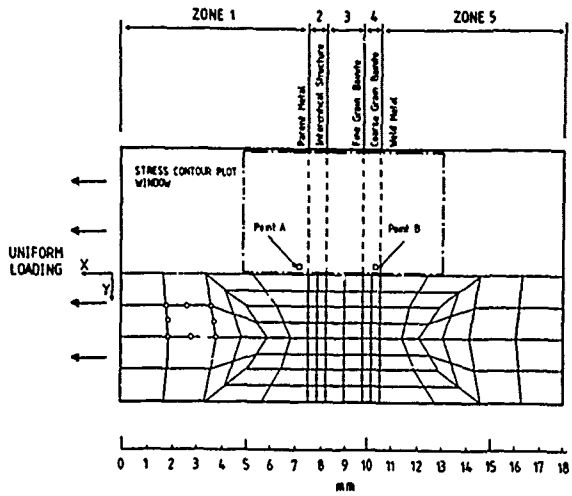


Fig. 7 Discretization of the weld zone by eight noded isoparametric elements. The properties of zones 1 to 5 are given in Table 1.

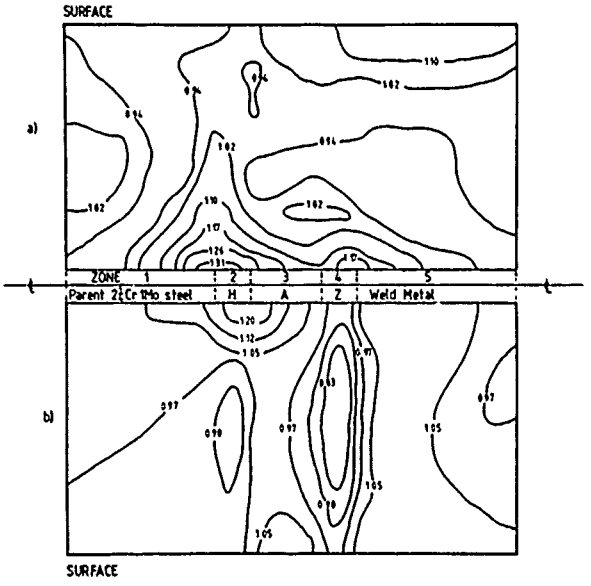


Fig. 8 Contours of the ratio of stress at a point to the initial (elastic) uniform stress. Number of time step increments is 64 (16ks). Initial uniform stress = 250 MPa. (a) is for maximum principal stress, (b) is for effective stress.

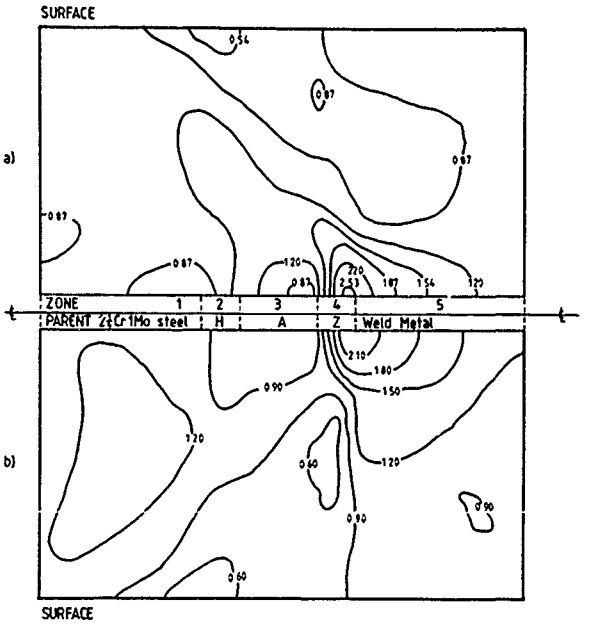


Fig. 9 Contours of the ratio of stress at a point to the initial uniform (elastic) stress. Number of time step increments is 64 (550ks). Initial uniform stress = 100 MPa. (a) is for maximum principal stress, (b) is for effective stress.

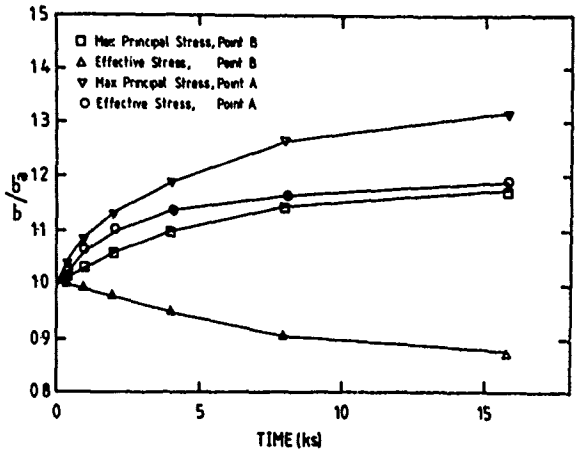


Fig. 10 Ratio of stress ($\sigma$) to initial uniform stress ($\sigma_a$) for points A and B (Figure 7) as a function of time for a uniform loading of 250 MPa at 838K.

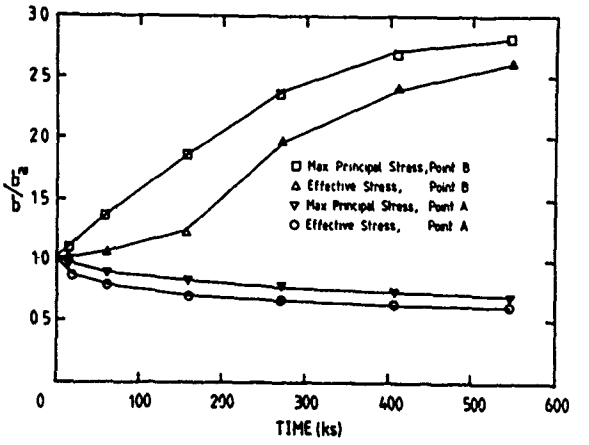


Fig. 11 Ratio of stress ($\sigma$) to initial uniform stress ($\sigma_a$) for points A and B (Figure 7) as a function of time for a uniform loading of 100 MPa at 838K.

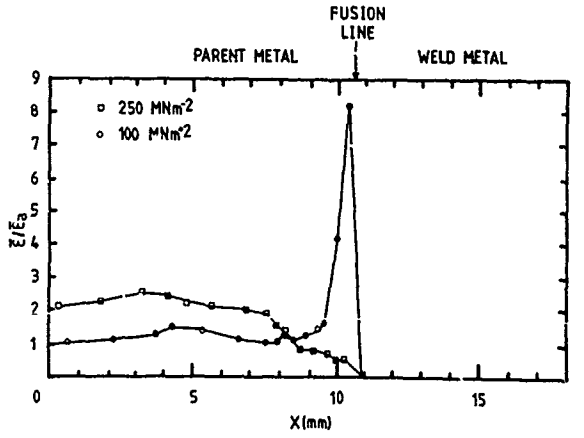


Fig. 12 Ratio of the average effective strain ($\bar{\varepsilon}$) to the overall average strain ($\bar{\varepsilon}_a$) as a function of position along the gauge length (x) for weld testpieces tested at 838K and 100 MPa and 250 MPa.

# CONTINUUM DAMAGE MECHANICS (CDM) - A NEW DESIGN TOOL

J. Hult

Professor Hult is in the Division of Solid Mechanics at Chalmers University of Technology, Gothenburg, Sweden.

SYNOPSIS

The basic ideas and concepts in Continuum Damage Mechanics (CDM) are outlined. One of the main purposes of CDM is to predict the carrying capacity of structures under load. The conditions for final failure are therefore discussed in some detail with reference to the behaviour of a fibre bundle under uniaxial tension.

## INTRODUCTION

The important influence of defects on the load carrying capacity in solids has long been recognized, as found in material tests and incorporated in modern theories of plasticity and fracture. Three areas of applied mechanics have evolved, where a certain type of mechanical defect is a central concept:

Dislocation Mechanics forms the basis for understanding plastic deformation in metals. Likewise Fracture Mechanics forms the basis for understanding fracture in solids with preexisting sharp cracks of finite size. The term Damage Mechanics has been coined in this tradition. It deals with the effect on the load carrying capacity of distributed small cracklike defects or voids.

Even though the defects themselves are discrete entities their joint effect may be described in continuum mechanical terms. Since the purpose of damage mechanics is to predict macroscopic properties, such as the rupture strength or the creep rupture lifetime of damaged materials, a continuum model may be used to advantage. Hence the expression Continuum Damage Mechanics (CDM) has come into being (Janson & Hult 1977).

Present day CDM is based on ideas first presented thirty years ago by Kachanov. He addressed the problem of describing, in simple engineering terms, the conditions for brittle creep rupture such as occurs in many metals at elevated temperatures and low stresses (Kachanov 1958). Later development has branched out into two separate areas:

(1) micromechanical, physical analyses of processes causing damage formation and growth,

(2) macromechanical, engineering analyses of structural effects of damage formation and growth.

For a long time work in these two areas proceeded in parallel with only slight interaction. As shown in recent reviews of the field (Cocks and Ashby 1982, Krajcinovic 1984, Lemaitre and Chaboche 1985, Bazant 1986, Murakami 1987, Lemaitre and Krajcinovic 1988, and others) the two areas of study have lately developed in directions to close the gap between micro and macro.

The present paper outlines, briefly, the basic concepts in CDM and then proceeds to discuss in some detail the conditions for final failure in structural components subject to damage formation and growth.

## Elementary damage mechanics

### a) Brittle creep rupture

In order to describe the gradual decay of the material structure which is observed to occur in many metals after long time exposure to stress and high temperature Kachanov (1958) introduced a scalar field variable $\psi$ denoted 'continuity', such that $\psi = 1$ describes a completely virgin material, whereas $\psi = 0$ describes a state of complete destruction.

Kachanov also postulated a relation governing the decrease of $\psi(t)$ as caused by the stress:

$$\frac{d\psi}{dt} = -f\left(\frac{\sigma}{\psi}\right) \qquad (1)$$

For any given stress history $\sigma(t)$ the magnitude of $\psi(t)$ may then be determined, considering the initial condition $\psi(0)=1$. The load carrying capacity of the material is exhausted when $\psi=0$ and the corresponding time is found to be

$$t_R(\sigma) = \sigma \cdot \int_{\sigma}^{\infty} \frac{dx}{x^2 \cdot f(x)} \qquad (2)$$

If, in particular,

$$f(x) = C x^{\nu} \qquad (3)$$

then

$$t_R(\sigma) = \frac{1}{(1+\nu) C \sigma^{\nu}} \qquad (4)$$

which is represented by a straight line in a $\log\sigma$ vs. $\log t_R$ diagram (Fig. 1).

It has been shown (Hult 1988) that for a step-up load sequence as shown in Fig. 2

$$\int_0^{t_R^*} \frac{dt}{t_R[\sigma(t)]} \lesseqgtr 1 \qquad (5)$$

according as

$$\frac{d}{dx}\left[\frac{f'(x)}{f(x)}\right] + \frac{1}{x}\cdot\frac{f'(x)}{f(x)} \gtreqless 0 \qquad (6)$$

Equality, i.e.

$$\int_0^{t_R^*} \frac{dt}{t_R[\sigma(t)]} = 1 \qquad (7)$$

requires $f(x)$ to be a power function. Hence the "linear life fraction rule" (7), LFR for short, holds if the creep rupture plot is a straight line as in Fig. 1.

For a reversed step loading sequence, i.e. a step-down load, corresponding relations hold, but in reversed order. Again the linear life fraction rule (7) holds for a power law material. This may be shown to be the case for any loading history such as indicated in Fig. 3. From LFR then follows the rupture time

$$t_R^* = t_{Rn}(\sigma_n) - \sum_{i=1}^{n-1} T_i\left[\left(\frac{\sigma_i}{\sigma_n}\right)^{\nu} - 1\right] \qquad (8)$$

where $t_{Rn}(\sigma_n)$ is the rupture time corresponding to the load $\sigma_n$ as given by (4) and where $n$ is such that

$$0 < t_{Rn} - \sum_{i=1}^{n-1} T_i\left(\frac{\sigma_i}{\sigma_n}\right)^{\nu} < T_n \qquad (9)$$

Since the $\log t_R$ vs. $\log\sigma$ relation is closely linear for many materials (8) should yield a good estimate of the creep rupture lifetime under varying loading programs.

b) Scalar or tensorial damage

The complementary quantity (Rabotnov 1969)

$$\omega \equiv 1 - \psi \qquad (10)$$

has later been adopted by several writers as a measure of the 'damage' caused to the material structure. Another common designation is $D$ .

In uniaxial tension damage can be represented by a single scalar field quantity. Multiaxial stresses may however result in damage configurations which require more than one field quantity for full characterization. Extensive, both experimental and theoretical, studies (Murakami and Ohno 1981, Hayhurst 1983, Betten 1983, Krajcinovic 1984, Lemaitre and Chaboche 1985, and several others) have resulted in various tensorial representations of multiaxial damage effects.

c) Ductile creep rupture

Assuming damage to influence also the creep deformation Rabotnov (1969) postulated the following modified form for the secondary creep law due to Norton:

$$\frac{d\varepsilon}{dt} = B\left(\frac{\sigma}{1-\omega}\right)^{n} \qquad (11)$$

This creep law and the corresponding damage law

$$\frac{d\omega}{dt} = C\left(\frac{\sigma}{1-\omega}\right)^{\nu} \qquad (12)$$

may be combined to describe the development of strain and damage in a creep test under constant load. Creep rupture is assumed to occur at time $t_R$ when $\omega = 1$.

The corresponding creep rupture plot is shown in Fig. 4, where the two limiting cases of purely ductile creep rupture ($C=0$), analysed by Hoff (1953) and the purely brittle creep rupture ($B=0$), analysed by Kachanov (1958), are indicated as limiting asymptotes.

d) Damage micromechanics

Early geometric interpretations of the damage measure $\omega$ directly in terms of 'remaining load carrying area' tended to oversimplify the problem at hand. Obviously the effect caused by cavities being formed in the material must depend on the shape, size and distribution of these cavities and also on the constitutive properties of the material itself. Recent development of analytical

and numerical methods to calculate strength and stiffness of cavitated materials, cf. Mura (1987), has made it possible to relate the damage measure to various cavity configurations.

A damage measure $\omega$ may then be implicitly defined by rewriting the constitutive equation of an undamaged material

$$L[\varepsilon] = M[\sigma] \tag{13}$$

in the form

$$L[\varepsilon] = M\left[\frac{\sigma}{1-\omega}\right] \tag{14}$$

Such results have been reported by Duva and Hutchinson (1984), Jansson and Stigh (1986), and several others.

e) Damage growth

Early experimental studies (Dyson and McLean 1972, Dyson 1983, and others) have shown how cavities are nucleated and grow in size under various conditions of stress and temperature. These results have also been incorporated in various models to describe accelerated damage growth (Budiansky, Hutchinson and Slutsky 1982, and others).

Conditions for final failure

Kachanov (1958) postulated brittle creep rupture to occur when the continuity has decreased to zero. The corresponding critical damage as given by (10) is corresponding to unlimited rates of strain and damage as given by (11) and (12). Obviously $\omega = 1$ must be an upper limit to the rupture damage.

Micrographs of cross sections close to the rupture location in creep test specimens usually show traces of damage in the form of small voids, microcracks, etc. The volume fraction of these cavities is however quite small, in contrast to the assumption of complete loss of continuity as implied by the rupture criterion $\Psi = 0$ i.e. $\omega = 1$. Rupture does indeed occur earlier, at a lower value of $\omega$, because a state is reached when stable equilibrium cannot be maintained.

The creation of voids which later merge to form small cracks causes the stresses to redistribute. The load has to find new paths through the body; when certain parts are deloaded due to cavity formation others have to take on higher stresses.

A continuum mechanical analysis of this process is prohibitive, and therefore simplified mechanical models have been studied, which give an insight into the general problem. One such model consists of a set of parallel bars or fibres loaded in uniaxial tension. All fibres suffer the same strain, and there is no sideways interaction between them. A load of prescribed time history is applied and the ensuing stress-time history in the individual fibres is recorded.

a) Probability analysis

In his probabilistic study of strength of materials Weibull (1939 a,b) considered the load carrying capacity of a system as in Fig. 5, where the fibres were ascribed a probability of survival at stress

$$P(\sigma) = \exp\left[-(\sigma/\sigma_m)^m\right] \tag{15}$$

If, at a certain state, $r$ fibres out of the total number $n$ have ruptured, then the probability of survival may be stated as

$$P(\sigma) = \frac{n-r}{n} = 1 - c \tag{16}$$

where $c = r/n$ is the rupture ratio, i.e. the fraction of ruptured fibres. With denoting the nominal stress, referred to the undamaged system, the stress carried by the surviving fibres is

$$\sigma = \sigma_0 \frac{n}{n-r} = \frac{\sigma_0}{1-c} \tag{17}$$

From (15), (16) and (17) follows

$$\frac{\sigma_0}{\sigma_m} = (1-c)\left[-\ln(1-c)\right]^{1/m} \tag{18}$$

This is a relation between the rupture ratio and the applied load , shown in Fig. 6. When the load increases from zero the rupture ratio increases slowly at first and then more rapidly. Eventually a critical state $(\sigma_0^*, c^*)$ is reached, when $dc/d\sigma_0 \to \infty$. If the load is increased above the critical stress level, equilibrium cannot be maintained and final rupture occurs, cf. Lundberg and Hult (1982).

The mean rupture stress of the undamaged fibre bundle is

$$\bar{\sigma}_{0U} = \int_0^\infty P(\sigma_0)\,d\sigma_0 = \sigma_m \cdot \Gamma(1+1/m) \tag{19}$$

The critical rupture ratio and the critical stress ratio are found to depend upon the Weibull exponent as follows

| m | 1 | 3 | 10 | 20 | 100 | ∞ |
|---|---|---|---|---|---|---|
| $c^*$ | 0.63 | 0.28 | 0.10 | 0.05 | 0.01 | 0 |
| $\sigma_0^*/\bar{\sigma}_{0U}$ | 0.37 | 0.56 | 0.76 | 0.84 | 0.95 | 1 |

The limiting case $m = \infty$ corresponds to the case of the fibres having zero rupture probability below stress $\sigma_m$ and zero survival probability above $\sigma_m$. The quantity $c^*$ may be interpreted as a measure of damage immediately before final rupture. The ratio $\sigma_0/(1-c)$ in (17)

has an exact counterpart in the expressions (11) and (13). The main conclusion from this study is that the critical damage $c^* \ll 1$ for values of corresponding to brittle materials (Weibull quotes $3 < m < 30$).

b) General fibre bundle

Increasing interest in fibre composites has led to further studies of fibre bundles, cf. Chrzanowski and Hult (1987) for references.

The mathematical analysis becomes simpler if the fibre bundle is modelled as a continuum (infinitely many fibres). Hult and Travnicek (1983) studied such a model (Fig. 7), where stiffness (E) and strength (U) were both assumed to vary linearly across the bundle

$$E(x) = \bar{E}\left[1+\mu(2x-1)\right] \qquad (20)$$

$$U(x) = \bar{U}\left[1+\nu(2x-1)\right] \qquad (21)$$

Here $\bar{E}$ and $\bar{U}$ denote the mean values of stiffness and strength, and $\mu$ and $\nu$ are measures of their nonuniformities.

The fibres may be imagined to be rearranged sideways such that rupture proceeds from one edge monotonically towards the other edge. The fraction of ruptured fibres will be denoted $c$ as above. The following expression is then obtained for the applied stress $\sigma_o$ in terms of the rupture ratio $c$, if $\mu < \nu$

$$\sigma_o(c) = \bar{U}\,\frac{(1-c+\mu c-\mu c^2)(1-\nu+2\nu c)}{1-\mu+2\mu c} \qquad (22)$$

as shown by Fig. 8. Rupturing starts at the load level $\sigma_o'$ and the rupture ratio then increases with increasing load just as for the probabilistic analysis above. The slope $\alpha$ may be positive (stable fracturing up to $\sigma_o^*$) or negative (unstable fracturing starting at $\sigma_o'$; this occurs at small values of $\mu$ and $\nu$). The critical rupture ratio falls in the interval

$$0 < c^* < 0.55 \qquad (23)$$

a result which, again, contradicts the rupture criterion $\omega = 1$.

Progressive creep rupture may also be analysed by this model. Assuming the linearly viscous creep law

$$\dot{\varepsilon} = S/M \qquad (24)$$

where $S$ denotes the fibre load divided by the actual cross sectional area, and where

$$M(x) = \bar{M}\left[1+\lambda(2x-1)\right] \qquad (25)$$

whereas $U(x)$ is given by (21) the results in Figs 9 and 10 were obtained (Chrzanowski and Hult 1987). Four modes of rupture (A through D) are identified to occur, determined by the magnitudes of the non uniformity parameters $\lambda$ and $\nu$. For small $\nu$ rupture will occur in a 'brittle', non gradual, manner. This may occur after a certain 'incubation' time $t_i$ (A), or immediately upon load application (B). For larger magnitudes of $\nu$ rupture will be of a ductile nature, occurring gradually, either after an incubation time $t_i$ (C), or upon load application (D). The critical rupture ratio $c^*$, in all these cases, falls in the interval (23).

## Conclusion

The results obtained from the different, probabilistic as well as deterministic, analyses of fibre bundles show great similarities as regards the mechanical behaviour under increasing load. The critical rupture ratio as well as the final rupture load, i.e. the load carrying capacity of the bundle, both depend strongly on the variability of the fibre properties.

The concept of an incubation time, before which no damage appears, shown here for a fibre bundle with small variability in rupture strength, is well known from observations on creep test specimens.

Summing up, this may be interpreted to imply that the critical damage causing final rupture in an engineering component subject to creep loading is also dependent upon local variations in constitutive properties. Further study of this dependence will make Continuum Damage Mechanics a more reliable tool for predicting creep rupture lifetimes as well as the static rupture load.

## References


Bazant,Z.P., Appl.Mech.Rev. 39:5 (1986), 675-705.

Betten,J., J. de Mécanique théorique et appliquée 2:1 (1883), 13-32.

Budiansky,B., Hutchinson, J.W., Slutsky,S., In 'Mechanics of Solids', Pergamon Press, Oxford 1982.

Chrzanowski, M., Hult, J., Engng. Fracture Mech. 28:5/6 (1987), 681-688.

Cocks, A.C.F., Ashby, M.F., Progress in Material Science 27 (1982), 189-244.

Duva, J.M., Hutchinson, J.W., Mechanics of Materials 3 (1984), 41-54.

Dyson, B.F., McLean, D., Metal Science J. 6 (1972), 220-223.

Dyson, B.F., Scripta Metall 17 (1983), 31-37.

Hayhurst, D.R., In 'Engineering Approaches to High Temperature Design', Pineridge Press, Swansea 1983.

Hoff, N.J. J.Appl.Mech. 20 (1953), 105-108.

Hult, J., Travnicek, L., J. de Mécanique théorique et appliquée 2:4 (1983), 643-657.

Hult, J., In 'Applied Solid Mechanics 2', Elsevier Applied Science Publ. 1988.
Janson, J., Hult, J., J. de Mécanique Appliquée 1:1 (1977), 69-84.
Jansson, S., Stigh, U., J.Appl.Mech. 52 (1985), 609-614.
Kachanov, L.M., Izv.Akad.Nauk.SSR, Otd.Tekhn. N.8 (1958), 26-31.
Krajcinovic, D., Appl.Mech.Rev. 37 (1984), 1-6.
Lemaitre, J., Krajcinovic, D., CISM course 1986. To be published 1988.
Lemaitre, J., Chaboche, J.-L., Mécanique des Matériaux Solides. Dunod, Paris 1985.
Lundborg, N., Hult, J., Mechanics Research Communications 9:5 (1982), 343-347.
Mura, T., Micromechanics of Defects in Solids, 2.ed., Nijhoff, Dordrecht 1987.
Murakami, S., Ohno, N., In 'Creep in Structures', Springer, Berlin 1981.
Murakami, S., JSME 30 (1987), 701-710.
Rabotnov, Yu.N., Proc. XII Int.Congr. Appl.Mech., Springer, Berlin 1969.
Weibull, W., IVA Proc. 151, 153, Stockholm 1939 a,b.

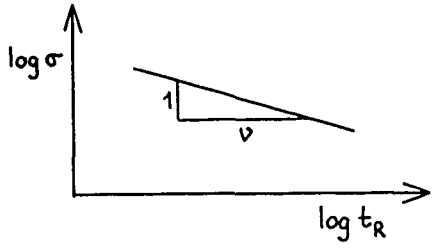


Fig. 1. Brittle creep rupture lifetime versus applied stress.

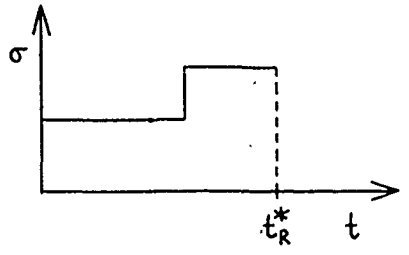


Fig. 2. Step-up loading sequence. Creep rupture occurs at time $t_R^*$.

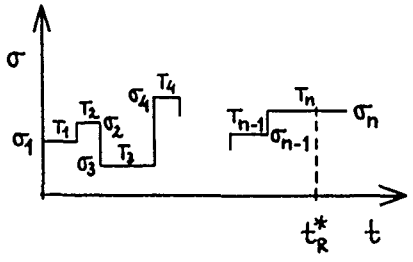


Fig. 3. Arbitrary loading sequence. Duration of stress $\sigma_k$ is $T_k$ Creep rupture occurs at time $t_R^*$.

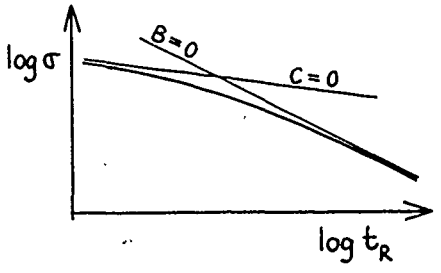


Fig. 4. Ductile and brittle creep rupture lifetime $t_R$ versus applied stress $\sigma$.

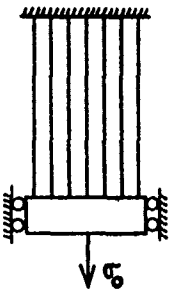


Fig. 5. Fibre bundle under tension.

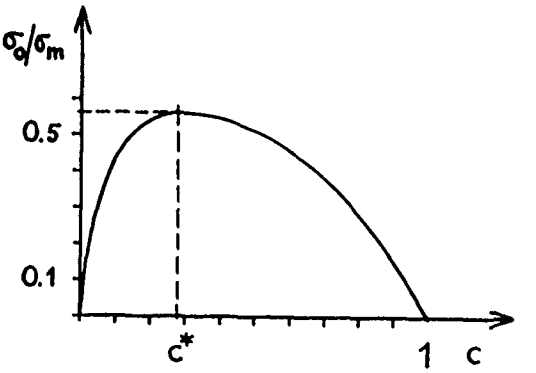


Fig. 6. Dependence of rupture ratio c upon load $\sigma_0$ applied to fibre bundle.

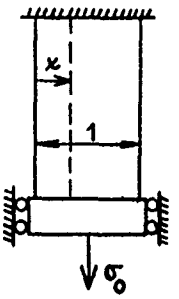


Fig. 7. Fibre continuum under tension. Local fibre identified by location x.

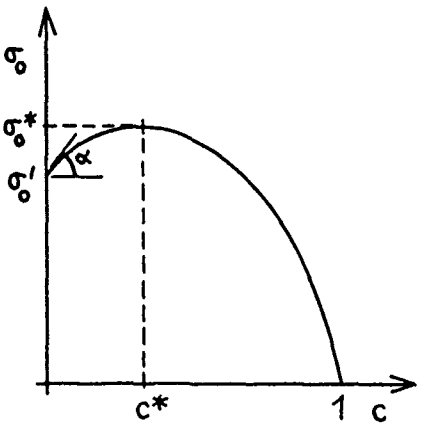


Fig. 8. Dependence of rupture ratio c upon load $\sigma_0$ applied to fibre continuum.

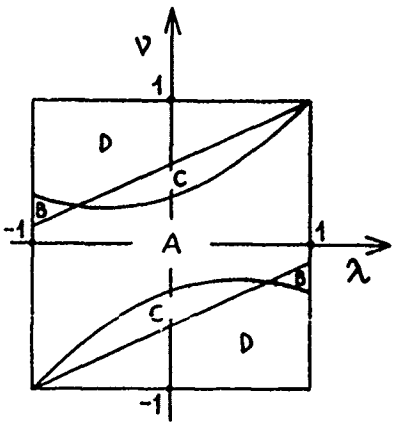


Fig. 9. Creep rupture mode map. A,B,C,D refer to rupture modes shown in Fig. 10.

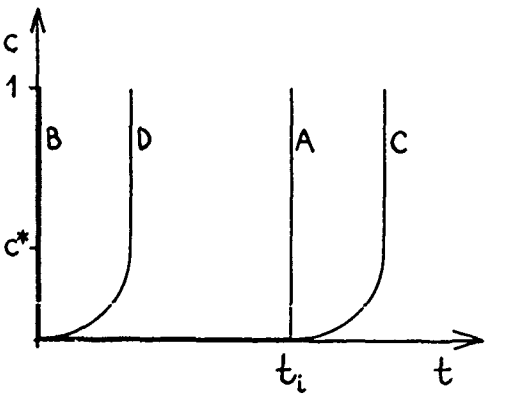


Fig. 10. Creep rupture modes: Immediate (instant B, gradual D) or Delayed (instant A, gradual C) with incubation time $t_i$.

□

# DUCTILE FRACTURE

B. A. Bilby, M. R. Goldthorpe, I. C. Howard and
Z. H. Li

Professor Bilby, Dr. Howard and Mr. Li are in the Department of Mechanical Engineering, University of Sheffield. Dr. Goldthorpe is with the Central Electricity Generating Board at Wythenshaw, Manchester.

## SYNOPSIS

The paper contains the results of large-strain elastic-plastic analyses of a group of specimen geometries. The results have been used to examine the questions of the size requirements for fracture toughness testing of ductile materials and the validity of single parameter characterisation of crack tip fields. The size requirements for testing appear to be conservation for many commonly used structure materials but there are reservations about some materials of which high strength weld metals may be an example. A two parameter characterisation of the crack tip field is demonstrated to be very effective for the centre-cracked panel and it should prove equally beneficial for those geometries which have similarly low values of constraint.

## INTRODUCTION

The assessment of fracture in ductile materials depends primarily upon the possession of measurement of certain material characteristics. The resistance of a ductile material to the propagation of a crack is conventionally measured in a J-test (ASTM, 1981). J is a load-related parameter that characterises the mechanical state of the crack tip material in the sense of rate of change of work input per unit crack advance. In certain geometries, for example the single edge notch bend specimen, its value is related to the work input at the loading pin of the machine deforming the specimen. It has, therefore, the unique quality of being both measurable in a conventional engineering test and able to characterise the crack tip material.

Figure 1 shows, in diagramatic form, the shape of a typical J-resistance curve with an indication underneath of the microstructural changes responsible for it. An initially sharp fatigue crack blunts as the specimen containing it is made to deform. This produces a region of crack "growth" which is the extension of the tip as a consequence of its homogeneous blunting. The amount of growth is directly proportional to J, and the "blunting line" so produced is represented in the ASTM standard by the equation

$$J = 2\sigma_y \Delta a \qquad (1)$$

where $\sigma_y$ is the yield stress of the material.

This blunting concentrates strain to a very great degree in the material ahead of the tip and also subjects it to a large hydrostatic tension. If the interfaces around weakly bonded particles had not previously failed they would do so once they become enveloped in this field, and a void is shown growing in this region. Eventually this void coalesces with the blunting crack tip, more often than not by some micromechanism on a smaller scale than that of the major void forming particles. This is the beginning of real crack growth, and the value of J at which it occurs is given a special name, $J_{IC}$ the value for crack initiation. $J_{IC}$ is a material property when it is measured in specimens that are thick enough to ensure conditions of plane strain and which are not so small that they fail to ensure proper constraint of the material at the tip of the track.

Continued deformation of the specimen causes further growth and coalescence of voids, and the spreading of plasticity further out into the specimen as a consequence makes the value of J rise. This rising "resistance curve", J-resistance or J-R curve is also a material characteristic under certain conditions analogous to those on $J_{IC}$ and also as long as the crack growth, $\Delta a$, is not too large.

The assessment of cracked structures depends upon comparing the value of the applied crack driving parameter with the resistance of the material to the initiation or growth of the crack. American practice has centred around the handbooks of Kumar et al (1981, 1984) which give values for J (and CTOD) for a range of geometrical configurations and different rates of strain-hardening. This J-based approach is also the foundation of of the latest version of the R6 procedures (Milne et al, 1986) developed within the Central Electricity Generating Board. Option 3 is the standard upon which is set the easier assessment routes of Options 1 and 2, and so one could regard the FAD of R6 as essentially based on the use of a J-resistance curve as the characteristic of material failure.

Several issues arising from all this now present themselves. They all concern the problem of when a single parameter (J or COD) can

be expected to characterise uniquely the state of material near to the crack tip, and what can be done about it when that characterisation fails. Primary interest currently centres upon the size requirements for $J_{IC}$ testing. This will be described in the following section. A further issue has, actually, been evident for longer than the potential limitations of the size requirements for testing. This is the way in which cracking can develop quite differently in components made of the same material but whose crack tips suffer different amounts of plastic constraint usually measured by the ratio of hydrostatic to the equivalent stress in the crack tip field. For example, Hancock and Cowling (1980) discovered that cracks in HY80 steel began to grow at values of COD differing by a factor of 10 in specimens subjected to radically different degrees of plastic constraint. The issue of constraint will be dealt with in a subsequent section.

## SIZE EFFECTS IN ELASTIC PLASTIC FRACTURE

The ASTM (1981) procedure for $J_{IC}$ testing demands that the specimen thickness B and the ligament b ahead of the crack tip must satisfy

$$B,\ b > 25\ \frac{J_{IC}}{\sigma_F} \qquad (2)$$

for the test to be valid. A similar criterion is set in the procedures of Neale et al (1985), but $J_{IC}$ in (1) is replaced by $J_{max}$, the maximum value of J which satisfies the validity requirements above. This value may, in fact, be reached only after a substantial ambount of ductile crack growth. $\sigma_F$ in the inequality is the mean of the 0.2% proof stress and the tensile strength of the material under test.

The fact that testing small ductile specimens (much smaller than those required to satisfy the demands of the tests of brittle fracture (British Standards Institution (1977) and ASTM (1983)) might require limitations on size was first noted by Paris (1972). An answer to this question was provided by McMeeking and Parkes (1979), Shih and German (1981) and Shih (1985), to the effect that the dimensionless group $M = b\sigma_o/J$ should be at least 25 in a specimen of hardening material where deformation in the ligament was dominated by bending.

We have re-examined these questions by performing a large number of finite deformation, elastic plastic analyses of two-dimensional models of the conventional test specimens. These are the single edge crack bend (SECB) specimen and the compact tension (CT) specimen. Dimensions are shown in Figure 2, which also gives those of other geometries to be discussed later in the paper. Figure 3 shows the region of the mesh surrounding the tip of the notch in one of our analyses. We have followed McMeeking (1977) in performing our large-strain elastic-plastic calculations on a model with a notch of finite, but small, root radius. The level of refinement of the meshes used ranged from one having a ratio of crack length to undeformed notch width of 500 (to obtain a solution for large scale yielding) up to a ratio of 4500 (to obtain a solution for small scale yielding (SSY)). Four-noded isoparametric elements were used throughout each mesh.

The material obeyed the von Mises yield criterion and the Prandtl-Reuss flow rule. The initial yield stress was $\sigma_o$. The ratio $E/\sigma_o$ was 300 and Poisson's ratio, $\nu$, was 0.3. Most of our work has been with non-hardening material, the most "non-elastic" of all time-independent responses. The effects of hardening have been included by studying a material which hardens via a power law connecting the effective stress, $\bar{\tau}$, and the logarithmic plastic strain $\bar{e}^p$ in the form

$$\frac{\bar{\tau}}{\sigma_o} = \left( \frac{\bar{\tau}}{\sigma_o} + \frac{3G\bar{e}p}{\sigma_o} \right)^n \qquad (3)$$

We report here data obtained when $n = 0.2$.

The results can be assessed by examining Figures 4(a) and (b) which show the states of stress in the SECB geometry directly ahead of the tip of the crack for two degrees of hardening (non-hardening and with a hardening exponent of $n = 0.2$). The pattern of stress in the region dominated by blunting (i.e. $R/\delta \leq 2$) is remarkedly insensitive to the value of M, but there is a significant trend away from the full line, that of small scale yielding (SSY), for the smaller values of M appropriate to small fully plastic specimens. The strain goes the other way, in that the major variation with M occurs in the region dominated by blunting. Outside that it is small.

One criterion, suggested by Shih (1985), to decide upon the value of M below which single-parameter control of the tip has been lost is to require that the stress at a distance of three crack openings ahead of the tip be within 90% of the value at the corresponding position for SSY conditions. The data of Figures 4(a) and (b) then show that this criterion is met when $M > 27$ in non-hardening material and when $M > 25$ is hardening material with $n = 0.2$. There is a considerable degree of subjectivity in any criterion of this kind. For example, if we are more stringent, and demand that the pattern of stress is approximately the same as SSY over distances of $R/\delta$ up to 10 then we would conclude that single parameter control is lost if $M \leq 150$ in non-hardening material and $M \leq 100$ in hardening material with $n = 0.2$.

Although the use of Shih's criterion appears to give strong support to the limitations of in-plane size of the standard for $J_{IC}$ testing, there are several features of the development of ductile damage which the criterion fails to address. Models of void growth in ductile steels predict an exponential dependence of the void growth rate on hydrostatic stress. Furthermore, the size to which a void may grow depends on the whole history of stress and strain at the site of the void from the moment the void is enveloped by the plastic zone growing from the crack tip. Relatively small deviations of stresses from the small scale yielding values may therefore give rise to large changes in the void growth rate. The accumulation of these differences during the history of void growth may enlarge these changes even further.

We have examined these questions using the model of Rice and Tracey (1969) by combining their expression

$$\frac{\dot{R}}{R} = C\,\dot{\varepsilon}^p \exp\left( \frac{3}{2}\,\frac{\sigma_m^{\infty}}{\sigma_y} \right) \qquad (4)$$

for the rate of growth of a spherical void of

radius R with the near-tip stresses and strains of our finite element analyses of specific cracked geometries. The analysis identifies the remote stress $\sigma_m^\infty$ and strain $\epsilon^p$ of the model of Rice and Tracey with the prediction of the finite element analysis at the point where the void is imagined to be. The simple model neglects void interactions, which would cause it to overestimate fracture strains in tensile specimens (Howard and Willoughby (1981), Anderson (1977) and McMeeking (1977)). But, more importantly, it neglects any interaction between the mechanical fields in the material ahead of the blunting tip and the voids that grow within them, redistributing them and weakening the material. However, it does address the important issues of the effect of mean stress on void growth and failure, and the history dependence of processes of ductile failure.

Figure 5 shows a set of data obtained from the analysis of void growth in three sizes of SECB specimen of non-hardening material at applied loads corresponding to the same value of the applied J. What is shown is the size R to which an initially spherical void of radius $R_o$ grows at a position X ahead of the tip. The abscissa is normalised with the current value of the crack opening displacement. If the data from a specimen stimulate SSY then they should lie on top of the SSY line. The curves of void growth are close to, and slightly above, the line of small scale yielding if M is bigger than 114. The data of M = 45 are different, lying below the SSY line if $X/\delta$ is big enough and above it otherwise. The point of cross-over is about $X/\delta = 1.7$.

Similar analyses have been performed on the compact specimen. Briefly, the pattern of stress near the tip of a blunting crack in this specimen rises above the SSY line as deformation proceeds and the extent of yielding increases. The specimen is over-constrained in comparison with SSY, and might be expected to produce conservative data on the fracture properties of materials. This suspicion is borne out in the results of our studies of void growth in this specimen, although the scale of investigation has not, as yet, been as extensive as that for the SECB geometry. At high values ($\lesssim 60$) of M, the curves for the growth of voids lie above that of SSY for the range ($0 \lesssim X/\delta \lesssim 10$) of relative distances investigated. This is also true for smaller values of M if $X/\delta$ is small to moderate, but these curves now fall below the SSY line at large $X/\delta$, the transition point decreasing with M as in the SECB geometry.

Our studies of void growth, limited to non-hardening material, suggest that an M value of about 120 in the SECB geometry suffices to ensure conditions in which the growth of void is done to that of SSY. The trend for compact specimens is similar, but our data are not extensive enough to estimate a value of M.

However, the trend is clear for both geometries when M is so small that there is no longer any close simulation of SSY. The curves of void growth lie <u>above</u> that for SSY if $X/\delta$ is less than some value about 2. These values of $X/\delta$ are of interest in predicting the initiation of crack growth in many ductile materials, for, as Knott (1980) shows, these values correspond to the ratio of inter-particle spacing to initiation COD observed. This evidence supports the assumption that the currently in-plane size requirements for $J_{IC}$ testing give conservation test data in comparison to those that would be obtained from large specimens.

However, there are materials, of which high strength weld metals are an example, (Knott, 1980) for which values of $X/\delta$ greater than 2 at initiation appear to be appropriate. Testing these materials in small specimens might be dangerous. The relatively low toughness exhibited by these materials is probably due to void growth being curtailed early by the formation of shear bands or other micromechanisms of failure, and the void growth occurs mainly in those parts of the plastic zone relatively remote from the tip where the full constraint simulating SSY does not occur.

## TWO-PARAMETER CHARACTERISATION OF CRACK TIP FIELDS

There are certain geometries, of which the centrally cracked panel (CCT) is the most notorious, in which control of the crack tip field by a single parameter is lost at rather low loads. Indeed, the CCT geometry is so poorly constrained that single parameter control of the crack tip material has already been lost at loads low enough to satisfy the requirement of the LEFM plane strain fracture toughness test (Larsson and Carlsson, 1973).

The mechanical reasons behind this are illustrated in Figures 6 (a) and (b) which show in the different symbols the drop in stress near the crack tip as plasticity is spread in this specimen. The lines through the data points are the predictions of a two-parameter characterisation of this geometry using the applied stress intensity factor K and the elastic T-term as the parameters.

Briefly T is the second term in the eigenfunction expansion (Williams, 1957) of the elastic field ahead of the crack tip. It is a field of constant stress parallel to the flanks of the crack. Its value is sensitive to specimen shape and loading, and it has been evaluated for a range of specimen geometries by Leevers and Radon (1982), Cardew et al. (1984), Goldthorpe (1986) and Kfouri (1986). The full lines in Figures 6 are the result of a modified boundary layer analysis for the appropriate values of K and T; that is, an analysis on elastic plastic material in a large circular region containing an effectively semi-infinite crack. This was performed here by a finite element method in which displacements were specified on the outer boundary equal to those of the elastic K and T fields combined.

The agreement is very good, clear evidence that a two-parameter characterisation of this geometry is effective at loads very close to the collapse state. These effects are exemplified further in Figure 7 which shows how well the growth of a void near the tip of a crack in a CCP is predicted by that in the modified boundary layer problem loaded to similar values of K and the same value of T. A further demonstration of the power of the two parameter approach to this geometry is given in Figures 8 and 9 which are for a CCP loaded biaxially so that the value of T is zero. For the particular geometry chosen this requires a ratio of the biaxial stress to the applied stress of $\lambda = 1.378$. The data for stress now overlie each other at all values of applied load and the size to which a void grows in these fields is also very similar for different loads, particularly in the materially important region where $X/\delta \lesssim 2$.

There is now mounting evidence that a single parameter may often be inadequate as a means of

characterising the mechanical state of a crack tip. For example, tests on the fatigue performance of materials subjected to biaxial loading (Brown and Miller (1982)) show that there may be an order-of-magnitude change in the rate of crack growth at the same nominal ΔK but differing biaxial loadings. Furthermore, a recent reappraisal by Priest (1986) of a range of tests to determine the fracture toughness of materials by the currently accepted standards (ASTM (1981), BSI (1977) for $K_{IC}$ testing concludes that the in-plane size requirement is, in many materials, not stringent enough to ensure characterisation of the crack tip material by K alone. Priest's remedy was to invoke ad hoc plastic zone corrections which bring the test data towards a materially constant value. Interestingly, the data from specimens which failed to give size-dependent results gave $K_{IC}$ values on the low side, a further piece of evidence for the hypothesis that tests with excessive plasticity gives conservative data in comparison with SSY for the initiation of crack growth.

## DISCUSSION

There appears to be strong evidence in support of the assumption that the conventional in-plane size requirement for $J_{IC}$ testing should produce test data in most ductile materials that are conservative in comparison with those obtained from large SSY specimens. However, there may be materials, for example high strength weld metal, where tests on small plastic specimens might produce over-optimistic initiation data. Experimental work on size requirements for $J_{IC}$ testing has concentrated upon materials that are likely to be conservative. This point will not be resolved until an experimental programme has been undertaken on the effects of specimen size on low toughness material.

Conservative data provides confidence when it is used in safety assessments on structures that are actually or potentially flawed. Safety factors are under-estimated and the structure is actually safer than the assessment suggests. This might not be so when the assessment is to find the maximum flaw size that would survive a proof test. Current practice uses mean data for this purpose.

A two-parameter characterisation of the crack tip is likely to prove of value to the assessment of fatigue and other processes of sub-critical crack growth and to a re-appraisal of the currently acccepted tests of brittle fracture which have recently been called into question by Priest (1986) and Sinclair and Chambers (1987). There is also considerable potential for its use in the characterisation of certain flaws in ductile material. For example, arguments of leak-before-break in thin-walled pressurised components would often use a geometry similar to the CCP reported in this paper. The lack of constraint on this geometry makes it much more resistant to the initiation of crack growth than the compact specimen. Yet data from this latter geometry is invariably used in assessments of structural integrity. There is a chance that a perfectly safe vessel may be condemmed by the use of high constraint, lower bound data collected in testing geometries. It is therefore highly desirable for tests to be undertaken to measure the differing effects of constrain on the initiation and growth of cracks in a well characterised ductile material.

## ACKNOWLEDGMENTS

The work reported here was conducted as part of a research project funded by H.M. Nuclear Installations Inspectorate to which we are indebted for permission to publish. The views expressed here are those of the authors alone and the permission to publish does not necessarily imply any endorsement of those views by the Nuclear Installations Inspectorate. The finite element calculations were carried out using the TOMECH program developed at the University of Sheffield.

## REFERENCES

Andersson, H. 1977. Analysis of a model of void growth and coalescence ahead of a moving crack tip, J. Mech. Phys. Solid, 25, 217-233.

ASTM. 1981. Standard Test for $J_{IC}$, a Measure of Fracture Toughness. Annual Book of ASTM Standards, E813-81, American Society for Testing and Materials, Philadelphia, (Pa), USA.

ASTM. 1983. Standard Test Method for Plane-Strain Fracture Toughness of Metallic Materials. Annual Book of ASTM Standards, E399-83, American Society for Testing and Materials, Philadelphia, (Pa), USA.

British Standards Institution. 1977. Methods of Test for Plain Strain Fracture Toughness ($K_{IC}$) of Metallic Materials, BS 5447:1977. British Standards Institution, London.

Brown, M. W. and Miller, K. J. 1984. Mode I fatigue crack growth under biaxial stress at room and elevated temperature. In: Brown, M. W. and Miller K. J. (Eds.), Multiaxial Fatigue, ASTM, STP 853. American Society for Testing and Materials, Philadelphia, 135-152.

Cardew, G. E., Goldthorpe, M. R., Howard, I. C. and Kfouri, A. P. 1984. On the elastic T-term. In: Bilby, B. A., Miller, K. J. and Willis, J. R. (Eds), Fundamental of Deformation and Fracture, Cambridge University Press, Cambridge, 465-476.

Goldthorpe, M. R. 1986. An Elastic-Plastic Finite Element Program with Applications to Cracked Bodies. Ph.D. thesis, Department of Mechanical Engineering, University of Sheffield, Sheffield.

Hancock, J. W. and Cowling, M. J. 1980. Role of state of stress in crack-tip failure processes. Metal Science, 14, 293-304.

Howard, I. C. and Willoughby, A. A. 1981. Mechanics and mechanisms of ductile fracture, in Developments of Fracture Mechanics - 2, Ed. Chell, G. G., Applied Science Publishers, Barking, 39-99.

Kfouri, A. P. 1986. Some evaluations of the elastic T-term using Eshelby's method. Int. J. of Fracture, 30, 301-315.

Knott, J. F. 1980. Michomechanics of Fibrous Crack Extension in Engineering Alloys. Metal Science, 14, 327-336.

Kumar, V., German, M. D. and Shih, C. F. 1981. An Engineering Approach for Elastic-Plastic

Fracture Analysis. Topical Report No. EPRI NP-1931, Research Project 1237-1, General Electric Company, Schenectady (NY), USA.

Kumar, V., German, M. D., Wilkening, W. W., Andrews, W. R., deLorenzi, H. G. and Mowbray, D.F. 1984. Advances in Elastic-Plastic Fracture Analysis. Report No. EPRI NP-3607, Research Project 1237-1, General Electric Company, Schenectady (NY), USA.

Larsson, S. G. and Carlsson, A. J. 1973. Influence of non-singular stress terms and specimen geometry on small-scale yielding at crack tips in elastic-plastic materials. J. Mech. Phys. Solids, 21, 447-473.

Leevers, P. S. and Radon, J. C. 1982. Inherent stress biaxiality in various fracture specimen geometries. Int. J. Fracture, 19, 311-325.

McMeeking, R. M. 1977. Finite deformation analysis of crack-tip opening in elastic-plastic materials and implications for fracture. J. Mech. Phys. Solids, 25, 357-381.

McMeeking, R. M. and Parks, D. M. 1979. On criteria for J-dominance of crack-tip fields in large-scale yielding. In: Landes J. D. et al. (Eds). Elastic-Plastic Fracture, ASTM STP 668, American Society for Testing and Materials, Philadelphia (Pa), USA, 175-194.

Milne, I., Ainsworth, R. A., Dowling, A. R. and Stewart, A. T. 1986. Assessment of the Integrity of Structures Containing Defects. CEGB Report No. R/H/R6 - Rev. 3.

Neale, B. K., Curry, D. A., Green, G., Haigh, J. R. and Akhurst, K. N. 1985. A procedure for the determination of the fracture resistance of ductile steels. Int. J. Pres. Ves. and Piping, 20, 155-179.

Paris, P. C. 1972. Discussion following the paper by Begley and Landes. In: Fracture Toughness, ASTM STP 514, American Society for Testing and Materials, Philadelphia (Pa), USA, 1-23.

Priest, A. H. 1986. Size effects in fracture toughness testing, RAE, Farnborough, 10/11/86, Institution of Mechanical Engineers, London, pp 53-61.

Shih, C. F. 1985. J-dominance under plain strain fully plastic conditions: the edge crack panel subject to combined tension and bending. Int. J. Fracture, 29, 73-84.

Shih, C. F. and German, M. D. 1981. Requirements for a one parameter characterisation of crack tip fields by the HRR singularity. Int. J. Fracture, 17, 27-43.

Sinclair, A. H. and Chambers, A. E. 1987. Strength size effects and fracture mechanics; what does the physical evidence say. Engineering Fracture Mechanics, 26, 279-310.

Williams, M. L. 1957. On the stress distribution at the base of a stationary crack. J. Appl. Mech., 24, 109-114.

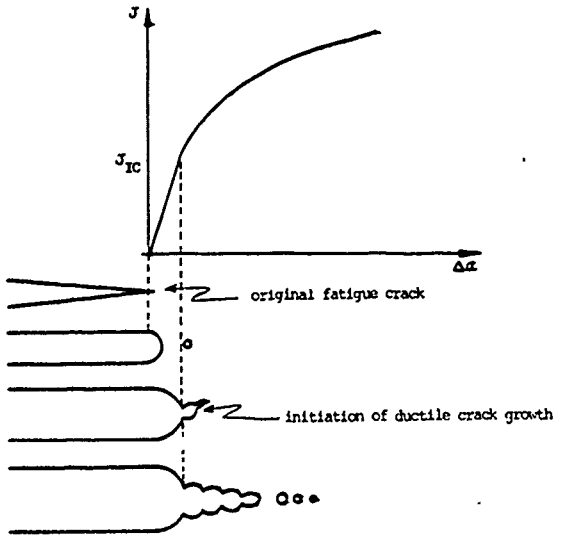


Figure 1. Schematic representation of a resistance curve with the microstructural changes that may give rise to it.

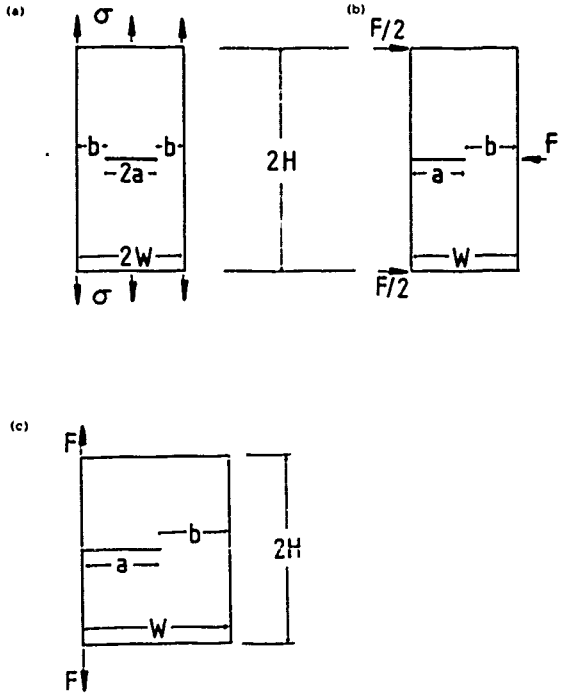


Figure 2. The specimen geometries that were analysed. (a) CCT, (b) SECB, (c) CT.

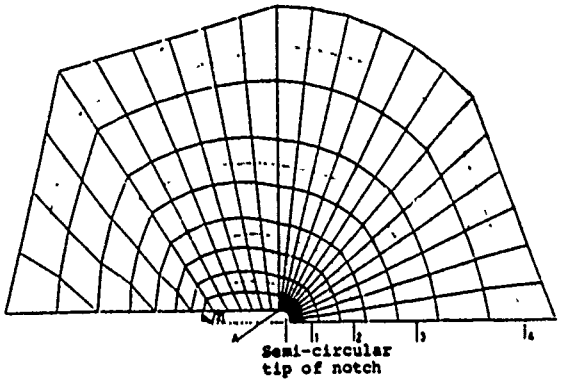


Figure 3. The finite element mesh surrounding the notch tip.

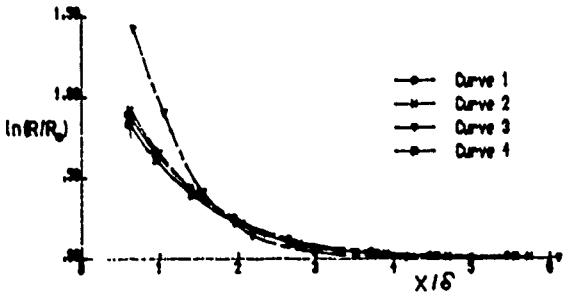


Figure 5. The relative size to which a void grows in the SECB specimen as a function of normalised distance ahead of the notch tip. All values are an applied J of about 8.8 in program units. Curve 1 - M = 446; Curve 2 - M = 114; Curve 3 - M = 45; Curve 4 - small scale yielding.

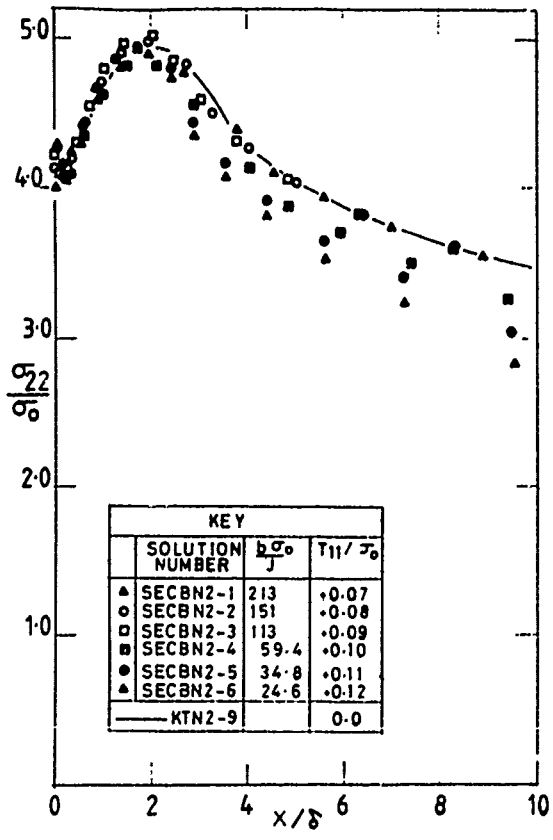


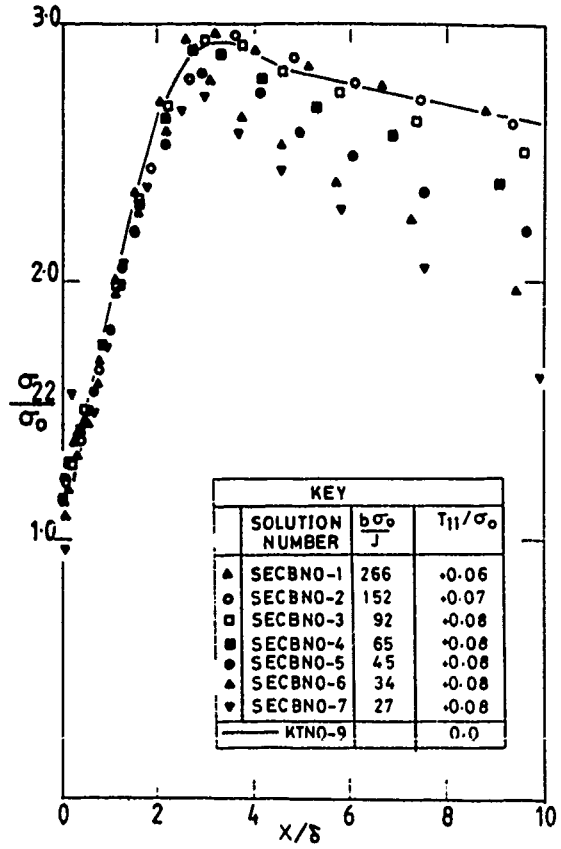


Figure 4. Variation of stress directly ahead of the notch tip for the SECB specimen with a/W = 0.5, H/W = 2. LEFT - n = 0.2. RIGHT - non-hardening.

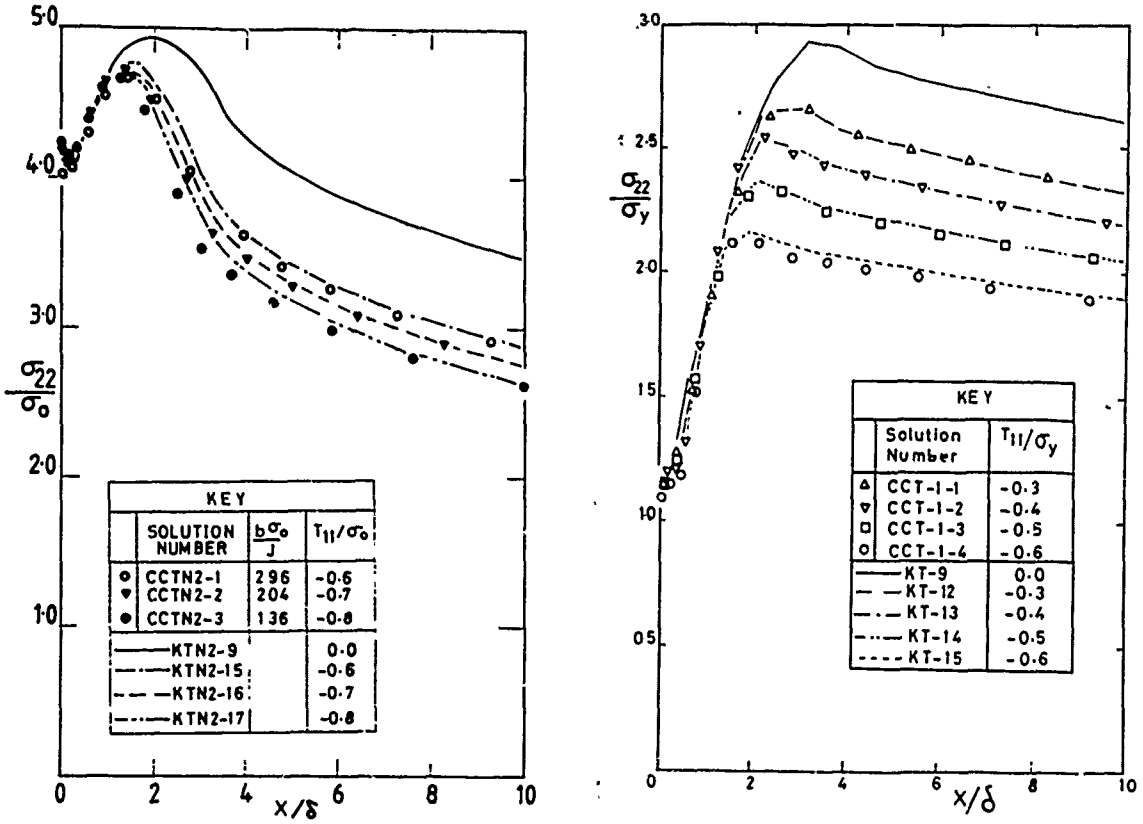


Figures 6. Variation of stress directly ahead of the notch tip for the CCT specimen with a/W = 0.5, H/W = 2. LEFT - n = 0.2. RIGHT - non-hardening.

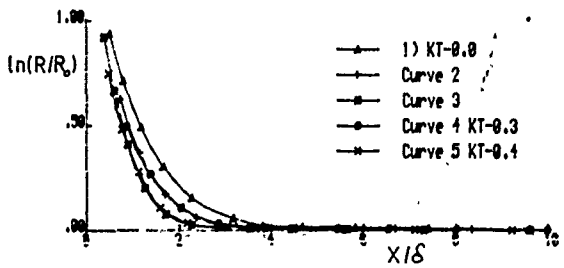


Figure 7. The relative size to which a void grows in the CCT specimen as a function of the notch tip. Curve 1 - small scale yielding; Curves 2 and 3 - specimen data, 2 with M = 1266 and T = -0.3, 3 with M = 698 and T = -0.4; Curves 4 and 5 - modified boundary layer data. 2 with T = -0.3, 3 with T = -0.4.

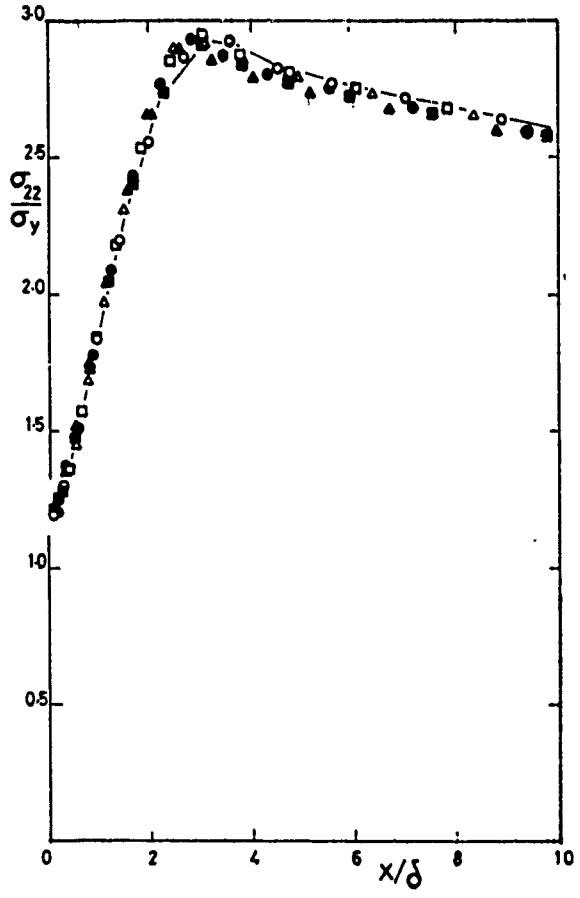


Figure 8. Variation of stress directly ahead of the notch tip for the CCT specimen biaxially loaded so that T = 0. a/W = 0.5, H/W = 1, non-hardening material.

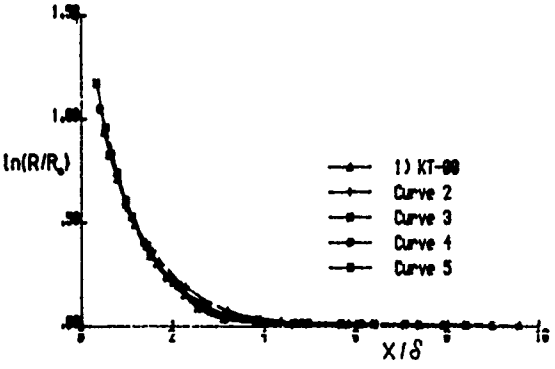


Figure 9. The relative size to which a void grows in the CCT specimen loaded as in Figure 8. Curve 1 - SSY; 2 - M = 556; 3 - M = 348; 4 - M = 237; 5 - M = 193.

# EFFICIENT REPRESENTATION OF FRACTURE MECHANICS KNOWLEDGE FOR DESIGN APPLICATION

Douglas L. Marriott

Professor Marriott is in the Design and Materials Division of the Mechanical Engineering Department at the University of Illinois at Urbana/Champaign, Illinois, USA.

SYNOPSIS

This paper examines the problem of why state-of-the-art fracture mechanics is not utilised more often in design. Sometimes the knowledge is too cumbersome to be integrated into the design process. Secondly, research findings on idealised and partial systems may be conceptually wrong in the context of a real component with a very complex geometry. This can be misleading to designers, and wastes resources. Examples are given to illustrate the type of information that is useful in design, and how it can be represented more conveniently for design application.

## INTRODUCTION

Any field of knowledge is incomplete. At best it is a collection of loosely related models. At worst these models can be unrelated, inconsistent or even contradictory.

Given this fragmentary state, the value of any particular model can only be judged on how well it serves its own limited purpose. This means in practice that there is generally no body of knowledge with universal applicability.

It is not widely recognised that the value of information depends very much on the use to which it is put. It is commonly assumed that any form of knowledge is somehow beneficial simply by virtue of its existence. The difficulty of transferring knowledge from one purpose to another is nowhere experienced more acutely than in trying to relate the knowledge of specialists and research workers to design decisionmaking.

This is not simply a matter of communication, or "technology transfer". Sometimes there is no relevant technology to transfer. The knowledge possessed by the specialist may not intersect in any way with the needs of the design engineer because their viewpoints are different.

Fracture is a very good example of the disparity between specialist knowledge and the information required to deal with problems as part of the design process.

This paper will try to illustrate this difference with the help of some examples taken from service experience. It will then offer some possibilities for restructuring existing models of fracture so that they can be applied more usefully.

## DIFFERENCES BETWEEN SPECIALIST- AND DESIGN-RELATED KNOWLEDGE IN FRACTURE

Case studies are a very valuable source of information on the causes of component failure, and several collections have been published in recent years [1,2,3].

Not surprisingly, much of the information in these reports is concerned with identifying the cause of failure. It is disappointing to find how little of this information is helpful to the designer in avoiding failure in the first place however.

For instance, service failure data has often been cited to verify the applicability of fracture mechanics to failure analysis[2], but this does not necessarily prove fracture mechanics to be a reliable tool in failure prevention.

For example, the Tippi Oy ammonia vessel failure in Finland[4] was caused by a heat treatment error which led to grossly different material properties from those assumed at the time of construction. Applying the most sophisticated fracture analysis methods available today, this vessel would have been rated safe, even given the 6mm defect found at the fracture initiation site. Although fracture mechanics was able to explain the failure, it was unable to predict it because data essential to the analysis could only be obtained from the failure itself.

Similar examples are contained in other case studies[1,2,3]. A recurring theme is that the data needed to perform a sensible failure analysis invariably comes to light only as a result of the failure itself, and would not be accessible to the designer before-the-fact short of 100% testing to destruction of everything - which is not a very productive way of operating.

A second example, which is typical of a large number of service failures, is the Triomf pressure vessel, which exploded in Potchefstroom, South Africa, in 1974, killing 18 people[5]. This failure showed no evidence whatever of a macroscopic defect at the fracture initiation site. Given that the material in question was severely degraded, with a brittle-ductile transition temperature well over 100°F, a minimum lower shelf fracture toughness of, say, 20 MPa.m$^{\frac{1}{2}}$, would require a defect size of approximately 1mm

to initiate fracture. No such defect was reported, even after microscopic examination.

This is not an isolated case. Out of about 80 examples of brittle failure in ASM and British Engine reports[1,3], less than half are reported to have an identifiable cracklike defect.

Strain age embrittlement and untempered martensite are typical metallurgical causes of failure which frequently show no indications of an initial defect. About 10% of the examples in the ASM Metals Handbook on Failure Analysis and Prevention are caused by untempered martensite alone[1], so the problem is not a negligible one.

High acuity notches, but blunt compared with cracks, are another problem. It should be remembered the probably the most frequent cause of brittle fracture experienced anywhere is the common-or-garden Charpy Vee Notch (CVN) test. Fracture mechanics can still not deal with this problem very comfortably.

Fracture mechanics has limitations when it comes to design. In some cases the data needed to do a fracture analysis are not available at the design stage for very fundamental reasons, and in others, fracture mechanics is simply not enough.

If fracture is to be designed out, rather than analysing it when it happens - which is too late - serious thought needs to be given to the type of information that will be appropriate to the job. The tools used by a fracture analyst cannot merely be transplanted into design and expected to work.

Detailed finite element based fracture analysis, for instance, which might work for one load case, is not economically feasible for comprehensive evaluation of the large number of critical elements found in a typical power plant, consisting as it does of literally hundreds of fracture calculations, involving combinations of location, crack orientation, time and different thermal transients.

There is a need for simple, rapid methods of screening to identify truly critical locations which may then be subjected to more detailed analysis if necessary. Some examples are given in the following section of simple formulations of fracture problems which have been found to work reasonably well in practical situations.

## KNOWLEDGE OF FRACTURE REQUIRED FOR FAILURE PREVENTION

Phenomena like temper embrittlement and strain aging are significant causes of fracture in service, so that they cannot be ignored simply because they are not fully understood.

Fortunately, the difference between the knowledge needed to understand a problem, and the knowledge needed to avoid it, can work in in our favor. As a general principle, avoiding a problem requires far less technical knowledge than solving it - although not necessarily less skill.

Models of even the most complex metallurgical embrittling mechanisms can be created with sufficient capability to identify the risk of failure, regardless of the current state of understanding of the mechanism. The reason this knowledge is not used more often is that it is seldom available at the right place at the right time, and the right people cannot get hold of it.

A particularly economical form for representing material failure mechanisms is the Material Failure Logic Model (MFLM)[6]. As an example, strain age embrittlement can be represented as follows

IF Material is Carbon steel
  and Grade is no Al killed
  and Cold work > about 4%
  and Time is given for incubation
    (e.g. 100's of hours at ambient or
    10's of hours at 100 to 200°C)
  and Service temperature is near ambient
THEN Brittle fracture by Strain age
  Embrittlement is a risk

Other examples are given in Ref.[6]. These models do not necessarily reflect full understanding of the underlying mechanics, although they can do. They are built with the specific purpose of containing the minimum information needed to identify the possibility that the mechanism in question exists in the component life cycle. Once this is known, and assuming it can be found out early enough, there are usually many ways the problem can be sidestepped.

For instance, most MFLM's require several events to occur in sequence. Fig.1 shows a graphical representation of an MFLM which can be used to search a manufacturing process for the elements of a failure mechanism. Any action which removes one of those elements is a valid preventive measure. Strain age embrittlement can be avoided for instance by

a) choosing a different material.
or b) Desensitising the material with a post-coldwork heat treatment.
or c) Devising a special test to check for strain aging (Note - no standard fracture control test will pick this problem up).

It is believed that the MFLM can go some way toward eliminating the problem of technology transfer by providing a succinct form for presenting metallurgical information that is focussed on failure mode identification.

## EFFICIENT FORMULATION OF FRACTURE MECHANICS SOLUTIONS

Generic computational techniques, using contour integration around crack tips or virtual crack extensions, are essentially post-design verification tools which do not fit easily into the design process.

Handbooks such as Rook and Cartwright[7] are useful, but only if some guidelines exist to establish similarities between the sample solutions provided and real problems, because there is seldom an exact match. Unfortunately, these rules of similarity have not been established in fracture mechanics to the same degree as they have in more traditional branches of mechanics.

What follows appears to be a rather random assortment of results for "quick-and-dirty" fracture mechanics computations. The underlying purpose however, is to make a start on establishing some of these important rules of similarity.

### Linear Elastic Fracture Mechanics

Probably 90% of all practical fracture problems involve an edge crack in a steep gradient stress field. A method ideally suited to this problem is the Weight Function[8]. This method calculates the stress intensity as the weighted average of the stress over the crack face, as calculated in the uncracked structure.

It is also potentially a very easy one to implement in design, because stress distributions can be obtained for the most complex geometries on a routine basis today, using finite element analysis (FEA). However, this fact is not as widely known among designers as it could be.

A very versatile weight function for an edge crack in a finite width plate has been developed by Bueckner[8] (see Fig.2). This is not particularly difficult to apply, if there is only one crack to consider.

From a design point of view however, even this simple formulation is too cumbersome at times.

A common question asked by design engineers is how fine a FEA mesh should be in order to get acceptable accuracy in fracture analysis, because FEA is notoriously unreliable in computing near-surface stresses. This information cannot be obtained by direct inspection from Bueckner's result.

A little bit of playing with the result for different geometries brings out some interesting insights. Simply drawing out the weight function is informative in itself. Fig.3 shows the weight functions appropriate to internal and edge cracks. By inspection, the major contribution to the stress intensity is provided by stresses in the immediate vicinity of the crack tip itself. Also, the weight function is almost constant over the outside half of an edge crack, which means that the exact shape of the stresses in this area is not important, as long as equilibrium is satisfied on average.

For many practical purposes a linear stress gradient, tangential to the stress curve at the crack tip (Fig.4a) gives sufficiently accurate results for most purposes. The approximation can be written as

$$K = 1.13(0.61S_T+0.39S_M)(\pi a)^{\frac{1}{2}}$$

An easier approximation to remember, which actually turns out to be more accurate when one includes the fact that most cracks are semi-elliptical anyway, is the Two-Third/One-Third Rule

$$K = 1.13(2/3S_T+1/3S_M)(\pi a)^{\frac{1}{2}}$$

If more sharply varying stress profiles are important, as in crack growth under thermal transients, Bueckner's solution can be integrated for a general power law stress variation giving the results shown in Fig.4b. For all but the first term representing constant stress, the stress intensity is not sensitive to the stress profile. In fact it is almost a unique function of the average stress on the crack face. This means that it is not necessary to be too precise about stress distributions as long as equilibrium is satisfied in the large.

By rights, the weight function is a function of the part geometry. If this were a significant factor the method would be no more use in design than other direct methods of stress intensity calculation. Fortunately, it seems that weight functions are not very geometry sensitive. Their practical value lies in the ability to use a few standard functions approximately for complex shapes.

A particularly common question, for instance, is whether the weight function for a crack in a flat surface can be used to estimate the stress intensity at the root of the notch. What is the effect of front wall curvature in other words?

The answer can be found by comparing two geometries, an edge crack, depth a, under uniform stress, $S_\infty$, and an infinitely deep crack, with a uniform stress, $S_\infty$, over a segment of crack, length a measured from the crack tip. The solutions to these two extreme cases are given in Fig.5. Clearly they bound all possible notch profiles, and it is reasonable to expect that the stress intensity for a crack at the root of a notch will lie between the two limiting cases. An average edge effect coefficient of 1.01 is never out by more than 11%. This is a robust result because it holds for any concave geometry.

In practice infinitely long cracks are a rarity. Semi-elliptical edge cracks are much more common. Everything one needs to know about semi-elliptical cracks can be summed up in just a few formulae.

Semi-ellipticals crack modify the results for long cracks in just two important respects.

i) The ellipticity factor, Q, is an important factor which cannot be ignored[9], i.e.

$$K(\text{ellipse}) = S_\infty(\pi a/Q)^{\frac{1}{2}}$$
where Q approx. $= 1+1.464(a/c)^{1.65}$

ii) Ellipticity in an edge crack significantly reduces the back wall effect. For instance, the stress intensity of a ½ wall crack, with an aspect ratio a/c = 0.1 is only about 7% greater than a similar crack in a semi-infinite solid (see Ref[7] for instance). This is a big crack! The sensible approach to anything bigger would be to get rid of it - not analyse it. In contrast, the increase for a long edge crack is 200%, showing how much influence ellipticity can have.

It can be concluded that, for all practical purposes, the stress intensity generated by a typical crack (i.e. semi-elliptical, ½ wall thickness max.) is reasonably independent of the complexities of component geometry, and that standard weight functions for infinitely large solids can be applied with reasonable accuracy to geometries of practical interest.

The solution for a semi-elliptical crack in a gradient stress field has been obtained empirically by Newman and Raju using FEA[9]. Their solution, like Bueckner's, is easy to apply once, but it is tedious to go through many times, and it is difficult to draw inferences from it, mainly because it is complicated by including back wall effects.

By realising that backwall effects are limited in practical interest, the Newman/Raju result can be simplified considerably (see Fig.6).

It can be seen immediately that edge effects are not as important in 3 dimensional cracks as in 2 dimensional ones. It seems to be a recurring theme in fracture mechanics that the nearer one gets to a "real" crack, the less important the concerns generated by studying idealised plane cracks.

Secondly, the "2/3-1/3" Rule for plane cracks applies even better to semi- elliptical cracks, and is almost exact for a semicircle.

Linear stress gradients are sufficient for most practical problems but there are occasions where local stresses may be highly peaked in the vicinity of a crack, and a more complex,

2-dimensional distribution may be of interest. This problem can be dealt with relatively easily using a classical influence function for a long crack, as shown in Fig.7[10].

The simplicity of this function suggests that it could be very useful if it can be shown to be a reasonable approximation for crack profiles other than the infinitely long edge crack.

A moderately severe test is to apply it to a semi-circular crack (see Fig.7) under a constant stress. The result overestimates the classical solution by somewhere between 4 and 9%. It is expected that any intermediate crack shape will be approximated even more accurately.

This result has great practical significance. Combined with the finding that component geometry is not very critical, it means that the stress intensity for virtually any part-thickness crack, in any geometry, under any stress distribution, can be calculated with reasonable accuracy, say within 15%, using one simple influence function. This covers many of the cracks encountered in practice and the large majority of fatigue cracks.

## Post Yield Fracture Mechanics

LEFM is commonly assumed to be limited to nominal stresses less than about ½ yield. This is a serious limitation because component stresses are usually at least that magnitude. It is not surprising therefore that non-experts frequently question the utility of LEFM. Inelastic fracture parameters can also be estimated with reasonable accuracy.

### Estimation of J

Detailed nonlinear analysis involving J-integrals, or virtual crack extensions, are not serious alternatives for design work. Nor is the "engineering approach" developed by Kumar etal[11]. It is expressed awkwardly, confined to elementary shapes, and offers no guidance on how a designer might cope with a really complex shape, short of repeating the detailed analysis itself - which rather destroys the whole point of the exercise.

Bhandari and his coworkers offer an alternative approach[12] which incidently provides greater insight into the form of J, the nonlinear energy release rate. From detailed inelastic analysis of a variety of geometries, they found that J can be calculated quite accurately from the inelastic stress and strain distributions in the uncracked component, using elastic weight functions (see Fig.8).

For constant stress, $S_o$, Bhandari's approach reduces to the following expression for J.

$$J = 1.12^n S_o e \pi a$$

where $S_o$ = Stress in uncracked component
e = inelastic strain in uncracked component

This reduces to the familiar relationship

$$J = K^2/E$$

in the special case of linear elasticity.

By including the Irwin small scale correction, as representing the localised region of intense inhomogeneous plasticity around the crack tip, and an adjustment for Osgood-Ramberg hardening, a relationship can be found which is in close agreement with experimental data collected by EPRI, and the empirical EPRI design J curve as well[13] (see Fig.9).

This equation is a useful formulation for design purposes. It is compact, easy to remember and use, and conceptually it is a very natural extension of ideas already established in LEFM.

It appears, contrary to research findings using idealised test specimens, that inhomogeneous crack tip plasticity does not propagate indefinitely in complex components, but is constrained, by a number of mechanisms, to a zone about $\pi a$ in radius around the crack. These effects include 3-D effect, strain hardening and strain gradient fields. This fact was first observed several years ago, and incorporated in the Welding Institute COD Design Curve[14].

As long as real cracks can be considered constrained for practical purposes, post yield fracture mechanics is not nearly the problem it appears at first sight. As can be seen from Fig.9, J is approximated very well by LEFM up to strains of about twice the elastic limit, considerably more than the ½ yield suggested by rigorous treatments of the subject. Furthermore the approximation is an upper bound, which is always safe from the design point-of-view.

### Tearing Modulus

Paris's Tearing Modulus, T, as defined in Fig.10, is an important contribution to the understanding of unstable fracture in engineering materials[15]. Unfortunately it is a concept which has had no easy physical interpretation, up till now, and is therefore difficult to present to engineers who are not fracture experts.

The simplified formulation of T presented in the previous section can be used to show that materials experiencing stable tearing display two distinct types of behavior, depending on the crack size.

For cracks larger than some threshhold value, $a_o$, initiation can occur easily, but unstable propagation is prevented by the high slope of the J-resistence curve.

$$a_o = J_{ic}/(dJ_R/da)$$

For cracks less than this threshhold, fast fracture can occur, but only after reaching a critical strain, $e_{crit}$. This critical strain in terms of the yield strain, ey, is simply

$$e_{crit}/ey = T/k\pi$$

where geometry factor, k = ~1 to 2

Knowing T for a material, it is intuitively obvious how sensitive that material is to local strain, and this knowledge can be used to guide material selection, and to define how much care needs to be expended to avoid notches.

## CONCLUSIONS

1) Complex fracture mechanics techniques developed in idealised surroundings do not necessarily work in the field. Often the complex geometry is easier to deal with.
2) A flexible method of representing failure mechanisms, the MFLM, is presented. This method has possible applications in design for identifying failure mechanisms which cannot be predicted by fracture mechanics.
3) It is shown that Bueckner's Weight Function Method can be used as a practical tool for calculating fracture parameters in complex components. The reason is that Weight

Functions are not strongly geometry dependent, so that a few standard Weight Functions can be used for a wide range of geometries.

4) By exploring stress intensites caused by complex stress distributions, it is shown that the precise distribution on a crack profile is not important, as long as equilibrium is satisfied on average. This fact provides confidence in the results of fracture analyses using approximate stress distributions.

REFERENCES


1] ASM Metals Handbook, 9th ed, Vol.11., ASM International, Metals Park.

2] ASTM STP 918, "Case Histories Involving Fatigue and Fracture Mechanics", eds. C.M.Hudson and T.P.Rich, 1986.

3] British Engine Technical Reports, British Engine Insurance Co, published in compiled form by ASM International, Metals Park, Ohio.

4] T.Moisio, "Brittle Fracture in Failed Ammonia Plant",Metal Constr. and Br.Weld.J., Jan.1972.

5] R.J.Campbell,"Avoiding Fracture in Pressure Vessels", Proc. 1st South African Nat. Conf. on Fracture, Univ. of Witwatersrand, Johannesburg, November 1979, pp. 265-276.

6] D.L.Marriott and N.R.Miller, "Material Failure Logic Models - ...", Trans ASME, Vol.104, July 1982, pp. 626-634.

7] D.P.Rook and D.J.Cartwright, "Compendium of Stress Intensity Factors", HMSO, 1976.

8] H.F.Bueckner, "A Novel Principle for the Computation of Stress Intensity Factors", ZAMM, Vol.50, No.9, 1970, pp. 529-546.

9] J.C.Newman,Jr. and I.S.Raju, "An Empirical Stress Intensity Factor ...",Eng.Fract.Mech., Vol.15, 1981, pp. 185-192.

10] R.C.Labbens, J.Heliot and A.Pellisier-Tanon, "Weight Functions for 3-D Symmetrical Cracks", ASTM STP 601, 1976, pp. 448-470.

11] V.Kumar, M.D.German and C.F.Shih,"An Engineering Approach for Elastic Plastic Fracture Analysis",EPRI Palo Alto, Calif., Report No NP 1931, 1981.

12] S.Bhandari and S.Charif D'Ouazzane, "Establishment of Governing Parameters for Fatigue Crack Growth in Areas of High Nominal Strain",ASME Paper No 84-PVP-20, Presented at 1984 ASME PVP Conf., San Antonio, Texas, June 1984.

13] K.F.Shih, M.D.German and K.Kumar, "An Engineering Approach for Examining Crack Growth and Stability in Flawed Structures", Int.J.Pres.Ves. and Piping, 1981, pp. 159-196.

14] F.M.Burdekin and M.G.Dawes, "Practical Use of Linear Elastic and Yielding Fracture Mechanics ..", Conf. on Appl. of Fract.Mech., I.Mech.E, May 1971.WI

15] P.C.Paris et al, "Initial Experimental Investigation of Tearing Instability Theory",ASTM STP 668, 1979, pp. 5-36.


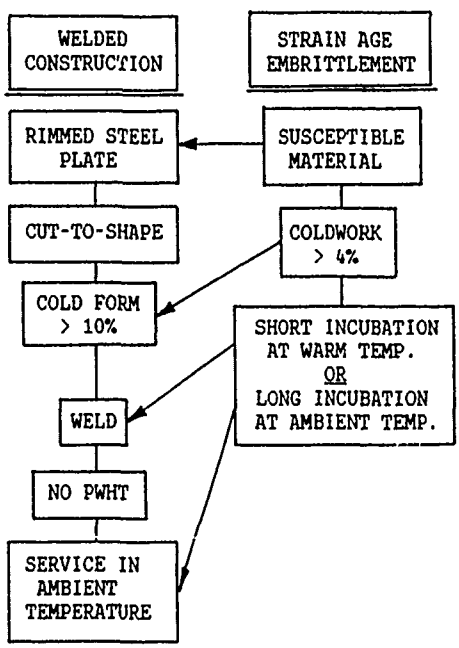


Fig.1 MATERIAL FAILURE LOGIC MODEL MATCHED WITH STEPS IN MANUFACTURING PROCESS

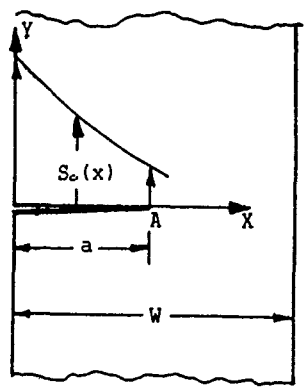


$$K = 2\int_0^a S_o(x).m(x,a)dx$$

$$m(x,a) = \frac{[1+A(a-x)/a+B((a-x)/a)^e]}{[2\pi(a-x)]^4}$$

$$A = 0.6147+17.18(a/W)^e+ 8.78(a/W)^e$$
$$B = 0.2502+ 3.29(a/W)^e+70.04(a/W)^e$$

Fig.2 BUECKNER'S WEIGHT FUNCTION FOR A LONG EDGE CRACK IN A FINITE WIDTH PLATE

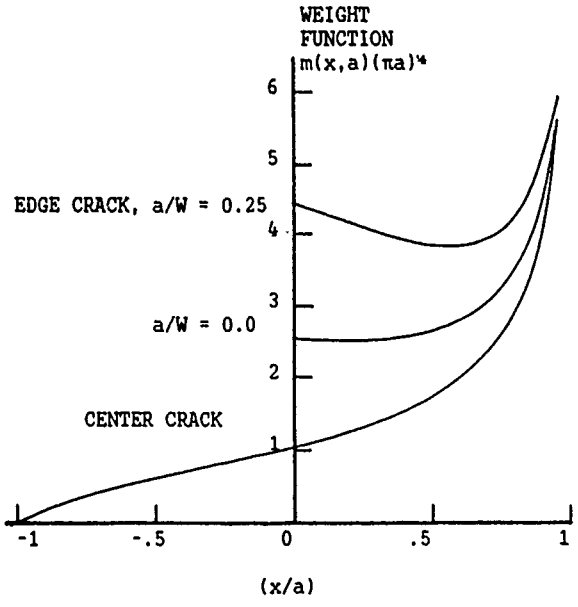


Fig.3 WEIGHT FUNCTIONS FOR CENTER AND EDGE CRACKS - BOTH CRACK FACES LOADED

A) LINEAR STRESS GRADIENT

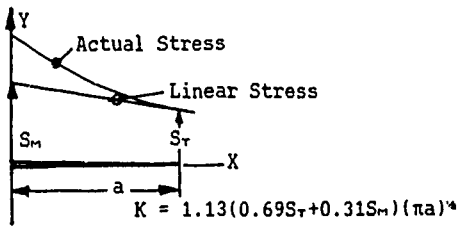


B) GENERALISED STRESS GRADIENT

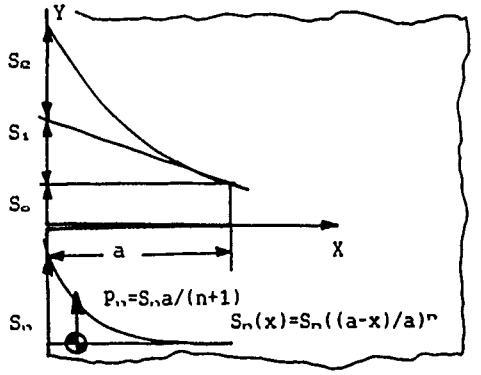


$k_n = K/(\pi a)^{1/2}$
$= 1.414 S_n \{2/(2n+1)+1.23/(2n+3)+0.50/(2n+5)\}$

| n | kn/Sn | kn/Pn |
|---|---|---|
| 0 | 1.129 | 1.129 |
| 1 | 0.443 | 0.885 |
| 2 | 0.284 | 0.852 |
| 3 | 0.211 | 0.842 |
| 100 | - | 0.839 |

Fig.4 STRESS INTENSITIES FOR TYPICAL STRESS PROFILES FOR AN EDGE CRACK

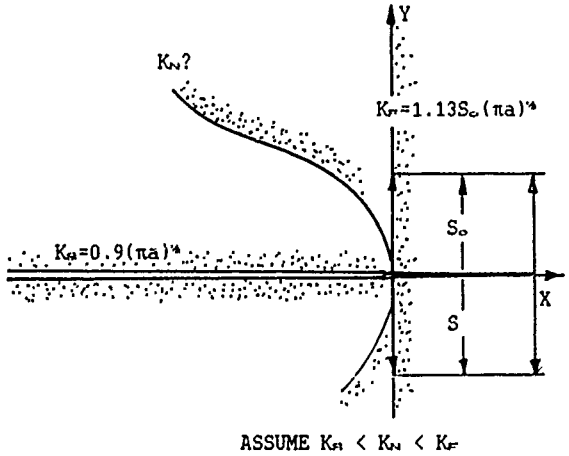


Fig.5 BOUNDING STRESS INTENSITIES FOR A CRACK AT THE ROOT OF A NOTCH

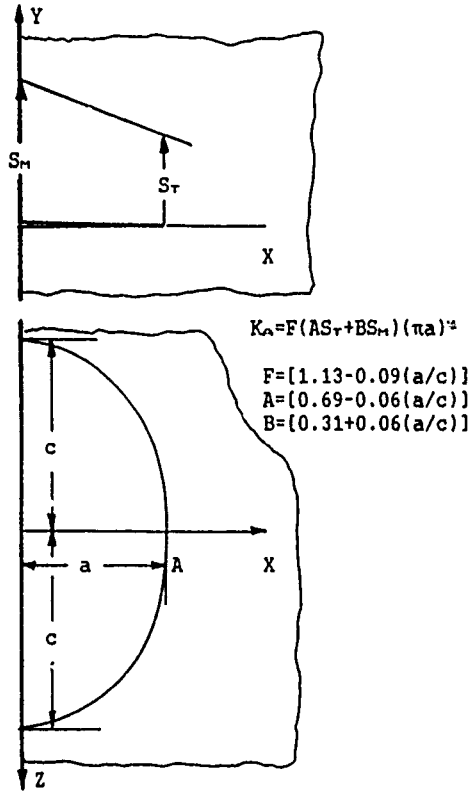


Fig.6 APPROXIMATE STRESS INTENSITY FOR AN ELLIPTICAL EDGE CRACK IN A LINEAR STRESS GRADIENT

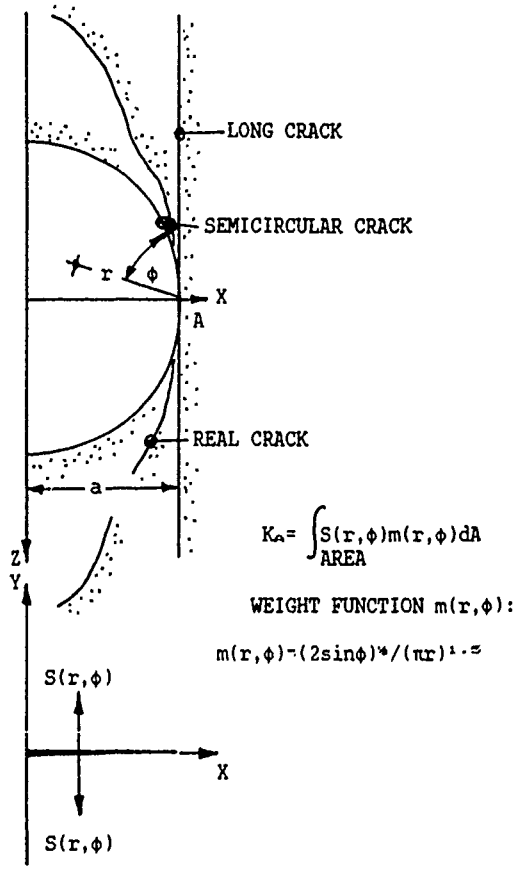


Fig.7 APPLICATION OF WEIGHT FUNCTION FOR A LONG CRACK TO ARBITRARY 3-D GEOMETRY

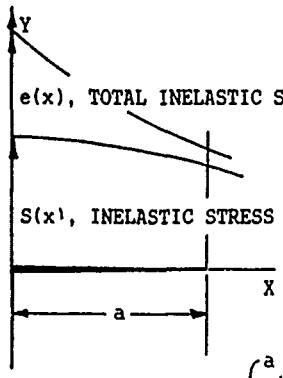


$$e_{eff} = \int_0^a e(x)m(x,a)dx$$

$$S_{eff} = \int_0^a S(x)m(x,a)dx$$

$$J = 1.25 S_{eff} e_{eff} \pi a$$

ALTERNATIVELY, IN TERMS OF $K_{IC}$:

$$K_{eff} = 1.12(S_{eff} e_{eff} \pi a)^{1/2}$$

Fig.8 BHANDARI'S APPROXIMATION FOR COMPUTATION OF INELASTIC FRACTURE PARAMETERS

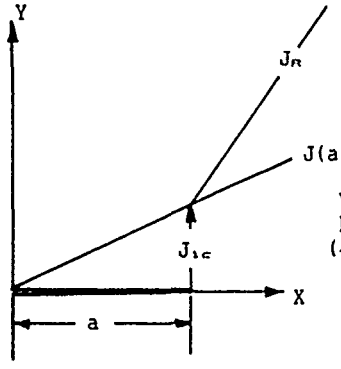


TEARING MODULUS, T: $E(dJ_R/da)/Y^2$

THRESHHOLD SIZE, $a_o$: $J_{Ic}/(dJ_R/da)$

WHEN $a = a_o$, $J(a) = J_{Ic}$
$dJ(a)/da = dJ_R/da$

FOR $a < a_o$, $e_{crit}/ey = T/k\pi$

Fig.10 SUMMARY OF TEARING MODULUS AND CRITICAL STRAIN FOR UNSTABLE FRACTURE

SCATTER IN EXPERIMENTAL DATA -

LEFM PREDICTION - - - -

EPRI EnJ CURVE ———

J DERIVED FROM BHANDARI ———

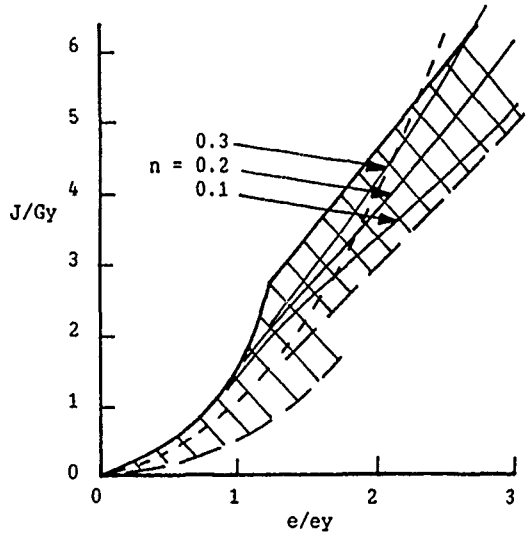


Gy = $Sy^2\pi a/E$
Sy = 0.2% Proof Stress
ey = 0.2% Plastic Strain
n = Strain Hardening Index

$$J_{eff} = 1.46 Sy.e.\pi a.F(e/ey)$$

where $F(e/ey) = (2(e/ey)-1)^n$

Alternative Form: $K_{eff} = (EJ_{eff})^{1/2}$

Fig.9 COMPARISON OF APPROXIMATE J WITH EXPERIMENTAL DATA FROM [13]

# CREEP OF METAL MATRIX COMPOSITES

M. McLean

Division of Materials Applications
National Physical Laboratory
Teddington, Middx. TW11 0LW

## SYNOPSIS

Possible mechanisms of time dependent deformation in metal matrix composites are considered and models relating to elastic fibres entrained in a metal matrix deforming by power law creep are developed. The theory which takes into account the end effects associated with short fibres and the development of different types of damage that eventually leads to fracture can account for the major features of creep data for metal matrix composites. The need for diagnostic tests to discriminate between different models is discussed.

## INTRODUCTION

One of the major attractions of metal-matrix composites is the potential increase in temperature capability for structural applications, compared with the metallic matrix, that can be achieved by sharing the load with a stronger reinforcing phase that is usually non-metallic[1]. Many current engineering alloys depend on the presence of dispersed phases to impart high temperature strength; these additions can be considered to modify rather than radically alter the creep characteristics of the host metal[2]. However, in the case of metal-matrix composites, particularly those reinforced with relatively high volume fractions of aligned fibres where the load is directly shared by the constituent phases, the creep behaviour must take into account both the coupled deformation of the matrix and reinforcement and the degradation of the reinforcing phase. This can lead to quite different types of creep behaviour than is usually observed for metals that can render established measures of creep performance and extrapolation techniques quite inappropriate[3].

Many measures of mechanical performance of composites, including their creep behaviour, are sensitive to the detailed form and distribution of the reinforcing phase. Consequently, identification of the operative deformation mechanisms and the critical defects that reduce the creep resistance are essential to developing an appropriate physical model for creep. This paper extends a previous treatment[3,4] of the time dependent deformation of composites consisting of elastically extending fibres entrained in a creeping matrix that has the following additional features:

a) A variety of different types of physical damage that lead to fracture and their effects on the forms of the creep curves are considered, and

b) The models are framed in terms of physically significant internal state variable, consistent with the formalism of continium damage mechanics[5], that can be solved for arbitrary initial boundary conditions to account for, for example, residual internal stresses produced during processing.

The approach used in this paper will be to progressively increase the complexity of the composite microstructure being modelled and, where possible, to compare the predictions of the models with appropriate experimental data. The aim is to produce a realistic physical interpretation that can be evaluated numerically rather than to strive for full analytical descriptions. Having established the equations required to describe creep deformation in composites, expressed in terms of a wide range of physical parameters, a simpler set of constitutive laws can be defined. This approach has been described as "physically inspired empiricism" by Ashby[6] and has been used to describe creep deformation in more conventional engineering alloys by Ashby and Dyson[7] and in a joint NPL/University of Cambridge research programme[8,9].

## CONTINUOUS STABLE FIBRES

Consider a composite consisting of aligned fibres of infinite length and having a volume fraction $\varphi$ embeded in a metallic matrix. The fibres are assumed to be non-creeping, by virtue of the low homologous temperature, but to be subject to elastic deformation and the metal, in isolation, exhibits a steady-state creep rate $\dot{\epsilon}_m$ that is described by the usual power-law expression,

$$\dot{\epsilon}_m = \dot{\epsilon}_{mo} \left[ \frac{\sigma}{\sigma_{mo}} \right]^n \qquad (1)$$

where $\dot{\epsilon}_{mo}, \sigma_{mo}$ are reference constants, n is the stress exponent and $\sigma$ is the applied stress. When a tensile stress $\sigma$ is applied parallel to the fibres, then mechanical equilibrium is satisfied by the following rate equations.

$$\left.\begin{aligned} \dot{\epsilon}_f &= \frac{1}{E_f}\dot{\sigma}_f && \text{(a)}\\ \dot{\epsilon}_m &= \frac{1}{E_m}\dot{\sigma}_m + \dot{\epsilon}_{mo}\left[\frac{\sigma_m}{\sigma_{mo}}\right]^n && \text{(b)}\\ \dot{\epsilon}_f &= \dot{\epsilon}_m = \dot{\epsilon} && \text{(c)} \end{aligned}\right\} \quad (2)$$

where the subscripts f,m refer to fibre and matrix respectively and E is Youngs modulus. Material continuity requires that the fibre and matrix deform at the same rate which is achieved by redistribution of stresses which satisfy the rule of mixtures

$$\sigma = \sigma_f\varphi + \sigma_m(1-\varphi) \quad (3)$$

where $\varphi$ is the volume fraction of fibres.
Manipulation of Equations 2 and 3 gives coupled differential equations

$$\left.\begin{aligned} \dot{\epsilon} &= \alpha_1\dot{\epsilon}_m\left[1 - \frac{\varphi\sigma_f}{\sigma}\right] && \text{(a)}\\ \dot{\sigma}_f &= E_f\dot{\epsilon} && \text{(b)} \end{aligned}\right\} \quad (4)$$

where $\alpha_1 = (1-\varphi)^{-n}.(1-\varphi)E_m/((1-\varphi)E_m+\varphi E_f)$.

Equations 4 can be integrated subject to appropriate boundary conditions to give an analytical expression for $\epsilon(t)$; however for consistency with later developments this will be solved numerically in the following simplified form

$$\boxed{\begin{aligned} \dot{\epsilon} &= \alpha_1\dot{\epsilon}_m(1-S_1)^n\\ \dot{S}_1 &= H\dot{\epsilon} \end{aligned}} \quad (5)$$

where $S_1 = \varphi\sigma_f/\sigma$ may be regarded as a dimensionless internal stress that modifies the matrix creep behaviour and $H=\varphi E_f/\sigma$ is a strain hardening coefficient.

Equations 5 have been solved using values of the physical parameters appropriate to an aluminium matrix and 15% volume silicon carbide fibres. Examples of creep curves calculated for $\sigma$=150 MPa and T=473 K assuming initial internal stresses of $S_1$=0, 0.1 and - 0.1 are shown in Figure 1. These have the same forms as the analytical expressions described previously[3] (as they should). There is no steady state, but a progressively decreasing creep rate that asymptotically approaches a zero creep rate when the fibres fully support the applied stress (ie. S=1 or $\sigma_f = \sigma/\varphi$). The strain at which this is achieved is sensitive to the initial value of S(0).

Since there is no steady state creep rate, the power law expression is not appropriate to representing the stress and temperature dependence of creep rate. However, it is instructive to compare the creep rates at a specified strain as a function of stress. Figure 2 plots the calculated creep rates at 0.1, 0.2 and 0.3% strains as functions of stress on logarithmic scales; the distinct curve shows that a variable stress exponent would be required to fit these data to a power law creep law even when the matrix creep behaviour is characterised by a constant n emphasising the inappropriateness of conventional measures of creep performance.

## SHORT STABLE FIBRES

Kelly and Street[10] have considered the rheology of steady state matrix flow around short fibres. Considering an idealised element of the composite microstructure consisting of a typical fibre, of length $\ell$ and diameter d, with associated surrounding matrix (Figure 3), the shear strain rates can be defined in terms of the local axial velocities of the matrix. On a plane normal to and at a distance z from the centre of the fibre the shear strain rate $\dot{\gamma}_z$ can be expressed as follows.

$$\dot{\gamma}_z = \frac{1}{h}\left[\dot{u}_m - \dot{u}_f - \dot{u}_s\right] \quad (6)$$

where $h = \frac{1}{2}d\left[(0.95\,\varphi)^{-\frac{1}{2}} - 1\right]$

$= \frac{1}{2}$x (interfibre spacing) (7)

$\dot{u}_m$ is the matrix velocity at a distance h from the fibre, $\dot{u}_f$ is the fibre velocity and $\dot{u}_s$ is the sliding velocity between matrix and fibre. Equation 1 can be expressed in terms of shear stresses $\tau$ and strains $\gamma$.

$$\dot{\gamma} = \gamma_{mo}\left[\frac{\tau}{\tau_{mo}}\right]^n \quad (8)$$

where $\dot{\gamma}_{mo} = \frac{3}{2}\dot{\epsilon}_{mo}$ and $\tau_{mo} = \sigma_{mo}/2$.

Combining Equations 6, 7 and 8 leads to an expression for $\tau(z)$ which for the case of a perfect fibre/matrix bond and totally rigid fibres gives the following relationship

$$\tau(z) = \beta'\sigma_{mo}\left[\frac{\dot{\epsilon}}{\dot{\epsilon}_{mo}}\right]^{1/n}\left[\frac{z}{d}\right]^{1/n} \quad (9)$$

where $\beta' = \frac{1}{2}\left[\frac{4}{3}\right]^{1/n}\left[(0.95\,\varphi)^{-\frac{1}{2}} - 1\right]^{1/n}$

This shear stress transmits a tensile stress to the fibre $\sigma_f$ that increases from 0 at the fibre ends to a maximum value at the centre of the fibres as shown schematically in Figure 3.

$$\sigma_f = \int_{\ell/2}^{z}\frac{\pi d\tau dz}{\pi\left[\frac{d}{2}\right]^2} = 4\beta'\sigma_m\left[\frac{n}{n+1}\right]\left[\left[\frac{\ell}{2d}\right]^{\frac{n+1}{n}} - \left[\frac{z}{d}\right]^{\frac{n+1}{n}}\right] \quad (10)$$

The average stress in the fibres due to the flowing matrix may be written as follows

$$\bar{\sigma}_f = \frac{2}{\ell}\int_0^{\ell/2} \sigma_f dz$$

$$= 4\beta' \sigma_m \left[\frac{n}{2n+1}\right]\left[\frac{\ell}{2d}\right]^{\frac{n+1}{n}} \qquad (11)$$

Combining Equation 11 with the rule of mixtures, the average stress on the matrix can be expressed in terms of the applied stress and $\bar{\sigma}_f$ and this leads to the following expression for creep rate.

$$\dot{\epsilon} = \alpha_2 \dot{\epsilon}_m (1-S_2)^n \qquad (12)$$

$$\text{where } S_2 = \frac{\varphi \bar{\sigma}_f}{\sigma} = \left[1 + \alpha_3 \left[\frac{\ell}{2d}\right]^{\frac{n+1}{n}}\right]^{-1} \qquad (13)$$

$$\alpha_2 = (1-\varphi)^{-n} \qquad (14)$$

$$\alpha_3 = \left[\frac{1-\varphi}{\varphi}\right] / 4\beta' \left[\frac{n}{2n+1}\right] \qquad (15)$$

When the fibre deforms, either by creep or elastically as is being considered here, the strain rates and internal stresses are reduced relative to the rigid fibre case. For elastically deforming fibres where the asymptotic strain rate is 0, Equation 12 continues to describe a steady state creep rate as $t\to\infty$; however, during the early stages of deformation the fibre strain rate must be taken into account. The following approximate treatment will overestimate the strains in the early stage of creep, but will approach the real situation at longer times.

The tensile stress distribution along the fibres can be approximated to a central zone, $\ell' = \ell - 2\delta$, which carries the full stress that would be associated with a continuously reinforced composite of reduced volume fraction $\varphi' < \varphi$ and two stress free ends of length $\delta$, as indicated in Figure 3, which can be defined to give the same average fibre stress as given by Equation 11.

$$\text{ie} \quad \bar{\sigma}_f \ell = \sigma_{cont} \ell' \qquad (16)$$

$$\text{where } \sigma_{cont} = \sigma_f(0) = 4\beta' \sigma_m \left[\frac{n}{n+1}\right]\left[\frac{\ell}{2d}\right]^{\frac{n+1}{n}} \qquad (17)$$

Manipulation of Equations 11 – 17 leads to the following relationships:

$$\left.\begin{aligned} \delta &= \tfrac{1}{2}\left[\frac{n}{2n+1}\right]\ell \qquad (18)\\ \varphi' &= \left[\frac{n+1}{2n+1}\right]\varphi \qquad (19)\\ \ell' &= \frac{n+1}{2n+1}\ell \qquad (20) \end{aligned}\right\}$$

We can now consider the central zone of the fibres to behave in exactly the same manner as in the continuous composites described in Section 2. The problem, however, is to determine how the deformations of the sub-elements combine to account for the creep of the composite microstructure and this depends on the detailed distribution of fibres. Figure 4 shows schematically two quite different combinations of the central and end zones and their influence on the matrix creep behaviour.

a) In Figure 4a the fibres are distributed so that the two contributions to creep can be considered to act in series with no interaction. Consequently each element carries the full applied stress and the Reuss averaging procedure is used. The creep behaviour can be described by a combination of Equations 5 and 12 suitably modified with the reduced volume fractions given by Equation 19.

$$\boxed{\begin{aligned} \dot{\epsilon} &= \alpha_1 \dot{\epsilon}_m (1-S_1)^n + \alpha_2 \dot{\epsilon}_m (1-S_2)^n \quad (a)\\ \dot{S}_1 &= H\alpha_1 \dot{\epsilon}_m (1-S_1)^n \quad (b) \end{aligned}} \qquad (21)$$

b) Figure 4b considers the situation where strain compatibility between the matrix and the entire fibre zone is required (ie. Voigt averaging). The creep rate of the elastic fibre plus end zones can be written

$$\dot{\epsilon} = \frac{\varphi'}{E_f}\dot{\sigma}_f + \alpha_2 \dot{\epsilon}_m \left[1 - \varphi \frac{\bar{\sigma}_f}{\sigma}\right]^n$$

or

$$\dot{\sigma}_f = \frac{E_f}{\varphi'}\dot{\epsilon} - \alpha_2 \frac{E_f}{\varphi'}\dot{\epsilon}_m \left[1 - \varphi \frac{\bar{\sigma}_f}{\sigma}\right]^n \qquad (22)$$

Combining Equations 4a and 22 leads to the alternative constitutive laws:

$$\boxed{\begin{aligned} \dot{\epsilon} &= \alpha_1 \dot{\epsilon}_m (1-S_1)^n \quad (a)\\ \dot{S}_1 &= H\dot{\epsilon} - R\dot{\epsilon}_m (1-s_2)^n \quad (b) \end{aligned}} \qquad (23)$$

where $R = \alpha_2 H$.

It is noteworthy that Equations 23 have the general form of a recovery controlled creep where the

hardening mechanism (here, elastic extension of the fibres) is balanced by a recovery process (flow around fibre ends) until a steady state is achieved when $S_1 = 0$. This leads to exactly the same steady state creep rate $\dot{\epsilon}_{ss}$ as is predicted by Equations 20.

$$\dot{\epsilon}_{ss} = \alpha_2 \dot{\epsilon}_m (1-S_2)^n \qquad (24)$$

Using values of parameters appropriate to an Al-SiC composite with 20% reinforcement, creep curves have been computed using both sets of constitutive equations representing the Reuss and Voigt formalisms. They give remarkably similar predictions of the creep curves (Figure 5a), but the stresses carried by the fibres are quite different in the two cases. The Reuss averageing approach is accompanied by a progressive increase in fibre stress such that $S_1 \to 1$ as $t \to \infty$; the Voigt equations however leads to a steady state value of $S_1$ (0.63 in this example) that decreases with decreasing fibre aspect ratio (Figure 5b). this is an important difference that has implications for the failure mechanisms and the anelastic behaviour that will be discussed more fully below.

Calculations have been carried out using both sets of equations and assuming different fibre aspect ratios and stress sensitivities for matrix creep. Typical results are shown in Figure 6. These clearly show that the creep performance of the composites deteriorates with decreasing fibre aspect ratio as, of course, they do. However, the sensitivity of creep behaviour to fibre aspect ratio depends on the matrix stress exponent n. Thus short fibres are predicted to be more effective in matrices characterised by a high n. This confirms the results of an earlier more approximate treatment(3).

## SHORT FIBRES WITH DAMAGE GENERATION

The model described above deals with the deformation of a composite material with a stable microstructure and predicts a decreasing creep rate with increasing strain that approaches 0 for continuous-fibre, and a finite steady state creep rate for short-fibre reinforced composites respectively. Final fracture depends on the initiation and growth of damage that can be defined as a degradation in the reinforcing microstructure, and this can influence the extent of deformation in the later stages of life. There can be many causes of microstructural changes in composites; for example, morphological changes due to spheroidisation(11) or fibre/matrix chemical interactions may be important in certain systems(12). However, the following discussion will assume chemical and thermodynamic stability, and will be restricted to mechanical instabilities due to fibre fragmentation.

We assume here that the initiating event of "fracture damage" is the fracture of an individual fibre. The nature of the development of damage following such a nucleation event is important in determining its interaction with the deformation processes and its effect on the shape of the creep curve. Figure 7 shows schematically three types of damage accumulation that may occur in composite materials and which will be discussed separately below.

a) Crack growth If the fibre diameter exceeds the critical crack length for propagation in the matrix for the applied stress, then fracture is rapid and damage is highly localised. Consequently, there is little effect on the shapes but an important effect on the extent of the creep curves. However, the nucleation event, viz. the fracture of the first fibre, is determined by the enhanced stress acting on the fibres $\sigma_f$ which is an elastic stress that scales with the elastic strain of the fibre. For continuous composites this is identical to the total axial strain - ie. elastic strain on loading plus time dependent strain. Thus, the creep strain to failure would be expected to decrease with increasing stress. The situation is more complex for short-fibre composites where the elastic stress in the fibres depends on the appropriate averaging procedure (Reuss or Voigt) and flow around fibre ends increases the total creep strain before fracture. Calculations with both Equations 21 and 23 indicate that for short fibres the creep strain before the fibre stress exceed a critical value increases with increasing applied stress.

b) Decreasing fibre aspect ratio If the matrix cavity associated with a fibre-break is unstable and is filled by plastic flow of the matrix, then the model developed in section 3 may be extended to consider the effect of a decreasing fibre aspect ratio ($\lambda = \ell/d$). We assume that the probability of a fibre break occurring depends on $\sigma_f$, the fibre stress, and that no breaks occur below a critical value $\sigma_f^{th}$. Some assumption must be made about the distribution of breaks with increasing stress; here we consider a simple relationship, but the model can be modified to deal with any arbitrary fracture statistics.

$$n = \text{no.of fibre breaks per unit length of fibre} = \exp\left[a\left[\sigma_f - \sigma_f^{th}\right]\right] - 1 \qquad (25)$$

If the initial fibre aspect ratio is $\lambda_o$, then the fibre aspect ratio can be written

$$\lambda = \lambda_o \exp\left[-a\left[\sigma_f - \sigma_f^{th}\right]\right] \qquad (26)$$

Fracture is taken to occur when $\lambda$ decreases to a minimum value $\lambda_f$ which allows evaluation of a

$$a = \frac{1}{\sigma_f^f - \sigma_f^{th}} \ln\left[\frac{\lambda_o}{\lambda_f}\right] \qquad (27)$$

From Equation 26,

$$\dot{\lambda} = -\frac{\lambda \ln(\lambda_o/\lambda_f)}{\sigma_f^f - \sigma_f^{th}} \cdot \dot{\sigma}_f \qquad (28)$$

This maybe combined with the Reuss Equations 21 to give a two state variable description of creep

$$\dot{\epsilon} = \alpha_1 \dot{\epsilon}_m (1-S_1)^n + \alpha_2 \dot{\epsilon}_m (1-S_2)^n \qquad (a)$$

$$\dot{S}_1 = H\alpha_1 \dot{\epsilon}_m (1-S_1)^n \qquad (b)$$

$$\dot{S}_2 = 0 \quad \text{for } S_1 < \frac{\varphi\sigma_f^{th}}{\sigma} \qquad (c)$$

$$\dot{S}_2 = -KS_2(1-S_2)\dot{S}_1 \quad \text{for } S_1 > \frac{\varphi\sigma_f^{th}}{\sigma} \qquad (d)$$

(29)

where $K = \left[\frac{n+1}{n}\right] \frac{\sigma}{\varphi} \frac{\ln(\lambda_o/\lambda_f)}{\sigma_f^f - \sigma_f^{th}}$

Figure 8 shows a computed creep curve obtained using Equations 29; the decreasing $\lambda$ contribution leads to a tertiary creep behaviour that is characteristic of alloys such as in-situ composites. Modification of the Voigt equations with variable $\lambda$ does not, as previously erroneously claimed[4], lead to tertiary creep. This is because the steady state value of $S_2$ (ie of $\sigma_f$) given by Equation 23b decreases with decreasing $\lambda$ so that the occurrence of a fibre fracture would make subsequent fractures less, rather than more, likely according to Equation 25.

c) Ductile tearing When the voids associated with cracked fibres or with decohesions at fibre ends are not filled by matrix, they will probably grow by void elongation at a rate determined by the surrounding creeping composite. A component of tertiary creep can, therefore be identified with the loss of internal section and the associated increase in stress that is caused by such creep controlled evolution of intra-grain voids. Cocks and Ashby[13] have considered the consequences of ductile tearing of a pre-existing density of voids; however this treatment is unlikely to be appropriate to the present case where fibre fractures and end decohesions are likely to occur continuously throughout the latter stages of deformation.

Since a stable void is incapable of supporting any load, the stress must be redistributed to the remaining sound material which will, consequently, deform at a faster rate. Assuming that the creation of such voids is proportional to the strain accumulated after a threshold value $\epsilon_{th}$, a damage parameter w can be defined that is simply related to the loss of internal load bearing section ($dA_{int}/A$). The change in stress and the associated creep rate can be expressed as follows

$$\frac{d\sigma}{\sigma} = -\frac{dA_{int}}{A} = k d\epsilon \qquad (30)$$

where k is a constant.

Integration and combination with the power-law expression for matrix creep yields:

$$\sigma = \sigma_i \exp(k\epsilon) \qquad (31)$$

$$\dot{\epsilon} = \dot{\epsilon}_i \exp(nk\epsilon) \qquad (32)$$

where the subscript i indicates the initial values before voids are formed. Equation 32 can be expressed:

$$\left.\begin{aligned} \dot{\epsilon} &= \dot{\epsilon}_i \exp(w) \\ \dot{w} &= k\dot{\epsilon} \end{aligned}\right\} \qquad (33)$$

Taking as suitable boundary conditions that w=0 before voids are formed and w=1 at fracture when the reinforcement is totally ineffective, then:

$$k = \frac{n\varphi}{(\epsilon_f - \epsilon_{th})} \qquad (34)$$

This is precisely the same argument as used by Dyson and Gibbons[14] to explain the dominant tertiary behaviour in low ductility superalloys in terms of the continuous creation of grain boundary cavities. Both the Reuss and Voigt formalisms can be modified to account for this effect; Equations 35 are the appropriate Voigt equations that account for void formation.

$$\boxed{\begin{aligned} \dot{\epsilon} &= \alpha_1 \dot{\epsilon}_m (1-S_1)^n \exp(w) \\ \dot{S}_1 &= H\alpha_1 \dot{\epsilon}_m (1-S_1)^n - R\dot{\epsilon}_m (1-S_2)^n \\ \dot{w} &= \frac{n\varphi\dot{\epsilon}}{(\epsilon_f - \epsilon_{th})} \end{aligned}} \qquad (35)$$

Figure 8 includes a creep curve calculated using Equations 35 that exhibits primary, minimum and tertiary creep behaviour. It is noteworthy that the void damage contribution to tertiary creep takes the same form as the equations derived to describe the intrinsic strain softening of metallic alloys due to dislocation accumulation where $n\varphi/\epsilon_f$ is replaced by a constant $C \sim 50$[8,15]. This latter factor may well also contribute to the behaviour of metal matrix composites, particularly those with particulte reinforcement. However, for low ductility materials where $n\varphi/(\epsilon_f - \epsilon_{th}) > 150$ the weakening by void creation is likely to be dominant.

## DISCUSSION

Although the theory has been developed to describe the composite creep behaviou. in terms of the deformation characteristics of the constituent phases, it must be emphasised that the deformation mechanisms operating in the individual phases when combined as a composite may be quite different from those operating in these materials in isolation. Such synergisms can lead to very substantial indirect strengthening which is quite different from the composite strengthening described in this paper and which is the most important factor in, for example, dispersion strengthening of metallic alloys. This is likely to be the dominant feature in particulate composites and will be an additional factor in fibre reinforced materials, particularly when the fibre dimensions are small. This makes it difficult to assess the validity of the model quantitatively.

Taking the approach of "physical inspired empiricism" that was discussed in the introduction, Equations 29 and 35 can each be regarded as alternative empirical descriptions of the creep curves, with five adjustable parameters, that have forms guided by physical reasoning.

$$\boxed{\begin{aligned} \dot{\epsilon} &= A_1(1-S_1)^n + B_1(1-S_2)^n \\ \dot{S}_1 &= C_1(1-S_1)^n \\ \dot{S}_2 &= -D_1 S_2 (1-S_2) S_1 \end{aligned}} \qquad (36)$$

and

$$\dot{\epsilon} = A_2(1-S_1)^n \exp(w)$$

$$\dot{S}_1 = B_2(1-S_1)^n - C_2 \qquad (37)$$

$$\dot{w} = D_2\dot{\epsilon}$$

Each set of equations has all the features required to describe a typical creep curve and, of course, they reduce to describe composites consisting of continuous and stable short fibres when appropriate terms are given a value of 0. A more detailed comparison of the predicted creep curves with experimental data is given elsewhere[16].

A random distribution of fibres will have different regions where Reuss and Voigt average equations will be appropriate; a full statistical treatment which combines these concepts is beyond the scope of the present paper. However, it would be of interest to determine which of the descriptions is dominant.

Although either equation set can adequately describe an isolated creep curve, they have quite different implications for more complex loading conditions. For example, the predicted responses following unloading for the two equation sets (Equations 36 and 37) applied to (i) continuous fibres, (ii) short stable fibres and (iii) short fibres with damage generation have quite different extents of anelastic recovery. This type of test has clear diagnostic value in discriminating between the rival models. To the author's knowledge, this type of data is not currently available.

## CONCLUSIONS

A theory of time-dependent deformation has been developed for an aligned fibre composite consisting of elastically extending fibres in a metal matrix subject to power-law creep. The model proposed takes into account the fibre dimensions and considers the effects of different types of damage generation on the creep characteristics.


## ACKNOWLEDGEMENT

The author thanks Dr Ana Barbosa for writing the software used to evaluate and display the calculated creep curves.


## REFERENCES


1. D.C. PHILLIPS, Proceedings of 6th International Conference on Composite Materials Volume 2, p.2.1 edited by F.L. Matthews et al. Elsevier Applied Science, 1988.
2. N.S. STOLOFF in "The Superalloys", edited by C.T. Sims and W.C. Hagel, Interscience, New York, 1979.
3. M. McLEAN, Proceedings of the 5th International Conference of Composite Materials, p.37, edited by W.C. Harrigan et al, The Metallurgical Society Inc., Warrendale, PA 1985.
4. M. McLEAN, Proceedings of the 4th Conference of the Irish Durability and Fracture Committee, p.202, edited by F.R. Montgomery, Queens University of Belfast, 1986.
5. J. HULT, this meeting.
6. M.F. ASHBY, Phil. Trans. Roy Society A322, 307 (1987).
7. M.F. ASHBY and B.F. DYSON, Advances in Fracture Research Volume 1, p.3, edited by S.R. Valluri et al., Pergamon Press 1984.
8. J.C. ION, A. BARBOSA, M.F. ASHBY, B.F. DYSON and M McLEAN. NPL Report No DMA(A)115, National Physical Laboratory, April 1986.
9. M. MALDINI, A. BARBOSA, B.F. DYSON and M. McLEAN. NPL Report No DMA(A)126, National Physical Laboratory, January 1987.
10. A. KELLY and K. STREET, Proc. Roy. Soc. A 328, 283 (1972).
11. M. McLEAN, Metals Science 12, 113 (1978).
12. R. WARREN and C-H. ANDERSON, Composites 15, 101 (1984).
13. A.C.F. COCKS and M.F. ASHBY, Progress in Materials Science. vol. 27, p.189 (1982).
14. B.F DYSON and T.B. GIBBONS, Acta. Met. 35, 2355 (1987).
15. B.F. DYSON and M McLEAN, Acta. Met. 17, 17 (1983).
16. M. McLEAN, Proceedings of Conference on High Temperature - High Performance Composites, Reno, Nevada 5-7 April 1988, Materials Research Society, to be published.

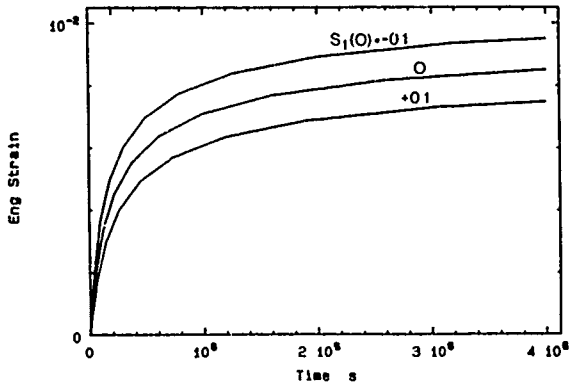


Figure 1 Creep curves for continuous composite with initial fibre stresses $S_1 = 0$, 0.1 and – 0.1 calculated from Equations 5 using parameters appropriate to Al–15% SiC. $\sigma$=150 MPa, T=473K.

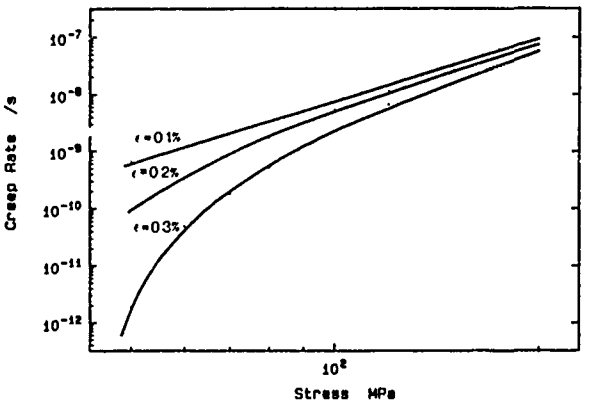


Figure 2 Calculated variations in creep rate at various strains as a function of applied stress for continuous composites. Parameters appropriate to Al–15% SiC at 473 K.

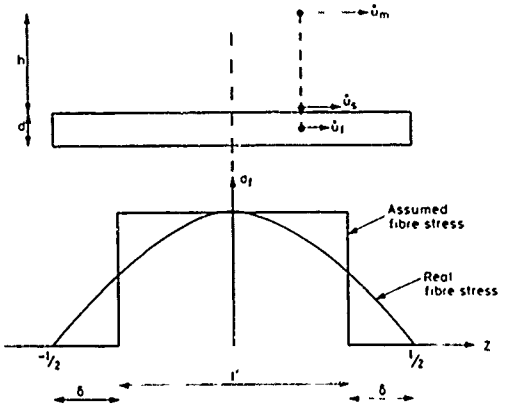


Figure 3 Schematic illustration of matrix flow around a short fibre showing the true and assumed distributions of tensile stress in the fibres.

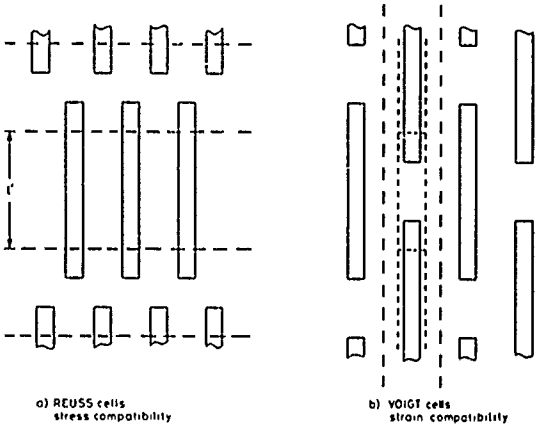


Figure 4 Schematic illustrations of fibre distributions and the different approaches to summing fibre deformation and end effects
a) Reuss averaging – constant stress
b) Voigt averaging – constant strain.

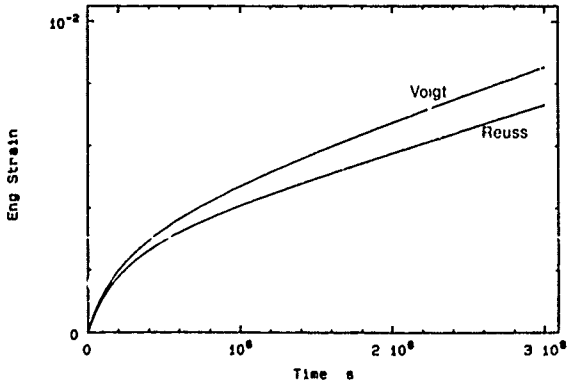


a) Calculated creep curves for short fibre reinforced composites using both Reuss and Voigt averaging procedures.

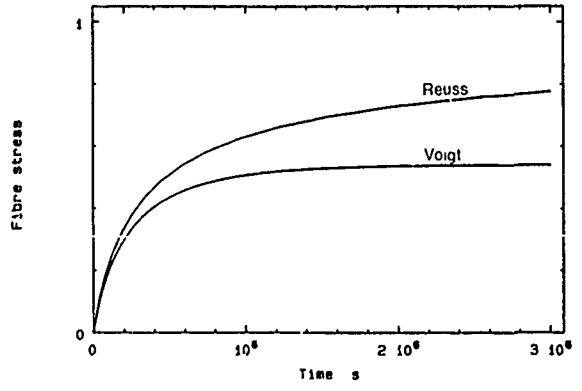


b) Variation in fibre stress associated with the two calculations. (Al–20% SiC, 100 MPa, 473 K).

Figure 5

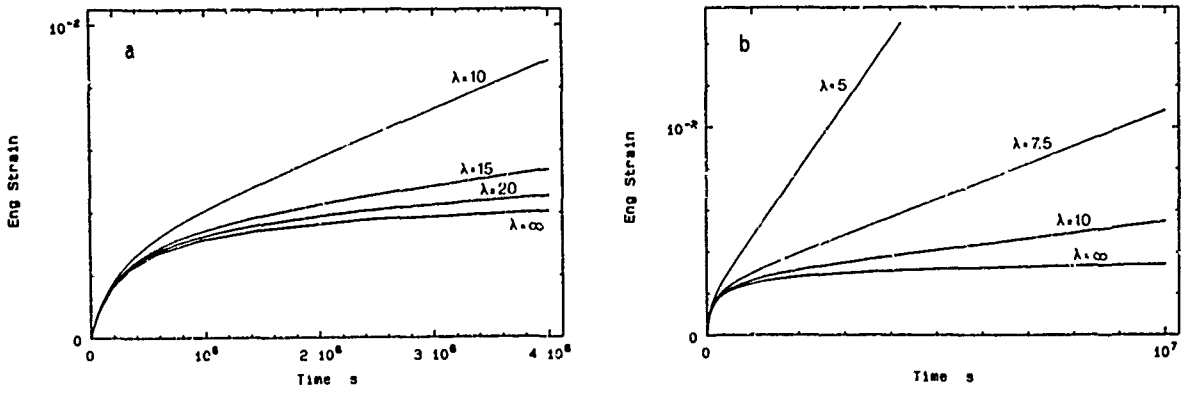


Figure 6 Calculated variation of creep curves with fibre aspect ratio using parameters appropriate to Al–20% SiC at 100 MPa and 473 K
a) n = 3 b) n = 6.

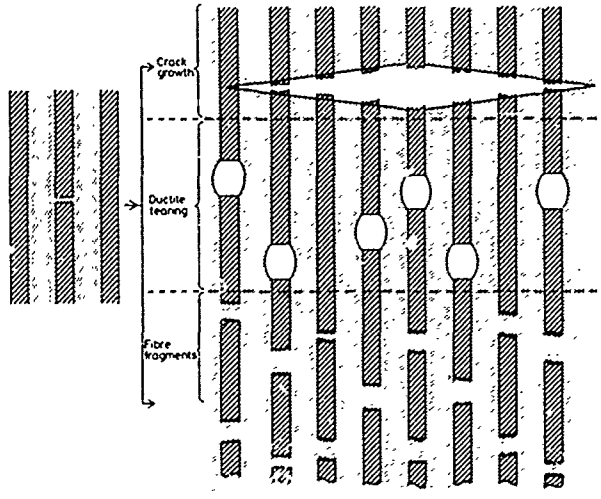


Figure 7 Schematic illustration of different modes of damage development.

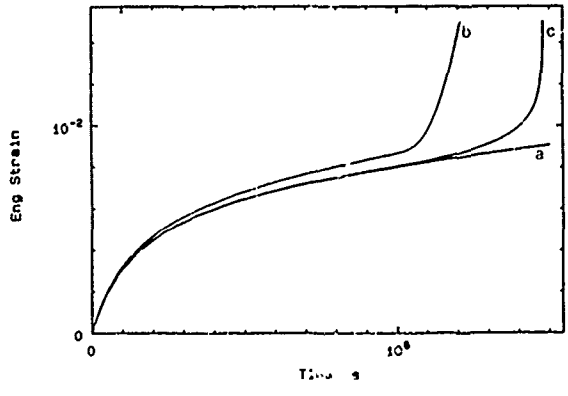


Figure 8 Calculated creep curves incorporating three different types of damage propagation.
a) crack growth (b) reducing fibre aspect ratio (c) void growth.

# MODELLING CREEP FRACTURE OF METALS FOR DESIGN

A.C.F. COCKS

Dr Cocks is in the Department of Engineering at the University of Leicester.

## SYNOPSIS

This paper examines the interaction between micromechanics, constitutive equations and component performance. The present state of the understanding of the micromechanisms of creep failure are reviewed and models describing these processes for multiaxial states of stress are presented. At the other extreme the process of design is examined and the type of information that is generally available to the designer is briefly reviewed. The constraints imposed on material constitutive laws by the microscopic degradation processes and the design procedure are discussed and situations are identified where the component response is largely insensitive to the details of the constitutive laws provided certain material characteristics are represented.

## INTRODUCTION

There are a number of reasons why one might wish to understand and model the response of a material. Here we are interested in using this understanding to develop material constitutive laws for component design, particularly the processes of material degradation leading to failure. A number of different approaches have been taken to obtain constitutive laws ranging from micromechanical to phenomenological methods. Before examining these approaches in any detail it is instructive to consider the types of questions that are posed in design and how answers are provided in other areas of study.

The basic questions asked during design are "will the component perform its function" and "what is the optimum configuration". To answer these questions the designer requires an understanding of the material phenomena involved and insight into how this behaviour influences component performance. Also, at least in the early stages of design, he needs to assess any effects of changes in shape on structural performance. Limit load and shakedown concepts have proved successful in providing the necessary information for structural components of ductile materials operating below the creep range. Although these techniques are based on a rather idealised view of material behaviour they provide conservative results, and the associated bounding techniques can be used at a number of different levels to aid the understanding of how a component performs.

If the effects of material hardening need to be investigated then provided the body experiences proportional loading the component response can be adequately predicted using an isotropic hardening model. If there is a high degree of non-proportional loading or large amounts of material rotation then a more elaborate material constitutive law might be required.

The important point to note about the above discussion is that the problem being analysed and information about structural performance required play an integral role in selecting the material constitutive relationships. There is no universal law and suitable approximations need to be made which provide an aequate description of the material response for the problem being considered.

We now return to the problem of creep failure and in the next section examine the type of information that is generally available to determine the material response. We then consider the different methods that have been proposed to represent this information. This is followed by an assessment of structural performance and an evaluation of the effect of choice of constitutive law on the predicted response.

## MATERIAL RESPONSE

Fig. 1 shows a typical creep curve for a uniaxial test conducted at constant stress. The major information that can be obtained from this type of curve is the steady-state creep-rate $\dot{\varepsilon}_{ss}$, the strain to failure $\varepsilon_f$ and the time to failure $t_f$. These quantities can be combined to form the parameter

$$\lambda = \frac{\varepsilon_f}{\dot{\varepsilon}_{ss} t_f} \qquad (1)$$

which was termed the creep damage tolerance by Ashby and Dyson [1]. If a series of constant stress creep tests are conducted at a number of

different stress states then the information from these tests can be presented in the form of an isochronous surface. This is a surface in stress space connecting stress states that result in the same time to failure. Fig. 2 shows two such surfaces obtained by Leckie and Hayhurst [2] for copper and an aluminium alloy. Copper fails according to a maximum principal stress criterion while the aluminium alloy obeys an effective stress criterion.

Any constitutive law developed for a material should reflect the form of the isochronous surface obtained experimentally and predict the correct value of $\lambda$ . It should be remembered, however, that the shape of the isochronous surface and the value of $\lambda$ can change as the stress and temperature ranges being considered change.

## MATERIAL MODELS

Constitutive laws describing material behaviour have either been developed from an understanding of the microscopic mechanisms responsible for deformation and failure or through the correlation of a set of experimental data. The phenomenological approach can either be adopted at the micro level, by, for example, correlating information on measured cavity population or used directly to model the macroscopic response. In many situations a combination of these methods is employed. In this section we review these different approaches and discuss the advantages and disadvantages of each.

Ashby and Dyson [1] have reviewed the different mechanisms of creep failure under uniaxial stress-states and associated a range of values of $\lambda$ with each mechanism. Here we focus on one particular class of mechanisms which has been studied extensively in the literature; namely, failure resulting from the nucleation, growth and coalescence of cavities to form grain boundary fissures. A number of authors have examined the extension of these models to multiaxial states of stress [3-6]. It is instructive to examine the processes of void nucleation, growth and coalescence in turn.

Most recent models of void nucleation treat it as a classical nucleation process involving the clustering of a number of vacancies at a stressed interface [7-10]. These models effectively predict a critical stress for nucleation, below which no voids nucleate and above which the rate of nucleation is so quick that it can be assumed that all the voids are nucleated early in the life of a component. This is at variance with experimental observation of the nucleation process where it is found that voids nucleate continuously throughout the lifetime of a component [11]. Also, the theoretical predictions of the critical stress tend to be large compared to stresses used in these tests. Attention has therefore focused on ways in which the required level of stress concentration can be achieved and how these can be developed over a period of time [10,12]. No clear models have, however, emerged from this work that provide a set of equations to use in the description of material behaviour.

Direct measurement of void and crack populations have proved more successful in providing an understanding of the nucleation process and equations for use in the development of constitutive equations. Studies of a number of materials have shown that the rate of nucleation of cavities is largely determined by the effective creep strain-rate [13,10]. During the early stages of creep a linear relationship between cavity density and creep-strain is often observed. At large strains a reduction in the rate of nucleation is observed as the number of possible nucleation sites becomes saturated and cavities coalesce. Chen and Argon [11] have also measured the influence of the orientation of a grain boundary on the void density for a 304 stainless steel. Their results indicate a linear dependence of the nucleation-rate on the stress normal to the grain boundary.

The mechanisms of void growth are better understood than those for nucleation and there is general acceptance as to the nature of these mechanisms and how they should be modelled. Void growth can be controlled by surface diffusion, grain-boundary diffusion, power-law creep of the surrounding matrix, or by any combination of these mechanisms [14]. In addition, creep of the surrounding grains can either accomodate or constrain the growth of the cavities [15]. During the life of a component the mechanisms of void growth can change and the stress local to a grain boundary can relax as the growth becomes constrained by the surrounding matrix material.

Cavity coalescence has received less attention than either nucleation or cavity growth. Provided a reasonable assumption is made about when coalescence occurs the resulting prediction of the time to failure is not strongly influenced by the details of the criterion used. A commonly used criterion is that a grain boundary fails if the area fraction of voids on the boundary exceeds 0.25 [14].

Tvergaard [4] has used the understanding gained from the above studies to construct a set of constitutive relationships for a damaging material He modified a result derived by Hutchinson [3] for a body containing a distribution of cracks to obtain an expression for the strain-rate under multiaxial states of stress:

$$\dot{\varepsilon}_{ij} = \frac{\partial \Phi}{\partial \sigma_{ij}} \qquad (2a)$$

$$\Phi = \frac{\dot{\varepsilon}_o}{n+1} \left(\frac{\sigma_e}{\sigma_o}\right)^{n+1} \left[ 1 + n\rho \left(\frac{\sigma_I - \sigma_N}{\sigma_e}\right)^2 \right] \qquad (2b)$$

where $\dot{\varepsilon}_o$ , $\sigma_o$ and $n$ are material constants, $\rho$ is a measure of the density of cavitated grain-boundaries which lie normal to the maximum principal stress $\sigma_I$ , $\sigma_N$ is the stress supported by the grain-bondaries and $\sigma_e$ is the von Mises effective stress.

Tvergaard [4] assumes that $\rho$ remains constant during the life of a component and determines $\sigma_N$ from compatibility constraints imposed on the deformation resulting from material plating onto the grain boundary as the voids grow by the surrounding material. If growth is unconstrained $\sigma_N = \sigma_I$ and there is no contribution to the strain-rate from the growing voids. Tvergaard [4] has constructed isochronous surfaces in plane stress space for a number of different nucleation

and void growth processes. Nucleation of cavities was assumed to be governed by an equation of the form

$$\dot{N} = \frac{\partial N}{\partial \varepsilon_e} \dot{\varepsilon}_e \qquad (3)$$

where $N$ is the number of cavities per unit area and $\varepsilon_e$ is the von Mises effective strain. Situations where $\partial N/\partial \varepsilon_e$ is either constant or is a function of stress $\sigma_N$ normal to the grain boundary were examined along with the different mechanisms of void growth described earlier. The majority of the isochronous surfaces he obtained are bounded by the two surfaces of Fig. 2.

Cocks and Leckie [5] noted that the process of void growth itself contributes very little to the tertiary stage of creep. It is only when void growth is fully constrained or the voids have linked to form a physical crack that there is an effect on the creep-rate. In these situations the potential of eqn. (2b) can be replaced by

$$\phi = \frac{\dot{\varepsilon}_o}{n+1} \left(\frac{\sigma_e}{\sigma_o}\right)^{n+1} \left[1 + n\rho \left(\frac{\sigma_I}{\sigma_e}\right)^2\right] \qquad (4)$$

where now $\rho$ is the density of crack-like features. They developed evolution laws for $\rho$ from an understanding of the mechanisms of void growth and assume that failure occurs when $\rho$ reaches a critical value. In this model it is assumed that not all the cracked boundaries are perpendicular to the direction of maximum principal stress.

Argon et al [6] have also used equation (4) to determine the creep rate of a damaged material. Like Tvergaard [4] they assume that all the failed boundaries are perpendicular to the direction of maximum principal stress and employ similar equations for the rate of growth of the voids. They also use eqn. (3) for the rate of nucleation of the cavities with $\frac{\partial N}{\partial \varepsilon_e} = \beta$ a constant. The value of $\beta$ is assumed to have a random distribution over all cavitating boundaries. This results in a rate of increase of $\rho$ over a period of time and failure is again assumed to occur when $\rho$ reaches a critical value.

There is broad agreement in these three models as to how the damage influences the deformation response of the material, but there are differences in how this damage is assumed to form and grow. The major difference lies in the choice of model for the nucleation of the cavities, reflecting the current level of understanding of this part of the process.

An alternative approach to the development of material constitutive laws was proposed by Kachanov [16] and extended to multiaxial states of stress by Leckie and Hayhurst [2]. In this formalisation the creep strain-rate is assumed to be a function of the stress $\sigma$ and a quantity $\omega$ which is a measure of the damage in the material. Leckie and Hayhurst [2] assume that the damage has the same influence on each component of strain-rate, and that there is zero dilitational strain as the damage grows. The strain rate potential is then given by an equation of the form

$$\phi = \frac{\dot{\varepsilon}_o}{n+1} \left(\frac{\sigma_e}{\sigma_o}\right)^{n+1} \frac{1}{(1-\omega)^{\phi}} \qquad (5)$$

and the damage is assumed to grow at a rate

$$\dot{\omega} = \frac{\dot{\omega}_o}{(1-\omega)^{\Psi}} \left(\frac{\chi(\sigma_{ij})}{\sigma_o}\right)^{\nu} \qquad (6)$$

where $\dot{\omega}_o$ , $\phi$ , $\Psi$ and $\nu$ are material quantities determined by examining the shape of a series of uniaxial creep curves [17] and $\chi(\sigma_{ij})$ is a function that describes the shape of the isochronous surface in stress space, and is equal to $\sigma_I$ for a maximum principal stress material and $\sigma_e$ for an effective stress material.

Although a number of authors have tried to assign a physical interpretation to $\omega$ this would be wrong. It is merely a parameter that is used to describe the shape of a creep curve and to represent the state of the material at a given instant in time.

A mechanistic approach has distinct advantages in component design. It provides an understanding of how changes in stress and temperature affect the performance of a material, and provides guidance in devising tests that are representative of conditions experienced in the design problem, thus permitting the extrapolation of this data to provide an assessment of the performance of a component. There are, however, two major difficulties to be overcome before this potential can be realised. At the present time the mechanisms of void nucleation are not fully understood. There is nothing inherently wrong with the approach adopted in the derivation of the equations described earlier, but there is no guarantee that the mechanism and the equations governing the nucleation process do not change when the stress and temperature differ from those employed in the laboratory. The second problem is that the equations that are currently adopted in the description of void growth tend to be rather elaborate and extensive numerical calculations need to be undertaken even to determine the material response under simple stress states. As a result, it is difficult to gain an understanding of those features of material behaviour that most influence the response of a component, and, at the same time, gain an insight into how the component performs.

The main attraction of the Kachenov approach is its relative simplicity. It also suffers, however, from the uncertainties that result when extrapolating from laboratory tests to the design situation.

## COMPONENT ANALYSIS

Tvergaard [18] has used the constitutive relationships centred on eqns. (2) and (3) to determine the response of a number of components. Hayhurst et al [19] have performed similar calculations employing equations (5) and (6). The major features of component response are similar in each case with damage initially accumulating in regions of stress concentration, leading to a local softening of the material and a gradual re-

distribution of stress as the damage zone spreads through the component. It would therefore appear that understanding the process of stress redistribution is an important part of the design process. Calculations of the type performed by Tvergaard [18] and Hayhurst et al [19], however, require a substantial amount of computing power even for relatively simple components.

In the Introduction we noted that simple models of material behaviour and relatively simple concepts of component analysis can provide information that is ideally suited to the design process. A particular example of this is the use of reference stress concepts [20] in creep deformation where the material information for use in design is obtained from a single prescribed material test. Using the Kachanov equations Ponter [21] has extended the reference stress concept to deal with creep failure, although the resulting bounds can, in certain circumstances, severely over-estimate the life of a component. An important result of Ponter's work [21] is the identification of a constant stress state that can be used to assess the life of a component. Cocks and Ponter [22] have recently re-examined this result by considering the response of a number of simple components.

One of the structures analysed by Cocks and Ponter [22] is the two-bar structure of Fig. 3, where the two bars are constrained to suffer the same extension under the action of the constant load $P$. Cocks and Ponter [22] examine the structural response in terms of a global damage parameter $\Omega$, which can be thought of as giving a measure of the extent of the damage in the structure in the same way that $\omega$ is a measure of the amount of damage in a uniaxial test specimen. Fig. 4 shows the variation of $\Omega$ with time for the two-bar structure, where $t_f^o$ is the time to failure in a uniaxial test at a constant stress $\sigma_o = P/2A$ where $A$ is the cross-sectional area of each bar. Also shown on Fig. 4 is the extrapolation of the initial rate to $\Omega = 0$, when failure occurs. Although stress redistribution occurs extrapolation of the initial rate of growth of the global damage, which is determined by the initial steady state stress distribution is the body, provides a good estimate of the life of the component. The reason for this is that for this problem, and many more structural situations, there is a high degree of kinematic constraint, and although the stresses redistribute, the pattern of deformation within the body remains largely unaltered. A result of this is that the damage tends to accumulate at a uniform rate in the body. Although these results were obtained for the Kachanov model the general features of structural behaviour are dictated by the configuration and the constraints imposed by the structure itself. As a result, the same procedure could be adopted to provide an assessment of the structural performance for other choices of material constitutive law.

For more complex structural configurations Cocks and Ponter [22] provide an alternative method of analysis. In general, failure occurs in a localised region of a structure. The collapse mechanism for a perfectly plastic material is used to identify the failure mechanism, and the stress distribution within the plastically deforming regions can be used to evaluate the time to failure of the component. As before, this method is based on an understanding of the structural phenomena and can be adapted to use any other constitutive law.

## CONCLUSIONS

In this paper we have examined a number of material constitutive laws for creep damaging materials. There is general agreement in the mechanistic approaches as to how damage affects the deformation response, when the damage is in the form of grain-boundary cavities and cracks, but, as a result of the current level of understanding of the processes which govern void nucleation, there is no generally accepted procedure for determining the rate of growth of this damage. If the mechanistic approach is to achieve its potential in providing suitable constitutive equations for component design, then a more complete understanding of the mechanisms of void nucleation is required.

The process of component assessment has also been considered, and, although stress redistribution occurs as a creeping structure damages, it has been shown how a uniform stress state can be used to provide an evaluation of structural performance. These methods are still in the process of development, particularly when using the mechanistic constitutive laws, but the procedures offer considerable advantages for use in design as they can be used at a number of different levels to provide an insight into how a component might perform.

## ACKNOWLEDGEMENTS

Financial support from the SERC during the course of this work is gratefully acknowledged.

## REFERENCES

[1] M.F. Ashby and B.F. Dyson, Creep damage mechanics and micromechanics, National Physical Laboratory Report DMA(A) 77, (1984)

[2] F.A. Leckie and D.R. Hayhurst, Proc. R. Soc. Lond. A, 340, (1974), 323.

[3] J.W. Hutchinson, Acta Metall., 31, (1983), 1079.

[4] V. Tvergaard, Acta Metall., 34, (1986).

[5] A.C.F. Cocks and F.A. Leckie, Adv. Applied Mech.

[6] A.S. Argon, C.W. Lau, B. Ozmat and D.M. Parks, Eshelby Memorial Volume.

[7] R. Raj and M.F. Ashby, Acta Metall., 23, (1975), 653.

[8] R. Raj, Acta Metall., 26, (1978), 995.

[9] M.H. Yoo and H. Trinkaus, Metall. Trans. A, 14, (1983), 547.

[10] A.S. Argon, in "Recent Advances in Creep and Fracture of Engineering Materials and Structures", eds. B. Wilshire and D.R.J. Owen, Pineridge Press, Swansea, U.K. (1982).

[11] I-W, Chen and A.S. Argon, Acta Metall., 29, (1981), 1321.

[12] A.C.F. Cocks, Acta Metall., 33, (1985), 129.

[13] B.F. Dyson and D. McLean, Metal Sci., 11, (1977), 37.

[14] A.C.F. Cocks and M.F. Ashby, Prog. Mat. Sci. 27, (1982) 189.

[15] B.F. Dyson, Can. Metal Quart., 18, (1979), 31.

[16] L.M. Kachanov, IZV. Akad. Nauk. SSSR Otdet Tekh. Nauk. No.8, (1958), 26.

[17] Yu N. Rabotnov, Creep problems in structural members (English translation by F.A. Leckie) North Holland, Amsterdam, (1969).

[18] V. Tvergaard, Analysis of creep rupture in a notch tensile bar, The Danish Centre for Applied Mathematics and Mechanisms report 300, (1985).

[19] D.R. Hayhurst, P.R. Diminer and C.J. Morrison, Phil. Trans. R. Soc. Lond. A, 311, (1984), 103.

[20] I.W. Goodall, F.A. Leckie, A.R.S. Ponter and C.H.A. Townley, Jnl. Eng. Mat. Tech., 101, (1979), 349.

[21] A.R.S. Ponter, Int. J. Mech. Sci., 19, (1977), 79.

[22] A.C.F. Cocks and A.R.S. Ponter, to appear Jnl. Nuc. Eng. Design.

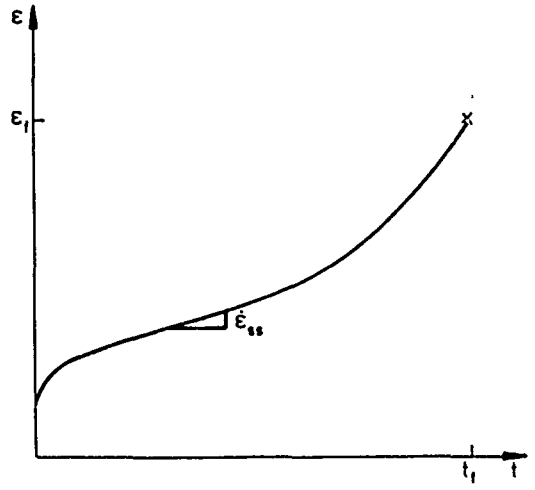


Fig. 1. A typical creep curve obtained from a uniaxial test at constant stress.

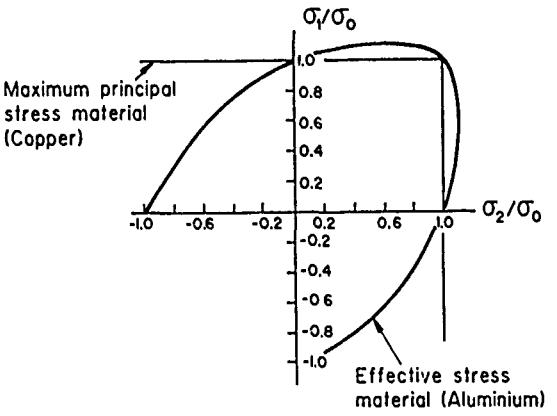


Fig. 2. Isochronous surfaces obtained by Leckie and Hayhurst [2] for copper and an aluminium alloy.

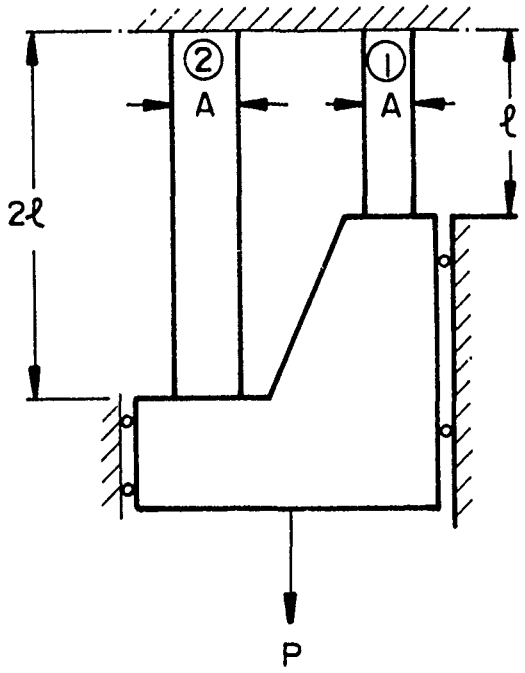


Fig. 3. A simple two-bar structure analysed by Cocks and Ponter [22].

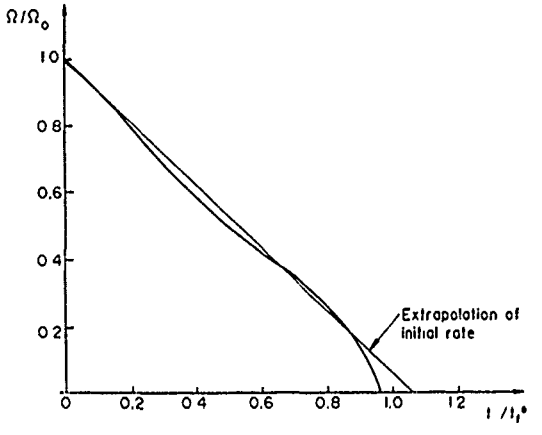


Fig. 4. The variation of global damage, $\Omega$, as a function of normalised time for the two-bar structure of Fig. 3.

# FATIGUE IN METALS--A CONTINUUM DAMAGE APPROACH

D. F. Socie and J. A. Bannantine

Department of Mechanical and Industrial Engineering
University of Illinois at Urbana-Champaign

## SYNOPSIS

Continuum damage approaches allow engineering estimates of fatigue life to be made without attempting to explicitly model the mechanics of the fatigue process. The employed models, however, must be representative of the observed damage and incorporate the dominant or controlling parameters consistent with the damage.

This paper presents observations that show that fatigue damage or cracking behavior depends upon loading mode, strain amplitude and material type. Correlation of test results using damaged models that are consistent with the observed cracking behavior show that successful multiaxial life predictions must be based upon observed damage.

## INTRODUCTION

The initiation and growth of cracks on a microscopic scale is a complicated metallurgical process. It is difficult to accurately describe and model this process in detail as evidenced by the wealth of literature on this subject. Despite the complexities, fatigue damage assessment for design of structures and components must be made. A continuum damage approach allows macroscopic damage models to be developed or appropriately selected based upon a qualitative understanding of the fatigue mechanisms.

To date, a large number of multiaxial fatigue damage models have been proposed. Stress, strain, and energy have all been proposed to correlate data for a wide variety of materials and loading conditions. In the low cycle fatigue region, equivalent strain [1-3], plastic work [4], plastic strain energy [5], and critical plane approaches [6-7] have been used to correlate the data. Although the importance of the damage development or cracking behavior has been recognized, the above multiaxial models have been proposed to correlate all materials and do not account for material differences in fatigue damage development. Material dependency is introduced only in constants required to fit each set of data.

The following paper reviews damage development observed in three different materials and discusses the impact this damage development has in the appropriate choice of a multiaxial fatigue damage model. The use of a continuum damage approach in design is discussed in light of these observations and correlation of experimental test data with continuum damage models is presented.

## BACKGROUND

Fatigue damage is a metallurgical process, which if unchecked, results in failure of a component or structure experiencing cycling loading. It is generally defined and quantified as the nucleation and growth of cracks.

Very early research [8] showed that in many metals, slip bands form and cracks subsequently initiate and develop in grains whose slip planes are most closely aligned with the maximum shear plane. Forsyth [9] designated crack initiation and growth on shear planes as Stage I growth. He reported that Stage I growth continues until reversal of dislocation movement is prevented. The crack may then turn and propagate in a Stage II direction, on a plane normal to the maximum principal stress. This has been shown to depend on the material [10].

Early research showing the material and stress state dependence of fatigue damage was performed by Gough [11]. He performed studies of the fatigue limit in bending and torsion and found that the ratio of the fatigue limit in torsion to that in bending varied with material tested. He proposed models that would reduce to the maximum shear stress theory for ductile materials and the maximum principal stress theory for brittle materials such as cast iron. Guest [12] also proposed a single model for both ductile and brittle materials with an adjustable constant that could change the theory from maximum shear stress to maximum principal stress. These models were among the first to incorporate the failure mode of the material in the damage model.

In the current paper, the fatigue damage dependency on material is further substantiated and the importance of choosing a model based upon the observed damage is discussed.

## EXPERIMENTAL PROCEDURE

Strain controlled tension and torsion tests were performed on AISI 304 stainless steel, SAE 1045 steel, and Inconel 718. The tubular specimens were tested in a computer controlled axial-torsional servo-hydraulic system with automated

test control and data acquisition. Strains were controlled using internal extensometry which allowed the outside surface to be monitored for crack formation and growth using acetate replicas. Additional material and specimen details, experimental data, and observations are given in Refs. [10,13,14].

## RESULTS

Detailed crack observations were made on the three materials. These materials exhibit different types of cracking behavior and represent extremes in the behavior observed in isotropic materials during tensile and torsional fatigue testing.

The behavior of the three materials in tension and torsion is summarized in Figs. 1-3. In these figures, the vertical axis is in terms of life fraction, $N/N_f$, and the horizontal scale is presented in terms of fatigue life, $N_f$, in cycles. The solid line represents the first observation of a surface crack of 100 μm and serves as a demarcation between crack nucleation and growth. It could be argued that nucleation occurs much earlier, say, for example, 10 μm. This would simply shift the line down without changing the qualitative phenomena represented by the plots. The dashed line represents the demarcation between crack growth on planes of maximum shear strain amplitude and crack growth on planes of maximum principal strain amplitude. Cracking behavior is categorized into three general regions, Regions A, B, and C. Region A denotes a failure mode that is dominated by shear crack growth. In Region B, shear crack nucleation is followed by crack growth on planes of maximum principal strain (Stage II planes). Crack nucleation dominates the fatigue life in Region C. Materials may exhibit cracking behavior that is representative of one, two, or all three of these regions. The cracking behavior of each of the three materials is discussed in detail below.

Stainless steel 304 tested in torsion exhibited cracking behavior which could be categorized into two regions, Region A and B, as shown in Fig. 1a. The stainless steel tested at high torsional strain levels exhibited behavior characteristic of Region A. Microcracks initiated on shear plane. Once initiated, the cracks become more distinct but showed no significant increase in length. A small amount of branching onto tensile planes (Stage II planes) was observed. Failure cracks grew on shear planes (Stage I) or tensile planes (Stage II) by a slow linking of previously initiated shear cracks. At lower values of strain, the stainless steel tested in torsion exhibited Region B behavior with large amounts of crack growth on tensile planes. A small number of cracks initiated on shear planes but quickly branched to tensile planes. Growth on these planes occurred by the propagation of the main crack rather than by a linking process.

In tension, the stainless steel exhibited no perceptible evidence of Stage I growth. As a result, no Region A behavior is shown in Fig. 1b. Scanning electron examination showed that the fracture surfaces appeared to be almost entirely dominated by Stage II growth.

The behavior of Inconel 718 is presented in Fig. 2. Unlike the stainless steel, which displayed mixed behavior, results of the Inconel 718 torsion tests showed that cracks initiated and remained on maximum shear planes. As shown in Fig. 2a, Region A behavior was observed in torsion for all values of shear strain investigated. Even at the lowest strain amplitude, in which the normal stress-strain response was essentially elastic, cracks initiated and remained on shear planes throughout the life. Crack density decreased in specimens tested at longer fatigue lives as it did in stainless steel, but no branching onto tensile planes was observed.

In Inconel 718 tested in tension, cracks remained on shear planes for the majority of fatigue life and a large zone of Region A behavior was observed as shown in Fig. 2b. Final failure in all tension tests was in a macroscopic tensile direction comprised of large portions of microscopic shear growth. Large amounts of shear growth were observed at failure for short and intermediate fatigue lives. Growth on Stage II planes occurred only late in life.

Damage accumulation in Inconel is shear dominated. This is attributed to localized shear deformation bands developed during cyclic loading. Reversed movement of dislocations progressively shears precipitates in these bands. Crack propagation then occurs along the bands with extensive shear crack growth throughout the fatigue life.

Two types of cracking systems have been observed in SAE 1045. One type, termed the Marco and Starkey [15], exhibits a large density of microcracks with the final failure occurring by a very rapid linking of these cracks. This type of damage occurred at high strain amplitudes. Alternatively, the S system, which exhibits one dominant crack that grows to failure, was observed at low strain amplitudes.

In torsion, at high amplitudes, the R system crack behavior was characteristic of Region A shown in Fig. 3a. In this region, the number of microcracks increased with the number of loading cycles. In addition, the surface length of microcracks, which appeared in the early stages of life, remained almost unchanged during the fatigue life. Darkness and clarity of the microcracks substantially increased with the increasing cycles. Cracks developed equally on both planes of maximum shear and were uniformly distributed over the entire gauge length. The failure was similar to that observed in the stainless steels at high amplitudes except that the linking of microcracks and final failure in 1045 occurred over a very few cycles, while the growth of the Region A failure crack in stainless steels occurred progressively throughout the life.

Region B behavior was observed in 1045 only at long lives. At the lowest strain amplitude, 0.26 percent, the crack branched and growth occurred on the tensile plane by a linking of previously initiated shear cracks. After a period of tensile growth, the crack linked with a large shear crack which had simultaneously developed. Final failure occurred by a mixture of Regions A and B behavior.

SAE 1045 tested in tension exhibited cracking behavior characteristic of both the R and S systems which developed on Stage II planes. As shown in Fig. 3b, microcracks initiated on shear planes at high amplitudes, in a manner representative of the R crack system. A very rapid linking of these microcracks occurred immediately prior to failure such that the failure crack was on tensile (Stage II) planes.

At low amplitudes, cracks initiated on shear planes but progressive growth occurred on Stage II planes.

In Region C, crack nucleation plays the dominant role. This region has been extensively studied by others. Nisitani [16] and Nisitani and Kawano [17] made observations of long life fatigue failures in low carbon steels. They concluded that at the fatigue limit, cracks formed within single grains but were unable to propagate into neighboring grains because of the differences in crystallographic orientation. This long life region should be controlled by cyclic shear stress. Tensile crack growth consumes a small portion of the total fatigue life. For low ductility materials containing flaws, non-propagating cracks should be considered and maximum principal strain amplitude is the controlling parameter.

## FATIGUE MODELS

A fatigue life estimate of a component of structure may be made using an appropriate continuum damage model selected after the failure mode has been identified. Each of the three regions of damage described above requires a separate damage model that is based on the observed cracking behavior. The following damage models are proposed, although it is important to note that alternative models could have been chosen. The models that are selected, however, must incorporate the dominant or controlling parameters for each region, as these below do, such as shear strain for Region A, tensile strain for Region B, and shear stress for Region C.

Region A:

$$\hat{\gamma} + \hat{\epsilon}_n + \hat{\sigma}_{no}/E = \gamma_f'(2N)^c + \tau_f'/G\ (2N)^b. \quad (1)$$

This model was proposed by Kandil, Brown and Miller [18] and modified by Socie, Kurath, and Koch [14] to include mean stress effects.

The right-hand side is the description of the strain life curve generated from torsion testing with the following nomenclature:

- $\gamma_f'$ shear fatigue ductility coefficient
- c fatigue ductility exponent
- $\tau_f'$ shear fatigue strength exponent
- b fatigue strength exponent
- G shear modulus
- 2N reversals to the formation of a 1.0 mm surface crack.

The terms on the left-hand side represent the loading parameters defined on the plane experiencing the largest range of cyclic shear strain and have the following definitions:

- $\hat{\gamma}$ maximum shear strain amplitude
- $\hat{\epsilon}_n$ tensile strain perpendicular to plane of the maximum shear strain amplitude
- $\hat{\sigma}_{no}$ mean stress perpendicular to the plane of maximum shear strain amplitude
- E elastic modulus.

Region B:

$$\sigma_1^{max}\ \epsilon_1 = \sigma_f'\ \epsilon_f'\ (2N)^{b+c} + \sigma_f'^2/E\ (2N)^{2b} \quad (2)$$

This model was originally proposed by Smith, Watson and Topper [19] for mean stress effects during uniaxial loading.

The right hand side is a description of the uniaxial strain life curve generated from tensile testing with the following nomenclature:

- $\epsilon_f'$ tensile fatigue ductility coefficient
- c fatigue ductility coefficient
- $\sigma_f'$ tensile fatigue strength exponent
- b fatigue strength exponent
- E elastic modulus
- 2N reversals to failure

The terms on the left-hand side represent the loading parameters and have the following definitions:

- $\Delta\epsilon_1/2$ Maximum principal strain amplitude
- $\sigma_1^{max}$ Maximum stress on the maximum principal strain plane

Region C:

$$\hat{\tau} + \hat{\sigma}_n = \sigma_f'(2N)^b \quad (3)$$

The right-hand side of the equation is the elastic portion of the uniaxial strain-life curve with the nomenclature the same as that given for Eq. (2). The terms on the left-hand side of the equation represent the loading parameters defined on the plane experiencing the largest range of cyclic shear stress and have the following definitions:

- $\hat{\tau}$ maximum shear stress amplitude
- $\hat{\sigma}_n$ normal stress on plane of maximum shear stress amplitude

This model was proposed by Findley [20] for long life fatigue with experimental verification for multiaxial fatigue presented.

A common feature of these damage models is that they are evaluated on a critical plane for crack nucleation and growth. They can easily be extended to complex non-proportional loading by evaluating the damage parameter on all planes to determine the plane experiencing the greatest fatigue damage and shortest expected fatigue life.

## DISCUSSION

Test data from uniaxial tests can be fit with any damage model by suitably adjusting the material constants. An example for IN 718 is given in Figs. 4a and 4b where shear strain (Eq. (1)) and tensile strain (Eq. (2)) are used to correlate the uniaxial test data, respectively. In the uniaxial case, no major difference is observed between the two models. The superiority of one model over the other is determined from tests results of more complicated loading situations.

A number of combined tension and torsion tests, under both in-phase and out-of-phase loading conditions, were performed on the AISI 304 stainless steel and the Inconel 718. Results of the stainless steel tests are correlated with the shear based damage parameters, Eq. (1), in Fig. 5a, and the tensile based parameter, Eq. (2), in Fig. 5b. Results of the Inconel tests are correlated in Figs. 6a and 6b with the same parameters, respectively. The poor correlation of the stainless steel with the shear based parameter, shown in Fig. 5a, is not surprising based on the cracking observations presented earlier. Since the damage developed in this material occurred on tensile planes, one would not expected a shear based parameter to correlate test results. Rather, it is expected that a tensile based model would results in better correlation. This is substantiated by the good correlation shown in Fig. 5b. Conversely, the Inconel which exhibited shear damage would not be expected to be correlated with a tensile based parameter. Instead one would expect that a shear based parameter would provide better correlations. This is shown to be the case in Fig. 6.

In Fig. 7 results of Inconel 718, SAE 1045, and stainless steel 304 are correlated with the tensile and shear models based upon the observed damage. The dashed line represents a factor of two in life. Correlation for the large amount of data is good.

Continuum damage approaches allow the designer or engineer to estimate the fatigue life of a component or structure based upon a qualitati e understanding of the fatigue process. In low cycle fatigue, cracking behavior (presented here as Region A and B behavior) is characterized by the development of a large number of microcracks that link to form a failure crack. To attempt to model the nucleation and growth of an individual crack would be impractical, if not impossible.

An alternative to the stress-strain continuum damage approach presented here is a fracture mechanics approach. In the fracture mechanics approach, crack growth could be defined as the average growth behavior of the microcracks. This average would integrate the nucleation and growth of the multiple microcracks as well as the linking process which results in a macroscopic crack. After the linking process, a standard fracture mechanics approach could be used to model the growth of the macroscopic crack. Some success has been achieved by Socie, et al. [21], for in-phase loading using this approach. However, difficulties arise using this method in estimating the stress intensity factor for the macroscopic crack surrounded by numerous microcracks.

## SUMMARY

Continuum approaches allow engineering estimates of fatigue life to be made without attempting to explicitly model the mechanics of the fatigue process. The employed models, however, must be representative of the observed damage and incorporate the dominant or controlling parameters consistent with the damage.

Observations presented here show that fatigue damage or cracking behavior depends upon loading mode, strain amplitude and material type. Successful multiaxial life predictions must be based upon observed damage. This as was shown by correlation of test results made using models that were consistent with the observed cracking behavior.

## REFERENCES

1. Taira, S., Inoue, J., and Takashashi, M., "Low Cycle Fatigue under Multiaxial Stress (in the Case of Combined Cyclic Tension-Compression and Cyclic Torsion in the Same Phase at Elevated Temperature)," The 10th Japan Congress on Testing Materials, 1967, pp. 18-23.

2. Pascoe, K. J., and DeVilliers, J. W. R., "Low Cycle Fatigue of Steels under Biaxial Strainings," J. Strain Analysis, 1967, Vol. 2, pp. 117-126.

3. Yokobori, T., Tamanouchi, H., and Tammamoto, S., "Low Cycle Fatigue of Thin-walled Hollow-cylinder Specimens of Mild Steel in Uniaxial and Torsional tests at Constant Strain Amplitude," Int. J. Fracture Mechanics, Vol. 1, 1965, pp. 3-13.

4. Garud, Y. W., 1979, "A New Approach to the Evaluation of Fatigue under Multiaxial Loadings," Methods for Predicting Material Life, ASME, 1979, pp. 247-263.

5. Ellyin, F., and Valaire, B., "High Strain Multiaxial Fatigue," ASME J. of Eng. Mat. and Tech., Vol. 104, 1982, pp. 165-171.

6. Brown, M. W., and Miller, J. J., "A Theory for Fatigue Failure under Multiaxial Stress and Strain Conditions," Proc., Inst. Mech. Eng., Vol. 187, 1973, pp. 746-755.

7. Lohr, R. D., and Ellison, E. G., "A Simple Theory for Low Cycle Multiaxial Fatigue," Fatigue of Eng. Mat. and Structures, 1980, Vol. 3, pp. 1-17.

8. Ewing, J. A., and Humfrey, J. C. W., "The Fracture of Metals under Repeated Alternations of Stress," Phil. Trans. Royal Soc., Vol. 200, 1903, pp. 241-253.

9. Forsyth, P. J. E., "A Two Stage Process of Fatigue Crack Growth," Proc., Symp. on Crack Propagation, Cranfield, England, 1961, pp. 76-94.

10. Bannantine, J. A., and Socie, D. F., "Observations of Cracking Behavior in Tension and Torsion Low Cycle Fatigue," ASTM Symposium on Low Cycle Fatigue-Directions for the Future, STP 942, 1985.

11. Gough, H. J., "Crystalline Structure in Relation to Failure of Metals - Especially Fatigue," Proc. ASTM 33, Part II, pp. 3-14.

12. Guest, J. J., "Recent Research on Combined Stress," Proc. Inst. Automobile Engrs., London, Vol. 35, 1940, pp. 33-72.

13. Hua, C. T., and Socie, D. F., "Fatigue Damage in 1045 Steel Under Variable Amplitude Biaxial Loading," Fatigue of Engineering Materials and Structures, Vol. 8, No. 2, 1985, pp. 101-114.

14. Socie, D. F., Kurath, P., and Koch, J. L., "A Multiaxial Fatigue Damage Parameter," Second International Conference on Multiaxial Fatigue, 1985.

15. Marco, A. M., and Starkey, W. L., "A Concept of Fatigue Damage," Trans. Am. Soc. Mech. Engrs., Vol. 76, 1954, pp. 627-632.

16. Nisitani, H., Japan Society of Mechanical Engineers Bulletin, Vol. 11, No. 48, 1968, pp. 947-957.

17. Nisitani, H., and Kawano, K., Japan Society of Mechanical Engineers Bulletin, Vol. 15, No. 82, 1972, pp. 433-438.

18. Kandil, F. A., Brown, M. W., and Miller, K. J., "Biaxial Low-Cycle Fatigue Fracture of 316 Stainless Steel at Elevated Temperatures," Book 280, The Metals Society, London, 1982, pp. 203-210.

19. Smith, R. N., Watson, P., and Topper, T. H., "A Stress-Strain Function for the Fatigue of Metals," Journal of Materials, JMLSA, Vol. 5, No. 4, 1970, pp. 767-778.

20. Findley, W. N., J. of Eng. for Ind. Trans., Amer. Soc. of Mech. Engrs., Series B, Vol. 81, 1959, pp. 301-306.

21. Socie, D. F., Worthem, D. F., and Hua, C. T., "Mixed Mode Small Crack Growth," Fatigue of Fract. Eng. Mater. Struct., Vol. 10, No. 1, 1987, pp. 1-16. press.

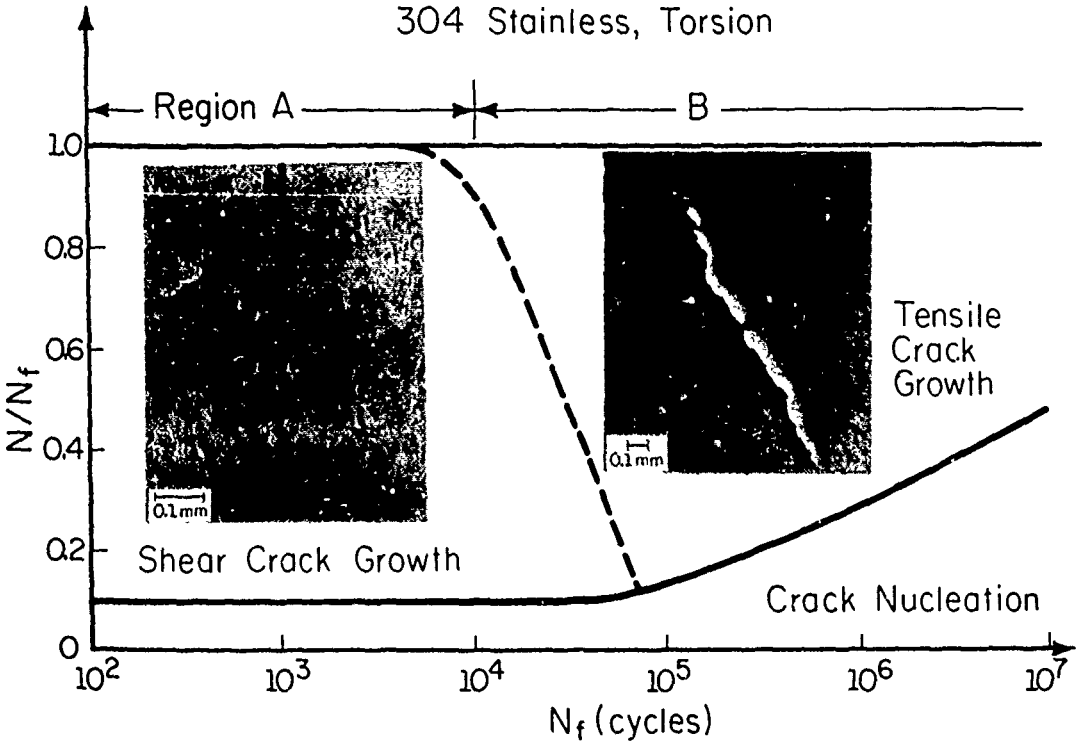


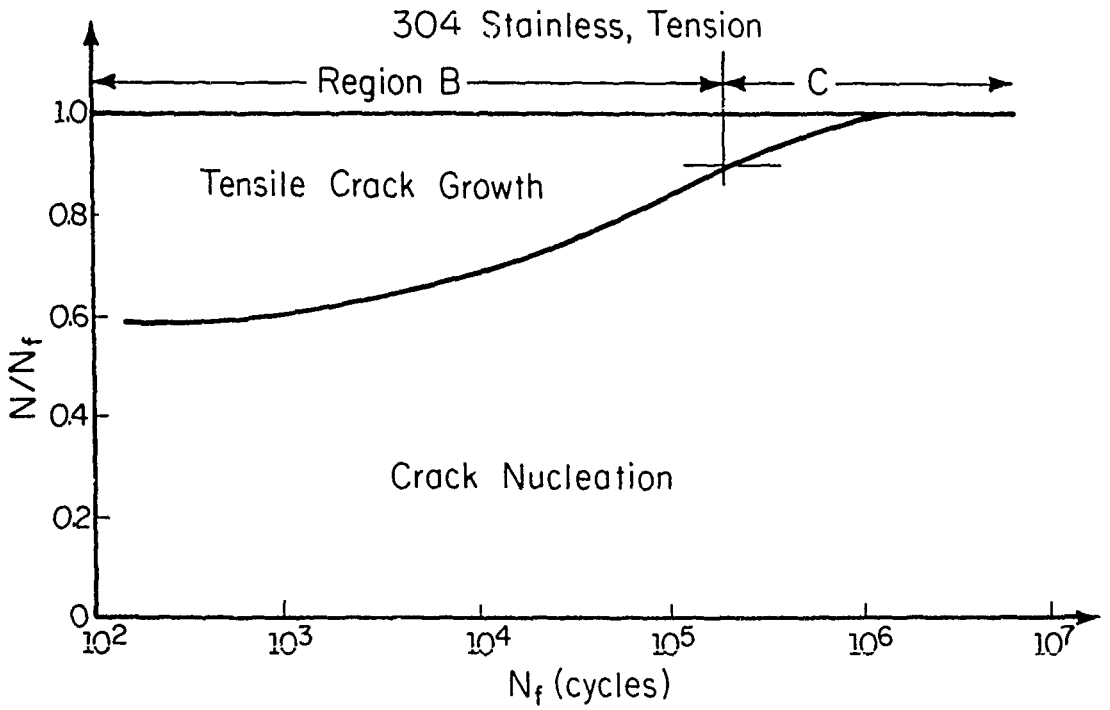


Figure 1 Cracking Behavior Observed in SS304
(a) Torsion (b) Tension

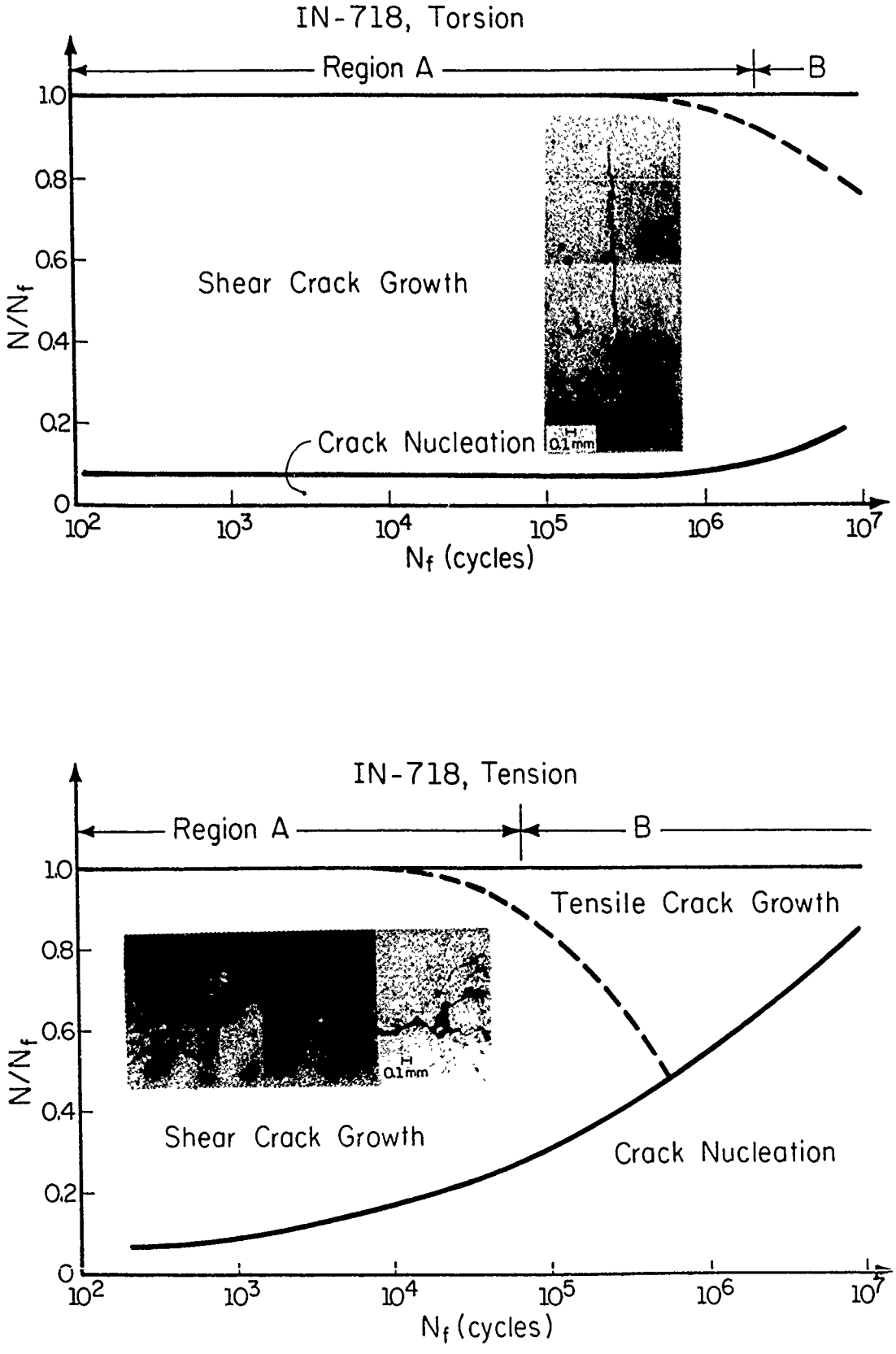


Figure 2 Cracking Behavior Observed in IN 718
(a) Torsion (b) Tension

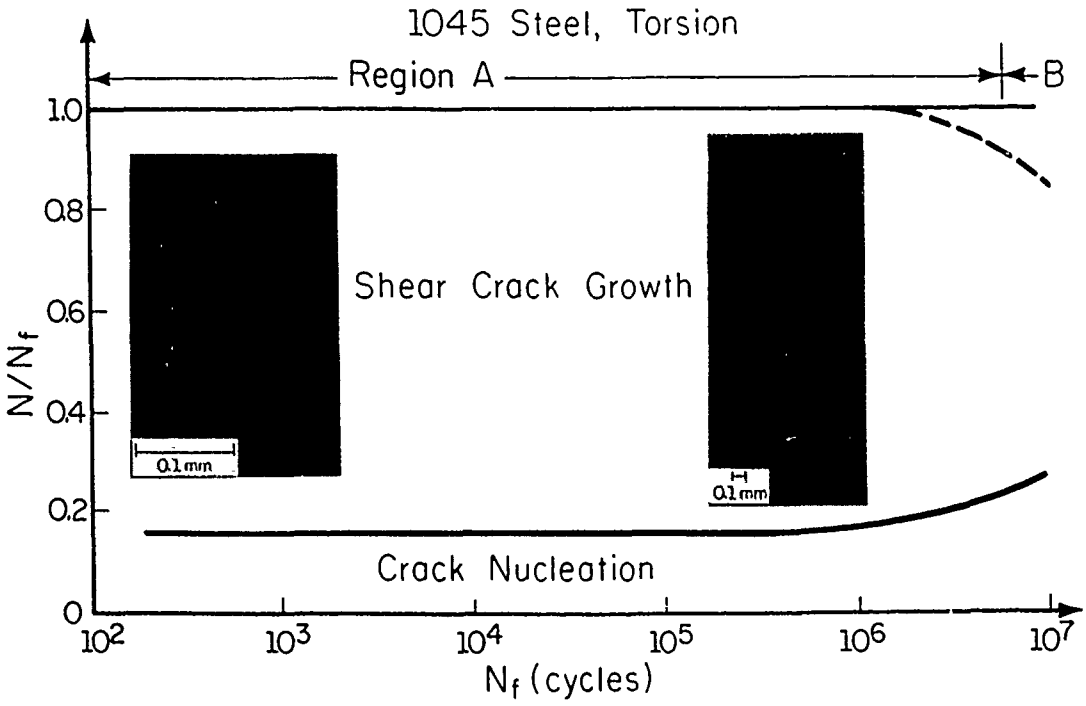


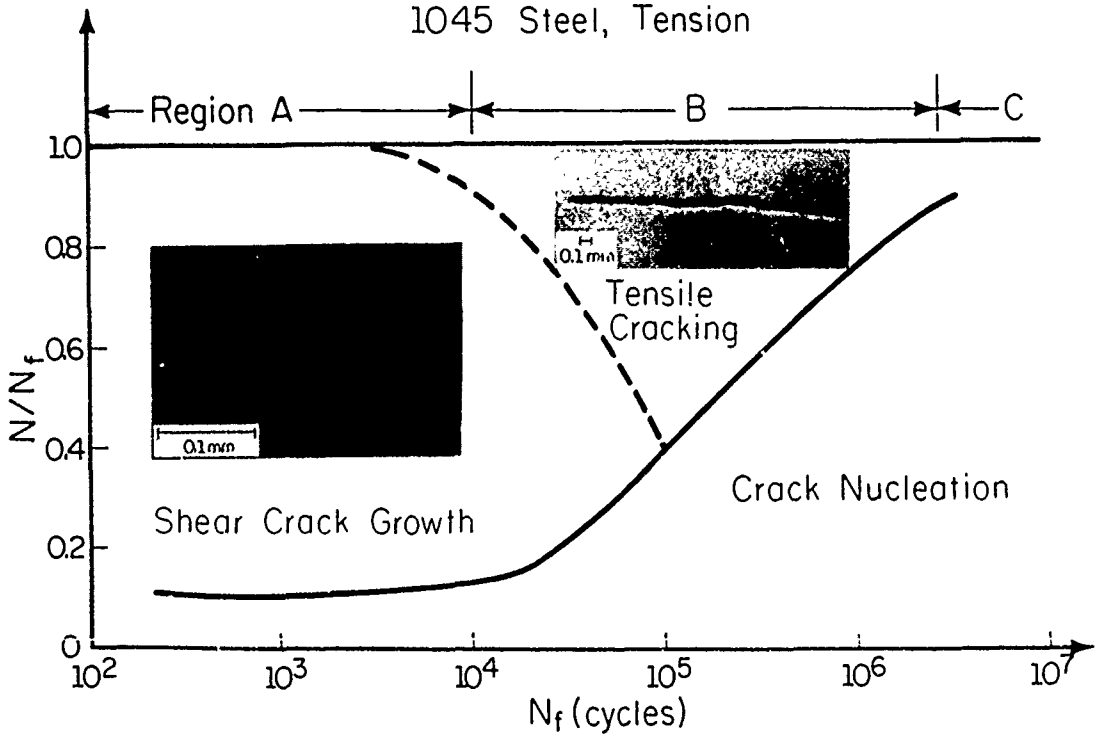


Figure 3 Cracking Behavior Observed inr SAE 1045
(a) Torsion (b) Tension

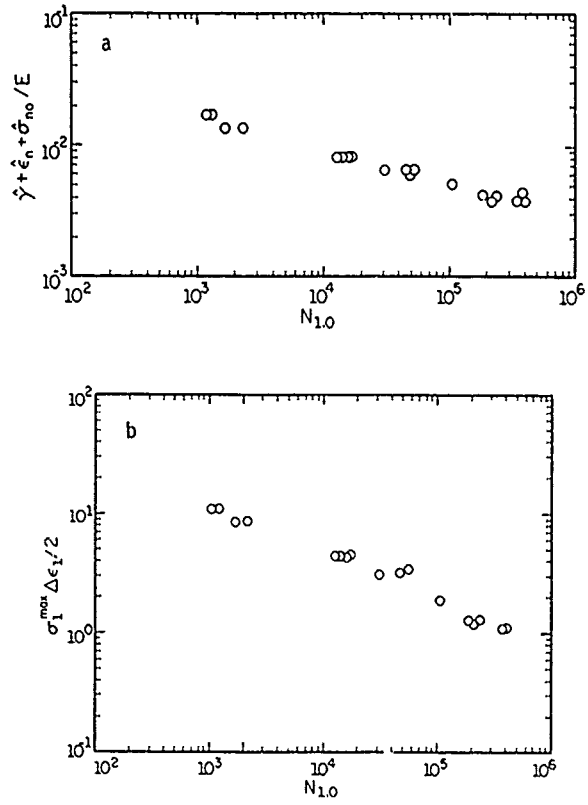


Figure 4 Uniaxial Data Correlation of Inccnel 718 with (a) Shear Strain Parameter (b) Tensile Strain Parameter

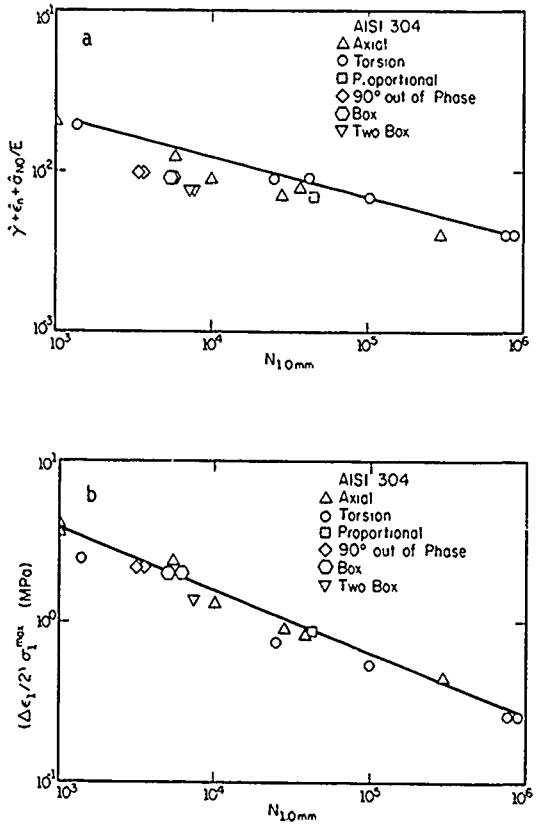


Figure 5 Correlations of SS 304 Test Data with (a) Shear Based Damage Parameter (b) Tensile Based Damage Parameter

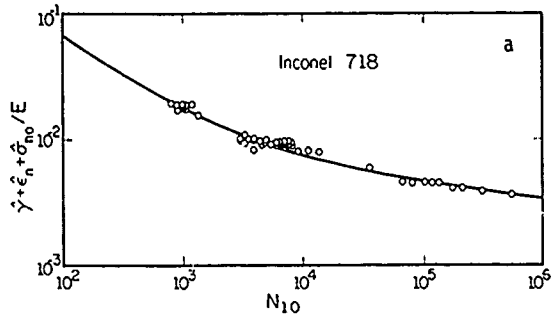


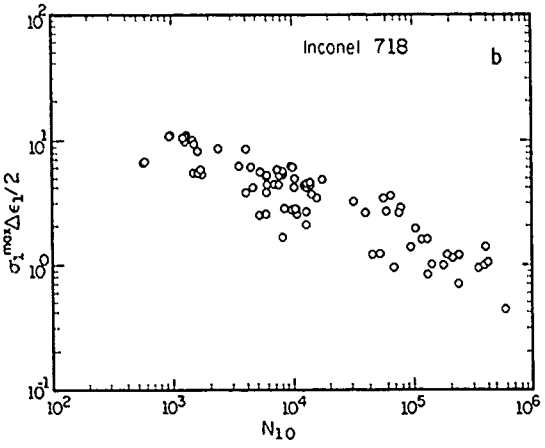


Figure 6 Correlation of Inconel 718 Test Data
(a) Shear Based Damage Parameter
(b) Tensile Based Damage Parameter

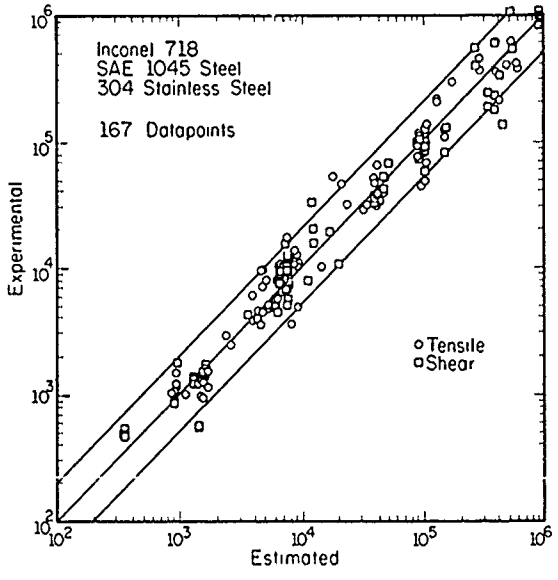


Figure 7 Correlation of Test Data Using Tensile and Shear Based Damage Parameters

# FATIGUE DAMAGE MECHANICS OF FIBRE COMPOSITES

Peter W R Beaumont

Dr Beaumont is a lecturer and the director of the Composite Materials Research Group in the University Engineering Department, Cambridge

## SYNOPSIS

The mechanics of fatigue damage in composite laminates is developed. Damage which results from such mechanisms as delamination and matrix cracking results in a loss of stiffness of the material. A change in stiffness is modelled in terms of the dominant mechanisms of failure and is used to monitor the accumulation of fatigue damage in the composite laminate. Catastrophic failure occurs when the damage exceeds a critical level which depends on the maximum stress in the cycle. These results can be applied to fatigue life prediction. However, life prediction for various block and random load sequences is less straightfoward. An acceleration in damage growth can be caused by block-loading interactions which can be included in the model empirically. Since the model considers the physical nature of damage, and empirically determines fatigue behaviour of composite laminates, the results can be extrapolated with far more confidence.

## INTRODUCTION

Fatigue damage in composite laminates accumulates with repeated load cycling and catastrophic failure occurs when a critical damage level is exceeded. Such damage can be in the form of fibre breakage, matrix cracking, splitting within plies and delamination between them. These modes of failure spread through the composite laminate until either the net section stress, (there is a loss of section caused by the damage), exceeds the tensile strength, or a crack of critical size, nucleated by the aggregation of microscopic damaging mechanisms, propagates catastrophically. The progressive accumulation of damage throughout the material's life-time is accompanied by changes in its stiffness.

Below, a damage accumulation model (Poursartip, Ashby and Beaumont, 1982, 1986; Poursartip, 1983) is proposed together with a general formulation based on fatigue damage and moduli changes. Next, experimental results are presented which identify and quantify damage mechanisms: delamination is dominant in a carbon fibre composite laminate and matrix cracking determines stiffness losses in a glass fibre composite laminate. These data are then used to determine a damage function, $f(D, R, \Delta\sigma)$, which shows the dependence of the damage accumulation rate, $dD/dN$, on the current level of damage, D, the load ratio, R, and the cyclic stress amplitude $\Delta\sigma$. This is a powerful approach: the function can be integrated for any stress history, $\Delta\sigma(N)$, to give, after N cycles, the current level of damage, D. Furthermore, when this damage exceeds a critical value, $D_f$, then catastrophic failure of the composite laminate takes place. Such a model has been used with some success to predict the S-N curve at constant and variable stress amplitude (Ogin, Smith and Beaumont, 1985a), and to predict the life-time for a variety of variable amplitude loading sequences (Poursartip and Beaumont, 1986).

The model is developed to show the relationship between stiffness changes and the accumulation of transverse-ply matrix cracks in a glass fibre composite laminate (Ogin, Smith and Beaumont, 1985a). The stress intensity factor, K, for a transverse-ply crack is derived and related to the rate of stiffness reduction using a Paris-type fatigue law (Ogin, Smith and Beaumont, 1985b).

## THE DAMAGE MODEL

Let the fatigue damage be measured by the variable data D. Cyclic loading causes the damage to increase from $D_i$ to $D_f$ at which point catastrophic failure of the composite laminate occurs. ($D_i$ is zero for undamaged material.) Assuming that the damage accumulation rate depends on the cyclic stress amplitude, $\Delta\sigma$, the load ratio, R, and on the current level of D, then:

$$\frac{dD}{dN} = f(\Delta\sigma, R, D) \qquad (1)$$

provided temperature, frequency, etc., are constant or have negligible effects. The life-time, $N_f$, (the number of cycles to increase D from $D_i$ to $D_f$) is therefore:

$$N_f = \int_{D_i}^{D_f} \frac{dD}{f(\Delta\sigma, R, D)} \qquad (2)$$

If a relation exists between, for example, the axial Young's modulus, E, of the composite laminate and the accumulated damage, D, we can write:

$$E = E_o g(D) \qquad (3)$$

where $E_o$ is the initial or unda aged modulus. Therefore:

$$\frac{1}{E_o}\frac{dE}{dD} = g'(D) \qquad (4)$$

where g' stands for the derivative of g with respect to D. Differentiating and substituting into Equation (1), we get:

$$\frac{1}{E_o}\frac{dE}{dN} = g'\left[g^{-1}\left(\frac{E}{E_o}\right)\right] f\left[\Delta\sigma, R, g^{-1}\left[\frac{E}{E_o}\right]\right] \qquad (5)$$

where $g^{-1}$ is the inverse of g:

$$D = g^{-1}\left(\frac{E}{E_o}\right) \qquad (6)$$

The function g(D) has to be established first, either experimentally or theoretically, before the function f can be determined. The function g(D) depends on the properties and lay-up of the composite laminate, not of how the damage, D, was introduced. Either a damage-accumulation function, $f(\Delta\sigma, R, D)$, is proposed, inserted into equation (5) and the result compared with experimental data, or data of $E/E_o$ is obtained as a function of N and, knowing g(D), the function $f(\Delta\sigma, R, D)$ is determined experimentally using:

$$f(\Delta\sigma, R, D) = \frac{1}{g'\left[g^{-1}\left(\frac{E}{E_o}\right)\right]} \frac{1}{E_o}\left(\frac{dE}{dN}\right) \qquad (7)$$

This is relatively straightforward; the right hand side of the equation is evaluated for different values of $\Delta\sigma$ at constant $E/E_o$ and R, for different values of R at constant $\Delta\sigma$ and $E/E_o$, and for different values of $E/E_o$ at constant $\Delta\sigma$ and R. The function f can then be determined from a plot of these results.

## THE DAMAGE MODEL APPLIED TO A QUASI-ISOTROPIC (45/90/-45/0)s CARBON FIBRE COMPOSITE LAMINATE

In the early stages of tension-tension fatigue, matrix cracks are observed in the 90 $^o$ plies, followed by matrix cracking of the 45 $^o$ plies, and then delamination crack growth between these off-axis layers. As fatigue damage progresses, delamination becomes the dominant mode of failure. Finally, fibre breakage and longitudinal splitting in the 0 $^o$ plies precedes final fracture (Poursartip, 1983; Poursartip, Ashby and Beaumont, 1986; Masters and Reifsnider, 1982).

The reduced (damaged) modulus, E, of the partially-delaminated composite laminate is given by (O'Brien, 1982):

$$E = E_o + (E^* - E_o)\frac{A}{A_o} \qquad (8)$$

where $E^*$ is the new modulus of a completely delaminated composite laminate into 2 (or more) separate sub-laminates (Fig. 1). Figure 2 shows a plot of normalised modulus, $E/E_o$, as a function of normalised delaminated area, $A/A_o$, where A is the actual delaminated area and $A_o$ is the total available interfacial area between plies. This empirical relation between the damaged modulus, E, and delaminated area, A, is clearly a linear one, with $E^* \approx 0.65E_o$ corresponding to complete delamination.

We can now define the damage parameter, D, as the normalised delaminated area $A/A_o$:

$$\left(\frac{A}{A_o}\right) = \frac{(E - E_o)}{(E^* - E_o)} \qquad (9)$$

and within the composite laminate only the 0 $^o$ plies remain undamaged. Thus the function g(D) in equation (3) can be expressed as:

$$g(D) = 1 - 0.35D \qquad (10)$$

for the $(45/90/-45/0)_s$ carbon fibre composite laminate.

Therefore:

$$D = 2.857\ (1 - E/E_o) \qquad (11)$$

and from equation (7):

$$f(\Delta\sigma, R, D) = -2.857\left(\frac{1}{E_o}\frac{dE}{dN}\right) \qquad (12)$$

### The damage rate as a function of stress amplitude

A typical set of data of $E/E_o$ versus N are shown in Figure 3. The modulus reduction rate is essentially linear. The damage rate, $dD/dN$, can be calculated using the derivative with respect to N of Equation (11):

$$\frac{dD}{dN} = -2.857\left[\frac{1}{E_o}\frac{dE}{dN}\right] \qquad (13)$$

Figure 4 shows experimental data of the damage rate, $dD/dN$ as a function of the stress range $\Delta\sigma$ for R = 0.1. Essentially, there are 3 regimes of behaviour:

(1) an apparent threshold stress of about 250 MPa below which no damage is detectable;

(2) between this threshold stress and cyclic stresses approaching the tensile strength of the composite laminate, the damage rate follows a power law relationship:

$$\frac{dD}{dN} = 9.2 \times 10^{-5}\left[\frac{\Delta\sigma}{\sigma_{TS}}\right]^{6.4} \qquad (14)$$

where $\sigma_{TS}$ = 586 MPa; and

(3) at stresses close to the tensile strength, $\sigma_{TS}$,

the damage rate is much higher than can be explained by the power law. Failure is now essentially a static one.

### The damage rate as a function of mean stress

Figure 5 shows data of damage rate, $dD/dN$, as a function of $\Delta\sigma$ for a range of values of R. For stresses close to the threshold stress, $\Delta\sigma$ = 220 MPa, for example, increasing the load ratio, R, from R = 0.1 to R = 0.53 accelerates the damage rate by a factor of 4 or more. At lower stress, $\Delta\sigma$ = 160 MPa, with R = 0.6, the damage rate can be predicted by extrapolation of the power law, as if no threshold stress existed. At even lower stresses, $\Delta\sigma$ < 120 MPa, where measurement of damage rates at R = 0.1 is difficult, an increase of load ratio, R > 0.5, produces a damage rate which appears independent of $\Delta\sigma$ and lies in the range $10^{-8}$ - $10^{-7}$ per cycle.

The data, replotted in the form $dD/dN$ versus mean stress, $\bar{\sigma}$, fit a power law relationship (Fig. 6). For stresses where $\Delta\sigma$ < 250 MPa:

$$\frac{dD}{dN} \propto (\bar{\sigma})^{2.7} \qquad (15a)$$

and for $\Delta\sigma$ > 250 MPa:

$$\frac{dD}{dN} \propto (\bar{\sigma})^{1.6} \qquad (15b)$$

The effect of mean stress, $\bar{\sigma}$, is such that:

$$\left[\frac{dD}{dN}\right]_{R > 0.1} = \left[\frac{dD}{dN}\right]_{R = 0.1} \times \left\{\frac{\bar{\sigma}\ (R > 0.1)}{\bar{\sigma}\ (R = 0.1)}\right\}^p \qquad (16)$$

where p = 2.7 at stresses below the threshold stress and p = 1.6 at stresses above the threshold stress.

### The terminal damage

The level of reduced (damaged) modulus at the fatigue life-time depends upon the maximum applied stress, $\sigma_{max}$ (Poursartip, Ashby and Beaumont, 1986).

Figure 7 shows the reduced modulus at failure is a linear function of $\sigma_{max}$. The reduced modulus (on the horizontal axis) is divided into 2 parts: for $(1 - E/E_o) < 0.35$, the damage due to delamination is $D_1$; for $(1 - E/E_o) > 0.35$, additional damage, $D_2$, is due to fibre breakage and splitting in the $0^o$ plies.

In the load-controlled fatigue experiments carried out by Poursartip (1983), the instantaneous strain, $\epsilon$, of the composite laminate increases as the damaged modulus, E, decreases with cycling, as one would expect. The fatigue life-time is reached when $\epsilon = \epsilon_c$. Under monotonic loading, assuming no modulus reduction, then:

$$\epsilon_c = \frac{\sigma_{TS}}{E_o} \qquad (17)$$

After some fatigue cycling at $\sigma_{max}$, the instantaneous strain is:

$$\epsilon = \frac{\sigma_{max}}{E} \qquad (18)$$

Since fast fracture occurs when $\epsilon$ during the fatigue cycle equals $\epsilon_c$, then, equating equations (17) and (18) and substituting for $D_f$ from equation (11), we have, at failure:

$$D_f = 2.857 \left[1 - \frac{E_f}{E_o}\right]$$

$$= 2.857 \left[1 - \frac{\sigma_{max}}{\sigma_{TS}}\right] \qquad (19)$$

The three broken lines in Figure 7 correspond to equation (19) where $\sigma_{TS}$ = 550, 600 and 650 MPa. The constant strain to failure criterion expains the data reasonably well.

Prediction of S-N curves

We can now substitute for $f\{\Delta\sigma, R, D\}$ from equations (14) and (16) into equations (1) and (2) which gives:

$$N_f = \int_{D_i}^{D_f} 1.1\times10^4 \left[\frac{\Delta\sigma}{\sigma_{TS}}\right]^{-6.4} \left\{\frac{\bar{\sigma}(R = 0.1)}{\bar{\sigma}(R > 0.1)}\right\}^P dD \qquad (20)$$

At the start of a constant-amplitude test $D_i = 0$. $D_f$ is determined using equation (19). We substitute for $\sigma_{max}$ and $\bar{\sigma}$ in terms of $\Delta\sigma$ and R. Integrating equation (20) and substituting from equation (19):

$$N_f = 3.11\times10^4 \left[\frac{\Delta\sigma}{\sigma_{TS}}\right]^{-6.4} \left[1.22\,\frac{1-R}{1+R}\right]^P \left[1 - \frac{\Delta\sigma}{(1-R)\sigma_{TS}}\right] \qquad (21)$$

Fig. 8 shows the S-N curve of the composite laminate for R = 0.1. The life-time prediction is shown by the solid lines, using equation (21) for $\sigma_{TS}$ = 550, 600 and 650 MPa. Good agreement between theory and experiment indicates consistency in our treatment of fatigue damage. Clearly, the low cycle fatigue behaviour is highly sensitive to changes in tensile strength.

Figure 9 shows the S-N curve when R = 0.5. In this example, only the number of cycles to failure were determined experimentally. Once again, agreement between theory and experiment reflects the validity of the model since these experimental results played no part in the determination of the constants in equations (14), (16), (19), (20), (21). The mean stress exponent in equation (21) was taken as p = 1.6, since the stress ranges of interest are high. Agreement between the predicted behaviour and measured data is good. Below 450 MPa, approaching the threshold stress, the predicted S-N curve is shown as a broken line, where $\sigma_{TS}$ = 600 MPa and p = 2.7 (high mean stress sensitivity).

Variable amplitude loading effects

Predicting life-time requires a knowledge of the average damage rate, $(dD/dN)_{av}$, and $D_f$ (equation 19). This critical damage, $D_f$, would be determined by the cycle with the highest maximum stress. Inserting an appropriate value of the tensile strength, $\sigma_{TS}$ into equation (19), between about 600 and 650 MPa, then:

$$0.476 < D_f < 0.659$$

In a series of block-loading experiments, (Poursartip and Beaumont, 1986), the measured value of $D_f$ is 0.644 which clearly falls between these limits.

Now consider two block loadings progressing for $N_1$ and $N_2$ cycles and having damage rates $(dD/dN)_1$ and $(dD/dN)_2$, respectively, where $(dD/dN)_{1,2}$ are determined using equation (14):

| | $N_{1,2}$ | $\Delta\sigma_{1,2}$ (MPa) | $R_{1,2}$ |
|---|---|---|---|
| Block 1 | 1000 | 395 | 0.2 |
| Block 2 | 2000 | 328 | 0.1 |

The total number of cycles in the block loading experiment is about 40,000.

Ignoring, for the time being, possible load interaction effects and assuming a linear sum of these damage rates, then:

$$\left[\frac{dD}{dN}\right]_{av} = \left[\frac{N_1}{N_1+N_2}\right]\left[\frac{dD}{dN}\right]_1 + \left[\frac{N_2}{N_1+N_2}\right]\left[\frac{dD}{dN}\right]_2 \qquad (22)$$

Using equation (14) to calculate $(dD/dN)_{1,2}$ and inserting these values into equation (22):

$$\left[\frac{dD}{dN}\right]_{av} = \frac{1}{3}(7.38\times10^{-6}) + \frac{2}{3}(2.25\times10^{-6})$$

$$= 4\times10^{-6} \text{ per cycle,}$$

which compares favourably with a measured average damage rate of $3.6\times10^{-6}$ per cycle (Poursartip and Beaumont, 1986). However, behaviour at low stress cannot necessarily be predicted from high stress range data. We now consider whether there are any load interaction effects when one block of cycles consists of small stress amplitude cycles.

Load interaction effects

Let an acceleration factor, A, due to load interaction be given by:

$$A = \frac{(dD/dN)_{obs}}{(dD/dN)_{pred}} \qquad (23)$$

where the predicted average damage rate, $(dD/dN)_{pred}$ is given by equation (22). If it turns out that A > 1, there is an acceleration in damage-rate; if A < 1, there is a retardation in damage-rate.

The results of a two-block loading sequence of experiments are shown in Figure 10 (Poursartip and Beaumont, 1986). To calculate $(dD/dN)_{pred}$ we used

measured values of $(dD/dN)_1 = 2\times10^{-6}$/cycle and $(dD/dN)_2 = 10^{-8}$/cycle. When the loading sequence contains less than 10% of the high stress amplitude cycles, then A = 2.8 (Fig. 10). Consequently, if we predict the damage rate for a wave form containing a large number of small amplitude cycles, then the linear summation of the individual damage rates (equation 22) will be a lower bound to the actual damage rate, at least 2 times too low.

## A MODIFIED DAMAGE MODEL APPLIED TO A CROSS-PLY $(0/90)_s$ GLASS FIBRE COMPOSITE LAMINATE

In tension-tension fatigue, the dominant mode of failure of a cross-ply glass fibre composite laminate is matrix cracking of the 90 $^{o}$ plies (Ogin, Smith and Beaumont, 1985a). Figure 11 is a schematic which shows a parallel array of idealised matrix cracks of average spacing 2s. In this case, the crack density, D ($= \frac{1}{2s}$), can be used as the damage parameter in the Poursartip, Ashby and Beaumont model:

$$\frac{dD}{dN} = f\ (\sigma_{max},\ D) \tag{24}$$

D uniquely defines the current level of damage due tc matrix cracking for a given set of test variables, load ratio R, frequency, temperature, and so forth.

The reduced (damaged) modulus, E, of the composite laminate as a result of matrix cracking is related to D in the following way (Steif, 1983):

$$E = E_o\ (1 - cD) \tag{25}$$

where $c = \frac{E_o}{E}\left[\frac{b+d}{b} - \frac{E_1}{E_o}\right]\frac{2}{\lambda}$, which equals 0.054 mm for this laminate:

$$\lambda = \left[\frac{3G(b+d)E_o}{d^2bE_2E_1}\right]^{\frac{1}{2}}\ ;\ \text{and}$$

$E_1$ and $E_2$ are the Young's moduli of the 0 $^{o}$ and 90 $^{o}$ plies of thickness b and d, respectively, and G is the shear modulus of the 90 $^{o}$ ply in the longitudinal direction (Figure 12).

Differentiating equation (25) with respect to the number of load cycles, N, and combining with equation (24):

$$-\frac{1}{cE_o}\frac{dE}{dN} = f\left[\sigma_{max},\ \frac{1}{c}\left(1 - \frac{E}{E_o}\right)\right] \tag{26}$$

As before, the difficulty is in finding the appropriate form of the function f.

One way of solving the problem is to consider the stored elastic strain energy, U, between 2 adjacent matrix cracks in the transverse ply (Ogin, Smith and Beaumont, 1985a):

$$U = \frac{K^2\sigma^2_{max}4sdW}{2E_2} \tag{27}$$

$K\sigma_{max}$ is that fraction of the applied stress on the laminate carried by the uncracked transverse ply and W is the laminate width.

The postulate is made, (which is supported by experimental data), that the total length, a, of all those matrix cracks increases with successive load cycles, and that the total crack growth rate obeys a power law function of the stored elastic strain energy, (Ogin, Smith and Beaumont, 1985a):

$$\frac{da}{dN} \propto (\sigma^2_{max}2s)^n \tag{28}$$

If we consider the average crack spacing, 2s, as a 'characteristic length', then the damage (crack) growth rate is proportional to some power of this characteristic distance. This is analogous to the Paris law of single crack mechanics of isotropic materials.

Since the crack density, E, is proportional to this total crack length, a, it follows, therefore, that:

$$\frac{dD}{dN} \propto \left[\frac{\sigma^2_{max}}{D}\right]^n \tag{29}$$

Alternatively, re-writing equation (29) in terms of the damaged modulus, E, (equation 25):

$$-\frac{1}{E_o}\frac{dE}{dN} \propto \left[\frac{\sigma^2_{max}}{E_o^2\ (1 - E/E_o)}\right]^n \tag{30}$$

where the introduction of the term $E_o^2$ makes the right hand side of the equation dimensionless. We now have a possible form of the function given by equation (26). The modulus reduction rate, $((-1/E_o)\ dE/dN)$, is simply the tangent to the experimental curve of $E/E_o$ versus N at any value of $E/E_o$ (Fig. 13). Figure 14 shows experimental data of reduced modulus over a range of maximum applied stress. The data fits a power law relation of the form:

$$-\frac{1}{E_o}\frac{dE}{dN} = A\left[\frac{\sigma^2_{max}}{E_o^2\ (1 - E/E_o)}\right]^n \tag{31}$$

where $A = 5.65 \times 10^4$ and n = 2.8.

It follows that the relationship between the current (damaged) modulus, E, the number of load cycles, N, and the maximum applied stress, $\sigma_{max}$, is:

$$\frac{E}{E_o} = 1 - \left[25.3\ \left(\frac{\sigma_{max}}{E_o}\right)^{1.48} N^{0.26}\right] \tag{32}$$

### The stress in a transverse ply containing matrix cracks

A cracked matrix of a transverse (90 $^{o}$) ply reduces the modulus of the composite laminate (equation 25) and affects the longitudinal stress, $\sigma_2$, in that 90 $^{o}$ ply (Ogin, Smith and Beaumont, 1984, 1985b). Now the average stored elastic strain energy between two neighbouring cracks (equation 27) can be more rigorously expressed as:

$$U = \frac{1}{V}\int_{-s}^{s}\left[\frac{\sigma_2^2\ W2d}{2E_2}\right]dx \tag{33}$$

where V is the volume of material between the 2 idealised matrix cracks spaced 2s apart (Fig. 11).

Given that, (from Steif's analysis described by Ogin, Smith and Beaumont, 1984):

$$\sigma_2 = \sigma\left[\frac{E_2}{E_o}\right]\left[1 - \frac{\cos h\ (\lambda_x)}{\cos h\ (\lambda_s)}\right] \tag{34}$$

where $\sigma$ is the applied stress on the laminate and integrating equation (33) gives:

$$U = \left[\frac{\sigma}{E_o}\right]^2 E_2 \frac{s}{k} \qquad (35)$$

approximately, for crack spacings between d and 3d, for which $E/E_o$ lies between 0.8 and 0.95. (k is a constant for a given value of $\lambda$ and is equal to 1.3 mm for this particular $(0/90)_s$ glass fibre composite laminate (Ogin, Smith and Beaumont, 1985b).

Re-writing the stored elastic strain energy, U, in terms of an average stress in the transverse ply, $\sigma_{av}$, and combining with equation (35), the average stress is given by:

$$\sigma_{av} = \frac{E_2}{E_o}\left(\frac{1}{k}\right)^{\frac{1}{2}} \sigma \sqrt{2s} \qquad (36)$$

Thus, $\sigma_{av}$ in the transverse ply falls off as the square root of the average crack spacing.

The stress intensity at the tip of a matrix crack

The re-distribution of localised stress around a tranverse ply crack relies on the adjacent intact $0^o$ plies. It follows, therefore, that there will be a localised stress disturbance close to the matrix crack tip only (Fig. 15). Since the size of this disturbance is roughly equal to one-half of the ply thickness, then an approximate expression for the crack tip stress intensity factor, K, is (Ogin, Smith and Beaumont, 1985b):

$$K = \sigma_{av} \sqrt{2d} \qquad (37)$$

This follows from recognising that the build-up of stress at the crack tip does not depend on crack length (Ogin, Smith and Beaumont, 1984). Combining equations (36) and (37):

$$K = \left[\frac{E_2}{E_o}\right]\left[\frac{2s}{k}\right]^{\frac{1}{2}} \sigma \sqrt{2d} \qquad (38)$$

Matrix crack growth rate

Equation (31) can now be interpreted in the form of the Paris law:

$$\frac{dz}{dN} = B K_{max}^m \qquad (39)$$

or using the total matrix crack length:

$$p\left(\frac{dz}{dN}\right) = p B K_{max}^m \qquad (40)$$

or

$$\frac{da}{dN} = p B K_{max}^m \qquad (41)$$

$dz/dN$ is the growth rate of a single matrix crack, p is a constant number of growing matrix cracks, (verified by experiment), and B and m are constants which depend on such variables as the load ratio R, mean stress, frequency, etc., and $da/dN$ is the total matrix crack growth rate.

Using the idealised model of a cracked laminate, the total matrix crack length, a, is given by:

$$a = \frac{WL}{2s} \qquad (42)$$

where W and L are the width and length of the composite laminate, respectively (Fig. 11). Re-writing equation (25):

$$\frac{E}{E_o} = 1 - \frac{c}{2s} \qquad (43)$$

Combining equation (43) with equation (42) and then differentiating with respect to N:

$$\frac{da}{dN} = \frac{WL}{c}\left[-\frac{1}{E_o}\left(\frac{dE}{dN}\right)\right] \qquad (44)$$

where $[-1/E_o (dE/dN)]$ is the tangent of the modulus reduction versus number of cycles curve at a given value of $E/E_o$.

From equation (38):

$$K_{max} \propto \sigma_{max} \sqrt{2s} \qquad (45)$$

Combining equations (41), (44) and (45) and substituting for the average crack spacing, 2s, (equation 43), we recover equation (31):

$$-\frac{1}{E_o}\left(\frac{dE}{dN}\right) = A\left[\frac{\sigma_{max}^2}{E_o^2 (1 - E/E_o)}\right]^n$$

Figure 16 shows a set of fatigue data plotted as total crack growth rate, $da/dN$, (equation 44) versus $K_{max}$, where $K_{max}$ is obtained by combining equations (38) and (43):

$$K_{max} = \left[\frac{E_2}{E_o}\right]\left[\frac{2\,dc}{k(1 - E/E_o)}\right]^{\frac{1}{2}} \sigma_{max} \qquad (46)$$

The value of c is 0.054 mm for this particular $(0/90)_s$ glass fibre composite laminate. While the range of $K_{max}$ between 0.3 and 1 MPa $\sqrt{m}$ is typical of sub-critical cracking in epoxy resins (Hertzberg and Manson, 1980), the corresponding total crack growth rates of the composite laminate are several orders of magnitude greater than observed for pure epoxy, some $10^{-4}$ - $10^{-2}$ mm/cycle. However, there are many hundreds of individual transverse ply cracks that contribute to the total crack growth, where the growth rate of any individual crack is very much smaller.

## FINAL COMMENTS

Composite structures generally spend much of their time in the 'non-linear' region of damage growth behaviour, precisely where threshold effects and load interaction effects have to be taken into account. The scatter in growth rates under these conditions is large for carbon fibre composite laminates, (for reasons that are not clear), so it is unrealistic to allow for these effects with anything more sophisticated than, say, an acceleration factor of 2 applied to the overall growth rate. This is considerably cruder than the retardation models used in fatigue crack propagation in metals, even though they are semi-empirical in nature as well. It is important to note that load interaction effects accelerate damage growth in composite laminates; the reverse is generally true for metals. Thus, with composite laminates, linear summation (equation 22) should not be used because it is non-conservative and dangerous (Poursartip and Beaumont, 1986).

In predicting the variable amplitude behaviour of the carbon fibre composite laminate, we assumed low values for the base growth rate and the load interaction acceleration factor, and for simplicity we did not include the mean stress effect in predicting fatigue life-term. As a result, we would expect our predicted

growth rates to be lower than those observed; this trend was born out. Nevertheless the predictions of the model are superior to Miner's rule (Poursartip and Beaumont, 1986). Since the model considers the physical nature of damage, and empirically determines the fatigue behaviour, the results can be extrapolated with far more confidence.

In general, the model predicts the fatigue behaviour of composite laminates with reasonable accuracy over a wide range of loading conditions. Furthermore, it not only provides a value for the life-time but it also predicts damage rates and failure levels, allowing for monitoring, up-dating, and assessment of the conditions of the composite laminate throughout the load cycling sequence.


## ACKNOWLEDGEMENTS

This work is primarily the result of studies of fatigue of composite laminates undertaken by Dr Anoush Pousartip and Dr Paul A. Smith, former graduate students, and Dr Stephen L. Ogin, former research fellow of the Composite Materials Research Group, Department of Engineering, University of Cambridge, England. I would like to praise them for the outstanding contributions they made to this subject as members of my research team. Also, I would like to thank Professor Michael F. Ashby for his contribution to the modelling and numerous invaluable discussions.

Parts of this work were financially supported by the Science and Engineering Research Council of Great Britain, the U.S. Army European Research Office in London, England, and the European Space Agency, Noordwijk, The Netherlands.


## REFERENCES


1. Hertzberg, R. W. and Manson, J. A., Fatigue of Engineering Plastics, Academic Press, Inc., New York, 1980.

2. Masters, J E., and Reifsnider, K. L., "An investigation of cumulative damage development in quasi-isotropic graphite-epoxy laminates", Damage in Composite Materials, ASTM STP 775, 1982, pp.40-62, (ed. by K. L. Reifsnider).

3. O'Brien, T. K.,"Characterisation of delamination onset and growth in a composite laminate", Damage in Composite Materials, ASTM STP 775, 1982, pp.140-167, (ed by K. L. Reifsnider).

4. Ogin, S. L., Smith, P. A., and Beaumont, P. W. R., "Transverse ply crack growth and associated stiffness reduction during the fatigue of a simple cross-ply laminate", CUED/MATS/TR.105 (September), Cambridge University Engineering Department, Cambridge, England.

5. Ogin, S. L., Smith, P. A., and Beaumont, P. W. R., "Matrix cracking and stiffness reduction during the fatigue of a $(0/90)_s$ GFRP laminate", Composite Science and Technology, 22, 1985a, pp.23-31.

6. Ogin, S. L., Smith, P. A., and Beaumont, P. W. R., "A stress intensity factor approach to the fatigue growth of transverse ply cracks", Composite Science and Technology, 24, 1985b, pp.47-59.

7. Poursartip, A., Ashby, M. F., and Beaumont, P. W. R., "Damage accumulation during the fatigue of composites", Scripta Metallurgica, 16 (5), 1982, p.601-606.

8. Poursartip, A., "Aspects of damage growth in fatigue of composites", 1983. Ph.D. Thesis, University of Cambridge, England.

9. Poursartip, A., Ashby, M. F., and Beaumont, P. W. R., "The fatigue damage mechanics of a carbon fibre composite laminate: I-Development of the model", Composites Science and Technology, 25, 1986a, pp.193-218.

10. Poursartip, A., and Beaumont, P. W. R., "The fatigue damage mechanics of a carbon fibre composite laminate: II-life prediction", Composites Science and Technology, 25, 1986b, pp.283-299.

11. Steif, P. S., 1983, private communication.


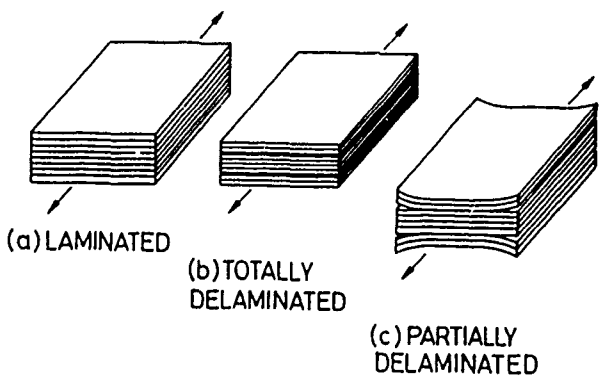


Fig. 1 O'Brien's model showing a composite laminate in various states of delamination, (after O'Brien, 1982).

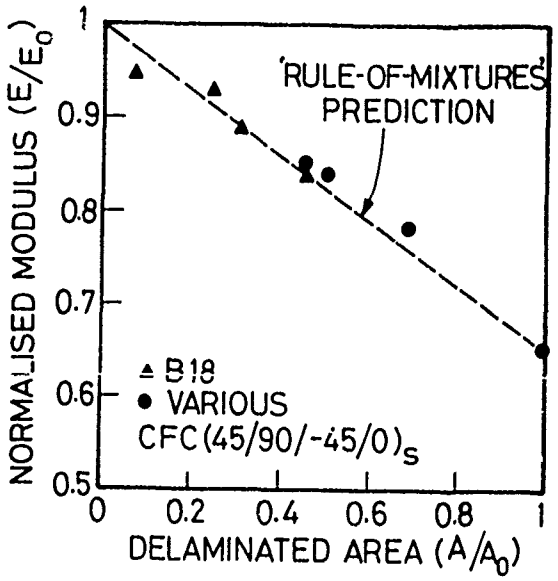


Fig. 2 Normalised modulus as a function of normalised delamination area.

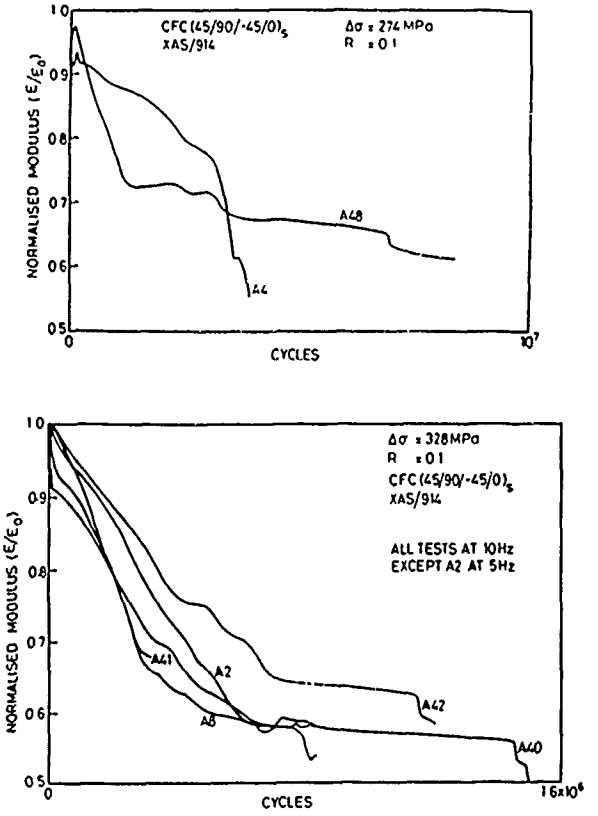


Fig. 3 Typical experimental plots of normalised modulus, $E/E_0$, versus number of cycles.

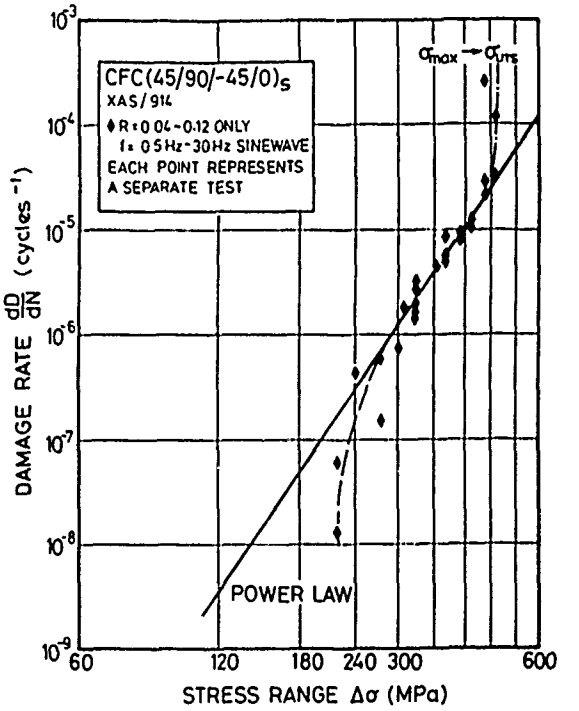


Fig. 4 The damage rate as a function of the applied stress range ($R \lesssim 0.12$).

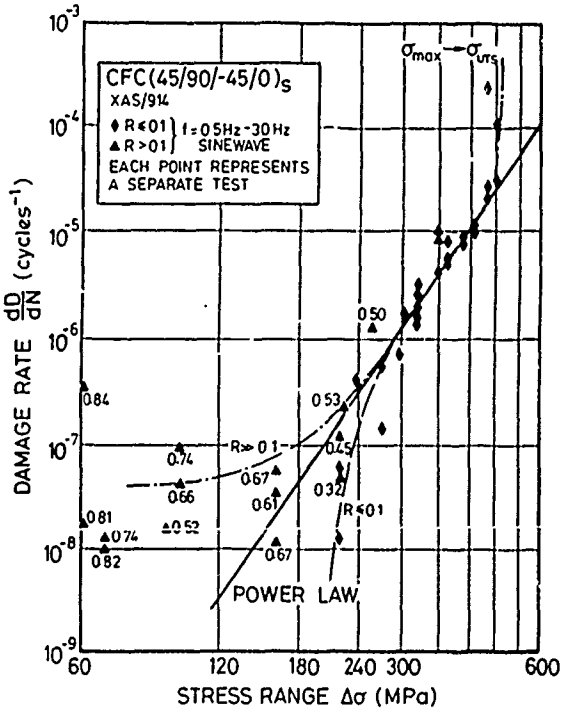


Fig 5 The damage rate as a function of the applied stress range for various values of load ratio R

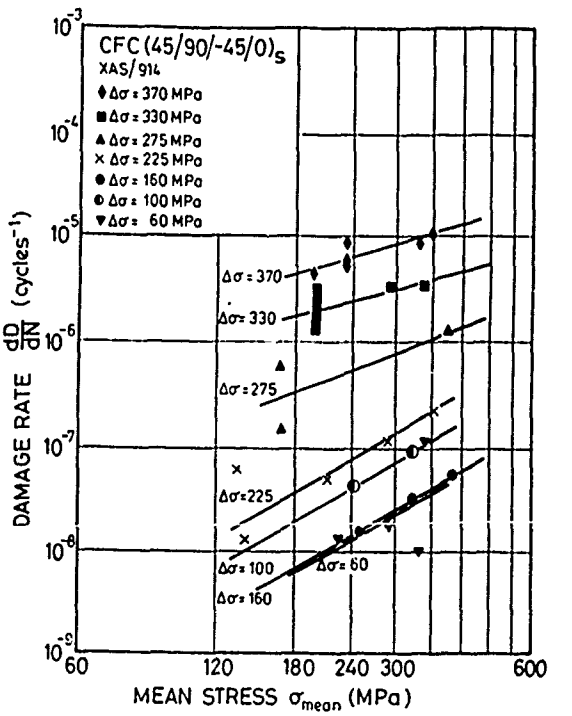


Fig. 6 The damage rate as a function of the applied mean stress.

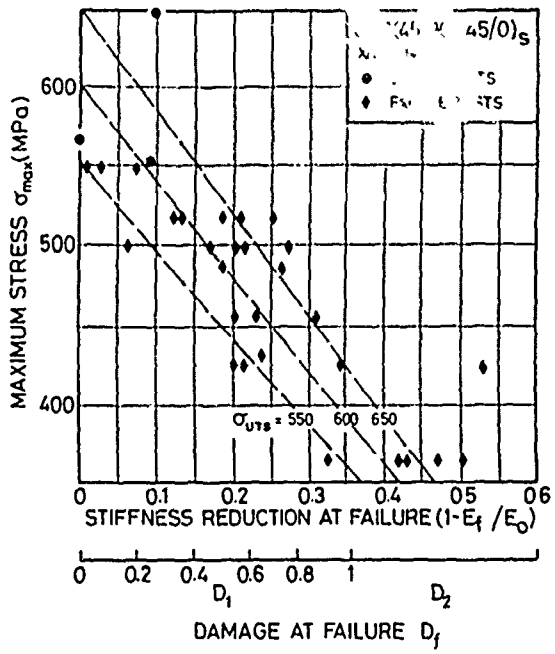


Fig. 7 Relation between maximum stress and stiffness reduction of damage at failure. The broken lines correspond to eqn (19).

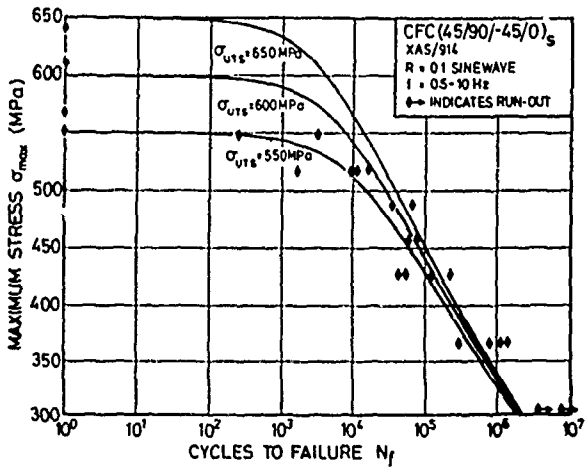


Fig. 8 S-N curve for tension-tension fatigue, (R = 0.1). The solid lines correspond to eqn (21).

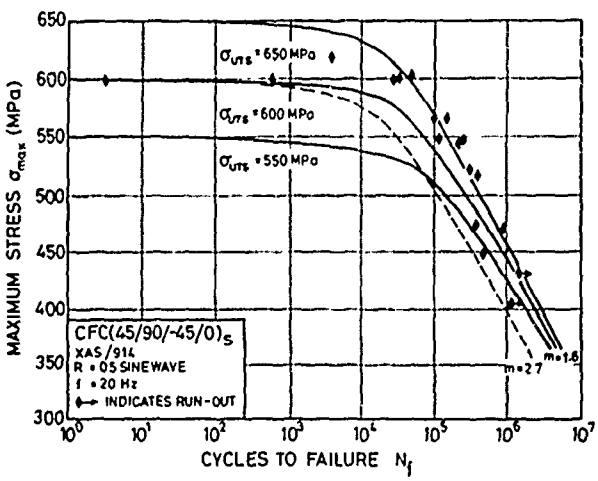


Fig. 9 S-N curve for tension-tension fatigue, (R = 0.5). The solid lines correspond to eqn (21). The broken line corresponds to a tensile strength of 600 MPa and p = 2.7 and a stress amplitude below 450 MPa.

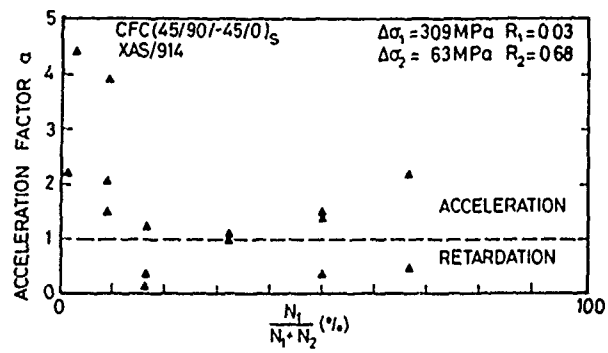


Fig. 10 Observed acceleration of growth rates in two-block loading fatigue tests as a function of the percentage of high load cycles.

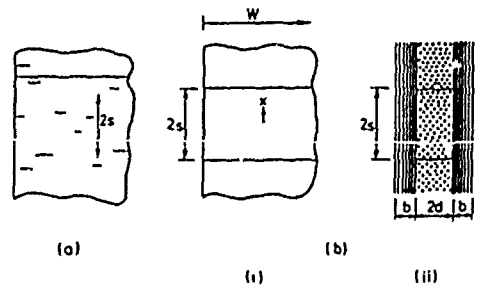


Fig. 11 A schematic of a cracked (0/90)s composite showing real and idealised geometry: (a) real crack distribution; (b) idealised crack distribution - 1 front view, 2 edge view.

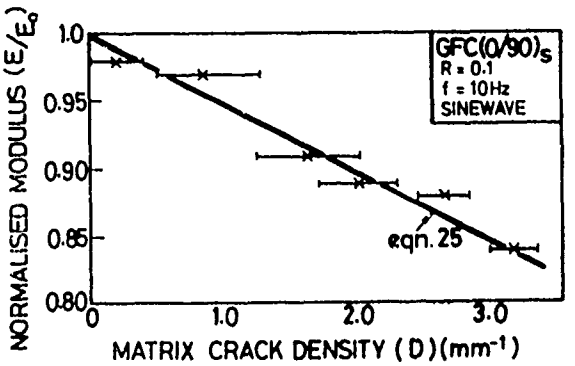


Fig. 12 Normalised modulus as a function of matrix crack density.

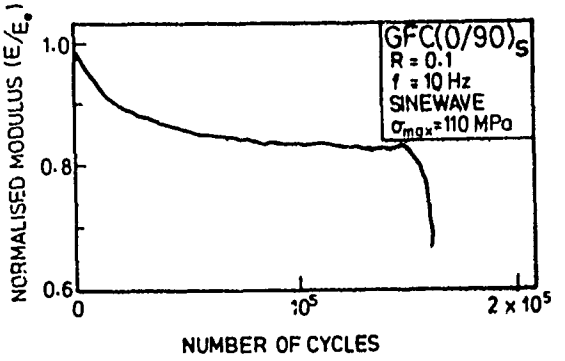


Fig. 13 A typical stiffness reduction curve for a (0/90)s glass fibre composite laminate.

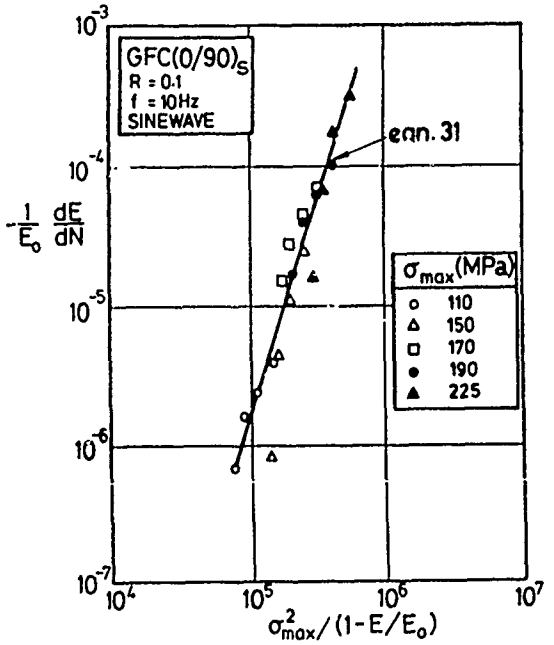


Fig. 14 A plot of maximum aplied stress and reduced stiffness. The solid line is predicted using equation (30).

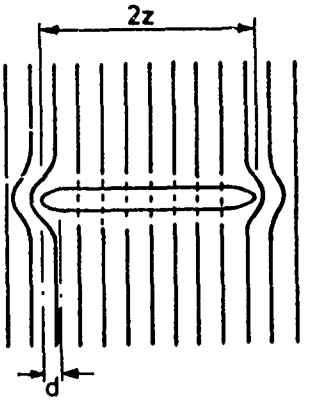


Fig. 15 Schematic of the stress distribution around a transverse ply crack-elevation of mid-plane of crack, length 2z. The dotted lines indicate load being diverted around the crack via the $0^o$ plies.

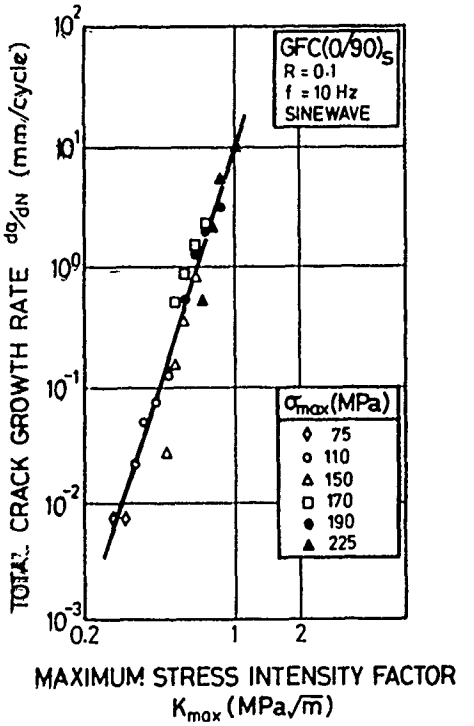


Fig. 16 Total crack growth rate in the transverse ply versus maximum stress intensity factor.

□

# PHYSICALLY-BASED CONSTITUTIVE EQUATIONS FOR CREEP AND PLASTICITY: CYCLIC DEFORMATION

G. A. Henshall and A. K. Miller

G. A. Henshall is a postdoctoral research associate in the Department of General Mechanics at the Technical University of Braunschweig, FRG; A. K. Miller is professor (research) in the Materials Science and Engineering Department at Stanford University, USA.

SYNOPSIS

The physical-phenomenological approach to modeling creep and plasticity, and its advantages compared with empirical or purely mechanistic methods, are discussed. To illustrate the physical-phenomenological approach, modeling of cyclic deformation is described in detail, with emphasis upon the Bauschinger effect, cyclic hardening, softening, and saturation. The mechanisms and physics of cyclic deformation are first reviewed, and then their implementation within the MATMOD-BSSOL constitutive equations is described. Finally, simulations and independent predictions using MATMOD-BSSOL are shown to compare favorably with a variety of cyclic data. Equally important, the internal behavior of the model is shown to be consistent with the physical processes believed to control cyclic deformation.

## 1) INTRODUCTION

Constitutive equations describe the mechanical behavior of materials through relationships among the macroscopic variables of stress, strain (or their rates), and temperature. For physically-based models the effects of the changing microstructure are also included in the description. Technologically there are many problems in which accurate predictions of nonelastic deformation are necessary for conditions involving wide variations in temperature, stress, and strain rate, including cyclic stresses and strains of varying amplitude and frequency. To handle such complex deformation histories, it has been recognized that the constitutive equations must have a physical or mechanistic basis [1-3]. Empirical approaches are simply not reliable for these complex problems because they do not account for the internal changes that occur in the material.

A great deal of work has been done to develop micro-mechanical or "first principles" models of nonelastic deformation. In such models the basic building blocks are quantitative equations governing specific elementary physical processes, and the variables in those equations are the actual physical entities involved, for example dislocation density, local internal stress, etc. These building blocks are assembled into models of more complex processes, but the key feature is that there is a discrete representation of the actual internal physical entities of importance. Although increasingly complex dislocation processes are represented in these models, they still treat only a limited number of phenomena [4]. Thus, first principles models have not led to general-purpose constitutive equations which can treat complex deformation histories [5]. Currently, therefore, the only reliable way to treat complex nonelastic deformation problems is with models developed through mechanistic-inspired phenomenology [1,5].

A brief description of the "physical-phenomenological" approach to constitutive modeling is presented here; a more complete discussion may be found elsewhere [3]. As first suggested by Hart [2], and now generally agreed, the proper way to handle the history dependence of nonelastic deformation is through a "unified" set of equations containing a single nonelastic strain rate variable, $\dot{\varepsilon}$. A "kinetic" equation is then written to describe the dependence of $\dot{\varepsilon}$ on the stress, temperature, and a small number of internal (or hidden) variables that represent the microstructure. These internal variables evolve during deformation, and are governed by separate "structure evolution" equations for their rates of change. The framework of the constitutive model is therefore:

$$\dot{\varepsilon} = f(\sigma, T, X), \qquad (1)$$

$$\dot{X} = g(\dot{\varepsilon}, T, X), \qquad (2)$$

where $\sigma$ is the stress, T is the absolute temperature, and X denotes the structure variables. The choice of internal structure variables is guided by the underlying mechanisms and physics of nonelastic deformation, which in most cases are related to dislocation motion [1,3,5]. In the MATMOD approach discussed in this paper, the concept is to have each structure variable represent one category of physical strengthening mechanisms. For example, some mechanisms strengthen the material in all directions, notably hardening due to overall forest dislocation density and subgrain size; other mechanisms, such as pile-ups or bowed subgrain walls, produce internal stresses that strengthen (or weaken) the material directionally. Thus, at least two types of internal structure variables are needed to represent these two different categories of strengthening. Fortunately, the number of categories of strengthening mechanisms is much less than the number of phenomena to be treated, so relatively few structure variables are needed.

In addition to the choice of variables, deformation physics governs the forms of the structure evolution equations. These equations are designed so that the behavior of the structure variables imitates what we believe to be the behavior of the actual physical variables under the same conditions. Once the mechanistically-inspired forms of the equations have been determined, actual algebraic expressions (applicable to the entire class of materials) are then derived by fitting a variety of mechanical test data. It is emphasized that these phenomenological equations are derived so that the behavior of both the externally-measured and the internal variables duplicate the observed response of real materials. This gives the model a degree of physical meaning and reliability which is not present in simple empirical equations. In summary, the data fitting provides the means for obtaining accurate simulations for a variety of simple histories, while the use of physics provides the means for obtaining reasonable predictions for complex loading histories.

Physical-phenomenological constitutive modeling is a broad topic. This paper focuses only upon cyclic deformation because of its technological importance, and because cyclic straining is often a part of more complex deformation histories [9]. In the following sections we first review the mechanisms and physics underlying cyclic behavior, including: the Bauschinger effect and hysteresis loop shape, and the related phenomena of cyclic hardening, softening, and saturation. The way in which these physical processes are represented within the MATMOD-BSSOL constitutive equations is then described. Finally, MATMOD-BSSOL calculations are compared with a variety of cyclic data to

demonstrate the capability of these equations to simulate cyclic deformation.

## 2) MECHANISMS AND PHYSICS OF CYCLIC DEFORMATION

### 2.1) Hysteresis Loop Shape and the Bauschinger Effect

Simulation of the correct stress-strain hysteresis loop shape, particularly the Bauschinger effect (B.E.), is technologically important, for example in fatigue modeling and life prediction. The B.E. is defined as the reduction in the magnitude of the stress necessary to begin nonelastic deformation in the "reverse" direction (e.g. compression) following prestraining in the "forward" direction (e.g. tension). The B.E. leads directly to the well-rounded hysteresis loops usually observed experimentally; in the absence of a B.E. reverse yielding would be sudden, with a sharp yield point [7].

It is generally accepted that the interaction of dislocations with the internal back stress fields of polarized dislocation structures accounts for the major portion of the B.E. [7]. As shown by TEM observations of curved primary dislocations in copper by Mughrabi [6], and postulated by many investigators, the magnitude of these back stresses is statistically distributed. Consistent with these observations, Lowe and Miller [8] have considered the effects of variations in the magnitude, spatial extent, and evolution kinetics of back stresses on the shape of the hysteresis loop. Their conclusions are described briefly below.

Reversing the direction of straining causes rapid rearrangement of the shorter-range back stresses, which arise from simple metastable dislocation configurations such as tangles and small pile-ups. The longer-range back stresses, however, are associated with more stable dislocation structures, such as bowed subgrain walls. Since these substructures rearrange slowly, the longer-range back stresses change slowly. This physical picture is supported by the data of Quesnel and Tsou [15] shown in Figure 1. Immediately following a reversal in the straining direction the internal back stress changes very rapidly, but as reversed straining proceeds the back stress changes more slowly. This disparity in the rates of internal back stress evolution leads to a smoothly curving hysteresis loop.

Colinearity of the back stress and strain rate directions is another physical concept that helps to explain the shape of the hysteresis loop, particularly in the microplastic regime. Following Lowe and Miller [8], changes in internal stress are expected to be slow when the internal stress and strain rate are parallel, or vectorially colinear, because dislocations must be activated through the existing internal stress field. Upon a stress reversal, however, the internal stress state changes rapidly, as shown in Figure 1, because the internal stress assists dislocation motion and associated structural changes. Specific mechanisms may involve dislocation or subgrain unbowing and lowering of pile-up intensity.

### 2.2) Cyclic Hardening, Softening, and Saturation

Three important and related cyclic phenomena are cyclic hardening, softening, and saturation. Cycling at a particular strain amplitude, $\Delta\varepsilon$, produces hardening or softening, and eventually leads to a stable, or saturated hysteresis loop. For wavy slip mode materials, for example Cu, Al, and Fe, the stable hysteresis loop is history-independent [11]. For these materials the cyclic saturation stress, $\sigma_{sat}$, (defined as half the saturated stress amplitude) depends only on the applied $\Delta\varepsilon$, and is substantially less than the monotonic steady state flow stress, $\sigma_{ss}$, for the same temperature and strain rate. The data of Abdel-Raouf and Plumtree [10] given in Figure 2 clearly show that cycling at a particular $\Delta\varepsilon$ leads to a unique saturated stress. In particular, note that the flow stress produced by 25% monotonic straining, which must be less than the steady state flow stress, is reduced by cycling at a strain amplitude of 2.8%.

The first clue to the physical causes of cyclic saturation comes from examining cyclic microstructures. The main features of these microstructures are the heterogeneous substructures produced, such as cells, veins, persistent slip bands (PSBs), etc. [7, 10-12]. All of these structures contribute to the isotropic strength of the material, and have a scale (e.g. cell size) that depends only upon $\Delta\varepsilon$ for a given temperature and strain rate [10,11]. Compared with monotonic microstructures, however, the cyclic ones are lower energy configurations [11,12]. Furthermore the internal back stresses produced by cyclic deformation are lower than those produced by monotonic deformation [7,11,12].

Based upon these observations, Miller [3] has proposed a simple, but plausible, physical picture explaining the dependence of $\sigma_{sat}$ on $\Delta\varepsilon$ and the fact that it is less than $\sigma_{ss}$. As deformation proceeds in a given direction, dislocations are forced against obstacles, building up back stresses. As these back stresses become more intense, dislocations climb and cross-slip around these obstacles, producing three-dimensional dislocation substructures, such as cells, and thus isotropic hardening. If deformation is monotonic, large back stresses can be built up, leading to substantial isotropic strength. When the direction of deformation is reversed, however, dislocations glide out of pile-ups and do not tend to climb and cross-slip until they form pile ups consistent with the new straining direction. In cyclic deformation the straining direction is repeatedly changed, and if $\Delta\varepsilon$ is small, the pile-ups (or other polarized structures) never become intense and there is little driving force for isotropic hardening. As $\Delta\varepsilon$ increases, the peak pile-up intensity (at the strain limits) increases, and there is more isotropic strengthening. This simple picture is consistent with the TEM observations made by Grosskreutz and Mughrabi [12] on Cu, Fe, and Al single crystals. These investigators found that secondary glide activity, which pins down sources of internal stress (such as pile-ups), is less during cyclic deformation than during monotonic straining. Since secondary slip is necessary to form heterogeneous substructures, this implies that the isotropic strength is also reduced by cyclic deformation. In summary, the peak back stress level is a unique function of $\Delta\varepsilon$ (for a given $\dot{\varepsilon}$ and T), and the isotropic strength is directly linked to the peak level of back stress.

If the stress has some value other than $\sigma_{sat}$ because of prior thermo-mechanical treatment, then cycling at a particular $\Delta\varepsilon$ will cause cyclic hardening or softening until the corresponding $\sigma_{sat}$ is reached. These changes in the stress are, of course, associated with microstructural changes. For example, Feltner and Laird [11] observed increases in cell size during cyclic softening of pure Cu, eventually leading to a cell size equal to that produced by cycling annealed Cu at the same reduced $\Delta\varepsilon$.

Figure 3 demonstrates another aspect of cyclic softening, namely the bias of the hysteresis loop in the direction of the strain immediately preceding cyclic straining at the lower $\Delta\varepsilon$. This behavior is apparent from the differences in the magnitudes of the positive and negative peak stresses, which persists for several cycles (see points 4 - 15 in Figure 3) This phenomenon is observed whether the prestrain was part of a larger amplitude cyclic history or monotonic straining. As shown by Lowe [13], decreases in the isotropic strength cause symmetric decreases in the cyclic peak stress Asymmetric decreases in the cyclic peak stress are therefore caused by back stresses biased in the direction of the prestrain These slowly relaxing (and therefore long range) back stresses then decay over a period of several cycles.

## 3) PHYSICAL-PHENOMENOLOGICAL MODELING OF CYCLIC DEFORMATION USING THE MATMOD APPROACH

The MATMOD (MATerials MODel) approach consists of a family of models developed over the past decade with the goal of treating complex deformation histories. The physical-phenomenological approach described in Section 1 was employed in developing all of these models. A full description of the evolution of MATMOD over the years has recently been given by Miller [3]; only the latest and most complete version, MATMOD-BSSOL, is presented in detail here. The methods used to model cyclic deformation with these equations were adopted from earlier versions of MATMOD [8,14].

The MATMOD-BSSOL (Back Stresses from SOLutes) equations are given in one-dimensional form in Figure 4. Note that $\dot{\varepsilon}$ represents the nonelastic strain rate, $\sigma$ the applied stress, T the absolute temperature, k Boltzman's constant, and sgn the "signum" function, except for the structure variables listed in Table 1, the remainder of the symbols represent material constants. The extension of these equations to three dimensions has been described elsewhere [16], and does not affect the present discussion. The three-dimensional version of the equations was in fact used for the calculations presented in Section 4. Derivation of the MATMOD-BSSOL equations and a full discussion of their capabilities has been given by Henshall [16] Only an overview of the model is presented here.

Following the format of equations (1) and (2), the nonelastic strain rate is given as a function of stress, temperature (through $\Theta$), and five internal structure variables in the kinetic equation at the top of Figure 4. Unlike most other models, temperature

appears explicitly in the equations through the physically meaningful Arrhenius-like $\Theta'$ terms. The material constants in the model are therefore temperature independent. This is important for modeling variable temperature deformation histories, as demonstrated by the authors through MATMOD simulations of thermal fatigue [17].

As discussed in Section 1 and summarized in Table 1, each of the five MATMOD-BSSOL structure variables represents a distinct category of strengthening mechanism, and corresponds to a particular feature of the microstructure. $F_{sol}$, which is a function only of the current nonelastic strain rate and temperature, allows the equations to simulate peaks in the curve of stress versus temperature that are associated with dynamic strain aging. The other structure variables represent features of the dislocation substructure that evolve during deformation. Rate equations for these variables are given in Figure 4, and follow the common (and physically meaningful) strain hardening-recovery format. Athermal plateaus in the curve of stress versus temperature, which are caused by solute additions, are simulated through the rapid hardening and mechanically activated recovery of $R_A$, the short range back stress variable. Steady state creep of Class I solid solution alloys with a stress exponent of three is represented through thermal recovery of $R_A$. The treatment of solute strengthening through the evolution of short range back stresses is the major conceptual difference between MATMOD-BSSOL and previous versions of MATMOD. Finally, it is emphasized that the equations cover a broad range of behavior, as summarized in Figure 5, even though the following discussion focuses only upon cyclic deformation.

3.1) The Bauschinger Effect

In keeping with the micro-mechanics described in Section 2, the B.E. is modeled through the back stress variables, $R_A$ and $R_B$, which are subtracted from the applied stress in the kinetic equation. Some of the older versions of MATMOD contain only a single back stress variable, leading to the prediction of square hysteresis loops (which is a problem with many constitutive models [9]). As discussed in Section 2, however, a statistical distribution of back stresses, with widely varying rearrangement kinetics, exists in real materials. Lowe and Miller [8] therefore introduced separate short range, $R_A$, and long range, $R_B$, back stress variables in the MATMOD-4V equations. This improvement has been retained in MATMOD-BSSOL. The rate equations shown in Figure 4 (and the values of the material constants) control the evolution kinetics of the back stress variables, and allow $R_A$ to change much more rapidly than $R_B$ following a reversal in the straining direction. Behavior similar to that shown in Figure 1 can therefore be simulated.

Following the method described by Lowe and Miller [8], colinearity of the back stress and strain rate is included in both the $\dot{R}_A$ and $\dot{R}_B$ equations. Consider, for example, the first two terms in the $\dot{R}_A$ equation:

$$\dot{R}_A \sim H_1 \dot{\varepsilon} - A_1 \left[\left(\frac{3}{2}|R_A|\right)^{m_1}\right] \cdot \frac{R_A|\dot{\varepsilon}|}{F_\rho} \quad , \qquad (3)$$

where $H_1$, $A_1$, and $m_1$ are material constants. The first term represents hardening, which is driven by the magnitude and direction of the nonelastic strain rate. The second term represents mechanically activated dynamic recovery. Straining in the positive strain rate direction increases the value of $R_A$, causing the dynamic recovery term to contribute negatively to $\dot{R}_A$ and hence to reduce $\dot{R}_A$. Upon a reversal in the direction of straining $\dot{\varepsilon}$ becomes negative, but the dynamic recovery expression continues at first to contribute negatively to $\dot{R}_A$ due to the presence of the absolute value of the strain rate. The dynamic recovery term therefore acts together with the hardening term to drive $R_A$ quickly toward zero, and eventually to negative values. Thus, when $R_A$ and $\dot{\varepsilon}$ are parallel (of similar sign for uniaxial deformation) the dynamic recovery term reduces the rate of hardening, but when $R_A$ and $\dot{\varepsilon}$ are anti-parallel the dynamic recovery term enhances the rate of change of $R_A$.

3.2) Cyclic Hardening, Softening, and Saturation

In the modeling of cyclic hardening, softening, and saturation, the major phenomena of interest are that $\sigma_{sat}$ is less than $\sigma_{ss}$, and that $\sigma_{sat}$ is a function only of $\Delta\varepsilon$. The physical picture of cyclic saturation given in the previous section suggests that these phenomena are caused by a coupling between isotropic strengthening and the level of back stress. In the MATMOD approach this coupling is represented through interactions between the structure variables in the evolution equations. Examination of Figure 4 shows that in MATMOD-BSSOL there are interactions between $\dot{F}_\lambda$ and $R_B$, $\dot{R}_B$ and $F_\lambda$, and $\dot{F}_\rho$ and $F_\lambda$. The interactions between $F_\lambda$ and $R_B$ represent the close connection between the evolution of long range back stresses and the formation of heterogeneous dislocation substructures [6,7,13]. The interaction with $F_\lambda$ in the $\dot{F}_\rho$ equation represents the relationship between dislocation density and subgrain size that has been observed in several cyclically saturated materials [12].

The structure variable interaction most critical in controlling cyclic saturation is present in the hardening term of the $\dot{F}_\lambda$ equation, which is given in equation (4):

$$\dot{F}_\lambda \sim H_4\left[C_4 + \frac{3}{2}|R_B| - \left(\frac{H_3}{A_3}\right) F_\lambda\right] |\dot{\varepsilon}| \quad , \qquad (4)$$

where $H_3$, $A_3$, $H_4$, and $C_4$ are material constants. The key feature of equation (4) is that the evolution rate of $F_\lambda$, the isotropic strengthening variable, is driven by the back stress variable $R_B$. The $-(H_3/A_3)F_\lambda$ term produces a dynamic equilibrium between $R_B$ and $F_\lambda$. Thus, as $R_B$ goes through a cycle, $F_\lambda$ increases or decreases until the negative contribution from this term exactly offsets the positive contribution from $C_4+3/2\cdot|R_B|$. With this equation, since the average and peak values of $R_B$ increase as $\Delta\varepsilon$ increases, the saturated value of $F_\lambda$ also increases with increasing $\Delta\varepsilon$. In addition, cyclic hardening or softening are simulated if $F_\lambda$ starts out at a value other than its unique saturated value for the imposed $\Delta\varepsilon$. Physically this is consistent with the changes in cell size observed by Feltner and Laird [11] during cyclic hardening and softening of Cu. It is also worth noting that directional strain softening can be modeled through equation (4), as previously shown by the authors [17].

The cyclically saturated value of $F_\rho$ is also a unique function of $\Delta\varepsilon$ and is lower that its steady state value. This behavior is produced by the simple interaction with $F_\lambda$ in the hardening term of the $\dot{F}_\rho$ equation. Phenomenologically, this interaction is especially important in modeling cyclic saturation at low strain amplitudes.

## 4) SIMULATIONS AND PREDICTIONS OF CYCLIC DEFORMATION

This section presents simulations and predictions of cyclic deformation performed, except in one case, using the MATMOD-BSSOL equations. The MATMOD-BSSOL material constants for pure aluminum used to produce these results are given in Table 2[1]. Before presenting the calculations, the terms "simulation" and "prediction" are defined. A simulation refers to calculations in which the data being simulated have been used to evaluate some of the material constants in the model. Predictions, on the other hand, are completely independent of the data against which they are compared. The results of independent predictions particularly demonstrate the extent to which the physics of deformation have been properly represented in the model.

Figure 6 compares the MATMOD-4V prediction of the room temperature hysteresis loop for pure Al deformed at a total strain amplitude of 1.77% with the data of Ziaai [7]. The overall shape of the hysteresis loop is well predicted. The accuracy of the predicted B.E. and initial microplasticity following a reversal in the straining direction is particularly noteworthy. These features of the hysteresis loop are accurately predicted because two independent back stress variables are present in the equations, just as in MATMOD-BSSOL. $R_A$ changes rapidly following a reversal in the direction of straining, particularly because of the colinearity term described in Section 3, and allows the model to simulate

[1] The MATMOD-BSSOL material constants have also been determined for Al-1% Mg, Al-3% Mg, Al-5% Mg [16], and for mild steel and two HSLA steels [19]. Approximate constants for Udimet 700, a Ni-base superalloy, have also been determined [20].

microplastic reverse yielding[2]. $R_B$ changes more slowly and allows the model to simulate the gradual curvature of the hysteresis loop later in the transient. In principle, MATMOD-BSSOL can also predict proper hysteresis loop shapes since it contains all of these ingredients. Unfortunately, the material constants used to date in the $R_A$ equation (which were chosen largely to give the proper temperature dependence of the flow stress at low strains) cause $R_A$ to change so rapidly following a strain reversal that the loops are overly square [16,17].

Figure 6 also demonstrates that MATMOD-4V is capable of predicting cyclic hardening. A demonstration of this capability in the MATMOD-BSSOL equations is provided in Figure 7. In this figure the calculated peak tensile stress is compared with the data of Ziaai [7] for pure aluminum deformed at room temperature. The calculations at $\Delta\varepsilon$=1.8% represent a simulation of the data, but the other calculations are independent predictions. The rate of cyclic hardening predicted by MATMOD-BSSOL is slightly low at the lowest $\Delta\varepsilon$ and too rapid at the largest $\Delta\varepsilon$. Cyclic hardening is simulated by MATMOD-BSSOL because the peak values of all the state variables increase toward their saturated values for that particular strain amplitude. The behavior of the model is therefore consistent with the increases in dislocation density and the formation of heterogeneous substructures observed in real materials and described in Section 2.

The saturated cyclic stress-strain curve for pure Al predicted using MATMOD-BSSOL is compared with the data of Ziaai [7] in Figure 8. The simulated monotonic $\sigma_{ss}$ is also shown in Figure 8 by the dashed line. Some constants in the model were evaluated from the value of $\sigma_{sat}$ at $\Delta\varepsilon$ = 1.8%, thus the overall level of the calculated curve is really a simulation. The slope and curvature of the MATMOD-BSSOL curve, however, are independent predictions of the model. MATMOD-BSSOL predicts that $\sigma_{sat}$ is less than $\sigma_{ss}$ and is a unique function of strain amplitude because of the structure variable interactions described in Section 3. The accuracy of the prediction indicates that the physical processes leading to cyclic saturation in pure aluminum have been well represented in the model.

Predictions of cyclic strain softening in cold-worked pure Al are given in Figure 9. These predictions were obtained by simulating a 30% tensile prestrain, resulting in a stress of approximately 70 MPa, and then cycling at a strain amplitude of 1%. The magnitudes of the positive and negative peak stresses have then been plotted as a function of the number of cycles. Large monotonic (or high amplitude cyclic) prestrains cause the MATMOD-BSSOL structure variables to be larger than their low $\Delta\varepsilon$ saturation values. Cycling at low strain amplitude therefore results in softening. As demonstrated elsewhere [16], the overall softening in Figure 9 is the result of a reduction in the peak values of $R_B$, $F_\rho$, and $F_\lambda$.

The bias of the hysteresis loop in the direction of the prior prestrain, which was discussed in Section 2 and illustrated in Figure 3, is also predicted. This behavior is indicated by the differences between the positive and negative peak stresses in Figure 9. The prestrain history for the data in Figure 3 was not the same as that used to produce the predictions shown in Figure 9, so quantitative comparisons between the two are not possible. Qualitatively, however, the predictions show the same behavior as the data, particularly regarding the dissipation of the bias after several cycles. As shown by Henshall [16], the bias in the peak stresses predicted by MATMOD-BSSOL is caused by a gradual decrease in the level of the long range back stress, $R_B$, over several cycles. Thus, the internal workings of the model, not just the predicted macroscopic behavior, are consistent with the behavior of real materials.

[2] Lowe and Miller [8] have also shown MATMOD-4V predictions of microplasticity during partial unloadings followed immediately by reloading in the original direction. The success of these predictions implies that the equations are capable of modeling low-temperature cyclic creep [18].

## 5) SUMMARY AND CONCLUSIONS

The physical-phenomenological approach to constitutive modeling has been described. For complex loading histories this approach has the advantages of providing more reliable extrapolations than empirical or purely phenomenological models, and the ability to treat a wider range of phenomena than purely mechanistic models. In general, physical-phenomenological models describe the dependence of a single nonelastic strain rate variable on the stress, temperature, and a small number of internal structure variables. Equations for the rates of change of these structure variables are developed to describe the evolution of the microstructure during deformation. The underlying physics and mechanisms of deformation are used to guide the choice of structure variables and the overall form of the equations. Phenomenological trends in mechanical test data are used to derive the specific algebraic expressions.

The mechanisms and physics of cyclic deformation have been reviewed, focusing on the Bauschinger effect, and cyclic hardening, softening, and saturation. The importance of internal back stresses that evolve at widely different rates, and the link between the back stress level and isotropic strengthening have been emphasized.

The MATMOD-BSSOL equations, which treat a very broad range of deformation behaviors, have been presented as the most recent version of the MATMOD family of constitutive equations. The blend of physics and phenomenology used to model cyclic deformation has been described. Emphasis has been placed upon the use of separate long range and short range back stress variables, and the interactions between the structure variables to produce a "saturated state" that is a function only of strain amplitude.

Finally, simulations and independent predictions using this model have been compared with a variety of cyclic data for pure aluminum. The calculations generally compare favorably with the data. Equally important, the internal behavior of the model is consistent with the physical processes believed to control cyclic deformation. It is this consistency between deformation physics and internal model behavior that provides the capability to successfully predict nonelastic deformation under complex thermo-mechanical loading conditions.

## REFERENCES


1) A.S. Argon, in Constitutive Equations in Plasticity, A.S. Argon, Ed., MIT Press, 1-22 (1975).
2) E.W. Hart, *Acta Met.*, **18**, 599-610 (1970).
3) A.K. Miller, in Unified Constitutive Equations for Creep and Plasticity, A.K. Miller, Ed., Applied Science Publishers, 139-219 (1987).
4) W.D. Nix, J.C. Gibeling, and D.A. Hughes, *Met. Trans.*, **16A**, 2215-2226 (1985).
5) E.W. Hart, *J. Eng. Matls. Tech.*, **106**, 322-325 (1984).
6) H. Mughrabi, in Constitutive Equations in Plasticity, A.S. Argon, Ed., MIT Press, 199 - 250 (1975).
7) A A. Ziaai-Moayyed, PhD Dissertation, Stanford University (1981).
8) T.C. Lowe and A.K. Miller, *J. Eng. Matls. Tech.*, **108**, 365-373 (1986).
9) K.P. Walker, NASA Report CR-165533 (1981).
10) C.E. Feltner and C. Laird, *Acta Met.*, **15**, 1621-1653 (1967).
11) H. Abdel-Raouf and A. Plumtree, *Met. Trans* , **2**, 1251-1254 (1971).
12) J C. Grosskreutz and H. Mughrabi, in Constitutive Equations in Plasticity, A.S. Argon, Ed., MIT Press, 251-326 (1975).
13) T. C. Lowe, PhD Dissertation, Stanford University (1981).
14) A.K. Miller, *J. Eng. Matls. Tech.*, **96H**, No. 2, 97-105 (1976).
15) J.C. Tsou and D.J. Quesnel, *Matls. Sci & Eng.*, **56**, p.289 (1982).
16) G A Henshall, PhD Dissertation, Stanford University (1987).
17) G.A. Henshall and A.K. Miller, Proc. Second International Conference on Low Cycle Fatigue and Elasto-Plastic Behavior of Materials, K.T. Rie Ed., Elsevier Applied Science Publishers, 184-191 (1987).
18) E. Krempl, *J. Mech. and Phys. Solids*, **27**, 363-375 (1979).
19) R. O. Adebanjo, PhD Dissertation, Stanford University (1987).
20) H. Wei, Masters Thesis, Stanford University (1988).

Table 1. Description of the MATMOD-BSSOL Structure Variables

| Variable | Definition | Microstructural Significance |
|---|---|---|
| $R_A$ | Short range back stresses | Bowing of individual dislocations, small dislocation pileups |
| $R_B$ | Long range back stresses | Bowing of subgrain walls, large pileups |
| $F_\rho$ | Isotropic strain hardening due to homogeneously distrubuted obstacles | Forest dislocations, small dislocation tangles, sessile dislocations |
| $F_\lambda$ | Isotropic strain hardening due to heterogeneously distrubuted obstacles | Subgrair , cells, large dislocation networks, persistent slip bands |
| $F_{sol}$ | Interactive solute strengthening | Mobile solutes that interact with strain hardening |

Table 2.
The MATMOD-BSSOL Material Constants foi Pure Aluminum

| | | | |
|---|---|---|---|
| B | $1.0 \times 10^4$ $s^{-1}$ | $A_1$ | $5.00 \times 10^{24}$ |
| d | 2.0 | $A_3$ | $1.50 \times 10^{-8}$ |
| $T_t$ | 461 K | $A_4$ | $5.50 \times 10^3$ |
| $Q^*$ | 35,500 cal/mol | $C_2$ | $1.25 \times 10^4$ |
| k | 1.987 cal/mol | $C_4$ | $1.50 \times 10^{-6}$ |
| $H_1$ | 5.0 | $C_5$ | $7.53 \times 10^7$ |
| $H_2$ | $3.33 \times 10^{-4}$ | $D_1$ | $6.00 \times 10^{22}$ |
| $H_3$ | $1.20 \times 10^{-3}$ | $D_2$ | $5.00 \times 10^3$ |
| $H_4$ | $4.00 \times 10^{-4}$ | $m_1$ | 8.0 |
| $G_2$ | $3.00 \times 10^{-5}$ | $m_2$ | 1.9 |
| $q_1$ | 3.1 | n | 5.0 |
| $q_3$ | 0.5 | | |

Notes:

1. $F_{sol,max}$ is set to 0 for pure metals; the other $F_{sol}$ constants are not needed.
2. $A_2$ is a function of $H_1$, $A_1$, $C_2$, and $m_1$ and is automatically computed [16].
3. Young's modulus: $E(T) = E_o + T \cdot E_1 + T^2 \cdot E_2$
   $E_o = 1.16 \times 10^4$ ksi, $E_1 = -4.392$ ksi/°K,
   $E_2 = -1.55 \times 10^{-3}$ ksi/°K$^2$

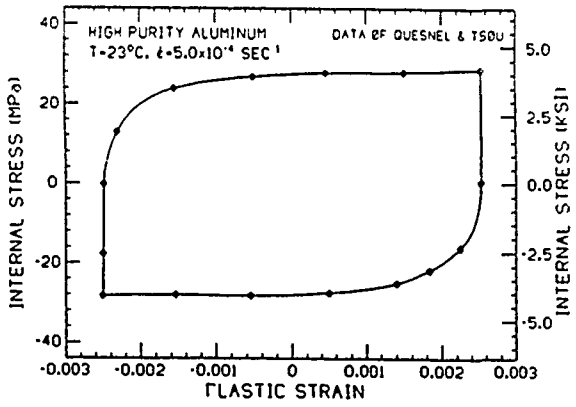


Fig. 1. Internal stress levels determined from stress relaxations initiated during saturated cyclic deformation. Data of Tsou and Quesnel [15]. (After Lowe and Miller [8]).

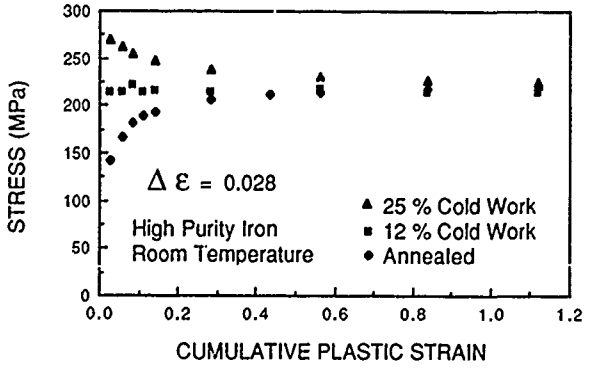


Fig. 2. Peak tensile stress as a function of accumulated plastic strain for iron deformed cyclically at room temperature. Data of Abdel-Raouf and Plumtree [10].

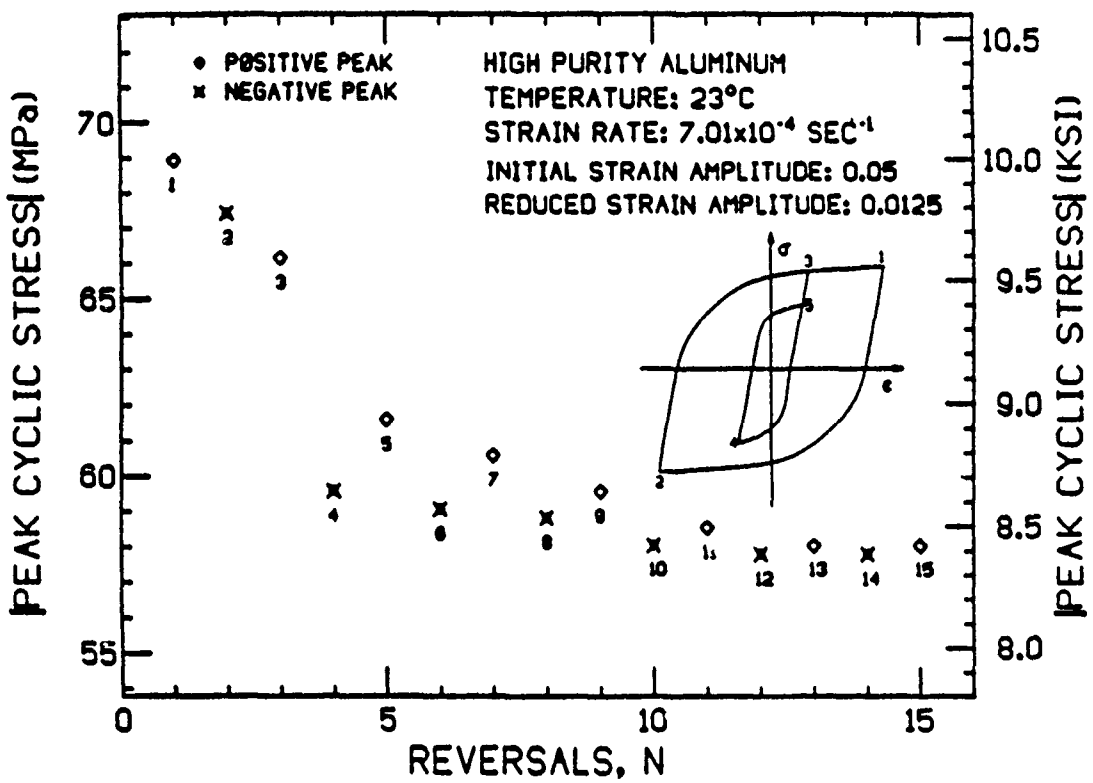


Fig. 3. The magnitudes of the tensile and compressive peak stresses during cyclic softening of aluminum. The imposed strain history is shown in the inset. Data of Lowe [13].

$$\dot{\varepsilon} = B\Theta' \left\{ \exp\left[ \frac{\left|\sigma/E - \frac{3}{2}(R_A + R_B)\right|}{\sqrt{F_\lambda + F_\rho(1 + F_{sol})}} \right] - 1 \right\}^d \quad \mathrm{sgn}\left[\sigma/E - \frac{3}{2}(R_A + R_B)\right]$$

$$\dot{R}_A = H_1 \dot{\varepsilon} - A_1 \left[ \left(\frac{3}{2}|R_A|\right)^{m_1} \right] \cdot \frac{R_A |\dot{\varepsilon}|}{F_\rho}$$

$$- H_1 B\Theta' D_1 \left[ \left(\frac{3}{2}|R_A|\right)^{q_1} \right] \left\{ 1 - \exp\left[ -D_2 \left(\frac{3}{2}|R_A|\right)^{m_2} \right] \right\} \cdot \mathrm{sgn}(R_A)$$

$$\dot{F}_\rho = H_2' |\dot{\varepsilon}| - H_2' B\Theta' \left\{ \exp\left[ A_2 F_\rho^{\left(\frac{1}{m_1+1}\right)} + C_2 \sqrt{F_\rho} \left[ \ln\left\{ \left(\frac{|\dot{\varepsilon}|}{B\Theta'}\right)^{1/d} \right\} \right] \right] \right\}^n$$

$$H_2' = H_2 \left[ G_2 - \left( F_\rho / F_\lambda^{q_3} \right) \right]$$

$$\dot{R}_B = H_3 \dot{\varepsilon} - \left( \frac{A_3 R_B |\dot{\varepsilon}|}{F_\lambda} \right)$$

$$\dot{F}_\lambda = H_4 \left[ C_4 + \frac{3}{2}|R_B| - \left(\frac{H_3}{A_3}\right) F_\lambda \right] |\dot{\varepsilon}|$$

$$- H_4 C_4 C_5 B\Theta' \left\{ \exp\left[ A_4 \sqrt{F_\lambda} \left( \ln\left\{ \left(\frac{|\dot{\varepsilon}|}{B\Theta'}\right)^{1/d} + 1 \right\} \right) \right] - 1 \right\}^n$$

$$F_{sol} = F_{sol,max} \exp\left[ -\left( \frac{\log(Z) - \log(Z_{max})}{\beta} \right)^2 \right] \quad ; \quad Z \equiv \frac{\dot{\varepsilon}}{\Theta'_{sol}}$$

$$\Theta' = \begin{cases} \exp\left\{ \left[ -\frac{Q^*}{kT_t} \right] \left[ \ln\left(\frac{T_t}{T}\right) + 1 \right] \right\} & ; T < T_t \\ \exp\left(-\frac{Q^*}{kT}\right) & ; T \geq T_t \end{cases}$$

$$\Theta'_{sol} = \exp\left(-\frac{Q_{sol}}{kT}\right)$$

Fig. 4. The one-dimensional MATMOD-BSSOL equations.

1. General "plasticity", including:
   (a) essentially elastic behavior followed by gradual yielding
   (b) strain rate sensitivity, including negative values for alloys deformed at intermediate temperatures, and large positive values for alloys deformed at high temperatures
   (c) temperature sensitivity, including peaks and plateaus for alloys

2. Steady state "creep", including:
   (a) power-law and power-law breakdown
   (b) Class I behavior with a constant stress exponent approximately equal to 3
   (c) change in stress exponent from 3 to 5 corresponding to the change from Class I to Class II behavior
   (d) dependence of the steady state creep rate on solute concentration

3. Cyclic stress-strain behavior, including:
   (a) Bauschinger effect
   (b) cyclic hardening and softening
   (c) shakedown to a saturated condition of constant stress or strain amplitude
   (d) hysteresis loop asymmetry

4. Primary creep, including:
   (a) the stress dependence of the primary creep strain

5. Recovery, including:
   (a) static recovery at high temperatures
   (b) dynamic recovery

6. Strain softening, including:
   (a) unidirectional strain softening
   (b) directional strain softening
   (c) cyclic strain softening

7. Complex histories, including:
   (a) stress changes
   (b) strain rate changes
   (c) temperature changes
   (d) creep-plasticity interaction
   (e) yield stress plateaus in cold-worked materials
   (f) multiaxial deformation

8. Interactions of all the above

Fig. 5. Summary of the phenomena modeled by the MATMOD-ESSOL constitutive equations.

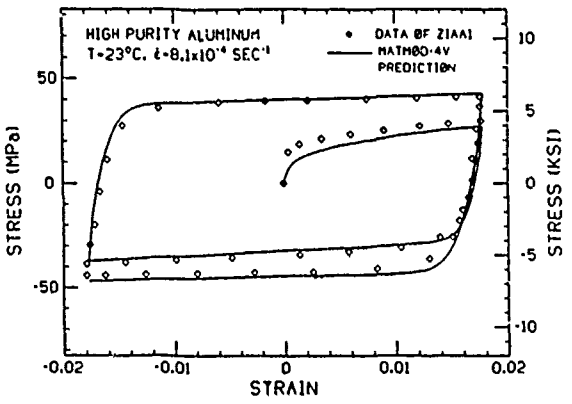


Fig. 6. Cyclic hysteresis loops for pure aluminum deformed at 296 K and a strain amplitude of 1.77%: MATMOD-4V predictions and data of Ziaai [7]. (After Lowe and Miller [8]).

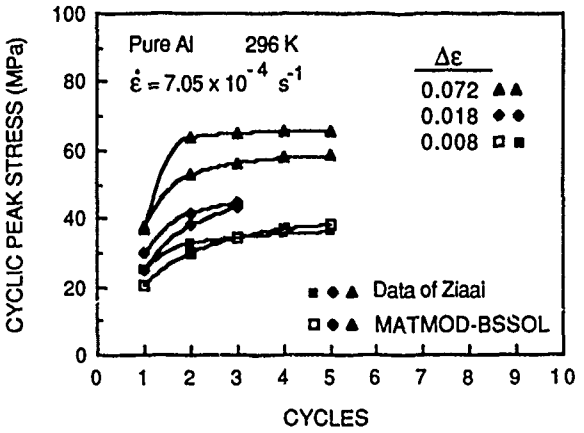


Fig. 7. MATMOD-BSSOL predictions of cyclic hardening for pure aluminum are compared with the data of Ziaai [7].

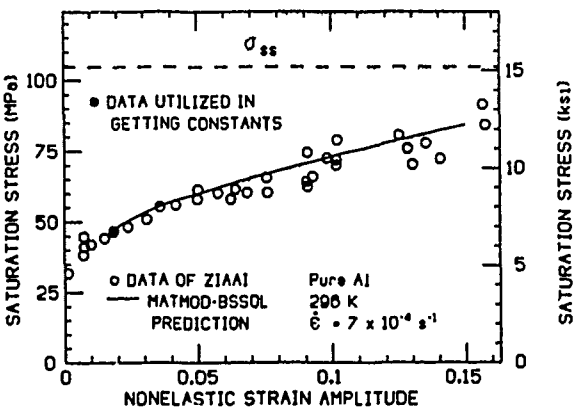


Fig. 8. The MATMOD-BSSOL prediction of the cyclic stress-strain curve for pure aluminum deformed at 296 K is compared with the data of Ziaai [7].

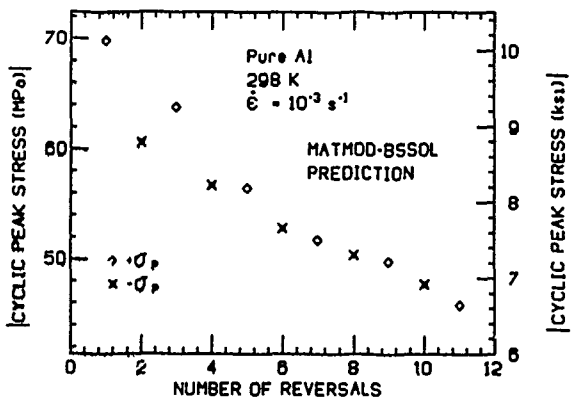


Fig. 9. The magnitudes of the tensile, $+\sigma_p$, and compressive, $-\sigma_p$, peak stresses for pure aluminum deformed cyclically at a strain amplitude of 1% following a 30% tensile prestrain.

# PHYSICAL MECHANISMS OF FRACTURE IN COMBINED CREEP AND FATIGUE

R. Hales

Dr. Hales is in the Technology, Planning and Research Division of the Central Electricity Generating Board at Berkeley Nuclear Laboratories, Berkeley, Gloucestershire.

SYNOPSIS

Early observations on creep-fatigue were interpreted in terms of modified fatigue processes. It is now recognised that for many engineering structures which have long projected lives the life limiting processes are controlled by creep. The way in which creep damage accumulates under strain controlled cyclic deformation is demonstrated. The factors which determine the failure mode are identified and the consequences of creep dominated failure for the assessment of engineering structures discussed.

## INTRODUCTION

About 35 years ago, thermal fatigue was identified as an important phenomenon which could limit the lifetime of components operating at high temperatures [1]. This stimulated the early systematic laboratory investigations which took two forms. The first measured the resistance of different materials to thermal-fatigue by thermally cycling carefully designed specimens [2]. The second extended contemporary studies of low cycle fatigue to temperatures at which time dependent deformation is observed [3]. The objective of the studies conducted in the intervening years has been to provide designers and engineers with detailed guidance on the endurance of materials under the appropriate conditions. These are often displacement controlled situations arising from changes in temperature, e.g. the start-up and shut down of power plant. More recently the objective has been to provide an understanding of the underlying mechanisms of failure and thereby improve our ability to extrapolate from the laboratory experience to long term service performance. In this paper our current understanding of these mechanisms will be described and it will be shown how that understanding can be used in assessing the performance of high temperature plant.

## CREEP-FATIGUE BEHAVIOUR

The behaviour of a wide range of metals and alloys under high temperature cyclic deformation has been widely reviewed elsewhere [4] but the most important features will be briefly recalled. Because most creep fatigue problems arise from secondary loading it is usual for experiments to be conducted under strain or quasi-strain control rather than under load control. Such experiments lead to the following observations.

(i) Rapid Continuous cycling at rates sufficiently fast to suppress time dependent deformation results in fatigue failures similar to those observed at ambient temperatures. In general, increasing the temperature leads to a slight reduction in endurance which is interpreted as being due to increased plastic strain, $\Delta\varepsilon_p$, for a given total cyclic strain range, $\Delta\varepsilon_t$. This behaviour is described by the Coffin-Manson equation [3,5].

$$N_f^{\beta}.\ \Delta\varepsilon_p = \text{Const} \qquad (1)$$

where $N_f$ is the number of cycles to failure, and $\beta$ is a materials constant. It should be noted that increasing the temperature does not universally result in increased plastic strain; e.g. type 316 stainless steel exhibits complex cyclic behaviour, hardening at some temperatures but not at others.

(ii) Frequency effects. As the strain rate is reduced, time-dependent deformation can occur, increasing still further the contribution of plastic strain. As the cyclic frequency is reduced the endurance generally reduces and this effect was first described by the frequency modified Coffin-Manson equation [6].

$$(N_f.\ \nu^{k-1})^{\beta}.\ \Delta\varepsilon_p = \text{const} \qquad (2)$$

where $\nu$ is the frequency and k reflects the frequency sensitivity of the material. If k=1 there is no frequency effect. This relationship takes no account of the wave shape nor does it take account of any change in mechanism which might occur. Provided that the loading pattern remains symmetrical, the reductions in endurance are generally small and most importantly the failure mechanism remains unaltered. The increased time spent at high temperature can result in structural changes including precipitation of a second phase or the formation

of a surface scale. In the latter case subsequent cycling can cause cracking of the surface layer, enhancing the initiation stage of fatigue failure [7]. In general, environmental effects will be frequency dependent but relatively insensitive to the precise nature of the loading cycle.

(iii) Asymmetric loading can be achieved either by imposing different strain rates in the tensile and compressive parts of the cycle or introducing one or more periods at consta strain. In the latter case elastic strain is converted to plastic strain at a variable decreasing rate by stress relaxation. The plastic strain rate is given by

$$\dot{\varepsilon}_p = -\frac{1}{E} \cdot \frac{d\sigma}{dt} \qquad (3)$$

which is controlled by a combination of glide and climb processes similar to those encountered in creep.

Asymmetric loading histories lead to the greatest reductions in endurance compared with continuous cycling especially when the slow strain rate deformation occurs under a tensile stress. An example of this is shown in Figure 1 in which it can be seen that at strain ranges greater than about 1% the presence of a 16 hour tensile dwell reduces the endurance compared with rapid cycl , (>>.1Hz) by a factor of about three but at lower strain ranges the reductions are even greater and can be as high as a factor of 15. Finally at about 0.1% strain range the endurance starts to approach the continuous cycling endurance. This complex behaviour can not be accounted for by a simple parametric equation of the form of equation 2 and a detailed understanding of the underlying processes is required.

(iv) Observations of Failure In general, symmetrical cyclic loading leads to a fatigue failure characterised by a transgranular crack, the faces of which are marked with striations. The striations record the extent of crack advance by shearing-off at the crack tip. Even when the strain rates are reduced and corresponding reductions of endurance are observed, the appearance of the fracture surface remains unchanged (Figure 2a). Upon increasing the contribution of tensile strain at 'slow' rates a change in the fracture mode is observed. Increasing areas of intergranular fracture appear until it is impossible to find striations at all. This change is accompanied by the production of intergranular cavities and wedge cracks throughout the structure (Figures 2b and c). This type of damage is usually associated with creep failures and its observation coincides with the most severe reductions in endurance.

## THE ROLE OF CREEP IN DETERMINING CYCLIC ENDURANCE

Several approaches to creep-fatigue have involved the concept that cyclic endurance is reduced by the accumulation of creep damage arising from time dependent deformation [9]. The change from transgranular fatigue crack growth to intergranular failure supports this idea. However, in the absence of a mechanistic description of the evolution of creep damage it is not clear how such processes can be assessed or how laboratory experience can be extrapolated to service conditions.

Mechanisms of creep failure have been widely studied but it is relatively recently that it has been appreciated that several different mechanisms can apply to the same material under different combinations of stress and temperature [10]. For many commercially important alloys and steels three mechanisms appear to be particularly important.

(i) At high stresses, under uniaxial loading, plastic hole growth leads to transgranular failure via the linkage of intra-granular cavities [11]

$$\dot{r} \propto r\,\dot{\varepsilon}$$

(ii) Diffusion controlled cavity growth leads to intergranular failure [12].

$$\dot{r} \propto \sigma_1$$

which gives failure times inversely proportional to maximum principal tensile stress.

(iii) Constrained cavity growth occurs at still lower stresses when the growth rate of intergranular cavities is limited by the deformation of the surrounding material [13].

$$\dot{r} \propto \dot{\varepsilon}/r^2$$

These changes in mechanism are often difficult to detect from the usual plot of log stress versus log time to rupture although the sigmoidal form of this curve is evidence of the phenomenon. Clearer evidence of the changes in mechanisms is obtained in a plot of strain to failure versus strain rate shown schematically in Figure 3. The regime where the ductility varies typically covers one to two orders of magnitude of strain rate which in power law creeping materials with a stress exponent ~ 6 which corresponds to a factor of about 1.5 on stress (hence the lack of sensitivity of the log stress versus log time plot).

It is important to note that, although the mechanisms controlling the rate of growth differ, all three mechanisms need a tensile stress to promote cavity growth. Beere and Roberts [14] have shown that if, as a result of a combination of temperature and strain-rate, either mechanism (i) plastic hole growth or mechanism (iii) constrained cavity growth, operate throughout the fatigue cycle no nett cavity growth can occur. This is because even if the time in tension is greater than the time in compression the strain is always fully reversed. In the case of diffusion controlled growth this is not true since the change in cavity size depends on time at a given stress. However the range of conditions over which diffusion is the rate controlling mechanism is narrow and it would be remarkable if all the examples of creep dominated failures in creep-fatigue coincided with this regime. To accumulate creep damage, therefore, it is necessary for different parts of the deformation cycle to occur at rates sufficiently different for the various growth mechanisms to operate. In particular it is necessary for the tensile component of the cycle to occur at rates which favour the most efficient cavity growth mechanisms.

## ASSESSMENT OF CREEP DAMAGE

By integrating the cavity growth and shrinkage during a complete creep fatigue cycle Beere and Roberts [14] demonstrated the rachetting growth of individual defects. Miller et al [15] have similary calculated the growth of arrays of cavities during a stress relaxation period at constant total strain to obtain the cyclic endurance. The critical parameter which determines the operating cavity growth mechanisms is $\dot{\varepsilon}/\sigma$ which decreases monotonically with hold time. In the case of both an austenitic and a ferritic steel it was shown that this decrease caused a change in cavity growth mechanisms from plastic void growth, through diffusion control to constrained cavity growth. Calculations of cyclic endurance based on these models give fair agreement with experiment but are very sensitive to the value selected for the cavity spacing and to a lesser degree on the value of the grain-boundary diffusion coefficient which can be subject to error.

For practical purposes it is preferable to calculate creep-damage from the measured monotonic creep properties of the material in question. This may be done on the basis of a time fraction or strain fraction approach. The former has been found convenient for the assessment of variable load controlled problems. The strain fraction or "ductility exhaustion" method is now preferred for assessment of creep damage in strain controlled situations having the virtue that strain is directly related to the most damaging mechanisms. During a period $t_h$ of stress relaxation at constant strain the damage accumulated per cycle, $D_c$, is given by

$$D_c = \int_0^{t_h} \frac{\dot{\varepsilon}_p}{\dot{\varepsilon}_f(\dot{\varepsilon}_p)} \, dt \qquad (4)$$

where $\dot{\varepsilon}_f(\dot{\varepsilon}_p)$ is defined by the creep failure illustrated in Figure 3. Although creep fatigue performance should ideally be gauged against the creep properties of the particular material it is not always possible and the creep damage must then be assessed from mean or lower bound properties. The time fraction approach to creep damage assessment under strain controlled conditions where the cavity growth is constrained leads to a paradox. Creep-resistant material which exhibits little stress relaxation will be assessed as highly creep damaged, although little or no creep strain is accumulated and conversely a material which relaxes quickly will be assessed as having little or no creep damage although substantial creep strain is accumulated.

## MEASUREMENT OF CREEP DAMAGE

The interpretation of creep damage as the growth and linkage of intergranular cavities is consistant with the observation of intergranular cavities and cracks whose preponderance increases with hold times under tensile load. Quantitative measurements have been made of intergranular creep damage which is defined as the length of grain boundary separated per unit area of section examined [16]. (For comparisons between different casts the measurements should also be normalised with respect to grain size). It has been found from numerous tests, some interrupted before failure, that the observed damage can be correlated with the damage function given in equation (4) as shown in Figure (4). For a limited number of tests performed at low strain ranges and with long hold times a condition of failure is given by

$$N_f \times D_c \cong 1 \qquad (5)$$

This criterion has been found to apply equally to austenitic [17] and ferritic steels [18].

The role of compressive creep deformation in reversing void growth has also been confirmed. Test cycles which include both tensile and compressive holds are slow and time consuming if continued to failure and therefore tests have been interrupted before failure. Combinations of dwells of 30 min/2min, 30 min/5min and 15/5min in tension and compression respectively were applied for 2000-3000 cycles. The resulting damage was measured as abovee and compared with the calculated damage. The measured damage correlated reasonably well with the nett damage, (i.e. damage due to tensile dwell minus damage due to compressive dwell) whereas the sum of the two processes overestimates damage by a factor between 5 and 10 depending on the relative durations of the dwells [16].

Finally it should be noted that a finite level of 'creep damage' must be accumulated before any microstructural damage is observed. This is regarded as the initiation phase of creep damage.

## CREEP-FATIGUE FAILURE MAPS

The mechanisms whereby the two processes, creep and fatigue, generate microstructural damage are now widely accepted. The interpretation of failure however has been obscured at varying times by conflicting results. Apparent inconsistencies have arisen because of mechanistic differences between classes of materials and because of variations in the detailed properties within an alloy specification. Similar differences have been observed in monotonic deformation and failure mechanisms. Ashby [10] has used a mapping technique to bound the conditions which give rise to each process. A similar technique has been developed to bound the creep fatigue behaviour and hence explain some of the variations observed.

Figure 5 shows a two dimensional section at a given hold-time through a 3-dimensional construction (tensile hold time is the third axis). Most materials show limited variability in continuous cycling fatigue endurance and a lower bound line can be drawn of the form of equation 1 and is the line abc in Figure 5. A similar relationship has been found to describe the number of cycles to cause a change from stage I to stage II crack growth [19] which can be regarded as a convenient measure of fatigue crack initiation in a smooth defect free specimen and is given by the line aed. Creep failure can be determined from a strain fraction rule and the line cdf can be computed from relatively short term tests using a parametric description of the stress relaxation behaviour and the creep ductility [17]. The general shape of the curve arises from the stress-strain

properties of the material; after yield the stress rises only slowly with increasing strain. Hence, as the strain range increases, the stress hardly changes and the accumulated strain per cycle changes by a correspondingly small amount. At strains near yield the stress changes much more rapidly with a corresponding sensitivity of endurance to strain range.

The condition for the nucleation of creep is much more difficult to define, but the metallographic observations in Figure 4, suggest that nucleation occurs at about 20% of the failure criterion and this definition has been used here to construct a line corresponding to the creep failure line reduced by a factor of 5 on the number of cycles.

In Figure 5 two regimes are clearly identifiable: at high strain ranges fatigue failure occurs before creep damage can nucleate and endurance is given by ab. Similarly at low strain ranges creep failure, defined by df, occurs before a fatigue crack initiates. It is important to realise that this criterion does not necessarily correspond to the separation of a test specimen into two halves, but is rather a level of damage which renders a component unfit for sevice [20]. It can be seen that the nature of any synergism between the two processes is reduced in importance since it can only occur over a narrow range of conditions defined by the area bcde. In the absence of any interaction the lines abc and cdf describe the cyclic endurance. The lowest endurance an interaction can cause is given by abe and edf. Models of creep fatigue interaction have been developed to describe crack growth but are not particularly well suited to the calculation of endurances in which the two types of damage are evolving continuously. From the evidence of the failure map it can be seen that any interaction is confined to a narrow set of conditions which are often outside the range of practical interest. Futher more plain specimen endurance is used in assessments based on initiation of a defect of acceptable dimensions and not on its subsequent growth.

In the absence of detailed creep fatigue data an estimate of the creep fatigue behaviour can be obtained from some basic materials properties as shown in Figure 6. As already explained the line AEDB is simply the continuous cycling fatigue endurance. Depending on the exact nature of the loading and the position of the dwell period in the cycle there is a limiting strain range below which relaxation strain cannot be regenerated. In the case of the normal experimental cycle, hold period at maximum tensile strain, irrespective of the duration of the hold periods or the number of cycles if the total strain range < the yield strain, $\varepsilon_y$, the creep strain is limited to $\varepsilon_y$. This will be less than the creep ductility, even in the most brittle materials, and sets a conservative lower limit below which creep failure cannot occur (line CD). At strain ranges which cause repeated cyclic yielding, the peak tensile stress is insensitive to total strain range. The relaxation strain $\varepsilon_r$ can be calculated for any dwell period from relatively simple relationships and a lower bound endurance is approximately given by

$$N_f = \varepsilon_{min}/\varepsilon_r \qquad (6)$$

which is plotted as EF. The solid line AECDB represents a conservative lower bound.

## DISCUSSION

The mechanisms which lead to the development of creep damage under strain controlled conditions described here allow a failure mechanism map of the type shown in Figure 5 to be drawn. An estimate of the lower bond endurance can also be made, as shown in Figure 6. The model also allows laboratory tests to be interpreted consistantly and extrapolated to service conditions.

(i) Extrapolation of test results Figure 5 clearly illustrates the potential dangers of extrapolating reductions in cycle endurance at high strain ranges (~2%) to low strain ranges. Even features tests with long hold times can give results which lead to non-conservative extrapolations. As already indicated this non-conservatism arises from the change in mechanisms encountered on reducing strain ranges. If accelerated tests are required, a more efficient strategy is often to test at temperatures higher than the service conditions thereby increasing the creep contribution in each cycle.

(ii) The Strain Rate Dependence of Ductility The effect of strain rate on ductility is crucial in determining creep fatigue effects. Some materials do not exhibit any strain rate dependence of the strain to failure. These materials usually fail at high ductilities by intra-granular void growth or by plastic instability. Neither of these processes can lead to failure under strain controlled cyclic deformation and therefore no significant reductions in endurance are anticipated. Any reductions in endurance are second order and arise from enhanced plastic strain range or environmental effects. Normalised and tempered 9Cr-1Mo ferritic steel exhibits this type of behaviour.

It is conceivable that under service conditions the tensile and compressive loading rates may be such that all the deformation is at a rate less than the transitional rate. Again no nett accumulation of creep damage is expected.

(iii) Creep-fatigue Interaction Because of the different gradients of the curves describing creep and fatigue failures, illustrated in figures 5 and 6, it can be seen that the relative contributions from the two processes change very quickly with changing strain range. It takes about 20% of the endurance to initiate each of the mechanisms and therefore the individual components of damage must be within a factor of about 5 of each other for a creep-fatigue interaction to occur. For steels used in power plant this regime is at strain ranges much greater than usually experienced. Creep-fatigue interactions become important in determining crack growth rates although even here many practical applications are dominated by one process or the other [21].

(iv) Multiaxial Effects Procedures for assessing the endurance of engineering components currently in use are extensions of codes previously developed for fatigue alone. Consequently multi-axial loading conditions are reduced to an equivalent uniaxial condition by the von Mises relationship. The equivalent strain range is then used to determine the creep-fatigue endurance from a uniaxial endurance curve. Models of multiaxial creep failure recognise two groups of materials; those whose failure is controlled by shear

stress and those whose failure is controlled by maximum principal stress [22]. The former group of materials corresponds to that already identified as failing by predominately ductile transgranular processes and which are therefore not expected to exhibit a creep-fatigue effect.

The behaviour of the second group of materials is controlled by the growth of intergranular voids. These defects do not grow under compressive stress and compressive stresses are not anticipated to contribute to failure under combined loading. Isochronous creep failure surfaces of these materials show large alleviations from the von Mises equivalent stress in the shear quadrant of bi-axial stress, approaching the maximum principal stress. However, the corresponding behaviour at a stress ratio of 2:1 produces a reduction of $2/\sqrt{3}$ in the equivalent stress from the von Mises criterion. This behaviour can also be predicted from the defect growth models. A plot of principal strain at failure as a function of equivalent strain-rate is shown schematically in Figure 7. The growth of voids under shear loading causes the diffusion controlled growth to occur at strain-rates approximately 2/3 of the corresponding uniaxial strain rate. Similarly bi-axial tension increases the transitional strain-rate by ~ 2. Torsional loading may very well exhibit further alleviations, the minimum ductility being greater than that for uniaxial loading because the number of cavity nuclei capable of growing under the reduced principal stress will be fewer than under uniaxial loading.

In extending uniaxial creep fatigue behaviour to multiaxial loading conditions it is necessary to assess the creep-damage for each loading contribution. The relaxation strain can be partitioned into component parts and only strains accumulated under tensile principal stresses should be considered to contribute to damage. The magnitude of that damage should be assessed against the ductility behaviour shown in Figure 7. Clearly assessment of loading combinations which included a compressive component could be conservatively assessed against uniaxial behaviour. However, the 15% reduction of equivalent stress in bi-axial tensile combinations can have serious implications, the reductions being much more severe when translated into strain ranges. Bi-axial tensile stresses often arise in the region of notch tips and hence further impair the performance beyond that anticipated from estimates of strain concentration.

(v) Assessment of Service Conditions The schematic diagram (Figure 6) emphasises the different processes which can lead to failure and hence indicate the most appropriate remedial action. The line CD is determined by the cyclic yield properties and the characteristics of the service cycle. It is not influenced by the creep ductility of the material. Failures predicted under service conditions close to CD can be avoided by changing the operating conditions i.e. an engineering solution is required.

By contrast, the line EF is controlled by the material properties in particular the ductility of the material. Service conditions which reduce the creep ductility for example irradiation or thermal ageing will reduce the number of cycles to failure. Similarly the position of this line is influenced by stress state. Hence, this behaviour is controlled by material properties and metallurgical solution is required.

## CONCLUSIONS

1. It is necessary to obtain a full understanding of the failure mechanisms and the factors which control them before a reliable estimate of long term endurance can be made.

2. In the case of many engineering materials, creep is the most important damage mechanisms and therefore due attention must be paid to the loading history and stress state.

3. The processes of creep and fatigue only co-exist over a narrow range of conditions and any interaction is of minor significance in determining the long term behaviour of engineering materials.

## Acknowledgement

This paper is published by permission of the Central Electricity Generating Board.

## References

1. Coffin, L.F., 1954, Trans ASME, 76A, 931.

2. Glenny, E., Northwood, J.E., Shaw, S.W.K. and Taylor, T.A., 1956-9, J. Inst. Metals, 87, 294.

3. Coffin, L.F. and Wesley, R.P., 1954, Trans ASME, 76A, 923.

4. Skelton, R.P., 1985, High Temperature Technology, 3, 179.

5. Manson, S.S., 1953, "Behaviour of Materials Under Thermal Stress", NACA-TN-2933.

6. Coffin, L.F., 1969, Proc. 2nd Int. Conf. Fracture, Brighton, p643.

7. Challenger, K.D., Miller, A.K. and Brinkman, C.R., 1981, J. Engng Mat. Technol., 103, 7.

8. Batte, A.D., Murphy, M.C. and Stringer, M.B., 1978, Metal Technol, 5, 405.

9. Wareing, J., 1983 "Mechanisms of high temperature fatigue and creep-fatigue failure in engineering materials", in "Fatigue at High Temperatures", ed. R.P. Skelton, London, Elsevier Applied Science, p135.

10. Ashby, M.F., 1978, Fracture-1CF4, University of Waterloo, 1.

11. Hancock, J., 1976, Met. Sci., 10, 319.

12. Speight, M.V. and Beere, W., 1975, Met. Sci., 9, 190.

13. Dyson, B.F., 1979, Can. Metall. A. 18, 31.

14. Beere, W. and Roberts, G., 1982, Acta Metall., 30, 571.

15. Miller, D.A., Hamm, C.D. and Philips, J.L., 1982, Mat. Sci., Engng, 53, 233.

16. Hales, R., 1984, Proc. Second Int. Conf. on Creep and Fracture of Engineering Materials and Structures, Part II., Swansea, Pineridge Press, p 1015.

17. Hales, R., 1983, Fatigue Engng. Mat. Struct., 6, 121.

18. Plumbridge, W.J., Dean, M.S. and Miller, D.A., 1982, Fatigue Engng. Mat. Str., 5, 101,

19. Maiya, P.S., 1979, Mat. Sci. Engng., 38 289.

20. Bocek, M., Armas, A. and Pel D., 1983, J. Nucl. Mat., 115, 159.

21. Nibkin, K.M. and Webster, G.A., 1984, Proc. Second Int. Conf. on Creep and Fracture of Engineering Materials and Structures, Part II., Swansea Pineridge Press, p. 1091.

22. Hayhurst, D.R. and Webster, G.A., 1986, Techniques for Multiaxial Creep Testing, ed. D.J. Gooch and I.M. How, Elsevier App. Sci. p. 137.

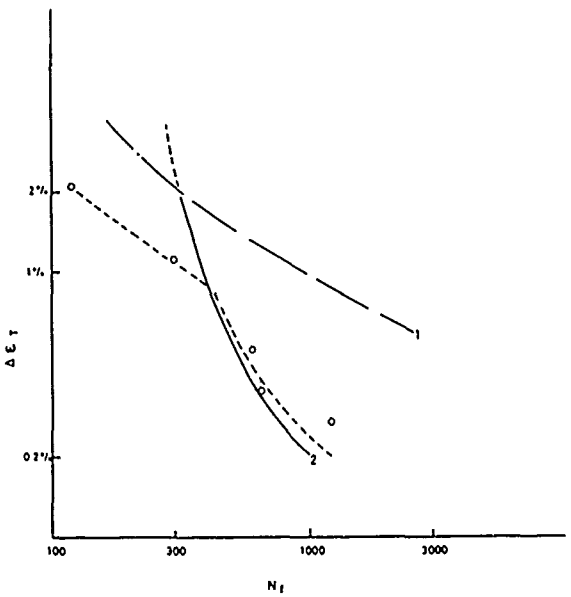


FIGURE 1 Cyclic Endurance of $^1/_2$ Cr-Mo-V [8]
(1) Continuous Cycling
(2) 16 hour hold.

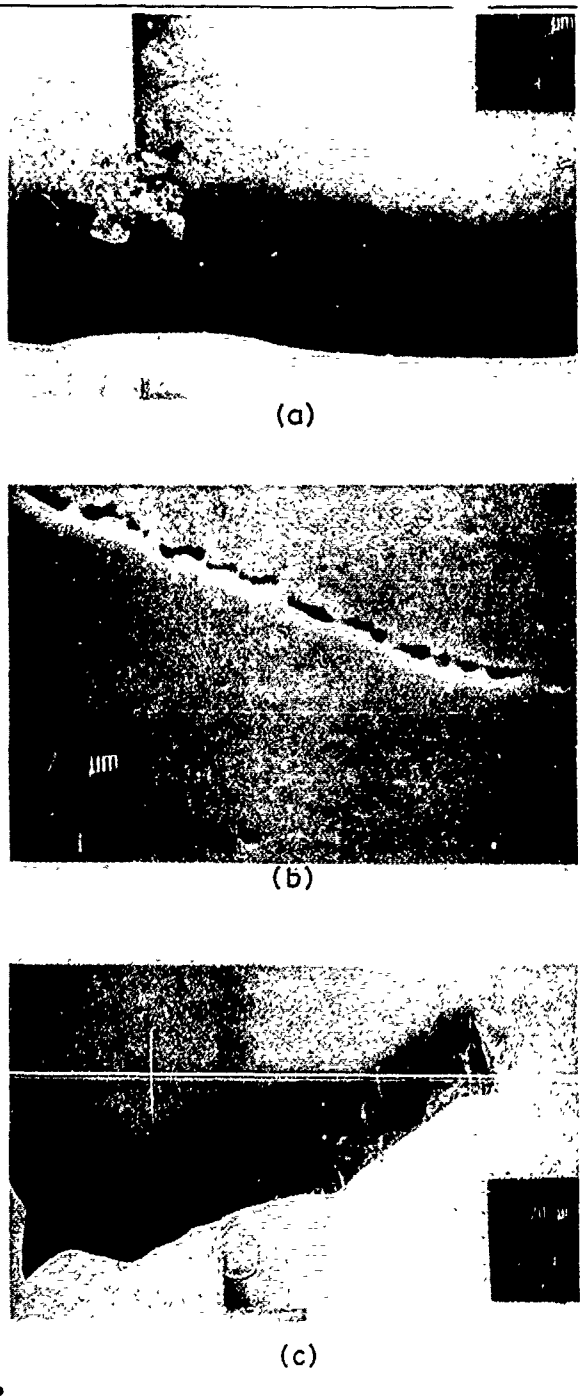


FIGURE 2 Metallographic features associated with (a) fatigue and (b and c) creep dominated failures.

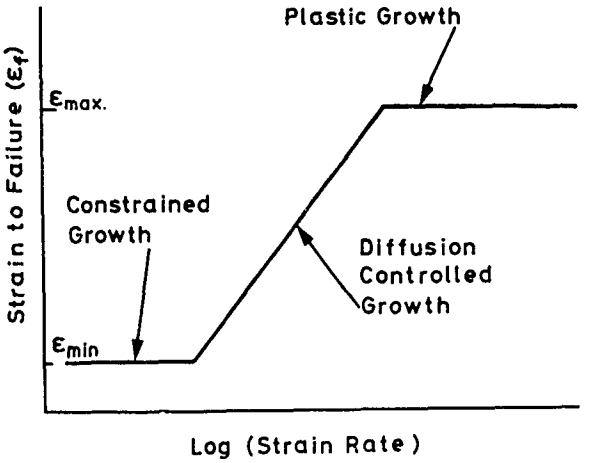


FIGURE 3 The relationship between ductility and strain rate in many structural materials.

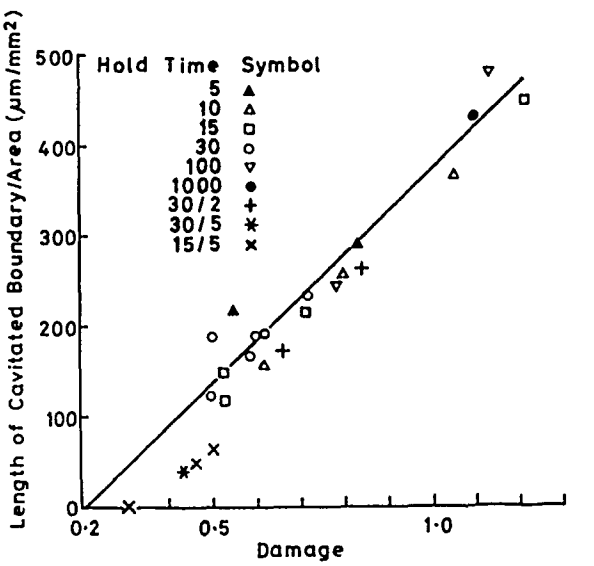


FIGURE 4 A plot of observed damage in 316 stainless steel as a function of damage calculated by the strain fraction method [16].

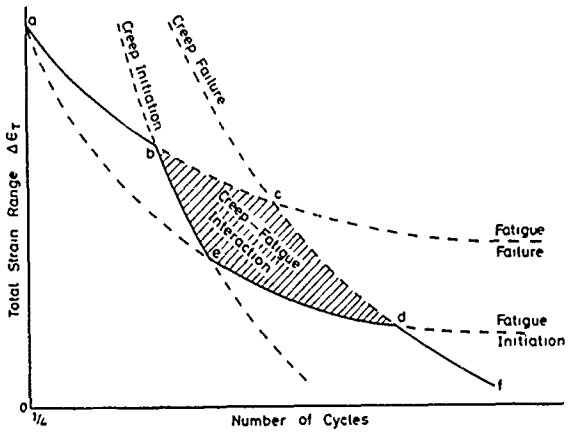


FIGURE 5 A mechanism map for constant hold time showing the conditions which lead to different types of failure.

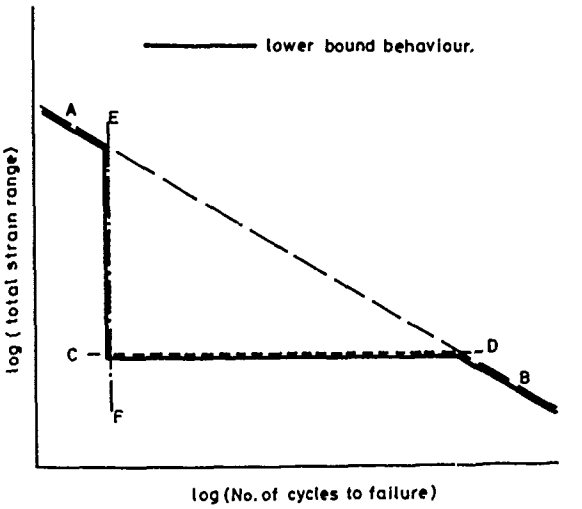


FIGURE 6 A schematic endurance curve derived from basic materials properties.

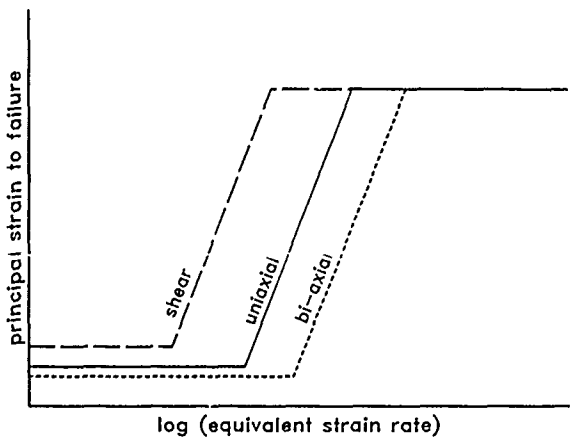


FIGURE 7 The effect of stress state on creep failure.

# ENVIRONMENTAL EFFECTS ON THE MECHANICAL PERFORMANCE OF FIBRE REINFORCED PLASTICS

Sarah M. Bishop

Dr Bishop is in the Materials and Structures Department at The Royal Aircraft Establishment, Farnborough, Hampshire, U.K.

## SYNOPSIS

Moisture and temperature generally affect the matrix-dominated properties of fibre-reinforced plastics. Results of ±45° tension tests on carbon-fibre/epoxy resin systems have been selected to illustrate the effects. The amount of moisture absorbed depends on relative humidity. Moisture causes the resin to swell, the glass transition temperature (Tg) to decrease and the behaviour to be more plastic. As a result the moduli decrease with temperature and moisture content but are greater for matrix resins with higher $T_g$. Low temperature excursions cause no degradation in mechanical performance. High temperature spiking results in significant increases in moisture absorption but no change in modulus; the additional moisture is thought to be stored in micro-cracks at the fibre-matrix interface. Failure strengths, however, depend on the interaction of several properties, the initial fibre-matrix bond strength, the degradation of the fibre-matrix bond strength (due to moisture, temperature and thermal spiking), the modulus of the resin and its glass transition temperature.

## INTRODUCTION

Fibre reinforced plastics are attractive for use in aerospace applications because they are lightweight, strong and stiff. The fibres orientated in defined directions provide tensile strength and stiffness in those directions whereas the plastic matrix provides load transfer between fibres, carries the shear loads and provides lateral support to fibres under compressive loads.

In a humid environment moisture diffuses slowly into the matrix such that the mechanical performance of the matrix maybe modified. Carbon-fibre properties are unaffected by moisture but the tensile strength of glass fibres has been shown to be reduced[1-4] by up to 20% as a result of moisture diffusing through the matrix. Generally it is the matrix-dominated properties such as shear and compression which are affected by moisture in a fibre reinforced plastic.

In this paper, the effects of various environemntal conditions (moisture and temperature) are described for the matrix-dominated properties of carbon-fibre reinforced plastics. Selected results are presented for four carbon-fibre/epoxy-resin systems A, B, C and D to illustrate the various environmental effects.

## MOISTURE ABSORPTION BEHAVIOUR

The rate of diffusion of moisture into the resin matrix increases with temperature. Generally, the diffusion coefficient, D, depends on the absolute temperature, T.

$$\log_e D \propto \frac{1}{T}$$

Initial moisture diffusion usually obeys Fick's law. For a fibre reinforced plastic laminate with both surfaces exposed to a constant environment, this can be expressed in terms of percentage moisture content by weight[5].

$$D = \pi \left(\frac{h}{4M_m}\right)^2 \left(\frac{M}{\sqrt{t}}\right)^2$$

Where M is the moisture content at the time, t, $M_m$ is the equilibrium (maximum) moisture content for that environment and h is the laminate thickness. The diffusion coefficient can be obtained from the slope of the initial linear portion of a plot of M against $\sqrt{t}$. $M_m$ generally depends only on the relative humidity of the environment and is independent of temperature providing the glass transition temperature of the resin is not exceeded. In practice the moisture content may not completely level off near the maximum value but continue to increase very slowly.

In Figure 1, typical moisture absorption curves at two temperatures are shown for a carbon-fibre reinforced plastic which was initially dry. The amount of moisture absorbed was determined by weighing.

Absorption of moisture causes the resin to swell resulting in dimensional changes in the fibre composite. A dry carbon-fibre laminate contains residual stresses which arise in manufacture during cooling following cure because of differential thermal expansion; the resin contracts more than the carbon fibres. Because carbon fibres are stiff, resin contraction cannot take place parallel to fibres and tensile residual stresses result in the resin. Residual stresses are particularly high in laminates where fibres in adjacent layers are at right angles to one another. Swelling of the resin on absorption of moisture relieves these residual stresses.

Absorbed moisture also lowers the glass transition temperature of the resin by roughly 20°C for every 1% by weight of moisture absorbed by the resin[4], ie roughly 60°C for 1% moisture in a typical carbon-fibre reinforced resin with a fibre volume fraction of 60%. This means that the degree of plastization of the resin which may occur with increase in temperature is greater when the resin is wet.

## MECHANICAL PERFORMANCE

In the experimental work described here, mechanical performance was assessed using a '±45° tension test'. Specimens (150 mm x 20 mm), cut with the length parallel to the 0° direction from 2 mm thick laminates with fibres orientated at +45° and -45°, were loaded in tension in the 0° direction. The specimens deformed in shear parallel to the fibre directions.

In Figures 2a and 2b plots of load against strain are shown up to failure for such ±45° specimens for various test temperatures between room temperature (RT) and 130°C. When the plots for the wet carbon-fibre/resin system (Figure 2b) are compared with those for the dry material (Figure 2a), it can be seen that at a particular load, greater strains were obtained with increased temperature in the wet case due to increased plasticity.

In Figure 3, the secant modulus at 1% strain of ±45° specimens has been plotted against moisture content for the carbon-fibre/resin system, A, conditioned to equilibrium (saturated) in various relative humidities. The modulus decreased with increased temperature and moisture content. When saturated at 90% relative humidity the modulus at 130°C was less than 25% of that for the dry material tested at room temperature. The glass transition temperature for the dry material had been determined to be 219°C; application of the rough rule described earlier indicates that at 130°C the glass transition temperature of the wet material had been exceeded.

In Figure 4, the secant modulus at 1% strain is plotted against moisture content for a different carbon-fibre/resin system C with a higher glass transition temperature when dry of 296°C. It can be seen that, although the moduli at the various temperatures were similar to those for resin system A when dry, when saturated at 90% RH, the modulus at 130°C was twice that for resin A, ie the glass transition temperature in the wet condition was higher for resin C and less plastic deformation had occurred.

The failure stresses for the same ±45° specimens are shown in Figures 5 and 6 for carbon fibre/resin systems A and C respectively. In Figure 5, temperatures up to 130°C had little effect on the failure stress of the dry material with resin A and at room temperature the failure stress was independent of moisture content. However, with increased moisture and temperature the failure stresses decreased from approximately 200 MPa to 140 MPa.

In Figure 6, different results were obtained for carbon-fibre/resin system C compared with resin system A. The failure stresses of the dry material were much lower and increased slightly with temperature. The failure stresses of the material tested at room temperature increased with moisture content. This behaviour suggested that residual stresses were being relieved by temperature and moisture thus making the material stronger. However the lay-up of the fibres and the cure temperatures were similar for both resin systems, which would imply that the residual stresses were similar in both cases. It was concluded that the shear strength was less for carbon-fibre/resin C; examination of the fracture surfaces showed considerably more splitting parallel to the fibres in resin C indicating a weaker fibre-matrix bond strength. With further increase in moisture and temperature the failure stresses for system C tended to decrease as for resin system A to a similar value at 130°C of 140 MPa for material saturated at 90% RH despite the higher modulus of resin C under these conditions (Figure 4). Again it was clear that the lower fibre-matrix bond strength contributed to failure. Thus failure in this material was not determined by plasticity of the matrix but mainly by fibre-matrix debonding.

In Figure 7 the fracture surfaces of two specimens of carbon-fibre/resin A are compared. It can be seen that the splitting was finer in the hot/wet case. The fracture of the dry specimen tested at room temperature tended to be more brittle and perpendicular to the load direction although some splitting occurred in the outer layer and near the specimen edge on inner layers. Failure of the hot/wet specimen tended to be parallel to the fibre directions at +45° and -45°. Further examination of the fracture surfaces of specimens with matrix resins A and C showed in both cases increased splitting with increased moisture content and increased splitting with increased temperature. The splitting was consistently more and finer for system C. Further evidence of degradation of the fibre/matrix interface by moisture was obtained microscopically from polished cross-sections of material conditioned in wet environments which had not been subjected to load or temperature. Some fibre-matrix debonding was observed in specimens conditioned at 90% RH.

Generally it was concluded that failure in shear was determined primarily by the fibre-matrix bond strength which decreased under hot and wet conditions. Of course, plasticity effects may have made some contribution to the failure, but it was apprent that increasing the glass transition temperature of the resin was not necessarily sufficient to increase shear strength although shear modulus was increased.

## LOW TEMPERATURE EXCURSIONS

In service an aircraft is subjected to low temperatures of approximately -55°C when flying at high altitude.

Experiments have been carried out to determine the performance of several carbon-fibre/epoxy-resins subjected to such low temperature excursions for half an hour daily, five days a week for a twenty week period. Different sets of specimens were initially conditioned to equilibrium in different relative humidities of 0, 50, 75 and 90% RH and then subjected to the twenty week exposure to low temperature (-55°C) excursions in a base climate of 75% RH (a typical humid North European climate). During this period moisture absorption and desorption were monitored and compared to that for material not subjected to low temperature excursions.

A small increase in equilibrium moisture content (approximately 5%) was observed but subsequent mechanical testing of ±45° specimens at temperatures from room temperature to 130°C

showed no change due to low temperature excursions in shear moduli, strengths or fracture surfaces.

It was thus established that cracking did not occur as a result of either freezing of water or increased residual stress effects due to greater differential thermal contractions occurring between carbon fibres and resin on cooling to -55°C. It is thought that water molecules diffusing through the resin become attached by hydrogen bonding to polar groups on the polymer molecules and do not conglomerate into groups that could freeze. The small increase in moisture absorption may be attributable to residual stress effects.

## THERMAL SPIKES

A supersonic aircraft may experience a sharp increase in temperature up to 132°C during a supersonic dash due to kinetic heating. Also reflected efflux from the engine of VTOL aircraft may cause high temperature spikes.

Experiments, similar to those for low temperature excursions have been carried out to assess the effects of high temperature spikes on the same carbon-fibre/epoxy-resin systems. Specimens were initially conditioned to equilibrium in different relative humidities of 0, 50, 75 or 90% RH and then moved to a base climate of 75% RH where they were subjected to a thermal spike of 132°C once a week for a period of twenty weeks. The specimens reached 132°C in six minutes and were then held at that temperature for one minute. Moisture absorption and desorption were monitored during the twenty week period and compared with that for control specimens stored in the same base climate without thermal spikes.

Thermal spiking resulted in a significant increase in moisture absorption. In Figure 8, plots of the moisture absorption are shown for spiked and control specimens for carbon-fibre/resin system D with a glass transition temperature of 232°C when dry. After twenty weeks all specimens had reached equilibrium in the base climate of 75% RH but the moisture contents of spiked specimens were approximately 50% higher than those of the controls. The equilibrium moisture contents were independent of the previous conditioning. For the different materials studied, the increases in moisture content due to thermal spiking ranged from 5% to 50% in the base climate of 75% RH.

Additional experiments showed that the moisture content increased with spike temperature and the increases were greater for base climates with higher humidities; the increase in moisture content for 132°C spikes ranged from 15% to 70% for the different materials in a base climate of 90% RH. The carbon-fibre/resin system C with the highest glass transition temperature when dry absorbed least additional moisture but generally for the systems studied there was little correlation between glass transition temperature and increase in moisture content when spiked.

The mechanical performance of the thermally-spiked specimens was assessed using the $\pm 45°$ tension test. In Figures 9 and 10 the results are shown for the carbon-fibre/resin system D spiked once a week at 132°C from a base climate of 75% RH. In Figure 9 the secant moduli at 1% strain for the spiked specimens are compared with the plot obtained for controls saturated at 75% RH. Despite the fact that the spiked specimens had absorbed 50% more moisture, no decrease in modulus was observed due to this. A similar result was found for the other materials studied and even when spiking occurred from a base climate of 90% RH the higher increased moisture contents had no effect on modulus.

In Figure 10, the failure stresses of the same $\pm 45°$ tension specimens are shown for carbon-fibre/resin system D. The failure stresses of spiked specimens of this system were consistently 10-15% lower than the controls saturated at 75% RH for all test temperatures; failure stresses for this sytem were similar for specimens spiked from a 90% RH climate. It appeared from examination of the fracture surfaces that the splitting was even finer and further degradation of the fibre-matrix interface had occurred.

Generally the overall reduction in failure stress were least for the two systems B and C with the highest glass transition temperatures (266°C and 296°C respectively when dry), which may be attributable to their higher moduli. However, for specimens spiked at 132°C from a 90% RH base climate, the highest failure stress of 140 MPa at a test temperature of 130°C was obtained for the system, B, with the second highest glass transition temperature when dry, despite the fact that the spiking had increased its moisture content by 50% to a value of 2.2% by weight; for systems A, C and D failure stresses of 125-130 MPa were obtained under the same conditions. Since the moduli were unaffected by the increased moisture content in all systems it is assumed that the extra moisture was held in micro-cracks at the fibre-matrix interface. The higher moduli of resins with higher glass transition temperatures appeared to reduce the effects on failure stress of degradation at the fibre-matrix interface but, because the initial strength of the fibre-matrix bond was lower for carbon-fibre/resin C, this system with the highest glass transition temperature did not perform the best.

Generally it was concluded that the shear strengths of carbon-fibre reinforced epoxy-resins exposed to moisture and high temperature spiking were dependent on the interactions of several properties, the initial fibre-matrix bond strength, degradation of the fibre-matrix bond, and the modulus and glass transition temperature of the resin system. These factors would also affect other 'so called' matrix-dominated properties such as compressive strength. Thus, when designing a fibre-reinforced composite material for the various environments to be met in use, it is important that all these factors are considered.

## CONCLUDING REMARKS

Carbon-fibre composite components are usually designed to operate at strain levels well below the failure stress. For a particular application, the matrix of the carbon-fibre reinforced plastic is chosen with a glass transition temperature high enough to maintain the required stiffness for the hot wet environments which will be experienced in use. However, for high performance use, it is not sufficient for the material designer to develop resins with high glass transition temperatures. Failure strengths of 'so called' matrix-dominated properties (shear and compression) are very dependent on the initial fibre-matrix bond strength and the degree of degradation of the fibre-matrix bond which occurs

due to moisture, temperature and thermal spiking effects. The material designer must therefore also optimize the properties of the fibre-matrix interface and develop an understanding of the causes of environmental degradation of the bond. This is an area where much research needs to be done.

ACKNOWLEDGMENTS

The author wishes to acknowledge the valuable contributions to the experimental work of Mr G. D. Howard, Royal Aircraft Establishment, Farnborough, and Mr P. J. Thompson and Mr I. Davies, sandwich students from Brunel University and Polytechnic of Wales respectively. Glass transition temperatures were determined by MBB, Ottobrunn, West Germany.



REFERENCES

1 L. Boniface, Dept. of Materials Science and Engineering, University of Surrey. Private communication.

2 Westland Helicopters, Yeovil. Private communication.

3 G. Dorey. Environmental degradation of composites. AGARD lecture series 124 (1982)

4 W. W. Wright. A review of the influence of absorbed moisture on the properties of composite materials based on epoxy-resins. RAE Technical Memorandum Mat 324 (1979)

5 C. Shen, G. S. Springer. Moisture absorption and desorption of composite materials. J. Composite Materials, 10, 2-20 (1976)

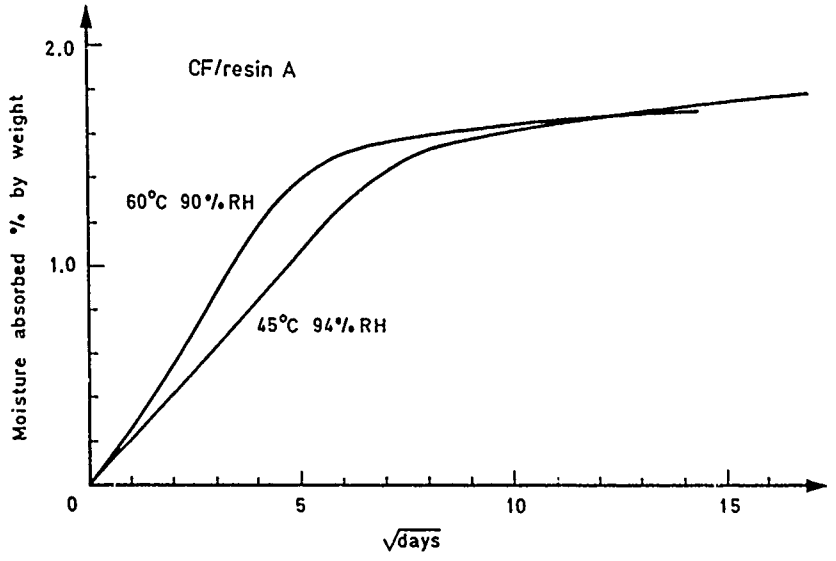


Figure 1 Plots of moisture absorption with time for a carbon-fibre reinforced epoxy-resin in 45°C 94% RH and 60°C 90% RH environments.

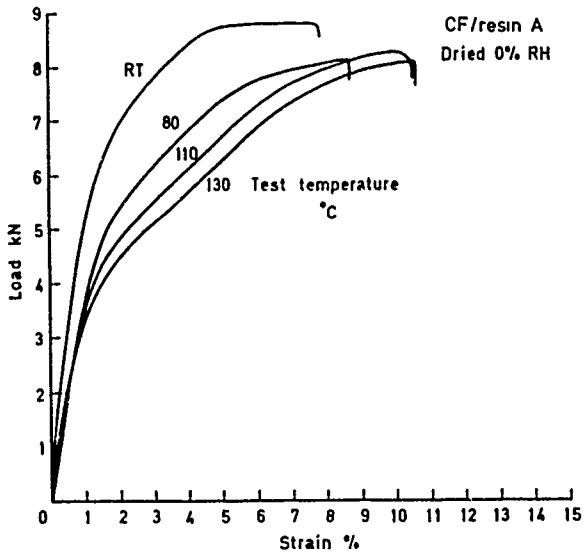


a

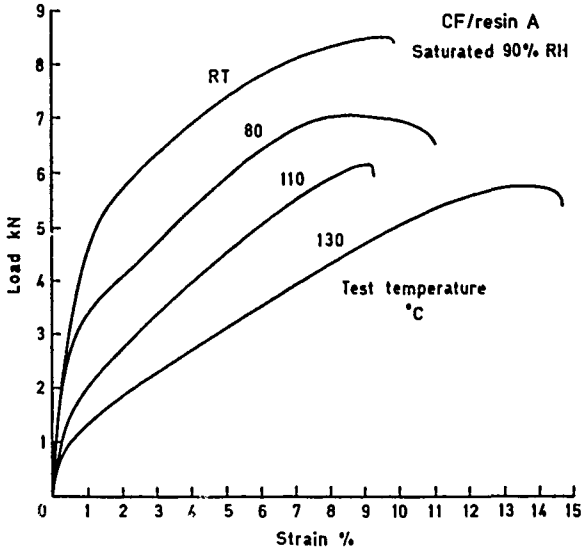


b

Figure 2 Plots of load against strain for ±45° specimens tested to failure at various temperatures (a) when dry (b) when saturated at 90% RH.

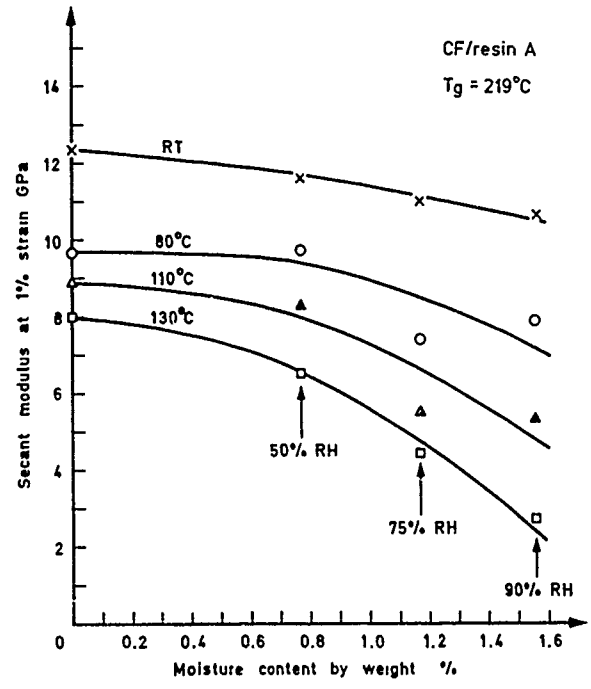


Figure 3 The secant moduli at 1% strain of ±45° tension specimens plotted against moisture content for carbon-fibre/resin A.

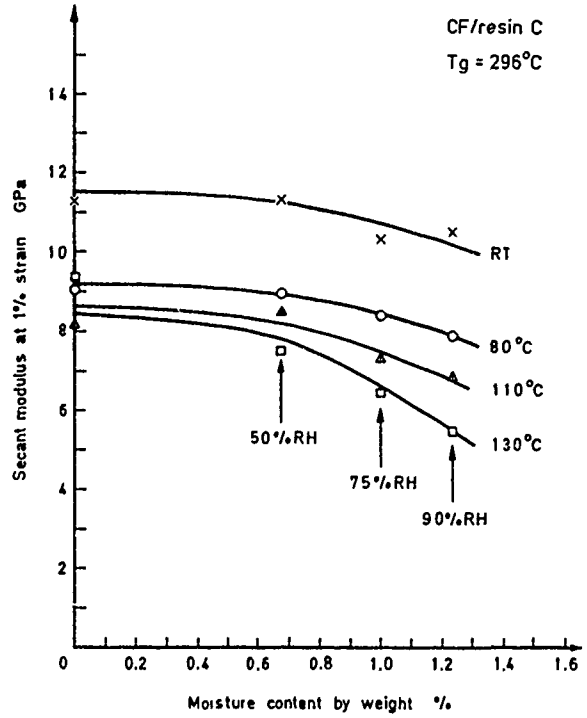


Figure 4 The secant moduli at 1% strain of ±45° tension specimens plotted against moisture content for carbon-fibre/resin C.

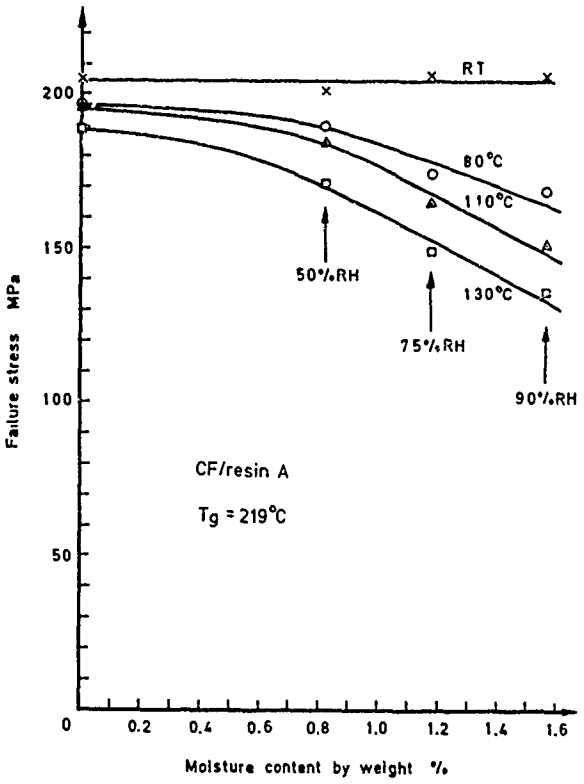


Figure 5 Failure stresses of ±45° tension specimens plotted against moisture content for carbon-fibre/resin A.

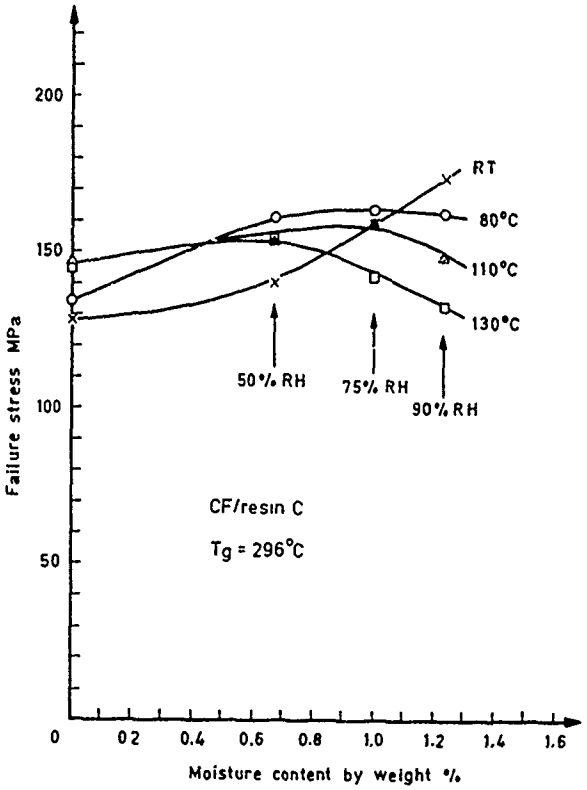


Figure 6 Failure stresses of ±45° tension specimens plotted against moisture content for carbon-fibre/resin C.

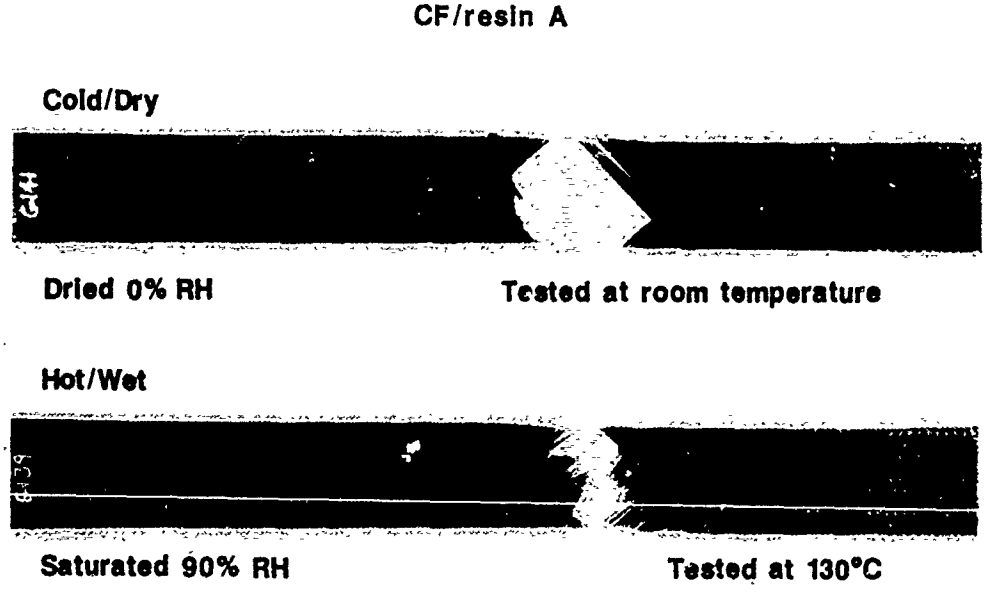


Figure 7 Comparison of fracture surfaces of a dry ±45° specimen tested at room temperature and a wet ±45° specimen tested at 130°C.

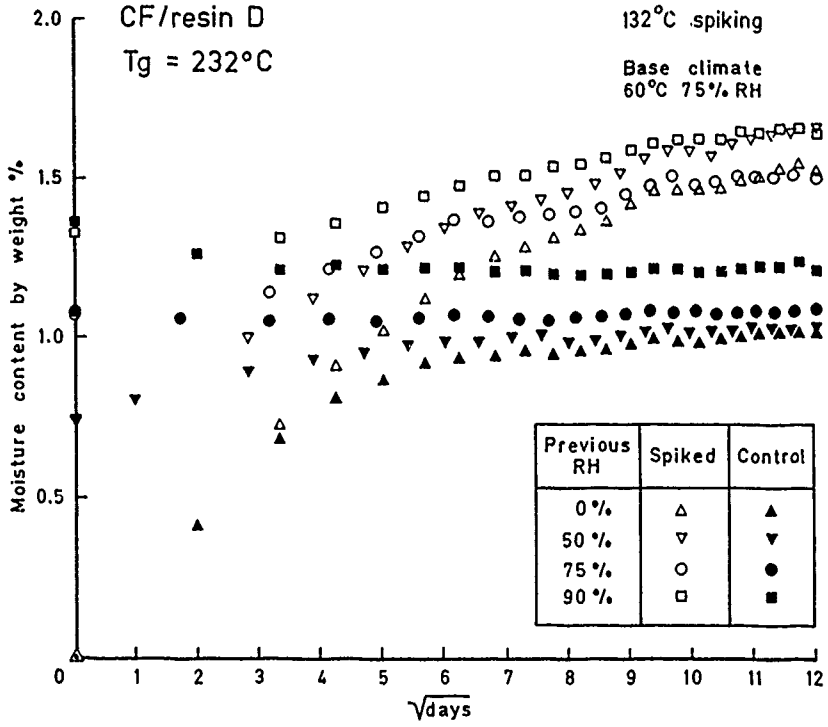


Figure 8 Comparison of moisture absorption of specimens spiked at 132°C and control specimens of carbon-fibre/resin D in a climate of 60°C 75% RH.

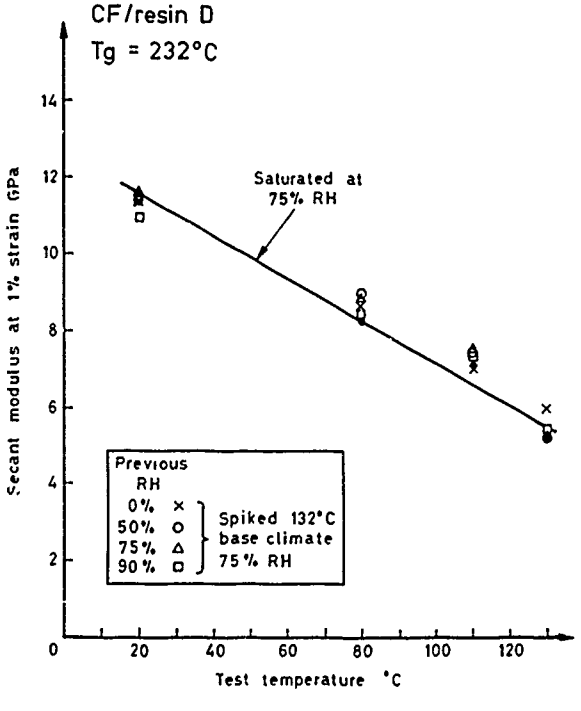


Figure 9 Secant moduli at 1% strain of ±45° specimens spiked at 132°C compared with plot for control specimens (straight line) in 75% RH climate.

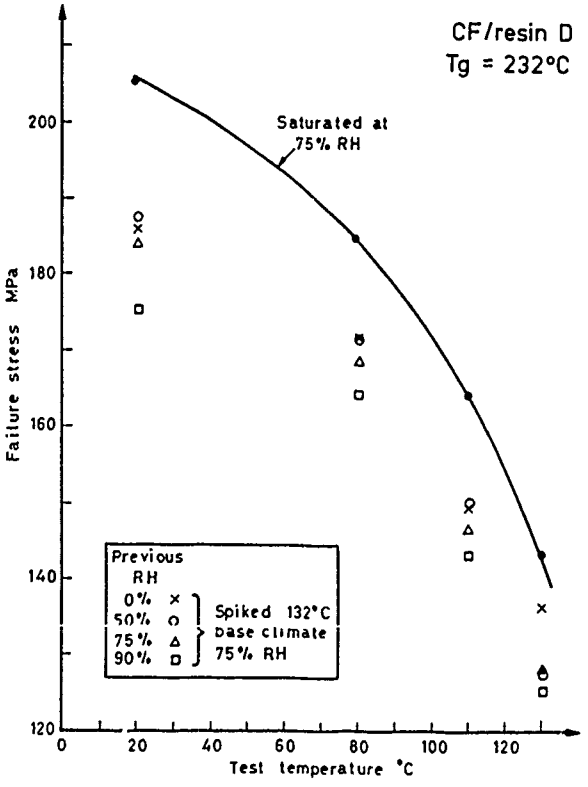


Figure 10 Failure stresses of ±45° specimens spiked at 132°C compared with plot for control specimens (curve) in climate of 75% RH.

# MODELLING SYNERGY BETWEEN CREEP AND CORROSION FOR ENGINEERING DESIGN

B F Dyson and S Osgerby

Dr Dyson and Mr Osgerby are in the Division of Materials Applications, National Physical Laboratory, Teddington, Middlesex TW11 0LW, England

## SYNOPSIS

When creep and corrosion of metallic alloys act concurrently, both creep rates and corrosion rates increase dramatically under certain situations: the principal parameters being the parabolic corrosion rate constant, the alloy's creep resistance and the section size. Physically-based mathematical modelling of this synergy can aid in the design process by enabling extrapolations of laboratory data to the conditions experienced in service. It is demonstrated how tertiary strain-softening alloys are much less affected than the steady state creeping alloys usually modelled. The synergy between creep and oxidation of low alloy ferritic steels, noted in the literature, has been accounted for quantitatively.

## INTRODUCTION AND DESIGN AGAINST ENVIRONMENTAL ATTACK

Load-bearing metallic components that are in service at temperatures where deformation is time-dependent, are usually designed on the basis of mechanical property data obtained from laboratory tests in air. The possibility of the laboratory atmosphere or the service environment interacting chemically with the alloy to induce mechanical degradation is not generally considered. Design procedures at their simplest level, require data obtained from laboratory uniaxial creep testing plotted as the stress to cause failure in a specified time. failure usually means reaching either a critical value of strain or the strain to cause rupture of the testpiece. For both cases, Fig 1 is a representative schematic of the data requirements: a design stress, $\sigma_D$, being defined by the specified lifetime, $t_D$.

Since there appears to be no equivalent procedure for taking account of environmental attack, we arbitrarily propose in this paper, that failure by this mechanism occurs when the load-bearing section has been reduced by 10%. A percentage figure being taken in order to accommodate the fact that components have a variety of section thicknesses. For a cylinder, the rate of attack in the absence of applied stress usually takes the form:

$$\dot{\omega} = \frac{1}{R}\left[\frac{K}{t}\right]^{\frac{1}{2}} = \frac{2K}{R^2\omega} \qquad (1)$$

K is a kinetic coefficient whose value depends on material and the mechanism of environmental (ie chemical) attack; t is the exposure time and R, the radius of the testpiece. $\omega = 2x/R$, where x, is the depth of chemical attack, is a dimensionless 'damage' parameter. To obtain a conservative (lower bound) estimate of the lifetime, $t_{f,E}$, limited by environmental attack in the absence of an applied stress, it is sensible to assume that the region delineated by $\omega$ cannot sustain load. Thus, using the integral of Eq (1) and putting $\omega = 0.1$:

$$t_{f,E} = 2.5 \times 10^{-3} \frac{R^2}{K} \qquad (2)$$

During the development and selection stages of the alloy, a design target would then be to ensure that $t_{f,E}$ was always greater than $t_D$, as indicated in Fig 1.

Such a simple approach to design takes no account of any possible synergy between creep and environmental attack; ie it assumes that stress does not influence the rate of chemical attack and that chemical attack does not change deformation rate or fracture resistance.

The objectives of this paper are to indicate how physically-based mathematical modelling of the synergy between creep and chemical-attack can aid the designer by providing guidance on the interpretation of laboratory data and by assisting in its extrapolation to service conditions of stress, environment chemistry, and section size. Although more than one mechanism of environmental attack will be considered, the paper focuses on the consequences of forming a well-defined corrosion product phase.

## MECHANISMS OF ENVIRONMENTAL ATTACK

There are two principal mechanisms enabling an active species in the environment to interact chemically with a metallic alloy. In one, the species, say oxygen, can diffuse into the metal, react with impurities to give a precipitate of an oxide; often solid but sometimes gaseous. For kinetic reasons, these oxides are likely to nucleate more frequently on grain boundaries. If gaseous, their continued growth can lead to internal disintegration of the alloy, even in the absence of stress. The most spectacular example is that of tough pitch copper heated in a hydrogen-containing environment to produce bubbles of water vapour. Another, is the technologically important generation of methane

bubbles when certain ferritic steels are heated in hydrogen-containing atmospheres, giving rise to so-called 'Hydrogen Attack'. Carbon dioxide bubbles have been identified in nickel/carbon alloys after exposure to oxygen-containing environments (1). In all cases, the application of a tensile creep stress facilitates a more rapid growth of these gas bubbles and results in a reduction of creep lifetime and ductility.

The other principal mechanism of attack is the formation of a surface phase of corrosion product; oxide, nitride, carbide. The formation of oxide corrosion products on the surface of high temperature engineering alloys is deliberate and the alloys are designed specifically to minimise their rates of growth; ie $|K|$ in Eq (1) is small. Nevertheless, as we shall see in the next section, there can be an unwelcome synergy when creep and oxidation occur simultaneously.

## PHYSICALLY-BASED MODELLING

The effects of chemical attack by the environment on creep rates and vice versa have been modelled approximately in the literature (2,3) by treating the damaged alloy as a cylindrical composite composed of a core of virgin material and an outer, environmentally-attacked zone. The primary assumptions being:

- o the chemically damaged region occupies the same volume as that of the alloy matrix it replaces
- o the interface between the damaged region and the alloy matrix is sharp, with spatially homogeneous material properties in each region
- o the intrinsic behaviour in creep in both regions is described by a constitutive law that depends only on stress and temperature. A Norton-type law being chosen for mathematical convenience:

$$\dot{\epsilon} = \dot{\epsilon}_o \left[ \frac{\sigma}{\sigma_o} \right]^n \qquad (3)$$

where $\dot{\epsilon}_o$ is a temperature-dependent creep parameter.

A number of equation-sets were developed (2,3), each taking the form:

$$\dot{\epsilon} = \dot{\epsilon} (\sigma\ T\ \omega) \qquad (4)$$

$$\left.\begin{aligned} \dot{\omega} &= \dot{\omega} (\sigma\ T\ \omega) \qquad (5a) \\ \text{or } \dot{\omega} &= \dot{\omega} (T\ \omega) \qquad (5b) \end{aligned}\right\}$$

The explicit forms of equations (4) and (5) depend on the detailed deformation and fracture characteristics of the two regions of the composite.

When the characteristics are such that a redistributed stationary state stress can be reached before fracture occurs, the composite creep rates and damage rates are given by (3):

$$\dot{\epsilon} = \dot{\epsilon}_o \left[ \frac{\sigma}{\sigma_o} \right]^n \left[ \frac{1}{1 - f\omega} \right]^n \qquad (6)$$

$$\dot{\omega} = \frac{2K}{R^2 \omega} \qquad (7)$$

K may be either the parabolic rate constant $K_p$, in the case of the formation of a corrosion phase, or a kinetic factor which, in the case of internal oxidation, carburisation or nitriding, includes the diffusion coefficient of the active species. The parameter:

$$f = [1 - (\dot{\epsilon}_{om} / \dot{\epsilon}_{op})^{1/n}]$$

is a measure of the relative creep strengths of the two regions, obtained by assuming that the stress index for creep in the two regions is the same. $\dot{\epsilon}_{om}$ and $\dot{\epsilon}_{op}$ are, respectively, the temperature dependent creep parameters for the matrix and outer zone. The two phases are identical in performance when $f = 0$. When the environmentally attacked region is the weaker (for example, when grain boundary bubble formation occurs) $f > 0$ and, in the limit of $f \to 1$, Eq (6) reduces to that given by Ashby and Dyson (2) for the case of zero load-bearing capacity. f becomes negative if the region is strengthened by, for example, internal oxidation, carburisation or nitriding.

A different equation-set is found when the chemically attacked region is stronger in creep but suffers spallation while still behaving elastically; ie before the redistributing stress reaches a value sufficiently high to cause creep. The damage rate now becomes faster than that given in Eq (7), as shown schematically in Fig 2. In order to obtain the new expression for $\dot{\omega}$, the thickness of oxide when it spalls, $x^*$, has to be calculated: there appears to be three relevant models.

### Strain energy model

Evans (4) was the first to suggest that the spallation criterion for oxides is that the strain energy per unit area should exceed the interfacial energy, $\gamma_i$: it is a necessary but insufficient criterion. Much later, Manning (5) used this criterion to demonstrate that for an elastic solid undergoing deformation at a rate $\dot{\epsilon}$, the critical thickness is given by:

$$x^* = \left[ \frac{15\ \gamma_i K_p^2}{4\ E \dot{\epsilon}^2} \right]^{\frac{1}{5}} \qquad (8)$$

Using Eq (1), this gives:

$$\dot{\omega} = \frac{2}{R} \left[ \frac{4\ E\ K_p^3}{15\ \gamma_i} \right]^{\frac{1}{5}} \dot{\epsilon}^{2/5} \qquad (9)$$

### Critical defect model

Brittle solids such as oxides, fracture because of the presence of intrinsic defects which require a probabilistic approach to fracture. However, for simplicity, we will assume a deterministic approach (equivalent to a high Weibull modulus) so that the fracture stress $\sigma^*$ is given by:

$$\sigma^* = \frac{K_{IC}}{\sqrt{\pi c}} \qquad (10)$$

where c is the (single) defect size.

Assuming, an ideally brittle solid as did Manning (5), then $K_{IC} = \sqrt{\pi\gamma E}$, where $\gamma$ is the oxide surface energy, then $\omega$ can be calculated using Eq (1), if through-thickness cracking is taken to be coincident with spallation. Two limiting conditions can be envisaged:

(i) $|c|$ is independent of oxide thickness, x. Then:

$$\dot{\omega} = \frac{2}{R}\left[\frac{K_p^2 E c}{\gamma}\right]^{\frac{1}{4}} \dot{\epsilon}^{1/2} \qquad (11)$$

Eq (11) is essentially the same as that used by Ashby and Dyson (2).

(ii) $|c|$ is proportional to the oxide thickness, ie $c = kx$. Now, from Eq (10)

$$\sigma^* \propto \frac{1}{\sqrt{x}} \qquad (12)$$

ie the critical stress is inversely proportional to the square root of the oxide thickness. Eq (12) is also predicted by the strain energy model and has received substantial experimental verification with ferritic steels (6).

Eq (12) leads to:

$$\dot{\omega} = \frac{2}{R}\left[\frac{K_p^3 E k}{\gamma}\right]^{\frac{1}{5}} \dot{\epsilon}^{2/5} \qquad (13)$$

Eq (13) is virtually identical to Eq (9).

Eq's (9), (11) and (13) can be rewritten in a convenient shorthand:

$$\dot{\omega} = \frac{2}{R} K\dot{\epsilon}^{\alpha} \qquad (14)$$

where the values of K and $\alpha$ are listed in Table 1.

TABLE 1

| Model | $\alpha$ | K |
|---|---|---|
| Strain Energy | $\frac{2}{3}$ | $\left[\frac{4K_p^3 E}{15\gamma_f}\right]^{\frac{1}{3}}$ |
| c = constant | $\frac{1}{2}$ | $\left[\frac{K_p^2 E c}{\gamma}\right]^{\frac{1}{4}}$ |
| c = k x | $\frac{2}{3}$ | $\left[\frac{K_p^3 E k}{\gamma}\right]^{\frac{1}{3}}$ |

With $K_p = 10^{-6}$ $mm^2h^{-1}$ (a typical value in the temperature range of interest), $K \simeq 0.1$ for the strain energy model.

The coincidence of spallation with through-thickness cracking, implied in the latter two models, can be understood when the probabilistic nature of fracture is taken into account. Cracking will occur over a range of stresses until the spacing between cracks is of the order of the thickness of the oxide. Since consequential tensile tractions are generated normal to the interface, the final appearance will be as shown schematically in Fig 3(b). A similar model for spalling has been proposed by Evans (7), except that shear cracking was proposed as the mechanism for the final spalling event.

Constitutive Equation for Strain-Softening Alloys

Many engineering alloys are best represented by a constitutive equation of the form:

$$\dot{\epsilon} = \dot{\epsilon}_o\left[\frac{\sigma}{\sigma_o}\right]^n \exp C\epsilon \qquad (15)$$

C is a parameter that characterises the rate of accumulation of tertiary creep strain. It has been suggested, and evidence presented for nickel-base superalloys (8), that C is a composite term given by:

$$C = C_{int} + n + n/3\epsilon_f \qquad (16)$$

where $C_{int}$ represents the contribution to tertiary creep due to the intrinsic mechanism of deformation; n is the contribution due to stress increasing with strain in a constant load test; and $n/3\epsilon_f$ is the maximum contribution from intergranular cavitation causing fracture. $C_{int}$ is zero for steady state creeping materials, such as pure metals and simple alloys.

The equation-set for modelling the synergy between creep of a strain-softening alloy and corrosion due to periodic spallation is:

$$\dot{\epsilon} = \dot{\epsilon}_o\left[\frac{\sigma}{\sigma_o}\right]^n \left[\frac{1}{1-\omega}\right]^n \exp C\epsilon \qquad (17)$$

$$\dot{\omega} = \frac{2}{R} K \dot{\epsilon}^{\alpha} \qquad (18)$$

Eq's (17) and (18) reduce to those given by Ashby and Dyson (2) when C = 0.

Integration under conditions of constant load/stress and temperature of Eq's (17) and (18) as a coupled pair yields strain as a function of time. The integration has to be performed numerically but an approximate analytical result can be found by dropping the term exp $C\epsilon$ in Eq (18), giving:

$$\dot{\omega} = \frac{2}{R} K\dot{\epsilon}_o^{\alpha}\left[\frac{\sigma}{\sigma_o}\right]^{\alpha n}\left[\frac{1}{1-\omega}\right]^{\alpha n} \qquad (19)$$

## MODEL PREDICTIONS

Integration of Eq's (17) and (19) at constant load and temperature gives:

$$\epsilon = -\frac{1}{C} \ln \left\{ 1 - \frac{RC\,\dot{\epsilon}_i^{1-\alpha}}{2K(n-\alpha n-1)} \left[ \left[ \frac{1}{1 - (1+\alpha n)\frac{2}{R} K \dot{\epsilon}_i^{\alpha} t} \right]^{\frac{n-\alpha n-1}{1+\alpha n}} - 1 \right] \right\} \quad (20)$$

where $\dot{\epsilon}_i = \dot{\epsilon}_o \left[\frac{\sigma}{\sigma_o}\right]^n$ is the initial creep rate.

$$\text{or} \quad \epsilon = -\frac{1}{C} \ln \left\{ 1 - C_{eff}\, \dot{\epsilon}_i t \right\} \quad (21)$$

where $C_{eff}$ is the effective C of the model composite: it is not of course a constant even at constant stress and temperature.

The accuracy of Eq (20) can be judged in Fig 4 by comparing it with the numerical solution of Eq's (17) and (18): it is adequate for most purposes.

Fig 5 demonstrates that corrosion exerts a greater influence on lifetime for a steady-state creeping material than for a strain-softening one: much smaller reductions in lifetime are found with the latter type of constitutive law.

The difficulty with creep/corrosion interactions as far as design is concerned is that laboratory stresses/temperatures are different from those found in service and therefore an extrapolation procedure is required. Figs 6 and 7 demonstrate the difficulties that can arise without access to an adequate extrapolation model. Both types of plot are used in the determination of remaining life of components. In Fig 6, lifetime is plotted as a function of stress for various values of the quotient K/R, equivalent to a factor of 20 span of section sizes. In Fig 7, lifetime at a given value of stress is plotted as a function of temperature. In this example, the activation energy for the parabolic corrosion rate constant has been taken to be less than that for creep, which accounts for the larger influence of corrosion at the lower temperature. The value of $Q(K_p)$ = 210 kJ/mole is that reported by Zhong and Zhang (9) for a low alloy steel containing aluminium and chromium.

## MODEL VALIDATION

There are only a few data in the literature which are suitable for attempting to validate the creep/corrosion model discussed in this paper. The most systematic and well-characterised set of information appears to be for the oxidation of low alloy ferritic steels. Fig 8 reproduces creep data on 1/2 CrMoV steel at 640°C, 43 MPa obtained in air and vacuum (10). We have used Eq's (17) and (18) to generate the two solid curves and it can be seen that agreement is quite good. A more demanding test is to predict the effect of changing the testpiece section size. Fig 9 reproduces data, again on 1/2 CrMoV steel, but tested at 675°C and 70 MPa using 4 widely different section sizes (10). Eq's (17) and (18) produce good fits to the experimental data.

Some further data on 1/2 CrMoV steel (11) are shown in Fig 10, where lifetime is plotted as a function of temperature. Again, Eq's (17) and (18) bound the data but in contrast to Fig 7, the model predicts less interaction at lower temperatures, because the activation energy for oxidation in this material is higher than for creep at temperatures greater than 600°C (12): at temperatures less than 600°C the reverse is true, as illustrated by the dashed/dotted line. The experimental data show no significant trend.

The paper has concentrated on the influence of stress-induced corrosion on creep life. However, as discussed in the Introduction, service lifetimes may also be limited by loss of load-bearing cross-section due to corrosion. In this case a slightly different picture emerges: Fig 11 has been constructed on the assumption that $t_{f,E} = 10^7$ h (see Fig 1), ie well in excess of the creep design lifetime of $10^5$ h at 40 MPa. At lower stresses spalling is seen to be life-limiting, but it has to be remembered that we have defined an arbitrary corrosion damage level of 0.1 and so Fig 11 must therefore be regarded only as informative until there is a design procedure for corrosion.

## CONCLUSIONS

1. For strain-softening alloys, the synergy between creep and corrosion by periodic spallation can be adequately modelled by numerical integration of two coupled differential Eq's (17) and (18) or by using an approximate analytical solution Eq (20), obtained from Eq's (17) and (19) (See Fig 4).

2. Corrosion effects on creep properties are predicted to be much greater for a steady state creep law than for a strain-softening law more appropriate to engineering materials.

3. The model has been validated on a published but limited experimental data-set on 1/2 CrMoV steel. Satisfactory agreement has been achieved in predicting the influence of section size at constant applied load and temperature as well as of test temperature at constant load and section size.

## ACKNOWLEDGEMENT

The authors would like to thank Dr A Barbosa for writing the computer program to enable numerical integration and graphical display of Eq's (17) and (18).

## REFERENCES

1. R.H. Bricknell and D.A. Woodford (1982) Acta Metall 30 257.

2. M.F. Ashby and B.F. Dyson (1984). Advances in Fracture Research (eds. S.R. Valluri et al) Vol 1 Pergamon Press p3.

3. B.F. Dyson and S. Osgerby (1987) Mat. Sci. & Tech. 3 545.

4. U.R. Evans (1948) "An Introduction to Metallic Corrosion" Edward Arnold, London p194.

5. M.I. Manning (1981) "Corrosion and Mechanical Stress at High Temperatures" Eds., V. Guttman and M. Merz Applied Science Publishers, London p326.

6. J. Armitt, D.R. Holmes, M.I. Manning, D.B. Meadowcroft and E. Metcalf (1978) "The spalling of steam grown oxide from superheater and reheater tube steels" EPRI Report FP 686.

7. H.E. Evans (1988) To appear in Mat. Sci. and Technology.

8. B.F. Dyson and T.B. Gibbons (1987) Acta Metall 35 2355.

9. Huang Zhen-Zhong and Zhu Ri-Zhang (1983) Proc. JIMIS - 3, 231.

10. B.J. Cane and R.D. Townsend (1985) "Flow and Fracture at Elevated Temperatures" ASM Ohio p279.

11. D.J. Gooch and R.D. Townsend (1986) Proc. EPRI conference "Life Assessment and Extension of Fossil Plants" Washington DC.

12. L.W. Pinder (1977) CEGB report SSD/MID/R58/77.

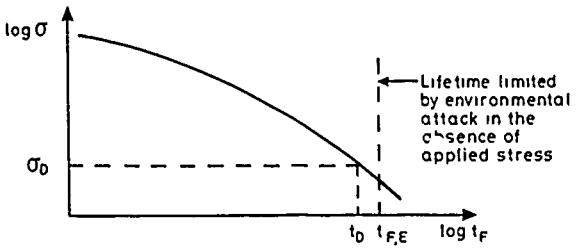


Fig 1: Schematic illustration of the relationship between the design failure time due to creep, $t_o$, and that due to environmental attack, $t_{f,E}$ in the absence of an applied stress.

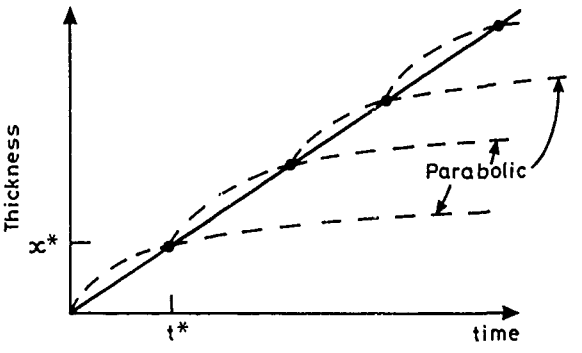


Fig 2: Periodic spallation after time t*, results in a much faster damage rate than given by parabolic rate kinetics: in this case, a pseudo linear rate.

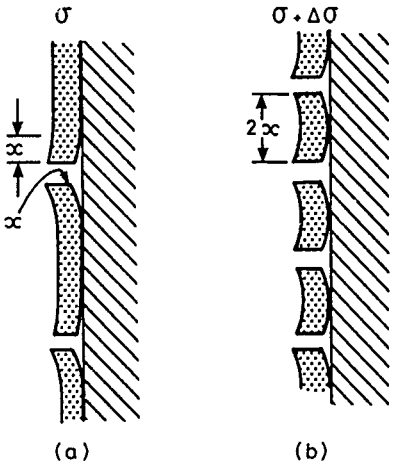


Fig 3: Schematic illustration of the mechanism by which through-thickness cracks in the oxide lead to spallation. In (a), the oxide is sustaining a stress $\sigma$ and has partially cracked and decohered. In (b), the stress has increased by $\Delta\sigma$ and the cracking density has saturated.

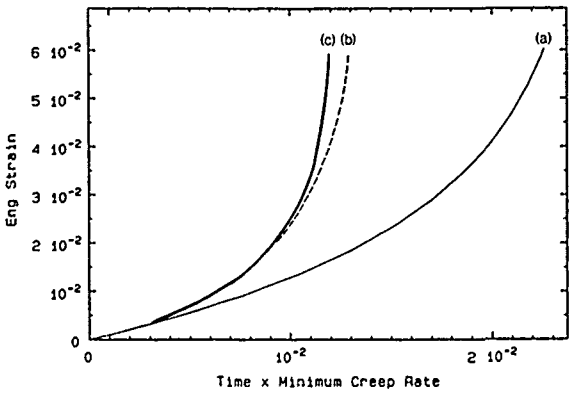


Fig 4: Comparison of approximate analytical solution (curve b) of creep/corrosion synergy using a strain-softening constitutive law with the exact numerical solution (curve c). Curve (a) is the Reference (no corrosion) curve. C = 40; K = 0.14; $\alpha$ = 0.5; R = 5 mm; n = 4.

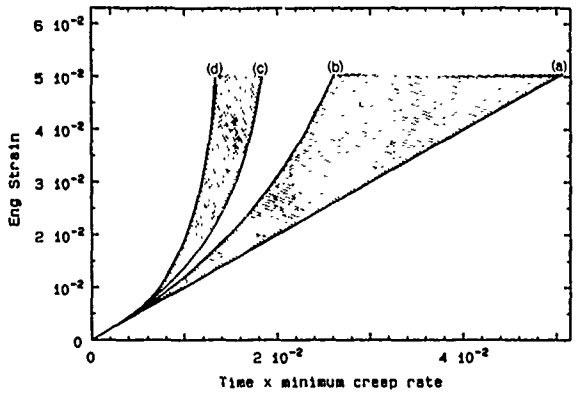


Fig 5: A plot of creep strain as a function of minimum (initial) strain rate × time; demonstrating that corrosion has a greater effect on lifetimes when the material obeys a steady state constitutive law rather than a strain-softening law. (a) and (c) are the Reference (no corrosion) curves for the two material classes. C = 50; K = 0.15; $\alpha$ = 0.5; R = 5 mm; n = 4.

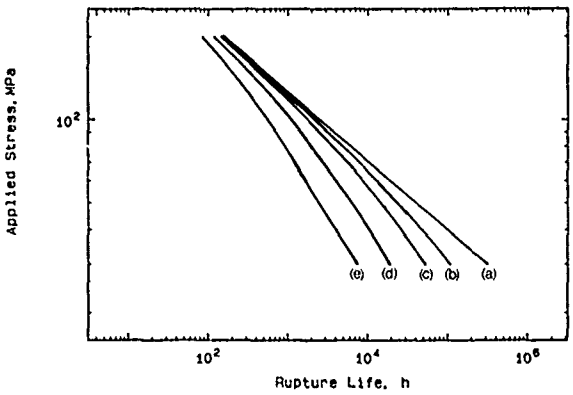


Fig 6: Plots of time to fracture as a function of stress for various values of the quotient K/R; C = 40; $\alpha$ = 0.5; n = 4; $\dot{\epsilon}_f$ = 0.1; K/R = 0(a), 0.004(b), 0.01(c), 0.03(d) and 0.08(e).

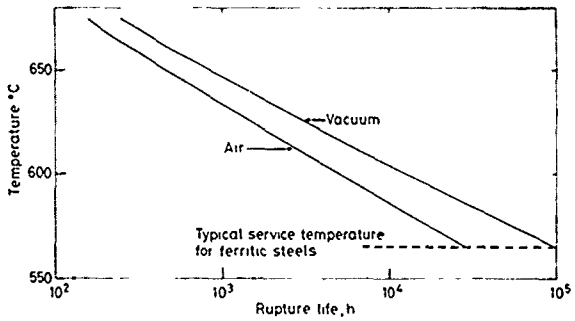


Fig 7: Plots of time to fracture as a function of temperature at constant load, illustrating that the effects of corrosion by periodic spallation become more important at lower temperatures for the case when the activation energy for corrosion is less than that for creep. C = 50; K (675°C) = 0.15; R = 2.5 mm; n = 4; Q (creep) = 360 kJ mole$^{-1}$; Q ($K_p$) = 210 kJ mole$^{-1}$.

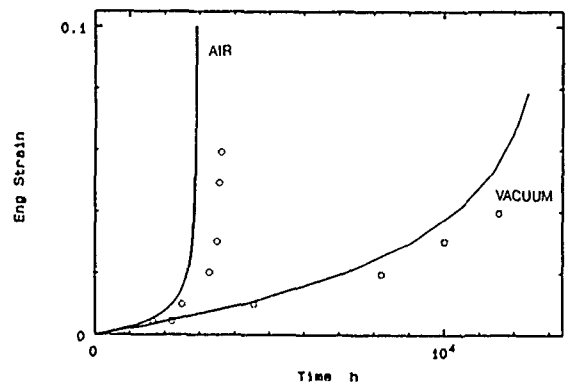


Fig 8: Comparison of model prediction and experimental data (10) on ½ CrMoV steel at 640°C and 43 MPa. C = 40; n = 4; K = 0.1; $\alpha$ = 0.5 and $\dot{\epsilon}_i = 1.9 \times 10^{-6} h^{-1}$.

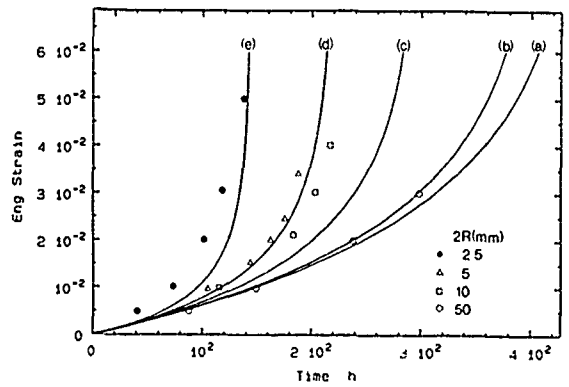


Fig 9: Comparison of model prediction and experimental data for the effect of section size on creep behaviour in the presence of oxidation by periodic spalling. C = 40; K = 0.14; $\alpha$ = 0.5; n = 4. (a) is the model vacuum curve. Curves (b) to (e) are model predictions for air tests using 2R = 50, 10, 5, 2.5 mm respectively.

Fig 10: Lifetime as a function of temperature at constant load in air and argon: comparison of model prediction and experimental data. C = 50; R = 2.5; n = 4; $\alpha$ = 0.5; $\dot{\epsilon}_i$(675°C) = 5 × $10^{-5}$ $h^{-1}$; K (675°C) = 0.15. Q ($K_p$) = 460 kJ $mole^{-1}$ (> 600°C), 110 kJ $mole^{-1}$ (< 600°C); Q (creep) = 360 kJ $mole^{-1}$.

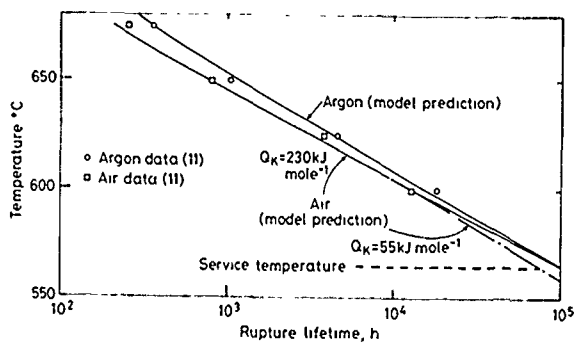


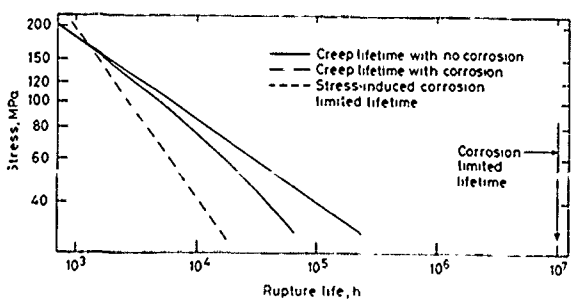


Fig 11: Demonstrating that lifetime can be limited by loss of section due to spallation. C = 40; K = 0.18; n = 4; R = 20 mm; $\epsilon_f$ = 0.1.

# DESIGN AND OPTIMIZATION OF EXPLOSIVE CLADDING PARAMETERS OF VARIOUS METAL COMBINATIONS AND CERAMIC

Dr. S.K. Salwan

Deputy Director
Central Mechanical Engineering Research Institute
Durgapur : INDIA

## INTRODUCTION

Explosive cladding offers real saving in materials usage because only a minimum layer of the more nobel and costly metal to resist an aggressive medium need be applied on a heavier and less costly load bearing substrate. Explosive welded products offer the designer unique option in material selection in term of possible bimetal system and bond integrity, including metal ceramic combinations. Control of welding paremeters results in a bond zone whose strength is equal to or greater than the weaker of the two metals.

## PROCESS

The stand off distance is a basic feature of explosive welding process, for it provides a gap across which the flyer plate may be accelerated to a sufficient velocity to generate the required pressure at collision point and condition of collision to be such as to produce jetting. The two types of configuration those are normally used i.e. one is parallel plate arrangement and second is preset angle arrangement were used for the experiment. Military plastic explosive was used and velocity of detonation was measured for various thickness of the compact rolled sheet. In order to obtain various explosive loading the weight of the explosive was varied by using corresponding thickness of the rolled sheet. The area of the weld selected was 15.2 cm x 7.62 cm. Rubber buffer of 3 mm thickness was used. The rubber has a hardness of 80 Hv the weight of the explosive has varied from 36 gm to 197 gm by having rolled sheets of 2 mm to 6 mm thickness in step of 0.5 mm.

TNT:NaCl (70:30) mixture was used for parallel plate arrangements. Ammonia-nitrate, TNT and Aluminium (80:15:5 by weight) was also used.

The tensile strength of the resulting explosive welds was measured using zero gauge length. Parameters for 12 metal combinations and one metal and ceramic combinations were optimised.

## DISCUSSION OF RESULTS/CONCLUSION

The following conclusion can be drawn :

a) The pressure at the interface must exceed the theoretical shear strength of the materials.

b) Minimum dynamic angle which must exceed is critical angle for jetting. No welding has occured below the critical angle.

c) Jet velocity must exceed the minimum value for proper scouring action and it is found to be between 0.5 to 0.7 times the bulk sound velocity.

d) For maximum weld strength it is seen from the experimental result that jet velocity is the best criterion because at jet velocity equal to the bulk sound velocity the maximum strength is obsdderved. It is good practive to keep $v_p \cot \beta/2 = C_p$.

e) The optimum kinetic energy per unit area of the impacting plate is approximately equal to theoretical shear strain energy per unit volume (proposed criterion).

f) There is no effect on increase in area of the weld on weld tensile strength. Area above 500 sq/cm was not tried due to limitation of firing sight.

g) The tensile strength showed fluctuation when the thickness was varied from 1.59 mm to 4.00 mm. This is due to the variation in impact energy.

h) When the thickness of parent plate was varied from 2 mm to 8 mm keeping the flyer plate thickness constant (3 mm), no change in tensile strength of the weld was oboserved.

## METALLURGICAL OBSERVATIONS

The unique microstructure generated is shown in Figs. 1,2,3. When viewed in the electron

microscope, the weld interface is the region of solid phase bond closely resembles an over size grain boundry between highly elongated grains of the two welded metals. The weld zone contain higher densities of dislocations and presumably higher concentration of point defects than the parent metals. Furthermore, effects of dynamic recovery and recrystallization have been observed near the weld interface as a result of heat generated by the collision.

The single most important factor which will govern mechanical behaviour after welding is the terminal microstructure. The microstructure difference reside primarily in the density and distribution of lattice defects such as dislocation vacancies and intersitials, stacking faults and mechanical twins. Stress corrosion resistance has been studied and related to terminal microstructure.

Fig. 1

Explosive welded joint between Titanium (top) and steel (bottom) in etched condition delimating regular crest and trough wavy interface with plastic deformation at Ti-steel junction

Fig. 2

Explosive welded joint between unetched steel (top) and etched Titanium (bottom) showing typical crest and trough wavy interface with plastic deformation of Titanium

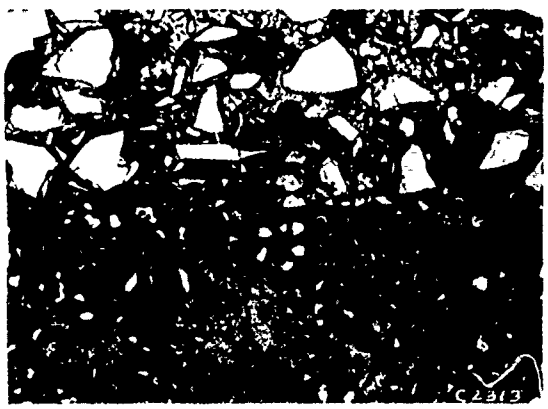

Fig. 3

Explosive welded joint between unetched aluminium (top) and unetched ceramic (bottom) delimating regular joining lines at the interface

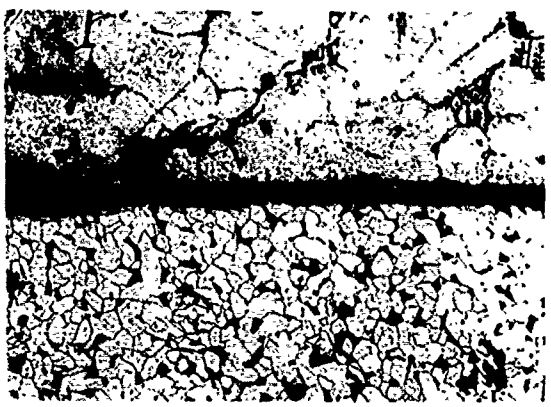

Fig. 4

Explosive welded joint between etched aluminium (top and etched steel (bottom) exhibiting regular joining line at the interface

J ROBERTS

# STRESS-STRAIN PROPERTY REFERENCE POINTS PROVIDING MEASURES OF MATERIAL RESILIENCE

Dr Roberts is in the Polymers Section of the Royal Armament Research and Development Establishment Fort Halstead Sevenoaks Kent.

## SYNOPSIS

An alternative presentation of the stress-strain data for plastic materials has been devised which defines three stages of mechanical deformation or degrees of material resilience.

It is suggested that such points could be useful aids in plastic materials selection and component design.

## INTRODUCTION

Plastic raterials are now being considered for an ever widening range of load bearing engineering applications. Their complex response when subjected to mechanical loads raises difficult materials selection and component design problems. As an aid in these areas three stress-strain reference points are proposed. Point A is a nominal elastic limit, point B an intermediate elastic-plastic limit and point C an initial yield limit.

The reference points are obtained using a graphical analysis of stress-strain data for as wide a range of temperatures and strain rates as possible. Data for all materials with an identifiable yield point can be considered.

## PROPOSED STRESS-STRAIN REFERENCE POINTS

The stresses and strains for the reference points are denoted $\sigma_A$, $\epsilon_A$ for point A, $\sigma_B$, $\epsilon_B$ for point B and $\sigma_C$, $\epsilon_C$ for point C. Values for these stresses and strains are obtained using the graphical constructions shown in Figs 1 and 2 (Ref 1) with data for cellulose acetate butyrate (Ref 2).

The procedure is:

a. From the stress-strain curve obtain the maximum stress $\sigma_D$ (Fig 1).

b. Plot valves of the ratio $\sigma/\sigma_D$ against $\log\epsilon$ and obtain values of $\epsilon_A$ and $\epsilon_C$ as limits to the transition region shown in Fig 2.

c. On the stress-strain curve (Fig 1) draw the secant modulus, $E_S$, for strain $\epsilon_A$. Extrapolate this modulus to the stress level $\sigma_D$ to give strain $\epsilon_B$.

d. Using the stress-strain curve obtain values of the stresses corresponding to strains $\epsilon_A$, $\epsilon_B$ and $\epsilon_C$.

It must be emphasised that the shape of a stress, strain curve and so the values of stress and strain do depend on the method of preparation of the test piece. For example, in many cases injection moulded narrow waisted dumbell tensile test pieces are used and there can be degrees of molecular orientation along the length of the specimen.

When matching the reference points with the temperature and rate of deformation required for a given application it is suggested that use be made of the observation that linear correlations are possible in each case. Thus, the variation of each reference point stress over a range of temperatures at a constant rate of strain can be described by a linear function of stress versus the square root of absoulute temperature. Again the variation of each stress over a range of strain rates at a constant temperature can be described by a linear function of stress versus $\log_e$ rate of deformation.

## THE PROPERTY REFERENCE POINTS AS MATERIAL RESILIENCE LIMITS

In the present context the term resilience is taken to be a measure of the degree of elasticity in the mechanical reponse of a material. It is noted that when the reference points are compared with cyclic stress-strain data (Ref 3) to a limit of the order of point A then the specimen recovers completely ie point A is a nominal elastic limit. For tests within the stress-strain range between points A and B there is limited residual strain whereas tests within the range between points B and C can result in a significant residual strain indicating that some plastic flow has occurred.

For plastic materials it is suggested that the stress $\sigma_C$ is a more appropriate maximum design limit than the yield stress $\sigma_D$.

## TENSILE CREEP LIMITS

Since the nominal elastic deformation limit, $\epsilon_A$, can correspond to an acceptable degree of resilience it is suggested it be used as the basis for the construction of creep curve limits useful in materials selection and component design.

From a set of creep curve data it is possible to construct a creep characteristic which gives the strain $\epsilon_A$ at the end of a required period of time.

## STRESS RELAXATION AND CRAZE INITIATION LIMITS

The strain $\epsilon_A$ also provides a useful working limit for stress relaxation applications. For example, it is noted that for polymethylmethacrylate a stress relaxation curve constructed for the strain $\epsilon_A$ not only ensures limited stress decay, it also avoids stress levels that cause crazing (Ref 4).

## DEWETTING IN PARTICULATE FILLED MATERIALS

It is assumed that the onset of dewetting is associated with the beginning of the breaking of the adhesive bonds between the explosive particles and binder material in polymer bonded explosives. The strain at the onset of dewetting, denoted $\epsilon_D$, has been taken (Ref 5) to be the point at which volume dilation reaches 0.1%. It is found that strain $\epsilon_B$ approximates to, or is less than, strain $\epsilon_D$ so that $\epsilon_B$ can provide a useful application limit.

## CONCLUSION

It is suggested that the proposed stress-strain property reference points can provide useful mechanical property limits for both the short and longer term loading of plastic materials.

## REFERENCES


1. Roberts J Plastics and Rubber Processing Applications - to be published.

2. Ely R E Plastics Techology November 1957 P900-903

3. Passaglia E and Knox J R Engineering Design for Plastics, Ed E Baer P143-198 Reinhold New York 1964.

4. Gotham K V Thermoplastics, Properties and Design Ed R M Ogorkiewicz P51-61 J Wiley London 1974.

5. Yee R Y and Martin E C Naval Weapons Centre, China Lake, USA, Report NWC TP-6619, Pt2, 1985 (unlimited).

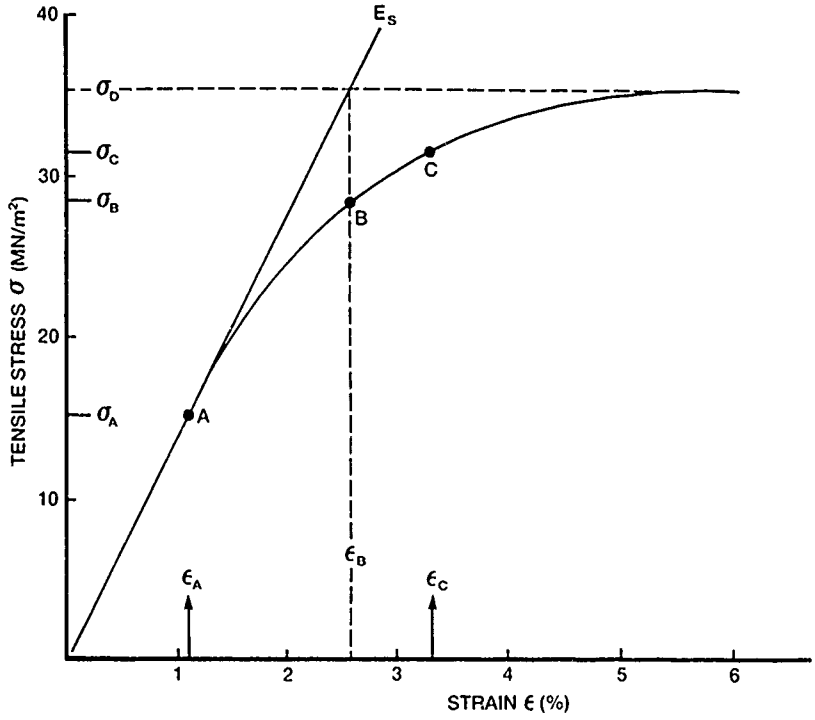


FIG 1 TENSILE STRESS STRAIN DATA FOR CELLULOSE ACETATE BUTYRATE (Ref 2)

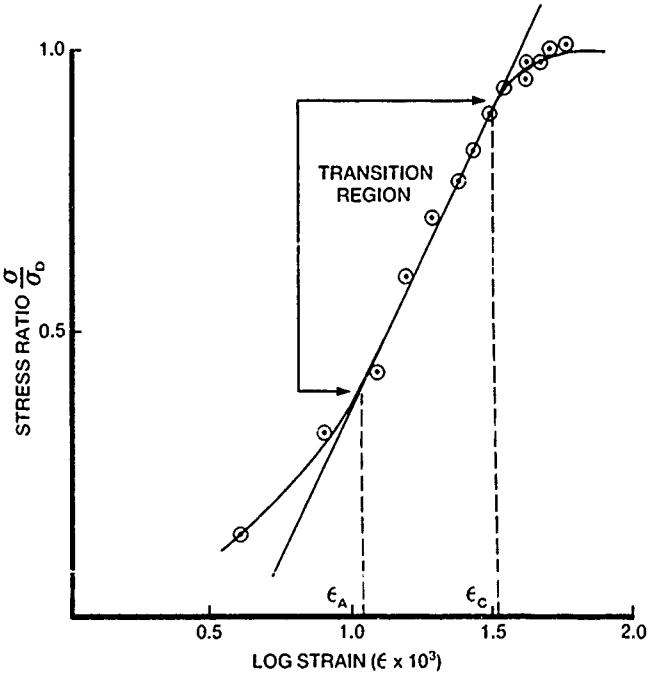


FIG 2 TENSILE STRESS RATIO,LOG STRAIN DATA FOR CELLULOSE ACETATE BUTYRATE

# 'VERTON' ADVANCED ENGINEERING PLASTICS : MATERIALS AND DESIGN

By Dr Mark G Styring and Mr G E Nutting, ICI Advanced Materials, 'Verton' Section, PO Box 90, Wilton Centre, Middlesbrough, Cleveland, TS6 8JE.

SYNOPSIS

This paper begins by describing the 'Verton' range of long-fibre-reinforced, engineering thermoplastic injection-moulding materials. They are manufactured by a recently-introduced technology for the impregnation of continuous fibres by thermoplastic resins. The end products display fibre lengths an order of magnitude greater than their short fibre-reinforced counterparts, with corresponding improvements in mechanical and other properties. This leads to applications in which metals are directly replaced. The first generation of 'Verton' materials were based on glass-reinforced nylon 66. The technology has been adapted to permit the impregnation of other fibre types, most notably aramid, with a range of resins, opening up exciting new possibilities for design engineers. The presentation at the Materials '88 conference takes the form of a poster session in which examples of 'Verton' materials and applications are on display, together with a practical demonstration of EPOS (Engineering Plastics on Screen). This is a software package, available through ICI Advanced Materials, which gives data on more than 600 grades of engineering plastics available through ICI, with more in-depth design information on certain materials, including 'Verton'.

## INTRODUCTION

The introduction of fibres into plastic materials is a means of producing composites having far superior mechanical properties to the unreinforced polymers. The mechanism of reinforcement is the transfer of the applied load through the relatively flexible plastic matrix to the stiff fibres. The amount of reinforcement is proportional to the length and amount of fibre in the matrix, to the strength of bonding between polymer and fibre and also to the stiffness and strength of the fibre itself. By far the most commonly-employed reinforcing fibre is glass, although carbon and aramid fibres are becoming increasingly accepted. Both thermosetting and thermoplastic resins can be reinforced, although this paper concentrates on the latter.

The technique of extrusion compounding to produce short-(0.2-0.4mm)-glass-fibre-reinforced thermoplastics was introduced a quarter century ago by ICI. Such materials display both extremely good mechanical properties, relatively low price and ease of processing, most commonly by injection moulding, which allows rapid production of parts requiring little or no finishing. At the other end of the materials spectrum, continuous-fibre-reinforced composites undoubtedly display the best mechanical properties, but the fabrication methods, e.g. hand lay-up and pultrusion, are normally slow and/or labour intensive, i.e.costly. The search for a material which could combine the superior mechanical properties of continuous-fibre composites with the ease of processing and cost effectiveness of short-fibre compounds lasted some 25 years. It was in 1985 that ICI launched the 'Verton' range of long-(10mm)glass-fibre-reinforced nylon 66 materials.

Early market acceptance has encouraged the development of grades of materials based on several other polymers and also such fibres as carbon and aramid.

## MANUFACTURE

'Verton' is manufactured by ICI's patented thermoplastic pultrusion process which ensures very good wet out and impregnation of fibre by polymer. This process produces continuous lace which is then chopped to pellets 10mm long. This length was chosen for an optimal balance between fibre length and ease of feeding in injection-moulding machines, although, in principle, any pellet length could be produced. 'Verton' lace, pellets and other 'off-spring' of this technology are shown in figure 1.

## PROCESSING

'Verton' materials can be processed on any conventional injection-moulding equipment, although certain features should be modified relative to short-fibre processing, to ensure optimal component properties. In all screw injection moulding machines, the polymer is melted by shear and conductive heating in the barrel, then the melt is injected at high speeds and pressures into the mould cavity. Inevitably some fibre breakdown occurs in such a process. The aim in processing 'Verton' is to keep this fibre attrition to a minimum, which is achieved simply by careful attention to screw design, machine settings and mould configuration.

## PROPERTIES

Most of the work so far published on 'Verton' compounds has been done on the nylon 66 variants. It is found that practically every measurable mechanical property, to a greater or lesser extent,

is enhanced relative to the short-fibre equivalent. The key to this lies in the residual fibre length in the moulding. This can be directly observed by pyrolysing the moulding and examining the "skeletal" remains.
Figure 2 shows a typical moulding, both before and after pyrolysis, where the "skeletal" remains are clearly visible and stand up under their own weight If moulded in short-fibre material, a pile of dust would remain. By adherence to moulding recommendations, residual fibre lengths are on average an order of magnitude greater than for short-fibre compounds. Figure 3 shows an example of the kind of property improvements achievable through long-fibre technology, on a plot of stiffness against impact strength.

APPLICATIONS

The improvement in mechanical properties, observed over a wide range of temperatures, combined with economics of processing and lack of corrosion, has led to the replacement of existing metal and thermoset components and in certain cases where parts traditionally moulded in short-fibre products are at the limit of their capabilities and where that extra margin of safety is required. Applications have so far been accepted in several industry areas.
In the automotive industry control pedals (see figure 4), connectors and transmission parts (see figure 5) have been made in 'Verton'. In the sports and leisure field, we see rackets, windsurfer parts, bicycle pedals and ski bindings. Electrical and electronics applications include switchgear and soldering apparatus and in power tools, housings and gear wheels have been made in 'Verton', to name a few of the applications.

VARIANTS

a) Glass Reinforced

Flame-retardant and hot oil/grease resistant versions of the nylon 66 material are available. A polypropylene version is available in commercial quantities. More recent product-development work has made available trial quantities of variants in nylon 6, nylon 6 10, PBT, PPS, polyurethane and polycarbonate. Each display improvements in properties over the short-fibre equivalents.

b) Aramid Reinforced

Aramid-reinforced versions show enhanced mechanical properties relative to the unfilled materials, though not yet to the same degree as their glass-reinforced counterparts. They do, however, possess outstanding wear properties. Composites available are based on nylon 66, polyurethane, polyester elastomer and polyacetal. For the nylon variant, wear resistance is between four and eight times better than for neat nylon and 70% better than glass-reinforced. The material is also forty times less abrasive than glass-reinforced nylon. Variants based on ICIs 'Victrex' polymers PES, PEEK and SRP are under development. Early evaluations show promise for these to become the ultimate thermoplastic bearing materials, owing to the high-temperature stability and chemical resistance of the resins.

c) Carbon-Reinforced

A carbon-fibre-reinforced nylon 66 material is available in trial quantities and 'Victrex' variants are under development.

EPOS DEVELOPMENTS

Figure 6 gives a schematic of how EPOS actually works. One can enter the system by searching for a material on the grounds of certain selection criteria such as price, chemical resistance, flammability rating and mechanical properties. The program lists any polymers which fall into the specified property ranges. The user can then access the data bank to obtain further information on supplier, chemical-resistance data, mechanical, thermal and general properties. All versions of EPOS have these features in common. Future versions will have, in addition, the facility to obtain further information on applications of a particular grade (a brief description and the reason for selection of that material), on processing, on metals replacement, on mould and product design. Further there is a fault finding guide for those experiencing problems during moulding.

---

Figure 1
'Verton' lace, pellets and other 'offspring'.
Figure 2
Typical moulding before and after pyrolysis.
Figure 3
Property improvements achievable on a plot of stiffness against impact strength.
Figure 4
Automotive control pedal.
Figure 5
Transmission selector plate on Jaguar car.
Figure 6
A schematic view of how EPOS' works.

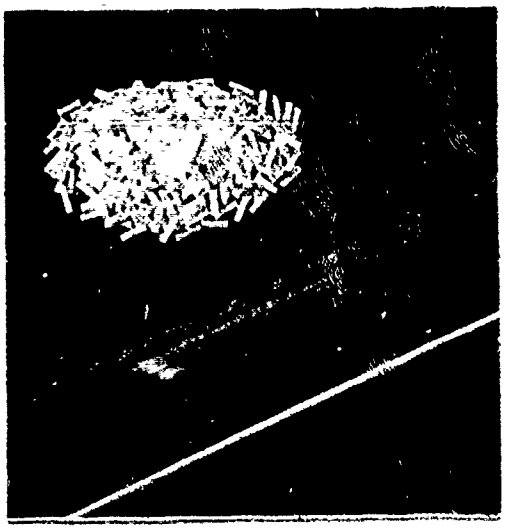

1

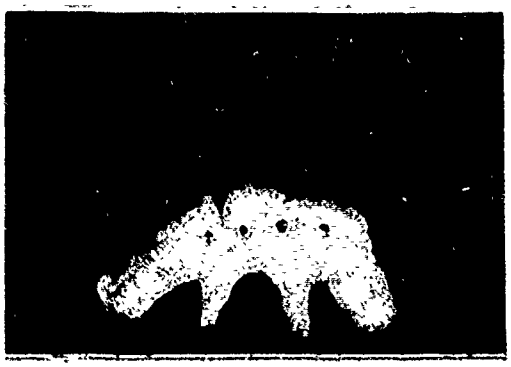

2

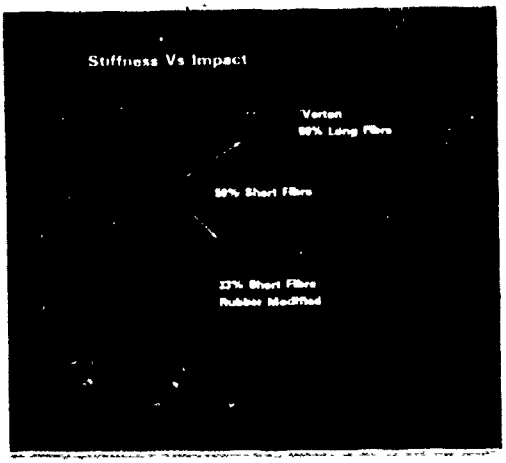
Stiffness Vs Impact
Verton
99% Long Fibre
50% Short Fibre
33% Short Fibre
Rubber Modified

3

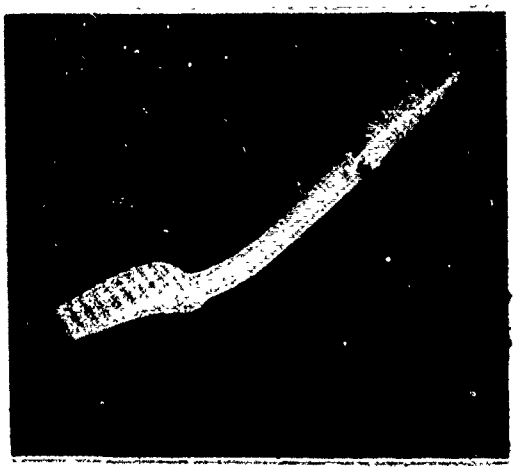

4

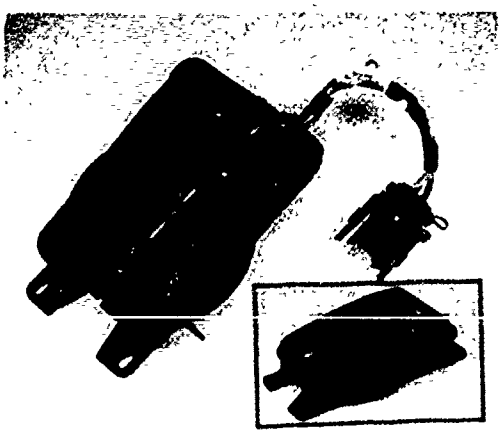

5

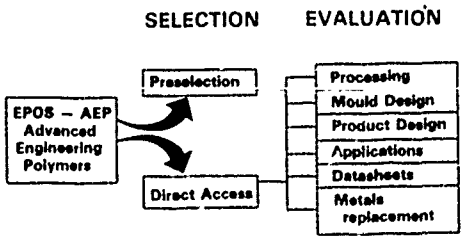
SELECTION
EVALUATION
EPOS – AEP
Advanced
Engineering
Polymers
Preselection
Direct Access
Processing
Mould Design
Product Design
Applications
Datasheets
Metals
replacement

6

# DYNAMIC RECOVERY IN AN Al-Li-Cu-Mg ALLOY

Xia Xiaoxin and John W. Martin

Oxford University Department of Metallurgy & Science of Materials

SYNOPSIS

A study has been made in alloy 8090 of varying the S-phase distribution either by varying the degree of prior stretch or by means of duplex ageing. A comparison has been made of work hardening rates (whr) in tension between 300K and 550K for each of the microstructures. Dynamic recovery is observed as a sudden fall in whr, and it has been found to occur at the lowest temperature (approx. 350K) in material subjected to the highest degree of prior stretch (7%), and at the highest temperatures (approx. 450K) in unstretched material. A dislocation model of dynamic recovery describes the experimental observations, and it is suggested that the dislocations introduced by the stretch are insufficiently pinned by the subsequent S-phase precipitation in this alloy.

## INTRODUCTION

This work is concerned with an Al-Li-Mg-Cu-Zr alloy designated 8090. The main strengthening phase is $\delta'$ ($Al_3Li$) which, being a coherent, ordered phase encourages planar slip which may lead to premature failure. Cu and Mg are added to promote the formation of S-phase ($Al_2CuMg$) which contributes to the strength and also has the effect of homogenizing the distribution of slip.

A more uniform distribution of the S-phase particles is produced if the alloy is plastically stretched prior to ageing. The dislocations introduced act as nucleation sites for the precipitation of S-phase particles. It has also been shown (1) that the distribution of S-phase may also be made homogeneous by means of a duplex heat-treatment introducing a period of natural ageing between solution treatment and artifical ageing. The object of the present research has been to study the effect of S-phase distribution and of prior stretch upon dynamic recovery on alloy 8090, as revealed by changes in work-hardening rate at elevated temperatures.

## EXPERIMENTAL PROCEDURE

The composition (wt %) of the alloy is as follows: Li 2.41, Cu 1.16, Mg 0.61, Zr 0.11, Fe 0.14, Si 0.10, Na 0.0015, balance Al. The material was in the form of rolled plate of 25 mm thickness.

A series of specimen blanks were solution-treated at 530°C for 1 hr, cold-water quenched and subjected to a plastic stretch of either 4% or 7%, and then aged to peak hardness (20 hr at 190°C).

A second series (coded D) of blanks were subjected to the following heat-treatment (1): solution treatment at 530°C for 1 hr followed by a water quench, natural ageing for 24 hr and a final artificial age of 24 hr at 190°C. A third series of blanks (coded N) were artificially aged as the second series, omitting the period of natural ageing.

Cylindrical tensile specimens of gauge length 18 mm and diameter 5 mm were machined from the blanks, such that their longitudinal axis was parallel to the rolling direction of the plate. Tensile tests were conducted over a range of temperatures between 300K and 550K at a strain rate of $1 \times 10^{-3}\ s^{-1}$, the specimens having been maintained at test temperature for 0.5 hr prior to testing.

## RESULTS

Fig.1a shows the S-phase in N material: the particles primarily decorate the stray dislocations present. In D material, fig.1b, there is an increased volume fraction of a fine, uniform array of S-phase in agreement with the observations of Flower et al (1). In stretched material, fig. 1c, there is a uniform array of S-phase, this time in association with the introduced dislocations.

The work-hardening rates (whr) were calculated from the gradient of the tensile curves at 0.2% plastic strain. Fig.2 shows the variation in the modulus-normalised whr with temperature. It may be seen that the stretched alloys exhibit a higher whr at room temperature than the unstretched materials, and that the D material had the lowest whr. With increase in test temperature, a sharp fall in whr is observed at around 450K in the unstretched (D and N) alloys, the 4% stretched material shows the fall at about 400K and the 7% stretched material at about 350K. It should be noted that these temperatures are all less than the final ageing temperature (463K), so are not associated with microstructural instability.

## DISCUSSION

At low temperature the dislocation substructure introduced by the stretch is evidently a potent source of work hardening, in that the highest whr is observed in the material subjected to the highest degree of stretch (7%).

With increase in temperature it appears that the dislocation substructure begins to act as a sink, so that the whr begins to fall first the 7% stretched material, while the D and N material exhibit the greatest resistance to dynamic recovery. Kocks (2) treats dynamic recovery as a balance between dislocation storage at a rate:

$$k_1\sqrt{\rho}/b$$

and dislocation annihilation at a rate:

$$k_2 l_r \rho / b$$

where $k_1$ and $k_2$ are constants, b the Burgers vector of the dislocations of density $\rho$ . lr is the length of dislocation annihilated per recovery event. The probability of softening events is assumed to be proportional to the total dislocation density, and so the rate of increase in dislocation density is :

$$d\rho/d\epsilon = (k_1\sqrt{\rho} - k_2 l_r \rho)/b$$

which becomes in terms of the whr ($\theta$):

$$\theta = \alpha\mu\, k_1/2 - (k_2 l_r/2b)\sigma$$

This relationship is idential to one postulated by Voce (3). By fitting the true stress-curves to polynomials, it is straightforward to determine the variation of $\theta$ with the true stress, and this is shown in fig.3. The Voce relationship is seen to be obeyed for a wide range of temperature and stress for the various structures studied.

With increasing temperature, the interaction cross-section of a moving dislocation will increase (4). The higher the degree of stretch, the higher the dislocation density, and thus the greater the probability of softening.

This model assumes that the degree of precipitation of S-phase at the dislocations upon ageing is insufficient to immobilise them. If the volume fraction of S-phase were increased sufficiently, it is possible that this effect of stretch upon dynamic recovery would not be observed, as complete dislocation pinning would obtain.


## ACKNOWLEDGEMENTS

The authors are grateful to Professor Sir P.B. Hirsch FRS for the laboratory facilities made available, and to the Procurement Executive MOD for the provision of material. One of us (X.X.) gratefully acknowledges the support of the Lee Hysan Foundation and St. Hilda's College, Oxford.


## REFERENCES


1. H.M. Flower, P.J. Gregson, C.N.J. Tite and A. Mukhopadhyay, Proc. Int. Conf. on "Aluminium Alloys, Their Physical and Mechanical Properties", Charlottesville, Va., June 1986, Vol.II: 743.

2. U.F. Kocks, Trans ASME J. Eng.Mat. Tech. (1976) 98: 76.

3. E. Voce, J. Inst. Metals (1948) 74: 537.

4. H. Mecking and G. Gottstein in 'Recrystallization of Metallic Materials' ed. F. Haessner, Riederer Verlag, Stuttgart, (1979): 195.


(a) (b) (c)

Fig.1 TEM micrographs showing the S-phase in (a) N material (bright field), (b) D material (dark field), and (c) 7% stretched materials (dark field).

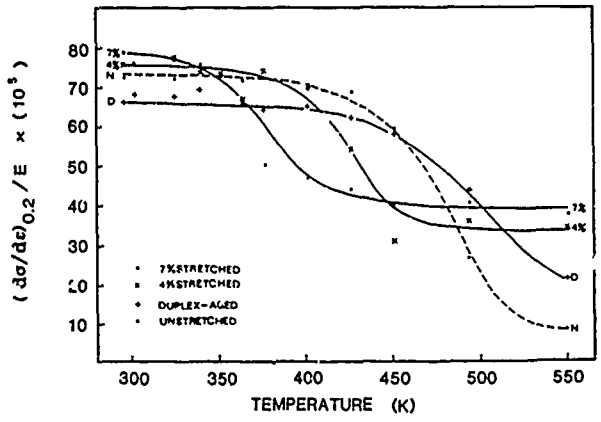


Fig.2 The variation in modulus-normalised work-hardening rate with temperature.

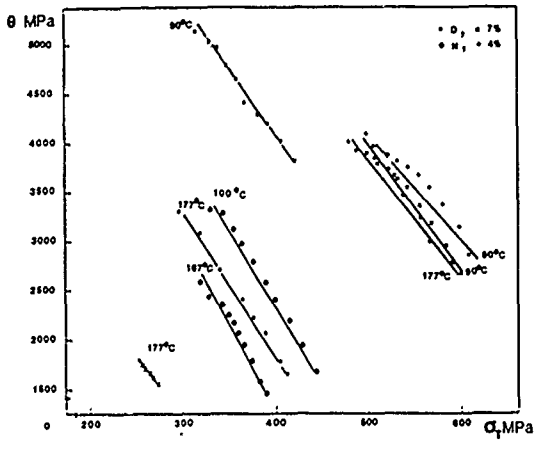


Fig.3. The variation in work-hardening rate with (true) flow stress.

K. NISHIDA and G.A. WEBSTER

# PREDICTION OF FAILURE BY CREEP CRACK GROWTH AND NET SECTION DAMAGE

Both Mr. Nishida and Dr. Webster are in the Department of Mechanical Engineering at Imperial College, London, SW7 2BX.

## SYNOPSIS

Failure by creep of components which contain an initial crack like defect is considered. A model is outlined in which local damage around the crack tip is allowed to interact with remote damage to predict failure by combined crack growth and net section rupture of a ½%Cr ½%Mo ¼%V steel pressure vessel which contained a full circumferential external defect.

## INTRODUCTION

Previous descriptions [1-4] of the failure of cracked components at elevated temperatures have assumed that the processes of crack growth and net section rupture proceed independently. Ligament damage ahead of the advancing crack was not considered to influence crack propagation rates cumulatively, although service exposed, rather than virgin, material properties have been employed in some remanent life assessments [4]. In this paper a model is outlined which allows interaction to take place between the crack growth and net section rupture mechanisms. The model is then applied to a practical example of an external circumferential crack growing in a pressure vessel [5,6].

## MODEL

Most models [7] of creep crack growth postulate a process zone at the crack tip as shown in Fig. 1. It is supposed that crack advance takes place when the creep ductility of the material in this region is exhausted. For a material in which creep strain rate $\dot{\varepsilon}$ and rupture life $t_r$ can be expressed in terms of stress $\sigma$ by

$$\dot{\varepsilon}/\dot{\varepsilon}_o = (\sigma/\sigma_o)^n \qquad (1)$$

and

$$t_r = \frac{\varepsilon_{fo}}{\dot{\varepsilon}_o}\left(\frac{\sigma_o}{\sigma}\right)^\nu \qquad (2)$$

where $\dot{\varepsilon}_o$, $\sigma_o$, n and $\nu$ are material constants and $\varepsilon_{fo}$ represents the material uni-axial creep ductility at stress $\sigma_o$, the model leads to a relationship between crack growth rate $\dot{a}$ and the creep fracture mechanics parameter C* of the form

$$\dot{a} = D_o C^{*\phi} \qquad (3)$$

where $\phi = \nu/(n+1)$ and $D_o$ is relatively insensitive to the process zone size $r_c$ (which can be taken to be approximately equal to the material grain size) but inversely proportional to the material creep ductility $\varepsilon^*_{fo}$ appropriate to the state of stress at the crack tip [7]. For plane stress conditions this can be taken as the uni-axial creep ductility $\varepsilon_{fo}$ and for plane strain conditions $\varepsilon_{fo}/50$.

When a crack propagates into undamaged material $D_o$ can be assumed to remain constant. However if damage accumulates in the uncracked ligament less ductility will be available to be exhausted in the process zone at the crack tip and, from eqns (1-3) it can be shown that, crack growth rate will increase proportionately to

$$\dot{a} = \frac{D_o}{[1 - t/t_r]} C^{*\phi} \qquad (4)$$

where $t/t_r$ is the fraction of life used up in the uncracked ligament.

## PRACTICAL APPLICATION

Equations (3) and (4) will be applied to predict crack growth in a plain cylinder of normalized and tempered ¼CrMoV steel tested under a constant internal pressure of 62.5 MPa at a temperature of 565°C [5,6]. Details of the vessel and notch dimensions are shown in Fig 2. The external circumferential notch C of initial depth 30 mm will be examined.

Relevant material properties are shown in Figs 3 and 4 and Table 1. The dashed lines in Fig 3 represent bounds to $D_o$ in eq (3). The material exhibited predominantly tertiary creep behaviour and Fig 4 shows minimum $\dot{\varepsilon}_{min}$ and average $\dot{\varepsilon}_A = \varepsilon_{fo}/t_r$ creep rates.

Calculations of crack growth in the vessel have been made for estimates of C* obtained from [9] using the average creep rate data. Two values of $\varepsilon^*_{fo} = 0.01$ and 0.02, to represent lower bound and average cracking properties, respectively, have been examined. The predictions are compared with experiment in Fig 5.

In Fig 5 the dotted lines represent the predictions of eq (3) which assumes no effect of damage in the uncracked ligament on crack growth whereas the solid lines incorporate the influence of net section damage described by eq (4). The effect of damage interaction is most marked towards the end of the test. It is apparent that the interaction model with $\varepsilon^*_{fo} = 0.02$ gives closest agreement with the experimental data. The initial high predicted cracking rate is a consequence of having used average creep rate $\dot{\varepsilon}_A$. Had minimum creep rate $\dot{\varepsilon}_{min}$ been employed approximately the correct initial cracking rate would have been obtained.

## CONCLUSIONS

Closer agreement between experiment and predictions is achieved when net section damage is incorporated into creep crack growth models. The effect will be most marked for small initial crack sizes.

## REFERENCES


1. AINSWORTH, R.A., CHELL, G.G., COLEMAN, M.C., GOODALL, I.W., GOOCH, D.J., HAIGH, J.R., KIMMINS , S.T. and NEATE, G.J. CEGB rep. no. TPRD/B/0784/R86.
2. WEBSTER, G.A., SMITH, D.J. and NIKBIN, K.M. Int. conf. on creep. Tokyo, 1986, JSME, p. 303-308.
3. SMITH, D.J.and WEBSTER, G.A. 'Creep and fracture of engineering materials and structures.' Inst. of Metals, 1987, p. 549-562.
4. WEBSTER G,A. 'High Temperature Crack Growth' I.Mech.E., 1987, p. 1-8.
5. COLEMAN, M.C., PRICE, A.T. AND WILLIAMS, J.A. in 'Fracture' (Ed. D.M.R. Taplin) Waterloo, Canada, 1977, vol 2, p. 649-662.
6. COLEMAN, M.C. in 'Advances in fracture' (Ed. D. Francois) Pergamon, Oxford, 1980, p 1235.
7. NIKBIN, K.M.,SMITH, D.J. and WEBSTER, G.A. Proc. Roy. Soc., 1984, A396, p. 183-197.
8. NEATE, G.J. Mat. Sci and Eng. 1986, vol 82, p. 59-76.
9. KUMAR, V, WILKENING, W.M., ANDREW, W.R., GERMAN, M.D., deLORENZI, H.G. and MOWBRAY, D.F. GE res. rep. SRD-82-048.


Table 1

Coefficients defining average creep properties at 565°C for ½CrMoV, normalized and tempered steel

| n | ν | $(h^{-1})$ | $\sigma_o$ (MPa) | $\varepsilon_{fo}$ | $r_c$ μm |
|---|---|---|---|---|---|
| 6.76 | 5 | $4.5\ 10^{-4}$ | 200 | 0.18 | 70 |

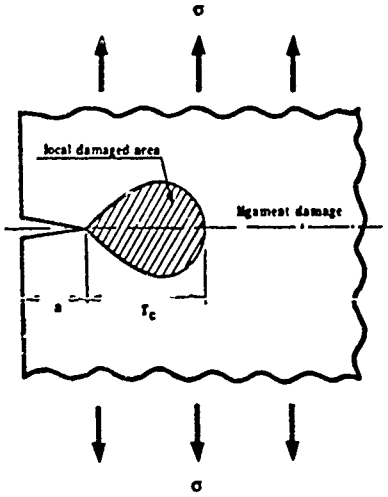


Fig. 1 Development of damage ahead of crack tip

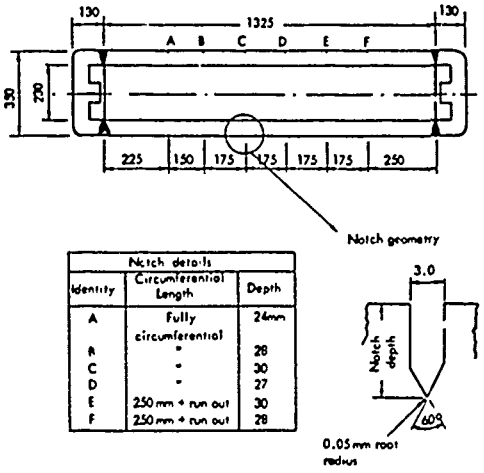


Fig. 2 Details of the circumferentially notched pressure vessel

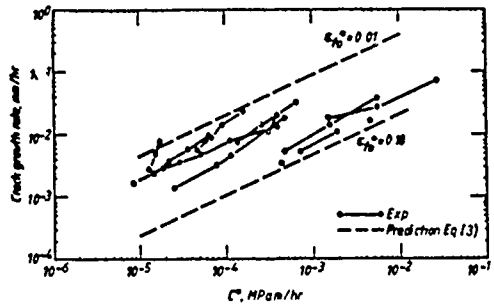


Fig. 3 Crack growth rates as a function of C*,for normalised and tempered 1/2 CrMoV (from Neate[8])

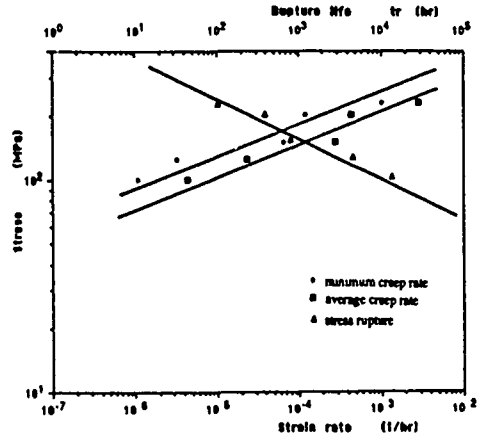


Fig. 4 Uniaxial creep data at 565°C for normalised and tempered 1/2 CrMoV steel

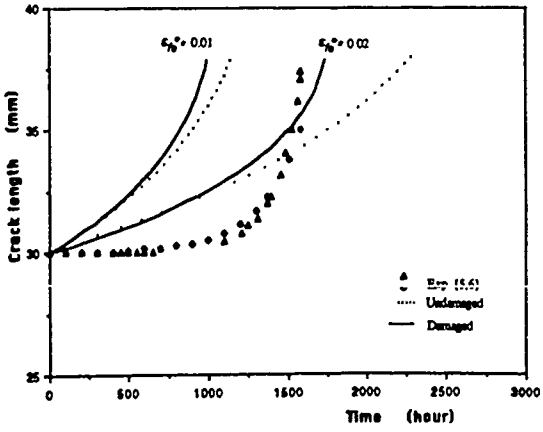


Fig. 5 Experimental and predicted crack growth from a circumferential crack in a 1/2 CrMoV pressure vessel

J. KNEZEVIC and J. L. HENSHALL

# ESTIMATION OF DESIGN LIFE FOR NOTCHED COMPONENTS SUBJECTED TO CREEP CRACKING USING A CONDITION PARAMETER BASED RELIABILITY APPROACH

Drs Knezevic and Henshall are in the Department of Engineering Science, University of Exeter, Exeter, Devon, EX4 4QF

## SYNOPSIS

Since the initial reports of crack growth under creep conditions [1,2], it has become apparent that this aspect of material behaviour must be incorporated into design and inspection methodologies for plants operating in the creep regime. The purpose of the present study is to demonstrate how the concepts and methods of reliability analysis [3,4] can be applied to creep crack growth. Comparison is made with the conventional deterministic approach to the problem.

## INTRODUCTION

An area of current concern with regard to the commercial steels being used in power-generating plant is to be able to provide good estimates of the remnant life of in-service components and pipework, particularly in the presence of macroscopic defects. These defects may grow under essentially constant load conditions to give failure. The mechanics of this creep crack propagation are complex and as yet incompletely determined, but depend on the interaction of both the material and stress state. The purpose of this paper is to outline a novel reliability-based approach that could be used to analyse in-service NDE flaw size data to provide quantifiable estimates of the remaining operational lifetime at a specified reliability level.

## EXPERIMENTAL DATA

The laboratory data utilised were obtained on six Double Edge Notched Tension specimens of AISI 316L stainless steel, which is commonly used in the power-generation and processing industries, using the procedures outlined in [5]. The test temperature was 909 K and the initial stress levels varied between 190 and 221 MPa. This stress variation was taken as being typical of that which might occur under operational conditions.

## CONVENTIONAL ANALYSIS OF RESULTS

For creep ductile materials the rate of crack growth is primarily dependent upon $C^*$, which is defined by:

$$C^* = \int_\Gamma \left\{ \left( \int_0^{\dot{\epsilon}_{ij}} \sigma_{ij} d\dot{\epsilon}_{ij} \right) dy - T_i \frac{du_i}{dx} ds \right\} \qquad (1)$$

Using the approach of Harper and Ellison [6], this can be shown to reduce to:

$$C^* = \frac{n}{n+1} \sigma_{net} \frac{d\Delta_c}{dt} \qquad (2)$$

for the DENT geometry, where $\sigma_{net}$ is the net section stress, $d\Delta_c/dt$ is the creep displacement rate at the loading pins, and n is the exponent in the Norton creep equation.

As can be seen from Figure 1, the crack growth rate data correlate well with $C^*$, and are well represented by the equation:

$$da/dt = 1.1 \times 10^{-8} (C^*)^{0.927} \qquad (3)$$

where the units of $C^*$ and $da/dt$ are $J\ m^{-2} s^{-1}$ and $m\ s^{-1}$ respectively.

The application of this data in the operational situation is however quite difficult and complex. Firstly, as is clear from equation (1), the calculation of $C^*$ for an arbitrary shaped defect in a multiaxial stress field requires considerable computational effort, particularly since displacement rates are not available in these situations. This is added to by the fact that since $C^*$ is a fairly complex function of both crack length and time, integration of an equation such as (3) to give the failure time is difficult. These factors are in addition to the usual problems of applying laboratory derived data to the material actually in-service, microstructural evolution of the material changing the properties, and the difficulties of defining the operational conditions precisely.

## RELIABILITY ANALYSIS OF RESULTS

It is proposed that the problems encountered above can be circumvented by adopting a probabilistic analysis and applying to flaw size data determined by NDE. A new approach to the calculation of reliability characteristics based on the probability distribution of relevant condition parameter, RCP, is presented in [3]. This is a parameter that describes the condition of the system/component at every instant of operating time. According to [3], reliability is defined as the probability that the relevant condition parameter will have a value between an initial value, RCPin, and the limiting value, RCPlim, thus:

$$R(t) = \int_{RCPin}^{RCPlim} f(RCP,t) dRCP \qquad (4)$$

where f(RCP,t) is the probability density function of RCP at time t. In this study the length of the creep crack is taken as the relevant condition parameter. In order to determine the reliability function defined by equation (4), it is necessary to provide a condition matrix which presents the set of numerical values of RCP

of several nominally identical systems/components obtained at several different instances of operating time, and to follow the methodology described in [4]. In this case the condition matrix (Fig. 2) consists of the measured values of the length of crack measured every 10 hours during the test for six specimens. The limit value adopted was 2.5 mm. The algorithm developed [4] was implemented in FORTRAN on a PRIME computer to determine the reliability function presented in Fig. 3, defined by a Weibull distribution, thus

$$R(t) = P(RCP, t < 2500) = exp(-t/96.6)^{42.6} \quad (5)$$

As the expected operating life of the system/component is equal to the area below reliability function, it is possible to estimate either the operating life at the design stage using laboratory data or the remnant life using inspection derived data, with this new approach. In this study the estimated safe operating life was 95 hours.

## Conclusions

This study would suggest that it is possible to use a probabilistic method for design and remnant lifetime estimates of failure by creep crack growth in operational conditions.

## References


1. Siverns, M. J. and Price A. T., Nature, 228, 1970, 760.
2. James, L. A., Int. J. Fracture, 8, 1972, 347.
3. Knezevic, J., Reliability Engineering, 19, 1987, 29.
4. Knezevic, J., Proc. of International Symposium on "Risk Analysis in Enviromental Impact Assessment, Milan, November 1987.
5. Henshall, J. L., Gee, M. G., Singh G. and Boyd G.A.C., ICM-3, Vol 2, 1980, 309.
6. Harper, M. P. and Ellison, E. G., J Strain Analysis, 12, 1977, 167.


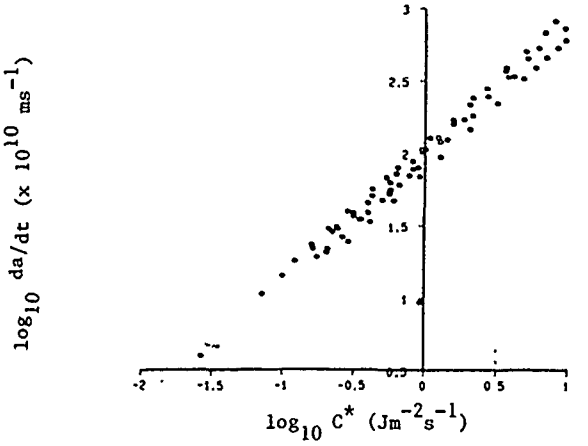


Figure 1. log crack growth rate vs log C*

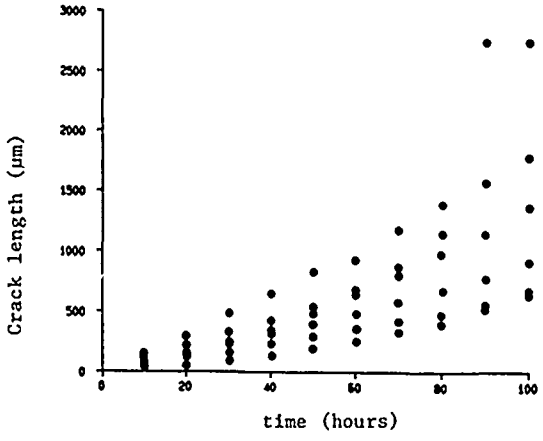


Figure 2. Crack length vs time

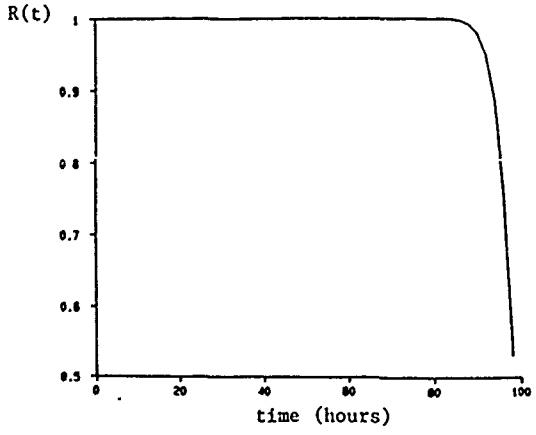


Figure 3. Reliability function vs. time

G. M. Carter, J. L. Henshall and R. M. Hooper

# CREEP OF ZIRCONIA CERAMICS BELOW 0.2 Tm

The authors are in the Department of Engineering Science, University of Exeter, Exeter, Devon.

## SYNOPSIS

Indentation creep has been observed in both polycrystalline and single crystal stabilised zirconia at low homologous temperature. The activation energy of the time-dependent plastic deformation process is derived and the implications for design are described.

## INTRODUCTION

Engineering ceramics are a class of inorganic compounds that are to be found in an increasing number of demanding applications, e. g. mechanical seals, bearings, tools, etc., where high strength, resistance to chemical attack and dimensional stability are necessary material properties [1,2].

Indentation and scratch hardness techniques are the most realistic simulative test procedures for materials evaluation for these applications. The most appropriate parameter is however not the conventional short-time hardness, but the indentation response under prolonged loading. The continuing penetration of an indenter, under constant load is refered to as indentation creep and the increase in the size of the impression is used as a measure of strain rate. The localised high hydrostatic stress beneath the indenter enables it to be used to observe creep in normally brittle materials where other test methods cause failure by fracture to occur before sufficiently high stresses can be attained.

The indentation creep behaviour of two types of cubic stabilised zirconia single crystal, a ceria stabilised TZP (tetragonal zirconia polycrystalline, 14.3 wt.% $CeO_2$) and a yttria stabilised polycrystalline cubic zirconia has been studied.

## EXPERIMENTAL

Single crystals of calcia stabilised (8.7 wt.%) and yttria stabilised (19.0 wt.%) zirconia were oriented by Laue back reflection analysis to give {111} faces. Small specimens of single and polycrystalline materials were taken and the faces to be indented were ground parallel prior to polishing with diamond paste to a 1/4 micron finish. Hardness measurements were made with a Knoop indenter and a load of 2.94N, with the long diagonal aligned parallel to ⟨110⟩ on the {111} single crystals [3]. The hardness tester had been modified for use with an optical microscope hot-stage to allow measurements to be made at elevated temperatures. A minimum of five indentations were made at dwell times of 1000s. or less and a minimum of three for times of 10000s ; all impressions were measured at x625 magnification to ±0.2 micrometres.

## RESULTS

Figures 1(a-d) show the variation of Knoop hardness with time at 290K and 573K. All materials show a decrease in hardness with both increasing time and temperature. The conventional short time hardness of the Yttria stabilised single crystal is slightly greater than the Calcia stabilised at R.T., but the hardness decreases more rapidly with increasing time and temperature. The polycrystalline and single crystal Y-CSZ have approximately similar hardness versus time behaviour at room temperature, but at 573K, there is a markedly greater decrease in the hardness of the polycrystalline material. The Ce-TZP, which has a much greater toughness than the other materials [4], is clearly far less hard and also at 573K shows a very rapid decrease in hardness of ca 25% in only 10000s.

## DISCUSSION

The significance of these results from the design aspect is that use of the short term room temperature hardness values may not be a good guide as to how the material will respond in operational service under relatively good design conditions, i.e. compressive loading and low temperatures, (600K locally. Hence it is necessary to develop a relationship between hardness and time/temperature to enable an improved design analysis procedure to be formulated.

Previous interpretation [5] of the hardness vs time/ temperature data collected on ceramic materials assumes a primary creep process with an associated stress exponent of 10, corresponding to a dislocation climb mechanism, with a conventional Arrhenius-type temperature dependence. The first method of determining the value of the activation energy, Q, requires that a plot of log $(H^{-3} - H_0^{-3})$ vs $\log(t^{\frac{1}{3}} - t_0^{\frac{1}{3}})$, where $H$ and $H_0$ are the hardness values measured at times $t$ and $t_0$, at constant temperature should have a slope of unity. Thus, from measurements made at constant time intervals at two different temperatures the creep activation energy Q, can be calculated from the intercepts. A second method of estimating the activation energy utilises plots of $\log(H_a^{-3} - H_0^{-3})$ vs. 1/T, where $H_a$ are the hardness values made at constant dwell times at temperatures $T$, which have gradients equal to Q/3R.

The results for the Yttria stabilised single- and polycrystal, and the Ceria stabilised TZP were found to fit the model tolerably well giving the activation energy values in Table I. However neither method of analysis was found to be appropriate for the Calcia stabilised single crystal. Since the model was based on the interpretation of hardness/time/temperature data for ceramic and metallic materials at test temperatures greater than

half the melting point, it is not surprising that it has limited applicability given the present low homologous temperatures.

The values obtained are very different from other workers values of activation energies, obtained from high temperature creep measurements, which give values in the range 326 - 646 kJ/mole.

## CONCLUSIONS

The results clearly demonstrate that there is a significant time and temperature dependence of the indentation hardness of both cubic and tetragonal phase stabilised Zirconia ceramics at low homologous temperatures ($\leq 0.2Tm$). The Atkins et al. model of indentation creep [5] has been selected as the most appropriate interpretation of the data, even at this low homologous temperature.

## REFERENCES


1. Engineering Ceramics as applied to Reciprocating Engines, NEL Report, East Kilbride, G75 0QU.
2. The World Market for Advanced Ceramics, B & MR Reports Ltd, Stockport SK6 8DX
3. Carter, G.M., Henshall, J.L and Hooper R.M., J Amer Ceram. Soc., in press.
4. Carter, G.M., Henshall, J.L. and Hooper R.M. in preparation
5. Atkins, A.G., Silverio, A and Tabor D., J Inst Met, 94, 1966, 369.


TABLE I

Activation Energy values for Low Temperature Indentation Creep.

| Material | First Analysis Method Q kJ/mole | Second Analysis Method Q kJ/mole |
|---|---|---|
| Yttria stab. polycrystal | 28.9 | 28.9 |
| Yttria stab. single-Xl. | 12.8 | 12.6 |
| Ce-TZP | 27.1 | 27.1 |

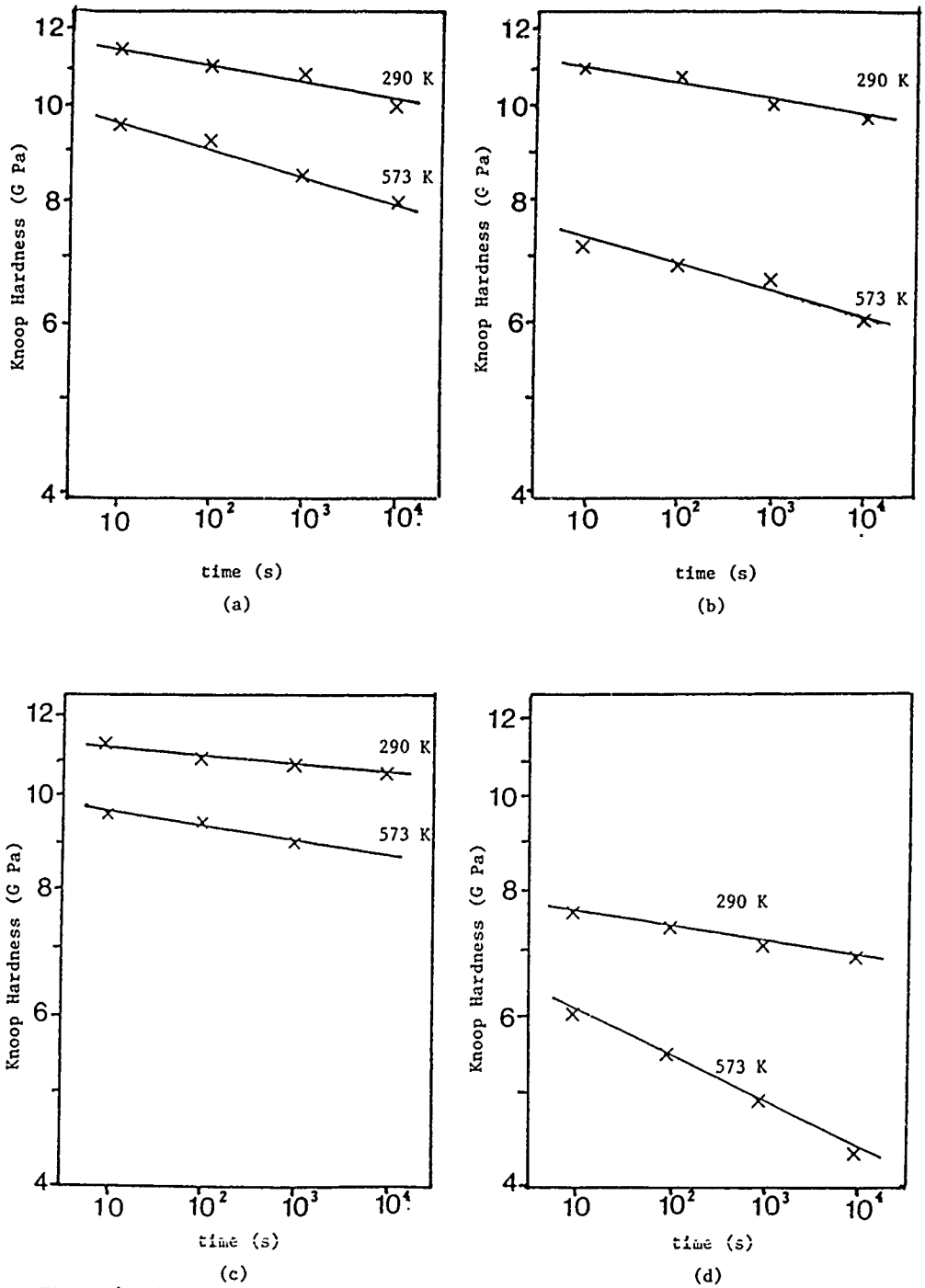


Figure 1. log Knoop hardness vs log time for
(a) Yttria stabilised cubic Zirconia single crystal.
(b) Yttria stabilised cubic Zirconia polycrystalline.
(c) Calcia stabilised cubic Zirconia single crystal.
(d) Ceria stabilised tetragonal Zirconia polycrystalline.

# THE SPECIFICATION AND INSTALLATION OF ALUMINA CERAMICS IN INDUSTRIAL WEAR

C.F. Paine

Morgan Roctec Ltd.,
Stourport-on-Severn.

ABSTRACT

The increasing cost of maintenance and loss of production caused by downtime of expensive capital equipment has meant that wear is now not just considered a fact of life. Engineers are becoming familiar with alternative materials such as ceramics which are finding an increasing market in industrial and process plant.

This paper will consider the use of alumina in engineering applications and discuss the selection, specification and installation of alumina ceramics.

INTRODUCTION

'Wear' defined as the removal of material is a phenomena which affects all industrial plants and processes. Very often wear is accepted as a 'fact of life' that cannot be stopped but can be budgetted for in maintenance schedules. The cost to industrial nations is very high. In 1975 Jost (1) stated that wear was costing the U.S.A. $100 million per annum. Although wear cannot be stopped, the rate of wear can be decreased substantially with the use of the 'best' wear resistant material correctly installed.

Wear can be divided into the following classes: abrasive, erosive, hydraulic, fretting and adhesive. For example in abrasive wear particles under load are sliding over a surface which could be particles 1-100mm of coal sliding down a chute at velocities of 2-5 m/s and erosive wear is caused by the impingement of small particles ( 20-800μm) at high velocities 15-65 m/s such as in the pneumatic conveying of pulverised coal. Many industrial situations involve the combination of different types of wear.

To select the best wear resistant material for any particular application, various factors need to be considered such as: operating temperature, corrosion effects, knowledge of wearing materials, relative cost to relative wear of alternative materials.

SELECTION OF MATERIALS

Classes of materials such as steels, cast irons, ceramics, cermets, plastics and elastomers are all used in wear resistant applications. The range is considerable not only between but within groups. This is important to note as often, for example, 'alumina' ceramics and 'polyurethane' are sometimes specified as one material. It is the purpose of this paper to discuss the selection and specification of alumina ceramics for the lining of pipes conveying particles pneumatically transported at 20-30 m/s i.e. erosive conditions.

WHAT ARE ALUMINA CERAMICS?

Most aluminas used in the wear resistant field have between 85 and 97% $Al_2O_3$, which consists of $Al_2O_3$ grains embedded in a glass/crystalline matrix comprising of a mixture of silicates. A typical production route involves milling and spray drying of the raw materials prior to die pressing and firing at 1400-1650°C.

It has seemed the practice to specify these materials on the basis of hardness, density and even alumina content alone, as a guideline to wear performance. This view is incorrect and the properties of the grain boundary matrix and the size of the alumina grains are equally important. Various models based on elastic-plastic erosion mechanisms have been proposed (2, 3, 4) relating the erosion volume loss (E) to both target and particle properties. The expressions are as follows:

$$E \propto Vo^{3.2}\ R^{3.7}\ \rho^{1.3}\ H^{-0.25}\ K_{IC}^{-1.3} \quad \text{(Ref.2)}$$

$$E \propto Vo^{2.4}\ R^{3.7}\ \rho^{1.2}\ H^{0.11}\ K_{IC}^{-1.3} \quad \text{(Ref.3)}$$

$$E \propto Vo^{2.8}\ R^{3.9}\ \rho^{1.4}\ H^{0.48}\ K_{IC}^{-1.9} \quad \text{(Ref.4)}$$

Vo - particle velocity  R - particle radius
$\rho$ - particle density  H - target hardness
$K_{IC}$ - target fracture toughness

The models do agree, at least qualitatively to distinguish between different material classes. However Dimond (5) has found that in comparing selected aluminas there is no correlation between any of the existing models, fundamental properties and erosion resistance. Tables 1 and 2 compare the properties of three aluminas used in wear resistant applications. It is noteworthy that alumina C with only 86% $Al_2O_3$ has a similar if not better erosion wear resistance than alumina A, a 97.5% $Al_2O_3$. It can be seen from the micrographs in Figs 1-3 that there are distinct differences in micro-structure; aluminas A and C having a smaller more uniform grain size of 2μm although they have different morphologies, compared to alumina B which has some larger grains up to 25μm. Some of the improved wear of alumina C must also be accounted for by a strong intergranular bond between the alumina grains. Hence the erosion wear of aluminas is significantly influenced by the microstructural properties and not necessarily the alumina content and other physical properties.

The results obtained are only applicable when considering impact erosion wear and should not be related to other wear regimes such as abrasive and hydraulic. These wear situations require an

accepted wear resistance test orientated to that particular application.

INSTALLATION OF CERAMICS

If ceramics are to be installed, the design has to ensure that the yield point of the ceramic is never reached or, if it is, the resultant crack does not enable tiles to fall out when installing alumina onto mild steel. The fact that the thermal expansion coefficient of the metal is twice that of alumina may need to be designed around. These problems can normally be overcome by using an appropriate fixing method such as:

* direct rigid bonding of the lining on the steel with a suitable adhesive
* bonding of the lining onto an elastomeric intermediate layer
* mechanical attachment
* self-supporting systems

Most ceramics are supplied as relatively small standard tiles which on installation result in joints between tiles. The joints cause areas of greatest wear. Fig.4. shows the problems that can exist using a brickwork pattern. This significantly reduces the effectiveness of the alumina lining. Joints lying parallel to the flow of material have given the expected increase in life over existing solutions. It is also important to minimise the gaps between tiles and if possible use an interlocking or tapered joint.

APPLICATION OF CERAMICS

If a typical application is considered; pneumatically conveying boiler ash of max size 3mm through 100mm bore bends at a design velocity of 25 m/s, it has been found that 6mm thick mild steel has lasted 15 days after a throughput of 120 tonnes. In laboratory testing using the equivalent ash, the 'best' alumina outperforms mild steel by a factor of 44 and the 'worst' grade of alumina by a factor of 8. The maximum weight acceptable means that only 12mm of ceramic is feasible and based on the above materials evaluation, a lined system would last for:

| 6mm Steel | 12mm 'best' alumina | 12mm 'worst' alumina | Total (days) |
|---|---|---|---|
| 15 | | | 15 |
| 15 | 1320 | | 1335 |
| 15 | | 240 | 255 |

if it is assumed life is proportional to thickness. If consideration is taken that once wear starts, impact angles, effects of joints, and hence wear rates increase, then the estimated lives for the 'best' and worst' alumina can be estimated to be 1,000 and 182 days respectively.

Possible installation solutions are:

a) For bends with a centre line radius to internal diameter 8, the bend can have a fabricated channel on the extrados of the bend lined with alumina tiles.

b) A square section bend can be fully lined with a square to round converter at the exit end (Fig.5). Fig.6. shows such a typical bend with a removable intrados plate to facilitate inspection.

c) Fig.7 shows a ceramic pipe constructed as a smooth tube or a lobster back form.

CONCLUSIONS

It has been shown that alumina ceramics can be used to replace metallic components to increase component life. In order to get the most benefit from ceramics in terms of cost/performance, it is necessary to design the component with ceramics in mind and not to design a metal component and then try and line it. It is of prime importance that design engineers and material scientists work in co-ordination to optimise the microstructure and physical properties through processing route and that components are designed to maximise the properties of the ceramic and not just the metallic replacements.

REFERENCES

1. Jost H.P. 'Principles of Technology' MacMillan, New York 1975.
2. Evans A.G., Gulden M.E., Rosenblatt M. Proc. R.Soc. London, A361(1706) 343-65 (1978).
3. Ruff A.W., Wiederhorn S.M. Treatise on Materials Science and Technology 16 1-67 (1979).
4. Wiederhorn S.M. Hockey B.J., J. Mat.Sci. 18 766-780 (1973).
5. Dimond C.R. Eurotrib '85 p.5 Paper 5.3 1/6-6/6 Elsevier-Science Publishers BV.

TABLE 1 - PROPERTIES OF ALUMINAS A, B AND C

| ALUMINA | %$Al_2O_3$ | Bulk Density ($g\ cm^{-3}$) | Hardness R45N | Hardness GPa | $K_{IC}$* ($M\ Pam^{\frac{1}{2}}$) |
|---|---|---|---|---|---|
| A | 97.5 | 3.80 | 84 | 15.7 | 3.2 |
| B | 97.0 | 3.81 | 82 | 14.8 | 3.4 |
| C | 86.0 | 3.51 | 75 | 9.5 | 2.8 |

* as measured by pyramid indentation.

TABLE 2 - EROSION DATA FOR ALUMINAS A, B AND C

Erodent 250μm $SiO_2$ Particle Velocity 45 m/s

Volume Loss ($cm^3\ 10^{-10}$) per impact

| ALUMINA | IMPINGEMENT ANGLE (DEGREES) 25 | 90 |
|---|---|---|
| A | 1.1 | 2.7 |
| B | 2.3 | 5.8 |
| C | 0.9 | 2.4 |


Fig.1. - ALUMINA A

Fig.2. - ALUMINA B

Fig.3. - ALUMINA C

Fig.4. - 'BRICKWORK' INSTALLATION IN PIPE BEND CONVEYING PULVERISED COAL

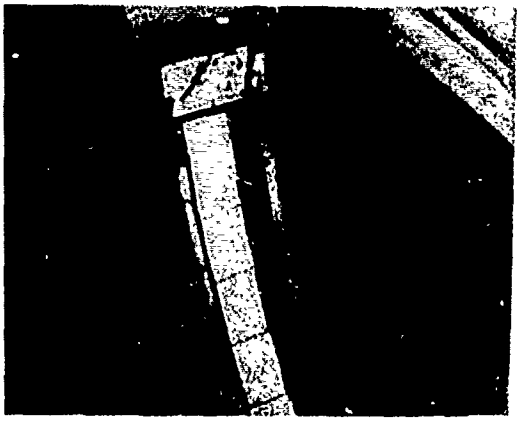

Fig.5. - BEND SHOWING INTRADOS REMOVED FOR INSPECTION

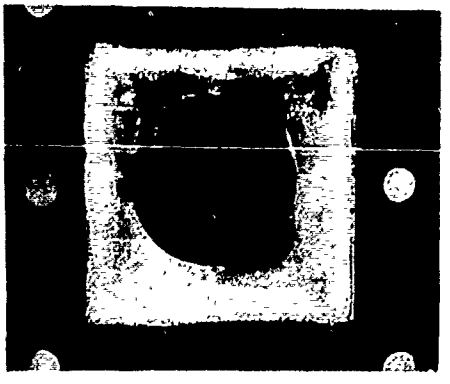

Fig.6. - SQUARE TO ROUND CONVERTER

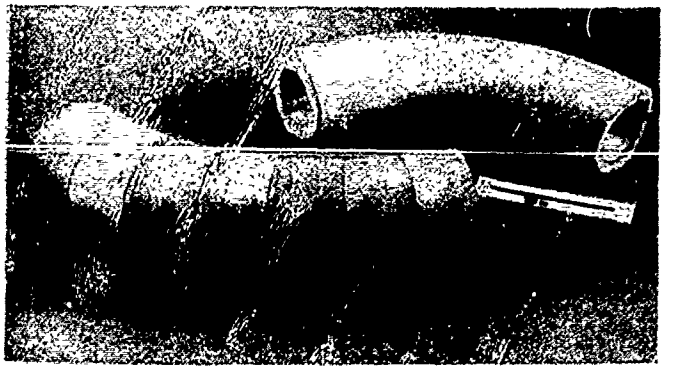

Fig.7. - SMOOTH CERAMIC TUBE AND LOBSTER PACKED BEND

P.J. BRIDGES and J.WILLIS

# NEW THINKING ON THE FUTURE OF HOT SHEET METAL FORMING

Dr. Bridges is Manager, Materials Group Technology, Inco Engineered Products Limited; Mr. Willis is a Consultant.

## INTRODUCTION

Hot sheet forming is a method of making a sheet fabrication using a single female die into which the shape is formed by gas pressure.

There is very accurate reproduction of the die shape and none of the spring back which can occur when conventional forming methods are used.

Broader acceptance of the process has been delayed by the high cost of superplastic materials, their slow forming speeds and the high die costs.

## DIES

Part costs on limited runs are sensitive to die costs. Dies cast in High Alumina cement give excellent finish and good dimensional accuracy without machining. Dies can be cast on 3 dimensional patterns or from an existing component.

## WELDED PREFABRICATION

Simple shapes such as boxes or cylinders can be cheaply and automatically welded, then formed to a more complex shape. Material such as IN-744 stainless, or Ti-6Al-4V Titanium have weld joints which are themselves superplastic. This technique can eliminate difficult post forming welds and attendant jigging problems. The hot forming process iteself also proves the integrity of the joint.

Recently developments in Plasma Keyhole welding indicate this technique may be extended to Aluminium alloys.

## MEMBRANE FORMING

Using a suitable superplastic diaphragm, non superplastic materials (of low cost) can be deep drawn into dies with reduced stretching and consequent lower cavitation. Thickness distribution of the part is more uniform and hence the blank may be of thinner material. In certain circumstances the diaphragm is reusable. Cavitation is also considerably reduced.

## NEW MATERIALS [1]

Metal Matrix composites, such as the New Al Alloys containing 20% SiC particles give elongations of $\approx$200% at forming speeds up to 1000%-/min. Alloy 2124 with 0.6Zr can give $\approx$ 500% elongation at similar forming speeds. The higher cost of these alloys may be offset by the potentially higher production rate, and the significantly better mechanical properties.

Ref.1. T.G. Nieh and J.Wadsworth. Superplasticity in Aerospace-Aluminium Cranfield August 1985.

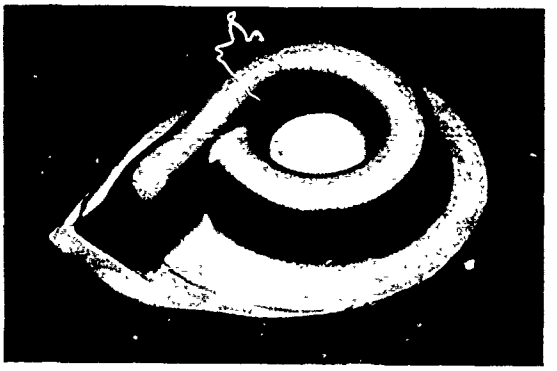

1 Pump cover in AA7475 formed in Ceramic Die
Size 370 x 300mm approx.

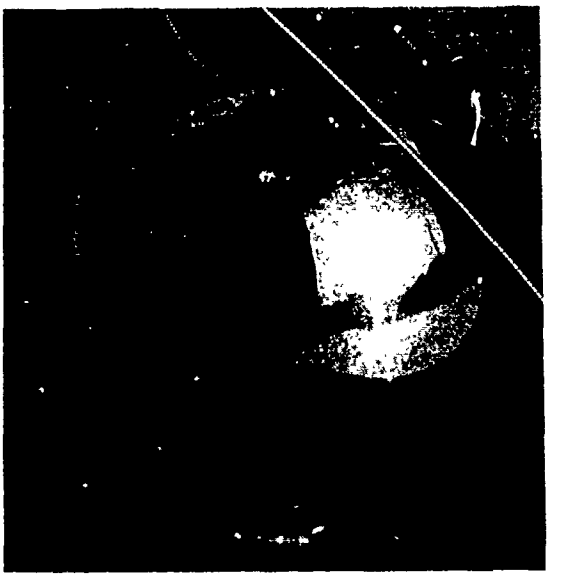

2

460mm diameter spherical loudspeaker cabinet made from closed ended welded cylinder of IN744 stainless steel.

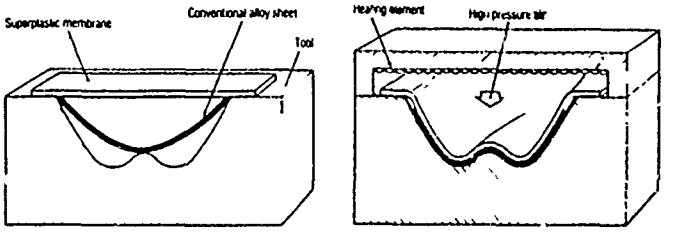


3 Principles of Membrane Forming

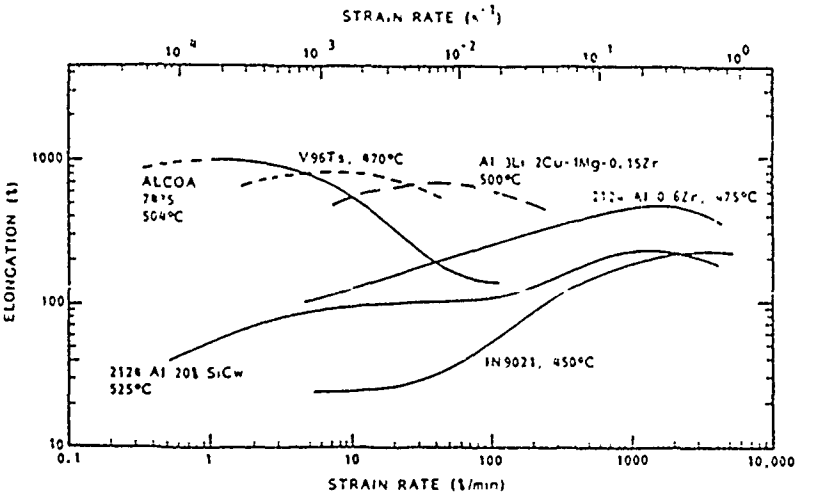


4 Strain rate/elongation characteristics of advanced aluminium alloys and composites (ref. 1)

# POST-PROCESSING OF CRACK INITIATION

J. LEMAITRE

Professeur à l' Université PARIS 6

**Laboratoire de Mécanique et Technologie**
(E.N.S. de Cachan/C.N.R.S./Université PARIS 6)
61, Avenue du Président Wilson - 94230 CACHAN (France)

The damage of a material submitted to any history of loading is always very localized at a scale below the one of the classical volume element in mechanics. This allows to consider that the coupling between the damage and the strain behaviors exists only at micro-scale. Then, a prediction of the conditions of crack initiation in structures may be set up in two steps.

In a first step, the stresses and the stresses fields can be calculated by classical elasticity, plasticity or viscoplasticity neglecting the coupling at macro-scale with the damage that is the damage dissipation in comparison to the strain energy.

In a second step, the maximum loaded macro-point is chosen as the one for which the damage equivalent stress is maximum and its strain history is considered as an imput in a micro-mechanics post-processor. The macro-volume element, strain loaded, is an elasto (visco) plastic matrix containing a micro-grain of the same material but weaker because of a lower yield stress taken as the fatigue limit and a damageable character represented, within the hypothesis of isotropy, by a scalar variable. The constitutive equations introduced at micro-scale are those of the standard materials, the coupling between strain and damage through the KACHANOV effective stress concept being done at the two levels of state variables and kinetic flux variables. The damage constitutive equation takes into account brittle, ductile, fatigue or creep damages. For a given history of three-dimensional state of macro-strain, the micro-strain and the damage are calculated within the hypothesis of strain compatibility of LIN TAYLOR.

This allows to consider this calculation of the integration in one point of the set of constitutive equations as a post-processor of a classical finite element code. The conditions for crack initiation are those corresponding to a critical value of the calculated damage.